Using the *Pseudomonas aeruginosa* T6SS as a protein shuttle to deliver effectors

Sarah Wettstädt

Department of Life Science

Imperial College London

This thesis is submitted in partial fulfilment of the

requirements for the degree of Doctor of Philosophy

Candidates declaration

I hereby declare that the work presented in this thesis is my own and that the contributions of others are duly acknowledged and appropriately referenced.

Copyright declaration

The copyright of this thesis rests with the author and is made available under a Creative Commons Attribution Non-Commercial No Derivatives licence. Researchers are free to copy, distribute or transmit the thesis on the condition that they attribute it, that they do not use it for commercial purposes and that they do not alter, transform or build upon it. For any reuse or redistribution, researchers must make clear to others the licence terms of this work.

Abstract

Pseudomonas aeruginosa is a dreadful opportunistic pathogen that can cause both acute and chronic infections in humans. This bacterium exhibits great abundance of virulence factors and has the ability to flourish in a wide range of environmental niches, partly due to its remarkable arsenal of protein secretion systems. The type VI secretion system (T6SS), is a contractile injection apparatus that translocates a spike loaded with various effectors directly into eukaryotic and prokaryotic target cells. *P. aeruginosa* can load either one of its three T6SSs with a variety of bullets by specific but different modes. This dissertation reveals work focussed on the molecular details of how effector delivery relies on the appropriate attachment onto the T6SS apparatus and spike.

Our work provides details on how the spike components of the T6SS can be manipulated to deliver effector proteins, which highlights an exceptional modularity for loading the T6SS nanoweapon. The spike, which punctures the bacterial cell envelope allowing effector transport, consists of a torch-like VgrG trimer on which sits a PAAR sharpening the VgrG tip. We show how various effectors can be fused directly to either of the two spike components and reach the supernatant or are delivered into target prey cells. Further, we reveal that effectors specifically bind to different parts of VgrG proteins and that these interactions not only lead to effector stabilisation, but also to their secretion. In summary, this work will give sound evidence that an effector delivered by the T6SS requires a chaperone module for stabilisation and an adaptor module for its connection to the T6SS spike.

Results from this thesis highlight the various modes that are at *P. aeruginosa'* s disposal to deliver its many T6SS effectors, which confer a significant advantage during bacterial competition. Overall, this work advances our understanding on the delivery mechanisms of T6SS effectors and thus, in general, of this fantastic nanomachine.

Acknowledgements

First of all, I thank Professor Alain Filloux for giving me the opportunity of doing a PhD in his lab under his supervision. It has been an absolute pleasure to be your student and learn from you to think critically and independently. Your mentorship was both encouraging and challenging, and always appropriate!

I want to extent my thanks to all lab members from the Filloux group. It was such a great and inspiring environment to work in for three years and I will certainly miss all the laughter in the lab! My biggest thanks go to Thomas Wood, without whom this PhD would have been half the fun! Thank you for being an awesome lab buddy and for always being a sounding board for my crazy ideas as well as for making lab weekends and long nights enjoyable and for teaching me about the English language and culture. I also would like to thank Dr Patricia Bernal and Dr Luke Allsopp, who were both great mentors for my professional development. Thank you for always having good advice for me for any question or problem that I had. I gratefully acknowledge Prof Erh-Min Lai for strains and antibodies, and also Dr Manda Yu and Dr Jer-Sheng Lin for making my stay in Taipei an amazing experience and for taking the time to help me in the lab as well as showing me around Taipei.

I must also thank my grandparents for their never-ending encouragement. Massive thanks go to my brother Robert, as well as Denise, Stefan, Susanna, Sven and Javi for supporting me throughout the last years and for believing in me, for pushing and distracting me whatever was more appropriate, for always having a place to crash for me or just for feeding me. I could have not tackled this without any of you!

Contents

Candidates declaration 2

Copyright declaration 3

Abstract 4

Acknowledgements 5

Contents 6

List of figures 13

List of tables 18

Abbreviations 19

1. Introduction 21

1.1. About *Pseudomonas aeruginosa* 21

1.1.1. The opportunistic pathogen *P. aeruginosa* 22

1.1.2. Antibiotic resistance 23

1.1.3. The diversity of *P. aeruginosa* strains 24

1.2. Protein secretion systems 25

1.2.1. Translocation across the inner membrane 26

1.2.2. Type I secretion system 28

1.2.3. Type II secretion system 30

1.2.4. Type III secretion system 35

1.2.5. Type IV secretion system 40

1.2.6. Type V secretion system 46

1.2.7. Polymorphic toxins 48

1.2.8. Contact-dependent growth inhibition 50

1.2.9. The type VII secretion system 54

1.3. The type VI secretion system in *P. aeruginosa* 55

1.3.1. The overall structure of the T6SS and mechanism of action 56

1.3.2. Spike composition 60
1.3.3. *P. aeruginosa* contains three T6SS clusters and up to 11 *vgrG* islands 63
1.3.4. Regulation of the T6SS in *P. aeruginosa* 66
1.3.5. Impact of the T6SS during interbacterial warfare 70
1.3.6. Effector activities 72
1.3.7. Effector delivery modes 78
1.4. Overview of this study 89
2. Experimental procedures 90
2.1. Bacterial strains and growth conditions 90
2.1.1. Bacterial strains 90
2.2. Molecular biology techniques 96
2.2.1. Genomic DNA extraction 96
2.2.2. Cloning PCRs 100
2.2.3. Colony PCRs 101
2.2.4. Restriction digestion and ligation 102
2.2.5. Mutagenesis and allelic exchange 103
2.2.6. Plasmid introduction into *P. aeruginosa* 110
2.3. Protein analysis 111
2.3.1. Secretion assays 111
2.3.2. SDS-PAGE and western blot 112
2.4. Interbacterial competition assays 113
2.5. Translocation assays 114
2.6. *In silico* analysis 115
3. Results:VgrGs can serve as delivery vehicles for a range of effector domains 117
3.1. Introduction 117
3.2. Aim of this chapter 118
3.3. Secretion assays as a read-out for chimera functionality 120
3.4. A canonical VgrG can secrete the extension domain from another evolved VgrG .. 121

3.4.1. VgrG1a-VgrG2b-CT is secreted 123
3.4.2. Comment: VgrG2b-CT has anti-bacterial activity 124
3.5. The unrelated passenger protein Bla_{TEM-1} can be delivered via the T6SS 126
3.5.1. Bla_{TEM-1} as a fusion to the canonical VgrG1a is secreted 126
3.5.2. Bla_{TEM-1} as a fusion to the canonical VgrG4b is secreted 128
3.5.3. VgrG proteins cannot deliver Bla_{TEM-1} into eukaryotic cells 131
3.6. Grafting an Hcp-dependent effector on a canonical VgrG 134
3.6.1. Tse2 as an extension domain of VgrG1a can reach the supernatant 135
3.6.2. Disrupting the interactions between Tse2 and Hcp1 in an attempt to increase secretion of the fusion VgrG1a-Tse2 137
3.6.3. Tse2 is likely delivered into prey cells when fused to VgrG1a 139
3.6.4. Summary: Rerouting an Hcp-dependent effector is rather challenging 141
3.7. Large T6SS effectors can be delivered when fused to canonical VgrGs 143
3.7.1. VgrG4b-PldA is secreted 145
3.7.2. VgrG4b can deliver covalently linked PldA into prey cells 146
3.7.3. Summary: Upgrading a cargo effector to an extension domain leads to an unstable but deliverable complex 148
3.8. Discussion 150
3.8.1. Evolved VgrG proteins can deliver a range of effector domains 150
3.8.2. Not every VgrG can puncture eukaryotic cell membranes 152
4. Results:PAAR proteins bind specific VgrG trimers and can carry effector domains 154
4.1. Introduction 154
4.2. Aim of this chapter 158
4.3. PAAR proteins guide VgrG trimer assembly and delivery 159
4.3.1. VgrG1a is secreted depending on its cognate PAAR effector 159
4.3.2. VgrG1a, VgrG1b and VgrG1c form heterotrimers 162
4.3.3. VgrG1a does not depend on VgrG1b or VgrG1c for secretion 163
4.4. PAAR proteins bind their cognate VgrG trimers via the last β-sheet 166

4.4.1. Analysing the interface between PAAR domains and VgrG trimers 166
4.4.2. Disrupting Tse7-binding to its cognate VgrG1b 172
4.4.3. Designing chimerae to study interactions between VgrG1a and the PAAR domain of Tse6 174
4.4.4. Full length VgrG1a is required to bind its cognate PAAR-domain 177
4.4.5. Summary: Full length VgrG1a is required to form a functional T6SS spike 182
4.5. PAAR proteins can carry heterologous effector domains 184
4.6. PAAR domains are part of large polymorphic toxins 187
4.6.1. PAAR folds in the N-termini of Rhs proteins connect them to the T6SS tip 187
4.6.2. Some evolved PAAR effectors contain N-terminal transmembrane domains and are delivered dependent on Eag proteins 192
4.7. Summary 195
4.8. Discussion 196
4.8.1. VgrG hetero-trimerisation 196
4.8.2. Formation of a functional T6SS tip requires a complete VgrG-PAAR assembly 197
4.8.3. VgrG1abc form stable multimers 198
4.8.4. Molecular details of the interactions between PAAR proteins and VgrG trimers 199
5. Results:T6SS effectors are specifically recruited by C-terminal domains of VgrG proteins 203
5.1. Introduction 203
5.2. Aim of this chapter 204
5.3. *P. aeruginosa* encodes two eukaryotic-like lipases 205
5.4. The *vgrG4b* and *vgrG5*-clusters are repressed by RsmA 207
5.5. Assessing delivery of T6SS substrates through secretion and inter-bacterial killing assays 209
5.6. Delivery of VgrG4b, PldA and PldB is dependent on the H2-T6SS 212
5.6.1. VgrG4b secretion is H2-T6SS dependent 212
5.6.2. PldA delivery is H2-T6SS dependent 213

5.6.3. PldB is delivered in an H2-T6SS-dependent manner 215
5.7. PldA and PldB are delivered via their cognate VgrGs 218
5.7.1. VgrG5 is essential for PldB delivery 219
5.7.2. VgrG4b is essential for delivery of PldA 221
5.8. T6SS effectors and their cognate VgrGs: challenging an exclusive specificity 223
5.8.1. Secretion of VgrG4b requires VgrG5 223
5.8.2. VgrG5 is additionally required for PldA delivery 225
5.8.3. Absence of VgrG4b does not impact PldB delivery 227
5.8.4. Discussion: Heterotrimers as a general advantage of the H2-T6SS machinery 228
5.9. The C-terminal TTR domains of VgrG4b and VgrG5 differ and are specific for recognition of PldA and PldB 232
5.9.1. Towards the function of TTR-like domains within VgrG proteins 232
5.9.2. Constructing chimerae to unravel the importance of C-terminal TTR-like domains of VgrG proteins 235
5.9.3. Modifying the C-terminus of VgrG5 abrogates delivery of PldB 238
5.9.4. Modifying the C-terminus of VgrG4b abrogates delivery of PldA 239
5.9.5. Effectors are stabilised by the C-terminal domains of their cognate VgrGs 241
5.9.6. VgrG4b cannot deliver PldB 243
5.9.7. Connecting PldA with VgrG5 via the C-terminus of VgrG4b 245
5.9.8. Summary: The C-termini of VgrG proteins are essential for effector delivery 250
5.10. Summary 253
5.11. Discussion 254
5.11.1. A PAAR protein recognises a specific interface at the end of a VgrG trimer 254
5.11.2. *P. aeruginosa* fires its bullets with different efficiencies 257
6. Results:Taps and their role in effector delivery 259
6.1. Introduction 259
6.2. Aim of this chapter 261

6.3. *P. aeruginosa* PA14 expresses a putative Tap-dependent Rhs effector that is auto-cleaved 262
6.3.1. RhsP2 is expressed and cleaved but not secreted 263
6.4. The Tap-dependent effector Tde1 from *A. tumefaciens* 266
6.4.1. *P. aeruginosa* cannot secrete the heterologous effector Tde1 267
6.4.2. Tde1 binds to the C-terminus of its cognate VgrG 269
6.4.3. Connecting an effector to the T6SS tip is not sufficient for its secretion 274
6.4.4. Does the tip get too bulky? 277
6.5. Bioinformatic analysis of recognition patterns within the VgrG-Tap complex 282
6.5.1. Tap-dependent effectors contain conserved and accessible cysteines 284
6.5.2. Tap-dependent effectors contain hydrophobic MIX-like motifs 287
6.5.3. VgrGs delivering Tap-dependent effectors contain conserved cysteines 288
6.5.4. Effector recruitment via disulphide bonds – a novel concept 290
6.5.5. Discussion: Using the chimeric nature of Taps to investigate Tap-dependent effector delivery 295
6.6. Summary 298
7. General discussion 299
7.1. Mix'n'match – finding the right adaptor to a chaperone 299
7.1.1. Concept A - Hcp rings can be adaptor and chaperone modules 302
7.1.2. Concept B - VgrG proteins can function as adaptor modules 303
7.1.3. Concept C - TTR-like domains serve as adaptor and chaperone modules 305
7.1.4. A PAAR domain functions as an adaptor 307
7.1.5. Concept H - Tap proteins function both as adaptor and chaperone 310
7.1.6. Adaptors and chaperones are common features of bacterial secretion systems . 313
7.2. Proteolytic cleavage of T6SS substrates 316
7.3. Molecular details of T6SS-mediated effector delivery 317
7.3.1. Space around the VgrG tip 317

7.3.2. Heterologous secretion is not a common feature of bacterial protein secretion systems 320
7.3.3. Basis of the “á la carte” effector delivery lies within the VgrG C-terminus 324
7.3.4. *P. aeruginosa* T6SS machineries can fire multiple VgrG-effector spikes 325
7.3.5. Specificity between VgrG and Hcp proteins 329
7.4. Conclusions 335
8. Bibliography 336
9. Appendix 349
9.1. Figure permissions 349

List of figures

Figure 1-1. Polypeptide export by the Sec machinery. 27
Figure 1-2. Model for protein export through the Tat translocase. 28
Figure 1-3. Model of substrate transfer mediated by the T1SS. 29
Figure 1-4. Structure of the secreton complex from EPEC. 31
Figure 1-5. Model of T2SS formation and substrate transport. 33
Figure 1-6. Structure of the chaperone Lif bound to its substrate LipA. 35
Figure 1-7. Model of the *P. aeruginosa* T3SS. 36
Figure 1-8. Model of T3SS translocon formation and substrate delivery. 37
Figure 1-9. T3SS effectors bind to dimers of their cognate chaperones. 39
Figure 1-10. Components of the T4SS machinery. 42
Figure 1-11. Types of the T5SS and their modularity. 47
Figure 1-12. Modularity of polymorphic toxins. 49
Figure 1-13. CDI-mediated toxin delivery. 51
Figure 1-14. CdiA is formed of multiple sub-domains with different functions. 53
Figure 1-15. Schematic of the T7SS. 55
Figure 1-16. Membrane complex of the T6SS. 57
Figure 1-17. Model of the T6SS and its activity. 59
Figure 1-18. The T6SS sheath forms a cogwheel-like tube. 60
Figure 1-19. The T6SS spike is structurally similar to the T4 spike. 62
Figure 1-20. The T6SS spike. 63
Figure 1-21. The three T6SS clusters present in *P. aeruginosa* strains PAK, PAO1, PA14. 64
Figure 1-22. *Pseudomonas aeruginosa* PAO1 contains three T6SS clusters and various remote *vgrG* and *paar* islands. 66
Figure 1-23. Schematic representation of networks regulating *P. aeruginosa* T6SS. 69
Figure 1-24. *P. putida* uses its T6SS to protect plants from pathogens. 72
Figure 1-25. T6SS-active bacteria inject anti-bacterial effectors into nearby competitors. 73
Figure 1-26. Structure of Tse2-Tsi2 complex. 78

Figure 1-27. Tse2 interacts with the inner lumen of Hcp hexamers. 79
Figure 1-28. Delivery mechanism of Hcp-dependent effectors. 80
Figure 1-29. Delivery mechanism of evolved spike components. 83
Figure 1-30. Eag proteins exhibit structural similarities to some immunity proteins. 85
Figure 1-31. Delivery mechanisms of effectors interacting with the C-termini of the spike. 87
Figure 2-1. Strategy to introduce gene fragments using overlap PCRs. 101
Figure 3-1. Concept of the here designed protein shuttle based on evolved VgrGs. 119
Figure 3-2. A representative figure for western blot analysis; *P. aeruginosa* PAKΔ*retS* expresses VgrG1a, VgrG1b and VgrG1c. 121
Figure 3-3. Design of a VgrG1a-VgrG2b-CT fusion protein. 123
Figure 3-4. VgrG1a-VgrG2b-CT is secreted into the supernatant. 124
Figure 3-5. Design of the VgrG1a-Bla_{TEM-1}-shuttle. 127
Figure 3-6. VgrG1a-Bla_{TEM-1} is secreted into the supernatant. 128
Figure 3-7. Employing VgrG4b in a protein shuttle. 129
Figure 3-8. VgrG4b-Bla_{TEM-1} is secreted into the supernatant. 130
Figure 3-9. Concept of Bla_{TEM-1}-based translocation assay. 132
Figure 3-10. VgrG1a-Bla_{TEM-1} and VgrG4b-Bla_{TEM-1} are not translocated into HeLa cells. 133
Figure 3-11. Design of the VgrG1a-Tse2 shuttle. 135
Figure 3-12. VgrG1a-Tse2 is weakly secreted into the supernatant. 136
Figure 3-13. VgrG1a-Tse2 is not secreted into the supernatant when strains interactions with Hcp1 are disrupted. 138
Figure 3-14. Concept of interbacterial competition assays. 140
Figure 3-15. VgrG1a-Tse2 can be delivered into prey cells in minor amounts. 141
Figure 3-16. Model of interference of interactions between the Hcp1 ring and Tse2 as part of a VgrG1a-Tse2 shuttle. 143
Figure 3-17. Design of a VgrG4b-PldA shuttle. 145
Figure 3-18. VgrG4b-PldA is secreted into the supernatant. 146
Figure 3-19. PldA can be delivered into prey cells as an extension domain of VgrG4b. 147
Figure 3-20. Model of non-covalent and covalent interactions between VgrG4b and PldA. 149
Figure 4-1. The VgrG spike of a T6SS. 155

Figure 4-2. *P. aeruginosa* H1-T6SS contains three PAAR protein. 158
Figure 4-3. VgrG1a is only secreted in presence of its cognate PAAR effector Tse6. 161
Figure 4-4. VgrG1a, VgrG1b and VgrG1c can form heterotrimers. 163
Figure 4-5. VgrG1a secretion is independent of Tse6, VgrG1b and VgrG1c. 165
Figure 4-6. PAAR proteins contain specific residues to bind their cognate VgrG trimers. 169
Figure 4-7. The last β-strand within VgrG proteins is conserved. 171
Figure 4-8. The PAAR domain of Tse7 sits on top of the VgrG1b-trimer. 173
Figure 4-9. Overview of design of the chimerae under investigation. 176
Figure 4-10. Chimerae between VgrG1a^{P} and VgrG1^{A} self-interact. 177
Figure 4-11. Only chimera A can form a functional T6SS spike. 179
Figure 4-12. Chimerae A and C can deliver Tse6 into prey cells. 181
Figure 4-13. Model of recruitment of Tse6 to the VgrG1a^{P} tip. 183
Figure 4-14. Cloning strategy for Tse6^{N}-Tse7^{C} shuttle. 185
Figure 4-15. Expression of Tse6^{N}-Tse7^{C} leads to a functional T6SS. 186
Figure 4-16. T6SS-dependent Rhs effectors are connected with the VgrG tip via their N-terminal PAAR domains. 189
Figure 4-17. Rhs domains form large shell-like forms that might wrap around VgrG spikes. 191
Figure 4-18. Eag-dependent effectors contain N-terminal transmembrane domains. 194
Figure 4-19. Comparison of the here characterised chimerae between VgrG1a^{P} and VgrG1^{A} with the truncation mutants used in the study by Bondage *et.al* 202
Figure 5-1. *P. aeruginosa* encodes the two lipases PldA and PldB. 207
Figure 5-2. VgrG4b, PldA and PldB are repressed by RsmA. 209
Figure 5-3. A representative figure of a western blot analysis 211
Figure 5-4. A representative plot of recovered cfu of prey strain 212
Figure 5-5. PldA delivery is H2-T6SS dependent. 215
Figure 5-6. PldB delivery is H2-T6SS dependent. 217
Figure 5-7. Delivery of PldB depends on VgrG5. 220
Figure 5-8. Delivery of PldA depends on VgrG4b. 222
Figure 5-9. VgrG4b delivery requires the gp5-/gp27-like domains of VgrG5. 225
Figure 5-10. Absence of VgrG5 impacts PldA delivery. 226

Figure 5-11. Delivery of PldB does not depend on VgrG4b. 228
Figure 5-12. Model of the heterotrimer formation resulted from this section. 231
Figure 5-13. Composition of VgrG proteins involved in delivering adaptor-less effectors. 233
Figure 5-14. The C-terminal domains of some VgrG proteins are homologues to transthyretin-like domains (TLD^{VgrG}). 235
Figure 5-15. Design of mutants to swap C-termini between VgrG4b and VgrG5. 237
Figure 5-16. Modifying the C-terminus of VgrG5 abrogates delivery of PldB. 239
Figure 5-17. Modifying the C-terminus of VgrG4b abrogates delivery of PldA. 240
Figure 5-18. Effectors are stabilised by the C-termini of their cognate VgrG proteins. 242
Figure 5-19. Co-expression of N-terminal VgrG5 does not support PldB secretion. 244
Figure 5-20. Substituting of the C-terminus of VgrG5 with the C-terminus of VgrG4b restores PldA secretion. 247
Figure 5-21. Swapping the VgrG vehicle for PldA secretion does not swap the T6SS machinery. 249
Figure 5-22. Model of the interactions between PldA and PldB and the C-terminal domains from their cognate VgrGs resulting in delivery shuttles of both effectors. 252
Figure 5-23. Models about contradictions in heterotrimer formation of VgrG4b and VgrG5. 256
Figure 6-1. Taps contain highly conserved motifs within their N-termini. 260
Figure 6-2. The hcp-2-operon of *P. aeruginosa* PA14 263
Figure 6-3. VgrG14 and RhsP2 are expressed in *P. aeruginosa* PA14. 265
Figure 6-4. Tde1 from *A. tumefaciens* is secreted dependent on the genes encoded in its cluster 267
Figure 6-5. *P. aeruginosa* cannot incorporate heterologous $VgrG1^{A}$ and secrete Tde1. 269
Figure 6-6. Overview of chimerae which were employed to connect Tde1 to the H1-T6SS in *P. aeruginosa*. 270
Figure 6-7. All chimerae interact with Tde1 in presence of Tap1. 272
Figure 6-8. All chimerae likely interact with Tde1 in presence of Tap1 *in vivo*. 273
Figure 6-9. *P. aeruginosa* is not able to secrete the heterologous effector Tde1. 276
Figure 6-10. Presence of Tde1 interferes with secretion of construct A. 279
Figure 6-11. Presence of Tde1 interferes with delivery of Tse6 into prey cells. 280
Figure 6-12. Model about the decoration of the VgrG1a/chimera A-tip in absence and presence of Tap-Tde1 282

Figure 6-13. Genetic environments of Tap-dependent effectors from *Vibrio cholerae*, *Pseudomonas aeruginosa* and *Agrobacterium tumefaciens.* 284
Figure 6-14. Tap-dependent effectors contain conserved cysteines. 285
Figure 6-15. Tap-dependent effectors contain easily accessible cysteines. 287
Figure 6-16. VgrGs delivering Tap effectors contain cysteine motifs. 290
Figure 6-17. Model of disulphide formation between a VgrG and its cognate Tap-dependent effector. 293
Figure 6-18. Strategy to elucidate the molecular mechanism of Tap-dependent effectors. 297
Figure 7-1. T6SS effectors are encoded together with their adaptor and chaperone module. 301
Figure 7-2. Evolved VgrGs might contain intramolecular chaperones within their linker regions. 305
Figure 7-3. PAAR domains work as adaptors, while the chaperones can be of various nature. 308
Figure 7-4. Effector proteins are chaperoned and connected to the T6SS tip by different mechanisms. 311
Figure 7-5. Predicted domains of RhsP2. 312
Figure 7-6. Space around the VgrG spike is limited. 319
Figure 7-7. Operons containing vgrG or paar genes within *P. aeruginosa* PAO1. 327

List of tables

Table 1-1. Chaperones involved in delivering protein secretion system substrates. 45

Table 2-1. Bacterial strains used in this study. 91

Table 2-2. Media supplements used in this work. 96

Table 2-3. Plasmids used in this study. 97

Table 2-4. Primers used in this study. 103

Table 2-5. Antibodies used in this study. 113

Table 3-1. Overview of known evolved VgrGs from the literature and from the current study. 151

Table 4-1. List of all PAAR proteins in *P. aeruginosa* PAO1 and their affiliations with a cognate VgrG. 156

Table 4-2. Interactions sites of characterised VgrG-PAAR pairs 172

Table 5-1. Sequence identities between VgrG proteins from *P. aeruginosa* PAO1. 224

Table 6-1. Overview of cysteine motifs within Tap-dependent effectors and their cognate VgrGs/PAARs. 291

Table 7-1. Overview of results from this thesis. 323

Table 7-2. VgrG spike compositions in *P. aeruginosa* PAO1. 329

Table 7-3. List of T6SS substrates and their activities and delivery modes. 331

Abbreviations

aa	Amino acids	PMF	Proton-motif-force
ABC	ATP-binding cassette	POTRA	Polypeptide transport-associated
ACD	Actin-cross linking	Rhs	Recombination hotspot
ATP	Adenosine 5'-triphosphate	RpoB	RNA-polymerase subunit b
BAM	β-barrel assembly machine	rpm	Rounds per minute
Bla	β-lactamase	RT	Room temperature
bp	basepair	SDS	Sodium dodecyl sulfate
BTH	Bacterial two hybrid	SOEing	Splicing by overlap extension
CDI	Contact-dependent growth inhibition	SRP	Signal-recognition particle
CF	Cystic fibrosis	tae	Type VI amidase effector
cfu	Colony forming units	tag	Type VI associated gene
Co-IP	Co-immunoprecipitation	tap	Type VI adaptor protein
CT	C-terminal	TBST	Tris-buffered saline solution with tween
dd	Double destilled	tde	Type VI DNase effector
DMEM	Dulbecco's modified Eagle medium	tdi	Type VI DNase immunity
DMF	Dimethylformamide	tec	Type VI effector chaperone
DUF	Domain of unknown function	tge	Type VI glycohydrolase effector
eag	Effector associated gene	TGS	Tris-glycine-SDS
GFP	Green fluorescent protein	TLD	Transthyretin-like domain
gp	Gene product	tle	Type VI lipase effector
GTP	Guanosine 5'-triphosphate	tli	Type VI lipase immunity
HA	Haemagglutinin	TLP	Transthyretin-like protein
HBSS	Hanks' Balanced Salt Solution	TSB	Tryptic soy broth
Hcp	Haemolysin co-regulated protein	TPS	Two-partner secretion
HEPES	4-(2-hydroxyethyl)-1-piperazineethanesulfonic acid	tse	Type VI effector
HRP	Horse radish peroxidase	tsi	Type VI immunity
IM	Inner membrane	tss	Type VI secretion system
IPTG	Isopropyl-β-D-thiogalactopyranoside	TTR	Transthyretin
LB	Lysogeny broth	T1SS	Type I secretion system

LC	Loading control	T2SS	Type II secretion system
MIX	Marker for type six	T3SS	Type III secretion system
$NAD(P)^+$	Nicotinamide adenine dinucleotide (phosphate)	T4CP	Type IV coupling protein
OD	Optical density	T4SS	Type IV secretion system
OM	Outer membrane	T5SS	Type V secretion system
PAAR	Proline-alanine-alanine-arginine	T6SS	Type VI secretion system
PAGE	Polyacrylamide gel electrophoresis	T7SS	Type VII secretion system
PDB	Protein data bank	Vgr	Valine-glycine rich
PBS	Phosphate-buffered saline	WT	Wildtype
PCR	Polymerase chain reaction	X-gal	5-bromo-4-chloro-3-indolyl-D-galactopyranoside
pld	Phospholipase D		

1. Introduction

1.1. About *Pseudomonas aeruginosa*

Pseudomonas aeruginosa is a motile rod-shaped Gram-negative bacterium, which is able to flourish in many environmental niches. It can grow at a wide temperature range between 4 ° and 43 °C while also being facultative anaerobe. *P. aeruginosa* has a genome of approximately 6.3 Mb, which encodes about 5600 open reading frames [1]. Within this high number of genes many encode for a variety of metabolic enzymes and even more importantly, a comprehensive set of regulatory proteins [2]. This metabolic diversity and highly complex regulatory network allow this bacterium a versatile lifestyle that lets it flourish in a variety of environments, like soil, aquatic environments, animals, plants, humans as well as artificial settings like clinical environments [3, 4].

P. aeruginosa is able to form biofilms, which are assemblies of microbial cells in an enclosed matrix of exopolysaccharides and other extracellular products known as “common goods” [4]. Furthermore, with the use of a polar flagellum and type IV pili, it can swim in liquid medium and twitch on solid surface, respectively. By employing both the flagellum and the type IV pili, *P. aeruginosa* can swarm. Swarming, which allows the bacterial cell to move on soft substrates, is considered as the social coordinated movement of a population after host cell attachment and before biofilm formation. With all these motile processes, *P. aeruginosa* is able to effectively colonise tissue and lead to various infections [5].

1.1.1. The opportunistic pathogen *P. aeruginosa*

As an opportunistic human pathogen, *P. aeruginosa* can cause multiple infections in humans. Interestingly, *P. aeruginosa* can switch between a planktonic and sessile lifestyle, with the former correlating with high motility and the latter with biofilm formation. These two lifestyles are regulated by a complex regulatory network, which will be focussed on in 1.3.3.

A planktonic motile lifestyle of *P. aeruginosa* goes along with a high cytotoxicity leading to acute infections like pneumonia occurring mainly in immune-compromised patients. These infections are initiated by binding of bacterial cells onto the mucosal barrier. Subsequently, cytotoxic virulence factors are translocated directly into eukaryotic cells or are released into the extracellular environment. These factors cause significant tissue damage allowing the pathogen to invade the host and spread rapidly [4].

On the contrary, chronic infections are common in the lungs of cystic fibrosis (CF) patients. CF results from a genetic defect in a gene encoding for a chloride channel regulating the hydration of the mucosal surface. This defect leads to a dehydrated environment within the CF lungs together with an overproduction of mucus and hampered pathogen clearance providing optimal growth conditions for *P. aeruginosa* and other airborne pathogens [6]. In this environment, *P. aeruginosa* is able to form mucoid biofilms that are accompanied by a low rate of cell motility and cytotoxicity [3]. These infections are most difficult to clear and because of the rising number of resistance mechanisms to antimicrobials, treatment becomes harder as well [2].

1.1.2. Antibiotic resistance

The WHO just published its first ever list of antibiotic-resistant “priority pathogens” with *P. aeruginosa* placed number 2. This critical status highlights the threat of *P. aeruginosa* being resistant to multiple antibiotics thus posing a great threat to human health. This list is further meant to focus the attention of governments and research towards the development of new antibiotics (WHO global priority pathogen list from 27th February 2017).

P. aeruginosa infections are highly resistant to a range of antibiotics by possessing multifactorial mechanisms of responses to various antimicrobials [7]. The low permeability of the outer membrane as well as the presence of multidrug efflux transporters inhibit the chances of a drug reaching its cellular target. The uptake rate of small molecules by specialised transporters, so-called porins, is comparably low and non-specific for antibiotics. Currently, only two porin transporters, OprF and OprD, are believed to allow the limited non-specific uptake of small substrates. On the other hand, *P. aeruginosa* encodes for a range of efflux pumps with overlapping specificities for antibiotics from different classes [8]. Thus, the slow uptake of antibiotics results in low concentrations within the cell so that efflux pumps can work efficiently since they are not overwhelmed with large antibiotic concentrations, ultimately resulting in effective resistance [9].

On another note, *P. aeruginosa* readily acquires resistance to antimicrobials by lateral gene transfer or chromosomal mutations [10]. This can lead to a constitutive expression of the chromosomal β-lactamase or the acquisition of plasmid-borne antibiotic-modifying enzymes [11]. These enzymes can alter the chemical structure of an antibiotic by transferring acetyl, phosphate or adenylyl groups and thus inactivating it. Alternatively, mutations in key residues within antibiotic targets change the conformation of the active site and thus inhibit antibiotic binding [7].

The long-term treatment with antibiotics ultimately resulted in the emergence of multi-drug resistant *P. aeruginosa* as well as other Gram-negative bacterial strains. The spread of antibiotic resistance between bacterial strains might render all currently used antibiotic ineffective even against trivial *P. aeruginosa* infections. At the moment, infections are efficiently treated by combination therapies using amino glycosides and polymyxin [12].

1.1.3. The diversity of *P. aeruginosa* strains

As the major reference strain, *P. aeruginosa* PAO1 has been maintained and studied in laboratories around the world. This led to an ongoing microevolution of genotypes and thus to the emergence of PAO1 sublines that was found to challenge reproducibility of research studies. Different PAO1 sublines from laboratories around the world were shown to carry additional mobile elements or deletions, thus showing different phenotypes in nutrient acquisition and virulence [3].

Other widely studied strains are PAK and the cytotoxic PA14, whose genome is slightly larger than the one from PAO1. PA14 carries additional pathogenicity islands encoding for example the virulence factor ExoU (see 1.2.4) that renders this strain more cytotoxic [13]. A taxonomic outlier is the *P. aeruginosa* strain PA7, which only shares 95 % of its genome with PAO1, containing 18 unique genomic islands while being deficient in various virulence factors as well as the whole type III secretion system locus (see 1.2.4).

More and more clinical isolates are obtained from lungs of CF patients and these variants are being sequenced and their phenotypes characterised. These studies attempt to pinpoint hot spots of mutations, such as genes related to transport and lipopolysaccharide modification to comprehend the ability of *P. aeruginosa* to cause infections [13]. Furthermore, a recent proteomic study of eleven clinical isolates from different *P. aeruginosa* infections

revealed the metabolic diversity of these strains. The authors found that the expression rates of 42 proteins were highly variable between isolates, with mainly proteins expressed in response to phosphate, iron or amino acids; factors, required for survival within the host and variable depending on the infection site. Interestingly, they also showed a high diversity in the expression of enzymes in metabolic fluxes, with niche-specific upregulations of the glyoxylate shunt or the Krebs cycle [14]. Together, these genomic and proteomic studies suggest how *P. aeruginosa* employs a range of strategies to survive in the host, while its capacity to cause infections is combinatorial and multifactorial.

1.2. Protein secretion systems

To cause infections in human hosts, pathogens deliver a range of virulence factors, called effectors, into the extracellular medium or directly into the host cell. Protein secretion in Gram-negative bacteria, like *P. aeruginosa,* is achieved upon transport across the bacterial cell envelope consisting of two membranes. Proteins destined for the extracellular medium need to cross both hydrophobic layers as well as the hydrophilic periplasmic space between them. To achieve this, bacteria have evolved to employ specialised nanomachines that deliver proteins of various properties not only into the extracellular medium but also into target cells. This secretion process can occur in either of two ways: in a one-step pathway, delivered directly from the cytoplasm, or in a two-step pathway, with a stop-over in the periplasm.

Proteins destined for the export with a special protein secretion system are generally called substrates. Secretion substrates usually contain a specific motif or secretion signal within their fold to distinguish them from the myriad of other cellular proteins [15]. This allows the specific recognition of substrates and their docking into the protein secretion machinery. The nature of important secretion pathways, which were classified under “types”, will be discussed here, with a special focus on the secretion mechanisms for substrates, substrate

specificity and the involvement of chaperones in their delivery. The type VI secretion system will be described in more detail in 1.3.

1.2.1. Translocation across the inner membrane

Some proteins are targeted to the periplasm because they contain an essential function in an extra-cytoplasmic compartment of the bacterial cell. To reach their destination they use one of the two pathways that specifically transport proteins from the bacterial cytoplasm into the periplasm. Once reached the periplasm, proteins can remain soluble in the periplasm or can be anchored to either of the two lipid membranes or they become substrates of a further secretion system as discussed below. Two pathways are known to facilitate translocation across the inner membrane, the Sec- and the Tat-pathway [16].

The Sec machinery consists of a cytoplasmic secretion-specific chaperone SecB, an ATPase SecA and an integral membrane complex, the SecYEG translocon [17]. Substrates recruited to the Sec machinery are unfolded and carry a N-terminal signal peptide that contain one or more positively charged residues followed by 8-12 hydrophobic residues. Proteins can be targeted to the Sec translocon in a co-translational or post-translational fashion (Figure 1-1). The ribonucleoprotein signal-recognition particle SRP recognises Sec targeted proteins co-translationally, as they are being produced from the ribosome. In contrast, the chaperone SecB recognises and binds to proteins post-translationally and maintains them in a secretion competent fold. In both pathways, the substrate is efficiently recruited to the cytoplasmic ATPase SecA that then associates with the translocation machinery and threads the unfolded protein through the SecYEG channel in a proton-motive force (PMF) dependent manner. Afterwards, substrates are converted into mature proteins by cleavage of the signal peptide after the Ala-X-Ala consensus sequence by signal peptidases [17, 18].

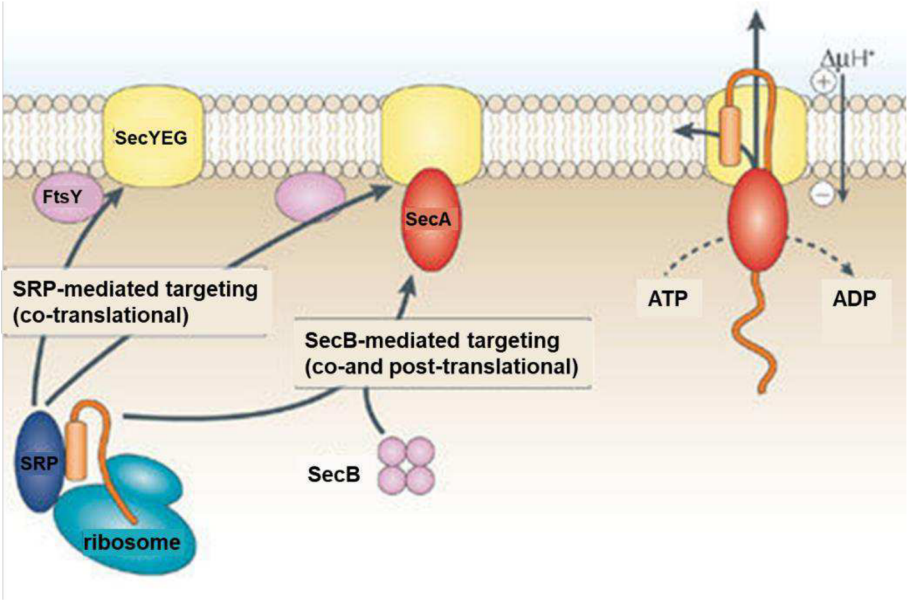


Figure 1-1. Polypeptide export by the Sec machinery.

Illustration of the characteristics of Sec-mediated protein translocation across the inner membrane. The translocase machinery consists of the SecYEG channel (yellow) and a cytoplasmic ATPase (red). Preproteins (orange) destined for Sec transport contain signal peptides that are recognised by the SRP (blue) co-translationally or SecB (pink) post-translationally. With either pathway, they are recruited towards the SecYEG machinery, where translocation across the inner membrane occurs. They can then fold at the *trans* side of the membrane or integrate into the lipid bilayer after signal peptide cleavage. This figure was adapted from [18] with permission from Springer Nature.

In contrast to the Sec pathway, the Tat translocon is able to mediate export of folded substrates. Tat-secreted substrates usually contain co-factors or metal ions that need to assemble with the folded proteins prior to translocation. The Tat translocase consists solely of an inner membrane complex of two to five different proteins termed TatA-E. The integral membrane translocase consists of TatA and TatC proteins. TatA monomers assemble to multimers of various numbers thus forming pores of different sizes and allowing the translocation of substrates of variable sizes. Tat substrates carry N-terminal signal sequences containing two conserved arginine residues thus leading to a positive charge in this region. The N-terminal signal sequence consists of a hydrophobic and a polar region followed by a conserved AXA motif. Substrate binding to the TatBC complex positions the signal peptide

close to TatC which is the prerequisite for substrate translocation (Figure 1-2). Once the substrate reaches the periplasm, its signal sequence is cleaved by the same signal peptidase as for Sec substrates and the mature protein is released into the periplasm [19].

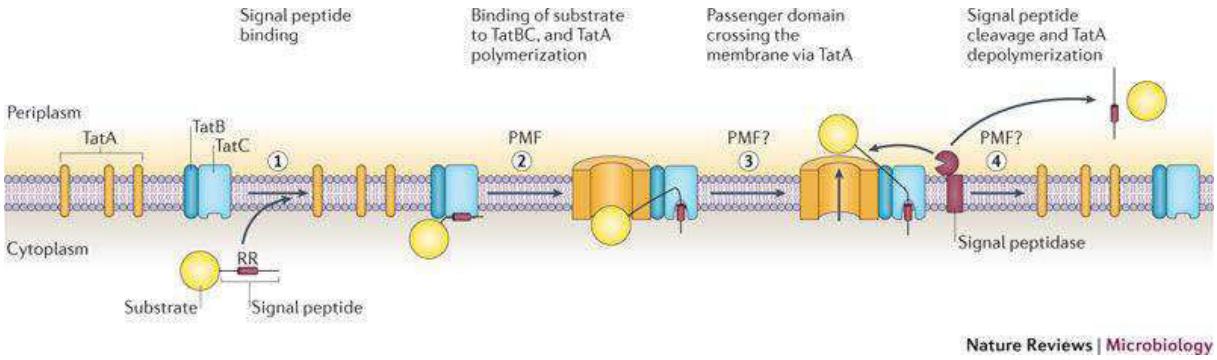


Figure 1-2. Model for protein export through the Tat translocase.

The Tat translocase consist of TatA (orange) multimers as well as TatB (blue) and TatC (cyan). TatB and TatC assemble and bind the signal peptide of a substrate protein (yellow) thus recruiting TatA and triggering its multimer formation. Translocation of the passenger domain of the substrate occurs in a PMF-dependent manner. The signal peptide is proteolytically cleaved releasing the substrate into the periplasm and TatABC dissociate. This figure was adapted from [19] with permission from Springer Nature.

1.2.2. Type I secretion system

The type I secretion system (T1SS) delivers unfolded proteins through the bacterial cell envelope in a single step. This simplest translocation mechanism is exemplified by the T1SS in *Escherichia coli* that exports the toxin HlyA and that has been studied in great detail [20]. The T1SS constitutes of an outer membrane protein TolC, an inner-membrane (IM) bound ATP-binding cassette (ABC)-transporter HlyB and a membrane fusion protein HlyD connecting the two components (Figure 1-3A). The trimeric TolC is embedded as a transmembrane β-barrel similar to porins thus forming a channel through the outer membrane.

HlyB, which is connected to TolC, is able to bind and hydrolyse ATP. This process is thought to provide the energy required for effector transport across the bacterial cell envelope [21].

P. aeruginosa contains two well characterised T1SSs. The Apr system is involved in the secretion of alkaline protease AprA and AprX [22], a protein of unknown function. Similar to other extracellular proteases, AprA is a well described virulence factor crucial for *Pseudomonas* infections [23]. The second T1SS system is involved in the uptake of iron by secreting the haemophore HasAp [24]. Due to its ability to sequester haem from haemoglobin and subsequently internalise this molecule, HasAp is considered a crucial component of *P. aeruginosa* infection establishment. Recently, another T1SS in *P. aeruginosa* was identified, which is homologous to the Lap system of *Pseudomonas putida* [25]. This system secretes LapG, a protease shown to play a role in biofilm formation and subsequent dispersal.

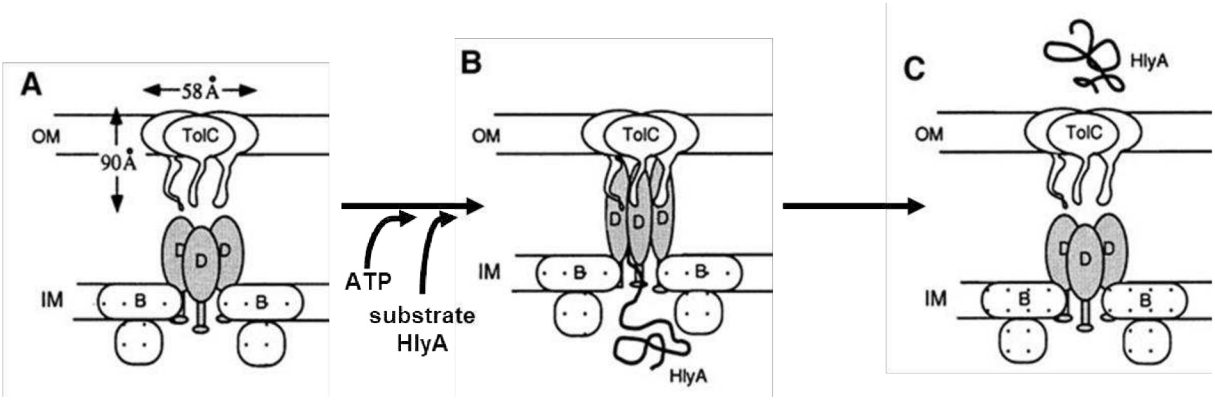


Figure 1-3. Model of substrate transfer mediated by the T1SS.

A: The outer membrane complex of the T1SS of *E. coli* consists of TolC and the inner membrane complex of HlyD and the traffic ATPase HlyB. B: Binding of the substrate HlyA to the IM complex triggers conformational changes in all three components from close to C: open subsequently allowing substrate channelling into the extracellular medium. Figure reproduced under a Creative Commons Attribution Licence from [26].

Effector delivery and specificity in the T1SS

The T1SS machinery delivers its substrates directly from the bacterial cytosol into the extracellular medium [16]. Unfolded T1SS effectors are targeted to the secretion machinery via a non-cleavable C-terminal secretion signal comprising 40 – 60 aa (Figure 1-3B) [27]. The C-terminal secretion signal containing a negatively charged amino acid followed by several hydrophobic ones is specifically recognised by the ABC transporter protein [24]. The secretion signal from HlyA was fused to a range of heterologous proteins, originally from *Corynebacterium diphtheria*, *Salmonella typhimurium* and *P. aeruginosa*. These fusion proteins were then shown to be recognised and exported by the TolC system in *E. coli* [28]. Interactions between substrate and transporter are thought to induce the assembly of a *trans*-periplasmic channel bridging the two complexes from the inner and outer membrane. Concomitant ATP binding and hydrolysis by the traffic ATPase then leads to substrate channelling through the T1SS and release into the extracellular medium (Figure 1-3C) [26, 29].

1.2.3. Type II secretion system

The type II secretion system (T2SS) exports proteins to the external environment in a two-step process after Sec- or Tat-dependent translocation into the periplasm. The T2SS comprises of four sub-complexes, together termed the secreton, spanning outer membrane, periplasm and inner membrane. Embedded in the outer membrane, the secretin sub-complex, of which a structure from enteropathogenic *E. coli* has just been published (Figure 1-4A) [30], forms a pore through which substrates are channelled. Its structure is unique among proteins found in the outer membrane due to its double β-architecture containing gates to regulate substrate secretion [30]. By reaching into the periplasm, the secretin forms a channel with the

inner-membrane sub-complex. This closed channel is called secretin vestibule and allows space for substrates (Figure 1-4B). Further, an assembly platform spanning the inner membrane interacts with a cytoplasmic traffic ATPase which energises the T2SS-dependent secretion process. Essential for secretion is also the pseudopilus that shows resemblance with the type IV pilus. The pseudopilus is made up of a major pilin and numerous minor pilins facilitating effector recognition, the whole complex forming a piston-like structure (Figure 1-5). This pseudopilus is anchored in the inner membrane and reaches into the periplasm. Activity of the ATPase drives the pseudopilus through the secretin channel, pushing out T2SS effectors (Figure 1-5) [31, 32].

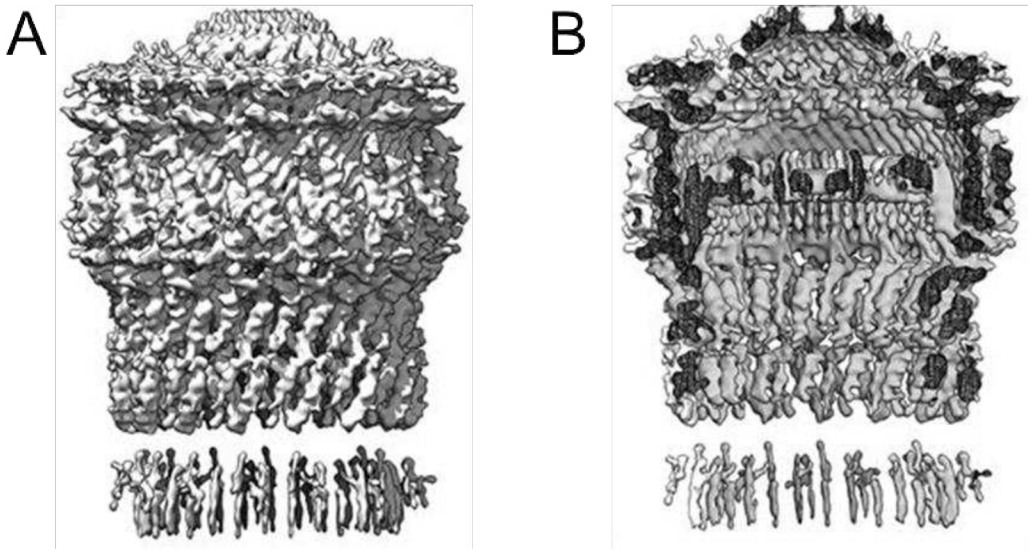


Figure 1-4. Structure of the secreton complex from EPEC.

A: Electron density map of the EPEC secreton and B: a slice through the map displaying the empty space within the secretion allowing accommodation of large substrates. Figure adapted from [30] with permission from Journal of Bacteriology.

P. aeruginosa employs three T2SS, the Txc, Xcp and the Hxc system, to secrete numerous hydrolysing enzymes and toxins [16, 33]. While the Hxc system was shown to secrete solely one substrate, which is the alkaline phosphatase LapA [34], many substrates

were associated with the Xcp system. These exoproteins have a broad diversity in enzymatic activities including the major extracellular protease LasB as well as many other proteases and lipases [35]. Interestingly, Exotoxin A (ToxA) is the only substrate released by *P. aeruginosa* T2SS into the extracellular medium, that is subsequently taken up by eukaryotic target cells. Once reached the host cytosol, ToxA modifies elongation factor 2, thus inhibiting protein synthesis and leading to host cell death [36].

Effector delivery and specificity of the T2SS

All T2SS substrates contain a signal peptide that direct them to either the Sec- or Tat-pathway, thus delivering them into the periplasm [32]. Once in the periplasm, the folded substrate is specifically recognised and recruited by the recruiter protein XcpP (Figure 1-5B). The substrate then moves into the periplasmic vestibule of the secretin where it interacts with the pseudopilus [31]. A growing pseudopilus expels the substrate through the secretin pore out of the cell (Figure 1-5C) [37]. The pilus is then retracted via a yet unknown mechanism and ready to be loaded with a new substrate [37].

The specific recognition of T2SS substrates is achieved by the recruiter protein XcpP. Interestingly, XcpP was shown not to interact with T2SS substrates from other T2SS systems even when originated from the same organism [37]. It is generally thought that up to three regions of 30-80 aa within the N-terminus of a T2SS substrate are needed for recognition by the cognate T2SS machinery [38]. A recent study into the delivery mechanism of PulA from *Klebsiella oxytoca* showed that two regions A and B, each of about 80 aa, are required for PulA translocation. In the same study, when the authors used a reporter enzyme and fused the two N-terminal regions A and B to it, they could detect secretion of the hybrid protein [38]. However, these two regions are not common in T2SS substrates, even though it is widely thought that the recognition principle by all T2SS might be similar. As substrates are

translocated in a folded conformation, it is generally understood that structural motifs on the protein surface would mediate specific binding to the XcpP [39].

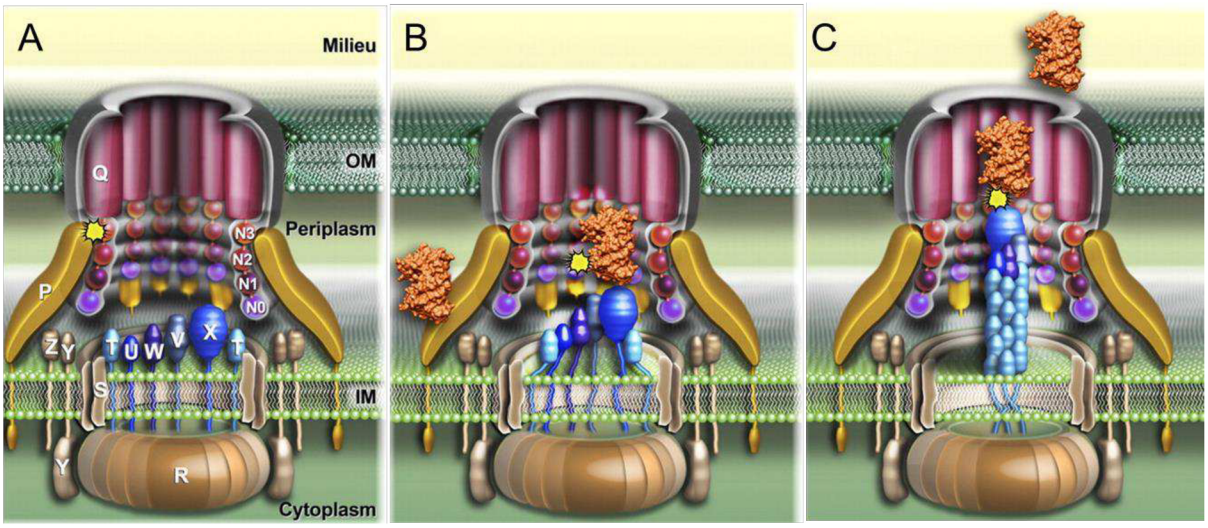


Figure 1-5. Model of T2SS formation and substrate transport.

A: Schematic representation of a T2SS secretion. Labelling follows the Xcp nomenclature of *P. aeruginosa*. B: A T2SS substrate (orange) engages with the secreton and is recruited into the vestibule, where it interacts with the pseudopilus (blue). C: Expulsion of the pseudopilus pushes the substrate through the outer membrane channel into the extracellular medium. This figure was adapted from [37].

In an attempt to achieve heterologous secretion from *Vibrio anguillarum*, Zhou and colleagues created chimerae between the signal peptide of a native T2SS substrate EmpA and heterologous proteins. A fusion between the N-terminal 40 aa of EmpA and the reporter protein GFP was shown to be secreted from *V. anguillarum*, however its T2SS-mediated secretion was not specifically demonstrated [40].

Chaperones required by certain T2SS effectors

In some organisms, secretion of several T2SS substrates were shown to be dependent on specific periplasmic chaperones (Table 1-1) [41-43]. The overall concept is that in absence of the cognate chaperones, substrates are not properly folded and prone to degradation by periplasmic proteases [42-44].

In *Burkholderia glumae*, the T2SS lipase LipA was shown to be correctly folded in the periplasm only upon interactions with its cognate chaperone lipase-foldase Lif. Interestingly, Lif contains a transmembrane domain anchoring it to the inner membrane while its C-terminal domain resides within the periplasm [43]. The structure of the Lif-LipA complex revealed an unusually extended folding platform for Lif (Figure 1-6A), which allows it to cover most of the protein surface of LipA as well as its active site (Figure 1-6B) [45]. Furthermore, in *Acinetobacter nosocomialis*, the metallo-peptidase CpaA was demonstrated to require the chaperone CpaB for its delivery via the T2SS [41]. Similarly to Lif, CpaB is membrane bound, although its N-terminal transmembrane domain was shown to be dispensable for CpaA secretion. This suggests that the N-terminal transmembrane domain likely functions to retain CpaB within the cell [44]. In contrast to proteins that function as chaperones for their cognate substrates, an intramolecular chaperone for the elastase LasB in *P. aeruginosa* has been described. The propeptide of LasB is involved in proper folding of the active enzyme, which is a prerequisite for secretion of LasB, as well as enzyme inhibition within the cell [46].

This highlights the dual and essential function of T2SS chaperones: by covering the active site, a chaperone inhibits the substrate's enzymatic activity, while also ensuring stabilisation of the protein and proper folding. Furthermore, it is thought that chaperones specifically channel their cognate substrates towards the secretin vestibule via a yet unknown mechanism [32].

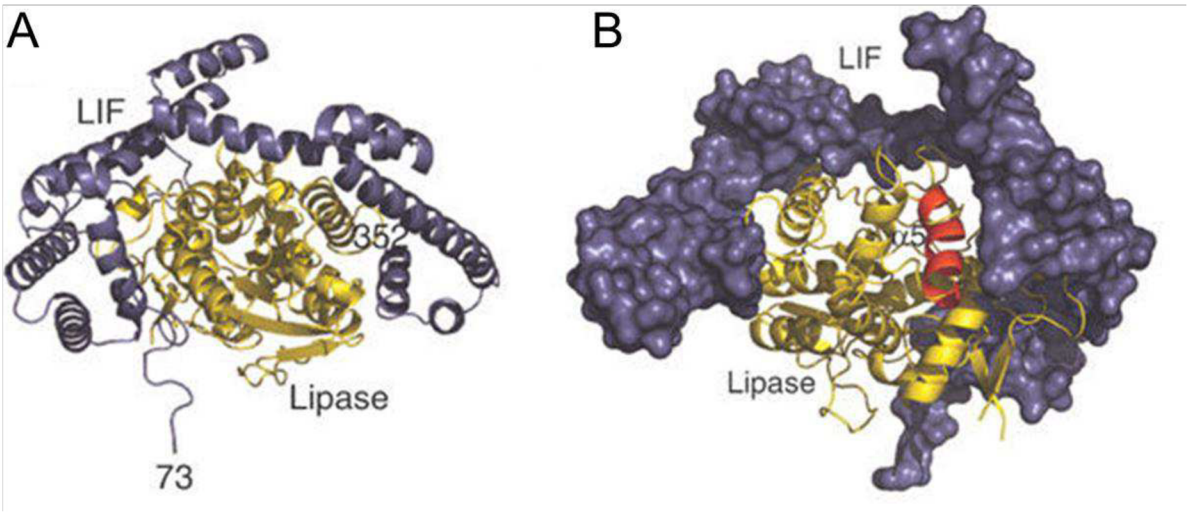


Figure 1-6. Structure of the chaperone Lif bound to its substrate LipA.

A: Ribbon view of the chaperone Lif (blue) completely covering the surface of its substrate LipA (yellow). B: Lif is shown in surface representation, while the helix containing the active site of LipA is coloured in red. This figure was adapted from [45] with permission from Nature Springer.

1.2.4. Type III secretion system

The type III secretion system (T3SS) is a macromolecular complex, the so-called injectosome, spanning the inner bacterial membrane, the periplasmic space, the outer membrane, the extracellular medium and the host cell membrane (Figure 1-7). This secretion system has the same evolutionary origin as the bacterial flagellum, however it evolved into a macromolecular syringe injecting effector proteins directly into eukaryotic target cells. The secretion complex of the T3SS consists of a secretin protein embedded in the bacterial envelope; with the secretion being from the same family as the one used by the T2SS (1.2.3). This secretin-mediated channel is connected to a hollow needle structure that protrudes from the bacterial cell surface (Figure 1-7). Anchoring of the needle to the bacterial membrane is mediated by a basal body which is composed of two inner and two outer rings [47]. The basal body channels T3SS substrates from the bacterial cytosol into the needle structure. By

sequential addition of single subunits into the needle structure, the tip grows towards the environment, until an accessory protein, a so-called molecular ruler, that measures the length of the needle in a yet undefined mechanism, triggers a substrate switch. Upon this switch and in contact with a host cell plasma membrane, two pore-forming proteins are translocated and inserted into the host cell plasma membrane, where they form the so-called translocon [47].

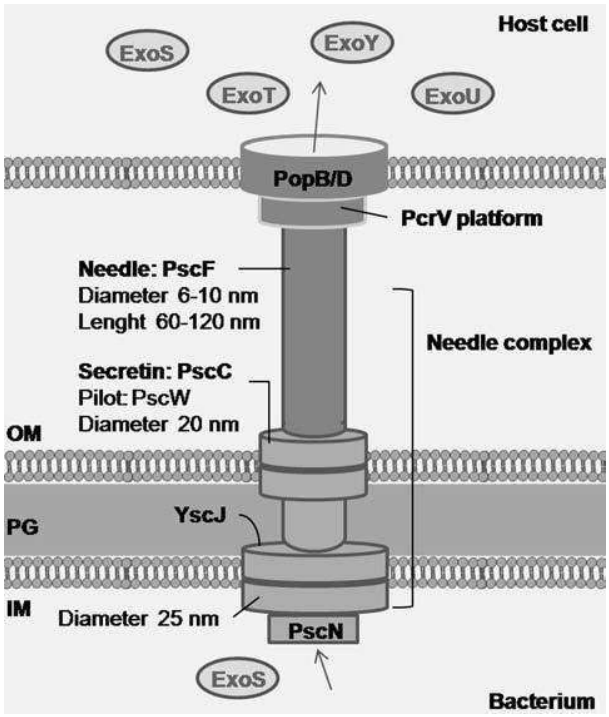


Figure 1-7. Model of the *P. aeruginosa* T3SS.

The T3SS is formed of a needle complex and a translocation apparatus as well as effector proteins that are delivered into the host cell cytosol. This figure was adapted from [48] with permission from the Copyright Clearance Centre.

P. aeruginosa utilises its T3SS to form a pore in the eukaryotic cell membrane and deliver its effector proteins (ExoS/T/U/Y) involved in cytotoxicity [16]. Just recently, in an *in silico* study, two new T3SS effectors of unknown function were proposed in *P. aeruginosa* PA14, however, further experimental work needs to prove their affiliation with the T3SS [49]. The fact, that only a few effector proteins are delivered via the T3SS is astounding considering

its importance for *P. aeruginosa* virulence and in comparison with the amount other pathogens deliver *via* their T3SS. While ExoS and ExoU are exclusive in different *P. aeruginosa* strains, they are both cytotoxic in eukaryotic cells and have major impacts on lung infections [50, 51]. Both ExoS and ExoT contain similar enzymatic activity, which is an N-terminal GTPase-activating and a C-terminal adenosine diphosphate ribosyl-transferase activity [52]. ExoU, which is the major T3SS effector, is a phospholipase while ExoY exhibits adenylyl cyclase activity [48]. Furthermore, the translocon was recently considered a T3SS effector itself. By inserting the two translocon proteins PopB and PopD into the host cell membrane, *P. aeruginosa* induces an ion exchange through this pore (Figure 1-8) thus inducing early T3SS-dependent dephosphorylation and deacetylation of histone H3 [53].

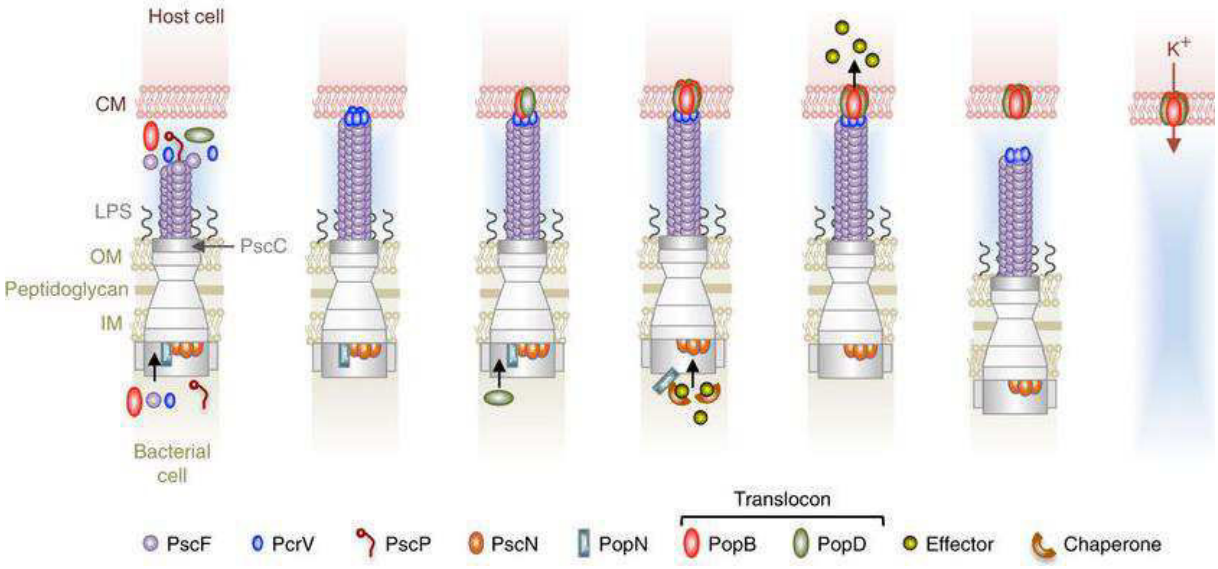


Figure 1-8. Model of T3SS translocon formation and substrate delivery.

The T3SS contacts host cell membranes and inserts the translocon proteins PopB and PopD into its membrane. This allows the delivery of substrates or effectors into the target cytosol. The T3SS needle rejects and leaves behind the translocon allowing K^+ efflux. This figure was adapted from [53] with permission from Springer Nature.

Effector delivery and specificity of the T3SS

T3SS substrates are thought to be delivered in a partially unfolded state. The unfolding is facilitated by a cytosolic ATPase that specifically recognises T3SS effectors. Effector recognition is mediated by a 20-25 aa long variable secretion motif at the N-terminus of the effector protein [47]. This secretion motif is enriched in serine and threonine residues, while no charged or hydrophobic residues are to be found within this region [54]. An interesting study also suggested that the secretion motif of the T3SS effector YopE from *Yersinia enterocolitica* lies within its mRNA [55]. This would suggest a co-translational delivery mechanism similar to the SRP-mediated Sec-pathway (1.2.1).

A couple of studies were able to demonstrate how the secretion motif mediates specificity for a certain T3SS machinery. *P. aeruginosa* was shown to secrete fusion proteins between the N-terminal 129, 96 and 54 aa of its T3SS substrate ExoS and heterologous passenger domains of various nature [56]. In another study, it was shown how *S. typhimurium* secreted chimeric proteins between the N-terminal 104 aa of its T3SS substrate SopE fused to reporter proteins or tumour antigens in a T3SS-dependent manner [57]. Interestingly, the T3SS machineries between *Yersinia pestis* and *S. typhimurium* are similarly enough that they could recognise and deliver substrates from the other organism [58]. On the basis of this finding, *Salmonella* strains were designed that recognised and delivered chimeric substrates between the N-terminal 138 aa from the *Y. pestis* T3SS substrate YopE and synthetic multi-domain proteins in a T3SS-dependent fashion [59].

Effector chaperones within the T3SS

Followed by a common N-terminal secretion motif, some T3SS effectors contain binding motifs or domains for cognate T3SS chaperones (Table 1-1) [60, 61]. These

chaperone binding domains of T3SS effectors wrap around their cognate chaperones by specifically binding to hydrophobic patches of the chaperone dimers (Figure 1-9) [61, 62]. This unusual conformation was revealed in recent studies showing the structures of the complex between the effector YopE and its chaperone SycE in *Yersinia pseudotuberculosis* (Figure 1-9B) [61] as well as SipA and InvB in *S. typhimurium* [63]. Thus, T3SS chaperones keep their effector proteins partially unfolded to maintain them in secretion-competent states before handing them over to the T3SS-specific ATPase [62]. The ATPase then dissociates the effector-chaperone complex and docks the effector into the cytosolic part of the T3SS apparatus [64]. This ultimately leads to effector translocation while the chaperone is retained within the bacterial cell [65].

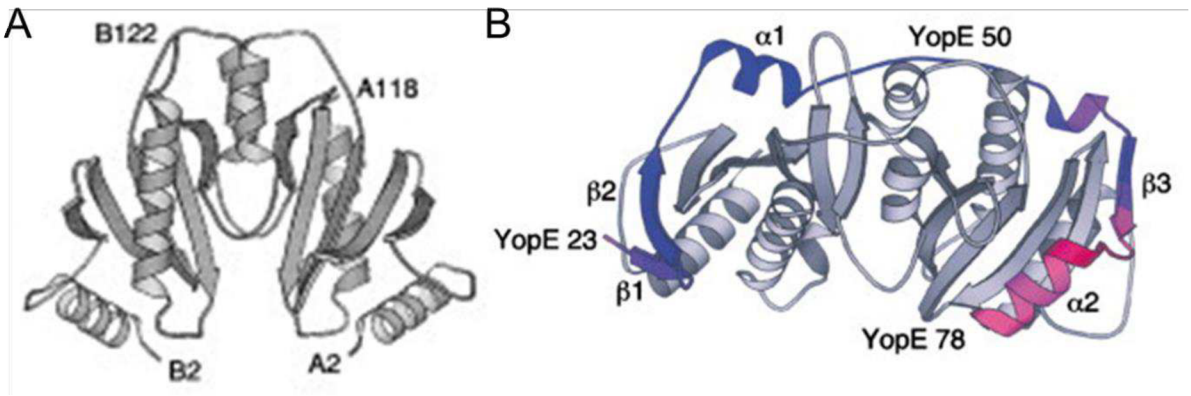


Figure 1-9. T3SS effectors bind to dimers of their cognate chaperones.

A: Ribbon model of the chaperone SycE from *Y. pseudotuberculosis*. B: Ribbon model of a SycE-YopE complex. Residues 23-78 of YopE (blue-red) encircles the SycE dimer (grey). This figure was adapted from [61].

Not in all cases is effector delivery completely abolished in absence of its cognate T3SS chaperone [66]. It was shown for YopE and YopH that their secretion was only reduced when they lacked their chaperone-binding domain [67]. Furthermore, effector chaperones of the T3SS are divided into two classes: while class IA chaperones associate with solely one

specific effector, class IB chaperones can bind several effectors [68]. Thus, class IA chaperones are considered more specialised, while class IB chaperones might represent a more generic and probably ancient form of T3SS chaperones [66]. Considering that not all effector chaperones are essential for effector recognition, it was hypothesised that chaperones might introduce a form of hierarchy into the effector delivery process. Thus, recognition of a chaperone-effector complex might impose a priority for chaperone-bound effectors, however, this hierarchical concept has not been fully proven yet [66].

Three of the four *P. aeruginosa* T3SS effectors are delivered in a chaperone-mediated fashion. While ExoS and ExoT share the same cytoplasmic chaperone SpcS [69], ExoU requires presence of SpcU for its delivery [70]. It was shown that SpcS binds to 45 specific amino acids within the N-terminal region of ExoS and ExoT [69], while ExoU contains a chaperone binding domain of about 120 aa for SpcU [71]. Interestingly, SpcS and SpcU are small acidic proteins that facilitate secretion of their cognate effectors, while also inhibiting their enzymatic activities. However, it remains prospect of future work to identify how the specific and also promiscuous binding to their cognate substrates is mediated.

1.2.5. Type IV secretion system

While many pathogens use the type IV secretion system (T4SS) in infection processes, *P. aeruginosa* lacks this machinery. Yet, for the purpose of completeness, the T4SS will be discussed here briefly. T4SS machineries are highly versatile, multi-functional and found in both Gram-positive and Gram-negative bacteria. They are involved in the uptake or export of DNA as well as protein substrates into a variety of bacterial, fungal, plant and human cell types or the extracellular medium [72]. Since the focus of this study is on the delivery of effector proteins, this section will cover the (protein) effector translocator group of T4SSs.

The best characterised T4SS is the VirB/D4 system in *Agrobacterium tumefaciens*, which delivers a fragment of oncogenic T-DNA as well as effector proteins directly into plant cells (Figure 1-10C). Integration of the bacterial DNA into the plant DNA leads to the tumorigenic Crown Gall disease [73]. Interestingly, a recent study just identified a T4SS in *Xanthomonas citri* that mediates contact-dependent killing of other Gram-negative bacteria [74]. This novel antibacterial machinery might form a special class of T4SS, whose detailed function has not been revealed yet.

T4SS are composed of an extracellular pilus, a core complex forming a channel from the outer to the inner membrane and three cytosolic ATPases (Figure 1-10). The core complex, formed of VirB7, 9, 10 (Figure 1-10C), builds a large 1 MDa complex spanning both the inner and the outer membrane (Figure 1-10A). Closed towards the outer membrane, the core complex encompasses two chambers forming a central channel that is open towards the cytoplasmic side [75] (Figure 1-10B). There it engages with the hexameric membrane-bound ATPase VirD4, termed type 4 coupling protein (T4CP) [73]. VirD4 is composed of three distinct domains: an N-terminal transmembrane domain connects it to the inner membrane complex; a nucleotide-binding domain provides energy for substrate translocation and the C-terminal substrate binding domain that specifically recognises T4SS substrates. Thus, the T4CP fulfils major roles in substrate recognition and binding, energising substrate transfer and connecting them to translocation channels [76].

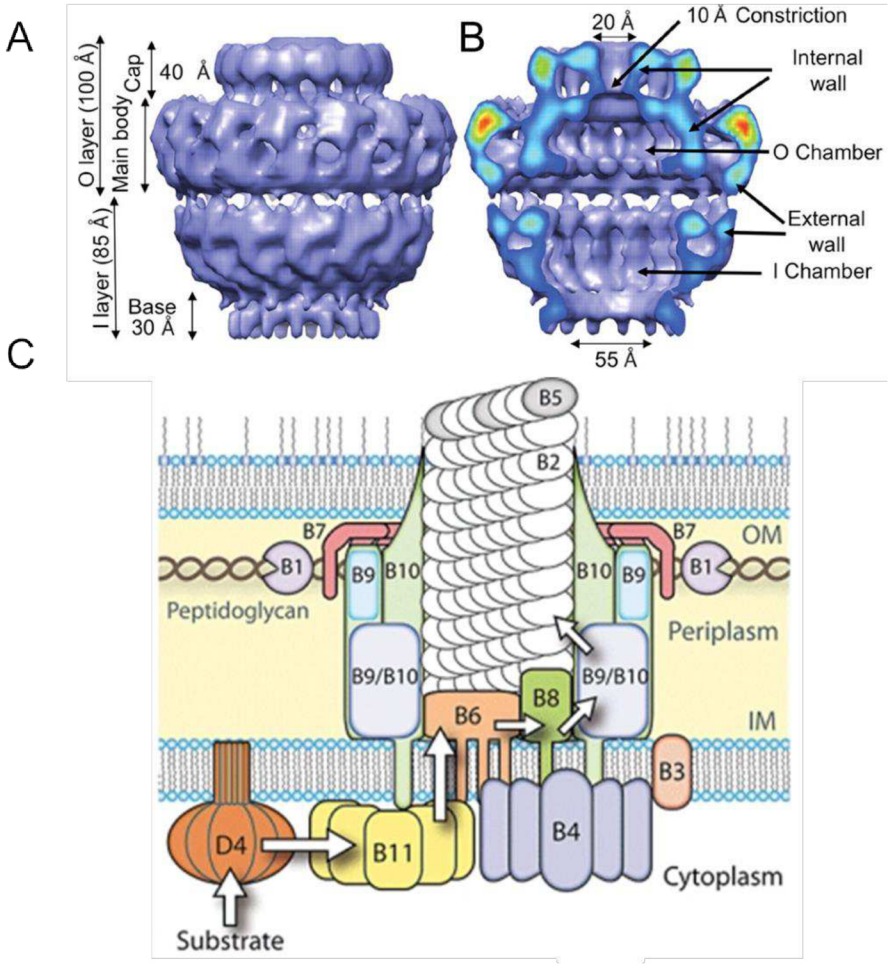


Figure 1-10. Components of the T4SS machinery.

A: Reconstruction of the cryo-EM structure of the T4SS core complex of *A. tumefaciens*. B: Cutaway side view displaying the available space of both O- and I- chambers. These figures are adapted from [77]. C: Schematic model depicting subunits of the VirB/D4 system from *A. tumefaciens*. The arrows indicate the way the substrate takes through the T4SS channel. This figure was adapted from [78] under the conditions provided by The American Association for the Advancement of Science and Copyright Clearance Centre.

Effector delivery and specificity in the T4SS

The T4CP, or VirD4 in *A. tumefaciens*, was suggested to serve as a substrate specificity checkpoint for cognate T4SS machineries [76]. The C-terminal substrate binding domain of VirD4 specifically recognises the signal sequence at the unstructured C-terminus

of T4SS substrates [73]. This signal sequence consists of clusters of positively charged arginine residues for the *A. tumefaciens* VirB/D4 substrates, or hydrophobic amino acids for *Legionella pneumophila* Dot/Icm substrates. For translocation of the CagA substrate from *Helicobacter pylori* through the Cag T4SS, a positively charged C-terminal tail as well as the N-terminal region was demonstrated to be crucial [79]. After binding to the T4CP, the T4SS substrate is handed over into the translocation channel in a process requiring ATP hydrolysis [73].

Specificity for T4SS substrates was shown on two different levels so far. In *A. tumefaciens*, fusion proteins were shown to be delivered that consisted of full-length VirE2 or VirF with N-terminal fused Cre recombinase as a reporter protein. The authors could then show how a fusion between Cre and the C-terminal 37 aa of VirE2 is specifically recognised and delivered by the T4SS [80]. Similarly, in *Bartonella henselae* it was demonstrated that its T4SS substrate BebD contains a C-terminal region of 183 aa that, when fused to Cre, mediates efficient substrate delivery in a T4SS-dependent manner [81]. Using a different concept, Whitaker and colleagues constructed chimeric T4CPs consisting of a N-terminal domain originated from *E. coli* and the core and C-terminal domains originated from *A. tumefaciens*, *Anaplasma phagocytophilum* or *Wolbachia pipientis*. The chimeric T4CPs were then shown to support the translocation of known T4SS substrates derived from *A. tumefaciens*, *A. phagocytophilum* and *W. pipientis,* respectively [76].

Effector chaperones within the T4SS

Recent evidence suggests, that some T4SS substrates are required to bind a chaperone in the cytosol prior to docking to the T4CP (Table 1-1) [82, 83]. In *A. tumefaciens*, delivery of the substrate VirE2 requires the presence of its downstream encoded chaperone VirE1, which, interestingly, exhibits several properties similar to the above described T3SS

effector chaperones (1.2.4) [73]. A translational coupling mechanism was described for this chaperone-effector pair to ensure the immediate binding of VirE1 to VirE2. The immediate stabilisation of VirE2 prevents formation of protein aggregates and maintains a translocation-competent state of VirE2 [84]. VirE1 binds to the N-terminus of VirE2, while the C-terminal domain of VirE2 is kept unoccupied for interactions with the T4CP VirD4 [82].

Furthermore, for the *H. pylori* substrate CagA it was demonstrated that it contains five internal motifs that specifically interact with its cognate chaperone CagF. Hence, it was suggested that multiple copies of CagF bind to CagA with high affinity. These interactions are further thought to maintain the labile CagA in a delivery-competent state while also recruiting it to the Cag-T4SS and thus facilitating substrate delivery [85].

After a substrate plugged into the T4CP, the chaperone is released and recycled to bind a new substrate protein [84]. This concept is similar to the role played by T2SS and T3SS chaperones; while they mainly function to stabilise their cognate substrates and channel them to the secretion apparatus, chaperones themselves are not delivered, but rather retained within the cell. However, it is not clear, whether all T4SS protein substrates require chaperones for their recognition and subsequent translocation or not.

Table 1-1. Chaperones involved in delivering protein secretion system substrates.

List of described T2SS, T3SS, T4SS and T7SS substrates that require interactions with a cognate chaperone for their delivery. When described, the interaction site within the substrate or the chaperon is listed. This table is however not an exhaustive list, but should rather exemplify the abundance of substrate chaperones within protein secretion systems.

organism	substrate	chaperone	interaction site	reference
T2SS				
B. glumae	LipA	Lif		[45]
A. nosocomialis	CpaA	CpaB		[41]
P. aeruginosa	LasB	LasB-propeptide		[46]
P. aeruginosa	LasA	LasA-propeptide		[86]
T3SS				
Y. pseudotuberculosis	YopE	SycE	60 N-term aa of YopE	[61]
Y. pseudotuberculosis	YopN	SycN		[66]
Y. pseudotuberculosis	YopH	SycH		[67]
Y. pseudotuberculosis	YopT	SycT		[66]
Shigella spp.	IpgD	IpgE		[66]
P. aeruginosa	ExoS	SpcS	45 N-term aa of ExoS	[69]
P. aeruginosa	ExoT	SpcS	45 N-term aa of ExoT	[69]
P. aeruginosa	ExoU	SpcU	120 N-term aa of ExoU	[70]
Salmonella spp.	SipA	InvB		[63]
Salmonella spp.	SptP	SicP		[63]
Salmonella spp.	SigD	SigE		[87]
EPEC	Tir	CesT		[87]
EPEC	EspF	CesF		[66]
T4SS				
A. tumefaciens	VirE2	VirE1	N-term of VirE2	[82, 84]
H. pylori	CagA	CagF	Five interfaces in CagA	[85]
L. pneumophila	SidA	IcmSW		[88]
L. pneumophila	SidB	IcmSW		[88]
L. pneumophila	SidC	IcmSW		[88]
L. pneumophila	SidD	IcmSW		[88]
L. pneumophila	SidE	IcmSW		[88]
L. pneumophila	SidG	IcmSW	C-term of SidG	[88]
L. pneumophila	SidH	IcmSW		[88]
T7SS				
S. aureus	EsaD	EsaE	N-term of EsaE	[89, 90]

1.2.6. Type V secretion system

The type V secretion system (T5SS) consists of two components that can be part of one polypeptide or exist as two different proteins (Figure 1-11). In any case, proteins of the T5SS reach the periplasm *via* a Sec-dependent translocation. For proteins, called autotransporters, since they carry all the information needed for the whole secretion process, the β-domain, which is called translocator domain, inserts into the outer membrane by forming a β-barrel channel. The second domain, the passenger domain, is then translocated through the channel into the extracellular medium [91]. Depending on the sub-type of T5SS, the two components can be two different proteins (T5bSS), hence also called two-partner secretion pathway (TPS), or one single polypeptide. These contain either a C-terminal (T5eSS) or N-terminal passenger domain that can remain attached to the barrel-pore (T5aSS, T5cSS), thus called autotransporters, or cleaved and released into the supernatant (T5dSS) (Figure 1-11). The passenger domains are in most cases long and fibrous polymorphic structures, while their C-terminal enzymatic domains vary depending on the sub-type and their function [91, 92].

P. aeruginosa does not employ all sub-types of T5SS [16], with EstA being the only characterised autotransporter. EstA, which is not cleaved from the bacterial surface, is an esterase. Its surface attachment allows the enzymatic domain to come in close contact to its substrate which is rhamnolipid [93]. This implies that EstA plays a role in motility and swarming as well as biofilm production. Additionally, the founding member of the T5dSS, that contains a C-terminal patatin-like domain, was recently described in *P. aeruginosa* [94]. Furthermore, two of the six T5bSS of *P. aeruginosa* are currently characterised, with LepA being a protease triggering host inflammatory responses, and CupB5 involved in the formation of CupB fimbriae [95]. Due to its involvement in inter-bacterial competitions, the T5bSS will be discussed here in detail.

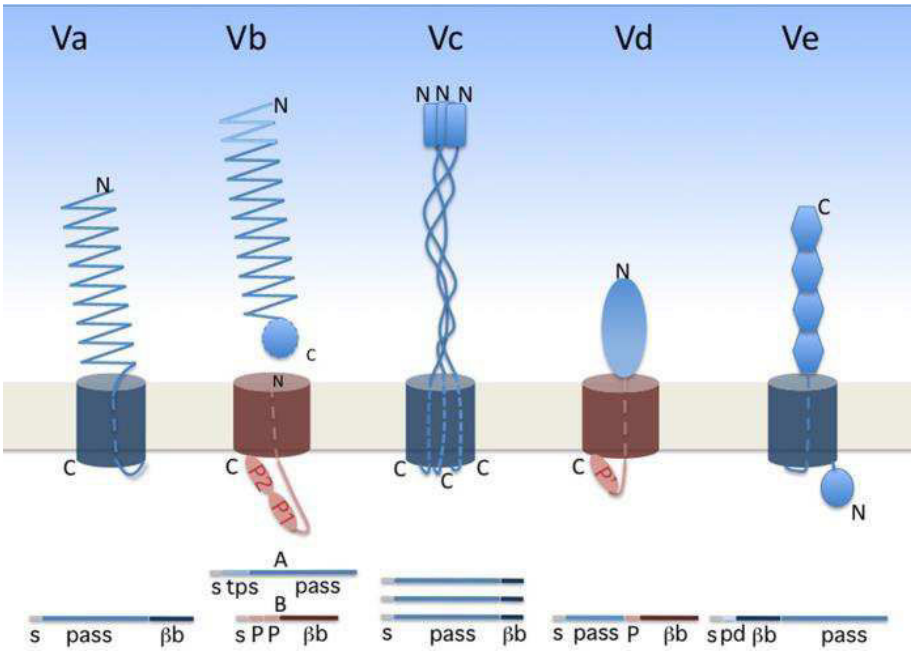


Figure 1-11. Types of the T5SS and their modularity.

The protein domains are sketched as in their final form after the secretion/integration process. T5aSSs and T5cSSs are produced as a single polypeptide with C-terminal β-barrel domains (blue) that integrate into the outer membrane. The T5bSSs are two proteins forming the transporter, being the TpsA for the passenger protein (blue), and TpsB as the transporter domain (red). T5dSSs are formed of single polypeptides with C-terminal β-barrel domains. T5eSSs are also formed of single polypeptides, but contain N-terminal β-barrel domains, thus called reverse autotransporters. This figure was adapted from [91] under the terms of the Creative Commons Attribution License.

T5bSS & two-partner secretion

Many bacteria employ the T5bSS, also termed two-partner secretion (TPS) system, to export toxins or adhesins. In most cases, the two genes involved in the TPS pathway form one operon [91]. Their gene products are TpsB, which forms a β-barrel channel in the outer membrane, and the passenger protein TpsA. TpsA contains an N-terminal TPS-domain that specifically recognises the POTRA (polypeptide transport-associated) domain of TpsB at the periplasmic side of the membrane. This ultimately leads to translocation of TpsA across the

outer membrane followed by additional cleavage. The mature TpsA then either remains anchored to the bacterial cell surface, or it is released into the extracellular medium [91].

Over the last years, several T5bSSs were identified in many pathogenic bacteria including *Serratia marcescens*, *Bordetella pertussis* and *Proteus mirabilis* where they export a range of cytolysins and adhesins. Interestingly, TPS operons in *Y. enterocolitica*, *Pasteurella multocida* and *P. aeruginosa* were shown to be upregulated upon host cell entry [91]. Additionally, in a range of bacteria T5bSSs were recently found to mediate inter-bacterial interactions leading to growth-inhibition as discussed below.

1.2.7. Polymorphic toxins

In the T5bSS as well as other protein secretion systems, different families of secreted multidomain toxins, termed polymorphic toxins, were identified. Generally, polymorphic toxins consist of a N-terminus that is related to a certain secretion system (Figure 1-12A, purple), and a C-terminal domain that harbours a toxin domain (red), which is delivered into neighbouring bacteria. A striking feature of polymorphic toxins is their modularity; any given N-terminal secretion domain can be found fused to distinct toxic domains (Figure 1-12B) and any given C-terminal toxic domain can be found fused to distinct secretion domains (Figure 1-12C). Also, the presence of orphan toxin-immunity modules (Figure 1-12A) allows the recombination with the 3' extremity of the full-length toxin to generate a new toxin using the same N-terminal domain. This allows the integration of novel toxin domains into the repertoire of a bacterium which can confer a competitive advantage against bugs that did not acquire the novel toxin module [96].

The typical locus of polymorphic toxin systems further includes an immunity gene (Figure 1-12A, cyan), located directly downstream of the toxin gene. The immunity gene

product protects the producing cell not only from autointoxication of the toxin, but also from incoming toxins produced by sibling cells. In some cases, the locus also contains additional genes that are involved in the secretion of the toxin [96].

The N-terminal secretion domain can be of various nature and size. Filamentous toxins contain core repeats of several domains of the same family, like recombination hotspot (Rhs)/YD- or filamentous hemagglutinin repeats [96]. One well characterised example is the CdiA protein as part of the contact-dependent inhibition system as described below, while Rhs toxins were previously associated with the T6SS and will be subject of later discussion (1.3.7).

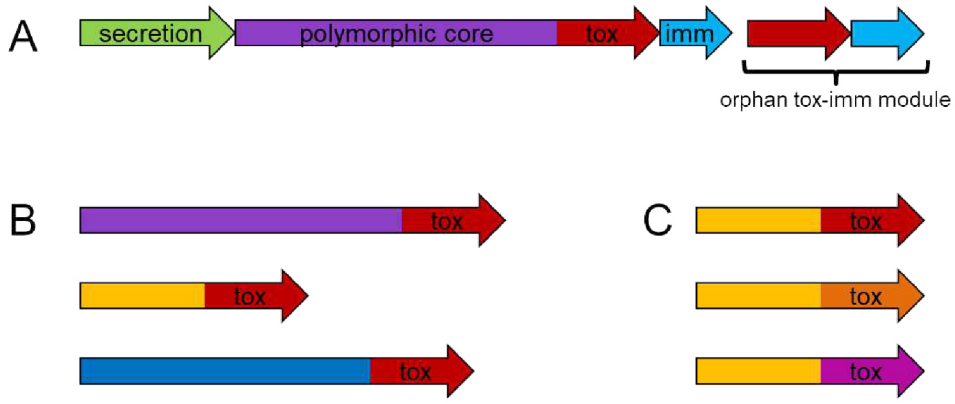


Figure 1-12. Modularity of polymorphic toxins.

A: General genetic organisation of polymorphic toxin-immunity modules. A gene encodes a protein that is involved in the secretion (green) of the downstream encoded toxin, whose N-terminus (purple) determines the affiliation with the secretion system and the C-terminus harbours the toxin domain (red). Downstream encoded is the cognate immunity (cyan) for the toxin with in some cases following orphan toxin-immunity modules. B: Modularity of polymorphic toxins. Any given N-terminus (purple, yellow, blue) can be fused to a distinct C-terminal toxin domain (red). C: Modularity of polymorphic toxins. Any given toxin domain (red, orange, pink) can be fused to a distinct N-terminal domain (yellow).

1.2.8. Contact-dependent growth inhibition

The contact-dependent growth inhibition (CDI) system is a specific type of T5bSS and involves two proteins. CdiB, the corresponding TpsB, forms a β-barrel channel in the outer membrane, while CdiA, the TpsA, is translocated through the outer membrane and attached to the bacterial surface (Figure 1-13) [97]. The polymorphic CdiA proteins contain toxic domains of various enzymatic activities within their C-termini that are delivered into neighbouring target cells. For the producing cell to also be protected from this toxic effect, corresponding immunity proteins, CdiI, are required that neutralise the toxic CdiA. These CdiI proteins are generally encoded downstream of the *cdiA* gene and in an operon with *cdiB,* similar to the operon sketched in Figure 1-12A. If the target cell does not express the cognate immunity protein for the incoming toxin, growth inhibition occurs in an extent depending on the enzymatic effect of the toxin (Figure 1-13).

The first CDI system described was in *E. coli* EC93 strain that inhibited the growth of other *E. coli* strains that did not produce the CDI system [98]. Different toxin domains were described and are usually strain specific; for example, the CdiA from *Enterobacter cloacae* was shown to cleave 16S ribosomal RNA to disrupt protein synthesis in the target cell [99]. Interestingly, CdiA from *E. coli* UPEC 536 contains tRNase activity while CdiA from *E. coli* EC93 forms pores in the inner membrane [100]. Thus, closely related bacterial species can outcompete each other to ensure their own survival (Figure 1-13).

Furthermore, the adhesive properties of CdiA were shown to promote collaborative behaviour between sibling cells. This aggregative behaviour was shown to be associated with biofilm formation in several species, such as *P. aeruginosa*, in which several CDI systems were identified but not fully characterised yet [101]. It is noteworthy, that cooperative behaviour mediated by the CDI is only provided when a cell contains the corresponding immunity for the

incoming CdiA toxin. Thus, biofilms only embrace bacterial cells from the same species, while susceptible and thus non-isogenic bacteria are excluded [97].

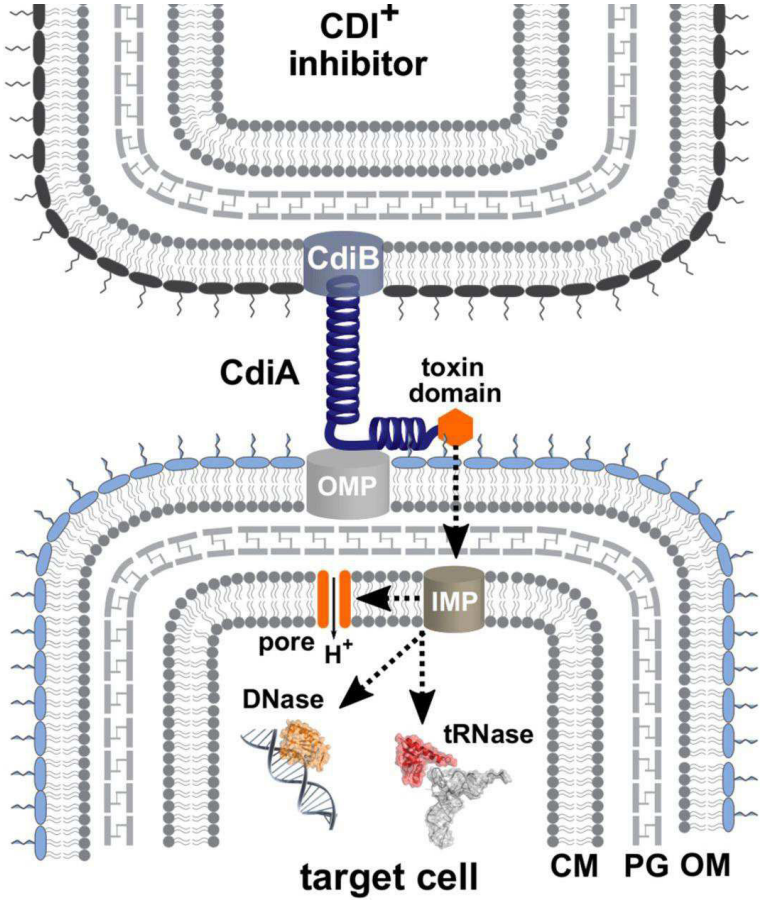


Figure 1-13. CDI-mediated toxin delivery.

Components of the CDI system are exported via the Sec-pathway. CdiB is inserted in the outer membrane and CdiA contacts its periplasmic POTRA domain following CdiA translocation. CdiA protrudes from the bacterial cell surface and contacts a neighbouring cell by binding a receptor. CdiA-CT is cleaved and enters the target cell, where it encounters its cellular target and exerts a toxic effect. This figure was adapted from [97] with granted permission from Portland Press Limited.

Effector delivery via the CDI

Polymorphic CdiA toxins are large rigid multi-domain proteins on the bacterial surface, that carry C-terminal toxin domains [102]. Generally, a CdiA protein consists of a cleavable signal sequence for Sec-mediated delivery across the inner membrane, a TPS transport domain for TpsB recognition and a core of rigid FHA repeats (Figure 1-14A). Recent work has identified a variable receptor binding domain between the highly conserved FHA-1 and FHA-2 domains within CdiA proteins from different species. The core domain is differentiated by a 4-aa long VENN motif, whose function in toxin maturation is still unclear. The C-terminal domain of CdiA (CdiA-CT) further contains two domains [103]: The N-terminal translocation domain and the toxic C-terminal domain (Figure 1-14A).

Recent research tried to outline the delivery of the toxin domain into target cells, while not all molecular steps are well understood yet. It was shown in *E. coli* EC93 that CdiA binds to a key subunit of the outer-membrane β-barrel assembly machine (BAM) complex, while this receptor seems to vary between species [104]. Furthermore, it was shown that in absence of the receptor protein on the target cell surface, inhibition occurs at a lower level [104]. Binding of CdiA to the target cell surface is mediated by its receptor binding domain (Figure 1-13), however, the actual translocation step remains elusive while it seems clear that cleavage of CdiA-CT occurs. Once in the periplasm, the strain-specific N-terminal translocation domain of CdiA-CT is thought to interact with a membrane protein governing its translocation across the inner membrane of target cells [103]. In a recent study, Hayes and co-workers designed a chimeric CdiA based on the two CdiA-CTs from *E. coli* EC869 and *E. coli* EC3006 (Figure 1-14A). While CdiA-CT^{EC3006} contains an N-terminal PtsG domain, that mediates translocation across the inner membrane dependent on the protein PtsG, and a C-terminal tRNase domain, CdiA-CT^{EC869} contains an N-terminal YciB domain, an unknown inner membrane protein, and a C-terminal DNase domain. They then swapped the C-terminal toxic domains from *E. coli* EC3006 with the one from *E. coli* EC869 (Figure 1-14C) and proved that this chimera was

delivered into target prey cells in a process dependent on PtsG [103]. LIttle is known about the actual translocation step, but potentially it involves the electrochemical gradient as a driving force [103, 105]. Once reached the target cytosol, some CdiA-CTs require activation by interacting with essential cell components like EF-Tu or AcrB [104] while the current hypothesis states that this interaction might lead to stabilisation of the CdiA-CT toxin [106].

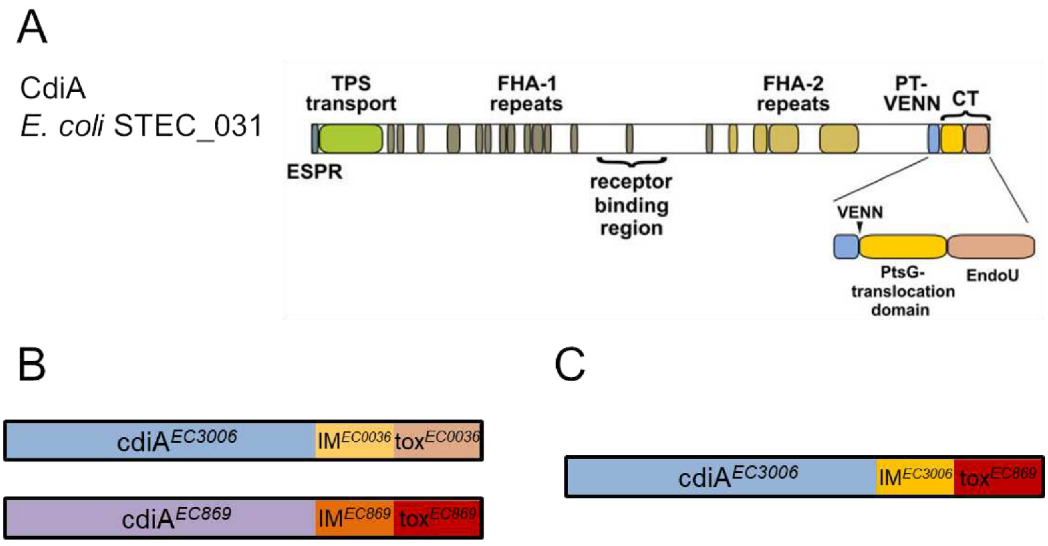


Figure 1-14. CdiA is formed of multiple sub-domains with different functions.

A: Modularity of CdiA. The N-terminal signal peptide ESPR (blue) mediates translocation across the inner membrane. The TPS transport domain (green) is crucial for binding to TpsB in the periplasm, resulting in its translocation across the outer membrane. FHA-1 and FHA-2 (browns) repeats are predicted to form rigid β-structures. The pretoxin-VENN motif (light blue) distinguishes the core domain from the C-terminal toxin domain (CdiA-CT), which is further composed of two variable domains: The N-terminal translocation domain (yellow) and very C-terminal toxic domain (red). This figure was adapted from [97] with granted permission from Portland Press Limited. B: $CdiA^{EC003}$ (blue) consists of a N-terminal PtsG domain (IM, yellow) of CdiA-CT, that directs it to the specific inner membrane receptor PtsG, and a toxic tRNase domain (tox, light brown). The closely related strain *E. coli* EC869 produces a CdiA protein (purple) with an N-terminal YciB domain (orange) within its CdiA-CT and a DNase domain (red). C: A chimeric protein was designed and showed to be delivered that contained the CdiA core domain and the PtsG domain from *E. coli* EC3006 as well as the toxic domain from *E. coli* EC869 [103].

1.2.9. The type VII secretion system

The type VII secretion system (T7SS) has only been identified in *Mycobacteria*, *Actinobacteria* and *Firmicutes* and shown to play a role in virulence [107]. However, due to recent findings of its impact on bacterial warfare in *Staphylococcus aureus* and its modularity of effector delivery mechanisms [90], the T7SS will be briefly introduced here.

Six core components were shown to assemble the T7SS/Ess complex in *S. aureus* [108, 109]. Three membrane-bound components, EsaA, EssA and EssB are essential for T7SS activity as well as a secreted protein EsxA and a predicted cytoplasmic protein EsaB (Figure 1-15A). A membrane-bound hexameric ATPase EssC was shown to provide energy and is also involved in effector delivery [108], even though, the detailed effector delivery mechanism is still unclear. The T7SS substrate EsaD, that varies between different *S. aureus* strains, is a polymorphic toxin with a C-terminal nuclease domain [90]. Downstream of *esaD*, the corresponding immunity *esaG* is encoded that protects the producing cell from EsaD toxicity [90]. In the mycobacterial T7SS, substrates contain a YxxxD/E signal sequence needed for recognition by the ATPase [110]. Binding of the effector to the C-terminus of the ATPase leads to an increase of ATPase activity which ultimately results in effector delivery [90, 111]. However, it is currently not clear, how well conserved this signal sequence is between the T7SS of *Mycobacteria* and *S. aureus*. Furthermore, in *S. aureus* it was recently revealed that secretion of the substrate EsaD requires binding to a cognate chaperone EsaE (Figure 1-15B) [89]. EsaE binds EsaD at its the N-terminus, thus stabilising the protein and mediating its secretion by recruiting it to the T7SS apparatus [89, 90]. In contrast to other protein secretion systems, the chaperone was here shown to be delivered together with the substrate [90].

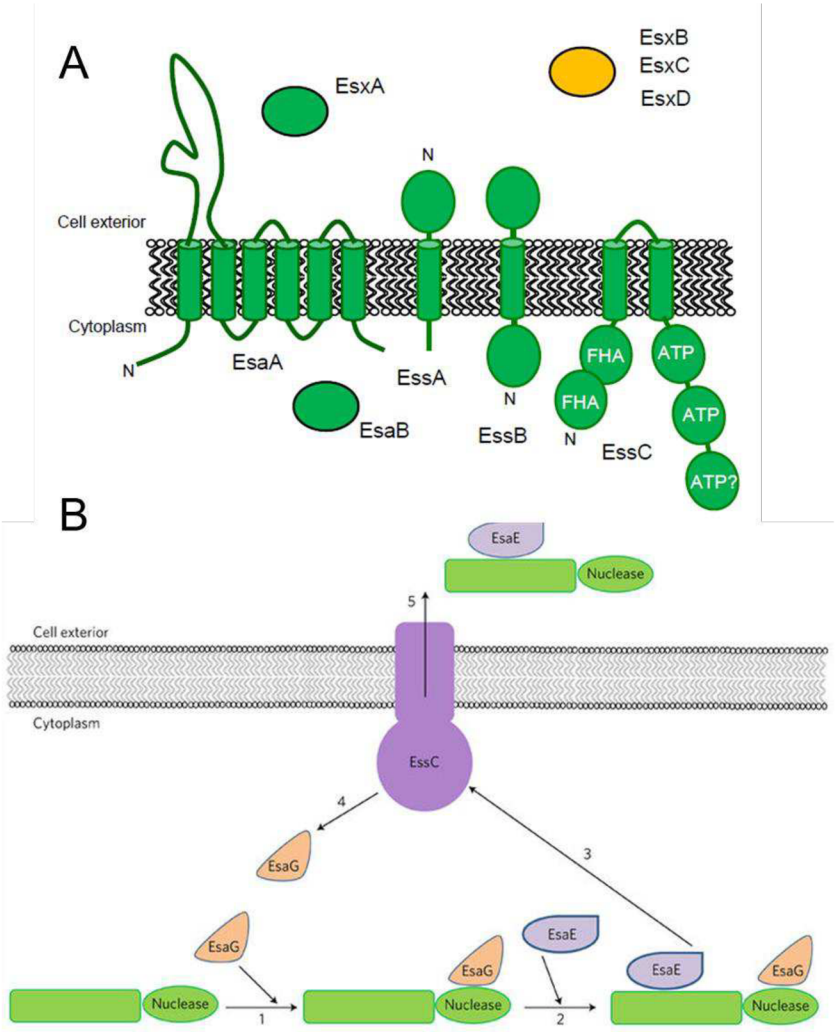


Figure 1-15. Schematic of the T7SS.

A: Subunits forming a T7SS machinery in *S. aureus*. Shown are the localisation and predicted topologies of Ess components. B: Model for delivery mechanism of EsaD (green). After synthesis of EsaD, it is bound by EsaG (orange) at its toxic domain. The chaperone EsaE (purple) recruits the toxin-immunity complex and targets it towards the secretion machinery followed by translocation of the chaperone and the toxin. This figure was adapted from [90] with permission from Springer Nature.

1.3. The type VI secretion system in *P. aeruginosa*

The type VI secretion system (T6SS) is a dynamic protein secretion system that is found in about 25 % of Gram-negative bacteria [112]. Its remarkable resemblance with the

bacteriophage T4 facilitated research into this fascinating machine and progress in understanding its function and assembly. However, while bacteriophage T4 injects DNA from the extracellular medium into a target bacterium, bacteria use the T6SS to drive effectors directly into target cells that can be of bacterial and eukaryotic nature [113]. This allows the bacterium to inhibit growth of competing bacteria in a contact-dependent manner or modulate host cell metabolism to facilitate its own survival. *P. aeruginosa* encodes three T6SS clusters (H1-, H2-, H3-T6SS), each of them able to assemble a unique machinery and deliver its own effector proteins [114]. This section aims to describe the architecture, function and payload of this protein secretion system.

1.3.1. The overall structure of the T6SS and mechanism of action

The membrane complex

Of the 13 essential T6SS components, three have been shown to reside in the cell envelope. Tss (type VI secretion system) L and TssM form the membrane complex anchored in the inner membrane, while TssJ connects the whole complex to the outer membrane (Figure 1-16) [115]. TssL contains a large cytoplasmic domain anchored to the inner membrane via one transmembrane helix [116]. The large TssM protein is formed of four structural segments: a cytoplasmic domain is inserted in the inner membrane through three transmembrane helices, followed by a periplasmic domain and a C-terminal beta domain [117]. Interestingly, in *S. marcescens* the periplasmic domain was shown to contain a disulphide bond for efficient functionality [118]. The TssM beta domain interacts with TssJ which is a lipoprotein attached to the outer membrane [117], thus connecting the membrane complex to the outer membrane. The negative stain EM structure of the TssJ-TssL-TssM-complex was determined and showed that ten copies of TssJ-TssM pillars span the periplasm contacting the inner membrane via

five TssL dimers (Figure 1-16) [115]. Despite this comprehensive knowledge about the assembly of the membrane complex, it has not been elucidated whether a pore is formed in the outer membrane and how a potential opening might be regulated. However, preliminary evidence suggests that the periplasmic domain of TssM would change its conformation to allow crossing of the T6SS spike into the extracellular medium [115]. Assembly of the T6SS machinery starts with TssJ and thus the membrane complex is considered a nucleation factor, to which the baseplate docks [119].

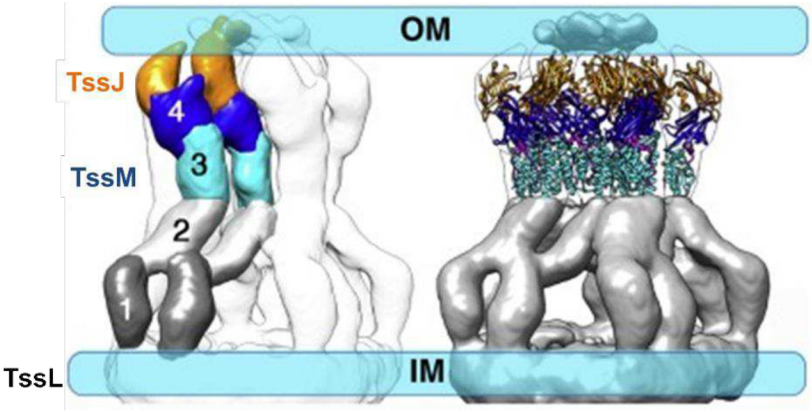


Figure 1-16. Membrane complex of the T6SS.

The TssJLM complex is anchored to the outer membrane via the lipoprotein TssJ. TssJ (orange) interacts with the periplasmic domains of TssM (blue) that is anchored to the inner membrane via its transmembrane domains (grey) where it contacts TssL. This figure was adapted from [115] with permission from Elsevier and the Copyright Clearance Centre.

The baseplate platform

The T6SS baseplate is considered a platform for assembly of the spike and the sheath and is thought to mediate sheath contraction and thus spike delivery through the membrane complex (Figure 1-17A). The baseplate consists of subunits of TssA, TssE, TssF, TssG, TssK and a VgrG [119, 120], which all resemble components of the baseplate of the bacteriophage

T4 [121]. The trimeric TssK was shown to interact with TssL from the membrane complex [122] but also to recruit TssF and TssG towards the baseplate while the function of TssE is still unclear [119]. Recent work from our lab showed that the dodecameric TssA1 from the H1-T6SS from *P. aeruginosa* interacts with TssK1, TssF1 and TssB1 and TssC1 from the sheath complex [120]. Different classes of TssA proteins were proposed to have different functions, with the TssA1-like proteins being part of the baseplate, while TssA2-like proteins contain C-terminal extensions. This extension might confer a TssA protein the function to prime and polymerise the T6SS contractile sheath as described by Zoued *et.al.* for the TssA in *E. coli* [123]. Hence, current evidence assigns TssA to be a genuine T6SS baseplate component.

The T6SS sheath

The T6SS sheath is a helical contractile tube composed of TssB and TssC subunits that are the homologues of the gene product (gp) 18 from bacteriophage T4 [124]. TssB and TssC interact via their so-called “handshake” domains to form long tubular and highly dynamic cogwheel-like structures (Figure 1-18) [125, 126]. The TssBC sheath further envelops the Hcp tube, which consists of head-to-tail stacked hexamers of Hcp (haemolysin co-regulated protein) [127]. The Hcp tube is topped by the so-called T6SS spike, which is discussed in more detail in 1.3.2 (Figure 1-17A) [128]. The T6SS sheath was shown to extend throughout the whole length of a bacterial cell [125], with the cell length being the limiting factor for sheath elongation [129]. The elongated sheath is in a meta-stable, high-energy state so that thermodynamically the contracted sheath represents the favoured low-energy state [130]. This energy collapse is predicted to release sufficient amount of energy to propel out the T6SS spike together with the Hcp tube (Figure 1-17B). Hence, Hcp is considered the landmark protein of the T6SS, since its presence in the supernatant fraction is the direct result of a functional T6SS machinery [131].

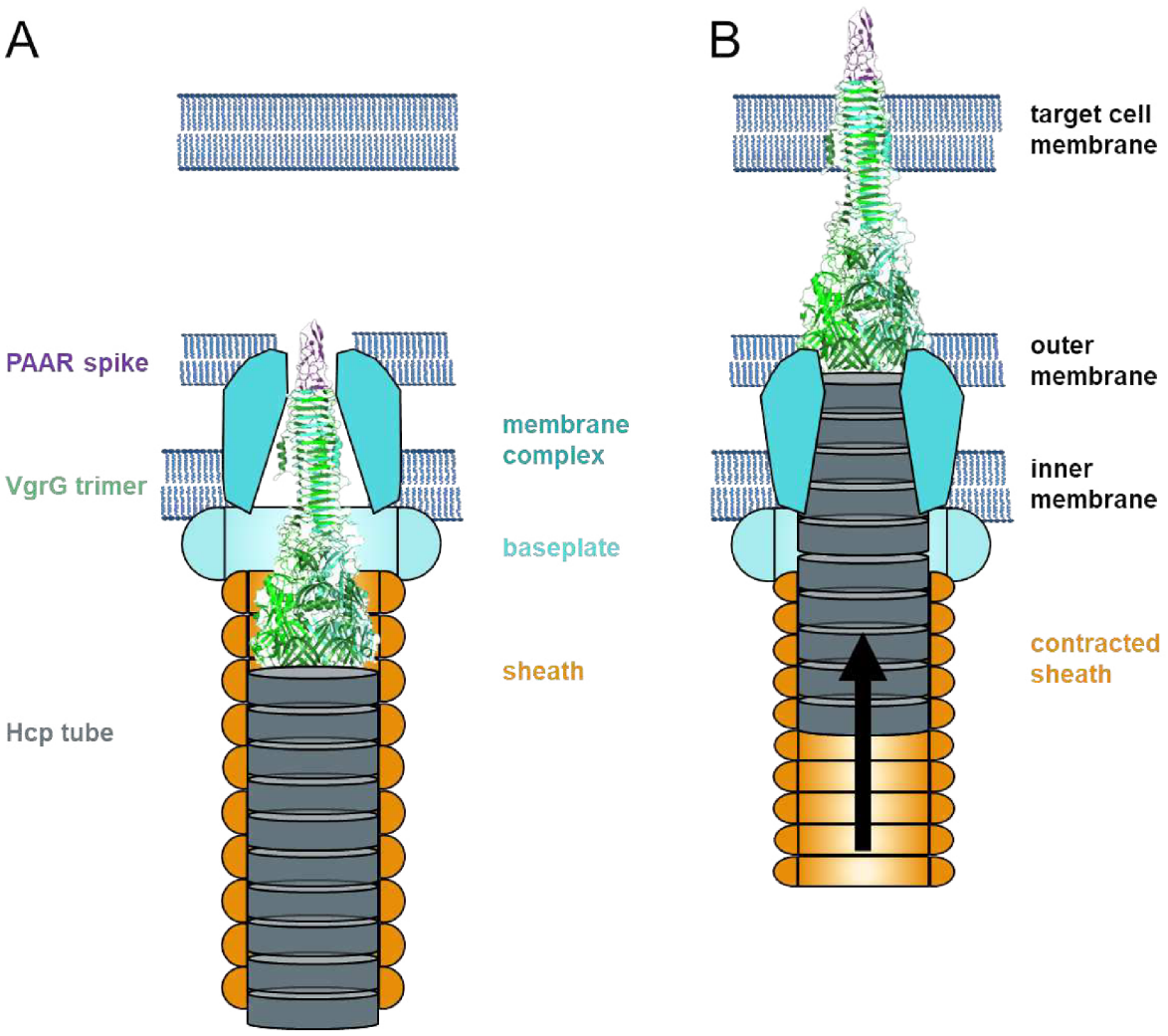


Figure 1-17. Model of the T6SS and its activity.

A: The membrane complex (blue) spans the bacterial cell envelope. The baseplate (cyan) is anchored to the inner membrane connecting to the cytosolic sheath (orange). Within the sheath, the Hcp tube (grey) is assembled, which is topped by the VgrG-PAAR spike (green-purple). B: Upon contraction of the sheath and likely opening of the membrane complex, the Hcp tube together with the VgrG-PAAR spike are propelled outside the cell and through the target cell membrane.

Activity and thus firing of the T6SS is thought to be triggered from the baseplate, that, *via* an unknown mechanism, leads to contraction of the TssBC sheath rendering the T6SS spike into a high-powered molecular drill puncturing the target membrane (Figure 1-17B) [132]. Upon contraction, a cytosolic ATPase ClpV is recruited towards the now exposed N-terminus of TssC and initiates depolymerisation of the TssBC tubule [133, 134]. This quick disassembly

then allows the re-association of the sheath for another round of T6SS firing [126]. A mutant lacking *clpV* still contains the ability to fire its T6SS machinery, however in many cases the efficiency was shown to be drastically reduced [126, 135]. Remarkably, not all organisms encode for ClpV proteins within their T6SS loci, for example the K2- and K3-T6SS of *P. putida* [136], and it remains to be investigated how these organisms energise their T6SS disassembly and thus functioning. Additionally, the closely related phages do not require ATPases, likely because they only fire once from the extracellular medium where no energy sources are available and they do not require rounds of disassembly and reassembly.

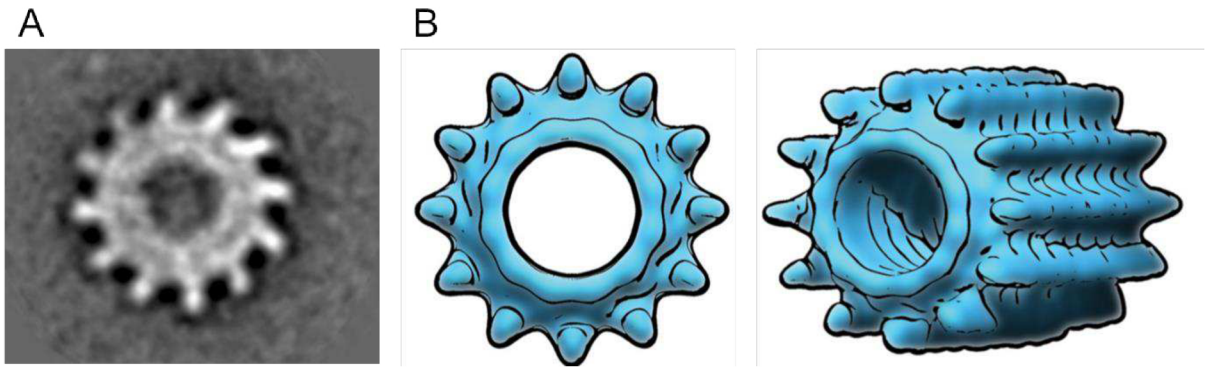


Figure 1-18. The T6SS sheath forms a cogwheel-like tube.

A: Negatively stained TssBC cogwheel structures with 12-fold symmetry. B: Model of the TssBC sheath on top and tilted view showing the 12-fold symmetry. This figure was adapted from [125] with permission from ASBMB journal and the Creative Common Attribution License.

1.3.2. Spike composition

The T6SS spike on top of the Hcp tube (Figure 1-17A) is composed of a trimer of VgrG (valine-glycine rich) proteins. VgrG proteins are homologues to the gp5 and gp27 that form the trimeric rigid torchlight-like spike of the bacteriophage T4 (Figure 1-19) [137]. A trimer of gp27 (Figure 1-19A, yellow, grey, purple) forms the cylindrical head of the spike to which a

trimer of gp5 (blue, red, green) is attached. In the bacteriophage, gp5 consists of an N-terminal lysozyme domain and a C-terminal needle-like spike formed of 18 intertwined β-sheets with conserved VXGXXXX motifs [137]. These β-sheets are hydrophobic and conserved, with a dominant glycine at position a (Figure 1-19B, highlighted in bold), asparagine or aspartic acid at position b and valine at position g [137]. The glycine at position a is thought to kink the polypeptide chain [137], allowing the β-sheets to form a cylindrical elongated structure. Intertwining of three gp5 monomers is facilitated by hydrogen bond formations between β-sheets from different monomers. This assembly results in the unique and sturdy spike structure [124, 138], highly stable and resistant to 10 % SDS as well as boiling [139, 140].

The C-terminal domain of a VgrG protein is exceptionally similarly structured to the C-terminal domain of gp5 from bacteriophage T4, hence called gp5-like, but it lacks the N-terminal lysozyme domain (Figure 1-20A). The organisation of the β-sheet forming octapeptides is highly similar (compare Figure 1-19B and C) [137] and, similarly to the bacteriophage T4, most VgrG proteins contain VXGXXXX or VGXXXXX motifs [139]. In any case, the conserved glycine at position a is prevalent in VgrG proteins, as exemplified by the C-terminal residues from *P. aeruginosa* VgrG1a (Figure 1-19C, highlighted in bold) [140]. It is worth mentioning at this point, that the last β-sheets in both bacteriophage T4 and VgrG1a are formed by similar sequences containing two hydrophobic amino acid residues, isoleucine or leucine (Figure 1-20B, C, bottom row).

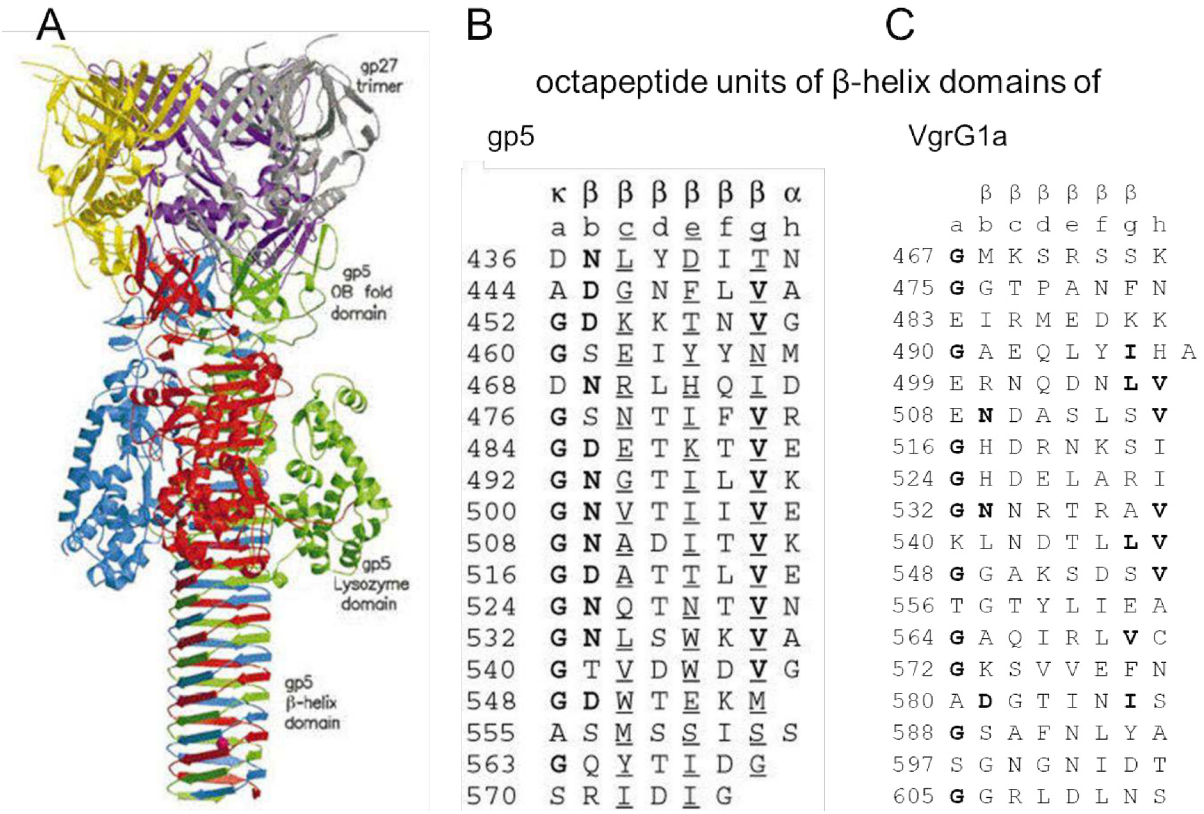


Figure 1-19. The T6SS spike is structurally similar to the T4 spike.

A: Structure of the trimeric gp27-gp5-complex from the bacteriophage T4. The three gp27 domains are coloured in yellow, purple and grey, while the three gp5 domains are coloured in blue, red and green. B, C: Alignments of amino acids residues forming the intertwined β-sheets in the C-terminus of B: gp5 of the bacteriophage T4 and C: the gp5-like domain of VgrG1a from *P. aeruginosa*. Highlighted in bold are amino acids that are conserved within the gp5 domains of bacteriophages. These figures were adapted from [137] with permission from Springer Nature.

On top of the T6SS VgrG trimer sits a conically shaped PAAR protein (Figure 1-20A, purple), that is structurally similar to the gp5.4 protein in bacteriophage T4 [141]. PAAR proteins harbour three highly conserved PAAR (proline-alanine-alanine-arginine) motifs as well as conserved histidine and cysteine residues that chelate a Zn ion (Figure 1-20B). The PAAR fold as well as the Zn ion are thought to stabilise this rigid conical shape that probably facilitates puncturing of target membranes [142]. As shown in Figure 1-20B, one PAAR protein

likely binds on top of one VgrG trimer in a way that it interacts with the last β-sheet derived from each VgrG monomer [141].

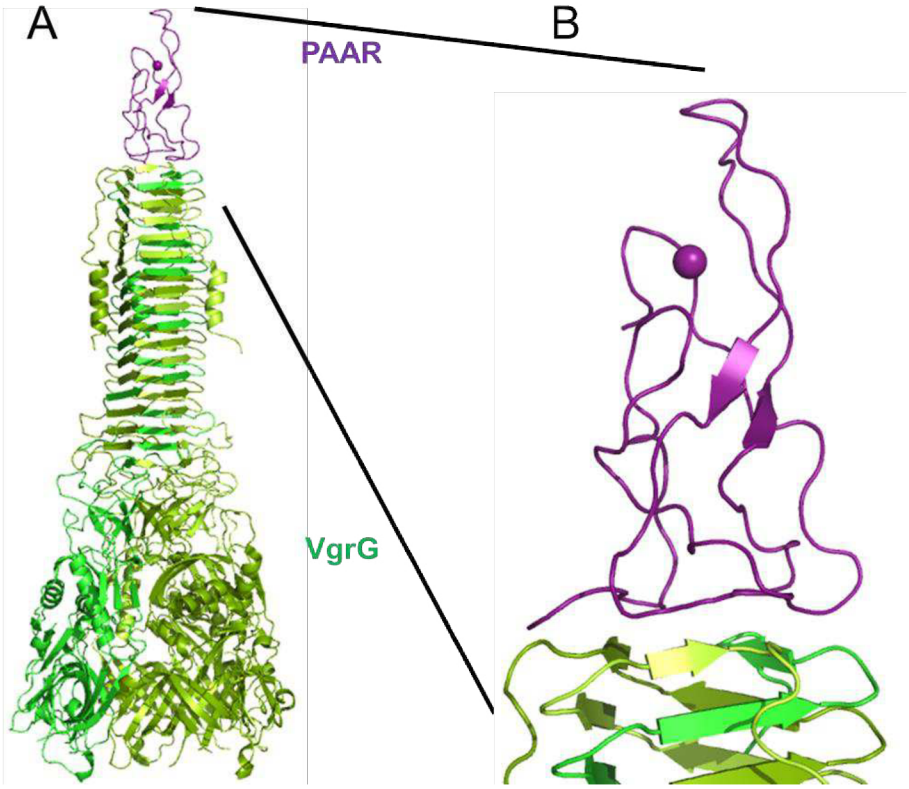


Figure 1-20. The T6SS spike.

A: The T6SS spike is composed of a trimer of VgrG proteins (green, VgrG1a from *P. aeruginosa* PDB: 4mtk) that form an intertwined needle structure. A PAAR protein (purple, model of the PAAR domain from Tse6) sits on top of the trimer. B: Close-up of the interaction surface between PAAR and VgrG. One PAAR protein binds to the blunt end of a VgrG trimer.

1.3.3. *P. aeruginosa* contains three T6SS clusters and up to 11 *vgrG* islands

Gram-negative bacteria can contain various numbers of T6SS clusters between one, like in *S. marcescens* [143], *Vibrio cholerae* [131], *A. tumefaciens* [144], up to five in *Y. pestis* [112] and even six in *Burkholderia pseudomallei* [145]. Each of *P. aeruginosa* 's T6SS clusters

contains all essential genes required to assemble a functional T6SS machinery (Figure 1-21) [114]. Within the H1-T6SS and H3-T6SS clusters, genes encoding Hcps (brown), the hallmark protein of the T6SS, VgrGs (green) and PAARs (purple), the essential spike components (1.3.2), are found that are functionally linked to the H1- and H3-T6SS machineries, respectively (Figure 1-21) [140, 146]. While in the PA14 genome *hcp2* is located upstream of *vgrG14* within the H2-T6SS cluster [147], this is not the case in PAO1. Here, three *hcp* genes, *hcpA*, *hcpB* and *hcpC*, are located together with *vgrG* and *paar* genes on remote gene islands (Figure 1-22). The two *vgrG* genes that are genetically linked to *hcpA* and *hcpC* were functionally linked with the H2-T6SS [146]. Due to a sequence identity of 99 % between *hcp2, hcpA*, *hcpB* and *hcpC*, it was thus assumed that they are all associated with the H2-T6SS [147].

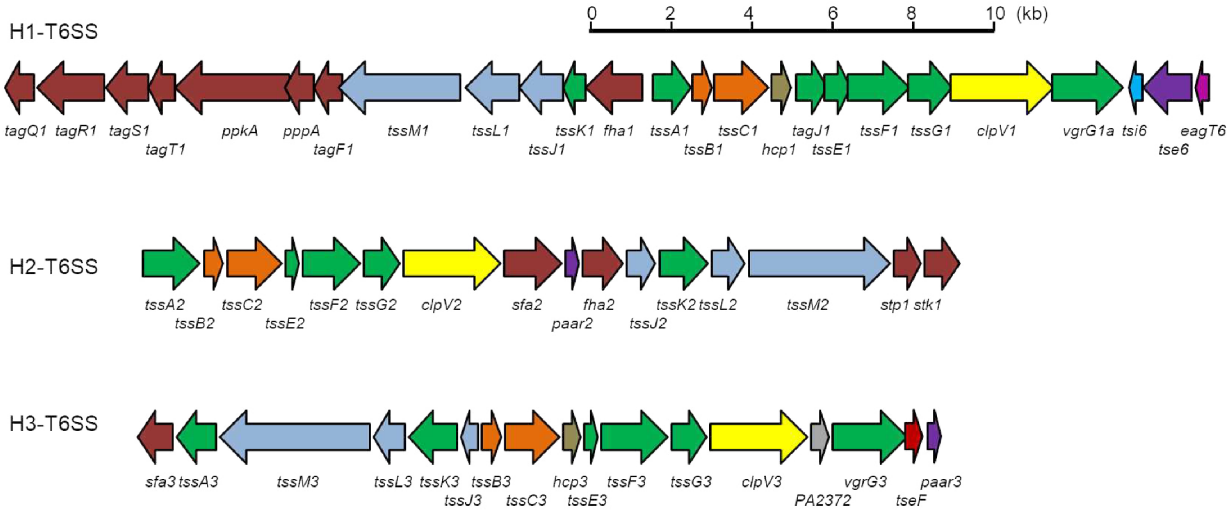


Figure 1-21. The three T6SS clusters present in *P. aeruginosa* strains PAK, PAO1, PA14.

Regulatory genes are shown in dark red; genes encoding for membrane complex proteins are shown in blue, for baseplates components in green, for sheath components in orange; *hcp* genes in brown and the ATPase encoding *clpV* genes in yellow, *paar* genes in purple, effectors in red and immunities in cyan and accessory genes in magenta.

In addition to the complete T6SS clusters, there are many remote gene islands, likely acquired via horizontal gene transfer, scattered around the genome, functionally linked to the T6SS and upregulated under the same conditions as the T6SS clusters [146, 147]. In most of these satellite islands, *vgrG* genes are located (Figure 1-22, green) and dependent on the strain, *P. aeruginosa* contains up to eleven different *vgrG* genes [140]. Encoded together with *vgrGs* are effector-immunity modules (red-cyan) as well as *paar* (purple) and accessory genes (magenta). In *P. aeruginosa* but also in many other organisms, it was shown that these gene products interact and facilitate delivery of the effector protein via one of the T6SS machineries, as will be discussed in 1.3.7.

In addition to various *vgrG* genes, also numerous *paar* genes are located within the *P. aeruginosa* genome. As discussed in detail in 1.3.2, a VgrG trimer topped with a PAAR forms the rigid puncturing spike of a T6SS, whose presence was shown to be a requirement for the formation of a functional T6SS [141, 148]. With the presence of that many different *vgrG* and *paar* genes, it becomes clear that *P. aeruginosa* can form various T6SS spikes consisting of diverse VgrG and PAAR proteins. On another note, it was established that one VgrG trimer requires the specific interaction with one cognate PAAR protein to form a functional T6SS spike and no non-cognate PAAR protein is able to substitute [141, 148]. This was shown not only in *P. aeruginosa*, as will be further discussed in 4.3, but also for the specific VgrG-PAAR pairs in *S. marcescens* [148] and *A. tumefaciens* [149]. Hence, a concept of specificity at the level of the VgrG-PAAR interface was proposed and will be subject of further discussion in 4.4.

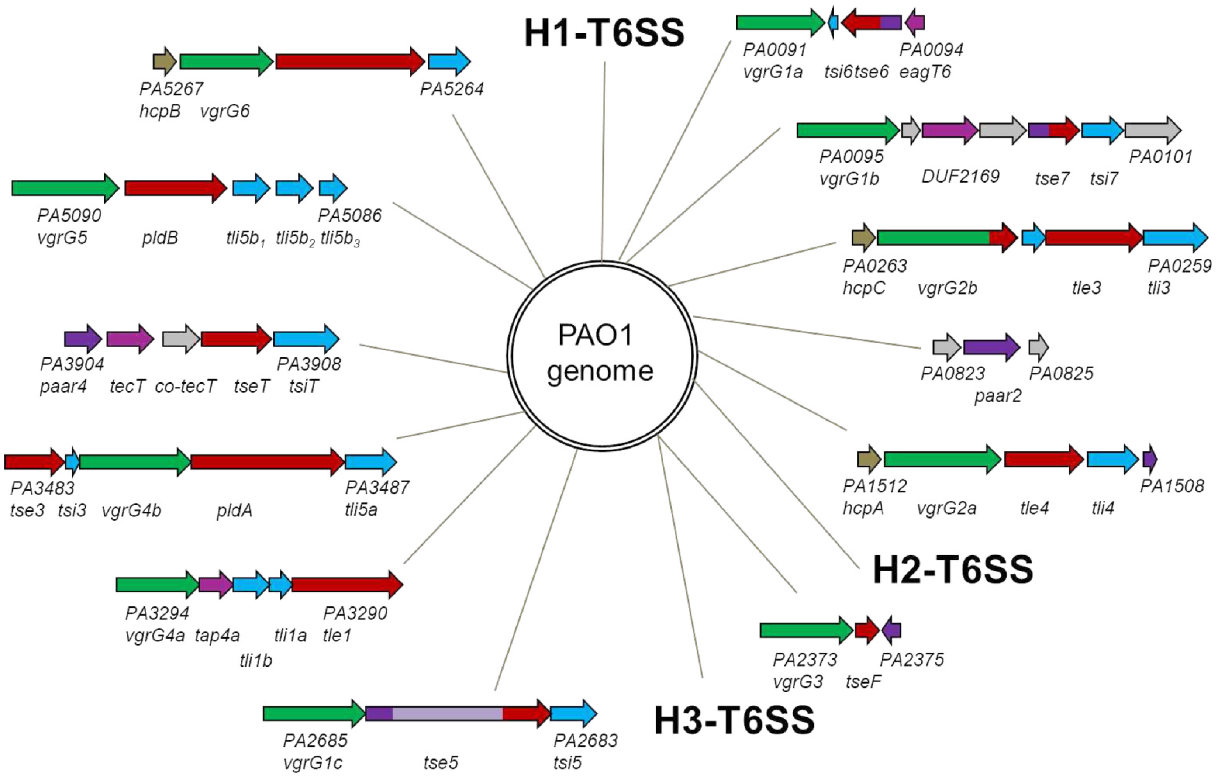


Figure 1-22. *Pseudomonas aeruginosa* PAO1 contains three T6SS clusters and various remote *vgrG* and *paar* islands.

Gene clusters are depicted relative to their location on the genome of PAO1. *vgrG* genes are shown in green; genes encoding for effectors or putative effectors are shown in red; their cognate immunity genes in cyan; genes encoding PAAR domains are shown in purple, Rhs domains in light purple; genes encoding for adaptor proteins are shown in magenta and *hcp* genes are shown in brown while genes of unknown function are shown in grey.

1.3.4. Regulation of the T6SS in *P. aeruginosa*

Due to the versatility and potency of this nanomachine, organisms need to tightly regulate T6SS production and assembly. Many bacteria were shown to upregulate T6SS expression upon encounter of antibiotics [150], host cell factors like bile [151], or nutrient limitations imitating the host cell environment [152]. In contrast, other bacteria like *A. tumefaciens* or *S. marcescens* do not seem to require an additional trigger for T6SS production and assembly [153, 154]. In any case, the identified regulatory networks for T6SS

activation in different organisms are numerous and highly complex. Since in our study we will employ the T6SS of *P. aeruginosa*, at this point we will solely cover the regulatory circuits of its T6SS activation essential for this study.

Post-translational regulation of the H1-T6SS

The regulation and the functionality of the H1-T6SS cluster from *P. aeruginosa* has been studied in great details. Within the H1-T6SS cluster, a set of regulatory genes is located, that are shown in red in Figure 1-21 and that encode for TagQRST, PpkA, PppA, TagF and Fha1, that are all required for post-translational regulation of the H1-T6SS. Activation of the H1-T6SS cluster is conditional on the phosphorylation status of Fha1, which can either reside in a complex with ClpV1 or TagF. Interaction with TagF1 sequesters Fha1 and thus represses T6SS activity [155]. Upon phosphorylation of Fha1, the ClpV1-Fha1 complex is recruited to the membrane and triggers H1-T6SS activity [156]. Phosphorylation of Fha1 is mediated by the serine/threonine protein kinase PpkA, whose activity is counteracted by the phosphatase PppA [156]. Activity of PpkA is further potentiated by the cell-envelope-associated TagQRST regulatory system, although the exact details of this signal transduction system are uncertain [157, 158]. It was shown by Casabona *et.al.* though that this phosphorelay system is stimulated by growth on the surface [157].

Tit-for-Tat

P. aeruginosa is further able to respond to the T6SS activity of adjacent competing cells with an increase in its own T6SS activity. This phenomenon was termed as “T6SS duelling” and is understood as a mechanism occurring in mixed populations within the same ecological niche [113]. With this mechanism *P. aeruginosa* is able to attack and kill *V. cholerae*

when the latter expresses a T6SS, while killing was shown to be a lot less efficient when *V. cholerae* did not produce a T6SS. This tit-for-tat killing was proposed to be a counter attack mechanism that is only employed once *P. aeruginosa* senses danger from a competing bacterium [113].

Since Basler and colleagues showed that this duelling behaviour of *P. aeruginosa* is abolished upon deletion of *pppA*, the tit-for-tat mechanism was linked to the TagQRST regulation circuit as discussed above. Basler and colleagues hypothesised that sensing of an incoming T6SS attack, likely *via* membrane stress, activates the TagQRST regulatory system [113] which could then result in recruitment of the ClpV1-Fha complex to where the incoming attack was sensed [156]. This would lead to a quick counterattack with T6SS firing precisely at the point of the initial attack thus immediately outcompeting the predatory neighbouring cell [113].

The Gac/Rsm-cascade and global T6SS regulation

One pathway to control all three T6SS clusters in *P. aeruginosa* is the Gac/Rsm network (Figure 1-23) [146]. RsmA (Figure 1-23, bright red) is a translational repressor of a myriad of messenger RNAs [159] and when sequestered by two small non-coding RNAs, RsmY and RsmZ, de-repression of T6SS genes occurs [160]. Transcription of RsmY and RsmZ is activated by phosphorylated GacA (dark green), the response regulator of the GacS/GacA two-component system [160]. Homodimerisation of GacS (green) maintains the auto-phosphorylated and activated state of GacS [161], which is inhibited upon hetero-dimerisation with RetS (Figure 1-23, red), a membrane-bound hybrid-sensor responding to an unknown environmental signal [160]. In addition to T6SS components, RetS regulates the switch between the planktonic and sessile lifestyle. RetS positively controls expression of genes required for cytotoxicity and acute infections and negatively controls genes essential

for biofilm formation, T6SS and maintaining chronic infections (1.1.1) [161, 162]. Thus, much research into the H1-T6SS cluster was conducted in *P. aeruginosa* PAK deleted in *retS*, as this mutant showed elevated levels of expression of the H1-T6SS and its associated effectors (Table 7-3) [140, 163].

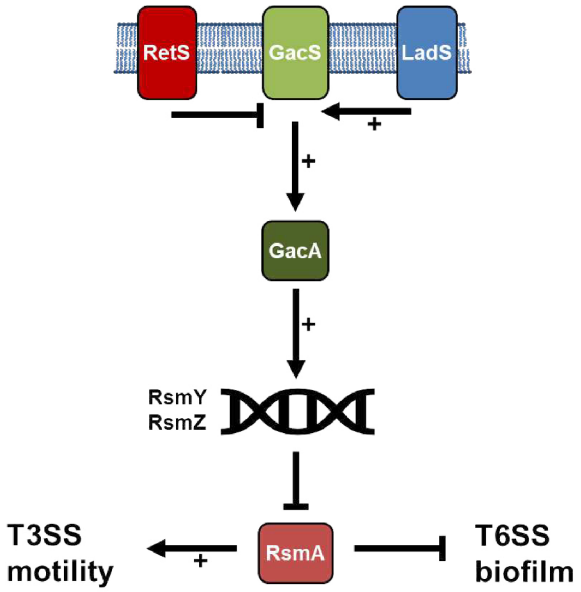


Figure 1-23. Schematic representation of networks regulating *P. aeruginosa* T6SS.

All three T6SS clusters of *P. aeruginosa* are regulated by the Gac/Rsm-cascade. RetS (red) forms heterodimers with GacS (green) thus inhibiting its autophosphorylation. Upon an unknown signal, GacS is free to form homodimers leading to its autophosphorylation, which activates the response regulator GacA (dark green) and thus in turn activates transcription of the small non-coding RNAs RsmY and RsmZ. These sequester RsmA (bright red) and inhibit its activity. Thus, T3SS and motility and genes required for acute infection process are repressed, while genes for T6SS, biofilm and the chronic infection process are activated. This figure was adapted from [162].

Until now, many signals have been described that feed into this highly complicated regulatory cascade. For example, it was shown by our lab, that sub-inhibitory kanamycin concentrations activate the H1-T6SS in a Gac/Rsm-dependent manner, however, the authors were not successful in demonstrating the molecular details of this mechanism [150]. Furthermore, a study by the Mougous group showed that lysed kin cells act as a danger signal,

which they termed PARA for *P. aeruginosa* response to antagonism, that is supposedly sensed by the Gac/Rsm pathway and then leads to elevated T6SS activity. Again, the authors could not pinpoint the molecular details of this signalling mechanism, but suggested that released components of lysed cells might serve as a signal to activate the Gac/Rsm pathway [164]. Additionally, a recent study from our lab showed a drastic impact of temperature on T6SS component production. Using western blot analysis, we followed production of Hcp proteins associated with each of the three T6SS cluster and detected elevated levels of Hcp1, HcpABC and Hcp3 when *P. aeruginosa* was grown at 25 °C in comparison to growth at 37 °C [146]. These regulatory mechanisms allow bacteria appropriate responses to the changing environments or competitors.

1.3.5. Impact of the T6SS during interbacterial warfare

In polymicrobial environments within human or plant hosts, bacteria are constantly at war with competitors for resources. Thus, the T6SS represents an important molecular device in the interbacterial warfare to acquire nutrients, new territory or foreign DNA. Recent research by the Blokesch group proved, that in *V. cholerae* upon T6SS-mediated killing, its competence regulon is highly induced. This strategy allows *V. cholerae* to take up released DNA from killed prey cells thereby enhancing horizontal gene transfer and bacterial evolution [165]. On another note, bacteria use the T6SS to acquire public goods, as in *P. aeruginosa* it was recently shown that the T6SS effector TseF is involved in iron scavenging. The underlying mechanism for this is the integration of TseF into outer membrane vesicles, where TseF binds to iron-chelated PQS molecules and then mediates binding to a specific cell receptor on the bacterial surface. This somehow facilitates import of iron however the exact mechanism is yet unclear [166].

The most important aspect of the T6SS was shown to be involved in inter-bacterial killing and competition [167]. Commensal members of the human gut or plant microbiota encode T6SS machineries, that might provide the host with a protection against intruding pathogens and thus are beneficial for the host's health [136, 168]. For example, *P. putida*, a biocontrol strain, was shown to outcompete the plant pathogen *Xanthomonas campestris* in order to protect the plant from the pathogen's virulence (Figure 1-24) [136]. Specifically, *X. campestris* on its own was shown to establish necrosis on plant leaves (Figure 1-24B), while in a co-infiltration with *P. putida* strains, this phenotype was decreased (Figure 1-24D) and *X. campestris* survival lower (Figure 1-24C). A T6SS-defective *P. putida* strain, however, was not able to protect the plant in the same extent as monitored with an established necrosis (Figure 1-24F) and higher *X. campestris* survival (Figure 1-24E), thus suggesting that *P. putida's* biocontrol ability is provoked by its T6SSs.

Much research has further been conducted demonstrating that the T6SS has a high impact on the human gut microbiome. The commensal *Bacteroides fragilis* possesses three T6SS architectures that are used to mediate potent inter-strain competition to an extent where its role in shaping the human gut microbiota is widely accepted [169, 170]. For example, a commensal *B. fragilis* strain can antagonise various *Bacteroidales* species [171] and was also shown to protect the mouse gut from acquisition of enterotoxigenic *B. fragilis* strains [172]. In contrast, it was also shown that Gram-negative enteric pathogens, like *V. cholerae* and *Citrobacter rodentium*, can outcompete other bacteria *in vitro*. However, it is not well understood yet, whether in the gut environment, the bacterium would have the same outcompeting ability [168]. Remarkably, *Salmonella enterica* serovar Typhimurium was shown to effectively kill the commensal *Klebsiella oxytoca* both *in vitro* and in the mouse gut using its T6SS [173]. Furthermore, in another study it was suggested that the T6SS of the enteric pathogen *Shigella sonnei* confers an advantage over the commensals *E. coli* and *Shigella flexneri* [174]. Hence, the authors reasoned that the global prevalence of *S. sonnei* is due to the presence of a T6SS, while it is absent in *S. flexneri*, conferring a competitive advantage.

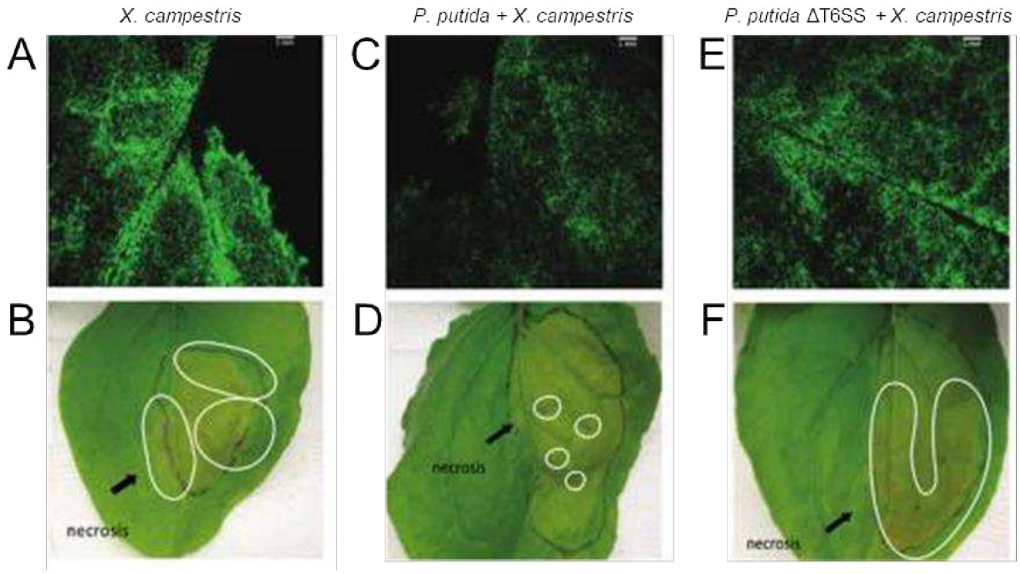


Figure 1-24. *P. putida* uses its T6SS to protect plants from pathogens.

X. campestris, labelled with GFP (A), is able to establish necrosis in plant cells (B). When plants are infiltrated with a mixture of *P. putida* and *X. campestris*, *P. putida* is able restrict the growth of *X. campestris* (C) and thus the necrosis mediated by this pathogen (D). When plants were infiltrated with a mixture of *P. putida* defective for all three T6SS machineries and *X. campestris*, necrosis occurs in larger portions (F) while survival of *X. campestris* is higher as well (E). This figure was adapted from [136] with permission under the terms of the Creative Commons CC.

P. aeruginosa was shown to kill *A. tumefaciens in vitro*, while *A. tumefaciens* was able to trigger a lethal counterattack once the killing was performed *in planta* [153]. Furthermore, *P. aeruginosa* was shown to outcompete *E. coli* [146, 175], *V. cholerae* and *Acinetobacter baylyi* [113]. This predatory behaviour of *P. aeruginosa* is most likely due to the presence of three T6SS machineries, each one of them equipped with a set of anti-bacterial weapons.

1.3.6. Effector activities

Antibacterial toxins delivered by the T6SS can target multiple cellular functions. Importantly, to protect itself from toxicity, bacteria always produce a corresponding immunity

(Figure 1-25A, cyan) that is generally encoded together with the toxin gene [176]. It is generally understood that the immunity protein neutralises the toxin (red) by occluding the catalytic site of the effector [177, 178]. Presence of immunity proteins is also understood to protect an organism from intoxication by neighbouring sibling cells (Figure 1-25B) [179]. Otherwise, a T6SS-active organism, the attacker, delivers a toxin into a neighbouring cell lacking the corresponding immunity, henceforth called prey strain, allowing the toxin to find its cellular target and exert toxicity leading to cell death (Figure 1-25C).

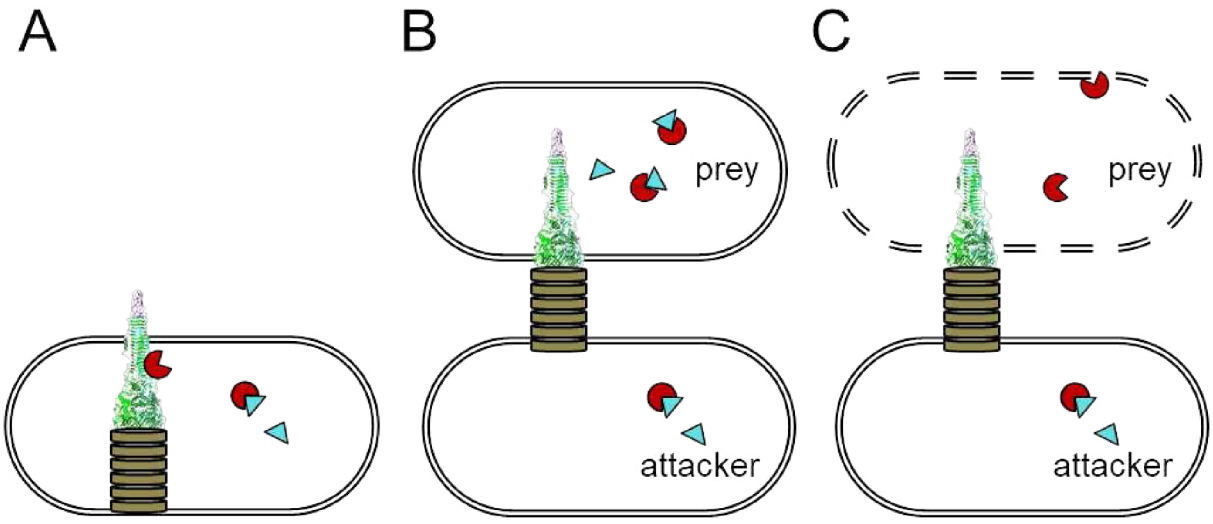


Figure 1-25. T6SS-active bacteria inject anti-bacterial effectors into nearby competitors.

A: A T6SS-active cell expresses the T6SS machinery (green spike) and loads it with an antibacterial toxin (red). By producing the cognate immunity (cyan), the cell is protected from toxicity. B, C: A T6SS-active cell, the attacker, assembles and fires its T6SS and injects an anti-bacterial toxin into the neighbouring cell, the prey cell. B: The prey expresses the cognate immunity to the injected toxin, binds and neutralises it and survives. C: The prey cell lacks the cognate immunity, allowing the injected toxin to find its cellular target and exert its toxic effect. Lysis of the prey occurs.

Even though, exported proteins that have an impact on eukaryotic host cells are generally called effectors, in the T6SS field all substrates of the T6SS are generally referred to as effectors. This might be due to the dual function of some T6SS substrates, however,

henceforth a T6SS effector is considered any T6SS substrate with an enzymatic activity. Anti-eukaryotic effector proteins will not be focus of this thesis, but for the matter of completeness, they will be briefly introduced here, before discussing antibacterial T6SS substrates and effector delivery mechanisms (1.3.7) in greater detail.

Anti-eukaryotic effectors

Anti-eukaryotic T6SS effectors were shown to impede host cell functions and promote immune evasion to successfully establish infections, which is similarly described for the T3SS and the T4SS [180]. Initially, the T6SS was identified due to the virulence of *V. cholerae* against the amoeba *Dictyostelium discoideum*, which involved the anti-eukaryotic effector VgrG-1 [131]. VgrG-1 was shown to cross-link actin cytoskeleton of both amoebae and macrophages after internalisation of the pathogen facilitating its own replication before resulting in host cell death [131, 181]. Furthermore, VgrG5 from *B. pseudomallei* was demonstrated to induce cell membrane fusion and thus intracellular spread of the bacterium, however its enzymatic activity has not been elucidated yet [182]. Another example of an anti-eukaryotic effector is VgrG1 from *Aeromonas hydrophila*, that was shown to induce cell apoptosis by ADP ribosylation of actin [183]. Additionally, TecA from *Burkholderia cenocepacia* was shown to deamidate Rho GTPases to modify the actin cytoskeleton of macrophages and thus reduce phagocytosis to trigger lung infection [184].

Additionally, *P. aeruginosa* contains one effector that was directly shown to modulate eukaryotic host cells. VgrG2b, which will be focussed on in 3.4, contains a C-terminal extension domain that is proposed to contain metallopeptidase activity. A recent study demonstrated that *P. aeruginosa* delivers VgrG2b into eukaryotic HeLa cells, where it interacts with components of the tubulin ring complex thus facilitating bacterial uptake in a microtubule-dependent manner [185]. Remarkably, recent data from our lab also demonstrated anti-

bacterial activity of VgrG2b with a periplasmic immunity protein encoded downstream (Thomas Wood, *personal communication*).

Membrane-targeting effectors

Many bacteria use the T6SS to deliver lipase effectors into both eukaryotic and bacterial target cells. These so called trans-kingdom effectors were shown to degrade both eukaryotic and bacterial membrane lipids thus compromising cell integrity [186, 187]. Tle effectors are likely to mediate membrane degradation from the periplasm, hence their cognate immunity proteins generally contain signal peptides sending them to the periplasm [186].

Currently, five distinct lipase families are described, of which four families exhibit the GXSXG motif, common for many lipases, while the fifth family contains dual HXKXXXXD motifs [186]. These are usually found in phospholipase D (Pld) enzymes, of which *P. aeruginosa* produces two, PldA and PldB [188], which will be focussed on in chapter 5. Additionally, *P. aeruginosa* encodes Tle4/TplE, as well as Tle1 and Tle3, all of them with phospholipase A activities [189, 190]. In *V. cholerae* [186], *Klebsiella pneumoniae* as well *Burkholderia thailandensis* [191], lipases were identified and shown to be delivered via their T6SS machineries.

Pore-forming toxins without any enzymatic activity have also been described to be delivered by a T6SS. For example, VasX from *V. cholerae* was proposed to insert itself into the inner membrane of a target prey cell, thus dissipating its membrane potential and resulting in cell death [192]. Pore-forming activity was also implied for Tse4 in *P. aeruginosa* as it efficiently induces permeability of the inner membrane [193], however a molecular mechanism for its toxicity has not been elucidated yet.

Cell wall targeting effectors

A very important target for antibacterial strategies is peptidoglycan. T6SS effectors targeting peptidoglycan are potent T6SS toxins implemented by many bacteria, as for example Tae2 from *B. thailandensis* [189], and Ssp1 and Ssp2 from *S. marcescens* [194, 195]. *P. aeruginosa* expresses at least two peptidoglycan-hydrolases, namely Tse1 and Tse3 that were both shown to be efficiently delivered into target bacteria resulting in cell death [163, 176]. Interestingly, a recent study by the Coulthurst lab revealed that upon delivery of the amidase effectors Ssp2 and Ssp4, the periplasmic DsbA from the target cell introduces disulphide bonds to activate the effectors. This strategy allows *S. marcescens* and probably other organisms to hijack the target cell's resources for toxicity [118]. Intoxication of amidases and peptidoglycan hydrolases from sibling cells is prevented by the production of immunity proteins that reside in the periplasm [196, 197]. As known for periplasmic proteins, some immunity proteins, for example Rap1a and Rap2a as the cognate immunities to the *S. marcescens* amidases Ssp1 and Ssp2, were shown to contain disulphide bonds [118]. Considering that T6SS substrates most likely do not face the periplasm during the secretion process (1.3.1), their presence is mainly required to protect the cell from injected toxins [198].

DNA-targeting effectors

Due to the omnipresence of DNA in all living species, it represents a potent target for antibacterial strategies. This is exemplified by the fact that many CdiA toxins contain nuclease domains within their C-termini (1.2.8). Also in T6SS-active organisms, several DNA-targeting toxins were identified and characterised. For instance, *P. aeruginosa* was recently confirmed by our lab to deliver its nuclease Tse7 into neighbouring bacteria (P. Pissaridou, *under review*). *A. tumefaciens* was shown to produce and deliver the DNase Tde1 into *E. coli* or *P. aeruginosa* to gain a competitive advantage [153]. Tde1 as well as its delivery mode will be

subject of further discussion in 0. Interestingly, nuclease domains were also demonstrated to be present in the ubiquitous Rhs toxins that are connected to the T6SS. *Dickeya dadantii* produces and delivers the two Rhs effectors, RhsA and RhsB, that contain C-terminal NS_2 and HNH-endonuclease domains, respectively. Expression of both toxic domains in *E. coli* was associated with a loss of DNA staining, while co-expressing the downstream encoded immunity proteins rescued *E. coli* survival [199]. Rhs2 from *S. marcescens* also exhibits DNase activity based on its C-terminal HNH endonuclease domain, with RhsI2 being the cognate immunity protein [200].

Bacterial cell-function inhibiting effectors

A new toxin family, delivered by bacteria using both T6SS and T7SS (1.2.9), was recently proposed by Whitney's group, the NADase effector family, or termed Tne for type VI NADase effector [201]. These enzymes were shown to degrade $NAD(P)^+$ thus depleting prey cells of this essential cofactor resulting in cell stasis. The founding member of this family, Tne2, was shown to be delivered by *P. protegens* to inhibit the growth of bacterial competitors [201]. Another well characterised example is Tse6 from *P. aeruginosa* which was demonstrated to be delivered into target cells where it hydrolyses NAD^+ and $NADP^+$ leading to cell stasis [202]. Additionally, the structure of Tse2 from *P. aeruginosa* in complex with its immunity Tsi2 was solved (Figure 1-26) with Tse2 displaying intriguing resemblance to mono-ADP-ribosyltransferase toxins like the cholera or diphtheria toxin [203] and being toxic in both prokaryotic and eukaryotic cells [163].

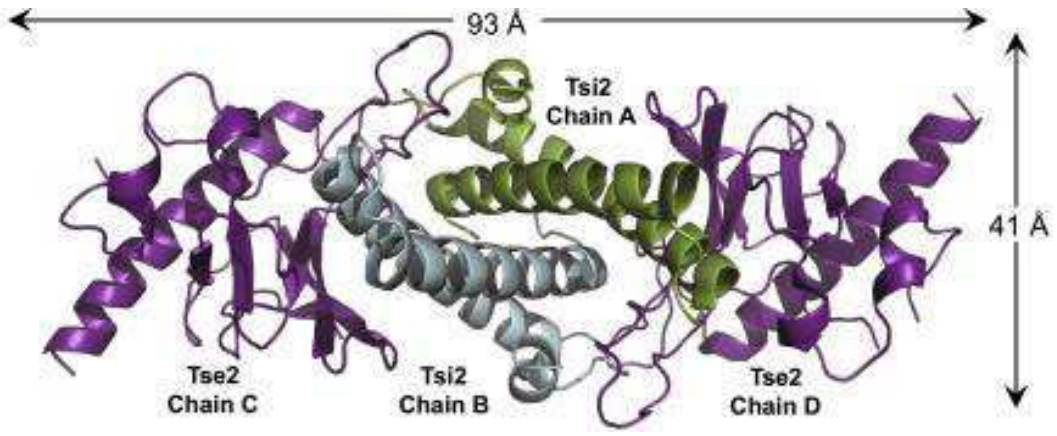


Figure 1-26. Structure of Tse2-Tsi2 complex.

A dimer of Tsi2 (grey, green) interacts with two monomers of Tse2 (purple). This figure was adapted from [203] with permission from Elsevier and the Copyright Clearance Centre.

1.3.7. Effector delivery modes

As indicated in 1.3.3, in many cases, effector genes are encoded together with *vgrG, paar* or *hcp* genes. In some cases, the effector is part of a gene encoding for a structural component and thus production leads to an evolved VgrG-, PAAR-, or Hcp-effector. If separated, a genetic link between an effector gene and a gene encoding for a T6SS component suggests a functional link. Indeed, the delivery of many effectors was shown to be dependent on the nearby encoded T6SS component, be it VgrG, PAAR or Hcp protein. This concept was coined “á la carte” effector delivery and suggests that a cargo effector is connected to a specific, or rather cognate, VgrG tip via non-covalent interactions [175]. In some cases, the presence of so called adaptor or chaperone proteins are required to connect effectors to the T6SS spike. Here, we will introduce the currently known players that facilitate effector delivery via the T6SS in a structured manner. However, one needs to take into account that for some effectors overlap between different delivery concepts occurs and the T6SS tip

is likely decorated with a range of effectors connected in various modes. Some of the delivery concepts will be presented in more detail throughout this thesis where appropriate.

Hcp-dependent effectors

Some T6SS effectors, as for example Tae in *A. tumefaciens* [144] and Ssp2 in *S. marcescens* [195], are encoded downstream of *hcp* genes. This genetic link already suggests a functional link and indeed it was shown that the secretion of these effectors generally correlates with cognate Hcp secretion [148, 149]. Remarkably, for Tse1, Tse2 and Tse3 of *P. aeruginosa* it was shown that they directly interact with Hcp1, even though neither of them are genetically linked to *hcp1* (Figure 1-21). Transmission electron microscopy of Tse2 and Hcp proteins provided evidence that Tse2 interacts with the inner surface of Hcp rings (Figure 1-27), thus supporting the unique model for effector transport within the Hcp1 lumen (Figure 1-28A) [204].

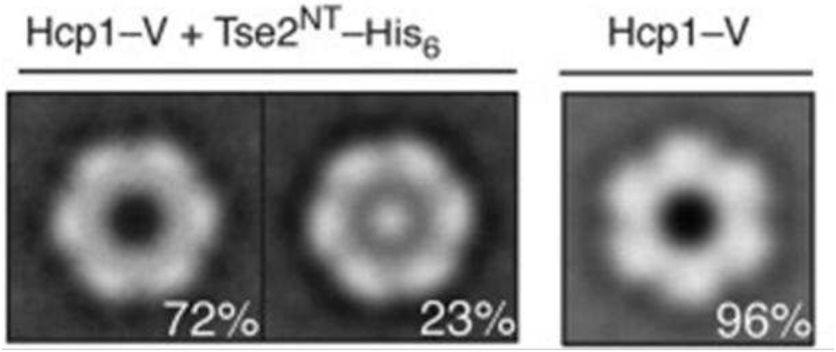


Figure 1-27. Tse2 interacts with the inner lumen of Hcp hexamers.

In 23 % of all particles, Tse2 was found assembled within the Hcp lumen. In 72 % or when Tse2 was not present, the lumen of the Hcp particles was empty. This figure was adapted from [204] with permission from Elsevier and the Copyright Clearance Centre.

The Hcp1 hexamers were shown to function as chaperones for Tse1, Tse2 and Tse3, due to instability of these effector proteins in absence of Hcp1. Furthermore, Silverman and colleagues demonstrated that conserved key residues within the Hcp lumen are responsible for the interactions with Tse2, which will be further introduced in 0. Thus, Hcp1 was described to function as a receptor that plugs an effector into the Hcp tube thus connecting the effector to the T6SS (Figure 1-28A) [204]. By driving the VgrG spike together with the Hcp tube into prey cells, the effector is thought to be released into the target cell [148, 204].

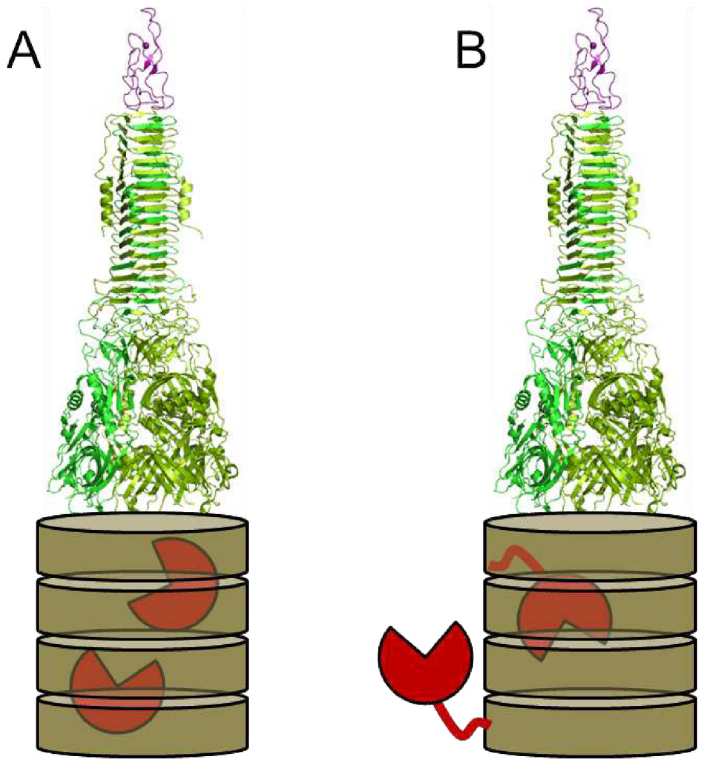


Figure 1-28. Delivery mechanism of Hcp-dependent effectors.

The VgrG-PAAR spike (green, purple) sits on top of an Hcp tube (brown). A: Effectors (red) are bound within the Hcp tube and are transported together. B: Effector domains are extension domains of Hcp proteins and can be accommodated within the Hcp tube or on the outside.

Evolved Hcp effectors

In different *Salmonella* and *E. coli* strains, *hcp* genes were identified with an unusual length. While the N-termini of these gene products harbour the Hcp domains, thus likely forming Hcp hexamers, the C-terminal domains contain toxic functions [205, 206]. Remarkably, *E. coli* STEC004 encodes five of these so called evolved Hcps, designated Hcp-ET1 to Hcp-ET5, with the C-terminal domains being DNase, lipase, as well as pore-forming colicin or pyocin domains. The authors verified that *E. coli* is able to deliver these toxic domains into target prey cells [206], however the molecular details remain prospect of future work. One could envisage that smaller domains like a DNase domain might be accommodated within the Hcp lumen in a similar fashion as the cargo effectors shown in Figure 1-28A. However, this is rather unlikely for the larger lipase domains, suggesting that these C-terminal extensions are accommodated around the Hcp tube and somehow within the TssBC sheath (Figure 1-28B).

Evolved VgrG effectors

All VgrG proteins contain gp5- and gp27-like domains and thus form the torch light structure required for a functional T6SS spike as introduced in 1.3.2. If a VgrG protein solely exhibits these two domains, it is called a canonical VgrG [207]. Some VgrG proteins, however, contain C-terminal extension domains, which usually comprise effector functions. As the founding example of evolved VgrGs, VgrG-1 from *V. cholerae* contains an actin-crosslinking domain within its C-terminus, that was shown to be dispensable for VgrG-1 secretion itself [181]. This supports the model that the torchlight structure of the VgrG is crucial for formation of a functional T6SS spike and that the C-terminal extension domain is delivered upon spike expulsion resulting in an effector-mediated phenotype (Figure 1-29A) [181]. This delivery mode will be focus of chapter 3.

Evolved PAAR effectors

Some polymorphous T6SS effectors carry PAAR- or PAAR-like domains within their N-termini and are thus called evolved PAAR effectors. Delivery of evolved PAARs was shown to be dependent on cognate VgrGs, with which the evolved PAAR is usually encoded [141, 149, 175, 208]. Evolved PAARs are plenty within T6SS active strains and the C-terminal toxin domains are of various nature. For instance, Tse6 from *P. aeruginosa* was shown to contain an N-terminal PAAR domain which assembles on top of the cognate VgrG1a tip as described in 1.3.2 and sketched in Figure 1-29B [202]. Its C-terminal $NAD(P)^+$ hydrolase domain is thought to float around the T6SS tip and was shown to be delivered in an "á la carte" piggy back ride together with the spike complex [141, 175, 202]. Additionally in *A. tumefaciens*, Tde2 contains a PAAR-like domain within its N-terminus which is thought to assemble on top of the cognate VgrG2 and thus connects the C-terminal nuclease to the T6SS tip [149].

Evolved PAAR-Rhs-effectors

Some T6SS effectors were identified that contain a huge core of Rhs/YD repeats that are ubiquitous among bacteria [175, 199, 200, 208, 209]. These polymorphic proteins of the Rhs/YD-protein family (1.2.7) consist of clade-specific N-terminal domains, huge core domains with numbers of YD repeats and enzymatic C-terminal domains of various lengths and activities [210, 211]. The YD-repeat domain has been demonstrated to fold into a massive shell-like form [212]. The C-terminal effector domain is separated from the core domain by 61 highly conserved amino acids that are involved in auto proteolysis releasing the effector domain [210, 213]. One might suggest that only the C-terminal effector domain is translocated into target prey cells, in a similar fashion as CdiA. Upon contact with the target cell, the C-terminal toxin domain of CdiA is cleaved and then translocated into the target cell (1.2.8).

Whether the same would be true for delivery of Rhs effectors via the T6SS requires further experimental work.

In the N-terminal domains of several Rhs effectors from *S. marcescens*, *P. aeruginosa* and *D. dadantii*, PAAR- or PAAR-like domains, were identified. Additionally, the delivery of these Rhs effectors was shown to be dependent on a cognate VgrG protein [148, 175, 199, 200, 208]. Hence, it is thought that the N-terminal PAAR domain of an Rhs effector connects to the VgrG tip in a similar fashion as an evolved PAAR effector [141]. This delivery mode and the fitting of Rhs effectors around the T6SS spike will be further discussed in 4.6.1.

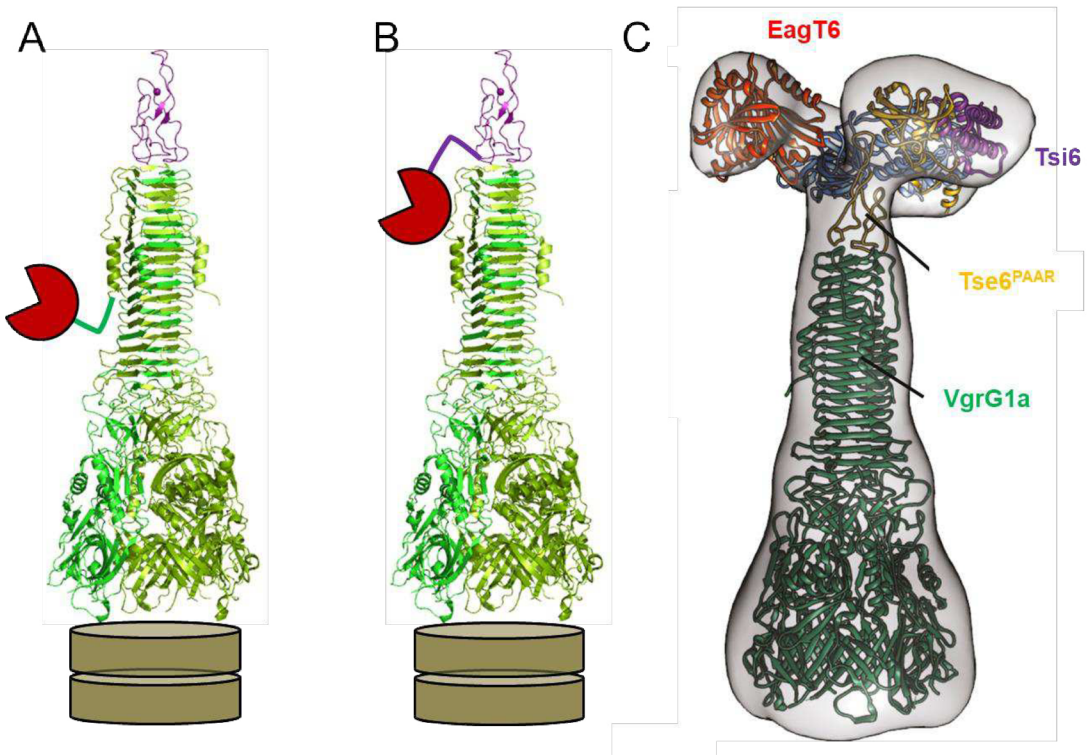


Figure 1-29. Delivery mechanism of evolved spike components.

A: An effector/extension domain (red) is part of the C-terminus of VgrG (green). B: An extension domain is part of a PAAR protein (purple). C: 3D density map of VgrG1a (green) with Tse6 fitted on top (yellow) bound with the immunity Tsi6 (blue) and the accessory protein EagT6 (red). This figure was adapted from [202] with permission from Elsevier and the Copyright Clearance Centre.

DUF1795/Eag-dependent effectors

Proteins of the Eag/DUF1795 family were shown to be essential for the delivery of several evolved PAAR and Rhs effectors. For example, delivery of *P. aeruginosa* Tse6 into target cells requires the accessory protein EagT6, which connects it somehow to the VgrG1a tip as shown with the structure of the VgrG1a-Tse6-EagT6 complex in Figure 1-29C [202]. Also in *S. marcescens,* delivery of the two Rhs effectors Rhs1 and Rhs2 was demonstrated to depend on their interactions with the cognate Eag proteins, EagR1 and EagR2, respectively [200]. Furthermore, the Coulthurst group could demonstrate that EagR1 and EagR2 specifically interact with hydrophobic fragments within the N-terminal domains of Rhs1 and Rhs2, respectively, suggesting this to be a common delivery mechanism of Eag-dependent effectors [148].

Interestingly, the structure of a dimer of EagT6, the chaperone for Tse6 in *P. aeruginosa*, exhibits a horse-shoe form (Figure 1-30, blue). The immunity proteins Tsi3 (Figure 1-30, green) as well as Tli4 from *P. aeruginosa* were shown to fold into a similar structure as EagT6. Since immunity proteins generally function to protect a cell from toxicity of the cognate effector proteins, one might suggest a similar role for Eag proteins. We will attempt to shed light on the importance of Eag proteins and their contribution to delivering their cognate effectors in 4.6.2.

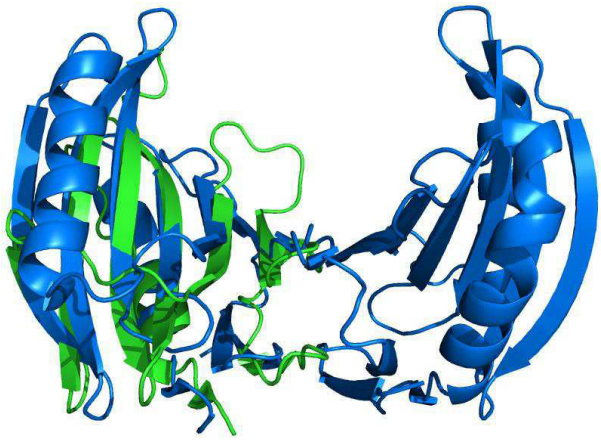


Figure 1-30. Eag proteins exhibit structural similarities to some immunity proteins.

The structure of the dimer of EagT6 is shown in blue (PDB: 1TU1). The structure of Tsi3 in green (PDB: 4N7S) displays structural homology with EagT6.

DUF2169-dependent effectors

DUF2169 proteins are prevalent in a few organisms and are genetically linked with *vgrG* and effector genes encoding for evolved PAAR effectors, like Tse7 in *P. aeruginosa* (Figure 1-22). Nevertheless, DUF2169 proteins have only been shown to be involved in effector delivery in *A. tumefaciens* so far [149]. Bondage and colleagues reported that a DUF2169 protein is needed for delivery of the downstream encoded evolved PAAR effector Tde2, while no molecular detail of the exact function of DUF2169 is known yet.

Effectors containing a MIX motif

One putative T6SS-recognition motif was identified and termed MIX for marker for type six secretion system by Salomon and colleagues. The authors identified the MIX motif in a range of T6SS effectors in various organisms and described them as three hydrophobic conserved sequences, which will be further discussed in 6.5.2. Different clades of MIX

effectors were identified and the genetic prevalence of MIX-containing effectors was shown not to depend on any specific T6SS component [214]. Remarkably, the authors could demonstrate that presence of the MIX motifs somehow allows for heterologous delivery of T6SS effectors. They showed that both *Vibrio alginolyticus* and *Vibrio parahaemolyticus* produce and deliver MIX effectors from the same clade. When they expressed the MIX effector Va02265 from *V. alginolyticus* in *V. parahaemolyticus*, delivery of the effector from the heterologous host into kin cells was monitored. However, the attempt of heterologous delivery from *V. cholerae*, that does not produce a MIX effector from that same clade, was unsuccessful [215]. This suggests that the MIX motif could be understood as a specific effector recognition motif, as not every organism seems to be able to recognise and incorporate MIX effectors into their T6SS machineries.

Effectors interacting with the C-termini of VgrG proteins

T6SS effectors were identified that solely contain an enzymatic activity without a MIX motif, an adaptor domain like a PAAR or an accessory gene encoded nearby. One of such, Tle1 from *E. coli* was shown to be delivered dependent on its upstream encoded VgrG1. Interestingly, VgrG1 contains a C-terminal transthyretin-like domain that was demonstrated to be crucial for Tle1 delivery [216]. Hence, the current working model states that an effector interacts with the C-terminus of its cognate VgrG, which recruits it towards the T6SS tip. Delivering the VgrG spike into target cells thus goes along with delivery of the effector in a piggy back ride (Figure 1-31A). *P. aeruginosa* encodes several effector proteins that are thought to be delivered in a similar fashion which will be focus of chapter 5.

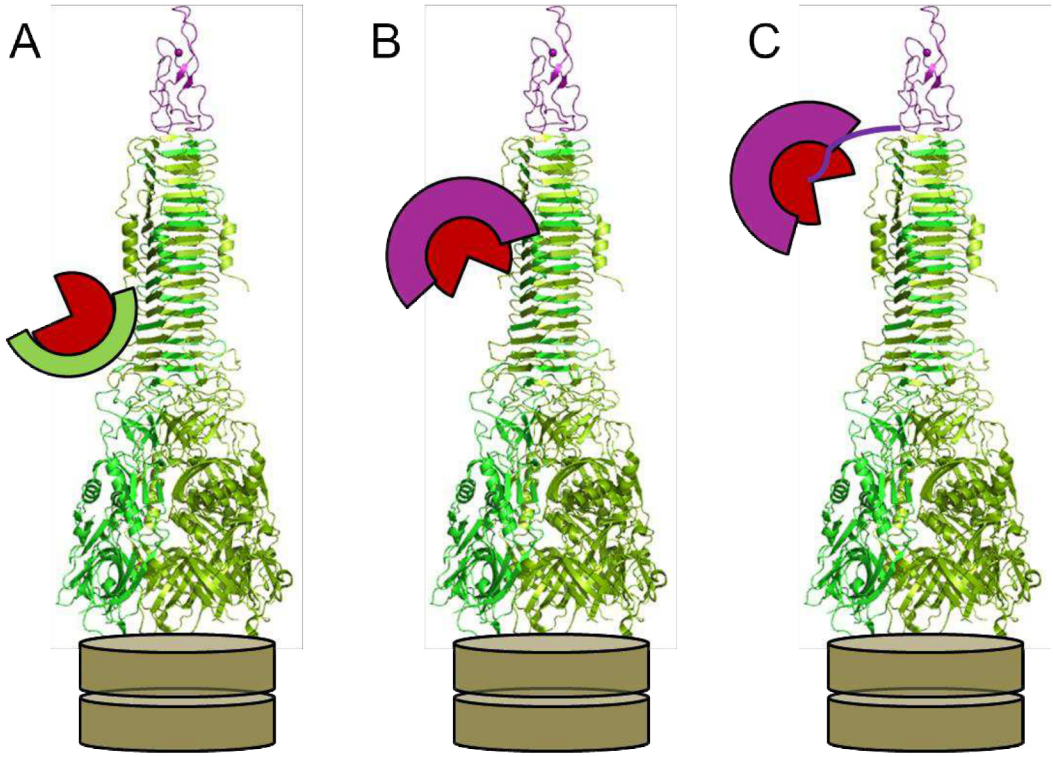


Figure 1-31. Delivery mechanisms of effectors interacting with the C-termini of the spike.

A: An effector (red) directly binds to the C-terminal domain (green block arc) of its cognate VgrG protein (green). B, C: An effector is stabilised by its cognate Tap (magenta), then the Tap-effector complex binds to the C-terminus of its cognate B: VgrG protein or C: PAAR protein (purple).

DUF4123/Tap/Tec-dependent effectors

Another set of T6SS effectors was described whose delivery depends on proteins from the DUF4123 family. These proteins are usually encoded together with the cognate effector and the secretion-mediating VgrG [149, 217]. Additionally, it was shown that presence of the DUF4123 protein is crucial for stability of the cognate effector, which is why some refer to them as chaperones [218]. Another function is to connect the effector to the VgrG spike, which is the reason for their label as adaptors [219]. In this study, we will term a DUF4123 protein a Tap for T6SS adaptor protein.

The delivery mechanisms of three Tap-dependent effectors were investigated in detail so far. TseL from *V. cholerae* was shown to be delivered in a Tap-1 (Tap-1^{Vcho}) dependent mechanism [217, 218], while delivery of Tde1 from *A. tumefaciens* was demonstrated to be dependent on its upstream encoded Tap1 (Tap1^{Atu}) [149] and TseT from *P. aeruginosa* is likely to be delivered via a complex of TecT and Co-TecT [220]. Both Tap-1^{Vcho} and Tap1^{Atu} were shown to interact with their cognate effectors resulting in stabilisation of the effector proteins. Furthermore, the Tap-effector complexes were shown to interact with C-terminal residues of their cognate VgrG proteins and these interactions are required to recruit the effectors to the T6SS tips (Figure 1-31B) [149, 217]. As for TseT, it was revealed that it does not interact with the C-terminus of a VgrG (Figure 1-31C), but of its nearby encoded PAAR protein PAAR4 (Figure 1-22) and that this interaction is required for TseT delivery [220]. The Tap is then thought to be released and retained within the cell as it was shown not be secreted [217]. The molecular details of Tap-dependent effector delivery will be discussed in more detail in chapter 6.

1.4. Overview of this study

This study aims at understanding the molecular mechanisms associated with effector recognition and assembly at the T6SS tip. By attempting to attain heterologous effector delivery, we want to shed light on the question of which components are essential to specifically connect an effector to the T6SS tip and investigate how a T6SS tip could be decorated with different effectors.

Each of the following results chapter will focus on another aspect of T6SS-mediated effector delivery. In chapter 3, we will put emphasis on evolved VgrG proteins and exploit the possibility to deliver any passenger domain as an extension domain of a canonical VgrG. Chapter 4 will then shift the focus towards PAAR proteins and their importance in the formation of functional T6SS spikes. We will also further explore the molecular details of VgrG-PAAR interactions. In chapter 5, we will investigate effectors that require non-covalent interactions with the C-terminal domains of VgrG proteins. Here, we aim to understand the molecular details of effector recognition and specificity. Chapter 6 will then broaden our knowledge on the involvement of Tap proteins in recruiting an effector towards the VgrG tip. In the last discussion chapter, we will then evaluate our results and attempt to integrate them into a broader model that could likely be valid for all secreted bacterial toxins.

2. Experimental procedures

2.1. Bacterial strains and growth conditions

2.1.1. Bacterial strains

The predominant bacterium of interest in this work is *P. aeruginosa*. Dependent on the T6SS-cluster that was being focussed on, work was done in strain PAK for H1-T6SS-dependent experiments, or in PAO1 for H2-T6SS-dependent experiments. A list of all employed bacterial strains in this work is presented in Table 2-1 and all plasmids are listed in Table 2-3.

P. aeruginosa cells were routinely cultured in tryptic soy broth (TSB, Oxoid) with ample aeration in Erlenmeyer flasks at 150 rpm in a reciprocal shaker at 37 °C. For time course experiments, such as secretion assays, *P. aeruginosa* strains were grown at 37 °C for H1-T6SS inducing conditions or at 25 °C for H2-T6SS inducing conditions at 180 rpm in an orbital shaker. Normalisation of culture turbidity was achieved by measuring the optical density of 1 ml culture at 600 nm (OD_{600}) with a CO8000 Biowave cell density meter (Biochrom). Strains were also cultivated on LB agar (Millipore) or Vogel-Bonner minimal medium (100 ml 10x stock: 200 mM magnesium sulfate heptahydrate, 2 g anhydrous citric acid, 10 g potassium phosphate dibasic and 3.5 g ammonium sodium phosphate dibasic tetrahydrate) where appropriate. *E. coli* strains were routinely grown in lysogeny broth (LB) (Miller; Millipore) or on LB agar (Millipore) at 37 °C, while *Agrobacterium tumefaciens* strains were grown at 28 °C. For long term storage, strains were stored in 40% (v/v) glycerol at -80 °C.

Table 2-1. Bacterial strains used in this study.

Strain	Characteristics	Source
P. aeruginosa		
PAKΔ*retS*	Wild type *P. aeruginosa* PAK strain with a deletion in *retS* (PA4856)	Lab collection
PAKΔ*retS*Δ*tse6tsi6*	PAKΔr*etS* with a deletion in *tse6* (*PA0093*) and *tsi6 (PA0092)*	This study
PAKΔ*retS*Δ*tse6tsi6 ::lacZ*	PAKΔr*etS* with a deletion in *tse6-tsi6* (*PA0093- PA0092*), chromosomal insertion of *lacZ* at *att* site	This study
PAKΔ*retS*Δ*vgrG1a*	PAKΔr*etS* with a deletion in *vgrG1a* (*PA0091*)	[140]
PAKΔr*etS*Δ*vgrG1a* Δ*tse6tsi6*	PAKΔr*etS* with deletions in *vgrG1a* (*PA0091*), *tse6-tsi6* (*PA0093- PA0092*),	This study
PAKΔ*retS*Δ*vgrG1a* Δv*grG1b*Δ*vgrG1c*	PAKΔr*etS* with deletions in *vgrG1a* (*PA0091*), *vgrG1b* (*PA0095*) and *vgrG1c* (*PA2685*)	[140]
PAKΔ*retS ::vgrG1a-vgrG1*^{Atu31}	PAKΔr*etS* with an insertion of gene portion corresponding *vgrG1*^{A31} before *vgrG1a* STOP codon	This study
PAKΔ*retS ::vgrG1a*^{605}*-vgrG1*^{Atu31}	PAKΔr*etS* with a substitution of gene portion corresponding to *vgrG1a*^{P39} with gene portion for *vgrG1*^{A31}	This study
PAKΔ*retS ::vgrG1a*^{614}*-vgrG1*^{Atu21}	PAKΔr*etS* with a substitution of gene portion corresponding to *vgrG1a*^{P28} with gene portion for *vgrG1*^{A21}	This study
PAKΔ*retS*Δ*vgrG1b*	PAKΔr*etS* with a deletion in *vgrG1b* (*PA0095*)	[140]
PAKΔ*retS*Δ*vgrG1b* Δ*PA0096-PA0101* Δ*vgrG1c*	PAKΔr*etS* with deletions of the *vgrG1b*-cluster (*PA0095-PA0101*) and *vgrG1c* (*PA2695*)	This study
PAKΔ*retS*Δ*vgrG1b* Δ*PA0096-PA0101* Δ*vgrG1c ::tse6*^{N}*-tse7*^{C}*-tsi7*	PAKΔr*etS* with deletions of the *vgrG1b*-cluster (*PA0095-PA0101*) and *vgrG1c* (*PA2695*), final 642 bp of *tse6-tsi6* (*PA0093- PA0092*), substituted with 393 bp of *tse7* (*PA0100*) and *tsi7* (*PA0099*)	This study
PAKΔ*retS*Δ*vgrG1b* Δ*PA0096-PA0101* Δ*vgrG1c*Δ*tssB1 ::tse6*^{N}*-tse7*^{C}*-tsi7*	PAKΔr*etS* with deletions of the *vgrG1b*-cluster (*PA0095-PA0101*) and *vgrG1c* (*PA2695*) and *tssB1* (*PA0083*) final 642 bp of *tse6-tsi6* (*PA0093- PA0092*), substituted with 393 bp of *tse7* (*PA0100*) and *tsi7* (*PA0099*)	This study
PAKΔ*retS*Δ*vgrG1b* Δ*tsei2*	PAKΔr*etS* with deletions in *vgrG1b* (*PA0095*) and *tse2- tsi2* (*PA2702-PA2703*),	This study
PAKΔ*retS*Δ*vgrG1b* Δ*tsei2::lacZ*	PAKΔr*etS* with deletions in *vgrG1b* (*PA0095*) and *tse2-tsi2 (PA2702-PA2703*), chromosomal insertion of *lacZ* at *att* site	This study
PAKΔ*retS*Δ*vgrG1b* Δ*tsei2*Δ*tssB1*	PAKΔr*etS* with deletions in *vgrG1b* (*PA0095*), *tssB1* (*PA0083*), *tse2-tsi2 (PA2702-PA2703*)	This study
PAKΔ*retS*Δ*vgrG1b* Δ*tsei2 ::vgrG1a-tse2tsi2*	PAKΔr*etS* with deletions in *vgrG1b* (*PA0095*) and *tse2-tsi2 (PA2702-PA2703),* insertion of gene portion for *tse2* and *tsi2* before *vgrG1a* (*PA0091*) STOP codon	This study
PAKΔ*retS*Δ*vgrG1b* Δ*tsei2*Δ*tssB1 ::vgrG1a-tse2tsi2*	PAKΔr*etS* with deletions in *vgrG1b* (*PA0095*), *tssB1* (*PA0083*), *tse2-tsi2 (PA2702-PA2703)*, insertion of gene	This study

Strain	Characteristics	Source
	portion for *tse2* and *tsi2* before *vgrG1a* (*PA0091*) STOP codon	
PAKΔ*retS*Δ*vgrG1b* Δ*tsei2::hcp1*^{S31Q}	PAKΔr*etS* with deletions in *vgrG1b* (*PA0095*) and *tse2-tsi2 (PA2702-PA2703*), point mutation (S31Q) in *hcp1* (*PA0085*)	This study
PAKΔ*retS*Δ*vgrG1b* Δ*tsei2* *::vgrG1a-tse2tsi2* *::hcp1*^{S31Q}	PAKΔr*etS* with deletions in *vgrG1b* (*PA0095*) and *tse2-tsi2 (PA2702-PA2703*), insertion of gene portion for *tse2* and *tsi2* before *vgrG1a* (*PA0091*) STOP codon, point mutation (S31Q) in *hcp1* (*PA0085*)	This study
PAKΔ*retS*Δ*vgrG1b* Δ*tsei2*Δ*tssB1* *::vgrG1a-tse2tsi2* *::hcp1*^{S31Q}	PAKΔr*etS* with deletions in *vgrG1b* (*PA0095*), *tssB1* (*PA0083*), *tse2-tsi2 (PA2702-PA2703*), insertion of gene portion for *tse2* and *tsi2* before *vgrG1a* (*PA0091*) STOP codon, point mutation (S31Q) in *hcp1* (*PA0085*)	This study
PAKΔ*retS*Δ*vgrG1b* Δ*tse6tsi6*	PAKΔr*etS* with deletions in *vgrG1b* (*PA0095*) and *tse6-tsi6* (*PA0093- PA0092*)	This study
PAKΔ*retS*Δ*vgrG1b* Δ*vgrG1c*	PAKΔr*etS* with a deletion in *vgrG1b* (*PA0095*) and *vgrG1c* (*PA2685*)	[140]
PAKΔ*retS*Δ*vgrG1b* Δ*vgrG1c*Δ*tse6tsi6*	PAKΔr*etS* with deletions in *vgrG1a* (*PA0091*), *vgrG1c* (*PA2685*), *tse6-tsi6* (*PA0093- PA0092*)	This study
PAKΔ*retS*Δ*vgrG1b* Δ*vgrG1c*Δ*tse6tsi6* *::lacZ*	PAKΔr*etS* with deletions in *vgrG1a* (*PA0091*), *vgrG1c* (*PA2685*), *tse6-tsi6* (*PA0093- PA0092*), chromosomal insertion of *lacZ* at *att* site	This study
PAKΔ*retS*Δ*vgrG1b* Δ*vgrG1c* *::vgrG1a-vgrG1*^{Atu31}	PAKΔr*etS* with deletions in *vgrG1b* (*PA0095*) and *vgrG1c* (*PA2685*), with an insertion of gene portion corresponding *vgrG1*^{A31} before *vgrG1a* STOP codon	This study
PAKΔ*retS*Δ*vgrG1b* Δ*vgrG1c* *::vgrG1a*^{605}*-vgrG1*^{Atu31}	PAKΔr*etS* with deletions in *vgrG1b* (*PA0095*) and *vgrG1c* (*PA2685*), with a substitution of gene portion corresponding to *vgrG1a*^{P39} with gene portion for *vgrG1*^{A31}	This study
PAKΔ*retS*Δ*vgrG1b* Δ*vgrG1c* *::vgrG1a*^{614}*-vgrG1*^{Atu21}	PAKΔr*etS* with deletions in *vgrG1b* (*PA0095*) and *vgrG1c* (*PA2685*), with a substitution of gene portion corresponding to *vgrG1a*^{P28} with gene portion for *vgrG1*^{A21}	This study
PAKΔ*retS*Δ*vgrG1c*	PAKΔr*etS* with a deletion in *vgrG1c* (*PA2685*)	[140]
PAKΔr*etS*Δ*vgrG1c* Δ*tse6tsi6*	PAKΔr*etS* with deletions in *vgrG1c* (*PA2685*), *tse6-tsi6* (*PA0093- PA0092*)	This study
PAKΔ*retS* *::vgrG1a-bla*$_{TEM-1}$	PAKΔr*etS* with an insertion of *bla*$_{TEM-1}$ before *vgrG1a (PA0091)* STOP codon	This study
PAKΔ*retS* *::vgrG1a-vgrG2b-CT*	PAKΔr*etS* with an insertion of gene 821 bp of *vgrG2b-CT* before *vgrG1a (PA0091)* STOP codon	This study
PAKΔ*retS*Δ*tse6tsi6*	PAKΔr*etS* with a deletion in *tse6-tsi6* (*PA0093- PA0092*)	This study
PAKΔ*retS*Δ*tssB1*	PAKΔr*etS* with deletion in *tssB1* (*PA0083*)	[221]
PAKΔ*retS*Δ*tssB1* *::vgrG1a- bla*$_{TEM-1}$	PAKΔr*etS* with deletion in *tssB1* (*PA0083*) and an insertion of *bla*$_{TEM-1}$ before *vgrG1a (PA0091)* STOP codon	This study
PAKΔ*retS*Δ*tssB1* *::vgrG1a-vgrG2b-CT*	PAKΔr*etS* with deletions in *tssB1* (*PA0083*) and an insertion of gene 821 bp of *vgrG2b-CT* before *vgrG1a (PA0091)* STOP codon	This study

Strain	Characteristics	Source
PAO1	PAO1 wild type strain	Lab collection
PAO1::*pldA-bla*$_{TEM-1}$	PAO1 with an insertion of *bla*$_{TEM-1}$ before *pldA (PA3487)* STOP codon	[146]
PAO1::*pldB-bla*$_{TEM-1}$	PAO1 with an insertion of *bla*$_{TEM-1}$ before *pldB (PA5089)* STOP codon	[146]
PAO1Δ*rsmA*	PAO1 wild type strain with deletion in *rsmA* (*PA0905*)	[146]
PAO1Δ*rsmA ::pldA-bla*$_{TEM-1}$	PAO1 with deletion in *rsmA* (*PA0905*) and an insertion of *bla*$_{TEM-1}$ before *pldA (PA3487)* STOP codon	[146]
PAO1Δ*rsmA ::pldB-bla*$_{TEM-1}$	PAO1 with deletion in *rsmA* (*PA0905*) and an insertion of *bla*$_{TEM-1}$ before *pldB (PA5089)* STOP codon	[146]
PAO1Δ*rsmA* Δ*pldAtli5a*	PAO1 with deletion in *rsmA* (*PA0905*), *pldA-tli5a* (*PA3487-PA3488*)	Thomas Wood
PAO1Δ*rsmA* Δ*pldAtli5a::lacZ*	PAO1 with deletion in *rsmA* (*PA0905*), *pldA-tli5a* (*PA3487-PA3488*), chromosomal insertion of *lacZ* at *att* site	Thomas Wood
PAO1Δ*rsmA* Δ*tlei5b*$_{123}$*::lacZ*	PAO1 with deletion in *rsmA* (*PA0905*), *pldB-tli5b*$_{123}$ (*PA5089-PA5086*), chromosomal insertion of *lacZ* at *att* site	Thomas Wood
PAO1Δ*rsmA*Δ*tssB2*	PAO1 with deletion in *rsmA* (*PA0905*) and *tssB2* (*PA1657*)	This study
PAO1Δ*rsmA*Δ*tssB2 ::vgrG4b-bla*$_{TEM-1}$	PAO1 with deletion in *rsmA* (*PA0905*), *tssB2* (*PA1657*) and an insertion of *bla*$_{TEM-1}$ before *vgrG4b (PA3486)* STOP codon	This study
PAO1Δ*rsmA* Δ*TAA*^{vgrG4b}*-ATG*^{pldA}	PAO1 with deletions in *rsmA* (*PA0905*), STOP codon of *vgrG4b (PA3486)* to START codon of *pldA (PA3487)*	This study
PAO1Δ*rsmA*Δ*tssE2*	PAO1 with deletions in *rsmA* (*PA0905*) and *tssE2* (*PA1657*)	Thomas Wood
PAO1Δ*rsmA*Δ*tssE2* Δ*TAA*^{vgrG4b}*-ATG*^{pldA}	PAO1 with deletions in *rsmA* (*PA0905*), STOP codon of *vgrG4b (PA3486)* to START codon of *pldA (PA3487)*	This study
PAO1Δ*rsmA*Δ*tssK3*	PAO1 with deletions in *rsmA* (*PA0905*) and *tssK3* (*PA2363*)	Thomas Wood
PAO1Δ*rsmA*Δ*tssE2 ::pldA-bla*$_{TEM-1}$	PAO1 with deletions in *rsmA* (*PA0905*), *tssE2* (*PA1657*) and an insertion of *bla*$_{TEM-1}$ before *pldA (PA3487)* STOP codon	[146]
PAO1Δ*rsmA*Δ*tssE2 ::pldB-bla*$_{TEM-1}$	PAO1 with deletions in *rsmA* (*PA0905*), *tssE2* (*PA1657*) and an insertion of *bla*$_{TEM-1}$ before *pldB (PA5089)* STOP codon	[146]
PAO1Δ*rsmA*Δ*tssK3 ::pldA-bla*$_{TEM-1}$	PAO1 with deletions in *rsmA* (*PA0905*), *tssK3* (*PA2363*) and an insertion of *bla*$_{TEM-1}$ before *pldA (PA3487)* STOP codon	This study
PAO1Δ*rsmA*Δ*vgrG4b*	PAO1 with deletions in *rsmA* (*PA0905*) and *vgrG4b* (*PA3486*)	[146]
PAO1Δ*rsmA*Δ*vgrG4b ::pldA-bla*$_{TEM-1}$	PAO1 with deletions in *rsmA* (*PA0905*), *vgrG4b* (*PA3486*) and an insertion of *bla*$_{TEM-1}$ before *pldA (PA3487)* STOP codon	[146]
PAO1Δ*rsmA*Δ*vgrG4b ::pldB-bla*$_{TEM-1}$	PAO1 with deletions in *rsmA* (*PA0905*), *vgrG4b* (*PA3486*) and an insertion of *bla*$_{TEM-1}$ before *pldB (PA5089)* STOP codon	This study

Strain	Characteristics	Source
PAO1Δ*rsmA ::vgrG4b-bla*$_{TEM-1}$	PAO1 with deletion in *rsmA* (*PA0905*) and an insertion of *bla*$_{TEM-1}$ before *vgrG4b (PA3486)* STOP codon	This study
PAO1Δ*rsmA*Δ*vgrG4b ::vgrG1a*^{606}*-vgrG4b*^{187} *::pldA-bla*$_{TEM-1}$	PAO1 with deletions in *rsmA* (*PA0905*), an insertion of *bla*$_{TEM-1}$ before *pldA (PA3487)* STOP codon and a substitution of gene portion corresponding to *vgrG1a*^{39} (*PA0091*) with gene portion for *vgrG4b*^{187} *(PA3486)*	This study
PAO1Δ*rsmA ::vgrG4b*^{618}*-vgrG5*^{169}	PAO1 with a deletion in *rsmA* (*PA0905*) and a substitution of gene portion corresponding to *vgrG4b*^{187} (*PA3486*) with gene portion for *vgrG5*^{169} *(PA5090)*	This study
PAO1Δ*rsmA ::vgrG4b*^{618}*-vgrG5*^{169} *::pldA-bla*$_{TEM-1}$	PAO1 with a deletion in *rsmA* (*PA0905*), an insertion of *bla*$_{TEM-1}$ before *pldA (PA3487)* STOP codon and a substitution of gene portion corresponding to *vgrG4b*^{187} (*PA3486*) with gene portion for *vgrG5*^{169} *(PA5090)*	This study
PAO1Δ*rsmA*Δ*vgrG4b ::vgrG5*^{623}*-vgrG4b*^{187}	PAO1 with deletions in *rsmA* (*PA0905*), *vgrG4b* (*PA3486*), and a substitution of gene portion corresponding to *vgrG4b*^{187} (*PA3486*) with gene portion for *vgrG5*^{169} *(PA5090)*	This study
PAO1Δ*rsmA*Δ*vgrG4b ::vgrG5*^{623}*-vgrG4b*^{187} *::pldA-bla*$_{TEM-1}$	PAO1 with deletions in *rsmA* (*PA0905*) and *vgrG4b* (*PA3486*), an insertion of *bla*$_{TEM-1}$ before *pldA (PA3487)* STOP codon and a substitution of gene portion corresponding to *vgrG4b*^{187} (*PA3486*) with gene portion for *vgrG5*^{169} *(PA5090)*	This study
PAO1Δ*rsmA*Δ*vgrG4b* Δ*tssE2 ::vgrG4b*^{618}*-vgrG5*^{169} *::pldA-bla*$_{TEM-1}$	PAO1 with deletions in *rsmA* (*PA0905*), *vgrG4b (PA3486), tssE2 (PA1657*) and an insertion of *bla*$_{TEM-1}$ before *pldA (PA3487)* STOP codon and a substitution of gene portion corresponding to *vgrG4b*^{187} (*PA3486*) with gene portion for *vgrG5*^{169} *(PA5090)*	This study
PAO1Δ*rsmA*Δ*vgrG4b* Δ*tssK3 ::vgrG4b*^{618}*-vgrG5*^{169} *::pldA-bla*$_{TEM-1}$	PAO1 with deletions in *rsmA* (*PA0905*), *vgrG4b (PA3486), tssK3 (PA2363*) and an insertion of *bla*$_{TEM-1}$ before *pldA (PA3487)* STOP codon and a substitution of gene portion corresponding to *vgrG4b*^{187} (*PA3486*) with gene portion for *vgrG5*^{169} *(PA5090)*	This study
PAO1Δ*rsmA*Δ*vgrG4b* Δ*vgrG5*	PAO1 with deletions in *rsmA* (*PA0905*), *vgrG4b (PA3486)* and *vgrG5 (PA5090)*	This study
PAO1Δ*rsmA*Δ*vgrG5*	PAO1 with deletions in *rsmA* (*PA0905*) and *vgrG5 (PA5090)*	This study
PAO1Δ*rsmA*Δ*vgrG5 ::pldA-bla*$_{TEM-1}$	PAO1 with deletions in *rsmA* (*PA0905*) and *vgrG5 (PA5090)* and an insertion of *bla*$_{TEM-1}$ before *pldA (PA3487)* STOP codon	This study
PAO1Δr*smA*Δ*vgrG5 ::pldB-bla*$_{TEM-1}$	PAO1 with deletions in *rsmA* (*PA0905*) and *vgrG5 (PA5090)* and an insertion of *bla*$_{TEM-1}$ before *pldB (PA5089)* STOP codon	This study
PAO1Δ*rsmA*Δ*vgrG5 ::vgrG4b*^{618}*-vgrG5*^{169}	PAO1 with deletions in *rsmA* (*PA0905*) and *vgrG5 (PA5090)* and a substitution of gene portion corresponding to *vgrG4b*^{187} (*PA3486*) with gene portion for *vgrG5*^{169} *(PA5090)*	This study
PAO1Δ*rsmA*Δ*vgrG5 ::vgrG4b*^{618}*-vgrG5*^{169} *::pldB-bla*$_{TEM-1}$	PAO1 with deletions in *rsmA* (*PA0905*) and *vgrG5 (PA5090),* a substitution of gene portion corresponding to *vgrG4b*^{187} (*PA3486*) with gene portion for *vgrG5*^{169} *(PA5090)* and an insertion of *bla*$_{TEM-1}$ before *pldB (PA5089)* STOP codon	This study

Strain	Characteristics	Source
PA14Δ*rsmA*	PA14 wild type strain with deletion in *rsmA* (*PA0905*)	[147]
PA14Δ*rsmA::rhsP2-V5*	PA14 with deletion in *rsmA* (*PA0905*) and insertion of gene sequence for V5-tag before STOP codon of *rhsP2* (*PA14_43100*)	[147]
PA14Δ*rsmA ::vgrG14-V5*	PA14 with deletion in *rsmA* (*PA0905*) and insertion of gene sequence for V5-tag before STOP codon of *vgrG14* (*PA14_43100*)	[147]
A. tumefaciens		
A. tumefaciens C58	C58 Wild type strain	Gift from Erh-Min Lai
E. coli		
DH5α	F– *endA1 glnV44 thi-1 recA1 relA1 gyrA96 deoR nupG purB20 φ80dlacZΔM15* Δ(*lacZYA-argF)U169, hsdR17*(rK– mK+), λ–	ThermoFisher
*Sm10*λpir	Host strain for Mini-CTX1 replication: *thi thr leu tonA lacY supE recA::RP4-2-Tc::Mu* (Km^R) λpir	[222]
*CC118*λpir	Host strain for pKNG101 replication: Δ(*ara-leu) araD ΔlacX74 galE galK-phoA20 thi-1 rpsE rpoB argE* (Sm^R) *recA1 Rfr λpir*	[223]
DHM1	*cya-854 recA1 gyrA96* (NaIR) *thi1 hsdR17 spoT1 rfbD1 glnV44*(*AS*)	[224]
1047	Helper strain for conjugation: (Km^R), *oriColE1 RK2- Mob+ RK2-Tra+*	[225]

Media were supplemented with antibiotics and other supplements when required at the concentrations listed in Table 2-2 unless otherwise stated. Supplements were dissolved in double-distilled water (ddH_2O), sterile filtered and kept at 4 °C in the short term or -20 °C in the long term, while those dissolved in ethanol or dimethylformamide (DMF) were always stored at -20 °C. Stock solutions of sterile 500 mM isopropyl-β-D-thiogalactopyranoside (IPTG) and 100 mg/ml 5-bromo-4-chloro-3-indolyl-D-galactopyranoside (X-gal) we stored at -20 °C.

Table 2-2. Media supplements used in this work.

Bacterium	Supplement	Solvent	Final concentration
P. aeruginosa	Carbenicillin (Cb)	ddH_20	100 µg/ml
	Gentamicin (Gm)	ddH_20	150 µg/ml
	Streptomycin (Sm)	ddH_20	1000 µg/ml
	Spectinomycin (Sp)	ddH_20	1000 µg/ml
	Tetracycline (Tc)	Ethanol	100 µg/ml
	X-Gal	DMF	100 µg/ml
E. coli	Ampicillin (Am)	ddH_20	50 µg/ml
	Carbenicillin (Cb)	ddH_20	50 µg/ml
	Gentamicin (Gm)	ddH_20	15 µg/ml
	Kanamycin (Km)	ddH_20	50 µg/ml
	Streptomycin (Sm)	ddH_20	50 µg/ml
	Spectinomycin (Sp)	ddH_20	50 µg/ml
	Tetracycline (Tc)	Ethanol	15 µg/ml
	IPTG	ddH_20	100 µg/ml
	X-Gal	DMF	40 µg/ml

2.2. Molecular biology techniques

2.2.1. Genomic DNA extraction

Genomic DNA was extracted from *P. aeruginosa* and *A. tumefaciens* cells using a PureLink Genomic DNA Mini Kit (ThermoFisher) using 500 µl of an overnight culture according to the manufacturer's instructions. DNA was eluted with 100 µl ddH2O and stored at -20 °C.

Table 2-3. Plasmids used in this study.

Plasmid	Characteristics	Source
Vectors for chromosomal mutagenesis		
pRK2013	Self-transmissible helper plasmid for three-partner conjugations, KmR	[225]
pKNG101	Non-replicative suicide vector to alter *P. aeruginosa* chromosome. *ori6K*, *mobRK2*, *sacB*, Sm^R	Lab collection
pKNG101::*hcp1*^{S31Q}	pKNG101 suicide plasmid to point mutate serine31 to aspartate of *hcp1,* Sm^R	This study
pKNG101::*pldA-bla*$_{TEM-1}$	pKNG101 suicide plasmid to integrate *bla*$_{TEM-1}$ to *pldA* gene, Sm^R	[146]
pKNG101::*pldB-bla*$_{TEM-1}$	pKNG101 suicide plasmid to integrate *bla*$_{TEM-1}$ to *pldB* gene, Sm^R	[146]
pKNG101 *::vgrG1a-bla*$_{TEM-1}$	pKNG101 suicide plasmid to integrate *bla*$_{TEM-1}$ to *vgrG1a* gene, Sm^R	This study
pKNG101 ::*vgrG1a-tse2tsi2*	pKNG101 suicide plasmid to integrate *tse2-tsi2* to *vgrG1a* gene, Sm^R	This study
pKNG101 ::*vgrG1a*^{606}*-vgrG4b*^{187}	pKNG101 suicide plasmid to substitute final 120 bp of *vgrG1a* with 561 bp from *vgrG4b,* Sm^R	This study
pKNG101 *::vgrG1a-vgrG2b-CT*	pKNG101 suicide plasmid to integrate *vgrG2b-CT* to *vgrG1a* gene, Sm^R	This study
pKNG101 ::*vgrG1a-vgrG1*^{Atu31}	pKNG101 suicide plasmid to integrate 93 bp of *vgrG1*^{Atu} before STOP codon of *vgrG1a,* Sm^R	This study
pKNG101 ::*vgrG1a*^{605}*-vgrG1*^{Atu31}	pKNG101 suicide plasmid to substitute final 114 bp of *vgrG1a* with 93 bp from *vgrG1*^{Atu,} Sm^R	This study
pKNG101 ::*vgrG1a*^{614}*-vgrG1*^{Atu31}	pKNG101 suicide plasmid to substitute final 95 bp of *vgrG1a* with 66 bp from *vgrG1*^{Atu,} Sm^R	This study
pKNG101 ::*vgrG4b-bla*$_{TEM-1}$	pKNG101 suicide plasmid to integrate *bla*$_{TEM-1}$ to *vgrG4b* gene, Sm^R	This study
pKNG101 ::*vgrG5*^{623}*-vgrG4b*^{187}	pKNG101 suicide plasmid to substitute final 493 bp of *vgrG5* with 564 bp from *vgrG4b,* Sm^R	This study
pKNG101 ::*vgrG4b*^{621}*-vgrG5*^{169}	pKNG101 suicide plasmid to substitute final 564 bp of vgrG4b with 493 bp from *vgrG5*, Sm^R	This study
pKNG101 ::*tse6*^{N}*-tse7*^{C}*-tsi7*	pKNG101 suicide plasmid to substitute 641 bp of *tse6* and *tsi6* with 393 bp of *tse7* and *tsi7,* Sm^R	This study
pKNG101 Δ*PA0096-PA0101*	pKNG101 suicide plasmid to delete genes downstream of *vgrG1b,* Sm^R	Panayiota Pissaridou
pKNG101Δ*rsmA*	pKNG101 suicide plasmid to delete *rsmA*, a master regulator, Sm^R	[146]
pKNG101Δ*tse2tsi2*	pKNG101 suicide plasmid to *tse2-tsi2*, an effector-immunity module, Sm^R	[175]

Plasmid	Characteristics	Source
pKNG101Δ*tse6tsi6*	pKNG101 suicide plasmid to *tse6-tsi6*, an effector-immunity module, Sm^R	This study
pKNG101Δ*tssB1*	pKNG101 suicide plasmid to delete *tssB1*, an essential sheath component of the H1-T6SS, Sm^R	[221]
pKNG101Δ*tssB2*	pKNG101 suicide plasmid to delete *tssB2*, an essential sheath component of the H2-T6SS, Sm^R	[146]
pKNG101Δ*tssE2*	pKNG101 suicide plasmid to delete *tssE2*, an essential sheath component of the H2-T6SS, Sm^R	[146]
pKNG101Δ*tssK3*	pKNG101 suicide plasmid to delete *tssK3*, an essential sheath component of the H3-T6SS, Sm^R	[146]
pKNG101Δ*vgrG1b*	pKNG101 suicide plasmid to delete *vgrG1b*, encoding one of the H1-T6SS-associated VgrGs, Sm^R	[140]
pKNG101Δ*vgrG4b*	pKNG101 suicide plasmid to delete *vgrG4b*, encoding one of the H2-T6SS-associated VgrGs, Sm^R	[146]
pKNG101 ΔTAA^{vgrG4b}-ATG^{pldA}	pKNG101 suicide plasmid to delete the STOP codon of *vgrG4b*, the intergenic region and the START codon of *pldA,* Sm^R	This study
pKNG101Δ*vgrG5*	pKNG101 suicide plasmid to delete *vgrG5*, encoding one of the H2-T6SS-associated VgrGs, Sm^R	This study
Cloning vectors		
pCR®-Blunt II-TOPO®	Subcloning vector for blunt-ended inserts, Km^R	ThermoFisher
Bacterial-two-hybrid vectors		
pKT25	BTH vector for C-terminal fusions with the T25 fragment of *Bordetella pertussis* adenylyl cyclase (CyaA), Km^R	[224]
pUT18C	BTH vector for C-terminal fusions with the T18 fragment of *B. pertussis* CyaA, Ap^R	[224]
pKT25-*zip*	BTH vector producing a C-terminal leucine zipper fusion with the T25 fragment of *B. pertussis* CyaA, Km^R	[224]
pUT18C-*zip*	BTH vector producing a C-terminal leucine zipper fusion with the T18 fragment of *B. pertussis* CyaA, Ap^R	[224]
pKT25 *vgrG1a*	BTH vector producing a C-terminal fusion of VgrG1a to T25-fragment of *B. pertussis* CyaA, Km^R	Lab collection
pUT18C *vgrG1a*	BTH vector producing a C-terminal fusion of VgrG1a to T18-fragment of *B. pertussis* CyaA, Am^R	Lab collection
pKT25 *vgrG1b*	BTH vector producing a C-terminal fusion of VgrG1b to T25-fragment of *B. pertussis* CyaA, Km^R	This study
pUT18C *vgrG1b*	BTH vector producing a C-terminal fusion of VgrG1b to T18-fragment of *B. pertussis* CyaA, Am^R	This study
pKT25 *vgrG1c*	BTH vector producing a C-terminal fusion of VgrG1c to T25-fragment of *B. pertussis* CyaA, Km^R	Lab collection
pUT18C *vgrG1c*	BTH vector producing a C-terminal fusion of VgrG1c to T18-fragment of *B. pertussis* CyaA, Am^R	Lab collection

Plasmid	Characteristics	Source
pKT25 *vgrG1a-vgrG1^{Atu31}*	BTH vector producing a C-terminal fusion of VgrG1a-vgrG1^{A31} to T25-fragment of *B. pertussis* CyaA, Km^{R}	This study
pUT18C *vgrG1a-vgrG1^{Atu31}*	BTH vector producing a C-terminal fusion of VgrG1a-vgrG1^{A31} to T18-fragment of *B. pertussis* CyaA, Am^{R}	This study
pKT25 *vgrG1a^{605}-vgrG1^{Atu31}*	BTH vector producing a C-terminal fusion of VgrG1a^{605}-vgrG1^{A31} to T25-fragment of *B. pertussis* CyaA, Km^{R}	This study
pUT18C *vgrG1a^{605}-vgrG1^{Atu31}*	BTH vector producing a C-terminal fusion of VgrG1a^{605}-vgrG1^{A31} to T18-fragment of *B. pertussis* CyaA, Am^{R}	This study
pKT25 *vgrG1a^{614}-vgrG1^{Atu31}*	BTH vector producing a C-terminal fusion of VgrG1a^{614}-vgrG1^{A31} to T25-fragment of *B. pertussis* CyaA, Km^{R}	This study
pUT18C *vgrG1a^{614}-vgrG1^{Atu31}*	BTH vector producing a C-terminal fusion of VgrG1a^{614}-vgrG1^{A31} to T18-fragment of *B. pertussis* CyaA, Am^{R}	This study
pKT25 *vgrG1^{Atu}*	BTH vector producing a C-terminal fusion of VgrG1^{A} to T25-fragment of *B. pertussis* CyaA, Km^{R}	This study
pUT18C *vgrG1^{Atu}*	BTH vector producing a C-terminal fusion of VgrG1a^{A} to T18-fragment of *B. pertussis* CyaA, Am^{R}	This study
pKT25 *tap1-tde1(HADA)*	BTH vector producing Tap1 and a C-terminal fusion of Tde1 to T25-fragment of *B. pertussis* CyaA, Km^{R}	This study
pUT18C *tap1-tde1(HADA)*	BTH vector producing Tap1 and a C-terminal fusion of Tde1 to T18-fragment of *B. pertussis* CyaA, Am^{R}	This study
pKT25 *tde1(HADA)*	BTH vector producing and a C-terminal fusion of Tde1 to T25-fragment of *B. pertussis* CyaA, Km^{R}	This study
pUT18C *tde1(HADA*)	BTH vector producing and a C-terminal fusion of Tde1 to T18-fragment of *B. pertussis* CyaA, Am^{R}	This study
Expression vectors		
pTrc200	Broad host range pVS1 derivative plasmid, *lacIq*, *pTrc* promoter, Sm^{R}/Sp^{R}	[226]; Gift from Erh-Min Lai
p *vgrG4b*	pTrc200 producing full length VgrG4b, Sm^{R}/Sp^{R}	This study
p *tap1-tde1-tdi1-paar*	pTrc200 producing Tap1-Tde1-Tdi1-PAAR from *A. tumefaciens,* Sm^{R}/Sp^{R}	[153]
p *tap1-tde1(HADA)-tdi1-paar*	pTrc200 producing Tap1-Tde1 (HADA)-Tdi1-PAAR from *A. tumefaciens,* Sm^{R}/Sp^{R}	[153]
pRL662	Broad host range pBBR1-derivative vector with a constitutive *PLAC* promoter, Gm^{R}	[153]
p *vgrG1^{Atu}*	pRL662 producing full-length VgrG1^{Atu,} Gm^{R}	[153]
pBBR1-mcs4	Broad host range vector, with constitutive *PLAC* promoter, Ap^{R}/Cb^{R}	[227]
p *vgrG5^{628}*-HA	pBBR1-MCS-4 encoding vgrG5628 with a C-terminal quadruple HA-tag, Ap^{R}, Cb^{R}	This study
miniCTX*::lacZ*	Mini-CTX1 harbouring the *lacZ* with a constitutive promoter, Tc^{R}	[228]

2.2.2. Cloning PCRs

Using 1 µl genomic DNA as a template, nucleotide sequences of interest were amplified by polymerase chain reaction (PCR) using 1 µl KOD Hot-Start DNA polymerase (Millipore) in a 50 µl reaction volume in thin-walled PCR tubes. Primers were designed using Primer3 [229] with an annealing temperature of 60 °C for amplifying *P. aeruginosa* or *A. tumefaciens* templates and 2 µl of each primer, synthesised by Sigma Aldrich, were added to the mixture. The reaction volume was completed with nuclease-free ddH_2O (AppliChem), 1 M betaine (Sigma Aldrich), 100 µM each dATP/dCTP/dTTP/dGTP (dNTP mix; Eurogentec), 1x KOD Hot-Start buffer (Millipore) and 1.5 mM magnesium sulfate. The PCR cycling conditions used were determined by the KOD Hot-Start instructions.

Splicing by overlap extension (SOEing) PCRs were undertaken to produce plasmids involved in chromosomal alteration of *P. aeruginosa*. As sketched in Figure 2-1, approximately 500 bp upstream and downstream of the locus of interest was amplified, using primers exF and upR and dnF and exR (Figure 2-1A, green). Primers upF and dnR (red) were designed to contain complementary sequences to the opposing side of the splice junction. Thus, two subsequent overlap extension PCR steps were undertaken, employing an equimolar ratio of the upstream and downstream fragments as the DNA template. This produces the altered locus to be introduced onto the chromosomal by allelic exchange (Figure 2-1B), described in section 2.2.5**.** Strains were screened with the relevant external primer pairs (not sketched). All primers used in this study were ordered from Sigma Aldrich and are listed in Table 2-4. PCR amplification products were confirmed by electrophoresis on 1 % (w/v) agarose gel (or 2 % if fragment was < 300 bp) alongside a Quick-Load Purple 2-log DNA ladder (NEB), stained with SafeView (NBS Biologicals) and visualised under ultraviolet light (Quantum; Vilber Lourmat).

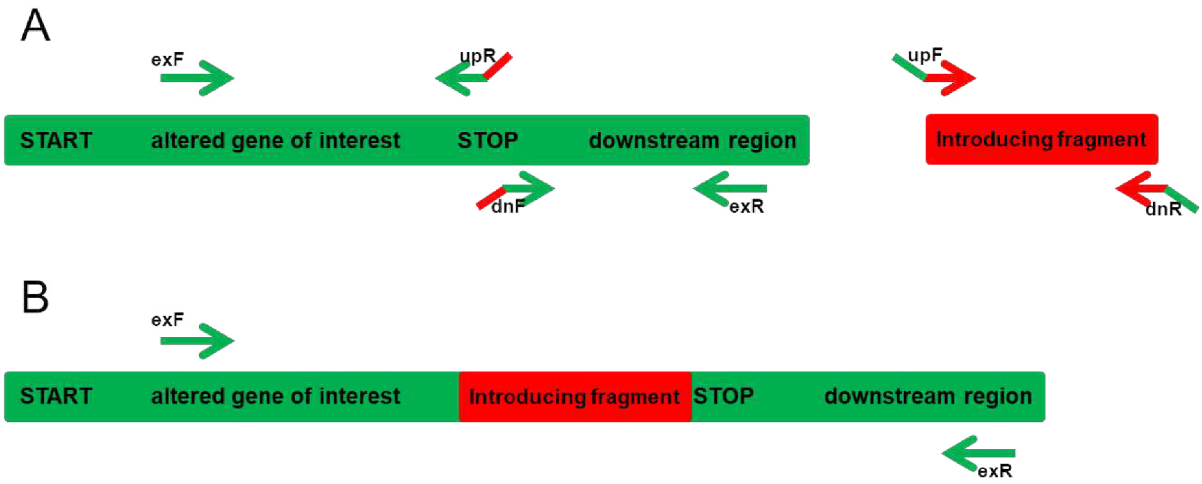


Figure 2-1. Strategy to introduce gene fragments using overlap PCRs.

A: 500 bp upstream and downstream of the introducing point, primers were designed (green, exF and exR, respectively). Two primers (upR and dnF, green-red) were designed to result in an upstream and downstream fragment containing the altered gene portion and an overlap region with the introducing fragment (red 3' end). Primers to amplify the introducing fragment (upF and dnR, red-green) were designed with an overlap for the altered gene of interest (green 3'). B: Two sets of overlapping PCRs were performed to finally result in a tri-partite gene product using primer exF and exR.

2.2.3. Colony PCRs

To screen plasmid constructions and strain generations, colony PCRs were employed. For screening of *E. coli* constructs, a single bacterial colony of interest was added to the PCR reaction mixture after replica plating. To screen *P. aeruginosa* mutants, colonies were resuspended in 20 µl sterile ddH_2O and two 10-minute freeze-thaw cycles at -80 °C to 95 °C were performed to lyse cells. The bacterial debris was pelleted by centrifugation at 13 000 *g* for 3 min and the supernatant, containing the DNA, was used in the reaction template. Colony PCR reactions with standard cycling conditions were done in 20 µl volumes with *Taq* DNA polymerase (NEB) and its standard *Taq* buffer, using 1 µl dimethyl sulfoxide instead of betaine to avoid nucleic acid secondary structure.

2.2.4. Restriction digestion and ligation

After amplification of the desired nucleotide sequences, they were cloned into plasmids. The sub-cloning vector pCR®-Blunt II-TOPO (ThermoFisher) was generally used to introduce restriction sites either site of the construct following the manufacturer's protocol. In some cases, sequences were restricted directly and ligated into the vector of interest. For digestions, 2 µg of purified DNA was incubated with 1 µl of each the required restriction enzyme (Roche) and 2 µl 10x associated buffer (Roche) plus other necessary supplements as stated by the manufacturer's instructions. Reaction mixes were incubated for 2 h at 37 °C, unless a different temperature was required. Digested DNA was purified by gel extraction using spin column purification (QIAgen) and the digested DNA fragments were ligated at a 3:1 insert/vector ratio in a 20 µl volume with 1 µl T4 DNA ligase (NEB) and 2 µl 10x T4 DNA ligase buffer (NEB) overnight at 16 °C.

Chemically competent *E. coli* cells, produced using a standard calcium chloride method, were transformed with ligation mixtures. Briefly, 50 µl competent cells were incubated on ice with the ligation mixture or plasmid for 30 min before a brief heat shock at 42 °C for 2 min. Cells were immediately removed to ice for 1 min before adding 500 µl TSB. Then, cells were incubated for phenotypic expression and outgrowth at 37 °C for 1 h before plating to LB agar containing the appropriate supplements to select for transformants during overnight incubation at 37 °C. Appearing colonies were screened by colony PCR as described above, positive colonies grown and their plasmids purified, using a MiniPrep kit (QIAgen), and confirmed by sequencing at GATC Biotech.

2.2.5. Mutagenesis and allelic exchange

Site-directed mutagenesis was conducted using SOEing PCR as in Figure 2-1. Alterations to the *P. aeruginosa* chromosome were conducted using the pKNG101 suicide vector as previously described [230]. Briefly, the mutated locus of interest was produced by SOEing PCR as described in 2.2.2 and ligated into the non-replicative pKNG101 plasmid and propagated in the CC118*λpir* strain of *E. coli*. The plasmid was mobilised into the *P. aeruginosa* recipient by three-partner conjugation, using 1047 pRK2013 as the helper strain. *P. aeruginosa* conjugants were selected on Vogel-Bonner medium containing streptomycin due to the ability of the recipient to metabolise citrate as its sole carbon source.

Conjugants were transferred to LB agar containing streptomycin to screen the resulting merodiploids by colony PCR. Two upstream and two downstream co-integrands were inoculated into flasks of 10 ml LB and grown at 30 °C for 2 h and 100 µl culture was plated onto an LB agar plate containing 20% (w/v) sucrose. The integrated pKNG101 vector backbone contains the *sacB* gene, conferring sucrose sensitivity. Hence, this counterselection step results in growth of those strains that successfully excised the vector. The mutants were incubated on the sucrose-containing media at room temperature for 72 h or until single colonies appeared. Colonies were replica-plated onto LB agar containing streptomycin, *Pseudomonas* isolation agar, and LB agar alone. Strains that have excised the plasmid would not grow on the streptomycin-supplemented media, but do on the other two. Strains displaying streptomycin-sensitivity were screened by colony PCR to assess mutant generation or reversion to the wild type genotype. Desired mutant colonies were streaked onto LB agar with and without streptomycin as well as *Pseudomonas* isolation agar and screened once more by colony PCR using an external primer pair to confirm construction of the mutant strain before stocking (Figure 2-1B).

Table 2-4. Primers used in this study.

Construct	Primer name	Code	Sequence
Cloning primers			
p *vgrG4b*	*vgrG4b* up	OAL3431	GCATACTCTAGAGTTGATCTGGTTGAGTTCCTTTTC
	vgrG4b down	OAL3432	GCATACGAGCTCTTTTCGAGAAACAGGGGACAG
p *vgrG5*^{628}-HA	*vgrG5*^{628} up	OAL4370	atgGTCGACGAATACGCCAGGAACGCAC
	vgrG5^{628} down	OAL4371	tagGCTAGCGCCGCCGCTGTTGATCATCA
Vector-screening primers			
pBBR1-mcs4	pBBR1-mcs4-F	OAL684	TGTAAAACGACGGCCAGT
	pBBR1-mcs4-R	OAL685	CAGGAAACAGCTATGACC
pKNG101	pKNG101_F	OAL682	CCCTGGATTTCACTGATGAG
	pKNG101_R	OAL683	CATATCACAACGTGCGTGGA
pTrc200	pTrc200_F	OAL2848	tttgcgccgacatcataacg
	pTrc200_R	OAL2849	gccaggcaaattctgttttatca
pUT18C	pUT18C_F	OAL190	GAAGTTCTCGCCGGATGTACTGGAAACGGT
	pUT18C_R	OAL191	TTGGCGGGTGTCGGGGCTGGCTTAACTATG
pKT25	pKT25_F	OAL192	TGGCGAAAGGGGGATGTGCTGCAAGGCGAT
	pKT25_R	OAL193	GTGACCAGCGGCGATTCGGTGACCGATTAC
Mutagenesis primers			
pKNG101 ::*hcp1*^{S31Q}	hcp1 S31Q F	OAL3072	GCTGGCATGGCAATGGGGCATGTCCC
	hcp1 S31Q R	OAL3073	GGGACATGCCCCATTGCCATGCCAGCACG
	hcp1 exF	OAL3076	CAACATCAACCGCTCCTTCAAG
	hcp1 exR	OAL3077	GCGGTGGAGTAGGTCTGTAC
pKNG101 ::*pldA-bla*$_{TEM-1}$	*pldA-bla*$_{TEM-1}$_exF	OAL2618	ACCGAACAGATCTACGTGCA
	pldA-bla$_{TEM-1}$_exR	OAL2900	CAGGATAAAGCCGATGGTGC
	pldA-bla$_{TEM-1}$_upF	OAL2613	AAGCATCGCACAGCGGCCAGCCT
	pldA-bla$_{TEM-1}$_upR	OAL2614	AGGCTGGCCGCTGTGCGATG
	pldA-bla$_{TEM-1}$_dnF	OAL2761	ATCGCACATGAAAAGGGTTTTGAT
	pldA-bla$_{TEM-1}$_dnR	OAL2899	TACCTTCGCAGTTTGGCATG

pKNG101 ::*pldB-bla*$_{TEM-1}$	*pldB-bla*$_{TEM-1}$_exF	OAL3210	ATGACTTGCGGGAAAAGCGG
	pldB-bla$_{TEM-1}$_exR	OAL3211	ACGGCGGCAGATGGTCTTTT
	pldB-bla$_{TEM-1}$_upF	OAL3206	CAAGATCGAGGCGCTCGAAG
	pldB-bla$_{TEM-1}$_upR	OAL3212	GTCAAAATCTTACGGTGGACGCGGCCAGCCTGGAAG
	pldB-bla$_{TEM-1}$_dnF	OAL3213	GCATCGCTCAGTCCACCGTTACCAATGCTTAATCAG
	pldB-bla$_{TEM-1}$_dnR	OAL3209	ACAGAGCACGGCCCAAAGTC
pKNG101 *::vgrG1a*-shuttles	*vgrG1a*_F	OAL3735	CGAGGAGATCTGGACCGAC
	*vgrG1a*_R	OAL3736	AAGGACATCGATCCTGCCG
pKNG101 *::vgrG1a-bla*$_{TEM-1}$	*vgrG1a-bla*$_{TEM-1}$_upF	OAL1347	GCTAGCcacccagaaacgctggtg
	vgrG1a-bla$_{TEM-1}$_dnR	OAL1348	GCTAGCttaccaatgcttaatcagtgag
pKNG101 ::*vgrG1a-tse2tsi2*	*vgrG1a-tse2tsi2*_upF	OAL1351	GCTAGCATGTCCTACGACTACGAGAA
	*vgrG1a-tse2tsi2*_dnR	OAL1352	GCTAGCCCGAAGACCATCTGTCGTTT
pKNG101 ::*vgrG1a*^{606}-*vgrG4b*^{187}	*::vgrG1a*^{606}-*vgrG4b*^{187}_upF	OAL4194	GGCCTGGCACGGATCAATG
	::vgrG1a^{606}-*vgrG4b*^{187}_upR	OAL4195	GTGCCAGGCCGCCGGTGTC
	::vgrG1a^{606}-*vgrG4b*^{187}_dnF	OAL4196	CAAGGACTGAGGCGGCGG
	::vgrG1a^{606}-*vgrG4b*^{187}_dnR	OAL4197	CCTCAGTCCTTGGCCAGTAG
pKNG101 *::vgrG1a-vgrG2b-CT*	*vgrG1a-vgrG2b-CT*_upF	OAL2731	AAGGGCACGCAGCGGCGGTT
	*vgrG1a-vgrG2b-CT*_upR	OAL2732	AACCGCCGCTGCGTGCCCTTCGCCG
	*vgrG1a-vgrG2b-CT*_dnF	OAL2733	GGGATACTGAGGCGGCGGCAT
	*vgrG1a-vgrG2b-CT*_dnR	OAL2734	ATGCCGCCGCCTCAGTATCCCGT

pKNG101 ::*vgrG1a-vgrG1^{Atu31}*	*vgrG1a-vgrG1^{Atu31}*_upF	OAL3125	CGGCGAAGGGCAACCAGATCAACTTC
	*vgrG1a-vgrG1^{Atu31}*_upR	OAL3124	GAAGTTGATCTGGTTGCCCTTCGCC
	*vgrG1a-vgrG1^{Atu31}*_dnF	OAL3119	CATCGACACCGGCAACCAGATCAA
	*vgrG1a-vgrG1^{Atu31}*_dnR	OAL3118	TTGATCTGGTTGCCGGTGTCGAT
pKNG101 ::*vgrG1a^{605}-vgrG1^{Atu31}*	*vgrG1a^{605}-vgrG1^{Atu31}*_upF	OAL3121	TCAGGATTTGATGAGGCGGC
	*vgrG1a^{605}-vgrG1^{Atu31}*_upR	OAL3120	CGCCGCCTCATCAAATCCTGAC
pKNG101 ::*vgrG1a^{614}-vgrG1^{Atu31}*	*vgrG1a^{614}-vgrG1^{Atu21}*_upF	OAL3699	CCGGCGGCCCAGGTGAAAG
	*vgrG1a^{614}-vgrG1^{Atu21}*_upR	OAL3698	CTGGGCCGCCGGAATTGAG
pKNG101 ::*vgrG4b-bla$_{TEM-1}$*	*vgrG4b-bla$_{TEM-1}$*_upF	OAL2603	CTGGCCAAGGACGCGGCCAGCCTG
	*vgrG4b-bla$_{TEM-1}$*_upR	OAL2604	CAGGCTGGCCGCGTCCTTGGCCAG
	*vgrG4b-bla$_{TEM-1}$*_dnF	OAL2608	GCATTGGTAATCCATGTTGCAGAA
	*vgrG4b-bla$_{TEM-1}$*_dnR	OAL2607	CAACATGGATTACCAATGCTTAATCAG
	*vgrG4b-bla$_{TEM-1}$*_exF	OAL2610	ATGACCAGAAGATCCGCGTC
	*vgrG4b-bla$_{TEM-1}$*_exF	OAL2611	CCGGGATTATAGGCGTCGTT
pKNG101 ::*vgrG5^{623}-vgrG4b^{187}*	*vgrG5^{623}-vgrG4b^{187}*_upF	OAL3679	GGCGCCCTGGCACGGATCAAT
	*vgrG5^{623}-vgrG4b^{187}*_upR	OAL3680	GTGCCAGGGCGCCGTCGAGGGTG
	*vgrG5^{623}-vgrG4b^{187}*_dnF	OAL3574	GCCAAGGACTGACAAGGATGAGC
	*vgrG5^{623}-vgrG4b^{187}*_dnR	OAL3575	TCCTTGTCAGTCCTTGGCCAGT
	*vgrG5^{623}-vgrG4b^{187}*_exF	OAL3569	CGAATGGAACGATCTCTGGC
	*vgrG5^{623}-vgrG4b^{187}*_exR	OAL3570	CTGTCGAGAGTGCGCTGG
	*vgrG4b^{621}-vgrG5^{169}*_upF	OAL3677	CGGCCCGCAGGTGATGATCAAC

pKNG101 ::*vgrG4b*^{621}-*vgrG5*^{169}	*vgrG4b*^{621}-*vgrG5*^{169}_upR	OAL3678	TCATCACCTGCGGGCCGCTGATGGC
	vgrG4b^{621}-*vgrG5*^{169}_dnF	OAL3567	CGCCATGAGCCAAGGACTGAT
	vgrG4b^{621}-*vgrG5*^{169}_dnR	OAL3568	CTCATGGCGTGGGCTCAT
	vgrG4b^{621}-*vgrG5*^{169}_exF	OAL3563	AGCGTCTTCAAGAGCCTCAG
	vgrG4b^{621}-*vgrG5*^{169}_exR	OAL3564	CTGGAAAGGTCGAACAGGGT
pKNG101 ::*tse6*^{N}-*tse7*^{C}-*tsi7*	*tse6*^{N}-*tse7*^{C}-*tsi7*_upF	OAL3992	CCGGAGAACTGAGCGCAACACCAT
	tse6^{N}-*tse7*^{C}-*tsi7*_upR	OAL3993	GGTGTTGCGCTCAGTTCTCCGG
	tse6^{N}-*tse7*^{C}-*tsi7*_dnF	OAL3994	GATGATGGGCCCTGGTCGCTGTAT
	tse6^{N}-*tse7*^{C}-*tsi7*_dnR	OAL3995	CGACCAGGGCCCATCATCAGG
pKNG101Δ*rsmA*	Δ*rsmA*_upF	OAL2276	ATATAGGGCCCCTTCAAGATCCTCGGGCCGATC
	Δ*rsmA*_upR	OAL2277	TGACGCCGAAATCAGCATTCCTTTCTC
	Δ*rsmA*_dnF	OAL2278	ATGCTGATTTCGGCGTCAACGCGCCGA
	Δ*rsmA*_dnR	OAL2279	ATATACCCGGGGCAACTGTCGATCCTTCGTCCG
	Δ*rsmA*_exF	OAL2280	GTCGAGTTCGCCGGCAAGTACAAC
	Δ*rsmA*_exR	OAL2281	CTTTCGGTATGGCGCACTCAGG
pKNG101 Δ*tse2tsi2*	Δ*tse2tsi2*_upF	OAL934	ACCACTGGTCGACGAAGAGGTGGAC
	Δ*tse2tsi2*_upR	OAL935	TCAGGATGCGTAGGACATGCGTGGACT
	Δ*tse2tsi2*_dnF	OAL936	ATGTCCTACGCATCCTGACGGCCCGTG
	Δ*tse2tsi2*_dnR	OAL937	CTTCAGCAGCAGCGCACCAGCTAC
	Δ*tse2tsi2*_exF	OAL1283	GCTGCTGCTCGGCCTGTTC
	Δ*tse2tsi2*_exR	OAL1284	AGGCGCCTGAACTGTTCGT
pKNG101 Δ*tse6tsi6*	Δ*tse6tsi6*_upF	OAL3348	TGAGGCGGCGGCATCCTGGCT
	Δ*tse6tsi6*_upR	OAL3349	AGCTGACCCGAGTACCACTGCAC
	Δ*tse6tsi6*_dnF	OAL3350	CGGTGCAGTGGTACTCGGGTC
	Δ*tse6tsi6*_dnR	OAL3351	ACATTCCGTAAAGCTTTTGTCCAG
	Δ*tse6tsi6*_exF	OAL3352	AGTTATACATCCACGCCGAGC

	Δ*tse6tsi6*_exR	OAL3353	GAAAGGGGAGATGCGTGACA
pKNG101 Δ*tssB1*	Δ*tssB1*_upF	OAL300	ATGCCCTGGCCATCGAGAG
	Δ*tssB1*_upR	OAL301	TTACGCCTGGCTTCCCATCTTGTTTCTCCC
	Δ*tssB1*_dnF	OAL302	ATGGGAAGCCAGGCGTAAGAGGATTCC
	Δ*tssB1*_dnR	OAL303	GGCGACTGGTCGAAGTAGTAGT
	Δ*tssB1*_exF	OAL304	ACCCCACCTTCCGTATCAAC
	Δ*tssB1*_exR	OAL305	CGATGTAGCGGGAGTCCT
pKNG101 Δ*tssB2*	Δ*tssB2*_upF	OAL1596	GCGCGGGATCCGGATCAGCGTCCATGTCATG
	Δ*tssB2*_upR	OAL1597	TCAGGCGTCTTTGGCCATGGCTTTTTC
	Δ*tssB2*_dnF	OAL1598	ATGGCCAAAGACGCCTGAGCCACCCCT
	Δ*tssB2*_dnR	OAL1599	CGCGCCCCGGGTGGAGACGTATTGCATCAGC
	Δ*tssB2*_exF	OAL1600	CAGGCGATGCGGGAAGTCGAAA
	Δ*tssB2*_exR	OAL1601	TCTGCCACTTGGCGAACTGC
pKNG101 Δ*tssE2*	Δ*tssE2*_upF	OAL3360	TGATCTAGAATCGAGACCAAGATCCCCAC
	Δ*tssE2*_upR	OAL3361	ACCTTCACCCTGCCGTATCCAGTCATG
	Δ*tssE2*_dnF	OAL3362	ATACGGCAGGGTGAAGGTCAGCTAAGGA
	Δ*tssE2*_dnR	OAL3363	TCAACTAGTAACTCGTCGTCCAGCTTCTG
	Δ*tssE2*_exF	OAL3364	CTTCGCCAAGTATCGCTGGT
	Δ*tssE2*_exR	OAL3365	TCAACTAGTCAGCAGGCACAGGTAGAGC
pKNG101 Δ*tssK3*	Δ*tssK3*_upF	OAL4076	AAAGGATCCAGGTGTCCGATACCGCTCATC
	Δ*tssK3*_upR	OAL4077	CTGCCTGACGGCAGCGACAACACCTAGAC
	Δ*tssK3*_dnF	OAL4078	GTCGCTGCCGTCAGGCAGAACACTCATACGAC
	Δ*tssK3*_dnR	OAL4079	TATACTAGTGAACCTGTCCTTGGCGATCC
	Δ*tssK3*_exF	OAL4080	AACCAGCATGAACAGGGTCG
	Δ*tssK3*_exR	OAL4081	CTTGTGCTGCGTACTCTCGG
pKNG101 Δ*vgrG1b*	Δ*vgrG1b*_upF	OAL2768	AATACCTGGCGCAGCATC
	Δ*vgrG1b*_upR	OAL2769	TCAGTTCTGAAGTGCCATGAAATCAT
	Δ*vgrG1b*_dnF	OAL2770	ATGGCACTTCAGAACTGAAGCGGC
	Δ*vgrG1b*_dnR	OAL2771	GTCGAGCCCCTGGTTGTAG
	Δ*vgrG1b*_exF	OAL2772	TTCTCGGCGTTTTCCAGTTG

	Δ*vgrG1b*_exR	OAL2773	GGCGTTCAACAGTTCCATGT
pKNG101 Δ*vgrG1b*-cluster	Δ*vgrG1b*-cluster_upF	OAL1997	CACTGGTAGTCGAGGAGCAC
	Δ*vgrG1b*-cluster_upR	OAL1998	TTCGTCGAATCCTTGATCCACGTCCATCA
	Δ*vgrG1b*-cluster_dnF	OAL1999	GATCAAGGATTCGACGAATTTCCCTGCAC
	Δ*vgrG1b*-cluster_dnR	OAL2000	GGGGAACTCTGGGTGATCA
	Δ*vgrG1b*-cluster_exF	OAL2001	CAGGGTCTGCATCGCCTG
	Δ*vgrG1b*-cluster_exR	OAL2002	ACCGTTCATCTGCCCGTAG
pKNG101 Δ*vgrG4b*	Δ*vgrG4b*_upF	OAL800	CCACGCCAACTGGAGGTC
	Δ*vgrG4b*_upR	OAL801	CGCAGCAACGTTGAACATCCGCTGTCC
	Δ*vgrG4b*_dnF	OAL802	ATGTTCAACGTTGCTGCGAAGGCGACC
	Δ*vgrG4b*_dnR	OAL803	ATAGCCGATGCGGTTGTC
	Δ*vgrG4b*_exF	OAL804	GCCTACGCCACCTTCCTCGA
	Δ*vgrG4b*_exR	OAL805	GCGCATGCAGCGTCAGGCTG
pKNG101 Δ*TAA*^{vgrG4b}-*ATG*^{pldA}	Δ*TAA*^{vgrG4b}-*ATG*^{pldA}_upF	OAL4111	CAAGGACCAGAAGAAGCCCTACAA
	Δ*TAA*^{vgrG4b}-*ATG*^{pldA}_upR	OAL4110	GGCTTCTTCTGGTCCTTGGCC
pKNG101 Δ*vgrG5*	Δ*vgrG5*_upF	OAL794	ACAGCCATGTGCTCAACG
	Δ*vgrG5*_upR	OAL795	GGTAGGCGTGGCGAACATTCACTGTCC
	Δ*vgrG5*_dnF	OAL796	ATGTTCGCCACGCCTACCGGCGCGACG
	Δ*vgrG5*_dnR	OAL797	CGCGATGAGGTTGAGGTT
	Δ*vgrG5*_exF	OAL798	CATGCGCTACCTGGCCGAAG
	Δ*vgrG5*_exR	OAL799	AGTCGCGGGTGAATATCTGC
pKNG101 Δ*pldAtli5a*	Δ*pldAtli5a*_upF	OAL3227	GCGATCAAGATGCCGTTGAC
	Δ*pldAtli5a*_upR	OAL3228	TACTTCTTCCTTCTTCTGCAACATGGATCAGTC
	Δ*pldAtli5a*_dnF	OAL3229	CAGAAGAAGGAAGAAGTACTGCCCCGCC
	Δ*pldAtli5a*_dnR	OAL3230	TTCTTCACCAGCATCTCGGT
	Δ*pldAtli5a*_exF	OAL3231	CCGGGCAGAAGATGGTGATC
	Δ*pldAtli5a*_exR	OAL3232	AGGACGATGCAATTGGTGGT

pKNG101 Δ*pldBtli5b*$_{123}$	Δ*pldBtli5b*$_{123}$_upF	OAL3233	CCTGAAGCAGCCGGAACA
	Δ*pldBtli5b*$_{123}$_upR	OAL3234	CCGCAAACCTATCCTCTGCCTCCTCATCC
	Δ*pldBtli5b*$_{123}$_dnF	OAL3235	CAGAGGATAGGTTTGCGGTTTGTACAGGT
	Δ*pldBtli5b*$_{123}$_dnR	OAL3236	TAGTGATCGAGGCAGGCATG
	Δ*pldBtli5b*$_{123}$_exF	OAL3237	GAACTGGCCACCTTGCATTC
	Δ*pldBtli5b*$_{123}$_exR	OAL3238	GGGCGACGAGATCCATTTCA
Bacterial-two-hybrid primers			
vgrG1a	*vgrG1a*_F	OAL3973	CCGGTCTAGAGCAACTGACCCGCCTGGTC
	*vgrG1a*_R	OAL1741	GCGCGGAATTCTCAGCCCTTCGCCGGCGG
vgrG1b	*vgrG1b*_F	OAL3825	gcgcTCTAGAATGGCACTTGCGCAACAG
	*vgrG1b*_R	OAL3826	tatacccgggtGTTCTGGAGGATCTTGCGTC
vgrG1c	*vgrG1c*_F	OAL1857	GCGCGTCTAGAGGTGGCTATTGGCCAGCCTTTC
	*vgrG1c*_R	OAL1858	GCGCGGAATTCtcaacagttgatatcgacattg
vgrG1^{Atu}	*vgrG1*^{Atu}_F	OAL3975	CCGGTCTAGAGAACGACCAGCCTTCGGTT
	vgrG1^{Atu}_R	OAL3974	ATATGGATCCTCAAATCCTGACAAACGGTG
tap1-tde1(HADA)	tap1-tde1_F	OAL3722	gcgcTCTAGAATGAACGACACACCCATAATTGATC
	tap1-tde1_R	OAL3723	ccggggatccAAAGACACCGGGACGTCAGG
tde1(HADA)	tap1-tde1_F	OAL3743	gcgcTCTAGAATGAGTGCGACGACAACTG

2.2.6. Plasmid introduction into *P. aeruginosa*

Integration of the Mini-CTX vectors was attained using three-partner conjugation from a Sm10*λpir* donor strain as described above. *P. aeruginosa* conjugants were selected using Vogel-Bonner medium containing tetracycline before screening by colony PCR.

Replicative plasmids were electroporated into *P. aeruginosa.* For this, 1 ml *P. aeruginosa* overnight culture was extensively washed with a sterile 300 mM sucrose

solution before incubating with 100 µg the plasmid of interest on ice for 30 min. The solution was transferred into 0.2 mm gap size electroporation cuvettes and electroporation was conducted at 2.5 kV, 200 Ω and 25 µF using a GenePulser (Bio-Rad) prior to immediate resuspension in 900 µl TSB and incubation at 37 °C for 1 h. Plasmid-containing cells were selected on antibiotic-containing LB agar plates.

2.3. Protein analysis

2.3.1. Secretion assays

Secretion assays were performed similarly to what has been described previously [140]. Cultures were subcultured from overnight cultures in TSB to OD_{600} 0.1 and grown as follows: to analyse H1-T6SS-dependent secretion, strains were grown at 37 °C to an OD of 5; to analyse H2-T6SS-dependent secretion, strains were grown at 25 ° to an OD of 4, unless otherwise stated. 1 OD of bacterial culture was harvested and spun down and served as the whole cell sample. Simultaneously, 13 ml culture was centrifuged at 4 000 *g* for 20 min at 4 °C to separate the bacterial cells from the culture supernatant. 10 ml of the supernatant was transferred into clean falcons and centrifuged again; 7 ml of the uppermost supernatant was transferred into clean falcons and centrifuged. To 1.8 ml supernatant fraction, we added 200 µl trichloroacetic acid to precipitate protein samples overnight at 4 °C. The protein precipitate was centrifugated at 16 000 *g* for 30 min at 4 °C and washed with cold 90% (v/v) acetone before centrifugation again. After removing the supernatant, the washed pellet was air-dried for 30 min and resuspended in 1x Laemmli buffer to an OD_{600} equivalent of 20.

2.3.2. SDS-PAGE and western blot

Bacterial cultures equivalents of an OD_{600} of 1 were harvested to serve as whole cell samples. Cells were pelleted by centrifugated at 8 000 *g* for 3 min before the culture supernatant was removed and 100 µl Laemmli buffer (4% (v/v) glycerol, 2% (w/v) sodium dodecyl sulfate (SDS), 60 mM Tris-HCl pH 6.8, 5 % (v/v) β-mercapto-ethanol and 0.002% (w/v) bromophenol blue) added. Samples were denatured by incubation at 95 °C for 15 min prior to electrophoresis in Tris-glycine-SDS (TGS) buffer (0.3% (w/v) Tris, 1.44% (w/v) glycine and 0.01% (w/v) SDS). Protein samples were separated by SDS-polyacrylamide gel electrophoresis (SDS-PAGE) at 160 V on 6%, 8%, 10%, 12% or 15% polyacrylamide gels, depending on the protein size resolution desired. Gels were prepared using Mini-PROTEAN Tetra handcast systems (Bio-Rad) with 10- or 15-well combs. A Precision Plus Protein Kaleidoscope Prestained Protein Standards marker (Bio-Rad) was used as a molecular weight marker for the loaded protein samples. Separated protein samples were analysed either by Coomassie staining (0.5% (w/v) Coomassie Brilliant Blue R250 (Sigma), 40% (v/v) methanol, 10% (v/v) acetic acid, 49.5% (v/v) ddH_2O) or western blot analysis.

For western blots, protein samples were transferred onto nitrocellulose membranes for probing with antibodies. Filter papers (Whatman), 0.2 µm nitrocellulose membrane (Amersham) and the electrophoresed gel were incubated in ice-cold transfer buffer (10% (v/v) TGS buffer, 20% (v/v) ethanol, 70% (v/v) ddH_2O), and the gel positioned on top of the membrane, sandwiched between six sheets of filter paper. Protein was transferred to the 90 x 110 mm membrane using a TransBlot SD semi-dry transfer cell (Bio-Rad) at 24 V and 0.18 A for 40-50 min depending on the size of the protein of interest.

Afterwards, the membrane was blocked in Tris-buffered saline solution with milk and tween (milk-TBST: 5% (w/v) skimmed milk powder (Sigma), 50 mM Tris-HCl pH 8.0, 150 mM NaCl, 0.1% (v/v) Tween-20) for 1 h. Then, the membrane was incubated with the antibodies

in milk-TBST overnight at 4 °C, followed by three 10-minute washes in TBST. The secondary antibody, conjugated to horse-radish peroxidase (HRP), was incubated with the membrane for 1 h, followed by three successive TBST washes. All antibodies used in this work are listed in Table 2-5. Western blots were developed by incubating the antibody-bound membrane with combined SuperSignal West Pico Chemiluminescent substrate (ThermoFisher) for 1 min. Protein bands were visualised using a LAS-3000 imager (Fujifilm).

Table 2-5. Antibodies used in this study.

Antibody	Host	Serum	Dilution	Reference
anti-TssB1	Rabbit	Polyclonal	1 in 1000	[221]
anti-TssB2	Rabbit	Polyclonal	1 in 1000	[147]
anti-RpoB	Mouse	Monoclonal	1 in 5000	Biolegend
anti-Hcp1	Rabbit	Polyclonal	1 in 1000	[140]
anti-Hcp2	Rabbit	Polyclonal	1 in 1000	[147]
anti-Hcp3	Rabbit	Polyclonal	1 in 1000	[146]
anti-LasB	Rabbit	Polyclonal	1 in 1000	Gift from Romé Voulhoux
anti-Bla_{TEM-1}	Mouse	Monoclonal	1 in 5000	Biolegend
anti-VgrG2b	Rabbit	Polyclonal	1 in 1000	[185]
anti-VgrG4b	Rabbit	Polyclonal	1 in 1000	[146]
anti-His6	Mouse	Monoclonal	1 in 1000	Sigma Aldrich
anti-Myc	Mouse	Monoclonal	1 in 1000	Millipore
anti-HA	Mouse	Monoclonal	1 in 1000	Biolegend
HRP-conjugated anti-rabbit	Goat	Polyclonal	1 in 5000	Sigma Aldrich
HRP-conjugated anti-mouse	Rabbit	Polyclonal	1 in 5000	Sigma Aldrich

2.4. Interbacterial competition assays

Interbacterial competition assays were conducted on solid media due to the contact-dependent killing of the T6SS. Prey *P. aeruginosa* strains contained the Mini-CTX-*lacZ* integrated at the *att* site, consequently giving rise to blue colonies on X-gal-containing media.

Overnight cultures in TSB were collected by centrifugation at 8 000 *g* for 3 min before washing twice in 1 ml sterile PBS and normalised to OD_{600} of 3.0. The OD_{600} was measured again for confirmation and 100 µl of attacker and 100 µl prey strains for a ratio of 1:1, or 100 µl of attacker and 20 µl of prey strains for a ratio of 5:1, were mixed. This mixture was centrifuged at 8 000 *g* for 3 min and 100 µl or 20 µl supernatant was removed to result in a competition mixture of the correct ratio of attacker and prey strains. 5 µl of each competition mix was spotted in duplicates onto LB-agar, the spots well dried and the Petri dish lids were secured using parafilm M (Bemis). Competition plates were inverted and incubated at 37 °C for 5 h for H1-T6SS-inducive killing and at 25 °C for 24 h for H2-T6SS-inducive killing.

The input competitions were serially diluted to 10^{-7}, plated on selective media for both attacker and prey (LB agar with 100 µg/ml X-gal for blue/white *P. aeruginosa* prey/attacker differentiation) and grown overnight at 37 °C to confirm the input ratios. Competition spots were gathered using 5 µl inoculation loops (VWR) and resuspended in 1 ml PBS. The competition output mixture was serially diluted to 10^{-7}, plated on selective media and grown overnight at 37 °C similarly to the input. Both attacker and prey colony forming units were enumerated on both input and output dilution plates. All competition assays were repeated three times unless otherwise stated and the mean cfu of survived prey strains obtained from all experiments with the standard deviation was plotted.

2.5. Translocation assays

HeLa cells were grown in low glucose Dulbecco's modified Eagle medium (DMEM; Sigma Aldrich) supplemented with 10 % heat-inactivated fetal calf serum (Gibco), 1% GlutaMAX (Gibco) and 1% non-essential amino acids (Gibco) in 75 cm^2 cell culture flasks (Nunc). Cells were grown at 37 °C in 5 % carbon dioxide, passaged at 70 % confluency. HeLa

cells were seeded in black 96-well plate with a transparent bottom at a density of 40'000 cells/well and incubated for 24 h at 37 °C/5 % CO_2.

2 OD of bacterial overnight culture was harvested and washed 2 times with sterile PBS and after the last washing step pellet was resuspended in 1 ml of 20 mM HEPES-HBSS solution pH 7.4. Bacterial solutions were diluted to an MOI of 100 with HEPES-HBSS.

After washing HeLa cells and wells of no-cell control twice with 200 µL PBS, 200 µL of bacterial solution was added to each well while 200 µL HEPES-HBSS served as non-infected and no-cell controls. Plates were centrifuged at 600 *g* for 5 minutes at RT and incubated at 37 °C/5 % CO_2 for 3 h. After equilibrating the cells to RT for 15 min, the supernatant was discarded and 180 µl HEPES-HBSS was added to each well together with 20 µL TEM substrate solution (see 3.5.3) prepared according to manufactures instructions (*life technologies*). After incubating the plate for 90 min wrapped in foil at RT, cells were washed three times with 200 µL HEPES-HBSS. Fluorescence was measured using Fluostar Optima plate reader at an excitation wavelength of 410 nm (10-nm band-pass), and emission recorded using 450-nm (blue fluorescence) and 520-nm (green fluorescence) filters. Raw data were normalised on uninfected background and the ratio calculated between cleaved (blue) and uncleaved (green) emission [231].

2.6. *In silico* analysis

All sequences were obtained from NCBI through BLASTp analysis of proteins. *P. aeruginosa* sequences were taken from www.pseudomonas.com before being confirmed with sequences from NCBI. Polypeptide alignments were done in Jalview [232] using the T-coffee server [233]. The prediction of transmembrane helices was undertaken using TMHMM server v2.0 [234]. Tertiary structure modelling of proteins was performed using the Phyre 2.0

server [235] and protein structures were visualised using PyMOL [236]. The statistical analyses described in this work were conducted using Prism 7.0 software (GraphPad).

3. Results:

VgrGs can serve as delivery vehicles for a range of effector domains

3.1. Introduction

The spike complex has a central function in the T6SS. The needle-like structure of a VgrG-PAAR spike facilitates the puncturing of target membranes thus allowing T6SS-related effectors to enter the target cell [141]. It further plays a key role in delivering effectors. Effectors can either directly interact with components of the spike complex, as discussed in later chapters, or they are directly fused to a spike component. While evolved PAAR effectors are highlighted in the next chapter, here we focus on the concept of evolved VgrGs.

While canonical VgrGs are only composed of the gp5- and gp27-like domains, as discussed in 1.3.2, evolved VgrGs contain C-terminal extension domains [207]. These extension domains usually harbour enzymatic activities, which in the case of *Pseudomonas aeruginosa, Vibrio cholerae, Burkholderia pseudomallei* or *Aeromonas hydrophila* are involved in host cell subversion to facilitate bacterial uptake [181-183, 185] (see also Table 3-1). So far, only one evolved VgrG with an antibacterial extension domain was characterised, namely VgrG-3 from *V. cholerae* [237, 238]. The C-terminal extension domain of VgrG-3 was shown to degrade peptidoglycan which is thought to confer a competitive advantage against neighbouring bacteria [237]. To avoid self-toxicity as well as VgrG-3-mediated toxicity by injection from neighbour cells, *V. cholerae* produces the immunity protein TsaB which tightly interacts with VgrG-3. Since VgrG-3 exhibits hydrolase activity, the authors speculated that VgrG-3 might mediate cleavage of glycans in the mucosal epithelium of the host. Thus, VgrG-

3-facilitated cleavage would allow *V. cholerae* the passage through the mucosa and VgrG-3 could also be considered as an anti-eukaryotic effector [237].

Two studies showed that a VgrG can not only deliver its own effector domain into eukaryotic or prokaryotic target cells but also a substituted heterologous effector domain [181, 238]. This highlights the dispensability of the extension domain for VgrG secretion and delivery. Hence, it is widely hypothesised that by delivering the VgrG spike into target cells, the covalently fused extension domain can reach the target cells as well [239]. However, it is currently unclear, whether a canonical VgrG could be manipulated to deliver any extension domain into eukaryotic or prokaryotic target cells. This concept would be the foundation for constructing a T6SS with a VgrG spike delivering any chosen passenger domain.

3.2. Aim of this chapter

Our overarching aim is to hijack the T6SS of *P. aeruginosa* to use it to carry passenger proteins of choice which will give us valuable clues about its delivery modes. The tip complex plays a crucial role in the delivery of T6SS effectors, which is why we want to focus on how the T6SS tip can be manipulated to achieve effector delivery. The tip complex consists of a trimer of VgrG proteins that come as canonical or evolved [140, 240]. Evolved VgrGs carry C-terminal extension domains that have enzymatic activities. This chapter hypothesises that a canonical VgrG can be converted to an evolved VgrG and deliver any chosen effector domain into the supernatant, eukaryotic or bacterial cells.

Our strategy is to extend canonical VgrGs by a range of effectors (see Figure 3-1) and have their delivery monitored by different read outs. We will investigate using biochemical methods whether bacterial cells are able to secrete the chimerae into the supernatant. With cell-based assays we will further examine whether our designed strains can deliver reporter

fusions into eukaryotic target cells. Additionally, to have a more physiologically relevant setting, we will determine whether the designed strains can deliver the fused extension domains into nearby target bacteria. Results from these experiments will give us valuable clues about the functionalities of constructed fusions and their applicability.

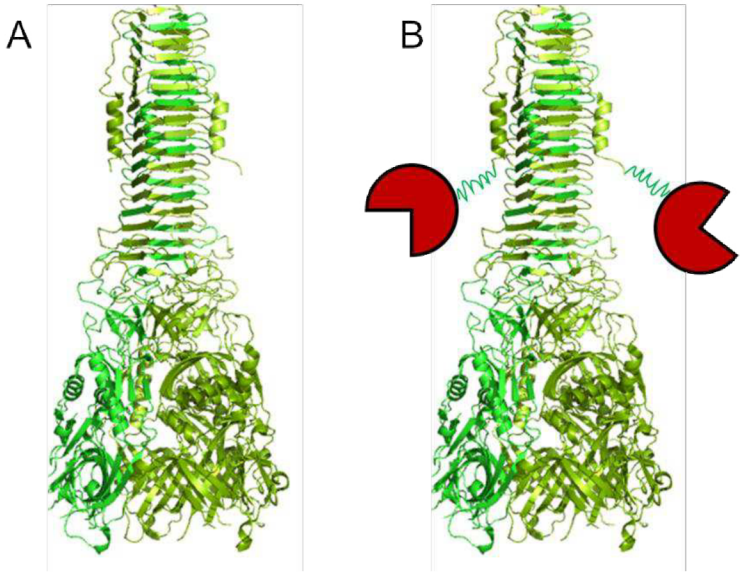


Figure 3-1. Concept of the here designed protein shuttle based on evolved VgrGs.

A: The canonical VgrG1a (green, pdb: 4mtk) forms a functional T6SS spike that is secreted, which will be the basis for the here constructed protein shuttle. B: By covalently fusing an effector domain (red) to the canonical VgrG1a, an evolved VgrG1a will be produced that carries a C-terminal extension domain.

Effector domains from various sources and with different enzymatic functions have been chosen, specifically the C-terminal extension domain of the evolved VgrG2b (VgrG2b-CT), the β-lactamase Bla_{TEM-1} from *E. coli* and the T6SS effectors Tse2 and PldA. In brief, Bla_{TEM-1} is completely unrelated to the T6SS, VgrG2b-CT is an effector domain from *P. aeruginosa* PAO1 [185], while PldA and Tse2 are *P. aeruginosa* cargo effectors delivered *via* a cognate VgrG [146] and Hcp [204], respectively. This strategic diversity is important to demonstrate that not only T6SS secreted effectors can be rerouted as extension domains of

unrelated VgrGs, but also that a completely unrelated protein like the Bla_{TEM-1} can be shuttled into the T6SS using a VgrG.

3.3. Secretion assays as a read-out for chimera functionality

Throughout this chapter, we will show results from the same kind of experiments to validate the functionalities of our chimerae. For all chimerae, we will perform secretion assays to monitor the production and the fate of the fusion proteins. Here, we will briefly explain the basics of secretion assays and how to interpret the results to avoid redundancy when explaining the rationale of experiments.

For secretion assays, growth conditions vary depending on the T6SS-machinery with which the VgrG of interest is associated. For H1-T6SS-inducing conditions, cells are grown at 37 °C until cultures reach on OD_{600} of approximately 5, while for H2-T6SS-inducing conditions, cells are grown at 25 °C until cultures reach an OD_{600} of approximately 4. Cells and supernatant were then separated by three centrifugation steps, the supernatant protein precipitated and washed and western blot analysis performed on both fractions. These experiments were repeated three times and one representative blot is shown in the current work. On representative figures showing western blots, as exemplified in Figure 3-2, different panels are shown with blots probed against various proteins as indicated on the right. The top panel shows a blot probed against the VgrG of interest, here VgrG1abc, while the panels below show further controls. Note, that the antibody against VgrG1abc recognises three species (lane 1), which are VgrG1b, VgrG1c as well as VgrG1a at about 93 kDa, 82 kDa and 72 kDa, respectively [140]. Lane 2 confirms the identity of the VgrG1a-band due to its absence in *vgrG1a* deficient strains. Production of the protein is shown in the whole cell fractions on the left, while secretion is visualised by the same bands in the supernatant fractions on the right. Note, that in the supernatant fractions, only VgrG1a and VgrG1c are detected (lane 3),

while the band corresponding to VgrG1b is missing, which also has been reported previously [140]. The cell lysis reporter RpoB (second panel) is not supposed to be detected in the supernatants (lanes 3 and 4) confirming that secretion of the protein of interest is specific and not due to leakage. The T6SS readout often uses Hcp secretion and dependent on the T6SS-association of the VgrG of interest, it will be a blot detecting Hcp1 or Hcp2, respectively. Figure 3-2 shows a membrane probed for Hcp1 (third panel), which is detected in the supernatant fractions of strains with a functional H1-T6SS machinery (lanes 3 and 4).

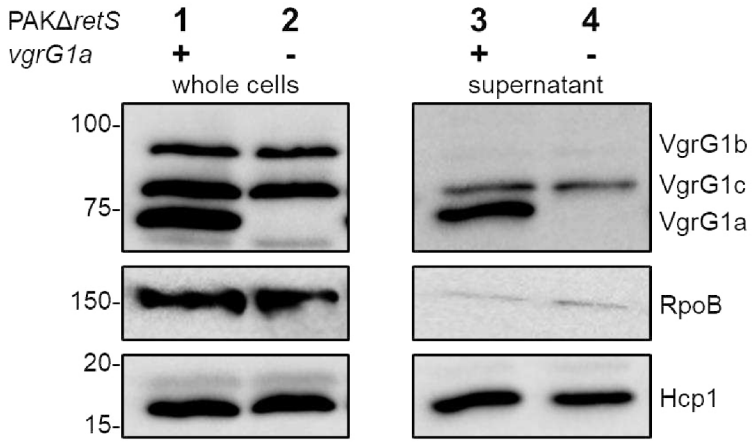


Figure 3-2. A representative figure for western blot analysis; *P. aeruginosa* PAKΔ*retS* expresses VgrG1a, VgrG1b and VgrG1c.

Representative figure of a western blot from a secretion assay of PAKΔ*retS* in presence (+) or absence (-) of *vgrG1a*. As a control for a functional H1-T6SS, membranes were blotted against Hcp1 (third panel). Antibodies were used against VgrG1abc, RpoB and Hcp1 as indicated on the right.

3.4. A canonical VgrG can secrete the extension domain from another evolved VgrG

Several VgrG proteins carry C-terminal extension domains with effector functions and are thus called evolved VgrGs [181-183, 185]. In *P. aeruginosa* PAO1 only one *vgrG* gene out

of ten found on the genome was identified to encode an evolved VgrG, VgrG2b. VgrG2b carries a DUF2345 domain as well as a C-terminal extension domain (VgrG2b-CT) and was shown to be secreted into the supernatant by the H2-T6SS (Thomas Wood, *unpublished data*) and translocated into HeLa cells [185]. It was further suggested by Bleves and colleagues, that once reached the eukaryotic cytosol, VgrG2b-CT binds its cellular target, microtubules, which ultimately facilitates actin-dependent internalisation of *P. aeruginosa* [185].

VgrG2b-CT comprises about 260 aa (Figure 3-3A, red underlined) whose structure was also recently solved by lab members (*not published*). The known extension domain comprises of a transthyretin- (TTR-) like domain (Figure 3-3A, bright green) and an enzymatic Zn-dependent metallopeptidase domain (red) [185].

This section aims at unravelling whether a canonical VgrG could be used to secrete VgrG2b-CT or whether secretion of VgrG2b-CT solely depends on VgrG2b as a vehicle. For this, we chose the canonical VgrG1a (Figure 3-3A), because an earlier study showed that secretion of VgrG1a is highly elevated in *P. aeruginosa* PAK carrying a deletion for *retS* [140]. Hence, we decided to fuse VgrG2b-CT covalently to VgrG1a by allelic exchange (Figure 3-3B). Mutants were constructed as follows: 500 bp upstream and downstream of the STOP codon of *vgrG1a* were amplified. The gene sequence for *vgrG2b-CT* was amplified with an overlap of 9 bp with both the upstream and downstream region. Two-step overlapping PCRs of each two gene fragments resulted in the amplification of the tri-partite gene sequence, which was cloned into the suicide vector *pKNG101*. This vector was conjugated into *P. aeruginosa* PAKΔ*retS*, where after two homologous recombination events, the gene sequence for *vgrG2b-CT* would substitute the STOP codon of *vgrG1a*, which would ultimately result in the *vgrG1a-vgrG2b-CT* fusion (Figure 3-3C).

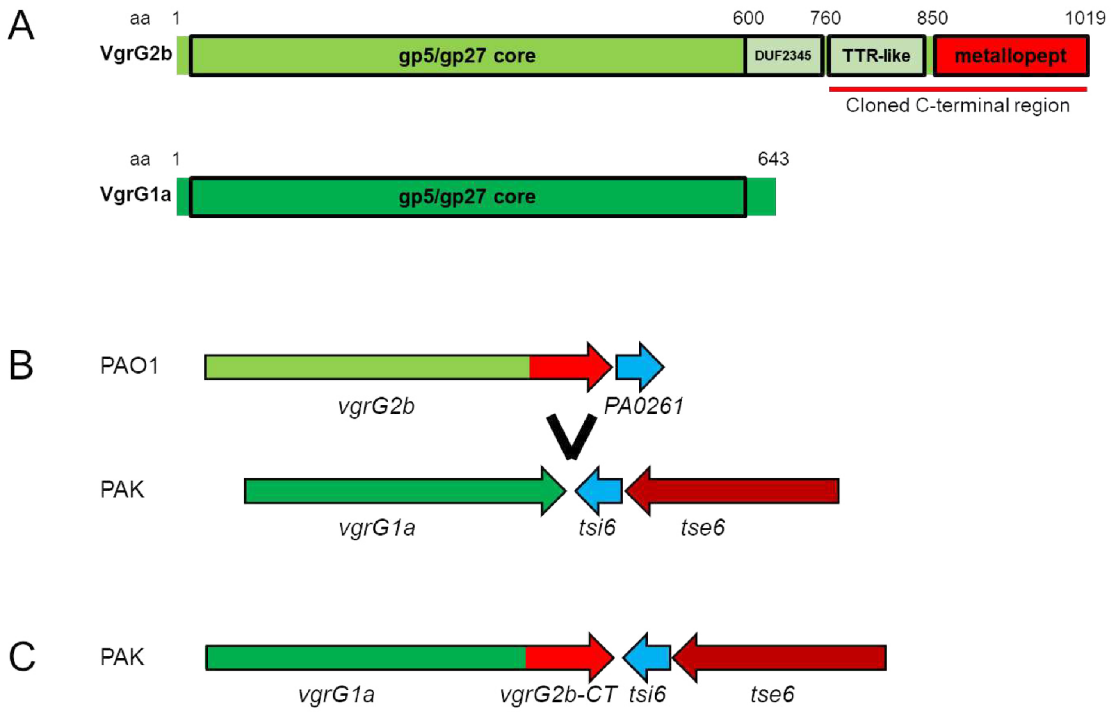


Figure 3-3. Design of a VgrG1a-VgrG2b-CT fusion protein.

A: Protein domains of VgrG2b and VgrG1a. The N-terminal part of both VgrG2b (bright green) and VgrG1a (green) are the gp5/gp27-like domains spanning the first approximately 610 aa. In VgrG2b, this region is followed by a DUF2345 and a transthyretin-like domain (grey-green). The C-terminal 170 aa comprise of the metallopeptidase domain (red). B: The *vgrG2b* gene (green-red) in *P. aeruginosa* PAO1 is followed by the immunity gene *PA0261* (cyan). In PAK, downstream of *vgrG1a* (green), *tse6* (dark red) and the immunity *tsi6* (cyan) are located. C: Design of mutants in which the STOP codon of *vgrG1a* was replaced with the gene sequence encoding VgrG2b-CT, while the downstream region of *vgrG1a* was unaltered.

3.4.1. VgrG1a-VgrG2b-CT is secreted

To investigate whether the canonical VgrG1a could deliver VgrG2b-CT into the supernatant, secretion assays were performed as described in 3.3. Here, the chimeric VgrG1a-VgrG2b-CT could be detected at approximately 100 kDa with a specific antibody against VgrG2b-CT (Figure 3-4, top panel, lane 3, asterisk). When probed with an antibody against VgrG1abc (second panel) against samples derived from strains expressing VgrG1a-

VgrG2b-CT, a shift in the VgrG1a band to approximately 100 kDa can be detected (asterisk, lane 3). Using both antibodies, the bands corresponding to VgrG1a-VgrG2b-CT could also be detected in the supernatant fractions of T6SS-active strains (red asterisks, lane 7), but not T6SS-defective strains (lane 8).

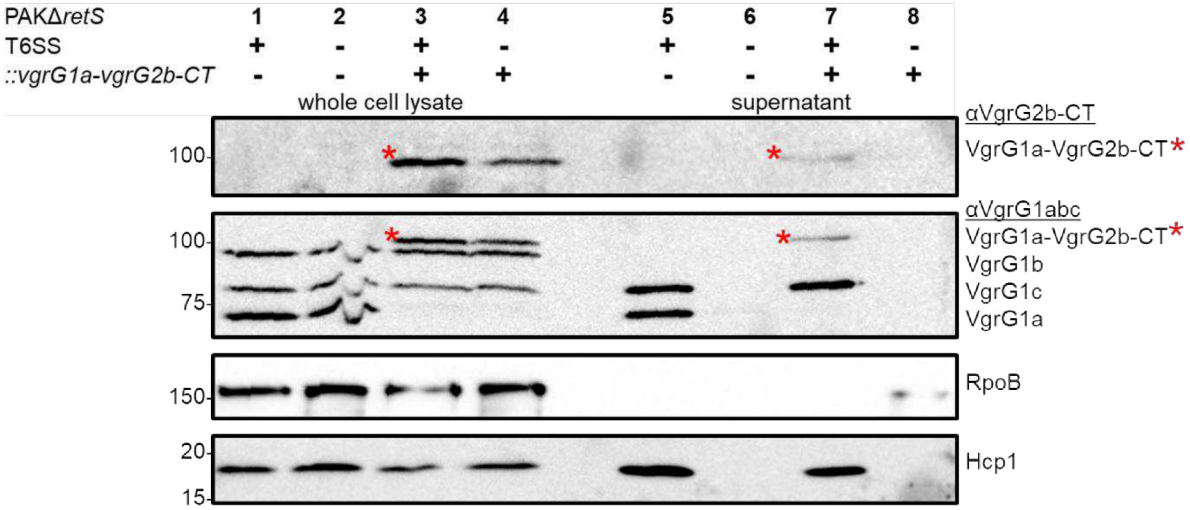


Figure 3-4. VgrG1a-VgrG2b-CT is secreted into the supernatant.

Representative figure of a western blot from a secretion assay of PAKΔ*retS* with an active (+) or inactive (-) H1-T6SS expressing VgrG1a-VgrG2b-CT (+). As a positive control for VgrG1a secretion, PAKΔ*retS* (lane 1) was included, while the negative expressed a defective H1-T6SS (lane 2). Antibodies were used against VgrG2b-CT, VgrG1abc, RpoB and Hcp1 as indicated on the right. Highlighted with red asterisks are the bands corresponding to VgrG1a-VgrG2b-CT.

3.4.2. Comment: VgrG2b-CT has anti-bacterial activity

Concurrently, research from current lab members showed that VgrG2b-CT exerts anti-bacterial toxicity when localised in the periplasm. Further, they confirmed that the small ORF downstream of *vgrG2b, PA0261,* confers immunity to VgrG2b (Figure 3-3A, cyan, Thomas Wood, *unpublished data*). In our mutants, however, we did not clone the proposed cognate

immunity gene for VgrG2b (Figure 3-3C) and surprisingly, the constructed mutants did not show any growth defects. This is rather unexpected, as the injection of T6SS effectors into sensitive sibling cells would result in killing and ultimately eradicating its own species [135, 241]. It could be that the delivery of VgrG2b-CT is not efficient enough in our experimental setup, however, we hypothesised three further possible scenarios.

The most obvious one being the idea that even though we observed secretion of the VgrG1a-VgrG2b-CT-chimera into the supernatant, it is not delivered into nearby sibling cells thus not having a detrimental effect on competing bacteria. This, however, would contradict recent work showing that VgrG1a delivers its cognate effector Tse6 into nearby prey bacteria and would raise the question why the C-terminal domain of VgrG1a cannot be delivered into nearby prey cells [175].

An alternative explanation might be, that VgrG1a-VgrG2b-CT is delivered into sibling cells, but even after delivery it does not face the periplasm. This might be due to immediate recruitment into the T6SS membrane complex thus firing the same chimera immediately again [239]. Alternatively, a recent study proposed the existence of a linker region between the gp5-/gp27-like domains and the C-terminal effector domain. This linker supposedly allows trafficking of the effector domain into the periplasm [238]. In VgrG2b, we were unable to identify this specific linker region, from which one might suggest that in our chimera we did not include this linker region, thus abrogating the trafficking of the effector domain into the periplasm.

Alternatively, even though *P. aeruginosa* PAK does not encode *vgrG2b*, it might be possible that it encodes its immunity or a heterologous immunity somewhere on the genome. It was shown in a few instances that some organisms carry immunity genes for effectors that they do not encode [219, 241, 242]. These could be remnants from lost effector-immunity modules or they were randomly acquired via horizontal gene transfer [219]. Thus, if

P. aeruginosa PAK somehow acquired such immunity gene for VgrG2b-CT, production of VgrG2b-CT would unlikely have a toxic effect on the cells.

3.5. The unrelated passenger protein Bla_{TEM-1} can be delivered *via* the T6SS

3.5.1. Bla_{TEM-1} as a fusion to the canonical VgrG1a is secreted

Next, we wanted to assess whether a completely unrelated effector domain can be channelled into the T6SS of *P. aeruginosa*. The mature Bla_{TEM-1}, lacking its peptide signal, was covalently fused to VgrG1a in a strategy as described for the VgrG1a-VgrG2b-CT fusion in 3.4. A linker peptide with the sequence GSTGST was included to introduce structural flexibility between the VgrG1a trimer and the effector domain (Figure 3-5B).

Secretion assays of H1-T6SS-active and H1-T6SS-inactive strains encoding the VgrG1a-Bla_{TEM-1} fusions were performed as described in 3.3 and a representative figure can be seen in Figure 3-6. Using an antibody against VgrG1abc (top panel), the chimeric VgrG1a-Bla_{TEM-1} appears as a larger product corresponding to the additional band at around 100 kDa (red asterisk, lane 2). The VgrG1a-Bla_{TEM-1} protein can be found in the supernatant fraction of T6SS-active strains (red asterisk, lane 6), but not of T6SS-inactive strains (lane 8). It is noteworthy, that, similar to the whole cell fraction (lane 2), a band corresponding to the original VgrG1a is observable in the supernatant fraction of T6SS-active strains (blue asterisk, lane 6). This band might result from chimera degradation and proteolytic cleavage of the Bla_{TEM-1} domain. This WT VgrG1a band is more pronounced in the supernatant as compared to whole cells which may suggest that the chimera is more prone to degradation once released from the cell.

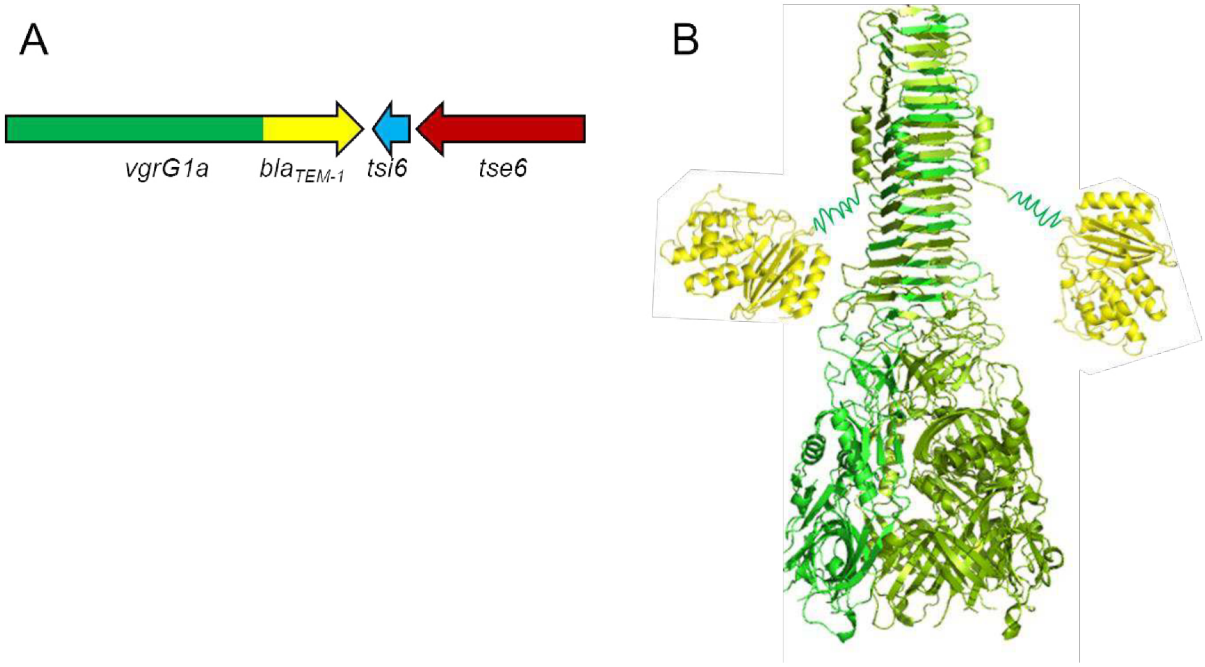


Figure 3-5. Design of the VgrG1a-Bla$_{TEM-1}$-shuttle.

A: Design of mutants in which the STOP codon of *vgrG1a* (green) was replaced with the gene sequence encoding *bla$_{TEM-1}$* (yellow). B: Model of a VgrG1a-bla$_{TEM-1}$ trimer. The Bla$_{TEM-1}$ domain (pdb: 1btl; yellow) is covalently fused to the C-terminus of VgrG1a (pdb: 4mtk; green) via a GSTGST linker (green line).

A faint band corresponding to VgrG1a can be detected in the supernatant fractions of T6SS-defective strains (Figure 3-5, top panel, lane 7), which does not correlate with Hcp1 secretion (bottom panel, lane 7). This phenomenon was observed previously in a study investigating the *P. aeruginosa* H1-T6SS function [125] and might be a general feature of H1-T6SS-inactive strains.

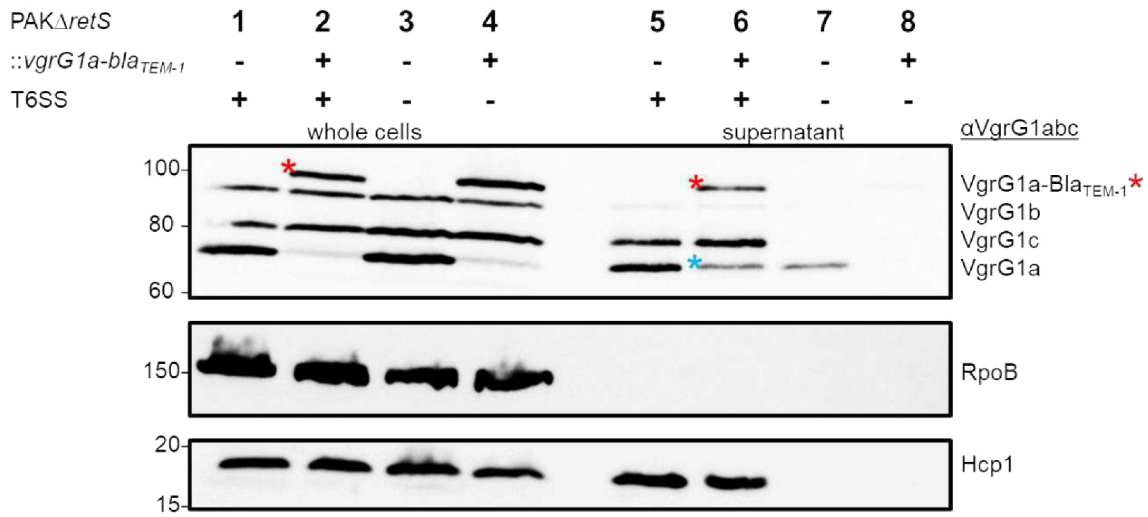


Figure 3-6. VgrG1a-Bla$_{TEM-1}$ is secreted into the supernatant.

Representative figure of a western blot from a secretion assay of PAKΔ*retS* with an active (+) or inactive (-) H1-T6SS encoding VgrG1a-Bla$_{TEM-1}$ (+). As a positive control for VgrG1a secretion, PAKΔ*retS* (lane 1) was included, while the negative expressed a defective H1-T6SS (lane 3). Antibodies were used against VgrG1abc, RpoB and Hcp1 as indicated on the right. Highlighted with red asterisks are bands corresponding to VgrG1a-Bla$_{TEM-1}$; highlighted with a blue asterisk is a degradation product corresponding to WT VgrG1a.

3.5.2. Bla$_{TEM-1}$ as a fusion to the canonical VgrG4b is secreted

To corroborate that any canonical VgrG is able to deliver the unrelated passenger domain Bla$_{TEM-1}$, it was fused to the canonical VgrG4b. VgrG4b is encoded on a remote *vgrG* island by *P. aeruginosa* PAO1 (Figure 3-7B) together with the effector-immunity module *pldA-tli5a*. VgrG4b and PldA were shown to be delivered by the H2-T6SS, while delivery of this VgrG-effector complex will be the main focus of chapter 5.7.2. In addition to the conserved gp5-/gp27-like domains (Figure 3-7A, green), VgrG4b contains a C-terminal TTR-like domain (bright green). This domain is considered not to be part of the needle-like structure of the VgrG, but rather a C-terminal extension without any enzymatic function [216]. Due to the

absence of an effector domain, VgrG4b is considered a canonical VgrG. Hence, this section aims at manipulating VgrG4b to deliver the passenger protein Bla_{TEM-1}.

To design the VgrG4b-Bla_{TEM-1} chimera, the gene sequence corresponding to *bla_{TEM-1}* was used to substitute the STOP codon of *vgrG4b* as described above (Figure 3-7C). These constructs were introduced into *P. aeruginosa* PAO1Δ*rsmA* as this regulatory mutant shows high levels of H2-T6SS activity and secretion assays were performed under H2-T6SS inducing conditions [146].

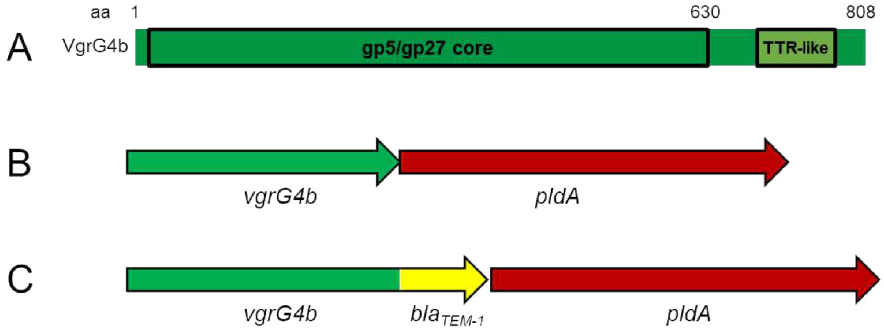


Figure 3-7. Employing VgrG4b in a protein shuttle.

A: Protein domains of VgrG4b. The N-terminal part of VgrG4b comprise of the gp5/gp27-like domains (green) spanning the first approximately 620 aa. This region is followed by a transthyretin (TTR)-like domain (bright green). B: The *vgrG4b* gene (green) is followed by the effector gene *pldA* (red). C: Design of mutants in which the STOP codon of *vgrG4b* was replaced with the gene sequence encoding Bla_{TEM-1} (yellow).

Figure 3-8 shows a representative figure of such secretion assay. Using an antibody against VgrG4b (top panel), VgrG4b can be readily detected in the whole cell fraction (lane 1) and in the supernatant (lane 5). The chimeric VgrG4b-Bla_{TEM-1} appears as a larger product corresponding to the band at around 120 kDa (lane 3). With an antibody against Bla_{TEM-1} (second panel) the same band was detected (lane 3). On the basis of the results from both antibodies, the VgrG4b-Bla_{TEM-1} protein can be found in the supernatant fraction of the T6SS-

active strains (lane 7), but not of the T6SS-inactive strains (lane 8). In the supernatant fraction of T6SS-active strains (lane 7) additional bands were detected suggesting degradation of the chimera. The degradation products in the top panel correspond to the size of WT VgrG4b, suggesting proteolytic cleavage of the Bla_{TEM-1} domain. Since WT VgrG4b could barely be detected in the whole cells, it suggests that the VgrG4b-Bla_{TEM-1} chimera is more prone to degradation once released from the cell.

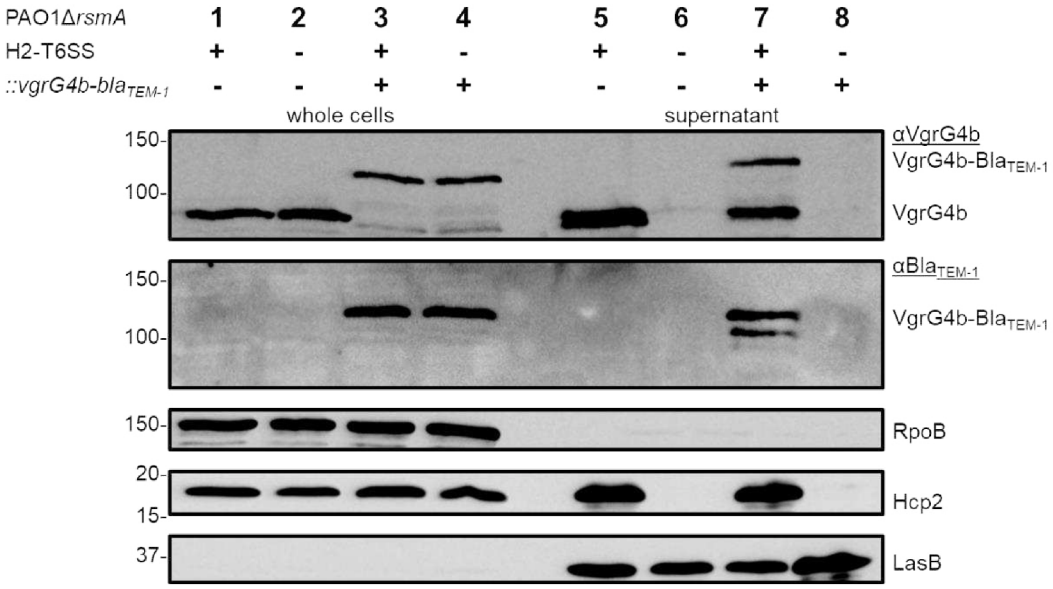


Figure 3-8. VgrG4b-Bla_{TEM-1} is secreted into the supernatant.

Representative figure of a western blot from a secretion assay of PAO1Δ*rsmA* with an active (+) or inactive (-) H2-T6SS encoding VgrG4b-Bla_{TEM-1} (+). As a positive control for VgrG4b secretion, PAO1Δ*rsmA* (lane 1) was included, while the negative control expressed a defective H2-T6SS (lane 2). Antibodies were used against VgrG4b, Bla_{TEM-1}, RpoB, Hcp1 and LasB as indicated on the right. Here, detection of LasB served as a supernatant loading control.

3.5.3. VgrG proteins cannot deliver Bla_{TEM-1} into eukaryotic cells

Since both VgrG1a-Bla_{TEM-1} and VgrG4b-Bla_{TEM-1} were shown to be secreted into the supernatant in a T6SS-dependent fashion, we asked whether such fusion could be delivered into a target cell. Since Bla_{TEM-1} is a common reporter enzyme to monitor translocation into eukaryotic cells [188, 243], it was assessed whether VgrG1a or VgrG4b could fulfil a role that will drive Bla_{TEM-1} all the way into the cytosol of HeLa cells.

The enzymatic activity of Bla_{TEM-1} is the readout for a cell-based translocation assay as sketched in Figure 3-9 [231]. HeLa cells are infected with bacteria with an MOI of 100 and incubated at 37 °C for 3 h. Supernatant is aspirated and fresh PBS added together with the substrate CCF2/AM. The substrate enters the cells, where cleavage by the translocated Bla_{TEM-1} occurs. After incubation at room temperature for 90 min, cells are extensively washed with PBS and fluorescence is measured using a Fluostar Optima plate reader. Uncleaved CCF2/AM has an excitation wavelength at 520 nm, while the cleaved form excites fluorescent light at 447 nm. Background fluorescence of no-cell control wells is subtracted and data are normalised on fluorescence of no-infection control wells and plotted.

As a positive control for this translocation assay, a fusion between Bla_{TEM-1} and the T6SS effector PldA was engineered. In a previous study by Jiang and colleagues it was shown that a PldA-Bla_{TEM-1} fusion is translocated into infected HeLa cells in a T6SS-dependent manner [188]. This could here be confirmed with an elevated translocation rate (Figure 3-10, lane 1). Our negative controls are either a mutant not encoding a Bla_{TEM-1} (lane 5) or a non-deliverable VgrG1a-Bla_{TEM-1} (lane 4). The test strains that express either VgrG4b-Bla_{TEM-1} (lane 2) or VgrG1a-Bla_{TEM-1} (lane 3) do not display any significant differences as compared to the negative controls, suggesting that no translocation of Bla_{TEM-1} occurred. Results obtained here reflect that the fusion proteins were unable to puncture the eukaryotic cell membrane. This could be a reasonable hypothesis for VgrG1a-Bla_{TEM-1}. However, in the case of VgrG4b-

Bla_{TEM-1} it is more surprising since, as the cognate VgrG for PldA [146], delivery of both proteins could be expected.

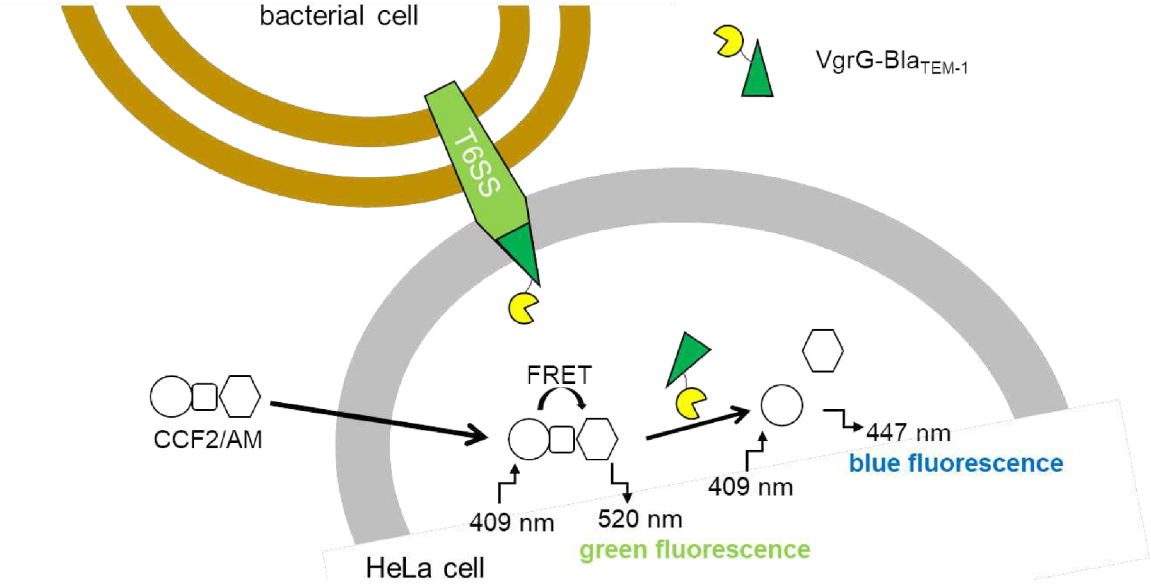


Figure 3-9. Concept of Bla_{TEM-1}-based translocation assay.

A bacterial cell uses a T6SS (bright green) to deliver its VgrG spike (green), which has a fused Bla_{TEM-1} (yellow), into HeLa cells. HeLa cells are loaded with the compound CCF2/AM which emits green fluorescence when excited at 409 nm. If Bla_{TEM-1} is injected into eukaryotic cells, it cleaves CCF2/AM, which leads to emission of blue fluorescent light. Adapted from [231].

Despite the fact that both chimeric VgrG4b-Bla_{TEM-1} and VgrG1a-Bla_{TEM-1} were secreted into the supernatant, we were unable to demonstrate that they could also be injected into eukaryotic cells. This could be due to the limitations of this experimental set-up. One obstacle of this assay is the fact that *P. aeruginosa* expresses a range of β-lactamases [7] that might already be delivered into eukaryotic target cells leading to a high background of cleaved substrate.

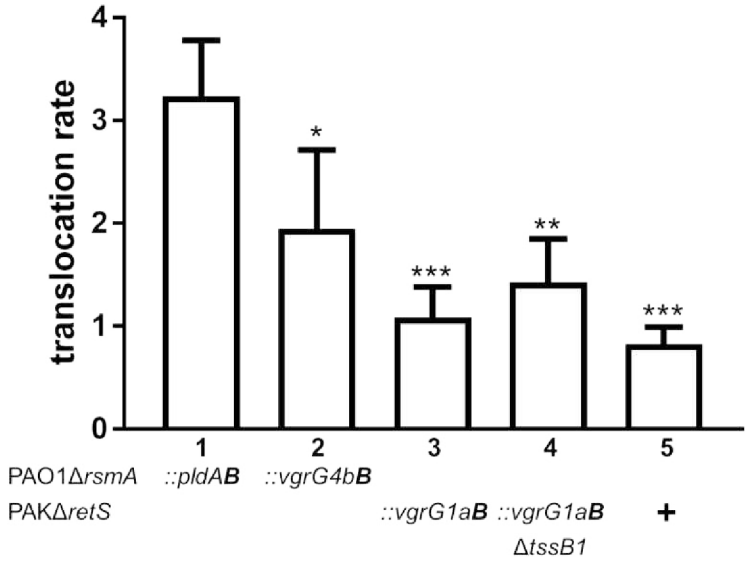


Figure 3-10. VgrG1a-Bla$_{TEM-1}$ and VgrG4b-Bla$_{TEM-1}$ are not translocated into HeLa cells.

HeLa cells were infected with *P. aeruginosa* strains for 3 h, washed and incubated with CCF2/AM substrate for 90 min. After extensive washing, emission of cells was measured. The translocation rate (emission of blue fluorescence / emission of green fluorescence) is here expressed for each sample in relation to the emission ratio of uninfected cells [244]. The positive control PldA-Bla$_{TEM-1}$ (::*pldA**B***, lane 1) was translocated, but not the negative control VgrG1a-Bla$_{TEM-1}$ (::*vgrG1a**B***) from T6SS-deficient strains (lane 4). An ordinary one-Way ANOVA analysis with Dunnett's multiple comparisons test of three independent experiments was conducted on the data set obtained from the positive control with *** $p<0.001$.

In comparison with other Bla$_{TEM-1}$-based translocation studies, the here obtained translocation rate of PldA-Bla$_{TEM-1}$ as a positive control was rather low. We adapted the here used protocol from a study by Schroeder and colleagues [244], in which translocation rates were obtained in ranges between 30 and 50. Here, the translocation rate for PldA-Bla$_{TEM-1}$ was 3, which is comparably low. However, this translocation rate is higher than the one obtained by Jiang *et. al.*, which was approximately 2, and from which the authors claimed translocation of PldA-Bla$_{TEM-1}$ [188]. It is noteworthy that Jiang and colleagues expressed PldA-Bla$_{TEM-1}$ from a plasmid while in this study we did not alter the chromosomal expression of the fusion. This variation of expression rate might indeed explain the altered translocation rate. Furthermore, the growth conditions for *P. aeruginosa* PAO1 need to be considered. We previously showed

that the H2-T6SS is highly activated when grown at 25 °C [146], while eukaryotic cells require to be incubated at 37 °C. Hence, the H2-T6SS, which delivers PldA, might not be activated in sufficient amount to result in an efficient PldA-Bla_{TEM-1} translocation. Considering these facts, PldA-Bla_{TEM-1} might not be a suitable control for this cell assay and thus we lack any option for an adequate positive control for this experiment.

3.6. Grafting an Hcp-dependent effector on a canonical VgrG

As discussed above, T6SS dependent effector delivery can have multiple facets. While many effectors are encoded together with *vgrG* genes and thus secreted in a VgrG-dependent fashion, there are a number of T6SS effectors that are encoded independent of *vgrGs* and instead together with *hcp* genes. These were proposed and in some instances shown to be delivered within the Hcp tube (Figure 3-16A) [149, 204]. In *P. aeruginosa*, four effectors are suggested to be delivered within the Hcp1 tube, which are Tse1, Tse2, Tse3 and Tse4 [204]. In the cases of Tse1 and Tse2, it is suggested that these effectors fold into small enough proteins that they can plug into the lumen of Hcp1 hexamers [203, 245, 246]. Similarly, Tse3 was demonstrated to adopt a lengthy structure that is thought to fit into the Hcp1 tube [196].

For this project, the T6SS effector Tse2 was chosen. Tse2 is most likely an ADP-ribosylase [203], that is toxic in both bacteria and eukaryotes [176]. Recent research showed that Tse2 is delivered by the H1-T6SS within the Hcp1 lumen and that stability of Tse2 highly depends on its interactions with Hcp1 [204]. On another note, Tse2 together with its immunity Tsi2 are not encoded near any T6SS components (Figure 3-11A), which corroborates a delivery mechanism concept independent of any VgrG. Here, the VgrG shuttle concept was challenged by attempting to deliver a Hcp-dependent T6SS effector as an extension domain of VgrG and thus uncouple the T6SS effector from Hcp as a vehicle.

3.6.1. Tse2 as an extension domain of VgrG1a can reach the supernatant

To monitor whether the canonical VgrG1a would be able to deliver Tse2 into the supernatant or bacterial preys, we followed the previous grafting strategy and fused *tse2* to *vgrG1a*. To avoid toxicity against sister cells, the cognate immunity *tsi2* was also cloned so that this gene now lies immediately downstream of the *vgrG1a-tse2* allele in the *vgrG1a* cluster. At the same time, the native *tse2tsi2* (*tsei2*) locus was deleted (Figure 3-11B). The chimera VgrG1a-Tse2 has an expected molecular size of about 91 kDa, which would then be similar to VgrG1b. Because the VgrG1abc-antibody also recognises VgrG1b (Figure 3-2), the *vgrG1a-tse2* chimerae were engineered in mutant strains lacking *vgrG1b*.

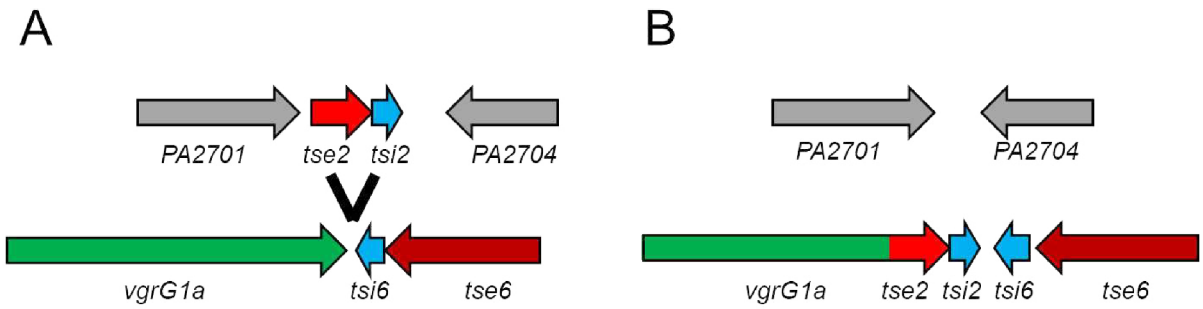


Figure 3-11. Design of the VgrG1a-Tse2 shuttle.

A: *P. aeruginosa* encodes *tse2tsi2* in a remote T6SS-independent locus. Downstream of *vgrG1a* (green), *tse6* (dark red) and the immunity *tsi6* (cyan) are located. B: For the VgrG1a-Tse2 shuttle, *tse2tsi2* were deleted in its native locus, while the gene sequence was used to substitute the STOP codon of *vgrG1a*.

As can be observed in Figure 3-12, top panel, lane 1, using an antibody against VgrG1abc, only VgrG1a and VgrG1c are detectable in whole cells of the parental strain. When strains carry *vgrG1a-tse2*, an additional band corresponding to VgrG1a-Tse2 appears (lane 2, red asterisk), while the intensity of the band for WT VgrG1a is weaker (blue asterisk). This

suggests that the chimera VgrG1a-Tse2 is expressed, but prone to proteolytic cleavage inside the cells. VgrG1a-Tse2 is also detectable in the supernatant of T6SS-active cells (lane 5, red asterisk), suggesting secretion of the chimera. A band corresponding to WT VgrG1a is also detectable in the supernatant fraction (lane 5, blue asterisk). However, it is not clear whether presence of VgrG1a in the supernatant results from cleavage of the chimera after secretion, or whether intracellularly cleaved VgrG1a is secreted. Additionally, in the supernatant fraction of T6SS-defective strains (lane 6), the three bands corresponding to VgrG1a-Tse2, VgrG1c and VgrG1a were faintly detected together with Hcp1 (third panel). Since in the same fraction no RpoA (second panel) was detected, cell lysis can be ruled out and may suggest residual T6SS activity. Tse3, another Hcp1-dependent effector, served as an additional control for Hcp1 secretion and thus T6SS functionality (bottom panel).

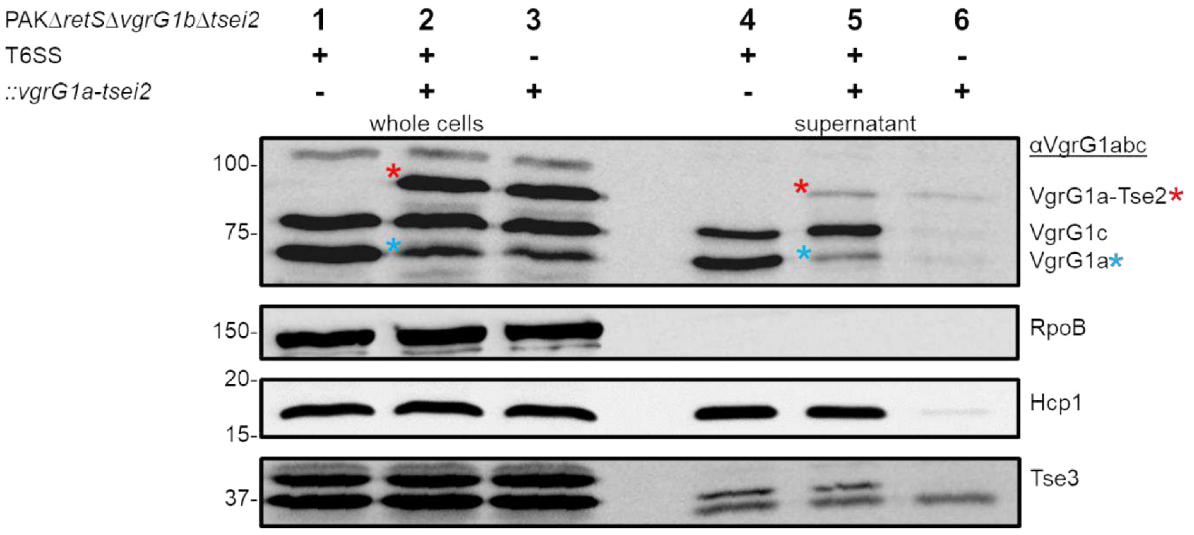


Figure 3-12. VgrG1a-Tse2 is weakly secreted into the supernatant.

Representative figure of a western blot from a secretion assay of PAKΔ*retS* with an active (+) or inactive (-) H1-T6SS encoding VgrG1a-Tse2 (+). As a positive control for VgrG1a secretion, PAKΔ*retS*Δ*vgrG1b*Δ*tsei2* (lane 1) was included. Antibodies were used against VgrG1abc, RpoA, Hcp1 and Tse3 as indicated on the right. Highlighted with red asterisks are bands corresponding to VgrG1a-Tse2, blue asterisks highlight degradation product corresponding to VgrG1a.

Secretion and stability of the VgrG1a-Tse2 chimera is thus far less clear and convincing as compared to VgrG1a-Bla_{TEM-1} (Figure 3-6) and VgrG1a-VgrG2b-CT (Figure 3-4). One possible issue here might be that the VgrG1a-Tse2 chimera is still able to interact with Hcp1 via its C-terminal extension Tse2. If this was the case, it would be possible that Hcp1 is recruited at the tip complex, which is then too bulky and secretion might get hampered.

3.6.2. Disrupting the interactions between Tse2 and Hcp1 in an attempt to increase secretion of the fusion VgrG1a-Tse2

To increase secretion of the VgrG1a-Tse2 chimera, we took advantage of a recent study about the interactions between Hcp1 and its cognate effectors [204]. Silverman *et. al* showed how stability and delivery of Tse2 is highly dependent on Hcp1 and pinpointed key interaction residues on the inside of the Hcp1 lumen. They showed that a range of highly conserved residues within the Hcp1 lumen are essential for interactions with Tse2 and by mutating each of these residues they confirmed that stability and secretion of Tse2 were drastically impaired. One of the strongest phenotypes had the mutant encoding $Hcp1^{S31Q}$ [204], which was thus selected for the current study. Strains were engineered that carried the S31Q substituted version in Hcp1. All above secretion assays were repeated but this time including mutants expressing $Hcp1^{S31Q}$ (Figure 3-13).

Secretion of VgrG1a, VgrG1c, Hcp or Tse3 is not affected when cells contain the hcp^{S31Q} variant (lanes 1 and 5). This is in good agreement with the previous study, in which it was shown that Tse3 secretion was not affected by the $hcp1^{S31Q}$ variant mutation [204]. In a context where *vgrG1a* was replaced by *vgrG1a-tse2* (lane 2), the band corresponding to VgrG1a-Tse2 (red asterisk) is more intense than the band corresponding to WT VgrG1a (blue asterisk) suggesting that the chimera is reasonably stable. However, upon introduction of the $hcp1^{S31Q}$ mutation (lane 3), stability of the chimera was decreased (red asterisk) with higher

abundance of a band corresponding to the size of WT VgrG1a (blue asterisk). This might be caused by the fact that Tse2 no longer interacts with the Hcp1^{S31Q} leading to destabilisation of the effector with subsequent degradation.

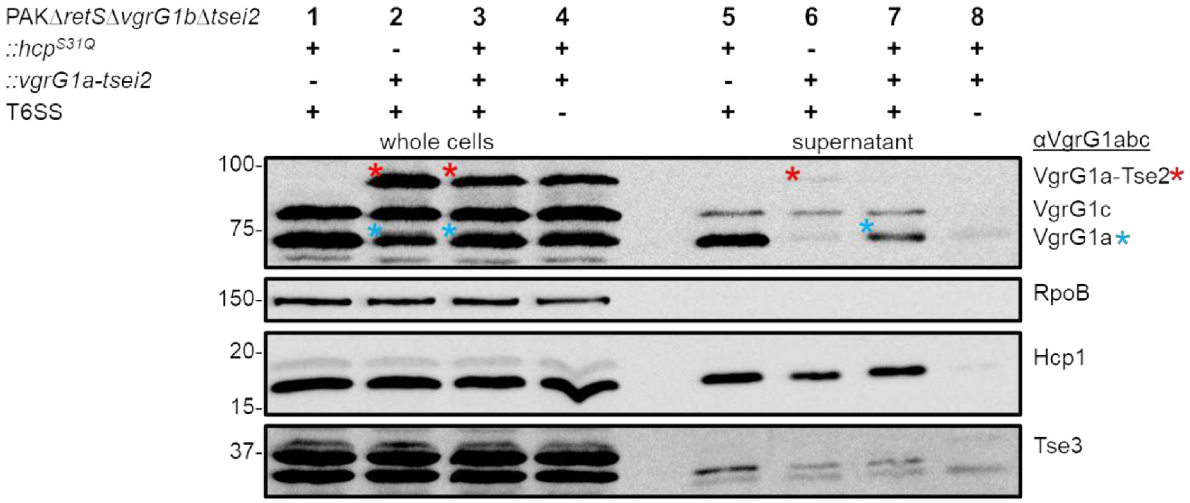


Figure 3-13. VgrG1a-Tse2 is not secreted into the supernatant when strains interactions with Hcp1 are disrupted.

Representative figure of a western blot from a secretion assay of PAKΔ*retS* encoding Hcp (-) or Hcp^{S31Q} (+) with an active (+) or inactive (-) H1-T6SS encoding VgrG1a-Tse2 (+). As a positive control for VgrG1a secretion, PAKΔ*retS*Δ*vgrG1b*Δ*tsei2*::*hcp1*^{S31Q} (lane 1) was included. Antibodies were used against VgrG1a, RpoB, Hcp1 and Tse3 as indicated on the right. Highlighted with asterisks are bands corresponding to VgrG1a-Tse2 (red) and degradation products corresponding to VgrG1a (blue).

In the supernatant fraction of strains carrying the WT *hcp* allele (lane 6), a weak band corresponding to VgrG1a-Tse2 (red asterisk) can be detected, as was the case in the experiment shown in Figure 3-12, lane 3. Secretion of the fusion is not detectable in strains containing the *hcp1*^{S31Q} mutation (lane 7). Interestingly, a rather intense band corresponding to WT VgrG1a is visible in the supernatant fraction of *hcp1*^{S31Q} mutants (blue asterisk). This leads to the hypothesis that either the abundantly cleaved VgrG1a in the cell is secreted, or that the VgrG1a-Tse2 fusion is secreted and then fully degraded, while the former hypothesis is likely correct.

3.6.3. Tse2 is likely delivered into prey cells when fused to VgrG1a

We have shown that Tse2 can be secreted in minor amounts when fused to VgrG1a, however, we also aimed at assessing whether Tse2 can be transported into target cells. Since Tse2 has antibacterial activity [176], we suspected that a more sensitive read-out than protein secretion would be to perform bacterial competition assays for which a protocol was established in our lab [247]. The concept of an interbacterial killing assay is sketched in Figure 3-14 and described below.

For effective interbacterial killing assays, prey cells were constructed that were sensitive to Tse2 by lacking the effector gene *tse2* and its cognate immunity gene *tsi2*. Prey cells then carried the gene encoding β-galactosidase at the *att* site under a constitutive promotor yielding blue colonies on LB-plates containing X-Gal. Prey strains were incubated with the attacking strain that encoded the fusion VgrG1a-Tse2. In the case of VgrG1a-Tse2 delivery into prey cells, Tse2 finds its cellular target within the prey cell and exerts its toxicity [176]. Prey cells lose cell integrity and die, which results in a decrease of blue cfu (Figure 3-14B).

Interbacterial competition assays were conducted by incubating prey cells and attacking cells in a 1:5 ratio for 5 h at 37 °C as a dried spot on an LB-agar plate. Afterwards, spots were harvested and resuspended in PBS and diluted to 10^{-7}. All dilutions were spotted on $LB^{X\text{-}Gal}$ in technical triplicates and incubated overnight at 37 °C. In the next days, blue appearing colonies were counted and plotted as can be seen in Figure 3-15.

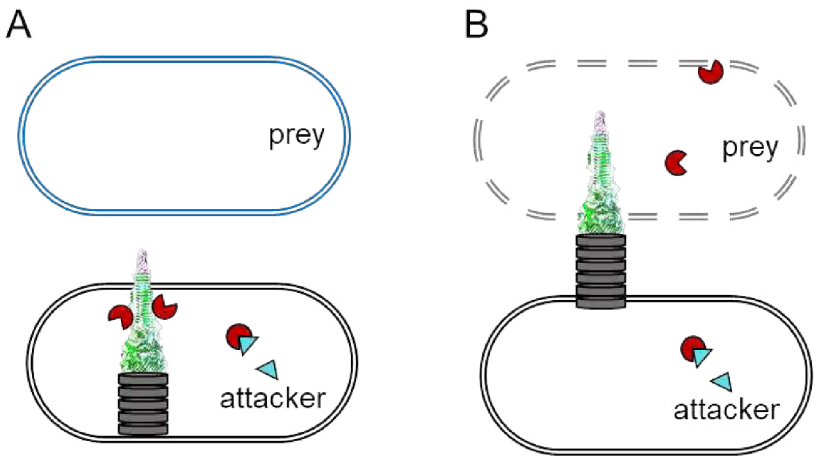


Figure 3-14. Concept of interbacterial competition assays.

The prey strain (blue) lacks the immunity gene for the effector under investigation (*tsi2* in this case). The attacker expresses an active T6SS and the VgrG fused to the effector under investigation (red, Tse2 in this case) as well as the corresponding immunities (cyan) to protect themselves from intoxication. A: The attacking strain is not able to deliver the fusion protein into the target prey cell. The prey cell survives and can be counted due to its apparent blue colour based on the expression of β-galactosidase and subsequent cleavage of X-Gal [247]. B: The attacking strain delivers the fusion protein with the toxic effector domain into prey cells, where no immunity protein neutralises it. The effector domain finds its cellular target and exerts its toxicity. Prey cells die (dashed line) and do not express β-galactosidase leading to decreased blue cfu.

The graph shows a plot of recovered prey numbers after contact with attacking strains. The prey strain lacked the native locus for *tse2tsi2*, hence it was sensitive to Tse2 delivery. When using the parental strain (PAKΔ*retS*Δ*vgrG1b,* lane 2) as an attacker as the positive control, the amount of recovered prey is significantly decreased as compared to the initial number counted in the absence of any attacker (lane 1) or in presence of an attacker lacking the *tsei2* locus (lane 3). This suggests that a suitable prey can be outcompeted due to Tse2 delivery. If the attacking strain expresses VgrG1a-Tse2, no significant killing is observed (lane 4). This suggests that even though VgrG1a-Tse2 was secreted in minor amounts, it does not seem to be delivered into prey cells.

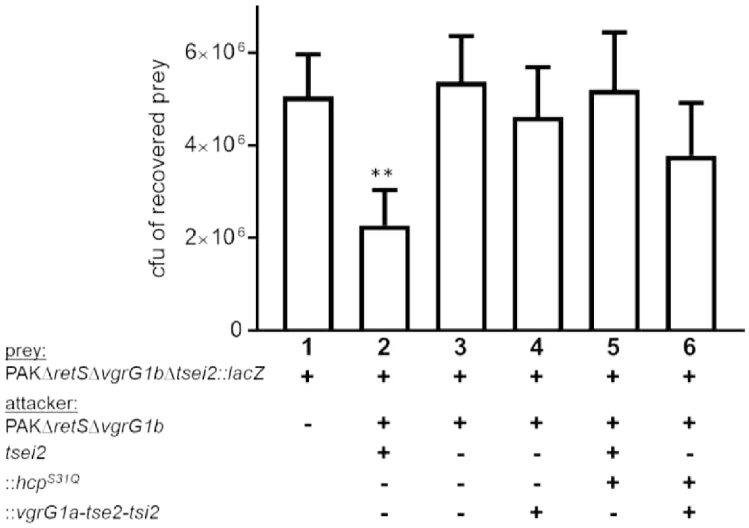


Figure 3-15. VgrG1a-Tse2 can be delivered into prey cells in minor amounts.

Plot of recovered cfu of prey strain PAKΔ*retS*Δ*vgrG1b*Δ*tsei2::lacZ* after contact with the attacker strain that encode WT Tse2 (+), encode Hcp1^{S31Q} (+) or encode the fusion VgrG1a-Tse2 (+) as indicated. As a positive control for Tse2-mediated killing, PAKΔ*retS*Δ*vgrG1b* was included (lane 2), while the negative controls lacked *tse2tsi2* (lane 3) or expressed the mutated Hcp^{S31Q} (lane 5). Spots were incubated for 5 h at 37 °C in a 5:1 ratio. One-Way ANOVA analysis with Dunnett's multiple comparisons test was conducted on data set obtained from recovered prey on their own with ** $p<0.01$.

When Hcp1 was mutated in the parental strain, so that Tse2 is no longer able to interact, more prey cells were recovered (lane 5). This confirms previous results, that Tse2 requires the interactions with Hcp1 to be delivered into target cells [204]. In this same background, if Tse2 instead is covalently linked to VgrG1a, then the attacker has a slight competitive advantage (lane 6). This would suggest that delivery of VgrG1a-Tse2 into prey cells could occur in small amounts when interactions with Hcp1 are disrupted.

3.6.4. Summary: Rerouting an Hcp-dependent effector is rather challenging

From the here obtained results, we can propose the following model which is summarised in Figure 3-16: In the parental strain (Figure 3-16A), Tse2 (red) is chaperoned by

Hcp1 (brown rings) via tight interactions mediated by highly conserved key residues [204]. This leads to recruitment of Tse2 into the Hcp1 tube, docking of the VgrG trimer (green) and subsequent Tse2 delivery [140]. Preliminary data suggest that Tse2 in complex with Hcp1 is folded due to its overall size that might fit into the lumen of a Hcp hexamer [203]. However, there is no data yet that shows a physiological state of this complex. When interactions between Tse2 and Hcp1 are abrogated due to the residual change within the Hcp lumen (Figure 3-16B), Tse2 is not incorporated into the Hcp1 tube and prone for degradation by proteases [204].

Fusing Tse2 covalently to the canonical VgrG1a (Figure 3-16C), does not alter its affinity for Hcp1. Thus, it most likely recruits Hcp hexamers to the T6SS tip. This might result in a large tip complex consisting of three VgrG1a-Tse2 monomers each binding at least one Hcp1 hexamer. Subsequently, VgrG1a-Tse2 is blocked inside the cells and can reach the supernatant or target cells only in minor amounts.

When we then disrupt the interactions between Tse2 and Hcp1 (Figure 3-16D), $Hcp1^{S31Q}$ no longer binds to Tse2 at the tip. This lack of protection by Hcp1 might result in Tse2 being completely exposed to cellular proteases [204], so that Tse2 is probably cleaved from the VgrG1a tip and degraded. This results in accumulation of WT VgrG1a followed by secretion of this species as seen in Figure 3-13.

Considering the here shown data are not conclusive, it can be simply suggested that rerouting T6SS effectors associated with Hcp proteins is not an applicable strategy. If the effector domain relies on its interactions with Hcp, it will either result in sterical hindrance or instability of the effector. Hence, an effector domain independent of a chaperone would be the optimal choice for further protein shuttles.

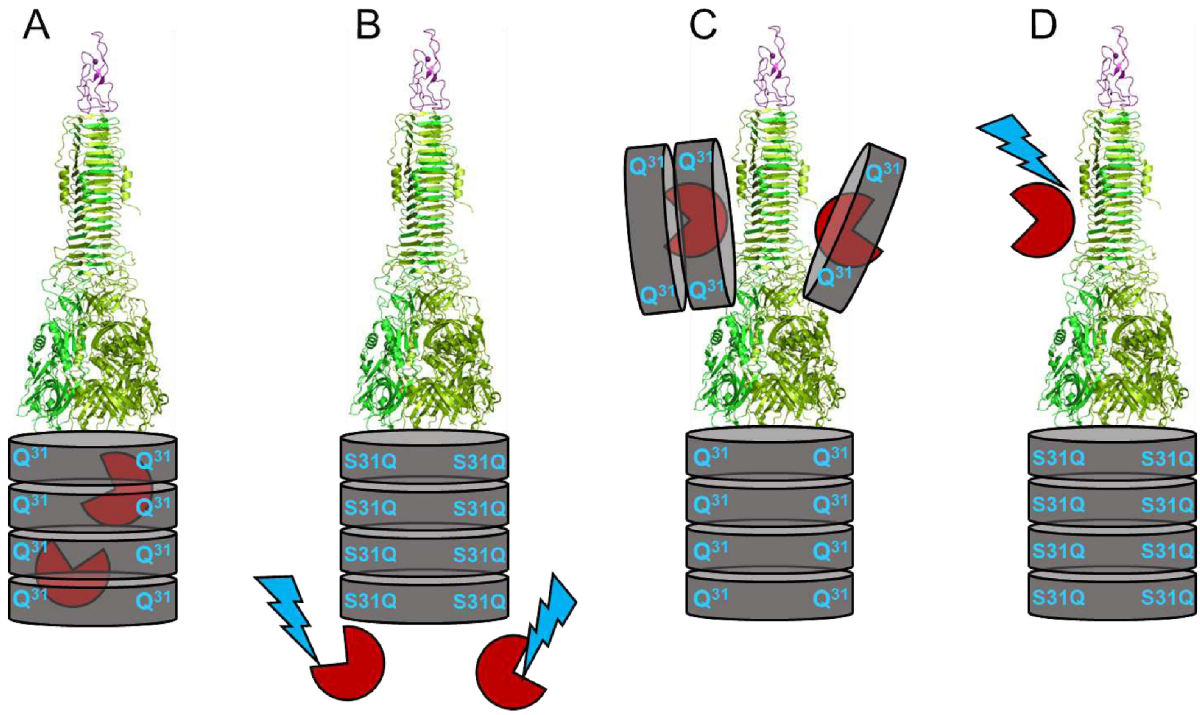


Figure 3-16. Model of interference of interactions between the Hcp1 ring (brown) and Tse2 (red) as part of a VgrG1a-Tse2 shuttle.

A: In the parental strain Tse2 interacts with the key conserved residues within the lumen of Hcp1 leading to stabilisation and subsequent delivery of Tse2. A trimer of VgrG proteins (green, PDB: 4mtk) sits on top of the Hcp1 tube. B: One key residue within the Hcp1 lumen (S31Q) mediating interactions with Tse2 is mutated. This prevents incorporation of Tse2 into the Hcp1 tube and renders it prone for proteolytic degradation (indicated by blue bolt). C: Tse2 is covalently fused to the canonical VgrG1a. Hcp1 molecules are recruited to the tip due to their high affinity for Tse2 leading to a bulky tip complex and blockage of the T6SS. D: One key residue within the Hcp1 lumen mediating interactions with Tse2 is mutated. This leads to destabilisation of Tse2 as C-terminal extension of VgrG1a, so that cleavage of Tse2 occurs and most likely degradation of the effector. WT VgrG1a is accumulated and can be incorporated into the T6SS complex and reach the supernatant. This model is based on the data obtained in this current study and the study shown by Silverman *et. al* [204].

3.7. Large T6SS effectors can be delivered when fused to canonical VgrGs

One aspect we wished to investigate is whether size restriction could apply to the concept of the VgrG shuttle. All previously fused effector domains to VgrG1a had sizes around

20-30 kDa, which correspond to the sizes of known effector domains in evolved VgrGs (see Table 3-1) [181-183, 185]. However, since the membrane complex around the VgrG tip supposedly harbours limited space for effectors [115], there might be sterical limitations as to the fused effector domain.

A literature research highlighted the presence of an antibacterial lipase, PldA, which is present in *P. aeruginosa* PAO1. PldA, which is about 120 kDa, was shown to be delivered into bacterial prey cells and eukaryotic HeLa cells [186, 188]. Hence, the aim of this project was to fuse PldA to VgrG1a in *P. aeruginosa* PAK, which naturally does not encode *pldA*. However, due to the size of the required gene fragment of the effector-immunity gene pair, cloning proved difficult and unsuccessful.

Encoded upstream of *pldA* is *vgrG4b* (Figure 3-17A), whose gene product, the canonical VgrG4b, was proven to be a useful vehicle to deliver Bla_{TEM-1} (see 3.5.2). Here, we reasoned that delivering PldA in a similar manner would be a challenging but likely task. Thus, we took advantage of the genetic link between *vgrG4b* and *pldA* to create a fusion that will encode a VgrG4b-PldA-shuttle. The *vgrG4b-pldA*-chimera was constructed by allelic exchange and by deleting the STOP codon of *vgrG4b*, the 9-bp intergenic region and the START codon of *pldA*, which would ultimately lead to the expression of a large fusion protein consisting of VgrG4b and PldA (Figure 3-17B). All mutants were confirmed by sequencing.

It is noteworthy that, in a later chapter of this thesis, we will show that delivery of PldA depends on VgrG4b, suggesting that these two proteins interact tightly with each other (see 5.7.2). Hence, it will be informative to analyse whether this state can be locked in a covalent interaction and still be functional. This will also give valuable clues about whether the covalent VgrG4b-PldA fusion has a comparable spatial arrangement as the secretion complex formed by non-covalent interactions.

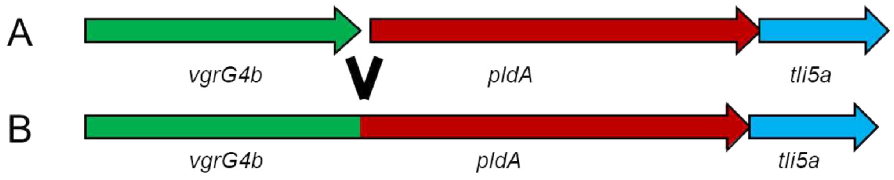


Figure 3-17. Design of a VgrG4b-PldA shuttle.

A: *vgrG4b* (green) is encoded upstream of *pldA* (red) and the cognate immunity *tli5a* (cyan). B: Strategy of VgrG4b-PldA-shuttle. STOP-codon of *vgrG4b*, intergenic region and START-codon of *pldA* were deleted to result in one gene product.

3.7.1. VgrG4b-PldA is secreted

To assess whether the fusion VgrG4b-PldA can be secreted from *P. aeruginosa*, secretion assays were performed. Because VgrG4b is secreted by the H2-T6SS [146], secretion assays were conducted under H2-T6SS inducing conditions as described in 3.3 and a representative figure can be seen in Figure 3-18.

Probing with an antibody against VgrG4b (top panel) resulted in the detection of WT VgrG4b in whole cell and supernatant fractions (lanes 1 and 5). Strains carrying the fusion VgrG4b-PldA expressed a larger protein corresponding to the expected size of VgrG4b-PldA at about 210 kDa (asterisk, lanes 3 and 4). The chimera can be detected in the supernatant fraction of H2-T6SS-active mutants (asterisk, lane 7) together with additional bands most likely representing degradation products. However, no such band can be detected in the supernatant fraction of T6SS-inactive mutants (lane 8) suggesting effective secretion of VgrG4b-PldA while the supernatant loading control LasB (bottom panel) is present in all supernatant fractions.

These results suggest that the covalent extension of a VgrG should not be an obstacle for the T6SS-dependent delivery of large proteins. This suggests that there is enough space

within the membrane complex of the H2-T6SS to accommodate the large PldA. However, it needs to be taken into account, that VgrG4b is naturally able to deliver PldA (see 5.7.2). From this, it can be assumed that space around the VgrG4b tip might be sufficient to accommodate the large PldA.

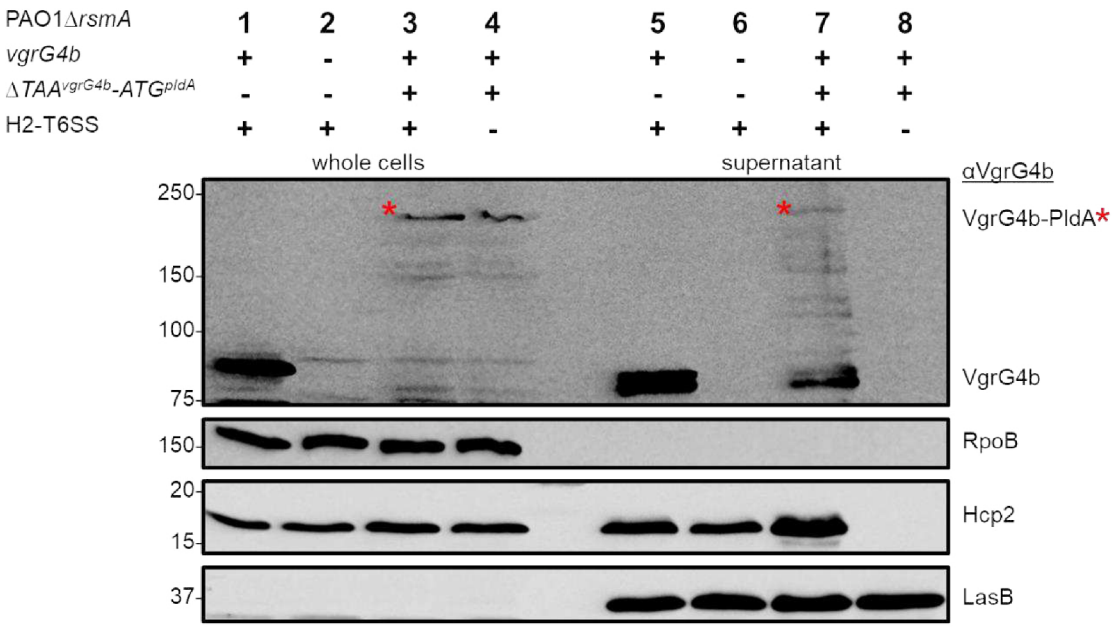


Figure 3-18. VgrG4b-PldA is secreted into the supernatant.

Representative figure of a western blot from a secretion assay of PAO1Δ*rsmA* with an active (+) or inactive (-) H2-T6SS encoding VgrG4b-PldA (+). As a positive control for VgrG4b secretion, PAO1Δ*rsmA* (lane 1) was included, while the negative control lacked *vgrG4b* (lane 2). Antibodies were used against VgrG4b, RpoB, Hcp2 and LasB as indicated on the right. Highlighted with red asterisks are bands corresponding to VgrG4b-PldA.

3.7.2. VgrG4b can deliver covalently linked PldA into prey cells

We have shown that the VgrG4b-PldA fusion is secreted in a T6SS-dependent manner. We further wanted to investigate whether such fusion could also be injected into bacterial prey

cells. Because PldA harbours anti-bacterial activity [186], we could use this as a basis for competition assays.

Prey cells were constructed that lacked *pldAtli5a*, which made them sensitive for PldA delivery. Because VgrG4b and PldA are delivered in a H2-T6SS dependent manner (see 5.6), competition assays were conducted under H2-T6SS inducing conditions [146]. Thus, attacker and prey cells were incubated for 24 h at 25 °C in a 1:1 ratio as a dried spot on an LB-agar plate [146]. Afterwards, spots were harvested and diluted to 10^{-7} before spotting all dilutions on $LB^{X\text{-}Gal}$. Due to the presence of β-galactosidase at the *att* site, prey colonies would turn blue. Recovered prey cfu were counted and plotted as can be seen in Figure 3-19.

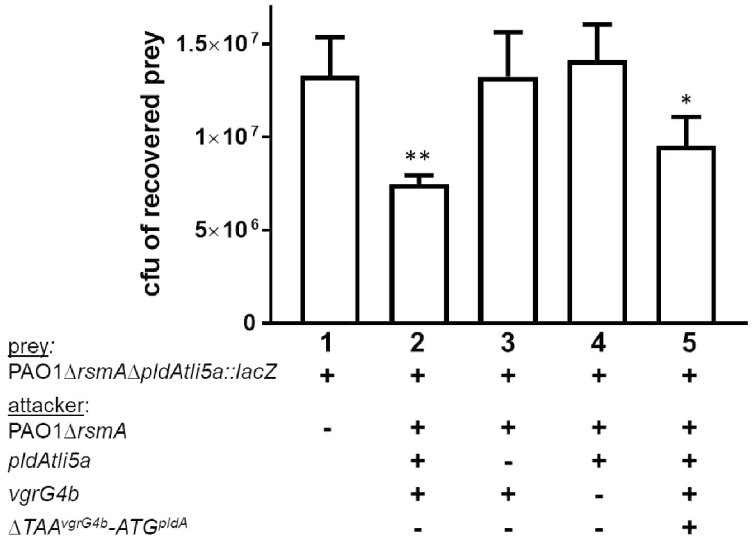


Figure 3-19. PldA can be delivered into prey cells as an extension domain of VgrG4b.

Plot of recovered cfu of prey strain PAO1Δ*rsmA*Δ*pldAtli5a::lacZ* after contact with the attacker strain encoding WT PldA (+), WT VgrG4b (+) or the fusion VgrG4b-PldA (+) as indicated. As a positive control for PldA-mediated killing, PAO1Δ*rsmA* was included (lane 2) while the negative controls lacked *pldAtli5a* (lane 3) or *vgrG4b* (lane 4). Spots were incubated for 24 h at 25 °C in a 1:1 ratio. One-Way ANOVA analysis with Dunnett's multiple comparisons test was conducted on the data set obtained from the recovered prey on its own with ** $p<0.01$.

As a positive control for PldA-mediated killing, the parental strain (PAO1Δ*rsmA*) was used as an attacker (lane 2). This led to a significant decrease in recovered prey as compared to the initial number counted in the absence of any attacker (lane 1). When the attacker lacked the *pldAtli5a* (lane 3) or *vgrG4b* (lane 4) locus, recovered prey count was significantly higher. This suggests that a prey can be outcompeted due to PldA delivery and that PldA delivery is VgrG4b-dependent, which will be the focus of a later chapter (see 5.7.2). If the attacking strain expresses the VgrG4b-PldA fusion protein, prey survival shows an intermediate phenotype (lane 5), but significant killing. This result suggests that VgrG4b-PldA is not only secreted, but can also be injected into bacterial target cells.

3.7.3. Summary: Upgrading a cargo effector to an extension domain leads to an unstable but deliverable complex

This is the first example showing how an anti-bacterial toxin could be connected to a T6SS tip as a C-terminal extension domain of a previously canonical VgrG (Figure 3-20). In the parental strain it is considered and will be proven in detail in chapter 5, that PldA tightly interacts with the C-terminal domain of VgrG4b (Figure 3-20A). This interaction, which is considered to be non-covalent [216], is the prerequisite for PldA delivery.

In our chimera fusion, we introduced a covalent bond between VgrG4b and PldA. In such fusion protein, PldA likely still interacts with the C-terminus of VgrG4b, as sketched in Figure 3-20B. However, one might reason that PldA and VgrG4b attempt to reach a configuration based on the WT-like non-covalent interaction and that this attempt might be sterically clogged by the covalent bond. Such a complex might not be highly stable resulting in degradation products as observed in the whole cell fractions of VgrG4b-PldA producing strains (Figure 3-18). One approach to surmount this issue could be to introduce a few

residues between VgrG4b and PldA to increase flexibility in the configuration of these two domains and thus stability of the complex.

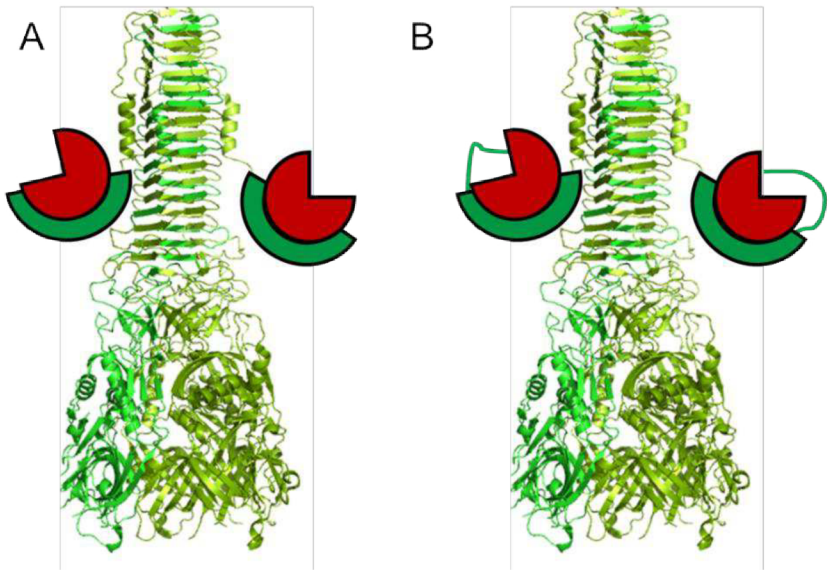


Figure 3-20. Model of non-covalent and covalent interactions between VgrG4b and PldA.

A: PldA (red) interacts tightly with the C-terminal domain (green arc) of VgrG4b, which are the requirements for its delivery, which will be intensely discussed in chapter 5. B: In the here designed effector shuttle, PldA is covalently linked to VgrG4b, as indicated by the green line, but might still interact with the C-terminal domain of VgrG4b. This spike complex is secreted and delivered into target prey cells.

Another concept that needs to be considered in this regard, is that a VgrG4b-PldA fusion protein does not seem to be very stable (Figure 3-18, lane 3). Cleavage most likely results in the accumulation of the two proteins VgrG4b and PldA. These two components could then interact similar to the WT configuration sketched in Figure 3-20. This WT-like complex can likely be delivered into prey cells leading to the same detrimental effect due to PldA toxicity. Using interbacterial competition assays we would be unable to distinguish these two scenarios of PldA delivery which thus remains a major obstacle of this study. Nevertheless, we could show how this now evolved VgrG4b protein was able to deliver the antibacterial

extension domain both into the supernatant and into target prey cells, which is a novel and unique aspect of T6SS-mediated effector delivery.

3.8. Discussion

This chapter demonstrates how VgrG proteins can be manipulated to connect an effector domain to a T6SS tip. We could show how effector domains from various sources and of various sizes can be connected to the T6SS tip of *P. aeruginosa*. This is the first study that further demonstrates how an artificially evolved VgrG can reach both the supernatant and target bacterial cells.

3.8.1. Evolved VgrG proteins can deliver a range of effector domains

Previous studies investigated secretion and translocation of evolved VgrGs. Some studies used β-lactamase as a reporter enzyme to follow the fate of VgrG proteins by monitoring translocation into eukaryotic cells [181, 183, 243]. In these cases, the β-lactamase domain was either used to extend the evolved VgrG or to substitute the extension domain thus proving that the effector domain is not essential for VgrG delivery [181] (see Table 3-1). In this current study, we were able to corroborate these findings by employing Bla_{TEM-1} as a reporter enzyme. We could further extend this knowledge by demonstrating that it is possible to extend a canonical VgrG with Bla_{TEM-1} or another effector domain and thus creating an artificially evolved VgrG.

Table 3-1. Overview of known evolved VgrGs from the literature and from the current study.

Names of the VgrGs are adapted from the literature with superscripted abbreviations corresponding to the organism the VgrG is derived from (*Paer - P. aeruginosa; Vcho – V. cholerae; Ahyd – A. hydrophila; Bpse – B. pseudomallei; Ftul – Francisella tularensis*). If no organism is mentioned, its source is *P. aeruginosa*. Artificially chimeric VgrGs with fused effector domains are highlighted with a grey background. The table lists the enzymatic activities of the extension domains and their size. It further highlights whether the evolved VgrG was found secreted in the supernatant and whether translocation in either eukaryotic or prokaryotic cells was shown.

evolved VgrG	effector domain	size	secreted?	delivered?	ref.
VgrG2b^{Paer}	metallo-peptidase	27 kDa	yes	HeLa cells	[185]
VgrG-1^{Vcho}	actin cross-linking	42 kDa	yes	J774 cells, CHO cells	[207, 248, 249]
VgrG-1$^{715\,Vcho}$-Bla	β-lactamase	30 kDa	yes	J774 cells	[181]
VgrG-1^{Vcho}-Bla	actin cross-linking β-lactamase	42 kDa 30 kDa	yes	J774 cells, CHO cells	[181]
VgrG-3^{Vcho}	peptidoglycan degrading	33 kDa	yes	prey cells	[237, 238]
VgrG3$^{708\,Vcho}$-NucSe1	nuclease	52 kDa		prey cells	[238]
VgrG1^{Ahyd}	actin ADP-ribosylating	23 kDa	yes	HeLa cells	[183]
VgrG1^{Ahyd}-Bla	actin ADP-ribosylating β-lactamase	23 kDa 30 kDa	yes	HeLa cells	[183]
VgrG5^{Bpse}	membrane fusion	37 kDa	yes		[182]
VgrG^{Ftul}-Bla	β-lactamase	30 kDa	yes	macrophages	[243]
VgrG1a-VgrG2b-CT	metallo-peptidase	27 kDa	yes		this study
VgrG1a-Bla$_{TEM-1}$	β-lactamase	30 kDa	yes	not HeLa	this study
VgrG4b-Bla$_{TEM-1}$	β-lactamase	30 kDa	yes	not HeLa	this study
VgrG1a-Tse2	putative ADP-ribosylating	18 kDa	minor	(prey cells)	this study
VgrG4b-PldA	lipase	122 kDa	yes	prey cells	this study

So far, only one evolved VgrG, VgrG-3^{Vcho}, has been shown to carry an antibacterial C-terminal extension domain which can be delivered into bacterial prey cells [237]. When the peptidoglycan hydrolase domain of VgrG-3^{Vcho} was substituted with a nuclease domain from *Salmonella enterica*, mutants expressing the resulting chimera VgrG3^{708Vcho}-NucSe1 were able to outcompete their parental strains [238]. This suggests that VgrG3^{Vcho} is able to deliver any covalently linked effector domain into target prey cells. However, in this current study, we showed that VgrG4b, which does not contain an extension domain, can be modified to deliver an antibacterial extension domain into target prey cells. So far, this is the first time shown that a VgrG can be equipped with an additional function, that is to deliver an effector domain.

3.8.2. Not every VgrG can puncture eukaryotic cell membranes

Four of the previously described evolved VgrG proteins were shown to carry effector domains targeting eukaryotic components [182, 183, 185, 207, 237, 238, 248, 249]. Three of these VgrG proteins were further shown to be translocated into eukaryotic cells themselves [181, 183, 185]. Additionally, the trans kingdom effectors PldA and PldB were previously demonstrated to be translocated into eukaryotic HeLa cells [188], which we could confirm here for PldA. Interestingly, when we also tested translocation of VgrG4b, which is the essential component for PldA delivery [146], we did not observe its translocation. Also, we did not monitor translocation of VgrG1a-Bla$_{TEM-1}$ into eukaryotic HeLa cells (3.5.3).

This led us to the assumption that not all VgrGs can be delivered into eukaryotic cells or can deliver associated effectors into eukaryotic cells. We have shown that the canonical VgrG1a and VgrG4b from *P. aeruginosa* are not delivered into eukaryotic cells, while the evolved VgrG2b is [185]. While VgrG1a solely constitutes of the gp5-/gp27-like domains (Figure 3-3A), VgrG4b additionally contains a transthyretin-like domain (Figure 3-7A) and VgrG2b on top of that a DUF2345 and a Zn-metallopeptidase domain (Figure 3-3A). Hence,

it would be interesting to unlock the molecular requirements of a VgrG protein that allows its translocation into eukaryotic cells. One option is to substitute different parts of the C-terminal domains of VgrG2b with Bla_{TEM-1} to determine which exact part is required for VgrG2b translocation into eukaryotic cells. This strategy would be similar to the work done by Ma *et.al.*, in which they substituted the ACD-domain from VgrG-1^{Vcho} with Bla_{TEM-1} and showed that the ACD-domain is not required for VgrG-1^{Vcho}-translocation [181]. Another approach could be to fuse different sections of the C-terminal domains of VgrG2b to either VgrG1a or VgrG4b together with the Bla_{TEM-1}-domain and test these chimerae for translocation into eukaryotic cells. This would allow the molecular dissection of VgrG domain determinants for eukaryotic cell translocation.

4. Results:

PAAR proteins bind specific VgrG trimers and can carry effector domains

4.1. Introduction

In the last chapter we showed how one component of the T6SS spike could be modified to carry heterologous effectors into the supernatant and into target cells. Here, we will focus on another component of the spike complex, which is the PAAR protein forming the piercing structure of the T6SS tip and we will investigate the molecular interactions between a PAAR domain and its cognate VgrG trimer.

PAAR proteins were shown to be essential components of the T6SS by further sharpening the torch-like structure of VgrG trimers (Figure 4-1A) [141, 148]. This rigid piercing device is thus crucial to puncture target membranes and allow the transport of effectors [141]. The conical shape of PAAR proteins is mediated by the intertwined assembly of three proline-alanine-alanine-arginine (PAAR)-motifs, which are found in protein domains of the families COG4104, DUF4150 and DUF4280 [141, 149, 250]. The PAAR fold is further stabilised by a zinc atom situated close to the cone's peak and stabilised by three histidine and one cysteine residue that are well conserved [141]. It is generally understood that one PAAR domain assembles on top of one VgrG trimer as indicated in Figure 4-1A [141]. These assemblies are thought to be mediated by specific interactions between one PAAR domain and one VgrG trimer, however, how this specificity is maintained remains elusive.

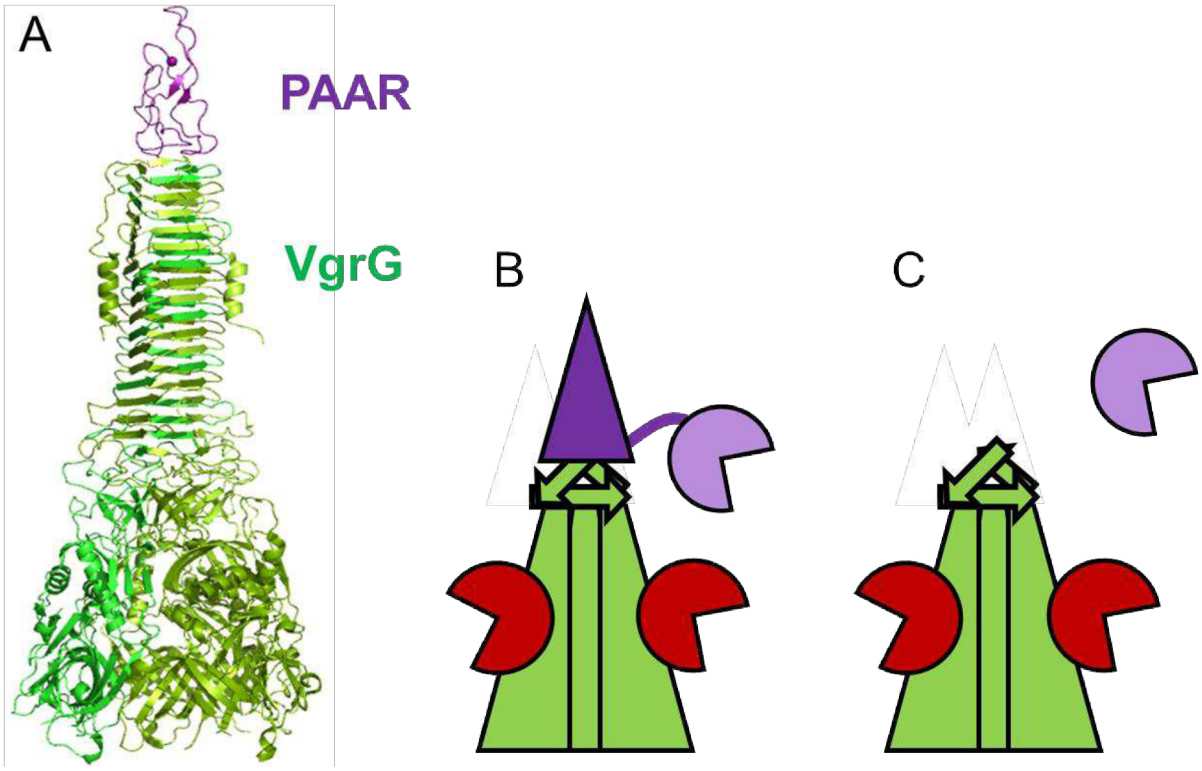


Figure 4-1. The VgrG spike of a T6SS.

A: The T6SS spike is composed of a trimer of VgrG proteins (green, PDB: 4mtk) that form an intertwined needle structure. A PAAR protein (purple, PDB: 4JUV) sits on top of the trimer. B: Model of a decorated T6SS spike. VgrG-dependent effectors (red) and PAAR-dependent effectors (bright purple) associate with the VgrG-PAAR spike and are delivered together with the spike complex [141]. C: In a *paar* mutant, the VgrG trimer might still assemble and recruit its cognate effectors. However, lack of the PAAR protein on top of the VgrG trimer abrogates delivery of the VgrG thus VgrG- and PAAR-associated effectors are not delivered leading to a non-toxic phenotype [148, 149].

PAAR proteins were classified into seven distinct groups, with three of them being relevant for this study [141]. Class 1 comprises PAAR proteins that solely contain PAAR domains and usually are of small sizes between 7 – 25 kDa. Class 2 and class 3 PAARs are polymorphous proteins containing C-terminal extension domains, while here we focus on evolved PAAR effectors, thus containing C-terminal effector domains. Classes 4 to 7 are PAAR proteins with N-terminal extensions of various functions and modular architectures similar to classes 1 to 3. In the case of class 2 PAARs, the N-terminus contains the PAAR fold, while the C-terminus is an effector domain (Figure 4-1B, bright purple). Class 3 PAARs

comprise Rhs proteins that contain N-terminal PAAR folds and additionally harbour massive Rhs repeat core domains prior to the C-terminal toxic domains [212]. Evolved PAAR effectors are thought to have dual functions: their N-terminal PAAR domains assemble on top of the VgrG trimer (Figure 4-1B) and thus facilitate puncturing of target membranes, while the C-terminal domains exert toxicity in the target cells.

Many organisms contain multiple *vgrG* and *paar* genes that are often genetically linked. In many organisms, functional links between these VgrG-PAAR pairs have been established as well [148, 149, 175]. Mutants lacking a PAAR protein or PAAR domain usually display phenotypes deficient for secretion of the cognate VgrG protein (Figure 4-1C), which was shown for the VgrG2b-PA1508 pair in *P. aeruginosa* (Thomas Wood, *unpublished data*). Further, it is a well established model that cognate effectors associate with VgrG-PAAR spikes (Figure 4-1B) [141, 149]. Thus, lack of VgrG delivery further results in abrogation of cognate effector delivery, which was the phenotypic readout for PAAR1 in *Agrobacterium tumefaciens* [149] as well as Rhs1 and Rhs2 in *Serratia marcescens* [148].

Table 4-1. List of all PAAR proteins in *P. aeruginosa* PAO1 and their affiliations with a cognate VgrG.

name	gene number	protein size	cognate VgrG
Tse6	PA0093	45 kDa	VgrG1a [175]
Tse7	PA0099	41 kDa	VgrG1b [175]
PAAR2	PA0824	18 kDa	?
PA1508	PA1508	9 kDa	VgrG2b (Thomas Wood, *unpublished*)
PA1659.1	PA1659.1	10 kDa	?
PA2375	PA2375	13 kDa	(VgrG3)
Tse5	PA2684	146 kDa	VgrG1c [175]
PAAR4	PA3904	13 kDa	VgrG4b, VgrG6 [220]

Interestingly, *P. aeruginosa* encodes a range of PAAR proteins as listed in Table 4-1, while their distribution on the *P. aeruginosa* chromosome can be seen in Figure 1-22. In a recent study about the "á la carte" effector delivery of the *P. aeruginosa* H1-T6SS, our group demonstrated that each VgrG affiliated with the H1-T6SS delivers a cognate PAAR effector [175]. Thus, *P. aeruginosa* fires its H1-T6SS machinery to deliver three different effectors. Specifically, VgrG1a is essential for delivery of the effector Tse6 (Figure 4-2A) which was demonstrated to contain $NAD(P)^+$-glycohydrolase activity [175, 202, 208]. Furthermore, it was shown that delivery of Tse6 also requires the gene product encoded downstream, EagT6 of the DUF1795 family, which has been characterised as an effector chaperone [148, 202]. Another evolved PAAR, Tse7, was shown to be delivered dependent on VgrG1b (Figure 4-2B) [175]. Present in the *vgrG1b* cluster are a number of additional genes, whose functions in Tse7 delivery have not been further characterised yet. Tse5/RhsP1, which is of the Rhs family of T6SS effectors, was shown to require presence of VgrG1c for its delivery (Figure 4-2C) [175, 208]. RhsP1 was proposed to contain an N-terminal cryptic PAAR fold that is thought to assemble on top of the VgrG trimer, while it is unclear how the rest of this massive protein is accommodated around the tip complex.

The ubiquitous presence of *paar* genes next to or within T6SS clusters or orphan operons assigns them an important and probably essential role in T6SS function and effector delivery. Some studies defined PAAR proteins as essential for VgrG delivery and thus effector delivery [141, 148]. Although the accepted concept is that PAAR proteins sit on top of VgrG trimers, and not only contribute to puncturing but possibly associate T6SS effectors to the tip, it is unclear what molecular role PAAR proteins play in the assembly of the VgrG spike and how interactions between PAAR domains and VgrG trimers are maintained.

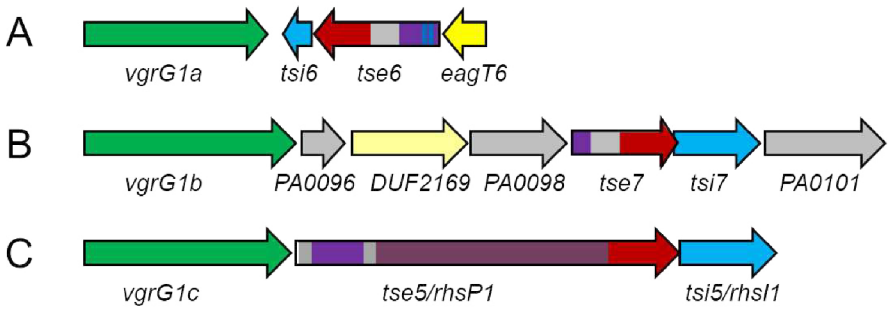


Figure 4-2. *P. aeruginosa* H1-T6SS contains three PAAR protein.

The three *vgrG* operons associated with the H1-T6SS cluster in *P. aeruginosa*. A: *vgrG1a* (green) is encoded upstream of the immunity gene *tsi6* (cyan), the corresponding PAAR effector gene *tse6* (red) and gene encoding for the DUF1795 chadaptor *eagT6* (yellow). B: the *vgrG1b*-cluster comprises of *vgrG1b* (green), a *DUF2169* chadaptor gene (bright yellow) and genes encoding the effector-immunity pair Tse7-Tsi7, together with three more genes whose production contain yet unknown functions (grey). C: *vgrG1c* (green) is encoded just upstream of a gene encoding for the Rhs effector Tse5 (red) and the cognate immunity gene *tsi5* (cyan).

4.2. Aim of this chapter

This study focusses on PAAR proteins and their role in VgrG assembly and effector delivery. In an attempt to design a protein shuttle based on a PAAR concept, we aim at delivering a heterologous effector domain using a well characterised PAAR domain as a vehicle.

Firstly, the concept of essentiality of the PAAR proteins in VgrG secretion will be supported by using the *P. aeruginosa* VgrG1a model. It will be shown that delivery of VgrG1a, the vehicle for the evolved PAAR Tse6, only occurs in presence of Tse6. We will also shed light on the concept of heterotrimer formation of VgrG proteins in *P. aeruginosa*.

Secondly, using bioinformatic analysis, this chapter will investigate possible interaction models between PAAR proteins and VgrG trimers. Multiple sequence alignments and

structural modelling will help determine specific amino acids that are essential for maintaining the binding of a PAAR protein to its cognate VgrG trimer. It will be tested whether the evolved PAAR Tse6 can still interact with a modified version of its cognate VgrG1a and whether VgrG1b can still interact with a modified version of the evolved cognate PAAR Tse7. These experiments will give valuable information about the interaction surface between VgrG and PAAR proteins.

Thirdly, the generated knowledge will be applied to investigate whether a PAAR domain can be adapted to deliver a non-cognate effector domain. The PAAR domain of Tse6 will be used to transport the effector domain of the evolved PAAR Tse7.

Finally, we will show that proteins of the ubiquitous Rhs-effector family are connected to the T6SS via N-terminal PAAR domains and we will shed some light on the involvement of Eag-adaptor proteins on PAAR effector delivery.

4.3. PAAR proteins guide VgrG trimer assembly and delivery

4.3.1. VgrG1a is secreted depending on its cognate PAAR effector

P. aeruginosa PAK encodes three homologous VgrG proteins, VgrG1a, VgrG1b and VgrG1c (VgrG1abc, Figure 4-2), that are all associated with the H1-T6SS cluster [140]. It has been shown in many studies from our lab, that the H1-T6SS and all the associated T6SS clusters, such as the *vgrG1c* orphan cluster, are highly expressed in a regulatory *retS* mutant, as described in 1.3.4 [251]. Hence, secretion of VgrG1abc could be investigated in this background using an antibody generated against purified VgrG1a but that recognises all three VgrG proteins as shown in Figure 4-3B, lane 1 [140].

Here, we further wished to investigate the concept of PAAR essentiality in T6SS function and subsequently the delivery of PAAR effectors by providing further experimental evidence. It is worth noticing that a read out for proper T6SS function could be the analysis of VgrG secretion, which would be found extracellularly only if membrane piercing has occurred [141]. Firstly, secretion of VgrG1a in the absence of its cognate PAAR effector Tse6 was investigated (Figure 4-3A). For this, a *P. aeruginosa* mutant lacking the *tsei6* toxin-immunity gene pair was engineered in the *retS* background and a secretion assay was performed under H1-T6SS-inducing conditions [140]. Briefly, cells were grown until they reached an OD_{600} of approximately 5 and the supernatant was separated from the whole cells by three centrifugation steps. Precipitation of proteins from the supernatant was followed by separation on SDS-PAGE gels, subsequent transfer onto nitrocellulose membranes and western blot analysis.

As can be seen in Figure 4-3, the antibody against VgrG1a nicely recognises the three proteins VgrG1abc at different sizes (lane 1). All three proteins are highly expressed, however in the supernatant only VgrG1a and VgrG1c are detected, not VgrG1b (lane 3), as shown in previous studies [140]. Interestingly, the band corresponding to VgrG1a is found in much lower amount in the supernatant fraction in the absence of Tse6 (lane 4), which is not the case for VgrG1c, thus suggesting that the presence of Tse6 is crucial for VgrG1a delivery. Multiple attempts to complement this phenotype by expressing *in trans* full length Tse6 or truncations corresponding to only the PAAR domain were unsuccessful (*data not shown*). This might be due to overexpression and the high hydrophobicity/insolubility of PAAR domains as discussed in 4.3. Additionally, in *S. marcescens* as well as *Acinetobacter baylyi* it was previously shown that a PAAR protein or PAAR effector is essential for secretion of the cognate VgrG [141, 148]. From our data shown here we also concluded that VgrG1a secretion efficiency depends on the presence of its cognate PAAR effector Tse6.

Figure 4-3 shows, that secretion of VgrG1a is highly impacted in absence of Tse6, however a band corresponding to VgrG1a is still detected in the supernatant of cells that do not produce Tse6 (lane 4). Due to the lack of RNA polymerase in the supernatant fraction (second panel), cell lysis can be excluded. One possible explanation could be that VgrG1a interacts with VgrG1b or VgrG1c and forms heterotrimers, as hypothesised in previous studies [140]. Such heterotrimer might then bind the cognate PAAR of VgrG1b or VgrG1c and thus result in VgrG1a secretion. It was decided to test this hypothesis, starting by assessing whether interactions between VgrG1a, VgrG1b and VgrG1c could actually occur.

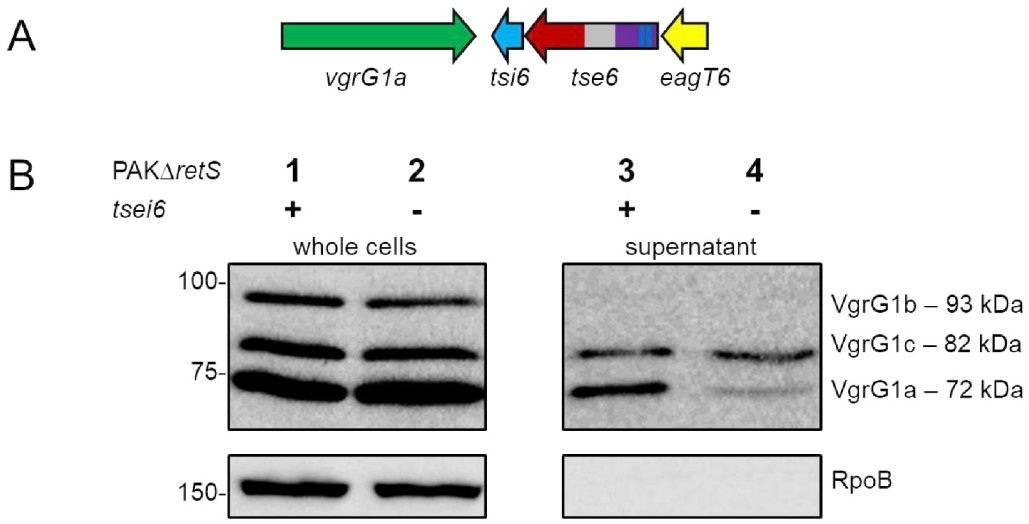


Figure 4-3. VgrG1a is only secreted in presence of its cognate PAAR effector Tse6.

A: *vgrG1a* (green) is encoded upstream of the immunity gene *tsi6* (cyan), the corresponding PAAR effector gene *tse6* (red) and gene encoding for the DUF1795 chaperone *eagT6* (yellow). B: Representative figure of a western blot from a secretion assay of PAKΔ*retS* in presence (+) or absence (-) of the native *tsei6* locus. As a positive control for VgrG1a secretion, PAKΔ*retS* (lane 1) was included. Antibodies were used against VgrG1abc and RpoB as indicated on the right.

4.3.2. VgrG1a, VgrG1b and VgrG1c form heterotrimers

The full length genes for *vgrG1a*, *vgrG1b* and *vgrG1c* were cloned into bacterial-two hybrid plasmids pUT18C and pKT25 containing the gene sequences for the T18- or T25-domains of the adenylate cyclase from *Bordetella pertussis* [224]. This would yield a gene product that contained the T18- or T25 domain at the N-terminus of the chimeric protein, while the C-terminal part would be the VgrG of interest. An appropriate combination of pUT18C and pKT25 plasmids were co-transformed into *Escherichia coli* and in case of interaction between two VgrG proteins of interest, the T18- and T25-domains would heterodimerise to form a functional adenylate cyclase. Enzyme activity results in accumulation of cAMP, which binds to the catabolite activator protein, which in turn results in the expression of β-galactosidase. The enzyme breaks the colorimetric substrate X-Gal, so that colonies appear blue on agar plates [224]. Overnight cultures of clones that carried combinations of *vgrG* plasmids or the empty vector control were spotted in duplicates on LB agar containing the appropriate antibiotics, IPTG and X-Gal. Plates were incubated at 30°C for 30 h and colonies observed.

One representative plate showing interactions between all three VgrGs is shown in Figure 4-4. All three VgrG proteins show a high degree of self-interaction, as indicated by the red boxes, while VgrG1a also interacts with VgrG1b and VgrG1c. However, this interaction only seemed to work in one direction of plasmids. Interaction between VgrG1a and VgrG1b is stronger than interactions between VgrG1a and VgrG1c, while VgrG1b and VgrG1c do not seem to interact. It needs to be stated at this point, that all of these results solely rely on visual observation and would need quantification to significantly conclude these findings.

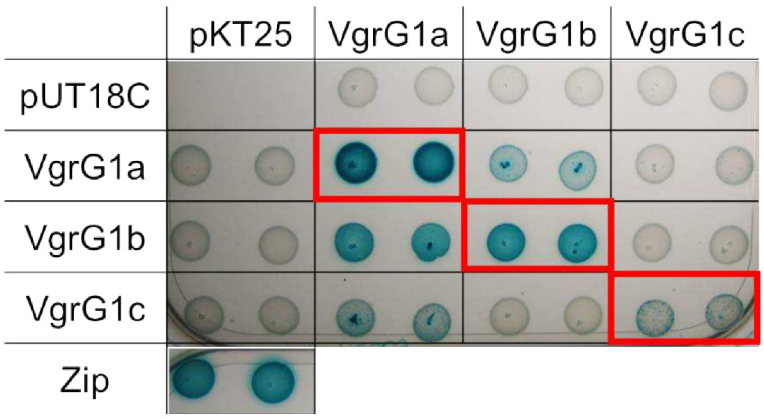


Figure 4-4. VgrG1a, VgrG1b and VgrG1c can form heterotrimers.

Bacterial-two-hybrid plate testing interactions between VgrG1a, VgrG1b and VgrG1c. Colonies contain plasmids expressing VgrG1a, VgrG1b and VgrG1c as indicated and were spotted in duplicates. Plasmids pUT18C or pKT25 contained the gene sequences for *vgrG1a, vgrG1b* or *vgrG1c* and were introduced in all possible combinations into DHM1 cells. Self-interactions are highlighted in red boxes, while empty vector controls can be seen in the top panel and first column. The zip control expressed a functional adenylate cyclase.

4.3.3. VgrG1a does not depend on VgrG1b or VgrG1c for secretion

Since VgrG1a can form heterotrimers with VgrG1b and VgrG1c *in vitro*, it was assumed that the cognate PAAR protein for VgrG1b, Tse7, or VgrG1c, RhsP1, could also mediate secretion of VgrG1a. In detail, if VgrG1a forms heterotrimers with VgrG1b, which from the bacterial two hybrid results is highly likely, Tse7 would need to be able to recognise a VgrG1a-VgrG1b heterocomplex. On the other hand, if VgrG1a forms heterotrimers with VgrG1c, RhsP1 would need to be able to recognise a VgrG1a-VgrG1c heterocomplex. To assess this, mutants with different combinations of deletions in *vgrG1b, vgrG1c, vgrG1a* and *tsei6* were engineered and secretion assays performed (Figure 4-5). If our hypothesis was correct, VgrG1a would not be found in the supernatant of those cells that did not express the VgrG that facilitates secretion of VgrG1a in the absence of Tse6.

As seen in Figure 4-3, VgrG1b, VgrG1c and VgrG1a are readily detectable in the whole cell fraction as monomers (Figure 4-5, second panel, lane 1) and as multimers (top panel), while VgrG1c and VgrG1a are clearly detected in the supernatant (second panel, lane 10). Interestingly, multimer formation inside the cells correlated with presence of both VgrG1a and Tse6 (lanes 1, 3, 5 and 7), while in the supernatant fraction multimer detection correlated with secretion of VgrG1a or VgrG1c (lanes 10-14, 16, 18). It has been demonstrated before and can be confirmed here, that the presence of either VgrG1a or VgrG1c is sufficient to form a functional H1-T6SS [140]. The panels showing secretion of Hcp1 and Tse3 confirm the functionality of the H1-T6SS. Lanes 2 and 11 show expression and secretion using a *vgrG1a* deletion mutant, so that VgrG1a bands can be distinguished from any unspecific band detected by the antibody.

As seen previously (Figure 4-3), the amount of VgrG1a inside the cells is not affected by the absence of Tse6 (lane 9), however, secretion of VgrG1a is massively decreased (lane 18). Furthermore, in the presence of Tse6, secretion of VgrG1a is not affected by the absence of VgrG1b (lane 12), VgrG1c (lane 14) or both (lane 16). We had hypothesised that the residual VgrG1a secretion observed in the absence of Tse6 (lane 18), could be further decreased in a background lacking VgrG1b (lane 13), VgrG1c (lane 15) or both (lane 17). Yet, no further decrease was observed, indicating that a VgrG1a homotrimer is likely able to pierce the membrane without its cognate PAAR, although inefficiently, and therefore be secreted.

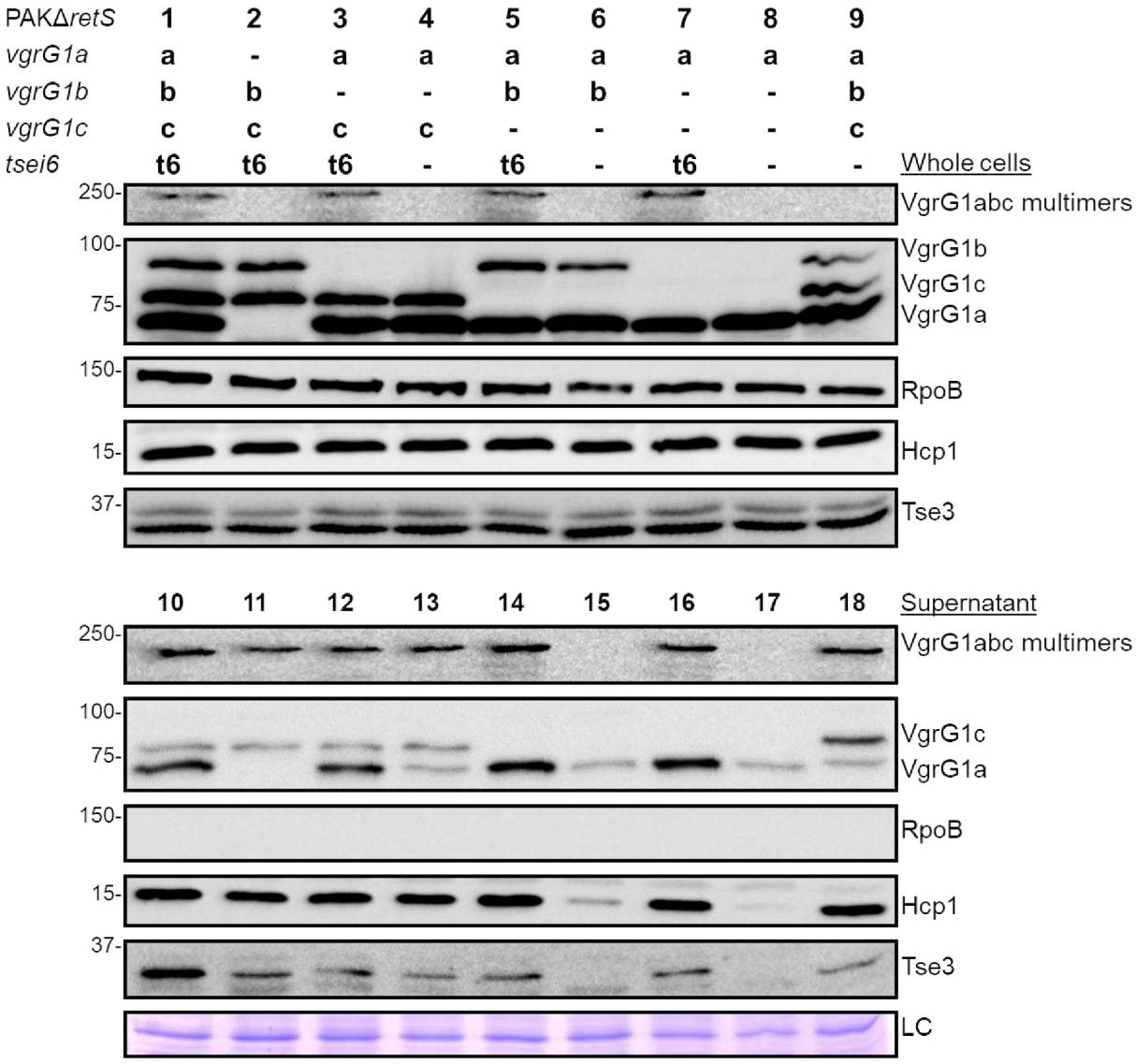


Figure 4-5. VgrG1a secretion is independent of Tse6, VgrG1b and VgrG1c.

Representative figure of a western blot from a secretion assay of PAKΔ*retS* in presence of *vgrG1a* (a), *vgrG1b* (b), *vgrG1c* (c) or *tsei6* (t6) or absence of either (-). As a positive control for VgrG1a secretion, PAKΔ*retS* (lane 1) was included. As a control for VgrG1a antibody detection PAKΔ*retS*Δ*vgrG1a* was included (lane 2), the negative control for VgrG1a secretion lacked *tsei6* (lane 18). Antibodies were used against VgrG1abc, recognising VgrG1abc multimers (top panel) or monomers (second panel), RpoB, Hcp1 and Tse3 as indicated on the right. A section from a Coomassie gel was included to assure equal loading of the supernatant fractions (LC). Secretion assays were performed at 37 °C.

Here, we provide evidence that VgrG1a secretion is massively reduced in absence of its cognate PAAR effector Tse6. These results are in good agreement with other studies

showing that indeed PAAR proteins are the prerequisite for VgrG and thus effector delivery [141, 148]. In *S. marcescens* three VgrG-PAAR assemblies were proposed between VgrG1 and PAAR1 and VgrG2 and one of the two Rhs effectors Rhs1 or Rhs2 [148]. For the *P. aeruginosa* H1-T6SS, we also propose three assemblies based on the findings here: VgrG1a-Tse6, VgrG1b-Tse7 and VgrG1c-Tse5. These functional pairs were already identified in previous studies as VgrG-effector pairs [175, 208], while here we specify them as VgrG-PAAR pairs with either the VgrG1a-Tse6 or VgrG1c-Tse5 being sufficient for the assembly of a functional T6SS tip.

Putting these data into a physiological setting, this mechanism can be understood as a protein-saving mechanism. In the case of Tse6 in *P. aeruginosa* [202] or Rhs1 and Rhs2 in *S. marcescens* [200], the PAAR protein carries an effector domain. These are thought to use their cognate VgrGs as vehicles to reach target cells [175, 202]. If the PAAR effector is missing in the cells, there is no rationale in delivering an empty VgrG spike into target cells without causing any damage. Thus, to recycle the protein and its building block, it is probably retained within the cells.

4.4. PAAR proteins bind their cognate VgrG trimers *via* the last β-sheet

4.4.1. Analysing the interface between PAAR domains and VgrG trimers

PAAR proteins are proposed to be essential parts of the T6SS machinery [141]. The reason would be that a VgrG trimer cannot by itself puncture the membrane and drive effector delivery. Instead, a cone-like PAAR domain or protein should be fitted at the tip of the torch-like structure of the VgrG trimer, thus sharpening the spike and allowing membrane piercing [141]. The flat bottom of the cone-shaped PAAR protein offers a large interaction

surface which is thought to bind the C-terminal blunt end of a VgrG trimer (Figure 4-6B). The very end of VgrG trimers was shown to be formed of three intertwined β-sheets [141], as indicated in Figure 4-1B. However, it is unclear whether these three β-sheets are required and sufficient to mediate specific binding to the cognate PAAR, bearing in mind that not all PAARs would fit on any VgrGs, and thus a level of specificity is expected.

For bioinformatical and structural analysis, PAAR proteins and PAAR domains of effectors were chosen, that were experimentally demonstrated to be involved in VgrG secretion [141, 149, 202] or are encoded in *P. aeruginosa* and *P. putida* [136]. A multiple sequence alignment shows conservation between those proteins (Figure 4-6A). To further pinpoint those amino acids mediating the binding to VgrG proteins we needed to revert to a more structural approach.

The structure of a gp5-PAAR (VgrG-2-VCA0105) complex of *V. cholerae* (pdb: 4jiv) has been solved previously [141], making it a valuable template for all models presented in this study. Above mentioned PAAR proteins or PAAR domains were structurally modelled with Phyre2 [235] and fitted onto the template from *V. cholerae* using PyMOL. Since the structure of VgrG1a from *P. aeruginosa* was also recently solved (pdb: 4mtk), we fitted this structure onto the gp5-template from *V. cholerae*. As can be seen in Figure 4-6B, the model of the PAAR domain of Tse6 (purple) fits nicely onto the blunt end of the VgrG1a trimer (green). We could readily identify the three highly conserved PAAR motifs that form the intertwined core of the PAAR fold (highlighted in red in both Figure 4-6A and B). Furthermore, we closely examined the interaction surface between the Tse6-model and VgrG1a. We identified three amino acid stretches of four residues at the bottom of the PAAR model that are in close proximity to VgrG1a (highlighted as blue sticks). When we mapped these amino acid stretches onto the multiple sequence alignment in Figure 4-6A, we observed that they clustered with similar stretches from other PAAR proteins (highlighted with blue lines). We then identified in other structural PAAR models these amino acids at the same location and listed them for each

PAAR protein in Table 4-2. Interestingly, these conserved stretches contain mainly hydrophobic amino acids and are in good agreement with other works that identified potential interactions sites within PAAR proteins [141, 220].

In the structural model in Figure 4-6B, one can observe that the PAAR domain sits on top of the blunt end of the VgrG trimer [141]. This blunt end corresponds to the three last intertwined β-sheets from each VgrG monomer (Figure 4-6B, green sticks). Thus, we asked whether there is a conserved binding motif within the last VgrG β-strand that would mediate specific binding to the cognate PAAR protein.

We sequence aligned the cognate VgrG proteins of the above analysed PAAR proteins as well as additional VgrG proteins that are known to bind PAAR domains. Figure 4-7A displays a high conservation throughout the first approximately 600 aa corresponding to the gp5-/gp27-like domains. We then mapped the last β-strand of VgrG1a from the structure onto the sequence alignment and surprisingly identified that these four amino acids are somewhat clustered together within VgrG proteins (Figure 4-7B, highlighted by a green line). Interestingly, in VgrG1b^{Paer}, VgrG1c^{Paer}, VgrG1^{Pput}, VgrGA^{Dda}, VgrG1^{Eco} and VgrG2^{Atu}, this area corresponds to the very C-terminus of the protein suggesting that indeed these four amino acids form the very last β-strand within these VgrG trimers [141]. Analysing these last β-strands from the different VgrG proteins, no conserved motif can be recognised, however mostly hydrophobic amino acids seem to be involved (Table 4-2). This not only agrees with previous studies [141, 149], but also with the fact that the interface from the PAAR protein exhibits mainly hydrophobic amino acids (Table 4-2).

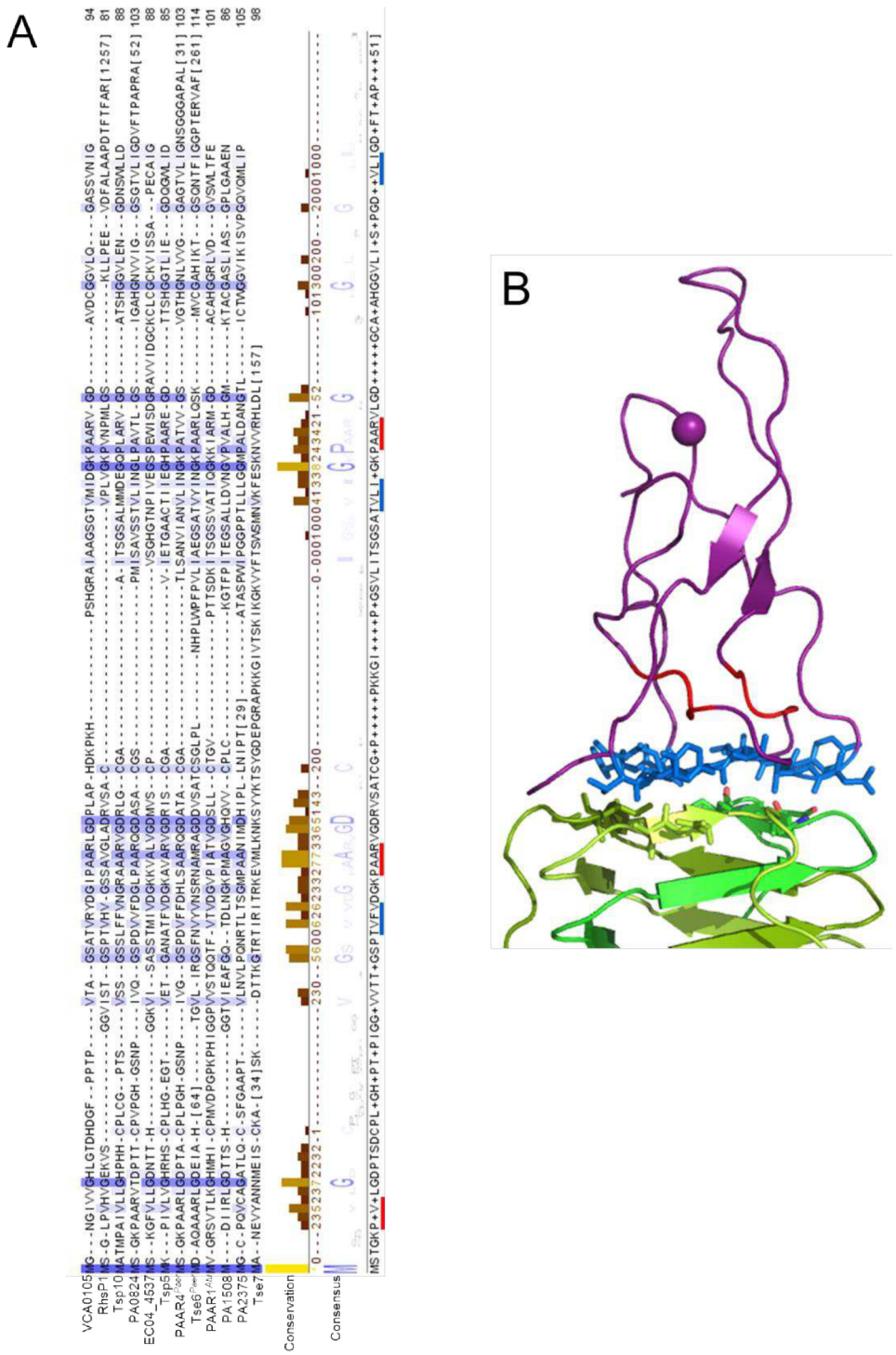


Figure 4-6. PAAR proteins contain specific residues to bind their cognate VgrG trimers.

A: Multiple sequence alignment of PAAR proteins. The highly conserved PAAR motifs are highlighted with a red line; amino acids interacting with the last β-strand of the VgrG trimer are highlighted with a blue line [141]. B: Model of the PAAR domain of Tse6 (purple) interacting with the last β-sheet of a VgrG1a trimer (pdb: 4mtk, green). The three conserved PAAR motifs are highlighted in red, while the residues involved in VgrG binding are highlighted as blue sticks. Green sticks highlight amino acids within VgrG1a that are involved in the interaction with the PAAR domain.

With the help of multiple sequence alignments and structural analysis, we were able to identify amino acids that are potentially involved in the interactions between PAAR and VgrG proteins. Since no conserved motifs could be identified in neither VgrG or PAAR proteins, the hypothesis would be that specific amino acid residues mediate specific interactions. This would underline how the PAAR domain of Tse6 specifically binds to the VgrG1a trimer and not to VgrG1b or VgrG1c (4.3.3) supporting the basic idea of the "á la carte" effector delivery concept [175]. Further, specific VgrG-PAAR interactions were also suggested in *A. tumefaciens* that expresses the functional VgrG1-PAAR1 and VgrG2-PAAR2-pairs [149]. Remarkably, a truncation version of VgrG1 would only interact with its cognate PAAR1 when it contained the amino acid sequence QINF of its putative last β-sheet [149]. Furthermore, the amino acid residues at the interfaces of VgrG1, VgrG2 and PAAR1, PAAR2 are distinct (Table 4-2), supporting our hypothesis that these regions mediate specificity.

Interestingly, PAAR2 and PAAR4 from *P. aeruginosa* exhibit similar amino acid residues in the regions predicted to be accessible for VgrG interactions (Table 4-2). Hence, we hypothesised that PAAR2 and PAAR4 might interact with the same cognate VgrG. Notably, a recent study showed that PAAR2 can functionally replace PAAR4 indicating that PAAR2 and PAAR4 bind and deliver the same VgrG trimer [220]. This, however, is not the first example in promiscuity of VgrG-PAAR pairs. In *S. marcescens*, it was shown that VgrG2 can bind and deliver two different PAAR-containing effectors, Rhs1^{Smar} and Rhs2^{Smar}, that additionally require interactions with two distinct Eag proteins, Eag1 and Eag2, respectively [148]. On the basis of these findings, we suggested that the interaction surface of the PAAR domains of Rhs1^{Smar} and Rhs2^{Smar} would be similar. Indeed, when analysing both PAAR domains, we observed that they contain identical or similar amino acid residues in two of the three regions predicted to interact with VgrG2^{Smar} (Table 4-2). The third interaction site is rather distinct and might be associated with the recruitment of the specific and cognate Eag protein [148].

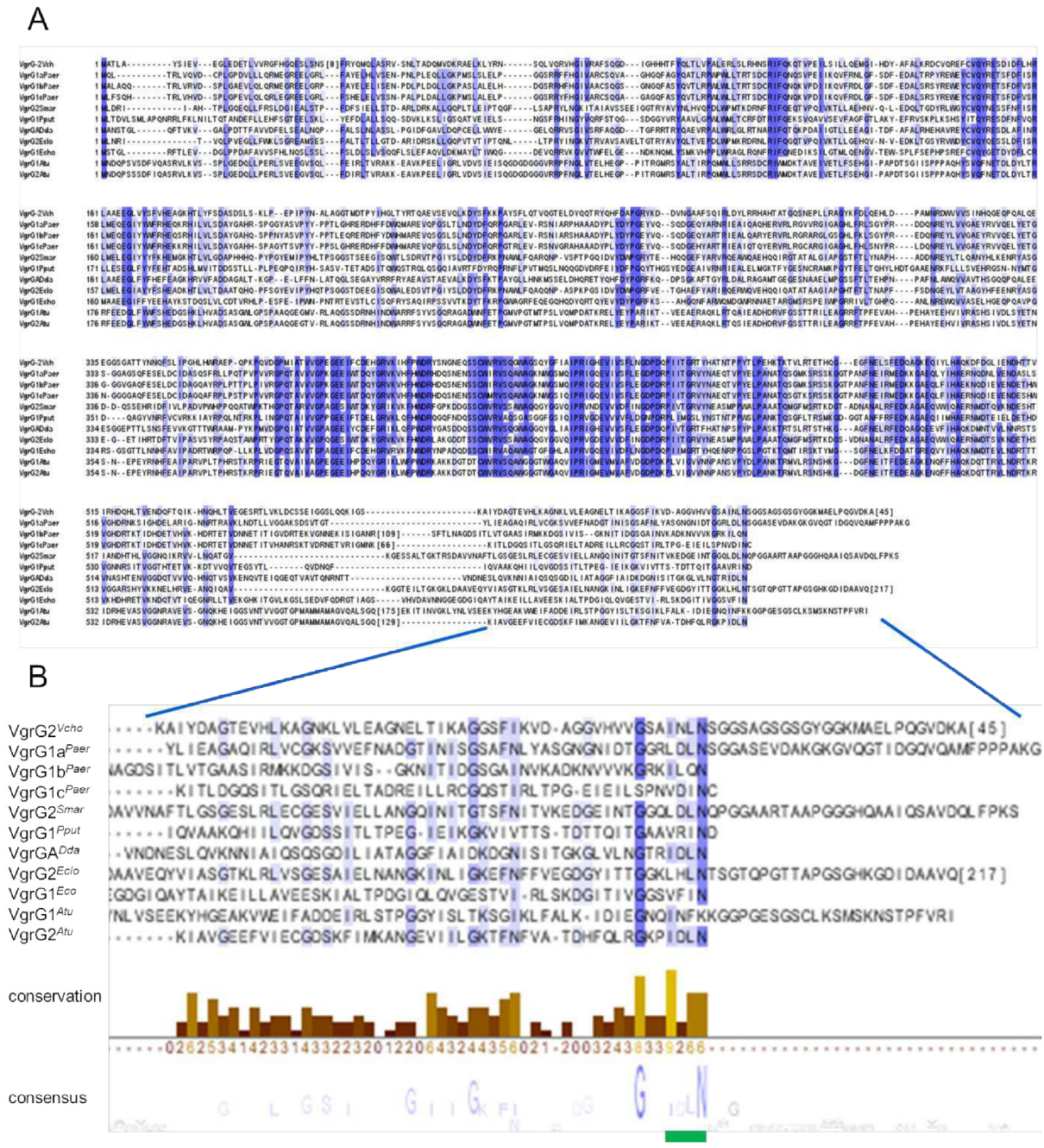


Figure 4-7. The last β-strand within VgrG proteins is conserved.

A: Multiple sequence alignment of VgrG proteins that are genetically associated with the PAAR proteins discussed in the previous paragraph. Identical amino acids are highlighted with blue boxes. B: Close-up of the sequence alignment from A on the C-terminal 50 amino acids highlighting a conserved amino acid stretch with a green line. This stretch corresponds to the putative last β sheet in VgrG trimers and might mediate the interactions with the cognate PAAR domain (Figure 4-6B).

Table 4-2. Interactions sites of characterised VgrG-PAAR pairs

This table lists amino acid residues that potentially mediate interactions between VgrG (see Figure 4-7A, green line) and PAAR proteins (Figure 4-6A, purple line). VgrG-2-VCA0105 from *V. cholerae* is the positive control for specific interactions according to [141] and the identified and putative VgrG-PAAR pairs from *P. aeruginosa*, *A. tumefaciens* and *S. marcescens*. Motifs in brackets state that the modelling was not very convincing due to variability in the lengths of the VgrG tips.

VgrG-PAAR pair	last VgrG β-strand	PAAR interaction sites			references
VgrG-2^{Vcho}-VCA0105	AINL	TVRY	TVMI	SVNI	[141]
VgrG1a-Tse6	RLDL	NVYV	TVYI	NTFI	[175]
VgrG1b-Tse7	(KILQ)	Not modelled	TIRI	NVFKE	[175]
VgrG1c-RhsP1	(NVDI)	TVHV	CPLV	ALAA	[175]
VgrG2b-PA1508	?	QTDL	LLDV	GAAE	Thomas Wood
VgrG4b-VgrG6-PAAR4	(LARI)/(NVRV)	DVFF	NVLI	TVLI	[220]
(VgrG4b-VgrG6-)PAAR2	(LARI)/(NVRV)	DVVF	TVLI	TVLI	[220]
VgrG3-PA2375	(LVKV)	RTLT	TLLL	QMLI	
VgrG1^{Atu}-PAAR1^{Atu}	QINF	FVTV	VATI	WLTF	[149]
VgrG2^{Atu}-PAAR2^{Atu}	PIDL	TWTT	KAMV	VESV	[149]
VgrG2^{Smar}-Rhs1^{Smar}	QLDL	NVFT	VFIN	NVQI	[148]
VgrG2^{Smar}-Rhs2^{Smar}	QLDL	NVFI	VSIN	VFIG	[148]

4.4.2. Disrupting Tse7-binding to its cognate VgrG1b

Ideally, the above model should be applied in an experimental context where the interactions between a PAAR domain with its cognate VgrG could be functionally assessed. The chosen example was VgrG1b of *P. aeruginosa*, which is proposed to be topped by the PAAR domain of its cognate effector Tse7 as discussed in 4.3. The VgrG1b trimer was modelled using Phyre 2 with VgrG1a (pdb:4mtk) as a template, however there is a caveat in this model. VgrG1a and VgrG1b have different sizes (compare protein bands in Figure 4-3) and protein prediction tools identified a weak similarity with a DUF2345 at the C-terminus of VgrG1b which might lead to an elongated VgrG1b tip [216]. Hence, the Phyre tool modelled

the overlapping amino acids of VgrG1b onto the template of VgrG1a while the remaining C-terminal amino acids were not fitted onto the VgrG1a structure and are not part of the model. If they fold into an extended β-prism shape based on the DUF2345 domain, as suggested in previous studies [216], it makes it impossible to predict the last β-strand forming the blunt end of the trimer. However, the PAAR domain of Tse7 could be modelled adequately and fitted on top of the VgrG1b model (Figure 4-8A).

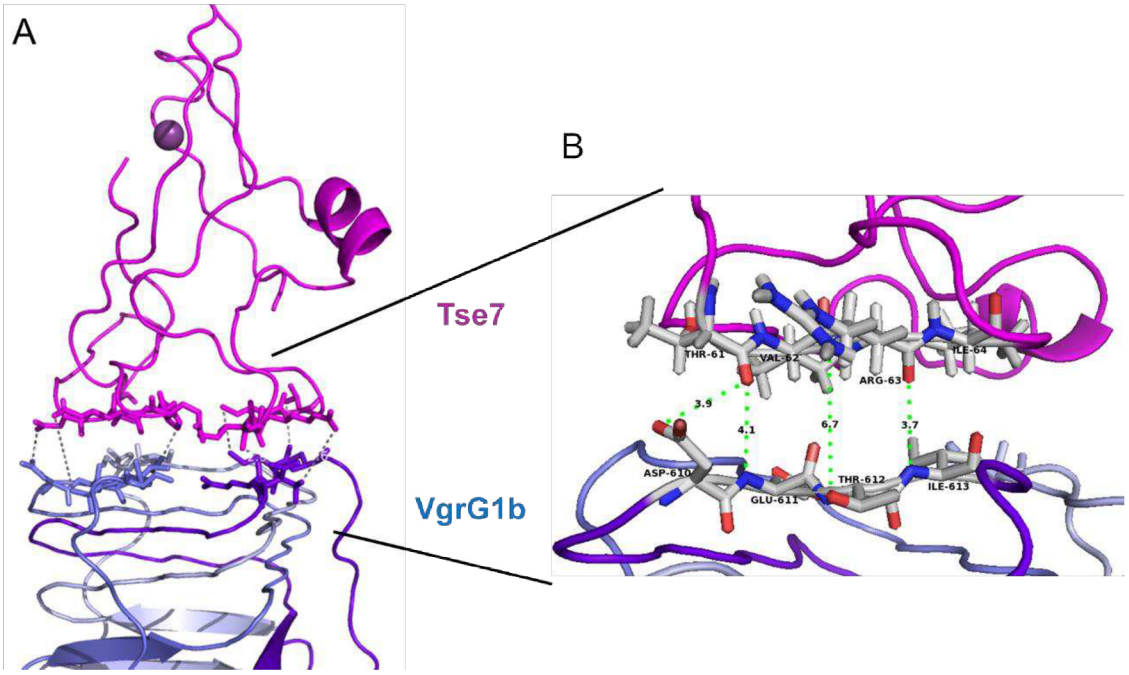


Figure 4-8. The PAAR domain of Tse7 sits on top of the VgrG1b-trimer.

A: Model of the PAAR domain of Tse7 (magenta) capping a VgrG1b trimer (blue, purple). B: Close-up of interacting surface between VgrG1b and Tse7. The whole bottom of the PAAR domain of Tse7 covers the surface assembled by the three last β-strand of the VgrG1b monomers. Distances between key residues in both proteins were measured using PyMOL and are solely based on the models of both proteins.

The docking of the PAAR domain of Tse7 onto the modelled VgrG1b trimer allowed the identification of key residues within the interface of VgrG1b and Tse7 (Figure 4-8B, Table 4-2). One of the interaction sites within the PAAR domain with the sequence T61-I62-R63-T64

was mutated to a sequence of AIQN to change the properties of those residues. This was hypothesised to disrupt the interface between VgrG1b and Tse7. Experiments to assess this hypothesis were conducted by another PhD student in the laboratory, Panayiota Pissaridou, and have shown that Tse7 carrying these mutations was not delivered into prey strains (*data not shown*) suggesting that the four amino acids T61-I64 are essential for the interaction and subsequent Tse7-VgrG1b-delivery (*co-authored publication under review at PNAS*). This result comes in supports of the model presented above and can likely be used as the basis for further experiments.

4.4.3. Designing chimerae to study interactions between VgrG1a and the PAAR domain of Tse6

As discussed in 4.3.1, delivery of the VgrG1a spike in *P. aeruginosa* is only triggered in presence of the cognate PAAR effector Tse6. Here, we further want to confirm our models obtained from the bioinformatic analysis (4.4.1) and want to prove which part of VgrG1a is essential for PAAR binding. The basis of this study are chimerae in which the interface at the tip of the trimer is compromised in a way that it may challenge the fit with the cognate PAAR effector.

Chimerae between two different VgrG proteins originated from two different organisms were engineered as described below and visualised in Figure 4-9. The main part, the gp5-/gp27-like domains, originates from VgrG1a from *P. aeruginosa*, here now labelled as VgrG1a^{P}, while the C-terminal part originates from VgrG1 from *A. tumefaciens*, from now on termed as VgrG1^{A}. On the basis of the recent study by Bondage and collaborators [149], we dissected the C-terminal domain of VgrG1^{A} into two parts. Residues 787 (green arrow labelled "B") to 794 (green arrow labelled "C") encompass the last VgrG1^{A} β-strand containing the sequence QINF (see Table 4-2 and Figure 4-9, red arrow labelled "PAAR"). The second part

corresponds to the extending amino acids after residue 795, that are thought to interact with the cognate effector Tde1, hence labelled “effector binding” in Figure 4-9.

In 4.4.1, we analysed the interaction surface between VgrG1a^{P} and its cognate Tse6 PAAR domain and together with the structure of VgrG1a^{P}, we identified the amino acids forming the last β-strand responsible for PAAR binding (Table 4-2). Thus, we designed three chimerae in which different parts of the C-terminal VgrG1a^{P} extension are substituted (Figure 4-9). Construct A (VgrG1a^{P}-G1^{A31}) contains the full length VgrG1a^{P} extended by 31 C-terminal amino acids from VgrG1^{A}. This extension includes amino acids that are possibly responsible for binding the cognate PAAR1^{A} and Tde1 [149]. Construct B (VgrG1a^{P605}-G1^{A31}) covers the first 605 amino acids from VgrG1a^{P} and the 31 C-terminal amino acids from VgrG1^{A}, with the swapping point indicated by the green arrow labelled “B” in Figure 4-9. Thus, the last β-sheet of VgrG1a^{P} is substituted by the putative last β-sheet of VgrG1^{A} Figure 4-7. Construct C (VgrG1a^{P614}-G1^{A21}) comprises of the first 614 amino acids from VgrG1a^{P} and the 21 C-terminal amino acids from VgrG1^{A} and the swapping point is indicated by the green arrow labelled “C” in Figure 4-9. This chimera includes the last β-sheet of VgrG1a^{P}, while the extending amino acids of VgrG1a^{P} are substituted by the proposed effector binding amino acids of VgrG1^{A}.

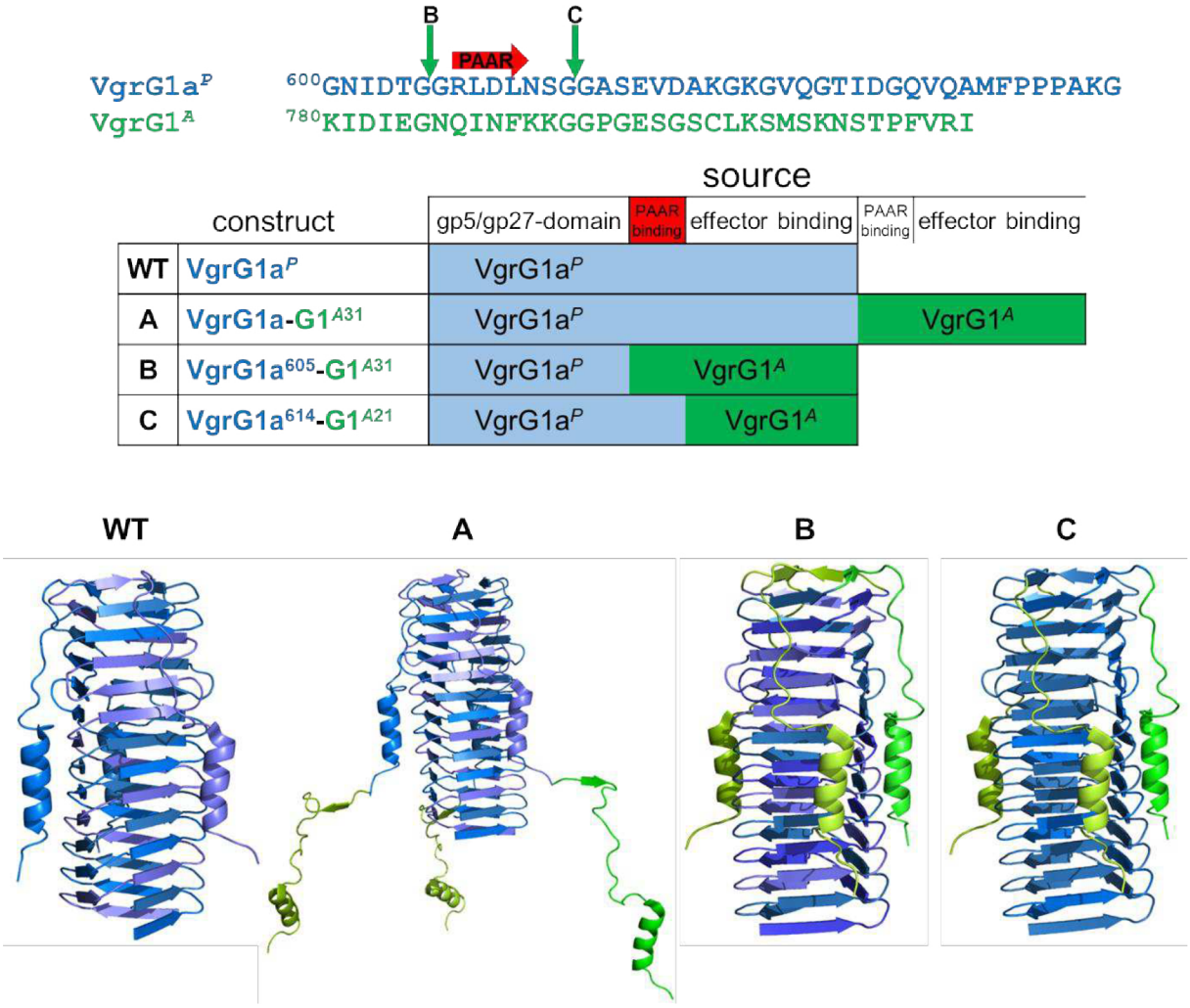


Figure 4-9. Overview of design of the chimerae under investigation.

The top panel represents the amino acid sequences of the C-terminal extensions of VgrG1a^P (blue) and VgrG1^A (green). The putative last β strand is highlighted with a red arrow. The location of the swaps for chimerae B and C are highlighted with green arrows. Structural models of the tips of the chimerae are shown in the bottom panel. WT corresponds to the full-length sequence of VgrG1a^P (blue). In construct A, the STOP codon of *vgrG1a*^{P} was replaced by the sequence corresponding to the last 31 aa of VgrG1^A (green) resulting in a bigger version of the protein. Construct B was designed by substituting the codon sequence of the last 35 aa of *vgrG1a*^{P} (green arrow "B" in the top panel) with the sequence corresponding to the last 31 aa of VgrG1^A (green). Construct C was designed by substituting the codon sequence of the last 29 aa of *vgrG1a*^{P} (green arrow "C" in the top panel) with the sequence corresponding to the last 21 aa of VgrG1^A (green).

4.4.4. Full length VgrG1a is required to bind its cognate PAAR-domain

As shown in 4.3.2, VgrG1a^{P} forms homotrimers, which is likely the basis for forming a PAAR-binding interface at the T6SS spike [141]. To understand whether the various VgrG1a^{P}-VgrG1^{A} chimerae would form functional trimers, the ability to self-interact was tested. The corresponding gene sequences were cloned into BTH plasmids, as described previously, resulting in gene products that contain N-terminal T25 and T18-adenylate cyclase domains fused to each of the VgrG variants. As observed on a LB-agar plate containing X-Gal in Figure 4-10, each single chimera was able to self-interact and likely to form a homotrimer.

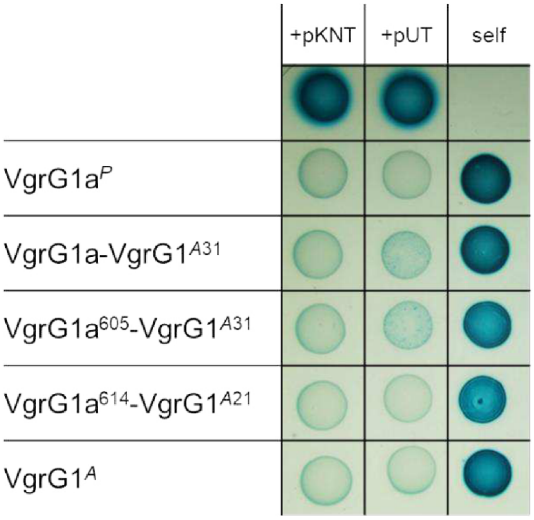


Figure 4-10. Chimerae between VgrG1a^{P} and VgrG1^{A} self-interact.

Bacterial two hybrid plate showing that chimerae between VgrG1a^{P} and VgrG1^{A} are self-interacting. Plasmids pUT18C or pKT25 contained the gene sequences for *vgrG1a* and derivates were introduced in all possible combinations into DHM1 cells. Self-interactions are highlighted in red boxes, while empty vector controls can be seen in the top panel and first column. The zip control expressed a functional adenylate cyclase.

Next, the chimerae were tested for their ability to bind Tse6 and henceforth an indirect readout was chosen by looking at secretion of the VgrG chimerae. For this, we engineered

strains that encoded one of the chimerae in absence (Figure 4-11A) or presence (Figure 4-11B) of the homologues VgrG1b and VgrG1c. This set of experiments will help us understand whether the presence of the other two spike proteins, VgrG1b and VgrG1c, has any influence on chimera secretion.

Independent of the presence of VgrG1b and VgrG1c, bands for VgrG1a^{P} (lanes 1 and 11) and all chimerae are readily detectable in the whole cell samples at approximately 75 kDa (lanes 3 - 5, 13 - 15). Due to the 31-amino acid extension in construct A (Figure 4-9), shifts in the size for construct A are clearly detectable (lanes 3 and 13, asterisks). The detected band for construct B is weaker than the one for VgrG1a^{P} (lanes 4 and 14), which could be due to instability of the chimera or decreased detection by the antibody after epitope modification.

As expected and shown previously (see 4.3.1), VgrG1a^{P} forms a functional T6SS in absence of VgrG1b and VgrG1c (Figure 4-11A) resulting in its secretion (top panel, lane 6) as well as secretion of the landmark protein Hcp1 and the Hcp1-dependent effector Tse3 (third and fourth panel). Similarly, construct A is secreted together with Hcp1 and Tse3, which suggests it is fully functional despite the C-terminal extension (lanes 8 and 18, asterisks). This is in good accordance with results from the previous chapter, which showed that VgrG1a^{P} with a C-terminal extension is secreted. Here, the extension is of smaller size, hence less impact on chimera secretion would be expected.

As a control and in the absence of all three VgrG1a, VgrG1b and VgrG1c, no Hcp1 and Tse3 are detected in the supernatant (lane 7) suggesting the H1-T6SS is non-functional. In contrast to construct A (lane 8), and although the constructs B and C were detected in the whole cell lysate samples, no effective secretion could be detected (lanes 9 and 10). Further, no Hcp1 and Tse3 were found in the supernatant (third and bottom panel), suggesting that chimerae B and C are unable to form functional H1-T6SSs. Neither chimerae B or C were

secreted in presence of VgrG1b and VgrG1c (lanes 19 and 20) confirming that they could not be transported as potential heterotrimers.

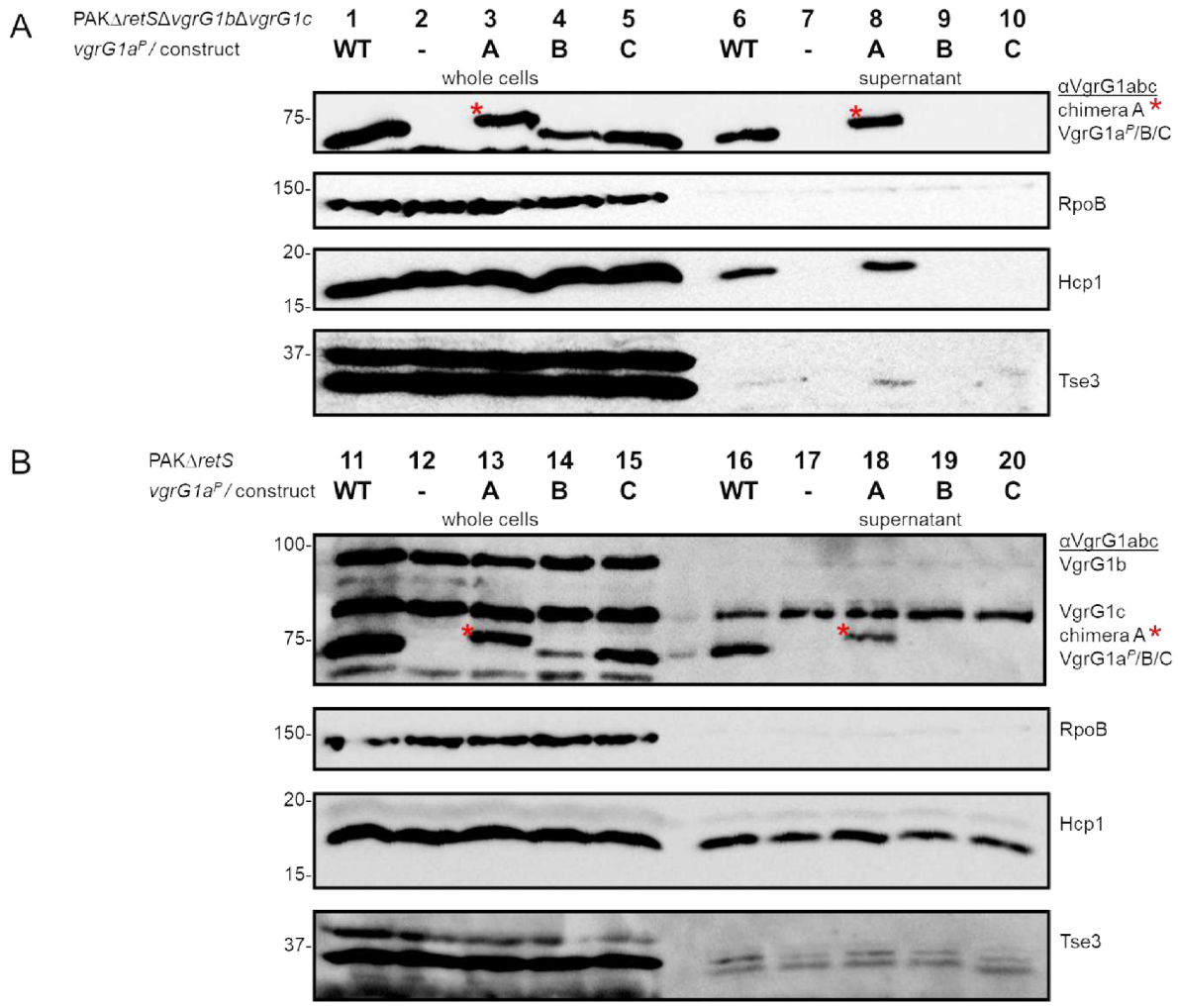


Figure 4-11. Only chimera A can form a functional T6SS spike.

Representative figures of western blots from secretion assay of (A) PAKΔ*retS*Δ*vgrG1b*Δ*vgrG1c* or (B) PAKΔ*retS* expressing WT VgrG1a (WT) or one of the chimerae (A/B/C). As positive controls for VgrG1a expression and secretion, the parental strains were each included (lanes 1, 6, 11 and 16). As a control for VgrG1a antibody detection, each of the parental strains lacking *vgrG1a* were included (lanes 2 and 12). Antibodies were used against VgrG1abc, RpoB, Hcp1 and Tse3 as indicated on the right. Highlighted with asterisks are the bands corresponding to chimera A.

Due to the observed secretion of construct A, one might suggest that this construct can bind the PAAR domain of Tse6. To prove this concept and further demonstrate the functionality of this chimera we wanted to assess whether it can deliver the Tse6 effector into prey cells. To do so, competition assays were performed against PAKΔ*retS* prey cells that lack genes for *tse6* and the cognate immunity *tsi6* (Figure 4-2A). Briefly, prey and attacking strains were incubated together for 5 h as a dried spot on a LB agar plate and afterwards the spots were recovered and diluted. All dilutions were spotted onto LB agar containing X-Gal. Due to the presence of a constitutive active β-galactosidase within the prey strain, surviving attacker and prey strains could be distinguished and quantified [247]. If the attacking strain delivers Tse6 into the prey cells, recovery of the prey is reduced due to the detrimental effect of Tse6 [175, 202].

Plots in Figure 4-12 show the cfu of recovered prey cells after grown in contact with attacker strains that expressed either of the chimerae in absence (Figure 4-12A) or presence (Figure 4-12B) of the homologues VgrG1b and VgrG1c. Again, we wanted to rule out that the presence of the other two spike proteins would have an impact on Tse6 delivery. High survival of the prey strains was ensured when they were growing on their own (lanes 1 and 7) or in contact with the attacking strains lacking *vgrG1a* (lanes 3 and 9). In the latter case, no Tse6 was delivered and thus survival of the prey was not compromised, which agrees with previous studies [175]. Independent of the presence of VgrG1b and VgrG1c, after contact with the parental strain, the number of recovered prey cells was significantly reduced due to delivery of Tse6 (lanes 2 and 8). Attacking strains expressing constructs A (lanes 4 and 10) or C (lanes 6 and 12) had competitive advantages similar to what was observed with the parental strain. When attacking strains expressed construct B (lanes 5 and 11), recovered prey cfu was high. This suggests that the two chimerae A and C could deliver Tse6 into prey cells, while this phenotype was abrogated in strains that expressed chimera B.

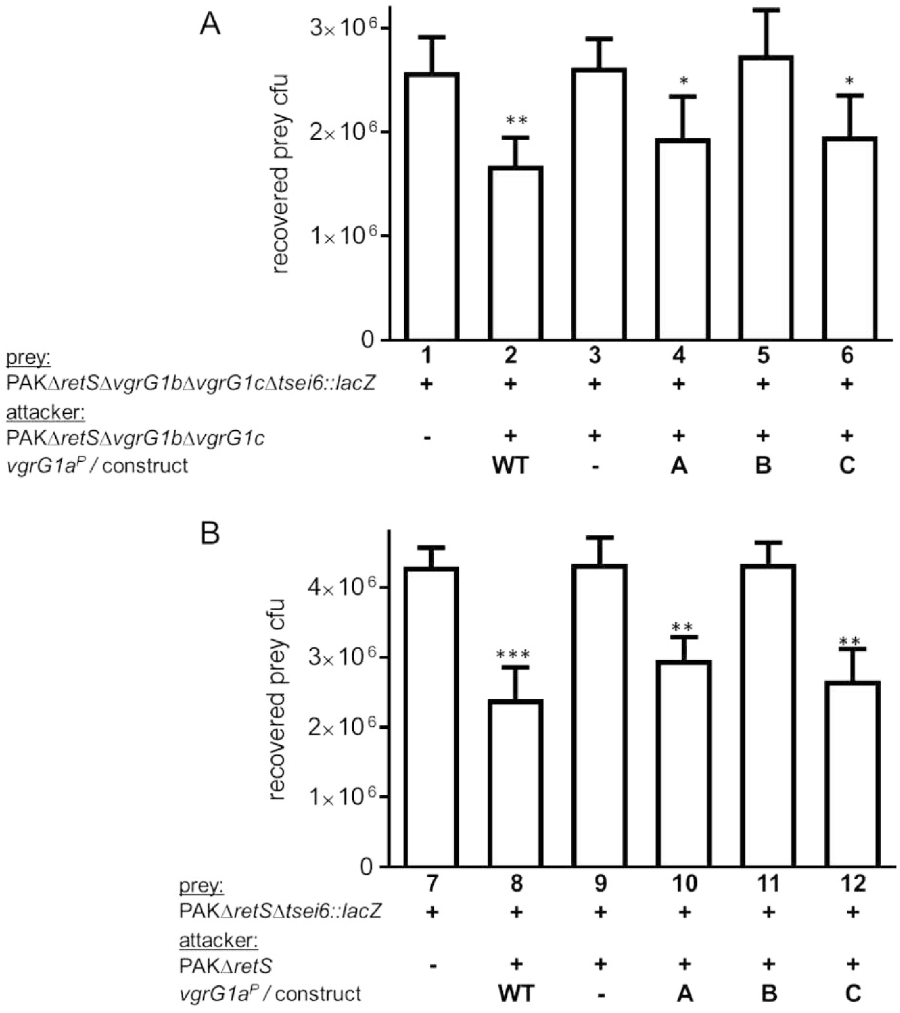


Figure 4-12. Chimerae A and C can deliver Tse6 into prey cells.

Plot of recovered cfu of prey strains (A) PAKΔ*retS*Δ*vgrG1b*Δ*vgrG1c*Δ*tsei6::lacZ* or (B) PAKΔ*retS*Δ*tsei6::lacZ* after contact with the attacker strain that encodes WT *vgrG1a* (WT), lacked native *vgrG1a* (-) or expressed one of the chimerae (A/B/C). As positive controls for Tse6 delivery, the parental strains were included (lanes 2 and 8), while the negative controls lacked *vgrG1a* (lanes 3 and 9). Spots were incubated for 5 h at 37 °C in a 5:1 ratio. Plots show the mean of at least three independent experiments and a one-way ANOVA analysis with Dunnett's multiple comparisons test was conducted on the data sets obtained from the recovered prey on their own (lanes 1 and 7) with *** $p<0.001$.

The two plots in Figure 4-12 show that prey survival seems to be variable dependent on the presence of VgrG1b and VgrG1c. Prey cells encoding VgrG1b and VgrG1c survive up to $4.5*10^6$ cfu, while in absence of VgrG1b and VgrG1c they only reach $3*10^6$ cfu, while the

experimental conditions were alike. This problem has not been addressed before and no explanation is apparent other than a growth defect of the *vgrG1b*-, *vgrG1c*-deficient mutants. However, since both experiments show the same result, we decided not to pursue this issue.

4.4.5. Summary: Full length VgrG1a is required to form a functional T6SS spike

In conclusion, this study supported previous research by Shneider *et.al* and demonstrated that the last β-sheet of the VgrG needle structure is essential for interactions with the cognate PAAR protein [141]. The here demonstrated results led us to propose a model about the interface of Tse6 and VgrG1a and how manipulating this region modifies the decoration of the tip (Figure 4-13).

In the parental strain (Figure 4-13A), it is believed that the N-terminal PAAR domain of Tse6 (orange) binds the blunt VgrG1a end (blue) *via* recognition of the three β-strands derived from each monomer [141]. Thus, the C-terminal effector domain of Tse6 is recruited towards the T6SS spike and can be propelled out of the cell [202]. The effector chaperone EagT6 (magenta) binds to the transmembrane helices of Tse6 thus stabilising the effector, which will be focussed on in 4.6.2. Similarly, chimera A contains full-length VgrG1a and thus its last β-sheet (Figure 4-9), which is most likely involved in PAAR binding. Hence, due to the same PAAR interface as the parental strain (Figure 4-13A), chimera A ought to have the same phenotype as WT VgrG1a^{P}. Indeed, we have evidence that chimera A recognises the cognate Tse6 and delivers it into target prey cells, which also led to secretion of chimera A.

As for chimera B, that contains a substituted PAAR interface from *A. tumefaciens* (Figure 4-13B), we expected PAAR binding to be affected. We confirmed this hypothesis with competition assays, in which delivery of the cognate Tse6 into prey cells could not be

monitored. This goes along with the fact that construct B was not secreted and thus most likely did not bind Tse6.

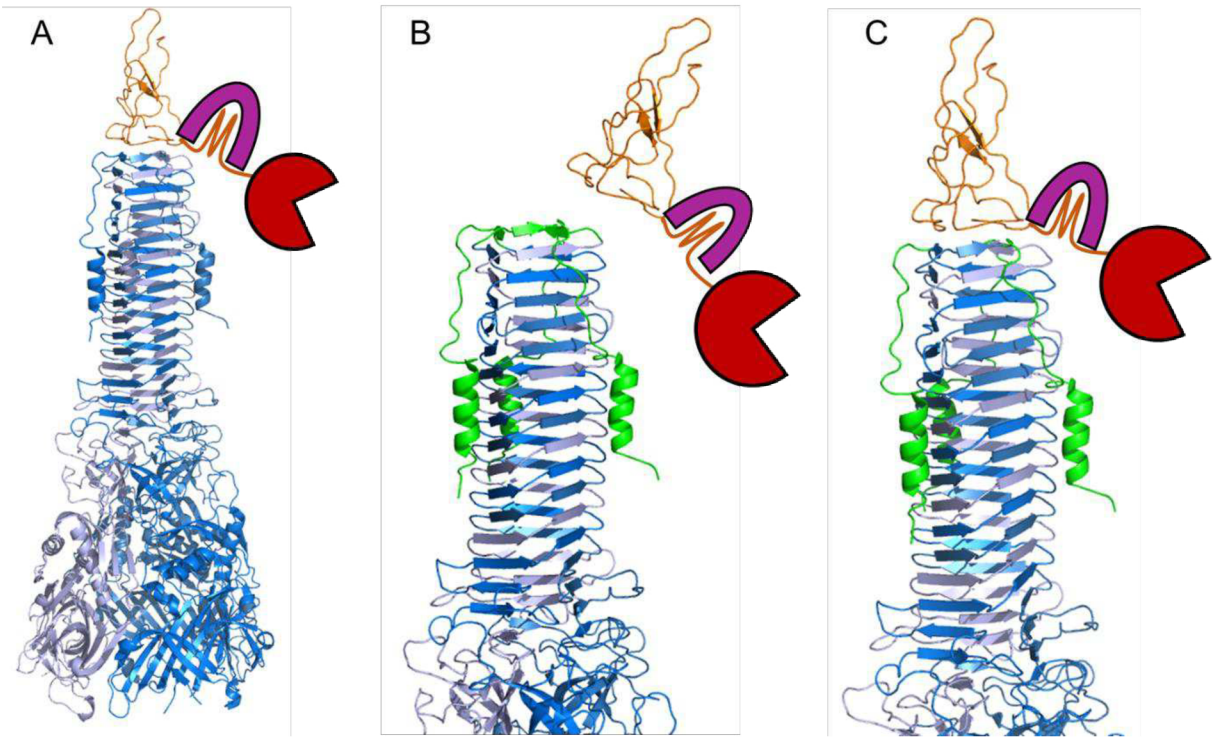


Figure 4-13. Model of recruitment of Tse6 to the VgrG1a^{P} tip.

A: Tse6 binds onto the VgrG1a^{P} tip (blue, PDB: 4mtk) via its N-terminal PAAR domain (orange, model based on PDB 4jiv). The chaperone EagT6 (magenta) binds Tse6 at its transmembrane domain. The C-terminal effector domain of Tse6 (red) is thus recruited to the T6 tip and delivered upon VgrG1a^{P} delivery. B: The last β-sheet and the C-terminal residues of VgrG1a^{P} are substituted with the corresponding residues from VgrG1^{A} (green) resulting in chimera B (VgrG1a^{P605}-G1^{A31}). The PAAR domain of Tse6 does not bind to the non-cognate β-sheet and thus Tse6 delivery is abrogated. C: The C-terminal residues of VgrG1a^{P} are substituted with the corresponding residues from VgrG1^{A} resulting in chimera C (VgrG1a^{P614}-G1^{A21}). The PAAR domain of Tse6 can bind to the cognate β-sheet and Tse6 is delivered.

Finally, chimera C contains the β-sheet that supposedly binds Tse6, although its very C-terminal end is replaced with the one from VgrG1^{A} (Figure 4-13C). Curiously, even though bacterial killing demonstrated that Tse6 is delivered into prey target cells, its own secretion

could not be detected. Since we observed that chimera C could not form a functional T6SS, its absence in the supernatant was not due to experimental shortcoming. These data suggest that the full length VgrG1a^{P} is needed to form a fully functional T6SS that delivers its cognate Tse6 into prey cells and leads to delivery of Hcp and Hcp-associated effectors. This further suggests that the very C-terminal residues of VgrG1a do have an impact on Tse6 binding, however the molecular details of this interaction remain elusive.

4.5. PAAR proteins can carry heterologous effector domains

Next, we wanted to employ the acquired knowledge in an attempt to construct a protein delivery system based on a PAAR protein. In a way similar to the previously described VgrG shuttle, the fact that PAAR proteins bind to VgrG tips could be the foundation to design a PAAR protein shuttle. Hence, it was decided to use the Tse6 PAAR effector and its dependency on VgrG1a (Figure 4-14A) and modify it in a way that it can deliver the toxic effector domain of Tse7 that usually depends on VgrG1b (Figure 4-14B).

We aimed at using the PAAR domain of Tse6 and fuse to it the C-terminal effector domain of Tse7, with the native C-terminal effector domain of Tse6 deleted (Figure 4-14C). According to structural data on Tse6 [202] and as shown in Figure 4-6B, the PAAR fold of Tse6 comprises the first 156 aa. However, complementation of Tse6 using only this PAAR domain was not successful (*data not shown*). Hence, we decided to include 50 aa of the non-functional linker region between the PAAR and the effector domain to give some structural flexibility to the fusion (Figure 4-14C, grey) [175, 202]. We engineered mutants that lacked *vgrG1c* and the whole *vgrG1b* cluster thus unable to express and deliver Tse7. In this background, the gene portion corresponding to the C-terminal effector domain of Tse6 and the cognate immunity gene *tsi6* was substituted with the gene portion encoding the C-terminal effector domain of Tse7 and its cognate immunity *tsi7* (Figure 4-14C).

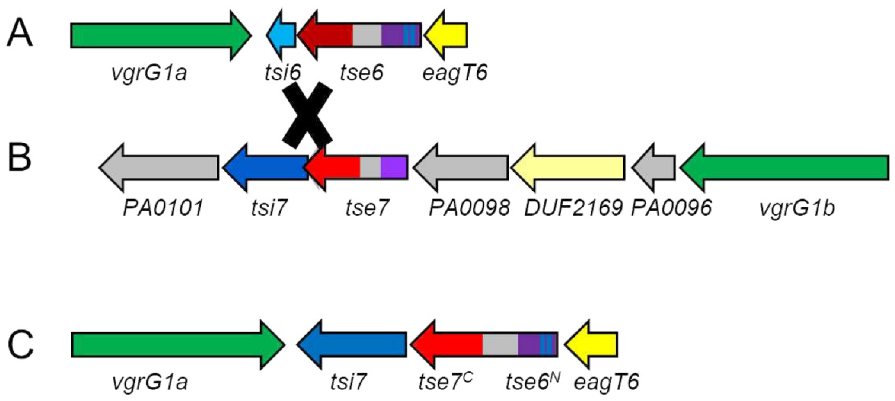


Figure 4-14. Cloning strategy for Tse6^{N}-Tse7^{C} shuttle.

A: *vgrG1a* (green) is encoded upstream of the immunity gene *tsi6* (cyan), the corresponding PAAR effector gene *tse6* (dark red) and a gene encoding for the DUF1795 chaperone *eagT6* (yellow). B: *vgrG1b* (green) is followed by a *DUF2169* adaptor gene (bright yellow) and genes encoding the effector-immunity pair Tse7-Tsi7 (red-blue), as well as three more genes of unknown functions (grey). C: The gene sequence corresponding to the C-terminal effector domain of Tse6 and the cognate immunity Tsi6 was substituted with the gene sequence corresponding to the C-terminal effector domain of Tse7 and the cognate immunity Tsi7 resulting in a Tse6^{N}-Tse7^{C} chimera.

A secretion assay was performed of strains that expressed the Tse6^{N}-Tse7^{C}-chimera in a T6SS-active or inactive background (Figure 4-15). In a western blot experiment, expression of the Tse6^{N}-Tse7^{C} chimera could be detected using an antibody against the V5-tag, that was included at the C-terminus of Tse7 (top panel). Tse6^{N}-Tse7^{C}-chimera production was weak, but detectable (lanes 2 and 3). No band for the chimera could be detected in the supernatant (lanes 5 and 6), however, VgrG1a was efficiently secreted into the supernatant both in the parental background with an intact *tse6* (lane 4) and in a context where it was replaced with the *tse6^{N}-tse7^{C}* fusion (lane 5). In absence of VgrG1b and VgrG1c, we have shown that VgrG1a can only form a functional H1-T6SS and thus secrete Hcp1 upon binding of its cognate PAAR protein, Tse6, which also leads to its own secretion (4.3.1). Hence, the detection of VgrG1a (second panel) and Hcp1 (bottom panel) in the supernatant fractions of cells expressing the Tse6^{N}-Tse7^{C}-chimera, suggests that a Tse6^{N}-Tse7^{C}-chimera still

executes its function, despite the fact that it was not detectable in the supernatant. This, again, might be due to the high hydrophobicity and thus insolubility of PAAR proteins.

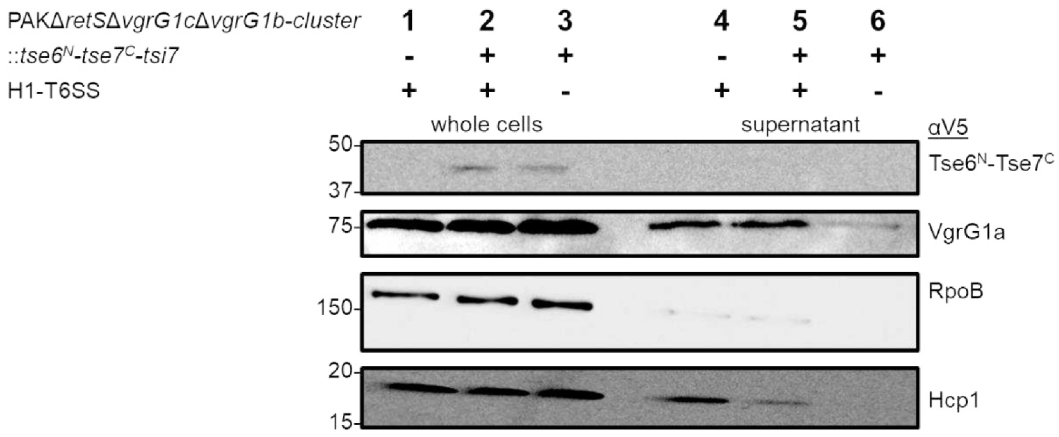


Figure 4-15. Expression of Tse6^{N}-Tse7^{C} leads to a functional T6SS.

Representative figure of western blots from secretion assay of PAKΔ*retS*Δ*vgrG1b-cluster*Δ*vgrG1c* encoding native *tsei6* (-) or the *tse6^{N}-tse7^{C}* chimera tagged with V5 (+). As a positive control for VgrG1a secretion, the parental strain was included (lane 4), while the negative control expressed a non-functional H1-T6SS (lane 6). Antibodies were used against V5, VgrG1abc, RpoB and Hcp1 as indicated on the right.

These results suggest that by swapping the C-terminal effector domain of Tse6 with the effector domain from a different source, Tse7, T6SS function might not be compromised. We could detect secreted VgrG1a in the supernatant fraction, however, this is only an indirect proof of delivery of the Tse6^{N}-Tse7^{C} chimera. This concept would need to be established with additional experiments, as for example interbacterial competition assays. In this case, prey strains would need to be engineered that lack both effector-immunity modules Tse6-Tsi6 and Tse7-Tsi7. Three attacker strains would then need to be tested. The positive control for Tse7-mediated killing would encompass a strain deleted for *tsei6*, but expressing and delivering Tse7 from its native locus. Due to Tse7 toxicity [175], this ought to lead to a decrease of prey survival. An attacking strain lacking both *tsei6* and *tsei7* would serve as a negative control as

being unable to deliver neither Tse7 or Tse6 into susceptible prey strains. The test strain would then be the one expressing the $Tse6^{N}$-$Tse7^{C}$-chimera, which might lead to a prey survival drop depending on its ability to deliver the chimera into prey cells. Yet, this PhD project did not encompass enough time to engineer appropriate strains and conduct the experiments.

4.6. PAAR domains are part of large polymorphic toxins

4.6.1. PAAR folds in the N-termini of Rhs proteins connect them to the T6SS tip

The previous sections highlighted the importance of the PAAR domain in T6SS assembly and VgrG binding. By swapping C-terminal effector domains of evolved PAAR effectors, we could further emphasise on the modularity of the T6SS. Here, we want to add another module to evolved PAAR effectors and discuss the family of Rhs effectors.

In addition to polymorphic PAAR effectors, in some organisms, toxins of the Rhs family have been associated with the T6SS [175, 199, 210, 211]. These ubiquitous proteins were shown to have toxic activity in a range of bacteria [252], however their physiological function remained long unclear. In a global study describing Rhs-effector diversification, it was proposed, that Rhs effectors can be classified into different clades based on their N-termini [210]. The N-terminal domain of a Rhs protein is differentiated by a hyper conserved RVVXXXXXXXG motif that is followed by a massive core domain of Rhs/YD repeats. After the Rhs core domain, another hyper conserved motif of about 60 aa follows, that serves as a border from the hyper variable toxic domain [210].

Interestingly, some Rhs effectors were connected to the T6SS and within their N-termini, PAAR motifs or cryptic, or hidden, PAAR motifs were identified [200, 208]. This allowed the assumption that Rhs effectors with N-terminal PAAR motifs are associated with

the T6SS. In this section, we want to address how delivery of Rhs effectors using the T6SS could be mediated. We selected Rhs effectors, that were experimentally proven to be connected with the T6SS or even with a specific VgrG, from various species [136, 148, 175, 199, 209]. Bioinformatic tools, like a multiple sequence alignment, confirmed the presence of the three PAAR motifs within the N-termini of these Rhs proteins (Figure 4-16A, highlighted by red lines). We could further identify the three same clusters of hydrophobic amino acids, highlighted with blue lines, as in Figure 4-6 that most likely mediate the interactions with the cognate VgrG protein. Firstly, this highlights the structural similarity between the N-terminal PAAR domains of evolved PAAR effectors and PAAR-containing Rhs effectors. Secondly, this finding implies a delivery mechanism very similar to the one of evolved PAAR effectors.

To confirm the PAAR fold as a general structural feature of Rhs effectors, the amino acid sequences prior to the diverging Rhs motif RVVXXXXXXXG [210], highlighted by a green line in Figure 4-16A, were modelled using the Phyre web tool [235]. For all tested Rhs proteins, structural simlarities with PAAR folds were identified within the N-termini. Chosen models of these PAAR domains of tested Rhs effectors were superimposed and can be seen in Figure 4-16B. We further could corroborate our hypothesis from 4.4.1, in which we stated that amino acids at the bottom interface of PAAR domains mediate specific interactions with the cognate VgrG. In the PAAR domains of RhsP1^{Paer}, Rhs1^{Smar} and Rhs2^{Smar}, we identified the putative VgrG-binding amino acid residues and listed them in Table 4-2. Furthermore, we observed that the modelled PAAR domain of RhsP1 (yellow model in Figure 4-16B) was smaller in comparison to other models. This is in good agreement with the sequence alignment in Figure 4-16A, which shows that RhsP1 shares the conserved PAAR motifs (highlighted with red lines) and the putatively VgrG-binding residues (highlighted with blue lines) with other PAAR domains, while the connecting regions are shortened. This raises the question whether the N-terminal PAAR domain of RhsP1 could have the same function as other PAAR domains which is piercing the membrane.

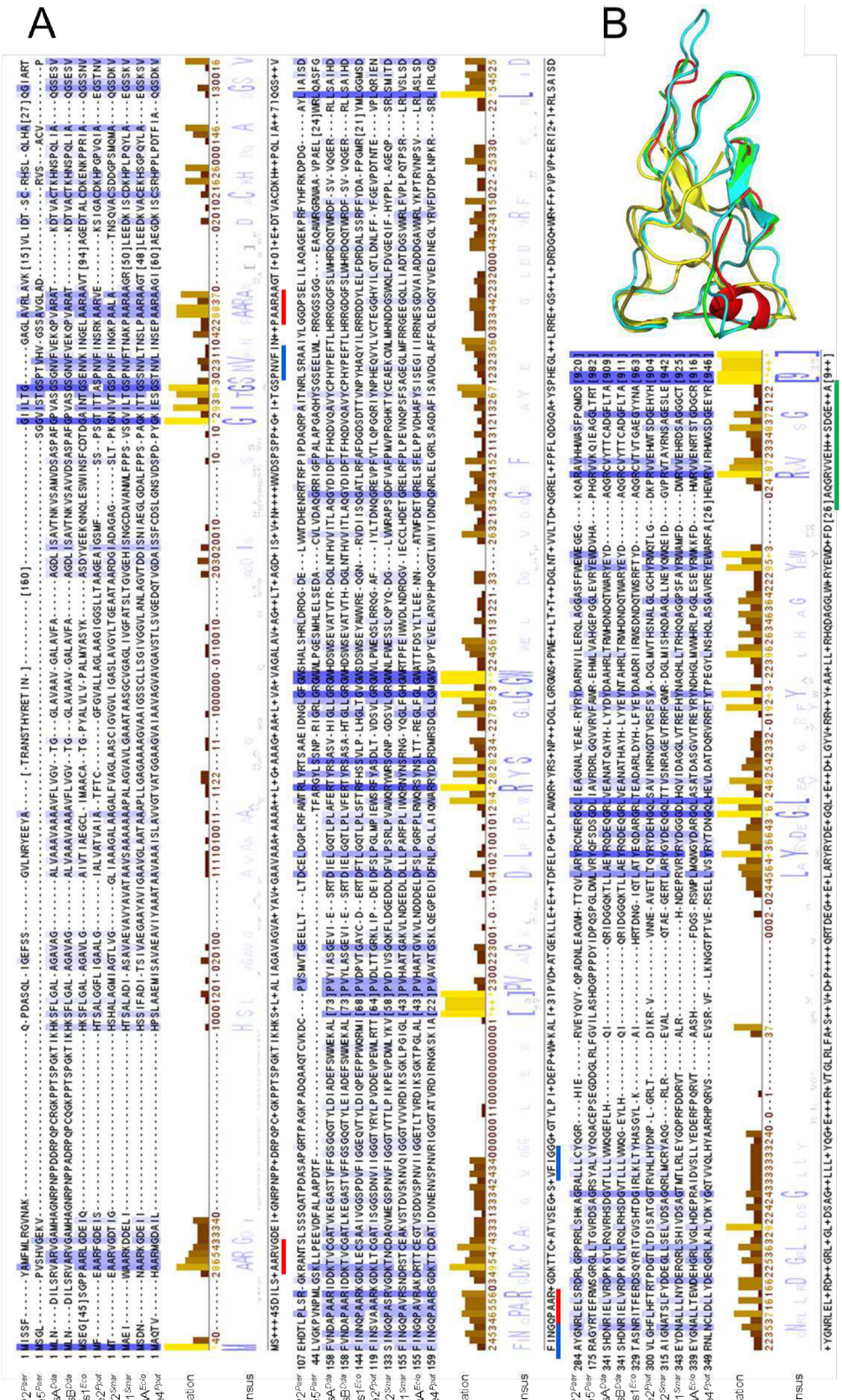


Figure 4-16. T6SS-dependent Rhs effectors are connected with the VgrG tip via their N-terminal PAAR domains.

A: Multiple sequence alignment of T6SS-dependent Rhs effectors. All effectors contain three PAAR- motifs in their N-termini (red lines), while three stretches of hydrophobic amino acids, highlighted with blue lines, correspond to those that are probably interacting with the VgrG trimer (see Figure 4-6). The conserved Rhs-motif RVXXXXXXG, that initiates the Rhs-core domain [210], is highlighted with a green line. B: Alignment of structural models as calculated by the Phyre web tool [235]. Analysed were the N-termini of RhsP1^{Paer} (yellow), Tke2^{Pput} (red), RhsA^{Ddan} (green) and Rhs1^{Smar} (cyan). All models show clear PAAR folds [141].

We have proposed a model of how the ubiquitous Rhs effectors might be connected to the T6SS tip and now the question is how are the large Rhs effectors delivered using the T6SS. The structure of the Rhs core domain of the ABC effector from *Yersinia entomophaga* was previously solved and showed that the Rhs core folds into a massive shell-like structure with hollow space in the middle (Figure 4-17A) [212]. When Rhs core domains from T6SS associated Rhs effectors were analysed with the Phyre web tool, they were all modelled on the template of the Rhs core domain of the ABC effector from *Y. entomophaga* with high confidence (*data not shown*). Examining these structural models, we also identified hollow space within the shell. Since it is assumed that the Rhs core is associated with the VgrG trimer, we then asked whether this hollow space could fit a VgrG trimer. Using the VgrG1c-RhsP1 pair from *P. aeruginosa* (Figure 4-2), we managed to build a model of a VgrG1c trimer (Figure 4-17B, green) and fitted the model of the PAAR domain of RhsP1 on top (purple). Further, the model of the Rhs core domain of RhsP1 (orange) could be accommodated around the VgrG1c trimer. This observation led us to the hypothesis, that Rhs effectors connect to the VgrG end via their N-terminal PAAR domains, while the large Rhs core wraps around the VgrG spike. This might lead to puncturing of the target cell membranes via the N-terminal PAAR proteins as discussed before. With delivery of the VgrG spike, the Rhs could be delivered as well. However, what remains elusive is, how the C-terminal toxin domain is accommodated around such tip. In the structural study by Busby *et.al*, it was suggested that the C-terminal domain is chaperoned within the hollow space of the Rhs core domain. Since in our model this hollow space would be occupied with the VgrG trimer, the C-terminal toxin domain would need to be

accommodated somewhere else within this complex. Future research should address this question, as it remains of upmost interest how these large and ubiquitous effectors make their way out of the producing cell and into target bacteria [210].

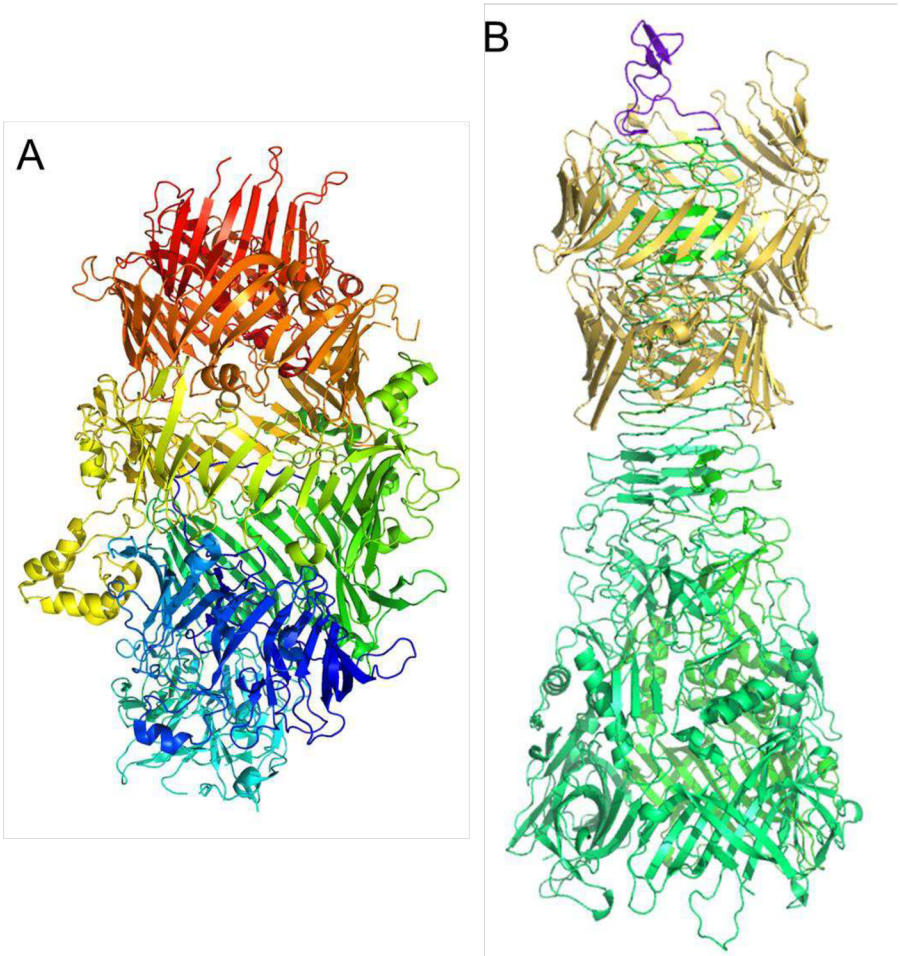


Figure 4-17. Rhs domains form large shell-like forms that might wrap around VgrG spikes.

A: Structure of Rhs core domain of the ABC toxin (pdb: 4igl) from *Yersinia entomophaga*. The ABC protein is coloured in a rainbow spectrum from red at the N-terminus to cyan at the C-terminus. B: Model of a complex between VgrG1c (green, model based on VgrG1a (PDB: 4mtk)) and RhsP1. The PAAR domain (purple, model based on PDB entry 4ku0) of RhsP1 assembles on top of the VgrG1c tip. The Rhs core domain (orange, model based on PDB entry: 4igl) was fitted around the VgrG1c tip.

4.6.2. Some evolved PAAR effectors contain N-terminal transmembrane domains and are delivered dependent on Eag proteins

The modularity of T6SS-mediated effector delivery can further be highlighted with the recent identification of effector chaperones [200, 217, 218]. In this section, we will focus on effector chaperones of the DUF1795 family, while chapter 6 will further develop on the function of effector chaperones derived from the DUF4123 family.

Proteins of the DUF1795 family, termed Eag for effector-associated gene, are small hydrophobic proteins usually encoded next to *paar* effector genes [200]. They were shown to play a crucial role in effector delivery with their absence resulting in abrogated delivery of the cognate PAAR effector [200]. A previous study by the Coulthurst lab in *S. marcescens* discovered that EagR1 and EagR2 bind the N-terminal regions of their cognate effectors Rhs1 and Rhs2, respectively; with this interaction being the prerequisite for effector delivery [148]. Interestingly, both Rhs1 and Rhs2 were predicted to contain N-terminal transmembrane helices [148] and so does the EagT6-dependent effector Tse6 [202]. Hence, we wanted to understand whether transmembrane helices are a common feature of Eag-dependent effectors which is why we analysed experimentally proven Eag-dependent effectors as well as effectors encoded next to *eag* genes from various organisms with bioinformatical tools.

In a multiple sequence alignment of Eag-dependent PAAR effectors, which is shown in Figure 4-18A, the three previously described PAAR motifs can be readily identified (highlighted with red lines). In this sequence alignment we further highlighted amino acid residues according to their chemical properties, with blue representing hydrophobic amino acids, red electrically charged and green polar residues. Using this colour scheme, a large hydrophobic insertion (highlighted with a blue line) can be identified between the first and the second PAAR motif which is only present in effectors encoded next to *eag* genes (compare with Figure 4-6). We further asked, whether this hydrophobic stretch could form transmembrane domains as

predicted for Rhs1^{Smar}, Rhs2^{Smar} and Tse6^{Paer}. A web tool for the prediction of transmembrane helices (http://www.cbs.dtu.dk/services/TMHMM/) convincingly identified transmembrane helices for all tested Eag effectors, as shown in Figure 4-18B. The two Eag-unrelated effectors Tse5^{Paer} and Tse7^{Paer} served as negative controls for this analysis and no transmembrane domains were identified in these two.

The identification of transmembrane domains within certain PAAR effectors might thus need a strict co-occurrence with Eag proteins. This finding is in good agreement with what has been described for Tse6^{Paer}, Rhs1^{Smar} and Rhs2^{Smar} [148, 202], while it was also shown that Eag proteins bind the N-terminal regions of their cognate effectors [148]. Because we predict that all Eag-dependent PAAR effectors contain N-terminal transmembrane helices, we hypothesise that the hydrophobic Eag proteins would specifically bind and chaperone these regions. This will probably prevent these hydrophobic regions from aggregation within the cell which in turn will stabilise the effector protein. One might also envision a role for Eag proteins which guides the effector and its transmembrane domains towards the membrane thus facilitating its insertion. This would give Eag proteins a similar role as periplasmic chaperones of the T2SS which are thought to guide their cognate effectors towards the membrane and thus the secretion vestibule [41].



Figure 4-18. Eag-dependent effectors contain N-terminal transmembrane domains.

A: Multiple sequence alignment of the N-termini of effectors that are encoded downstream of *eag* genes. Amino acid residues are colour coded according to their chemical properties; hydrophobic amino acids are blue, polar residues are green and charged residues are red. Highlighted with red lines are the three PAAR motifs, highlighted with a blue line is the putative transmembrane domain. B: Summary of analysis of transmembrane probability of Eag-dependent effectors based on http://www.cbs.dtu.dk/services/TMHMM/. All effectors contain at least one transmembrane domain within their N-terminal domain with high probabilities except for Tse5^{Paer} and Tse7^{Paer}, that are effectors independent of *eag* genes.

4.7. Summary

This chapter shed some light on the molecular details of PAAR functionality and binding to a T6SS spike as well as the modularity of T6SS-mediated effector delivery. First, we could show that in the absence of the PAAR effector Tse6, cells do not deliver the cognate VgrG1a anymore. We then identified residues responsible for VgrG-PAAR interactions and could verify our findings using two examples in which we manipulated the VgrG-PAAR interface. We modified the PAAR domain of Tse7 and showed that Tse7 is no longer delivered by its cognate VgrG1b probably due to the lack of interactions. Furthermore, we manipulated the last β-strand of VgrG1a which abolished Tse6 delivery. These results verified our bioinformatic-based models.

We then showed another aspect of T6SS modularity by demonstrating that a PAAR domain could deliver an effector domain similar to the VgrG shuttle in chapter 3. There, we showed that heterologous passenger domains can be connect to the T6SS spike via a covalent link with a VgrG, while here we used a PAAR domain as a vehicle to deliver an effector domain. Modularity of PAAR effectors was further highlighted by the fact that some evolved PAAR effectors additionally contain a big Rhs core domain and/or a transmembrane domain that requires an additional chaperone protein for effective delivery. The here outlined concepts can be further employed as tools to investigate T6SS-mediated effector delivery

using a similar approach of swapping an effector domain of an existing PAAR effector with a heterologous one and monitoring its delivery.

4.8. Discussion

4.8.1. VgrG hetero-trimerisation

This is the first study so far that investigates the formation of VgrG heterotrimers both *in vivo* and *in vitro*. Due to a sequence identity of 67 % and 76 % between VgrG1a and VgrG1b and VgrG1c, it was suggested that VgrG1a, VgrG1b and VgrG1c could interact and be secreted as heterotrimers [140]. Also in *V. cholerae* hetero-trimerisation between VgrG-1, VgrG-2 and VgrG-3 was proposed due to the finding that only VgrG-2 on its own can form a functional T6SS [207]. The authors suggested that the other two VgrGs would thus require interacting with VgrG-2 for their delivery.

Here, we wanted to establish whether the three homologues VgrG1a, VgrG1b and VgrG1c could form functional heterotrimers and could be secreted as such. Using a bacterial two hybrid approach, interactions between VgrG1a and VgrG1b as well as VgrG1a and VgrG1c were confirmed (Figure 4-4). However, using a direct read-out, we showed that secretion of VgrG1a is clearly independent of VgrG1b and VgrG1c (Figure 4-5). One explanation for this contradiction might lie in the different lengths of these three proteins that would result in the lack of recognition by a cognate PAAR protein.

VgrG1a, VgrG1b and VgrG1c are composed of 643 aa, 741 aa and 690 aa, respectively (compare band sizes corresponding to VgrG1a, VgrG1b and VgrG1c in Figure 4-3). The structure of VgrG1a was solved and showed that the gp5-corresponding needle-like part ends after the first 612 aa with the remaining 35 aa folding back into an extension arm

(Figure 4-1A) [253]. This needle-like structure is formed of intertwined β-sheets that stack on top of each other [253]. Secondary structure prediction tools predict β-sheets throughout the whole gp5-like domain until the C-termini of both VgrG1b and VgrG1c with low resemblance to a DUF2345 domain for VgrG1b [140]. This might mean that the VgrG1b and VgrG1c spikes are longer than a VgrG1a spike. This would be in good accordance to other structural studies that showed that phage spike proteins can have different lengths while still being functional [253]. Thus, heterologous interactions between VgrG1a and either VgrG1b or VgrG1c might lead to trimers with overhanging and thus loose or split ends. Such complex is unlikely to be recognised by one PAAR protein as most likely binding of three β-sheets originating from three VgrG monomers is required [141]. Hence, it can be proposed that heterotrimers between VgrG1a, VgrG1b and VgrG1c are formed within the cells, but these complexes might have other physiological functions, if any at all, than being T6 secretion components.

4.8.2. Formation of a functional T6SS tip requires a complete VgrG-PAAR assembly

This chapter provides deeper molecular insights into the requirements for a functional T6SS. Previous studies in *S. marcescens* and *A. baylyi* demonstrated that at least one VgrG protein and its cognate PAAR need to assemble to form a functional T6SS tip [141, 148]. In the case of *S. marcescens*, three such assemblies can form: (1) VgrG1 and its cognate PAAR1; (2.1) VgrG2 and Rhs1 or (2.2) VgrG2 and Rhs2. Each of the two PAAR domains of the Rhs effectors can top VgrG2 and thus form a functional spike complex. In *P. aeruginosa*, it was previously demonstrated, that each VgrG associated with the H1-T6SS, VgrG1a, VgrG1b or VgrG1c, can associate with their cognate PAAR effector, Tse6, Tse7 and Tse5, respectively [175]. Nevertheless, the authors showed and here we confirmed that presence of the VgrG1a-Tse6 complex is sufficient to form a functional H1-T6SS (Figure 4-5, lane 7) [140].

We could further approve that VgrG1c but not VgrG1b on its own is able to form a functional H1-T6SS (lanes 13 and 15). This suggests that VgrG1c associates with the PAAR domain of its cognate effector RhsP1 for delivery and this complex might get delivered in a fashion outlined in 4.6.1. We know from another study from our group that VgrG1b interacts with the PAAR domain of Tse7 (*under review at PNAS*), however it remains elusive why this complex on its own would not form a functional tip and what the requirements are for Tse7 delivery.

This feature also highlights another interesting strategy of the *P. aeruginosa* H1-T6SS. Only in the presence of VgrG1a or VgrG1c *P. aeruginosa* assembles its H1-T6SS machinery and fires a VgrG1a-Tse6 or VgrG1c-RhsP1 spike together with Hcp and thus Hcp-dependent effectors [140, 204]. This concomitant load of multiple effectors into prey cells is thought to have a highly efficient detrimental effect [175]. One can assume that delivering a VgrG1b-Tse7 spike together with Hcp-dependent effectors might not have such a lethal effect. Thus, Tse7 might not be considered a main weapon causing lots of damage, but rather an efficient add-on weapon to support killing of the prey in presence of more effective toxins. This would also fit the idea that the T6SS fires an effector cocktail in one shot thus causing as much damage as possible on their neighbouring competing bacteria [141, 193].

4.8.3. VgrG1abc form stable multimers

Multimerisation of VgrG complexes in *P. aeruginosa* has also been investigated before. A previous study from our group suggested that using the VgrG1abc antibody, multimers of VgrG1a and VgrG1c could be detected in both whole cell and supernatant fractions [140]. Here, we could confirm those data and propose that a VgrG trimer preferably forms in presence of its cognate PAAR protein under physiological conditions. This also suggests that the sample preparation and treatment with SDS is not sufficient to dissociate the spike components, which agrees with previous studies investigating the tip complex of other VgrG

proteins [139]. The top panel in Figure 4-5 displays multimers using the VgrG1abc antibody. In the whole cell fraction, detection of this band correlates with presence of both VgrG1a and Tse6 (lanes 1, 3, 5 and 7) suggesting that this band corresponds to an intracellular VgrG1a-Tse6 complex. In the supernatant fractions, however, multimers are detected in correlation with Hcp1 and Tse3 presence, thus correlating with a functional T6SS (lanes 10-14, 16 and 18). This implies that these bands correspond to trimers of either VgrG1a or VgrG1c or hetero-trimers of those. It is somewhat surprising why VgrG1c trimers are only detected in the supernatant fraction and not inside cells.

One possible explanation for this could be the model stated in Figure 4-17B. Here, we proposed that RhsP1 wraps around the VgrG1c trimer to form a functional spike. In a tight VgrG1c-RhsP1 complex, the antibody recognising epitope might be completely covered by the Rhs domain which would thus inhibit detection of this complex. This would also imply that a VgrG1c-RhsP1 complex is resistant to SDS-treatment. Once delivered into the supernatant, VgrG1c and RhsP1 might dissociate, due to changes in the environment for example the pH, thus allowing the antibody to specifically recognise VgrG1c trimers. To shed light on this issue, RhsP1 or only its Rhs domain could be deleted and western blot analysis performed on whole cells to analyse whether VgrG1c could then be detected.

4.8.4. Molecular details of the interactions between PAAR proteins and VgrG trimers

This study broadened our knowledge on the interaction sites between VgrG and PAAR proteins. We could precisely pinpoint at amino acid residues mediating these interactions within both PAAR and VgrG proteins and validated these by disrupting the specific interactions. We constructed three chimerae between VgrG1a^{P} and VgrG1^{A} as described in detail in 4.4.3 and shown in Figure 4-19.

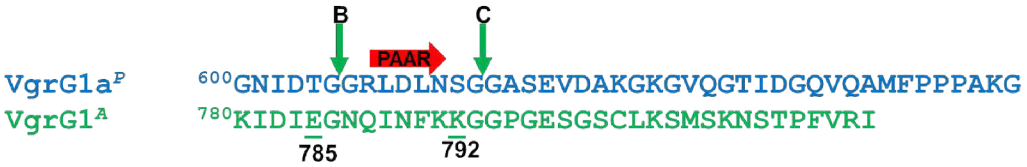
Here, we want to highlight contradictions between our findings and a recent study by Bondage *et.al*. [149], which was the basis for this current study. Bondage and colleagues engineered an *A. tumefaciens* mutant deficient for both *vgrG1* and *vgrG2* thus unable to form a functional T6SS. By expressing a range of truncation versions of VgrG1^{A}, the authors wanted to elucidate the molecular detail of PAAR- and effector binding by competition and secretion assays. On the basis of their findings, we dissected the C-terminal domain of VgrG1^{A} and constructed the chimerae for this study (4.4.3). Thus, the here designed chimerae and their truncations mutants share the same molecular binding platforms for the cognate PAAR domain and should thus display the same phenotypes regarding PAAR binding and spike assembly. However, we identified some inconsistencies with our results and listed them in Figure 4-19.

The study by Bondage *et.al.* used a truncation mutant VgrG1^{A792}, that was shortened after its last β-sheet, likely still able to bind its cognate PAAR1^{A} [149]. Thus, this construct would correspond to our chimera C, in which we substituted the C-terminal residues of VgrG1a^{P} after its last β-sheet (Figure 4-19). The authors showed that their truncation mutant did not bind the cognate PAAR1^{A} protein in a Co-IP, while its expression resulted in Hcp secretion, suggesting the formation of a functional T6SS tip. In contrast, our chimera C was indeed able to bind the cognate PAAR, as we could monitor Tse6-mediated killing (Figure 4-12). This is somewhat surprising, as both constructs contain the last β-sheet of the VgrG thus ought to be able to bind the cognate PAAR. Furthermore, here (see Figure 4-11A) and in other studies [141, 148] it was shown that the formation of a functional T6SS tip with subsequent Hcp secretion requires the formation of a complete VgrG-PAAR complex. Hence, it remains questionable how the truncation mutant VgrG1^{A792} could assemble a functional T6SS tip without binding its cognate PAAR1^{A} protein.

Bondage *et.al* used another truncation mutant, VgrG1^{A785}, that solely encompassed the gp5-/gp27-like domains of VgrG1^{A} [149]. Due to the lack of the last putative β-sheet in this

VgrG1^{A} construct, it could be hypothesised that the cognate PAAR1^{A} would not bind and they confirmed this with Co-IP. However, this truncated protein somehow formed a functional T6SS tip again resulting in Hcp1 secretion. In contrast, the corresponding chimera from our study, chimera B, was unable to deliver the cognate effector Tse6 (see Figure 4-12). This was expected as this chimera lacked the cognate β-sheet for PAAR binding (Figure 4-13B). We also could not detect any secreted Hcp when cells expressed this chimera (see Figure 4-11), suggesting that it was unable to form a functional T6SS tip. However, the fact that the VgrG1^{A785} construct would lead to Hcp secretion without binding its cognate PAAR contradicts our results as well as previous studies.

From these comparisons, it remains questionable how a VgrG mutant deficient for PAAR binding can form a functional T6SS spike. The fact that the authors expressed their truncation versions from plasmids might lead to altered T6SS activity or regulation, however it is unlikely that such basic mechanism as protein interaction could be affected by this condition. Another reasonable explanation could be the fact that VgrG1^{A} has an extended spike in comparison to other VgrG proteins [149]. This extension could have a facilitating role in puncturing the cell membrane to allow delivery of the VgrG-effector complex in absence of the cognate PAAR protein. However, this theory requires more profound molecular investigation.



	construct	gp5/gp27-domain	PAAR binding	effector binding	Hcp secretion	PAAR binding	effector delivery
WT	VgrG1a^{P}	VgrG1a^{P}			+	(+)	+
C	VgrG1a^{614}-G1^{Atu21}	VgrG1a^{P}		VgrG1^{A}	-	(+)	+
B	VgrG1a^{605}-G1^{Atu31}	VgrG1a^{P}		VgrG1^{A}	-	-	-
WT	VgrG1^{A}	VgrG1^{A}			+	+	+
792	VgrG1^{792}	VgrG1^{A}			+	-	-
785	VgrG1^{785}	VgrG1^{A}			+	-	-

Figure 4-19. Comparison of the here characterised chimerae between VgrG1a^{P} and VgrG1^{A} with the truncation mutants used in the study by Bondage *et.al* [149].

The top panel represents the amino acid sequences of the C-terminal extensions of VgrG1a^{P} (blue) and VgrG1^{A} (green). The putative last β strand is highlighted with a red arrow. The location of the swaps for chimerae B and C are highlighted with green arrows. Table: Both WT VgrG1a^{P} and VgrG1^{A} on their own can form functional T6SS tips leading to Hcp secretion and delivery of their cognate effectors [140, 149]. Chimera C in *P. aeruginosa* can deliver its cognate effector Tse6 into prey cells, but no Hcp1 secretion was detected suggesting a non-functional T6SS tip. Chimera B did not form a functional T6SS tip and did not deliver its cognate effector. Plusses for PAAR binding are in brackets as this is solely an indirect result from Tse6 delivery. The truncation mutants VgrG1^{785} and VgrG1^{792} from *A. tumefaciens* formed functional T6SS tips leading to Hcp secretion while PAAR binding could not be observed and delivery of the cognate effector was abrogated.

5. Results:

T6SS effectors are specifically recruited by C-terminal domains of VgrG proteins

5.1. Introduction

It is likely no longer needed to re-emphasise that effector delivery with the T6SS is highly versatile. In the previous chapters it is shown that effectors can be delivered as extension domains of T6SS structural components like VgrG- or PAAR-proteins (chapters 3 and 4, respectively). We confirmed that some T6SS effectors contain PAAR domains as adaptors that connect them to the T6SS machine by binding onto the blunt end of the VgrG trimer [141]. Other T6SS effectors do not contain such adaptor motif, but they manage to bind to the VgrG-PAAR spike. For some of these effectors, the involvement of additional adaptor or chaperone proteins of the DUF4123 family was demonstrated [149, 217, 218, 220], which we will focus on in chapter 6.

Here, we emphasise on T6SS effectors that do not exhibit any adaptor motif and whose delivery is independent of any adaptor protein. As one example for these adaptor-less T6SS effectors, the delivery mechanism of Tle1 from entero-aggregative *Escherichia coli* was studied [216]. In this work, Flaugnatti and collaborators demonstrated that the lipase Tle1 directly interacts with the C-terminus of its upstream encoded VgrG1. Interestingly, VgrG1 contains a C-terminal transthyretin (TTR)-like domain, which is present in a range of prokaryotic and eukaryotic species [254]. The authors could show that the TTR-like domain specifically binds the cognate Tle1 and that this interaction is mandatory for Tle1

delivery [216]. The presence of TTR-like domains in other VgrGs genetically linked to T6SS effectors adds another layer of modularity to the "á la carte" effector delivery concept.

In this chapter, we focus on the two *P. aeruginosa* T6SS lipase effectors PldA and PldB [186]. Recent research investigated their activities and substrate specificities [255] and their role in modulating the host response to facilitate internalisation [188]. In this very same study the authors also proposed that *P. aeruginosa* uses its H2-T6SS to deliver PldA into eukaryotic HeLa cells and its H3-T6SS to deliver PldB [188]. *pldA* and *pldB* are encoded downstream of two *vgrG* genes, *vgrG4b* and *vgrG5*, respectively (Figure 5-1A). Hence, we reasoned that we could use this genetic link to investigate the molecular details of PldA and PldB delivery and see whether this could be manipulated upon designing and engineering chimera and an original effector delivery shuttle.

5.2. Aim of this chapter

In the previous chapters, we broadened our knowledge on the molecular details of the delivery of effectors that were covalently fused to T6SS structural components as VgrG or PAAR proteins. In this chapter, the aim is to direct effectors to a specific region at the VgrG C-terminus so that T6SS shuttling occurs in a non-covalent VgrG-dependent fashion. This approach will also shed light on the delivery mechanisms of the two effectors PldA and PldB and their cognate VgrGs, VgrG4b and VgrG5, respectively.

Firstly, conditions in which PldA and PldB are expressed are investigated. Since no antibodies against PldA and PldB are currently available, both effector genes will be modified on the chromosome so that a chimeric protein with a Bla_{TEM-1} C-terminal extension is produced and detectable by western blot analysis. Secretion and interbacterial competition assays will

be performed to elucidate which of the H1-, H2- or H3-T6SS machinery in *P. aeruginosa* mediates delivery of these effectors.

We then aim to elucidate molecular details of T6SS effector delivery by investigating the role of the upstream *vgrGs* genes and assign a cognate VgrG to PldA and PldB. Further, we manipulate the VgrG C-termini to refine the specific binding domain towards the T6SS effectors. In the last part, we will attempt to redirect both effectors to a different VgrG as a vehicle to reach the target cells. This effector shuttling will be based on the direct interaction between a T6SS effector and the C-terminus of its cognate VgrG. Here, the VgrG tip can be modified to recruit and deliver alternative effectors and we will detail the limitations of this delivery concept.

5.3. *P. aeruginosa* encodes two eukaryotic-like lipases

As described in length in the introduction, *P. aeruginosa* contains multiple remote *vgrG* islands with various effector-immunity modules (see 1.3.3). Two distinct orphan *vgrG* clusters also carry genes encoding two previously characterised T6SS effectors PldA/Tle5a (PA3487) and PldB/Tle5b (PA5089), hereafter called PldA and PldB, respectively (Figure 5-1A).

Both PldA and PldB were shown to exert lipase activities based on their dual catalytic HxKxxxxD motifs, whose locations are highlighted in Figure 5-1B in red. PldA was demonstrated to have a wide substrate profile; it hydrolyses a range of phospholipids to generate the lipid phosphatidic acid [255]. By producing this signalling lipid, both PldA and PldB were proposed to induce the PI3K/Akt pathway resulting in actin rearrangement with subsequent *P. aeruginosa* internalisation [186, 188]. Thus, PldA and PldB are among the few T6SS effectors that are translocated into eukaryotic host cells and that impact them in the bacterium's favour [188].

For both lipase effectors, anti-bacterial activities based on membrane targeting were also observed. Both PldA and PldB were shown to be delivered into susceptible prey strains leading to prey killing [186, 188]. When prey strains expressed Tli5a, the corresponding immunity to PldA (Figure 5-1A), they acquired immunity to PldA-mediated killing [186]. Interestingly, expression of either one of the three immunities downstream of *pldB*, Tli5b$_1$, Tli5b$_2$ or Tli5b$_3$, confers resistance to PldB-mediated killing [188]. PldB and its series of immunity genes on the chromosome of *P. aeruginosa* is just one of many examples of T6SS effectors that are encoded together with more than one immunity protein. The physiological role of stockpiling immunity proteins is however far from understood. Notably, PldA and PldB are the founding members of trans-kingdom effectors due to their dual role in influencing both eukaryotic and prokaryotic targets.

Not much research has been done into the delivery mechanisms of PldA and PldB. To facilitate recognition of genes and gene products, we will use the same colour scheme for each gene or gene product throughout this chapter (Figure 5-1A). The gene/gene product *vgrG4b*/VgrG4b will be shown in green and *pldA*/PldA in bright green; *vgrG5*/VgrG5 will be depicted in blue and *pldB*/PldB in cyan. The *pldA* and *pldB* genes are located downstream of two *vgrGs* genes, *vgrG4b* and *vgrG5*, respectively, and no adaptor proteins are encoded nearby and neither PldA nor PldB contain any adaptor motifs (Figure 5-1A). Hence, it was hypothesised that PldA and PldB may directly connect to the VgrG tip, which will be the basis of this chapter.

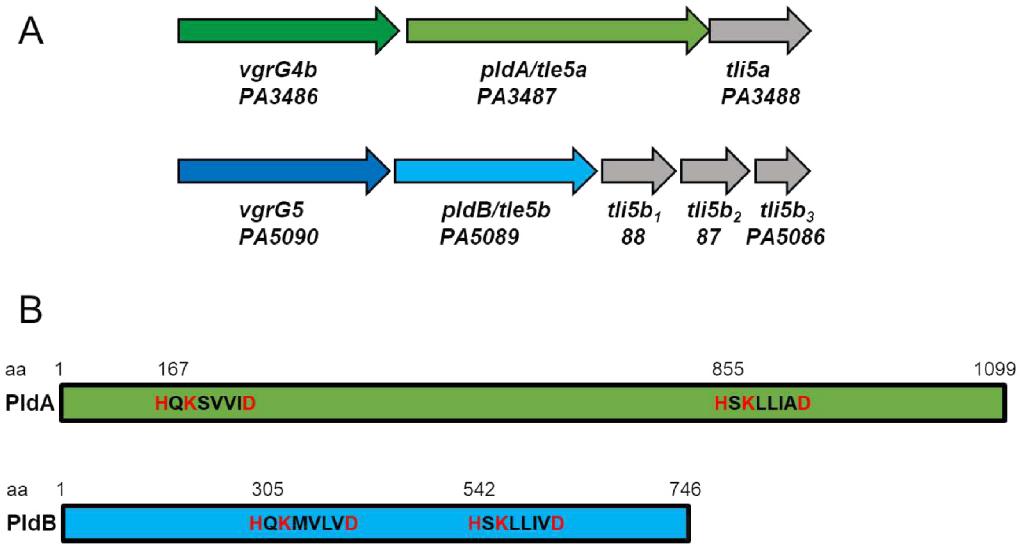


Figure 5-1. *P. aeruginosa* encodes the two lipases PldA and PldB.

The following colour code will be used throughout this chapter: *vgrG4b*/VgrG4b in green and *pldA*/PldA in bright green; *vgrG5*/VgrG5 in blue and *pldB*/PldB in cyan. A: *vgrG4b* and *vgrG5* operons. *vgrG4b* is encoded upstream of *pldA/tle5a* followed by the cognate immunity *tli5a* (grey). *vgrG5* is encoded upstream of *pldB*/*tle5b* followed by three cognate immunity genes *tli5b*$_1$, *tli5b*$_2$ and *tli5b*$_3$ (grey). B: Organisation of the lipases PldA (green) and PldB (cyan) showing the dual catalytic motifs and the conserved catalytic residues denoted in red.

5.4. The *vgrG4b* and *vgrG5*-clusters are repressed by RsmA

Before diving into the delivery mechanisms of PldA and PldB, we need to identify expression condition for both effectors. Previous studies investigating PldA- and PldB-mediated killing and translocation were conducted in *P. aeruginosa* strain PAO1 and expression conditions in those studies were 37 °C at the late exponential phase [186, 188]. However, using our lab PAO1 strain and the same conditions, we did not detect activation of any remote *vgrG* island or protein expression of T6SS components other than H1-T6SS associated (*data not shown*) [140]. This might probably be due to the high genomic divergence of different PAO1 strains used by different laboratories. This causes phenotypic variations in virulence and T6SS-mediated killing as discussed in length in a recent commentary [256]. On

the basis of these contradictions, we aimed at finding conditions under which the *vgrG4b*- and *vgrG5*-clusters are expressed to a level that allow phenotypic characterisation using the us available tools of secretion and interbacterial competition assays.

In a previous transcriptome study using the regulatory mutant *P. aeruginosa* PAO1Δ*rsmA*, it was observed that *vgrG4b* was upregulated when grown at 25 °C [257]. In our laboratory, Allsopp and collaborators [146] were also investigating, using unbiased approaches and transposon mutagenesis, regulatory mutants that are highly up-regulated for T6SS functions. Remarkably, it was found that a mutation in *rsmA* was up-regulating all 3 T6SSs but also all *vgrG* orphan clusters, including the *vgrG4b* cluster. In order to reconcile expression and protein production, we thus decided to probe the level of VgrG4b production in a mutant lacking *rsmA* by using a specific antibody against VgrG4b. Strikingly, when cells were grown at 25 °C, we clearly observed a band at a size corresponding to VgrG4b which is only visible in the strain lacking *rsmA*, but not in the PAO1 parental strain (Figure 5-2A).

Although expected, we further investigated whether in this very same background production of PldA and PldB could be detected. We thus engineered chromosomal chimera of these genes, so that they encode a fusion of PldA or PldB with a C-terminal extension being the β-lactamase effector domain (Bla_{TEM-1}). In a study conducted by Jiang and collaborators, they used similar protein fusions between PldA or PldB and Bla_{TEM-1} [188]. In that study, effector fusions were produced from a plasmid, while here, we introduced the fusions into the chromosome of both PAO1 and the isogenic *rsmA* mutant. Bacteria were grown in the same conditions as described above and proteins in whole cell fractions were analysed using western blotting and antibodies directed against β-lactamase.

Bands corresponding to the expected sizes of PldA-Bla_{TEM-1} (Figure 5-2B) and PldB-Bla_{TEM-1} (Figure 5-2C) were clearly detected and only visible in strains lacking *rsmA*. Specificity of the Bla_{TEM-1}-antibody could also be verified by using strains that did not encode for the β-

lactamase-fusion and in this case, no band is revealed. These data led us to conclude that RsmA represses genes from both the *vgrG4b* and *vgrG5* cluster and these results were recently published in a PNAS paper that I co-authored [146]. Hence, for all following experiments in this chapter, the parental strain we use is PAO1Δ*rsmA* and all new mutants were constructed in this background.

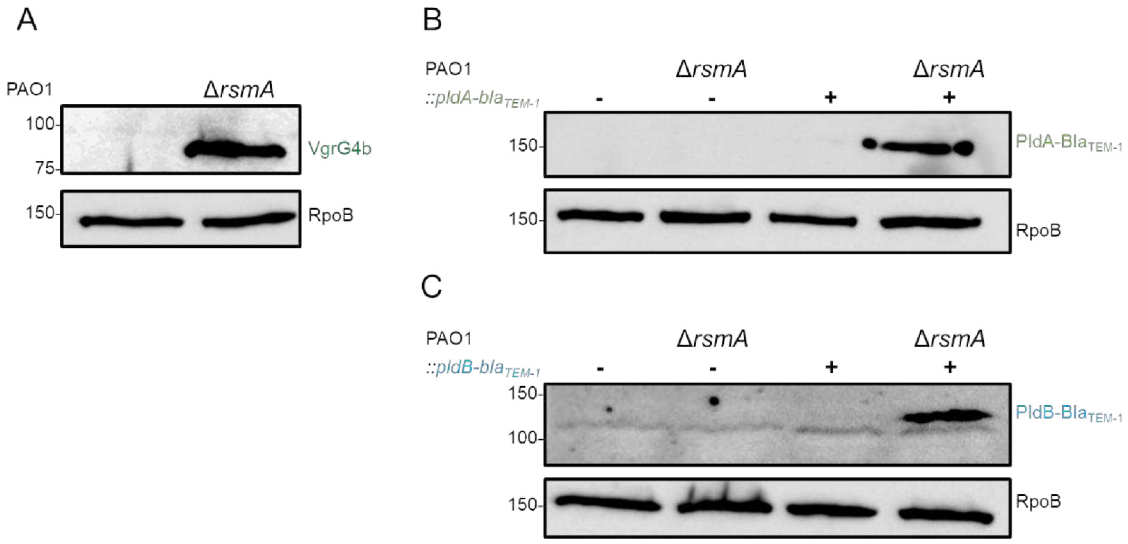


Figure 5-2. VgrG4b, PldA and PldB are repressed by RsmA.

Representative figures of western blots of whole cell lysates of PAO1 WT or with a deletion in *rsmA* (Δ*rsmA*) expressing $bla_{TEM\text{-}1}$ tagged versions of C: PldA (+) or D: PldB (+). Antibodies were used against RpoB and B: VgrG4b; C, D: $Bla_{TEM\text{-}1}$ as indicated on the right of each panel.

5.5. Assessing delivery of T6SS substrates through secretion and inter-bacterial killing assays

Throughout this chapter, we will show results from the same kind of experiments; secretion assays and inter-bacterial killing assays. While secretion assays are performed to monitor the production and the fate of any detectable protein, inter-bacterial killing assays are

more sensitive read-outs to monitor the delivery of a toxic component into a sensitive prey strain [247]. Here, we will briefly describe the basics of both experiments and how to interpret the results to avoid redundancy when explaining the rationale of experiments.

For secretion assays, strains of interest are grown at 25 °C due to induction of the H2-T6SS under these conditions [146] until the cultures reached an OD_{600} of approximately 4. Cells and supernatant are then separated by three centrifugation steps, the supernatant protein precipitated and washed and western blot analysis performed on both fractions. These experiments were repeated three times and one representative blot is shown for each experiment. On representative figures showing western blots, as exemplified in Figure 5-3, different panels are shown with blots probed against various proteins as indicated on the right. The top panel shows a blot of the protein of interest (here VgrG4b in green), while the panels below show further controls. Production of the protein is shown in the whole cell fractions on the left, while its secretion is visualised by the same bands in the supernatant fractions on the right. The cell lysis reporter RpoB (second panel) is not supposed to be detected in the supernatants (lanes 3 and 4) confirming that secretion of the protein of interest is specific and not due to leakage. Another protein, LasB (bottom panel), which relies on the T2SS and not the T6SS for secretion, is generally found in the supernatant fractions independent of the T6SS background. This confirms equal loading of the supernatant fractions. The T6SS readout often uses Hcp secretion and here we use Hcp2 (third panel) as the hallmark of H2-T6SS functionality. *P. aeruginosa* encodes three homologues, *hcpA, hcpB* and *hcpC*, that are grouped together as *hcp2*. These genes are found in satellite islands associated with the H2-T6SS (see also Figure 1-22) [146, 147]. Due to the high homology between HcpA, HcpB and HcpC, the Hcp2 antibody, which was raised against HcpA (PA1512), recognises all three species [147]. As seen in Figure 5-3, Hcp2 is only detected in the supernatant fractions of H2-T6SS active strains (lane 3), but not of H2-T6SS-inactive strains (lane 4), confirming T6SS functionality.

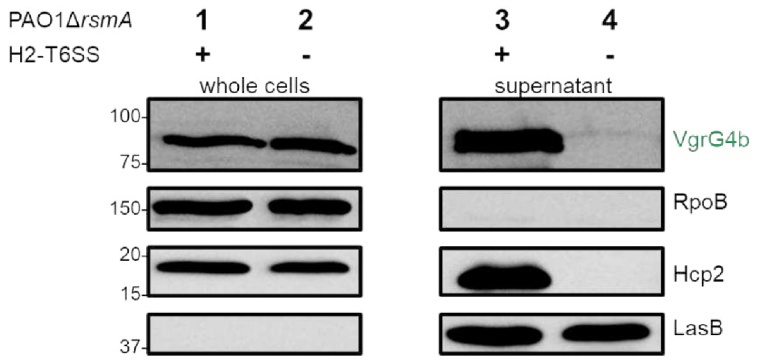


Figure 5-3. A representative figure of a western blot analysis; VgrG4b is secreted by the H2-T6SS.

Representative figure of a western blot from a secretion assay of PAO1Δ*rsmA* with an active (+) or inactive (-) H2-T6SS. As a control for a functional H2-T6SS, membranes were blotted against Hcp2 (third panel). Antibodies were used against VgrG4b-CT, RpoB, LasB and Hcp2 as indicated on the right.

To assess delivery of effectors into target prey cells, we perform competition assays based on the visual output of tagged prey strains [247]. Both PldA and PldB, the effectors of interest in this study, were shown to harbour anti-bacterial activities [186, 188], which is the basis for inter-bacterial competition assays. For this, prey strains were constructed that lacked the alleles for *pldA* or *pldB* and the cognate immunity genes, respectively. These strains expressed chromosomal β-galactosidase introduced at the *att* site resulting in blue colonies when grown on LB-agar containing X-Gal [247]. These strains were kindly provided by Thomas Wood. We then mix equal amounts of the prey strain with an attacking strain and incubate this mix as a dried spot on a LB-agar plate for 24 h at 25 °C. After resuspending the spot in PBS, the mixes are diluted and the dilutions grown on LB-agar containing X-Gal. Competition assays were repeated at least three times, the survived prey cfu counted and the mean plotted dependent on the attacker strain as exemplified in Figure 5-4.

In such plot, the first lane always shows the survival of the prey strain on its own after 24 h as a control for prey growth which is usually high. When the prey strain faced the positive

control (lane 2), which in most cases is the parental strain PAO1Δ*rsmA*, prey survival drops due to effector delivery. Lane 3 then usually shows survival of the prey when in contact with the negative control that somehow inhibits delivery of the effector of interest. In this case, prey survival is high as compared to lane 2, from which it can be concluded that no effector is being delivered into prey cells.

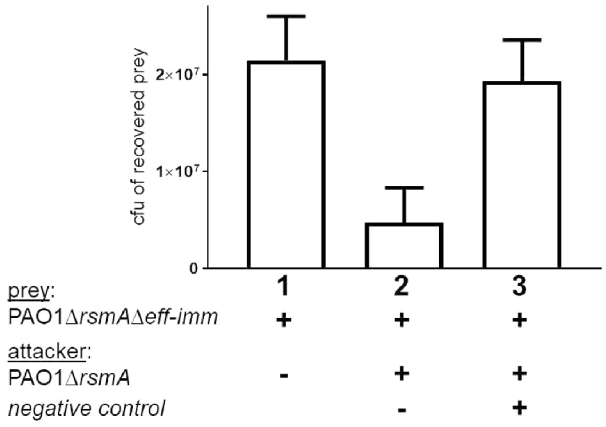


Figure 5-4. A representative plot of recovered cfu of prey strain PAO1Δ*rsmA*Δ*eff-imm::lacZ*.

5.6. Delivery of VgrG4b, PldA and PldB is dependent on the H2-T6SS

5.6.1. VgrG4b secretion is H2-T6SS dependent

Previous work from Jiang *et.al*, which was conducted concomitantly to our study, suggested that PldA was delivered in an H2-T6SS-dependent fashion. However, the tools in our lab are different, since we detect protein expression and secretion using a VgrG4b-specific antibody, while Jiang and collaborators showed their results using translocation assays [188].

We abstained from performing translocation assays due to the encountered drawbacks discussed in 3.5.3. Additionally, the mutants they used to show H2-T6SS association were deleted in *clpV2* which corresponds to the ATPase gene product of the H2-T6SS. Since deletion of *clpV* does not completely abolish functionality of a T6SS machinery [126, 133], we here preferred to use mutants that express a completely inactive T6SS machinery. We thus engineered an H2-T6SS-mutant lacking the essential sheath component TssB2 in PAO1Δ*rsmA* and performed a secretion assay which is shown in Figure 5-3. VgrG4b is detected in the whole cell fractions (lanes 1 and 2) and in the supernatant fraction of H2-T6SS-active strains (lane 3), but not of H2-T6SS-inactive strains (lane 4) suggesting that VgrG4b delivery requires H2-T6SS function. From this experiment, we concluded that the *vgrG4b* cluster is H2-T6SS-affiliated.

5.6.2. PldA delivery is H2-T6SS dependent

Since PldA is encoded within the *vgrG4b* cluster, it is expected that this effector is delivered in a H2-T6SS-dependent manner and in a VgrG4b-dependent manner, which will be focussed on later. Hence, we engineered a PAO1Δ*rsmA* strain that has an inactive H2-T6SS machinery. For reasons of comparability with experiments conducted by other lab members on this subject, we decided to inactivate the essential component TssE2 to result in an inactive H2-T6SS machinery for further experiments [146]. To visualise PldA in a secretion assay, we introduced on its chromosome the *bla*$_{TEM-1}$-tagged version of *pldA*. Secretion assays were performed as described in 5.5 and a representative figure is shown in Figure 5-5A. PldA-Bla$_{TEM-1}$ is detected in the whole cell fractions (top panel, lanes 3 and 4) and can only be detected in the supernatant fraction if the strain has an active H2-T6SS (lane 7). This band is missing in the supernatant fraction of a strain with an inactive H2-T6SS (lane 8).

We then assessed whether the H2-T6SS machinery could also mediate delivery of PldA into bacterial preys. As for attacking strains, we used either the parental strain or mutants thereof that additionally lacked an essential component of the H2-T6SS, *tssE2*, or of the H3-T6SS, *tssK3* (kindly provided by Thomas Wood). We decided to test for H3-T6SS-dependency of PldA, because it was suggested before that PldB was indeed delivered by the H3-T6SS [188]. To confirm that the H3-T6SS, however, has no impact on PldA delivery, we included this small aspect into our experiment.

When the prey strain was challenged against the parental strain, we observed a clear drop in cell number (Figure 5-5B, lane 10) as compared to the initial input (lane 9). Instead, after contact with an attacking strain that has a non-functional H2-T6SS, a high number of prey is recovered (lane 11), not significantly different from the initial input (lane 9) suggesting that PldA delivery was abrogated. Furthermore, when the prey was in contact with an attacking strain having a non-functional H3-T6SS, less prey cells were recovered (lane 12), just like with the parental strain (lane 10), thus indicating PldA delivery is H3-T6SS-independent and relies exclusively on the H2-T6SS.

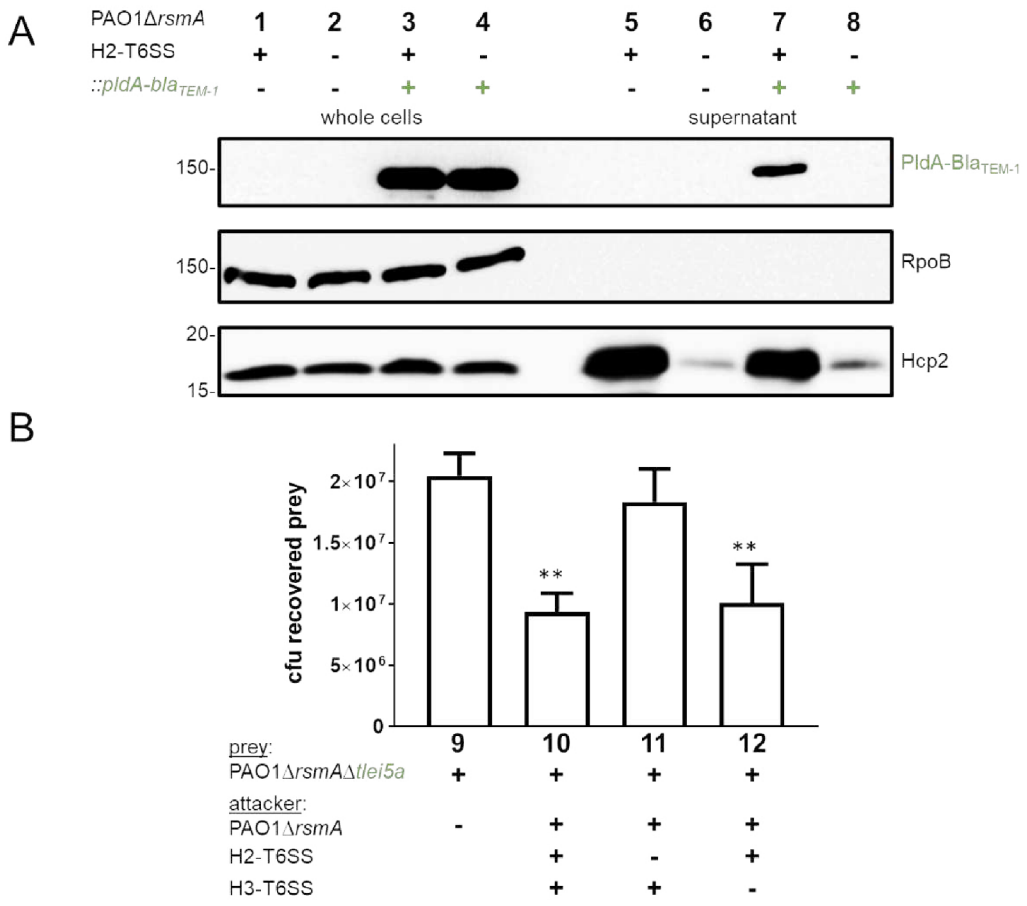


Figure 5-5. PldA delivery is H2-T6SS dependent.

A: Representative figure of a western blot from a secretion assay of PAO1Δ*rsmA* with an active (+) or inactive (-) H2-T6SS expressing a Bla_{TEM-1}-tagged version of PldA (+). As a control for a functional H2-T6SS, membranes were blotted against Hcp2 (third panel). Antibodies were used against Bla_{TEM-1}, RpoB and Hcp2 as indicated on the right. B: Plot of recovered cfu of prey strain PAO1Δ*rsmA*Δ*tlei5a::lacZ* after contact with the attacker strain that encoded a non-functional H2- or H3-T6SS (-). As a positive control for PldA-mediated killing, PAO1Δ*rsmA* was included (lane 10). Spots were incubated for 24 h at 25 °C in a 1:1 ratio. One-Way ANOVA analysis with Dunnett's multiple comparisons test was conducted on data set obtained from recovered prey on their own with ** $p<0.01$.

5.6.3. PldB is delivered in an H2-T6SS-dependent manner

The second cluster of interest for this study is the *vgrG5* cluster encoding the effector PldB (Figure 5-1A). Recent work by Jiang and collaborators suggested that the H3-T6SS is

responsible for PldB delivery into bacterial cells and eukaryotic cells [188]. Here, we followed the procedure we applied for VgrG4b/PldA and interrogated PldB T6SS-dependent secretion and PldB-dependent killing.

Secretion assays were performed using strains encoding a PldB-Bla_{TEM-1}-fusion engineered in a H2-T6SS-active and inactive background (Figure 5-6A). Using an antibody against Bla_{TEM-1}, we readily detected a band of approximately 120 kDa, which corresponds to the size of PldB-Bla_{TEM-1} in the whole cell fractions (lanes 1 and 2). In the supernatant fraction of a H2-T6SS-active strain (lanes 3), a band at around 80 kDa was detected. As our antibody is very specific, this suggests that PldB-Bla_{TEM-1} might be susceptible to proteolytic degradation after or during the secretion process. Interestingly, this band was absent in the supernatant fraction of H2-T6SS-inactive cells (lane 4). This suggests that PldB secretion is H2-T6SS-dependent and not H3-T6SS-dependent as previously proposed [188].

We then performed bacterial competition assays to confirm that PldB function has not been altered and to reassess both H2- and H3-T6SS-dependent delivery. We thus used H2-T6SS and H3-T6SS inactive mutants as attacking strains. As for the prey, they were engineered to lack *pldB* and all three immunities, rendering those strains susceptible for PldB delivery. Competition assays were conducted under the same conditions as described above and a plot can be seen in Figure 5-6B.

Upon challenge with the parental strain, prey survival is significantly decreased (lane 6), indicating that PldB has been successfully delivered. Instead, when the prey strain is in contact with an attacking strain that has a non-functional H2-T6SS, the number of prey recovered does not vary as compared with the initial input (compare lanes 7 and 5), suggesting that PldB delivery did not occur. Finally, after grown in contact with an attacking strain expressing a non-functional H3-T6SS, prey killing is very effective and comparable to the impact of the parental strain (compare lanes 6 and 8), indicating PldB delivery. This

confirms the obtained data from the secretion assay and thus contradicts previous data suggesting the H3-T6SS dependent transport of PldB [188].

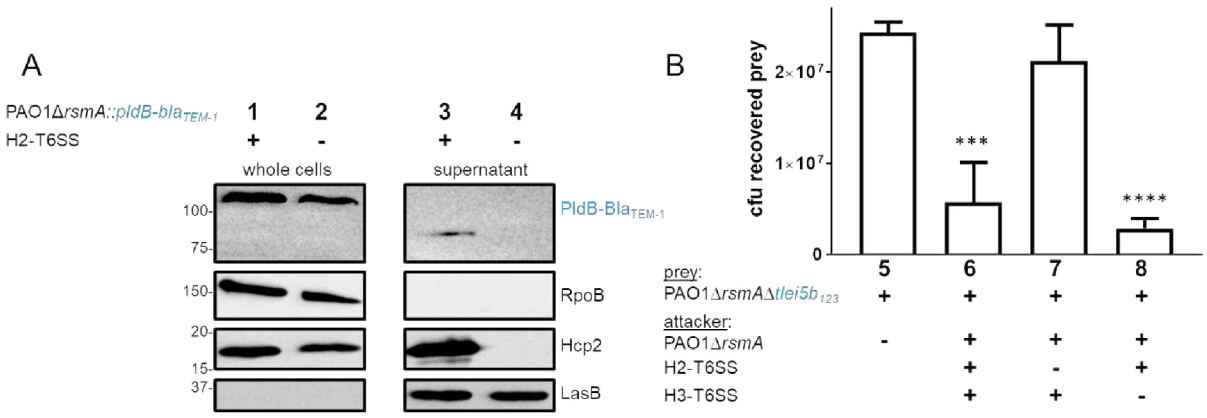


Figure 5-6. PldB delivery is H2-T6SS dependent.

A: Representative figure of a western blot from a secretion assay of PAO1Δ*rsmA* with an active (+) or inactive (-) H2-T6SS expressing a Bla_{TEM-1}-tagged version of PldB. As a control for a functional H2-T6SS, membranes were blotted against Hcp2 (third panel). Antibodies were used against Bla_{TEM-1}, RpoB, LasB and Hcp2 as indicated on the right. B: Plot of recovered cfu of prey strain PAO1Δ*rsmA*Δ*tlei5b*$_{123}$*::lacZ* after contact with the attacker strain that encoded a non-functional H2- or H3-T6SS (-). As a positive control for PldB-mediated killing, PAO1Δ*rsmA* was included (lane 6). Spots were incubated for 24 h at 25 °C in a 1:1 ratio. One-Way ANOVA analysis with Dunnett's multiple comparisons test was conducted on the data set obtained from recovered prey on its own with **** $p<0.0001$.

In summary, we found that the H2-T6SS machinery of *P. aeruginosa* mediates delivery of both PldA, as suggested before, and PldB. With the latter, it contrasts with the study by Jiang and colleagues. In their study, the authors have shown that ClpV3 and thus the H3-T6SS facilitates delivery of PldB [188]. Deletion of *clpV3*, an ATPase, is thought to be essential to recycle proteins of the H3-T6SS sheath, while minor activity of the H3-T6SS is given [221]. Here, we deleted an essential baseplate component of the H3-T6SS machinery, *tssK3* [146], which renders the H3-T6SS completely inactive. Additionally, while their conclusions were

mainly based on results from translocation assays and competition assays [188], we here used secretion assays to directly detect PldB-Bla_{TEM-1} with western blot analysis. Furthermore, competition assays in this current study were conducted at 25 °C using PAO1Δ*rsmA*, rather than 37 °C using PAO1 WT [188]. It is unlikely that the association of an effector to its cognate T6SS machinery may change depending on temperature. However, one possibility might be the contradiction of different PAO1 sublines [256], as mentioned above, that could lead to variations in the *vgrG5* gene and thus alters T6SS association. Another difference in experimental procedure is the expression of PldB-Bla_{TEM-1} from a plasmid as done by Jiang and colleagues [188] and not from the native locus as in this current study. The addition of antibiotics to the growth medium to maintain the plasmid could likely alter *P. aeruginosa* virulence and T6SS regulation and assembly, as seen in experiments in our lab (*data not shown*). On another note, different experimental procedures under alternative lab settings could be basis for the different experimental outcomes.

5.7. PldA and PldB are delivered *via* their cognate VgrGs

For various effectors, it has been shown that their delivery is mediated by a specific VgrG protein. Both the T6SS effector and the *vgrG* genes are usually clustered together in what has also been called orphan *vgrG* clusters [175, 200, 208, 216]. The genetic and physical linkage between VgrG and T6SS effectors has also led to the proposed concept of the "á la carte" delivery, suggesting one VgrG specifically recognises one effector [175]. As shown earlier, both *pldA* and *pldB* are located just downstream of *vgrG* genes, *vgrG4b* and *vgrG5*, respectively (Figure 5-1A). The accepted hypothesis would then be that delivery of PldA and PldB is mediated by the upstream encoded VgrGs.

To confirm whether the above is true, secretion assays were performed of strains that expressed Bla_{TEM-1}-tagged versions of PldA or PldB in presence or absence of their upstream

encoded VgrG. To support these results, competition assays were performed against prey cells that lacked genes for the effector-immunity pair as appropriate. As for the attacking strains, we will compare survival of prey after contact with WT or strains deleted for *vgrG4b*, *vgrG5* or both genes.

5.7.1. VgrG5 is essential for PldB delivery

First, we wanted to investigate the impact of VgrG5 on PldB delivery (Figure 5-7A). A representative figure of a secretion assay, as depicted in Figure 5-7B, shows secretion of PldB-Bla-$_{TEM-1}$ into the supernatant fraction from the parental strain (lane 3). Yet, no band for PldB-Bla-$_{TEM-1}$ was identified in the supernatant fraction of *vgrG5*-deleted cells (lane 4) suggesting that secretion of PldB-Bla$_{TEM-1}$ is abrogated in the absence of VgrG5. Note, that the secretion product of PldB-Bla$_{TEM-1}$ has a smaller size as compared to the band detected in the whole cells, which can also be seen in Figure 5-6, lane 3. Interestingly, a band of weaker intensity corresponding to PldB-Bla$_{TEM-1}$ is detected in the whole cell fraction of *vgrG5*-deleted strains (lane 2) while equal loading was confirmed upon analysis of the RpoB band control.

We have no antibody detecting VgrG5 as an available tool, but out of interest, we also monitored fate of VgrG4b in these experiments using a specific antibody. Remarkably, we observed that secretion of VgrG4b was abrogated in the absence of VgrG5 (lane 4), while its production was not impacted (lane 2). The absence of secreted VgrG4b is directly linked to the absence of VgrG5, while the overall H2-T6SS function does not seem to be impacted as confirmed with efficient secretion of Hcp2 (bottom panel). This is in good agreement with other studies showing that the H2-T6SS machinery recruits multiple VgrGs, such as VgrG2a, VgrG2b, VgrG4b and VgrG6, with one of them being sufficient for H2-T6SS activity even in absence of VgrG5 (Thomas Wood, *unpublished data*) [220].

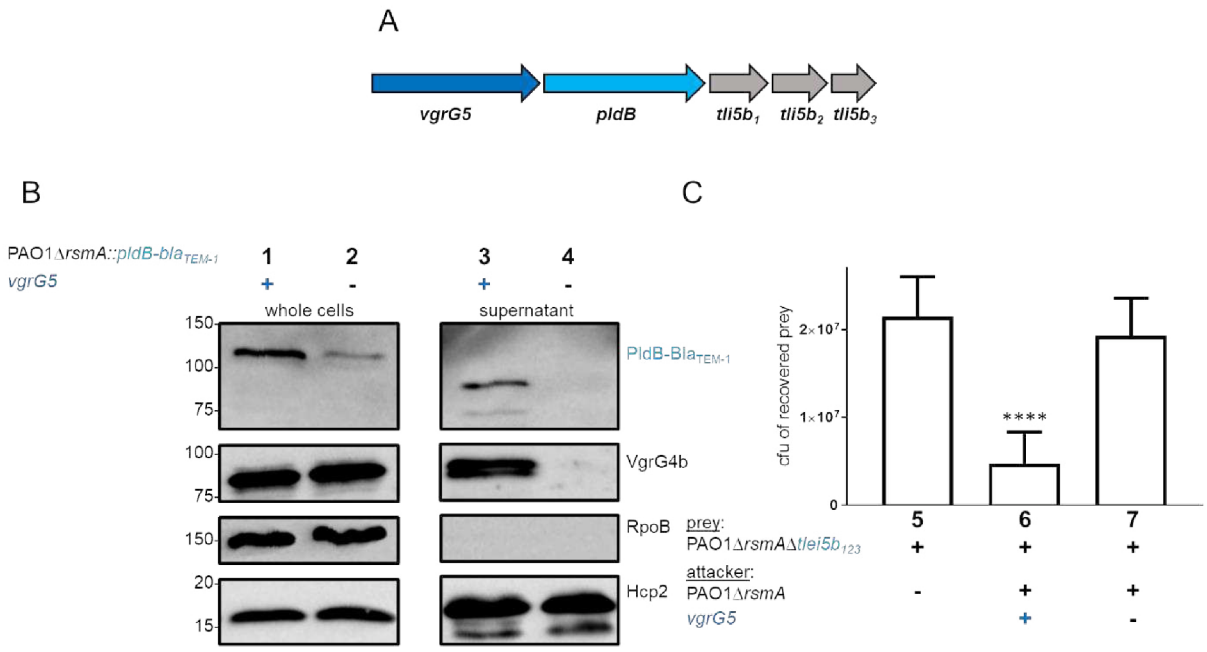


Figure 5-7. Delivery of PldB depends on VgrG5.

A: *vgrG5* (blue) is encoded directly upstream of *pldB* (cyan). B: Representative figure of a western blot from a secretion assay of PAO1Δ*rsmA* in absence (-) or presence (+) of the native *vgrG5* expressing a Bla_{TEM-1}-tagged version of PldB. As a control for VgrG secretion, membranes were blotted against VgrG4b (second panel). Antibodies were used against Bla_{TEM-1}, VgrG4b, RpoB, LasB and Hcp2 as indicated on the right. B: Plot of recovered cfu of prey strain PAO1Δ*rsmA*Δ*tlei5b*$_{123}$*::lacZ* after contact with the attacker strain that did not encode native *vgrG5* (-). As a positive control for PldB-mediated killing, PAO1Δ*rsmA* was included (lane 6). Spots were incubated for 24 h at 25 °C in a 1:1 ratio. One-Way ANOVA analysis with Dunnett's multiple comparisons test was conducted on the data set obtained from recovered prey on their own with **** $p<0.0001$.

Furthermore, we wanted to test VgrG5 impact on PldB delivery into prey cells. The plot in Figure 5-7C shows a mean of survival of the prey strain that was challenged against the parental strain (lane 6) or a strain lacking *vgrG5* (lane 7). When the prey strain faced an attacking strain that was deleted in *vgrG5*, recovered prey cfu was similar to survival of the prey on its own (lane 5). This indicates that delivery of PldB depends on the presence of VgrG5, which is in agreement with the above stated dogma and results from the secretion assay.

5.7.2. VgrG4b is essential for delivery of PldA

Next, we hypothesised that VgrG4b would mediate delivery of the downstream encoded gene product PldA (Figure 5-8A). Secretion assays showed the production (Figure 5-8B, lane 1) and the secretion (lane 4) of PldA-Bla_{TEM-1} from the parental strain. Remarkably, no cleavage product of PldA-Bla_{TEM-1} in the supernatant fraction was detected. The PldA-Bla_{TEM-1} band is detected in the whole cell fraction of *vgrG4b*-deleted strains (lane 2), but no band for PldA-Bla_{TEM-1} was identified in the supernatant fraction of *vgrG4b*-deleted cells (lane 5) suggesting that secretion of PldA-Bla_{TEM-1} is abrogated in the absence of VgrG4b. Absence of VgrG4b was also confirmed using an antibody against VgrG4b (second panel) and introduction of *vgrG4b in trans* (lane 3 and 6) restored production and secretion of PldA-Bla_{TEM-1} (top panel). Again, we could confirm that the H2-T6SS is indeed functional in the absence of *vgrG4b*, confirming data from other studies that further VgrGs are recruited to form a functional H2-T6SS machinery and thus result in Hcp2 secretion (lane 5) [220].

The plot in Figure 5-8C shows a mean of survival of the prey strain, lacking the immunity Tli5a and thus being susceptible for PldA delivery. Once challenged with the parental strain (lane 8), low amounts of prey cfu are recovered, suggesting effective PldA delivery. Yet, if the attacking strain is deleted for *vgrG4b* (lane 9), no such impact is detected indicating that PldA delivery depends on VgrG4b.

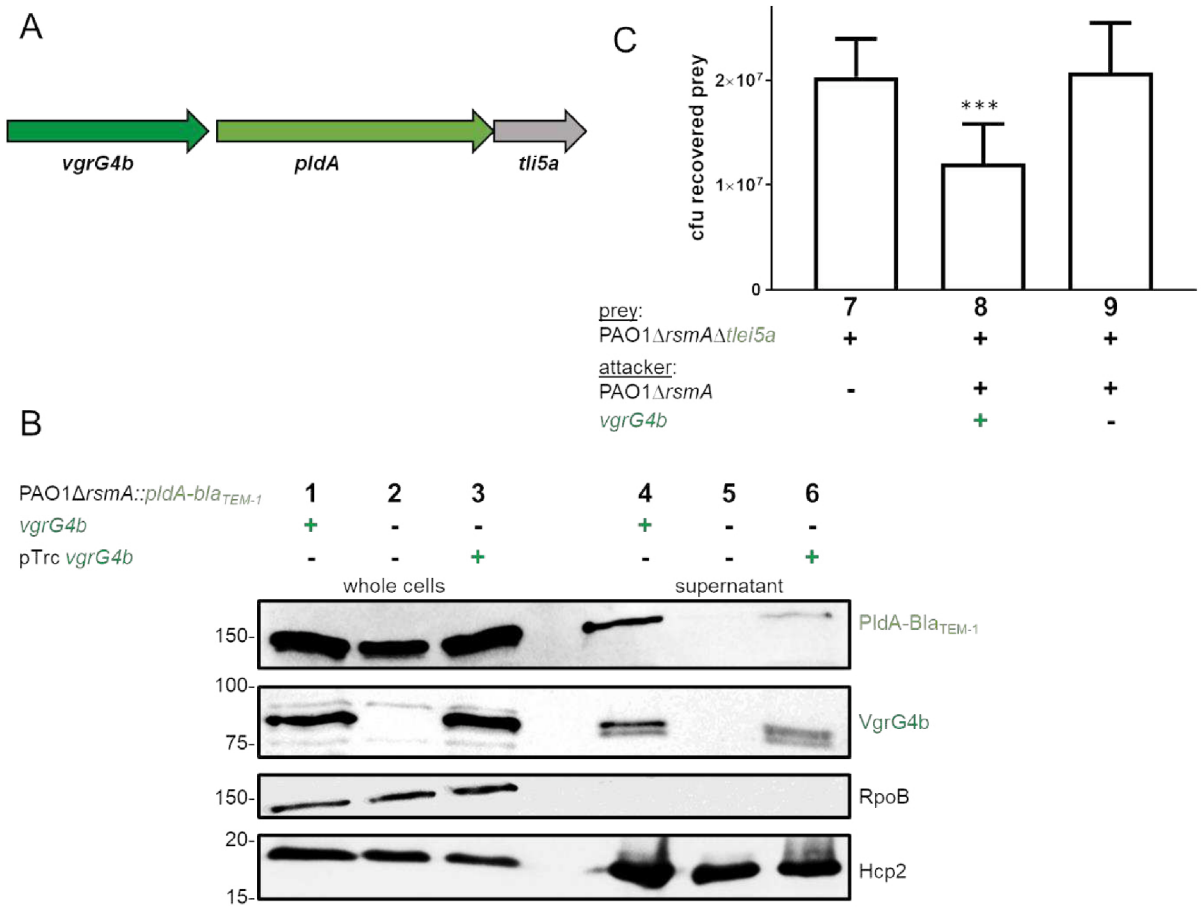


Figure 5-8. Delivery of PldA depends on VgrG4b.

A: *vgrG4b* (green) is encoded directly upstream of *pldA* (bright green). B: Representative figure of a western blot from a secretion assay of PAO1Δ*rsmA* in absence (-) or presence (+) of *vgrG4b* expressing a Bla_{TEM-1}-tagged version of PldB. Antibodies were used against Bla_{TEM-1}, VgrG4b, RpoB, and Hcp2 as indicated on the right. C: Plot of recovered cfu of prey strain PAO1Δ*rsmA*Δ*tlei5a::lacZ* after contact with the attacker strain lacking native *vgrG4b* (-). As a positive control for PldA-mediated killing, PAO1Δ*rsmA* was included (lane 8). Spots were incubated for 24 h at 25 °C in a 1:1 ratio. One-Way ANOVA analysis with Dunnett's multiple comparisons test was conducted on the data set obtained from recovered prey on its own with **** $p<0.0001$.

5.8. T6SS effectors and their cognate VgrGs: challenging an exclusive specificity

5.8.1. Secretion of VgrG4b requires VgrG5

Our data suggest that VgrG5 not only mediates delivery of PldB, but somehow affects VgrG4b secretion (Figure 5-7). This unexpected result led us to investigate the molecular details of this functional link. VgrG4b and VgrG5 share 69 % sequence identity within their gp5-/gp27-like domains, while sequence identities with gp5-/gp27-like domains from other *P. aeruginosa* VgrG proteins are lower with VgrG4a and VgrG6 being the exceptions (Table 5-1). The gp5-/gp27-like domains are known to mediate the intertwining and thus trimerisation of VgrG spikes [253]. Hence, the secretion defect of VgrG4b in absence of VgrG5 and the high sequence identities between these two proteins led us to postulate functional VgrG4b-VgrG5-heterotrimers. Just recently, experimental evidence suggested that VgrG4b and VgrG6 would form heterotrimers that deliver the cognate effector TseT [220]. This idea would be, based on the high sequence identity between these two proteins (Table 5-1), comparably reasonable. Furthermore, sequence identity between VgrG4a and VgrG4b is even higher, indicating interactions and thus hetero-trimerisation between these proteins. However, currently we lack any experimental evidence to support this concept.

Table 5-1. Sequence identities between VgrG proteins from *P. aeruginosa* PAO1.

Sequence identities between each two VgrG proteins were determined using the SIM alignment webtool (https://web.expasy.org/sim/). The VgrG listed in the middle was tested against VgrG5, for which the sequence identity in percent is listed on the left, and against VgrG4b, for which the sequence identity in percent is listed on the right. Sequence identities between VgrG4a, VgrG4b, VgrG5 and VgrG6 are highest suggesting interactions between these proteins.

Sequence identity with VgrG5	VgrG	Sequence identity with VgrG4b
37 %	**VgrG1a**	37 %
35 %	**VgrG1b**	34 %
35 %	**VgrG1c**	34 %
37 %	**VgrG2a**	35 %
37 %	**VgrG2b**	34 %
36 %	**VgrG3**	36 %
67 %	**VgrG4a**	97 %
70 %	**VgrG6**	73 %

We attempted to restore secretion of VgrG4b in a *vgrG5* mutant, but the attempt to clone the full-length version of VgrG5 was unsuccessful. Since the trimerisation of VgrG spikes solely requires the gp5-/gp27-like domains [253], we reasoned that expressing the gp5-/gp27-like domains of VgrG5 might be sufficient to form functional heterotrimers with VgrG4b and lead to its secretion. Hence, we decided to clone only the DNA region corresponding to the gp5-/gp27-like domains of VgrG5 resulting in the truncated version *vgrG5*^{628}. This construct would encompass the last β-strand of the VgrG trimer that is required to bind a cognate PAAR protein [141]. We also added a HA-tag to follow the protein by western blot and transformed the plasmid containing *vgrG5*^{628} into strains that lacked the native *vgrG5* locus and performed secretion assays (Figure 5-9).

As seen before, VgrG4b is expressed (top panel, lane 1) and secreted (lane 5) from the parental strain. In the absence of *vgrG5*, VgrG4b production is not affected (lane 3), but

its secretion is (lane 7). When strains expressed the gp5-/gp27-like domains of VgrG5 *in trans*, we could monitor the production of the protein with an anti-HA (second panel, lane 4) and its secretion (lane 8). Remarkably, we were then able to restore VgrG4b secretion in this context (top panel) suggesting that the gp5-/gp27-like domains of VgrG5 are sufficient to mediate secretion of VgrG4b.

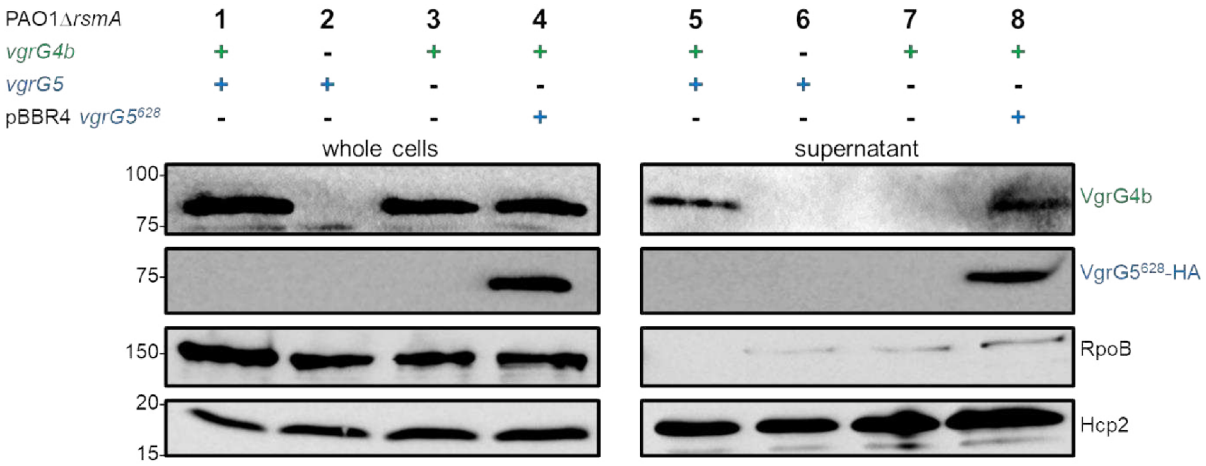


Figure 5-9. VgrG4b delivery requires the gp5-/gp27-like domains of VgrG5.

Representative figure of western blot from a secretion assay of PAO1Δ*rsmA* in absence (-) or presence (+) of the native *vgrG5* or *vgrG4b* or expressing an HA-tagged version of *vgrG5*^{628} *in trans* (+). Antibodies were used against VgrG4b, HA, RpoB and Hcp2 as indicated on the right.

5.8.2. VgrG5 is additionally required for PldA delivery

Since we have observed a functional link between VgrG5 and VgrG4b, we wanted to investigate whether this link would also have an impact on PldA delivery. Since VgrG4b secretion is dependent on the presence of VgrG5, we also wanted to establish whether VgrG5 would play a role in delivering PldA. Bacterial competition assays were performed against prey strains susceptible for PldA delivery, thus lacking the immunity Tli5a, while the attacking strain lacked either *vgrG4b, vgrG5,* both genes or expressed VgrG5^{628} (Figure 5-10A).

When prey strains were grown together with the parental strain as an attacker, it was outcompeted as expected (lane 2). If the attacking strains either lacked *vgrG4b, vgrG5* or both (lanes 3, 4 and 5), no such competition was observed. Furthermore, expressing VgrG5^{628} *in trans* did not result in PldA-mediated killing, suggesting that PldA delivery does not only require VgrG4b for delivery, but also VgrG5. It is noteworthy, that we only expressed the gp5-/gp27-like domains of VgrG5 and not the native full-length protein. It might be possible that the C-terminal region of VgrG5 is somehow required to mediate the delivery of PldA, which would be the appropriate control for this experiment.

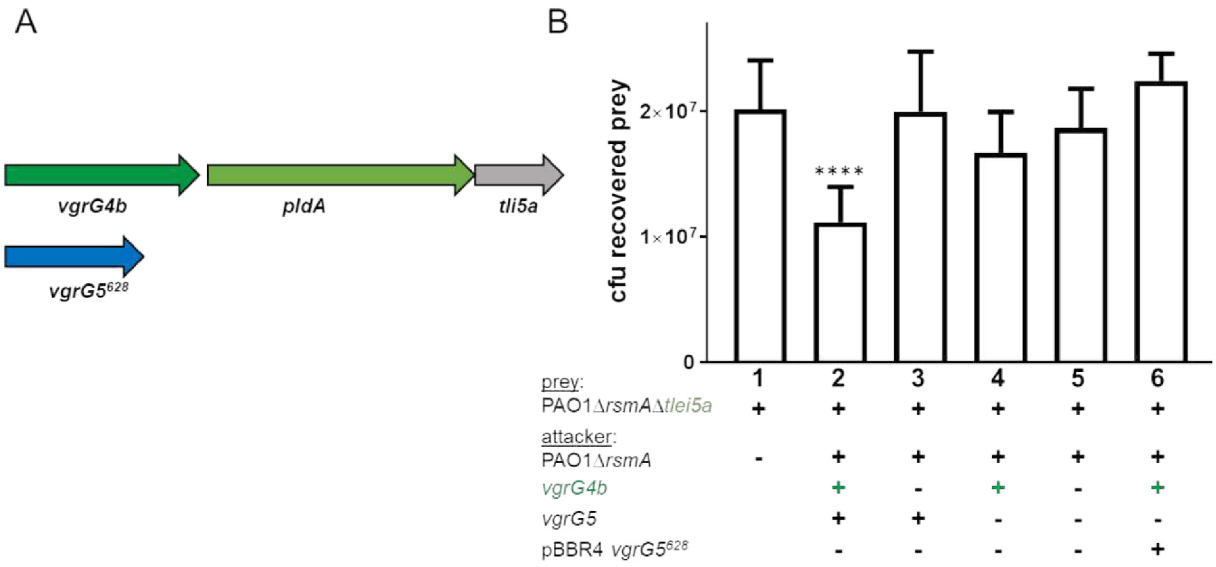


Figure 5-10. Absence of VgrG5 impacts PldA delivery.

A: Attacking strains either lacked *vgrG4b* (green, lane 3), *vgrG5*, both or expressed *vgrG5*^{628} *in trans* (lane 6). B: Plot of recovered cfu of prey strain PAO1Δ*rsmA*Δ*tlei5a::lacZ* after contact with the attacker strain encoding native *vgrG5* (+) and/or *vgrG4b* (+). As a positive control for PldA-mediated killing, PAO1Δ*rsmA* was included (lane 2), while the negative control lacked both *vgrG4b* and *vgrG5* (lane 5). Spots were incubated for 24 h at 25 °C in a 1:1 ratio. One-Way ANOVA analysis with Dunnett's multiple comparisons test was conducted on data set obtained from recovered prey on their own with **** $p<0.0001$.

5.8.3. Absence of VgrG4b does not impact PldB delivery

We observed an impact of absence of VgrG5 on PldA delivery. Next, we wanted to interrogate whether, *vice versa*, the absence of VgrG4b would have an influence on PldB delivery, since it just recently has been shown that absence of VgrG4b has an impact on the remotely encoded effector TseT [220]. Hence, we engineered mutants that express PldB-Bla_{TEM-1} in a *vgrG4b*-deleted background and conducted secretion assays (Figure 5-11A). These results were then confirmed with bacterial competition assays (Figure 5-11B).

Despite the poor quality of the blot with this particular experiment we could confirm that PldB-Bla_{TEM-1} requires VgrG5 for secretion (see arrow for truncated forms in lanes 4 and 5). The presence of VgrG4b was not needed (lane 5) and VgrG4b on its own cannot support PldB secretion (lane 6). It is also noteworthy that in absence of VgrG5, the level of produced PldB-Bla_{TEM-1} is slightly decreased (lane 3), which is not the case in the absence of VgrG4b (lane 2). Despite the low quality of the blots, all above conclusions were corroborated by the readout of the competition assay. Indeed PldB-dependent killing is clearly observable in the absence of VgrG4b (lane 10) but inexistent if VgrG5 is lacking (lanes 9 and 11).

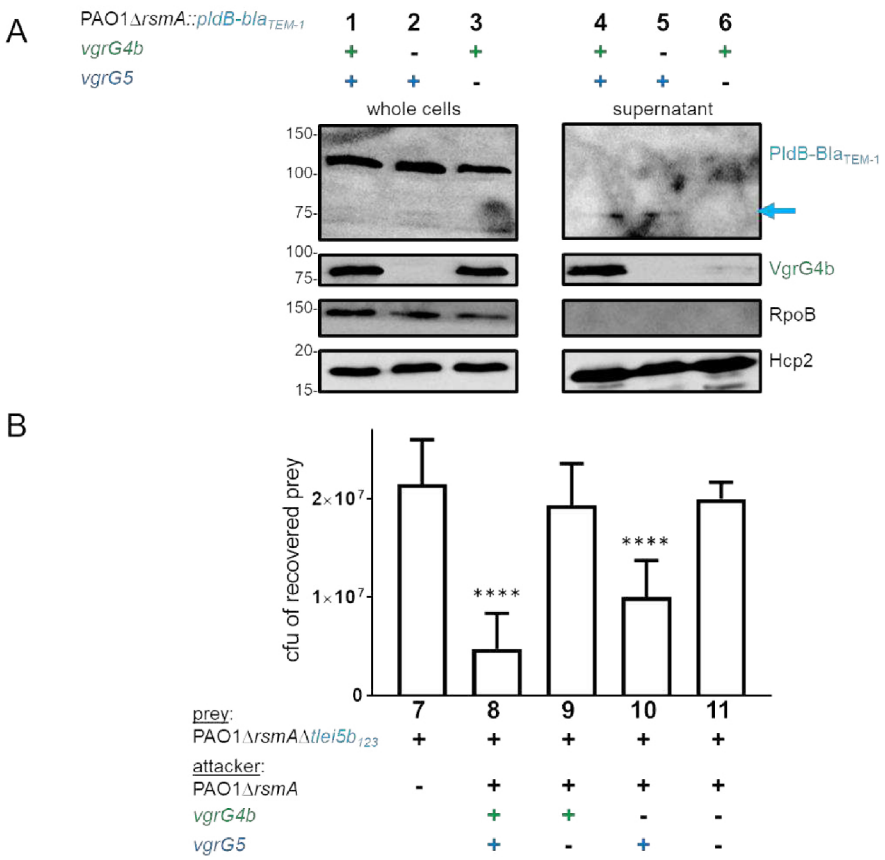


Figure 5-11. Delivery of PldB does not depend on VgrG4b.

A: Representative figure of western blot from a secretion assay of PAO1Δ*rsmA* in absence (-) or presence (+) of the native *vgrG5* or *vgrG4b* expressing a Bla_{TEM-1}-tagged version of PldB. Antibodies were used against Bla_{TEM-1}, VgrG4b, RpoB and Hcp2 as indicated on the right. B: Plot of recovered cfu of prey strain PAO1Δ*rsmA*Δ*tlei5b*$_{123}$*::lacZ* after contact with the attacker strain encoding native *vgrG5* (+) and/or *vgrG4b* (+). As a positive control for PldB-mediated killing, PAO1Δ*rsmA* was included (lane 8), while the negative control lacked both *vgrG4b* and *vgrG5* (lane 11). Spots were incubated for 24 h at 25 °C in a 1:1 ratio. One-Way ANOVA analysis with Dunnett's multiple comparisons test was conducted on data set obtained from recovered prey on their own with **** $p<0.0001$.

5.8.4. Discussion: Heterotrimers as a general advantage of the H2-T6SS machinery

In this chapter, we established a novel concept for T6SS-mediated effector delivery. We highlighted a remarkable interplay between VgrG4b and VgrG5 and examined how this

link impacts delivery of their cognate effectors. While we showed that delivery of PldB solely depends on its upstream encoded VgrG5, we observed that delivery of PldA not only depends on its upstream encoded VgrG4b but also on the distantly encoded VgrG5. This is in good agreement with a recent study showing that delivery of the effector TseT depends on two remotely encoded VgrG proteins, namely VgrG4b and VgrG6 [220].

In our model in Figure 5-12A, a heterotrimer of VgrG4b (green) and VgrG5 (blue) is possibly topped by one cognate PAAR (orange). The configuration of a VgrG4b-VgrG5-PAAR complex is a functional spike and secretion of VgrG4b, PldA (bright green) and PldB (cyan) have been experimentally verified. So far, there is no data on which of the PAAR proteins from *P. aeruginosa* could be the cognate one for this tip. The list of PAAR proteins in *P. aeruginosa* in Table 4-1 shows that we have not identified all functional VgrG-PAAR pairs and there are at least three reasonable candidates. Deletion mutants in any of the *paar* genes ought to be tested for their abilities to deliver PldA and PldB, which would give first hints about the PAAR dependencies of VgrG4b and VgrG5.

In the absence of VgrG4b (Figure 5-12B), we observed secretion of PldB (Figure 5-11), and could thus assume delivery of VgrG5, but no longer of PldA (Figure 5-8). We thus have to acknowledge that there is a functional T6SS tip, which is likely to be a homotrimer of VgrG5 together with a potential cognate PAAR, although we only have these indirect results that support this hypothesis.

In the absence of VgrG5 (Figure 5-12C), we made the striking observation that delivery of both PldA and PldB was abrogated. It was expected to observe an impact on PldB delivery due to the genetic link between *vgrG5* and *pldB*. However, the indirect influence of VgrG5 on PldA delivery was more unexpected but easily explained by the fact that in absence of VgrG5, VgrG4b as a vehicle was also not delivered. The absence of VgrG4b secretion either suggests that a VgrG4b homotrimer is unstable, or that a PAAR protein requires at least one β-strand

of VgrG5 to bind the trimer. This question should be addressed once the cognate PAAR protein for a VgrG5- and a VgrG4b-VgrG5 trimer has been identified. It might as well be the case, that one specific PAAR protein recognises a VgrG4b-VgrG5 heterotrimer, while another PAAR protein specifically binds VgrG5 homotrimers.

When we attempted to complement the *vgrG5* mutant by expressing the N-terminal region of VgrG5 (Figure 5-12D), we were able to restore secretion of VgrG4b (Figure 5-9). This would suggest that in this context, a heterotrimer of VgrG4b and VgrG5^{628} can be formed and the cognate PAAR most likely recognises this complex. Interestingly, although we could restore VgrG4b secretion, PldA delivery was not restored. This was unexpected, since VgrG4b seemed to be intact and therefore should recruit PldA and mediate its delivery. The only component missing in this context was the C-terminal region of VgrG5, which seems to have an impact on PldA delivery. One could envisage that another T6SS component, such as an adaptor or chaperone, binds the C-terminal region of VgrG5 and connects it with both VgrG4b and PldA. There is weak evidence suggesting that the chaperone TecT indeed binds a VgrG4b-VgrG6 heterotrimer connecting it to the effector TseT [220]. One might assume that these interactions are mediated by the C-termini of the VgrG proteins, thus a similar concept might be possible for a VgrG4b-VgrG5-PldA complex. On another note, we have not investigated PldB delivery using the *vgrG5^{628}* construct, as the impact of C-terminal regions of VgrG proteins will be the focus of the next section.

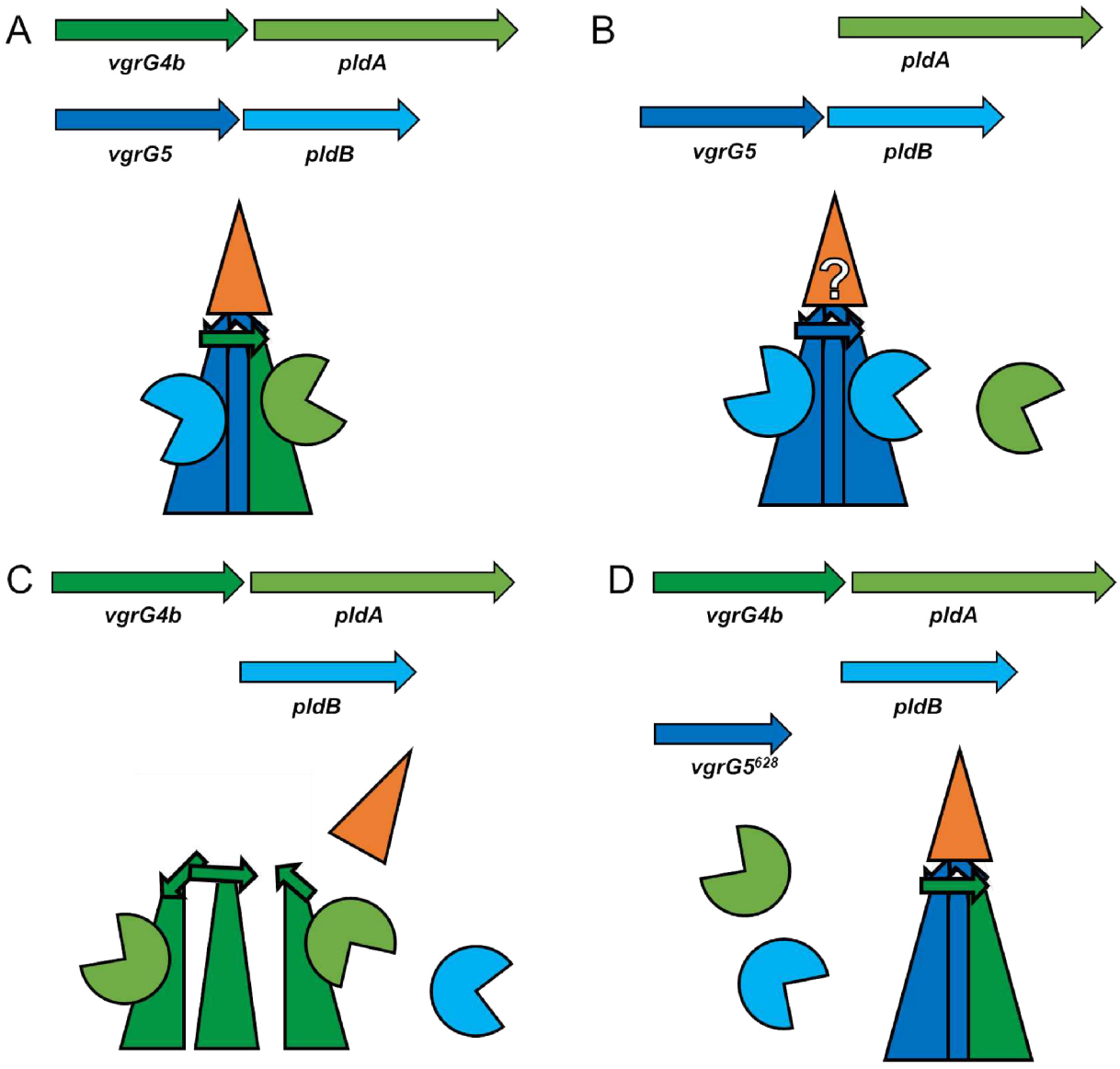


Figure 5-12. Model of the heterotrimer formation resulted from this section.

A: In *P. aeruginosa* WT, VgrG4b (green) and VgrG5 (blue) form a heterotrimer together with a putative cognate PAAR (orange) that is secreted. PldA (bright green) and PldB (cyan) are delivered. B: In the absence of VgrG5, VgrG4b on its own cannot form a functional T6 tip and is not secreted. PldB delivery is abrogated due to its missing cognate VgrG and PldA delivery is highly impacted due to the lack of a functional VgrG4b tip. C: In the absence of VgrG4b, PldA delivery is completely abrogated. VgrG5 might form a functional T6 tip, although this has not been proven. PldB is still delivered. D: Complementation of the N-terminus of VgrG5 leads to the formation of a functional VgrG4b-VgrG5 heterotrimer that is secreted. PldA, however, is not delivered.

5.9. The C-terminal TTR domains of VgrG4b and VgrG5 differ and are specific for recognition of PldA and PldB

5.9.1. Towards the function of TTR-like domains within VgrG proteins

VgrG4b and VgrG5 influence delivery of their cognate effectors PldA and PldB, respectively. We wanted to further characterise the VgrG region involved in specificity and use this information in an attempt to design protein delivery shuttles. As indicated, recent research into the delivery mechanism of Tle1 from entero-aggregative *Escherichia coli* showed that its cognate VgrG1^{Eco} contains a C-terminal TTR-like domain essential for Tle1 delivery [216]. Bioinformatic analysis of VgrG4b and VgrG5 led us to identify similar TTR-like domains within their C-termini. Other characterised VgrG proteins, particularly those encoded upstream of adaptor-less effector genes (Figure 5-13A), were closely examined. We identified TTR-like domains within the C-terminal regions of these VgrGs (bright green) and interestingly, in all cases the cognate effectors are lipases. In the cases of VgrG4b and VgrG5, a potential PAAR-binding site, identified by the conserved motif within the last putative β-strand, precedes the TTR-like domain (Figure 5-13B, purple). In VgrG proteins, that additionally contain DUF2345 domains (Figure 5-13A, grey areas), series of β-sheets are predicted throughout the DUF2345 domains (*data not shown*). This makes it impossible to exactly pinpoint the location of the PAAR-binding site within the C-terminus of these VgrG proteins. In any case, TTR-like domains are located at the very C-terminus of VgrG proteins (Figure 5-13B) and, due the absence of predicted series of β-sheets, they are unlikely to be part of the needle-like structure. This suggests that the TTR-like domain represents an extension of the VgrG protein which is not an effector domain as in the case of evolved VgrGs. However, the specific role of the TTR-like domain in the T6SS is still unclear and will be focus of this section.

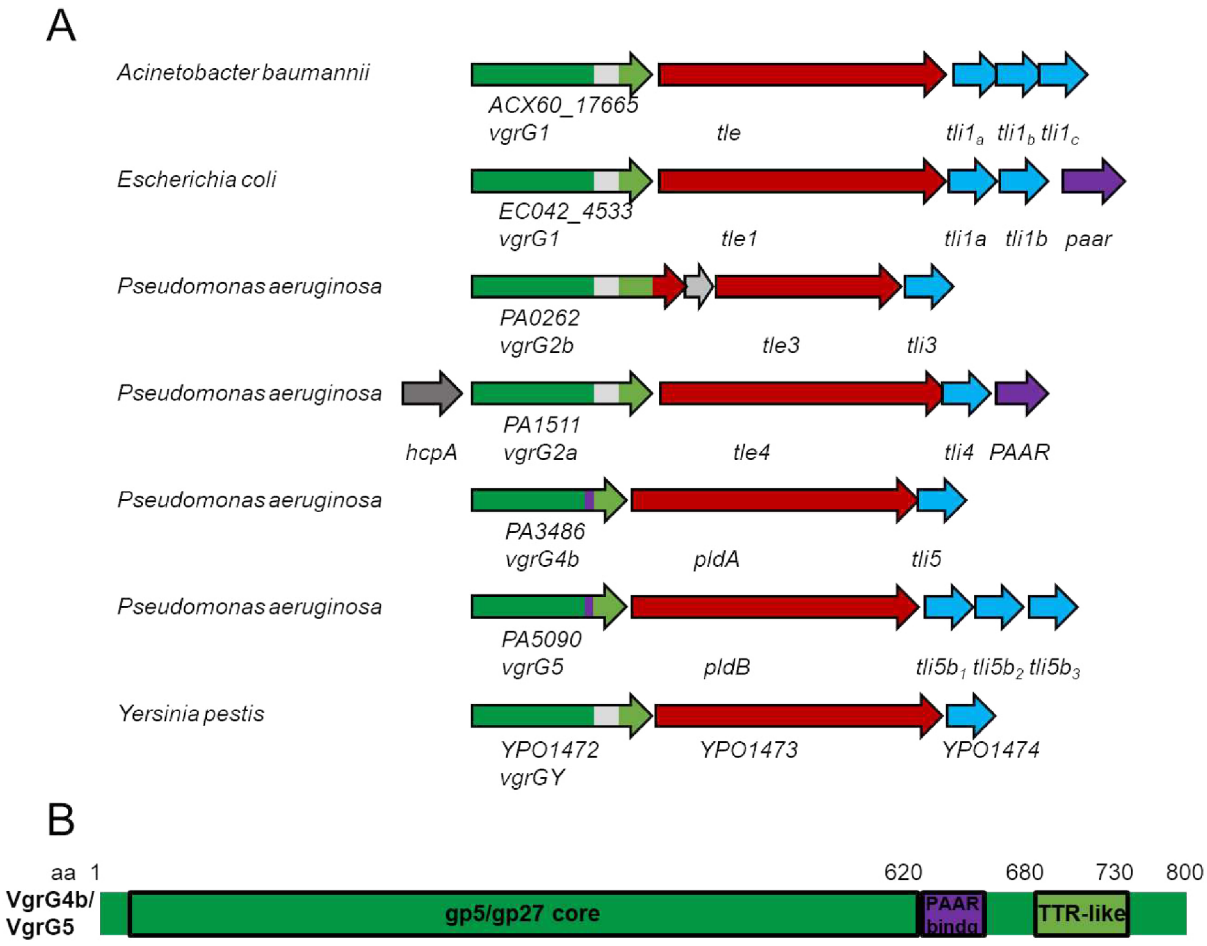


Figure 5-13. Composition of VgrG proteins involved in delivering adaptor-less effectors.

A: Genetic environments of effector genes (red) whose gene products do not contain any T6SS-related adaptors. *vgrG* genes are depicted in green, corresponding TTR-like domains and DUF2345 in bright green and grey-green, respectively; effector genes in red, immunities in cyan, *paar* genes in purple. B: VgrG4b and VgrG5 contain the core gp5-/gp27-like domains (green) followed by the PAAR-binding motif (purple) and a TTR-like domain (bright green).

On the basis of Phyre2 analysis [235], we identified transthyretin-like folds of approximately 110 aa in VgrG proteins that are encoded upstream of adaptor-less lipases as listed in Figure 5-13A. Originally, transthyretin-like proteins (TLPs) were structurally and mechanistically characterised in a range of bacteria. In contrast to human transthyretin, which is involved in the transport of holo-retinol binding protein and thyroxine [258, 259], bacterial TLPs are involved in purine metabolism [254, 260]. Both transthyretin and TLPs were shown

to form homo-tetramers [254]. However, it seems highly unlikely that C-terminal extension domains of VgrG proteins are involved in the transport of eukaryotic proteins or in purine metabolism.

To shed light on the functionality of these transthyretin-like domains within VgrG proteins ($TLDs^{VgrG}$), we aligned their amino acid sequence and structural models with those from *S. dublin* TLP (TLP^{Sdub}). Figure 5-14A shows that all $TLDs^{VgrG}$ display similar structural folds as TLP^{Sdub}, confirming the Phyre results [235]. Furthermore, a multiple sequence alignment showed that the amino acid sequences of $TLDs^{VgrG}$ are more similar within the N-terminus with TLP^{Sdub} and less within the C-terminus (Figure 5-14B). More specifically, four conserved motifs were previously identified in TLPs [261]. While the two N-terminal motifs (LDXXXG, GXTXXXG) are conserved within $TLDs^{VgrG}$ (red lines), the third motif (GXY) is barely recognisable (bright red line), while the C-terminal motif (YRGS) is only present in TLP^{Sdub} (faint red line). According to structural studies, the last two motifs are involved in the formation of homo-tetramers [261]. Hence, the lack of these conserved residues might be in agreement with the fact that $TLDs^{VgrG}$ are unlikely to form homo-tetramers. This is in agreement with the fact that VgrGs form trimers and thus tetramerisation is highly unlikely [253].

On another note, TLPs were demonstrated to harbour hydrolase activity mediated by two conserved histidine and one tyrosine residue, highlighted with red asterisks in Figure 5-14B [254]. These residues from the catalytic site of TLPs are not present in $TLDs^{VgrG}$, suggesting that $TLDs^{VgrG}$ do not bind and hydrolyse the same substrate as TLP^{Sdub}. This allows the assumption that $TLDs^{VgrG}$ are not involved in purine metabolism. Since TTR-like domains are found at the C-terminus of VgrG, a putative role would be effector recognition and delivery.

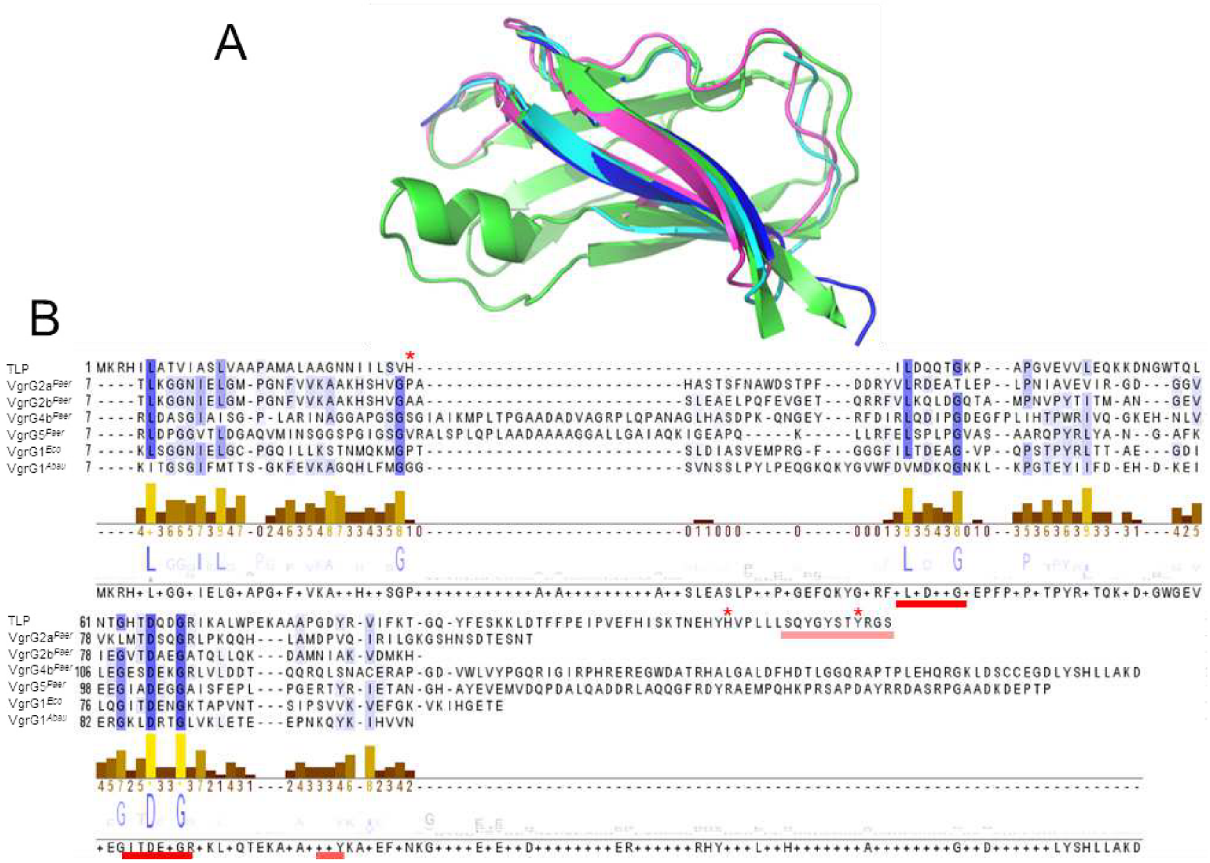


Figure 5-14. The C-terminal domains of some VgrG proteins are homologues to transthyretin-like domains (TLD^{VgrG}).

A: Structural alignments of models of the C-terminal domains of VgrG4b (blue), VgrG5 (cyan) and VgrG2b (pink) on the transthyretin-like protein (TLP) from *Salmonella dublin* (green, pdb: 2GPZ). B: Multiple sequence alignment of the transthyretin-like protein from *S. dublin* and homologues domains from VgrGs. Highlighted with red lines are the conserved TTR-like motifs shown on the consensus sequence, while the least conserved motif is only present in TLP^{Sdub} (fading red line). Red asterisks in TLP^{Sdub} highlight the conserved catalytic residues that are absent in TTR-like domains of VgrG proteins.

5.9.2. Constructing chimerae to unravel the importance of C-terminal TTR-like domains of VgrG proteins

In an attempt to confirm that specificity for an effector is mediated by the C-terminal TTR-like domain of a VgrG protein, we closely compared the amino acid sequences of VgrG4b and VgrG5 (Figure 5-15A). The gp27-/gp5-like domains comprise the first approximately

620 aa corresponding to the needle-shaped VgrG spike [253], which corresponds to the region prior to the red line in Figure 5-15A. Throughout these domains, VgrG4b and VgrG5 share a sequence identity of 69 % (https://web.expasy.org/sim/) with the amino acid identity highlighted by blue boxes. Beyond this point (beyond the red line), VgrG4b and VgrG5 start to diverge and the sequence identity drops to 25 % confirming that effector specificity likely relies on the C-terminus. From secondary structure predictions (data not shown), we speculated that the amino acid sequence highlighted by the purple line in Figure 5-15A corresponds to the PAAR-binding motifs of both VgrG4b and VgrG5, while the predicted TTR-like domain is highlighted with a green line.

Based on these findings, it was hypothesised that modification of the C-terminus of VgrG4b and VgrG5 would abrogate effector recognition and thus delivery of PldA and PldB, respectively. From now on, the term C-terminus of VgrG4b or VgrG5 corresponds to the protein region beyond the red line in Figure 5-15A. This region includes the putative PAAR-binding β-strand (highlighted with a purple line) and the TTR-like domain (highlighted with a bright green line). It was decided to swap the C-termini between VgrG4b and VgrG5 and monitor delivery of the cognate effectors. Specifically, the gene portion corresponding to the C-terminal 187 aa of VgrG4b was substituted with the gene portion corresponding to the C-terminal 169 aa of VgrG5. This would ultimately lead to the expression of a VgrG4b^{621}-VgrG5^{169}-chimera. To ensure that production of the downstream encoded PldA is not impacted by this substitution, the 30 bp upstream of its START codon were unchanged (Figure 5-15B). Similarly, to design a VgrG5^{623}-VgrG4b^{187}-chimera, the gene portion corresponding to the C-terminal 169 aa of VgrG5 was substituted with the gene portion corresponding to the C-terminal 187 aa of VgrG4b. PldB production was ensured not to be affected by leaving the 30 bp upstream of its START codon unchanged (Figure 5-15C).

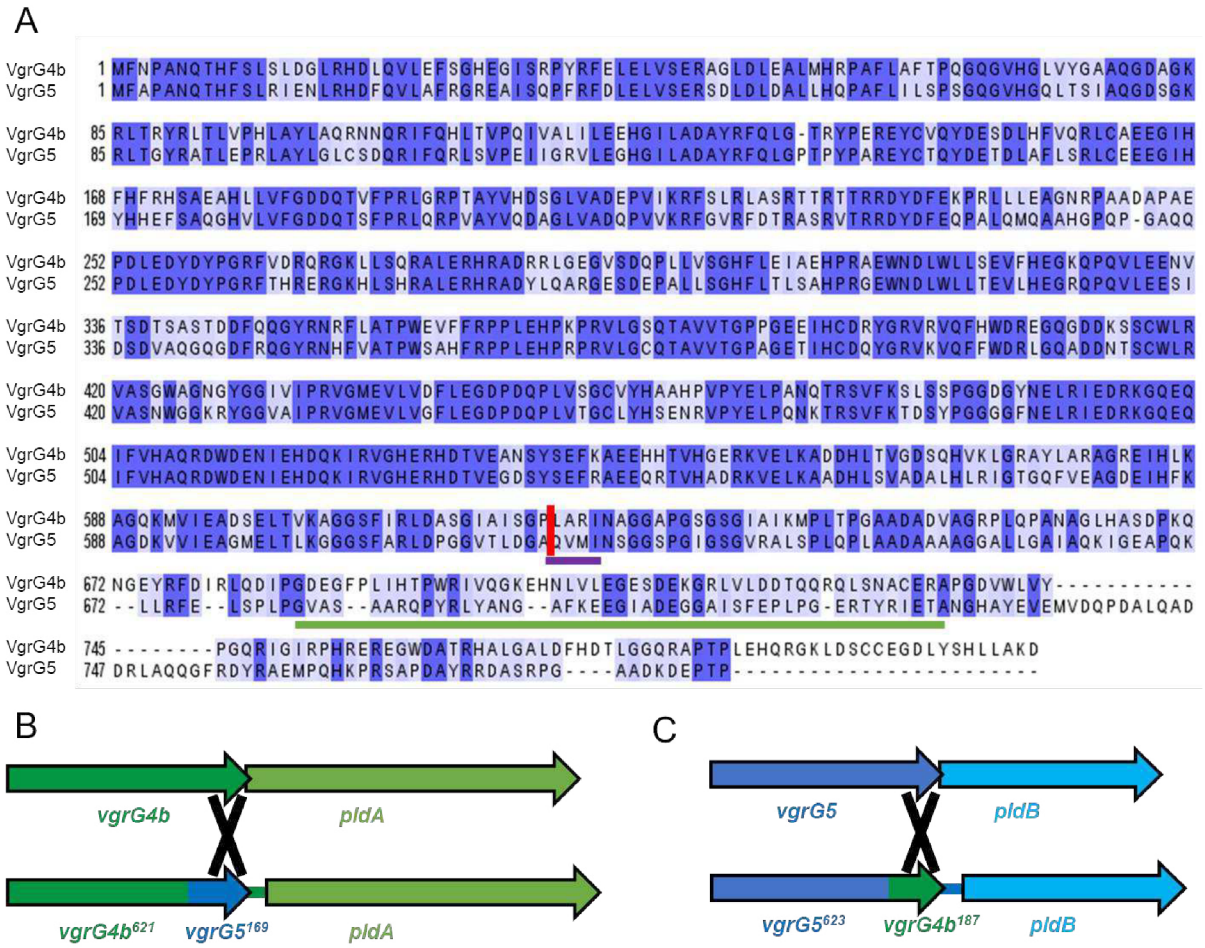


Figure 5-15. Design of mutants to swap C-termini between VgrG4b and VgrG5.

A: Multiple sequence alignment between VgrG4b and VgrG5. Highlighted with a purple line are the putative PAAR-binding sites; highlighted with a bright green line are the putative TTR-like domains. The red line indicates the location of the swap of the C-termini. B: WT *vgrG4b* (green) is followed by *pldA* (bright green). For this mutant, the gene sequence corresponding to the C-terminus of $vgrG5^{169}$ (blue) was used to substitute the gene sequence corresponding to the C-terminus of *vgrG4b*, while 30 bp upstream of the START codon of *pldA* was unchanged. C: WT *vgrG5* (blue) is followed by *pldB* (cyan). For this mutant, the gene sequence corresponding to the C-terminus of $vgrG4b^{187}$ was used to substitute the gene sequence corresponding to the C-terminus of *vgrG5*, while 30 bp upstream of the START codon of *pldB* was unchanged.

5.9.3. Modifying the C-terminus of VgrG5 abrogates delivery of PldB

We used strains that expressed the VgrG5^{623}-VgrG4b^{187}-chimera to understand whether the C-terminal substitution has an impact on PldB delivery (Figure 5-16A). To avoid cross-recognition with native VgrG4b, the construct was introduced into a *vgrG4b*-deficient background. Because our antibody against VgrG4b specifically recognises the C-terminal 190 residues of VgrG4b we first verified expression of the chimera (Figure 5-16B). Western blot analysis on whole cell samples expressing the chimera resulted in the detection of a band corresponding to the expected size of VgrG5^{623}-VgrG4b^{187} in a background lacking native VgrG4b (lane 3).

It was thus hypothesised that the lack of the effector-recognising domain of VgrG5, containing the TTR-like domain, would prevent PldB delivery. Competition assays were performed against PldB-sensitive prey strains (Figure 5-16C). While the positive control, the parental strain lacking *vgrG4b*, outcompeted the prey strain due to delivery of PldB (lane 5), the negative control lacking both *vgrG4b* and *vgrG5* did not have the same competitive advantage (lane 6). The tested strain expressing VgrG5^{623}-VgrG4b^{187} (lane 7) showed a similar phenotype as the negative control, suggesting that the lack of the C-terminus of VgrG5 abrogated PldB delivery.

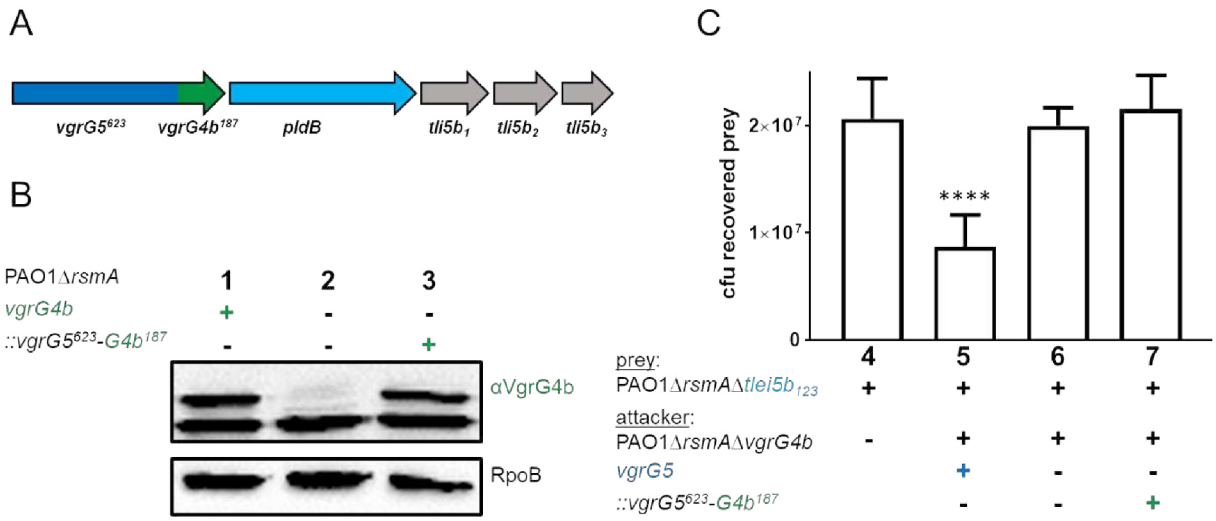


Figure 5-16. Modifying the C-terminus of VgrG5 abrogates delivery of PldB.

A: The here used mutants carry the gene sequence for a *vgrG5*^{623}-*vgrG4b*^{187}-chimera followed by *pldB* (cyan). B: Representative figure of a western blot from whole cell fractions of PAO1Δ*rsmA* encoding native *vgrG4b* (+) or the *vgrG5*^{623}-*vgrG4b*^{187}-chimera (+) to ensure expression of the chimera. Antibodies were used against VgrG4b-CT and RpoB as indicated on the right. C: Plot of recovered cfu of prey strain PAO1Δ*rsmA*Δ*tlei5b*$_{123}$::*lacZ* after contact with the attacker strain that encoded native *vgrG5* (+) or the *vgrG5*^{623}-*vgrG4b*^{187}-chimera (+). As a positive control for PldB-mediated killing, PAO1Δ*rsmA*Δ*vgrG4b* was included (lane 5), while the negative control lacked *vgrG5* (lane 6). Spots were incubated for 24 h at 25 °C in a 1:1 ratio. One-Way ANOVA analysis with Dunnett's multiple comparisons test was conducted on data set obtained from recovered prey on their own with **** $p<0.0001$.

5.9.4. Modifying the C-terminus of VgrG4b abrogates delivery of PldA

To examine whether the C-terminus of VgrG4b is essential for delivery of PldA, strains were engineered that carried the *vgrG4b*^{621}-*vgrG5*^{169}-chimera (Figure 5-17A). These chimerae were introduced into the parental background, as we showed before, that VgrG4b would not be secreted from *vgrG5* deficient strains (see 5.8.1). As the C-terminus of VgrG4b was not present in those cells, we had no tools to detect this chimera. We could simply assume its

production on the basis of the lack of a band corresponding to VgrG4b, since the chimera would no longer be detected by the anti-VgrG4b.

Competition assays were conducted with mutants that carried the *vgrG4b*^{621}-*vgrG5*^{169}-allele against PldA-sensitive prey strains of which a plot can be seen in Figure 5-17B. The tested strains expressing VgrG4b^{621}-VgrG5^{169} (lane 4) showed similar phenotypes as the negative control (lane 3) suggesting that the lack of the C-terminus of VgrG4b abrogated PldA delivery. However, since we have no mean to test production of the chimera, this result remains speculative.

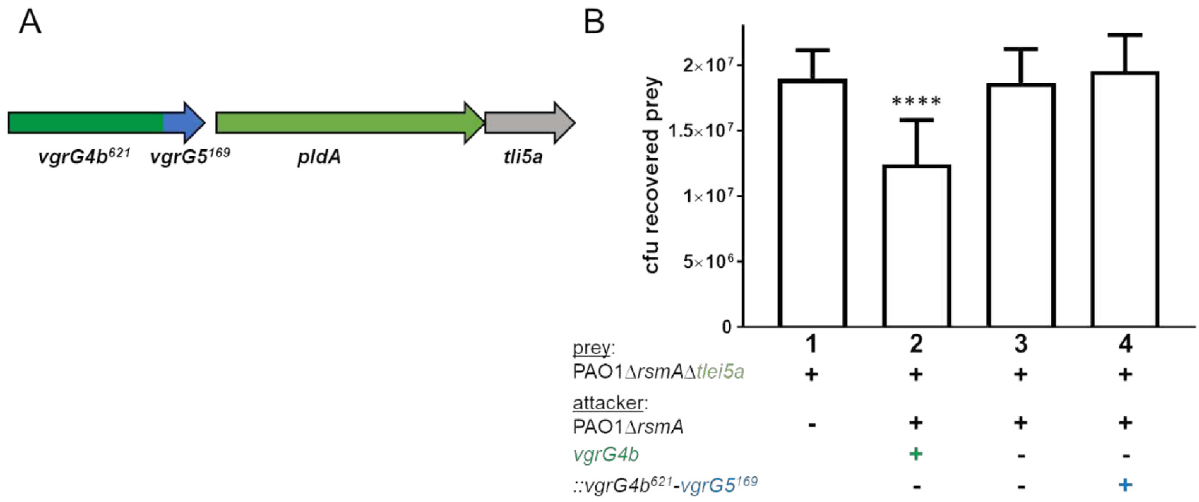


Figure 5-17. Modifying the C-terminus of VgrG4b abrogates delivery of PldA.

A: The here used mutants carry the gene sequence for a *vgrG4b*^{621}-*vgrG5*^{169}-chimera followed by *pldA* (green). B: Plot of recovered cfu of prey strain PAO1Δ*rsmA*Δ*tlei5a::lacZ* after contact with the attacker strain that encoded native *vgrG4b* (+) or the *vgrG4b*^{621}-*vgrG5*^{169}-chimera (+). As a positive control for PldA-mediated killing, PAO1Δ*rsmA* was included (lane 2), while the negative control lacked *vgrG4b* (lane 3). Spots were incubated for 24 h at 25 °C in a 1:1 ratio. One-Way ANOVA analysis with Dunnett's multiple comparisons test was conducted on data set obtained from recovered prey on their own with **** $p<0.0001$.

5.9.5. Effectors are stabilised by the C-terminal domains of their cognate VgrGs

In Figure 5-7 and Figure 5-8, as well as further obtained western blots not shown here we observed decreases of effector stability in the absence of the cognate VgrG protein. The finding, that an effector seemed to be less stable due to absence of its cognate VgrG, was rather puzzling. However, it was shown for another T6SS effector, Tde1 from *A. tumefaciens*, that it is more stable in presence of its cognate chaperone Tap1 [153].

This led us to introduce various chimerae into our PldA-Bla_{TEM-1}- or PldB-Bla_{TEM-1}-expressing strains. In a mutant expressing PldB-Bla_{TEM-1} we substituted the C-terminus of VgrG4b with the C-terminus of VgrG5 as described in 5.9.2 in a *vgrG5* deficient background (Figure 5-18A). We wanted to analyse whether the presence of the C-terminus of VgrG5 has a stabilising effect on PldB independent on the VgrG vehicle it is fused to. We also constructed a chimera between VgrG1a and substituted its C-terminus with the one from VgrG4b in a similar fashion as for the chimera between VgrG5 and VgrG4b (see 5.9.2). We introduced this construct into PldA-Bla_{TEM-1} producing strains to verify that the C-terminus of VgrG4b has a stabilising effect on PldA (Figure 5-18B). To ultimately point out that the C-terminus of VgrG4b stabilises PldA stability and to rule out any cross-specificity, we introduced both chimerae versions of VgrG4b and VgrG5 into PldA-Bla_{TEM-1} producing strains (Figure 5-18C).

For all experiments, cells were grown together with the parental strain and the strain lacking the cognate *vgrG* as controls. Whole cell lysates were blotted for the effectors with the Bla_{TEM-1}-antibody. In all cases, effector stabilities were highest in the parental strains (each top panel, lanes 2, 5 and 8). When the cognate VgrGs are absent, the corresponding bands for the effectors decrease in intensity (lanes 3, 6 and 9). Remarkably, whenever the C-terminus of the cognate VgrG was then present, but fused to another VgrG vehicle, the band corresponding to the effector intensified, suggesting stability of the effector proteins (lanes 4, 7 and 11). Equal loadings were confirmed with blots against RpoB (bottom panels), while

blotting against VgrG4b confirmed expression of chimerae that contained the C-terminal domain of VgrG4b (second panels).

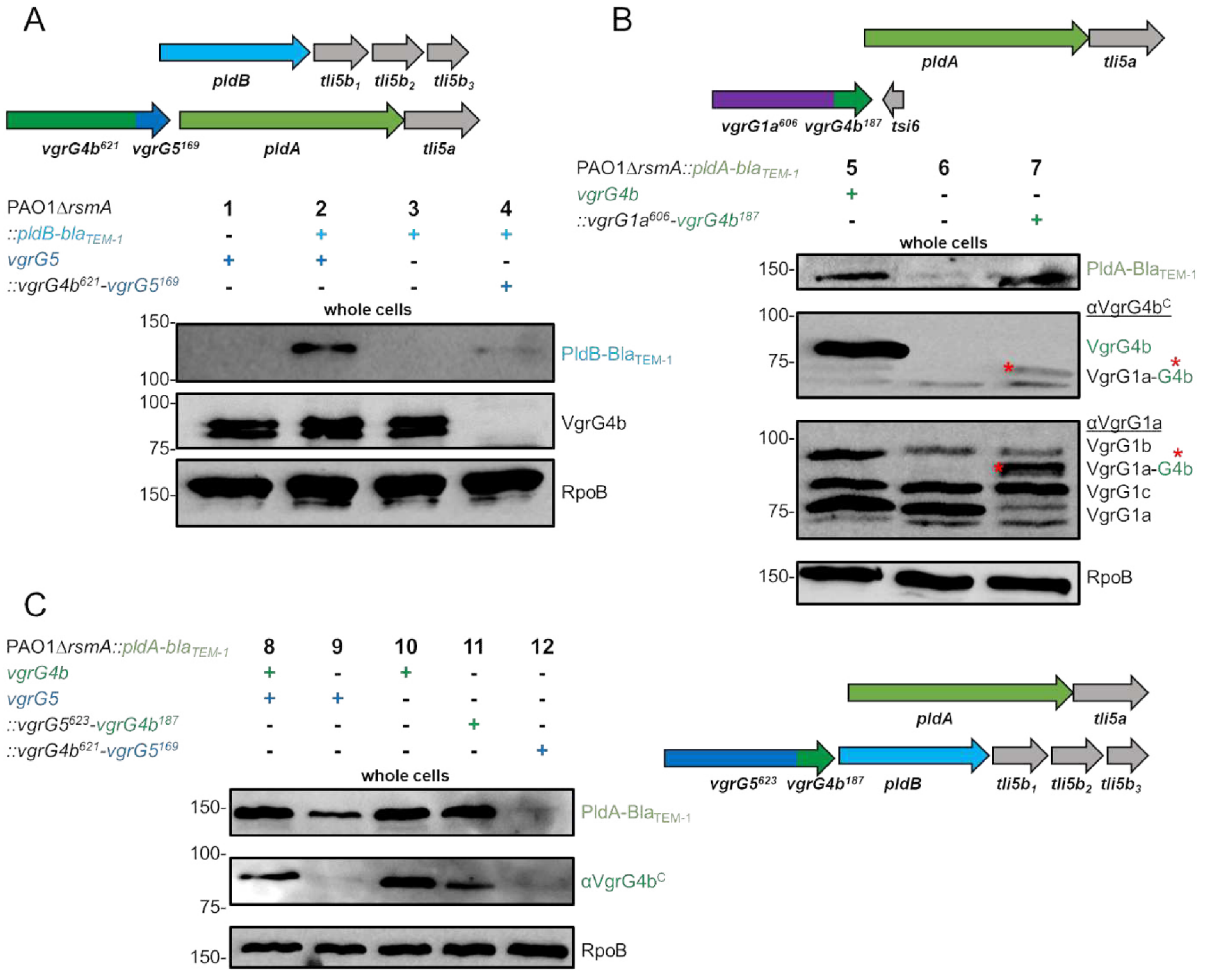


Figure 5-18. Effectors are stabilised by the C-termini of their cognate VgrG proteins.

Genetic backgrounds: mutants carry the gene sequences as sketched for all experiments. A: *vgrG4b*^{629}-*G5*^{169}-chimera instead of the native *vgrG4b* locus and in absence of the native *vgrG5* locus. B: *vgrG1a*^{606}-*G4b*^{187}-chimera instead of the native *vgrG1a* locus and in absence of the native *vgrG4b* locus. C: Native *vgrG4b* (+), native *vgrG5* (+), the *vgrG4b*^{629}-*G5*^{169}-chimera (+) or the *vgrG5*^{623}-*G4b*^{187}-chimera (+). Lower panels: Representative figures of western blots from whole cell fractions of A: PAO1Δ*rsmA::pldB-bla*$_{TEM-1}$ in presence of the native *vgrG5* (+) or encoding the *vgrG4b*^{629}-*G5*^{169}-chimera (+); B: PAO1Δ*rsmA::pldA-bla*$_{TEM-1}$ in presence of the native *vgrG4b* (+) or encoding the *vgrG1a*^{606}-*G4b*^{187}-chimera (+); C: PAO1Δ*rsmA::pldA*$_{TEM-1}$. Controls for effector stabilities are shown with the parental strains in A: lane 2, B: lane 5 and C: lane 8, while the negative controls lack the cognate *vgrG* loci A: lane 3, B: lane 6 and C: lane 9. Antibodies were used against Bla$_{TEM-1}$, VgrG4b-CT, VgrG1abc and RpoB as indicated on the right of each panel.

These figures support our hypothesis that the C-terminal regions of VgrG proteins specifically bind and stabilise the cognate effectors. On the basis of these results, we then wanted to test whether these specific interactions would be sufficient to mediate delivery of the cognate effector.

5.9.6. VgrG4b cannot deliver PldB

Figure 5-18A allows the assumption that the VgrG5 C-terminus as part of VgrG4b somehow interacts and stabilises PldB (top panel). However, we have shown in 5.7.1, that secretion of VgrG4b is abrogated in absence of VgrG5. One might assume that secretion of the VgrG4b^{621}-VgrG5^{169}-chimera in absence of VgrG5 is also compromised. Hence, we attempted to obtain proficient secretion of the VgrG4b^{621}-VgrG5^{169}-chimera by co-expressing VgrG5^{628}. This construct successfully facilitated secretion of VgrG4b in Figure 5-9, and we suspect it might have the same effect on VgrG4b^{621}-VgrG5^{169}. Since VgrG5^{628} lacks the C-terminal cognate domain to interact with PldB, it would solely facilitate secretion of VgrG4b^{621}-VgrG5^{169}, likely by forming a heterotrimer with the chimera, which in turn would mediate delivery of PldB that interacts with the C-terminus of the chimera (Figure 5-19A).

To follow PldB secretion, we performed secretion assays with strains that expressed the PldB-Bla$_{TEM-1}$-fusion and the VgrG4b^{621}-VgrG5^{169} and carried the plasmid for VgrG5^{628} (Figure 5-19B). Similarly to previous results, we detected PldB-Bla$_{TEM-1}$ in the whole cell fractions and a cleaved version in the supernatant fraction of the parental strain (top panel, lane 5). In none of the other supernatant fractions could we observe PldB-Bla$_{TEM-1}$ suggesting that our attempt to secrete the effector was unsuccessful. VgrG4b was secreted from the parental strain (second panel), but not in the absence of *vgrG5* (lane 6), while the chimera was not detected due to the lack of the C-terminal VgG4b domain (lanes 3 and 7).

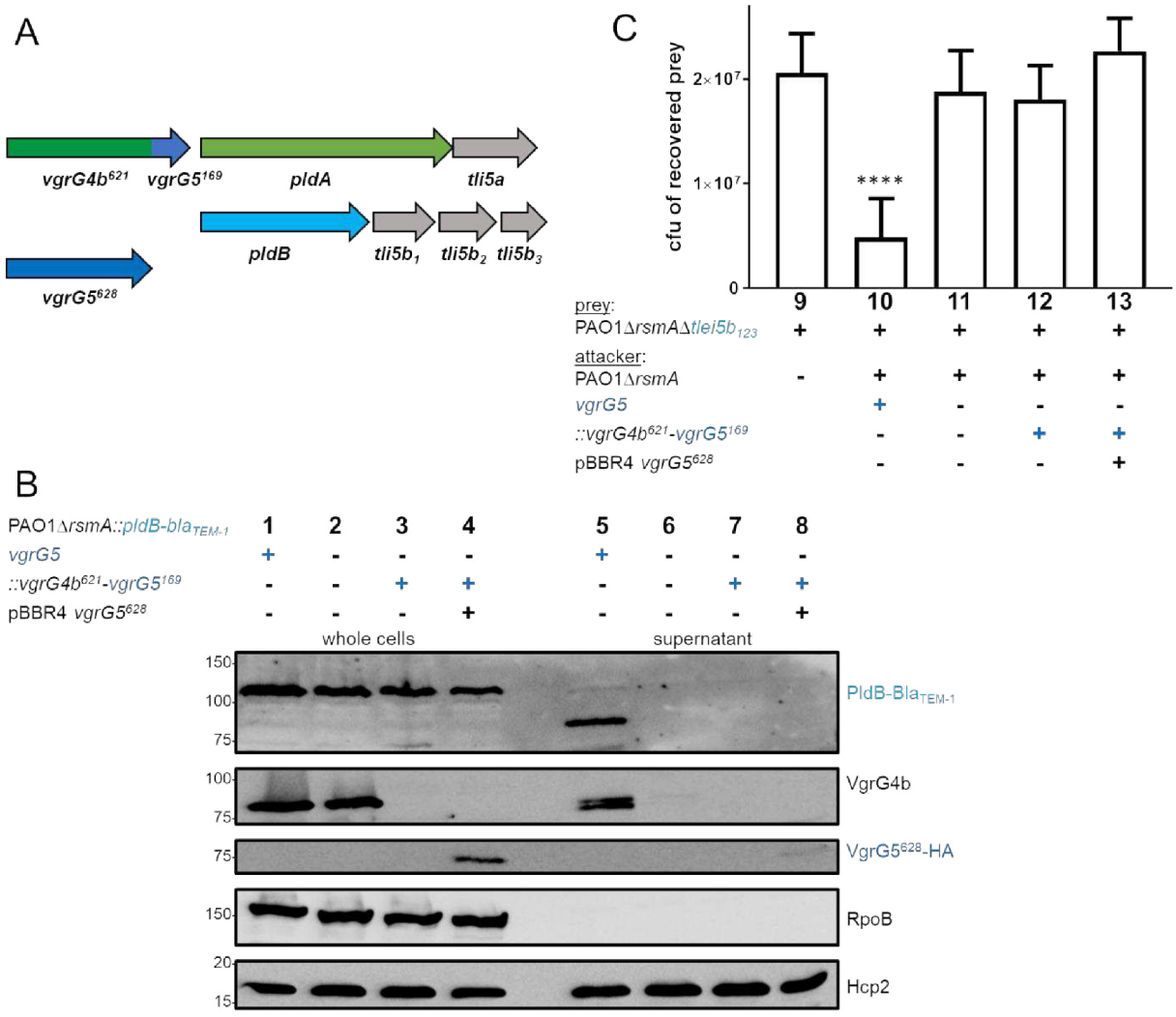


Figure 5-19. Co-expression of N-terminal VgrG5 does not support PldB secretion.

A: The here used mutants carry the gene sequence for a *vgrG4b*^{629}-*vgrG5*^{169}-chimera instead of the native *vgrG4b* locus, in absence of the native *vgrG5* locus and expressed an HA-tagged version of *vgrG5*^{628} from *pBBR1-mcs4*. B: Representative figure of a western blot of a secretion assay of PAO1Δ*rsmA::pldB-bla*$_{TEM-1}$ in presence (+) of the native *vgrG5* or encoding the *vgrG4b*^{629}-*vgrG5*^{169}-chimera (+) together with *pBBR1-mcs4 vgrG5*^{628} (+). Antibodies were used against Bla$_{TEM-1}$, VgrG4b, HA, Hcp2 and RpoB as indicated on the right. C: Plot of recovered cfu of prey strain PAO1Δ*rsmA*Δ*tlei5b*$_3$*::lacZ* after contact with the attacker strain that encoded native *vgrG5* (+) or the *vgrG4b*^{629}-*vgrG5*^{169}-chimera (+) or *pBBR1-mcs4 vgrG5*^{628} (+). As a positive control for PldB-mediated killing, PAO1Δ*rsmA* was included (lane 10), while the negative control lacked the native *vgrG5* locus (lane 11). Spots were incubated for 24 h at 25 °C in a 1:1 ratio. One-Way ANOVA analysis with Dunnett's multiple comparisons test was conducted on data set obtained from recovered prey on their own with **** $p<0.0001$.

When strains expressed VgrG5^{628} we could detect its production due to the presence of an HA-tag (third panel, lane 4), however secretion of this construct was massively compromised in comparison to previous results obtained in presence of WT VgrG4b (Figure 5-9). Detection of Hcp2 in the supernatant (bottom panel) suggested that presence of the VgrG4b^{621}-VgrG5^{169} chimera and/or VgrG5^{628} still resulted in a functional H2-T6SS machinery.

Competition assays against PldB-sensitive strains support these data (Figure 5-19C). Strains expressing VgrG4b^{621}-VgrG5^{169} in absence (lane 12) or presence of VgrG5^{628} (lane 13) showed a similar phenotype as the negative control (lane 11) suggesting that PldB delivery was abrogated.

5.9.7. Connecting PldA with VgrG5 *via* the C-terminus of VgrG4b

We confirmed in Figure 5-18B and C that the presence of the C-terminus of VgrG4b has a stabilising effect on PldA independent of the VgrG vehicle it is fused to. Hence, we asked whether this interaction would be sufficient to connect PldA to another VgrG tip and we tested VgrG1a and VgrG5. When we manipulated VgrG1a to carry the C-terminal domain of VgrG4b, we could see production of the chimera as shown in Figure 5-18B. However, due to the different inducing conditions of the H1-T6SS and the H2-T6SS in *P. aeruginosa* (37 °C and 25 °C, respectively [140, 146]), we did not observe secretion of both the H1-T6SS-dependent VgrG1a^{606}-VgrG4b^{187}-chimera and the H2-T6SS-dependent effector PldA-Bla$_{TEM-1}$ under the same conditions (*data not shown*). Due to this drawback, we focussed on connecting PldA with VgrG5, since these two components exhibit the same expression and secretion condition profile [146].

We tested strains expressing VgrG5^{623}-VgrG4b^{187} in secretion assays and monitored PldA-Bla$_{TEM-1}$ secretion (Figure 5-20B). As previously shown, when cells lacked *vgrG4b*, PldA-

Bla_{TEM-1} stability was massively compromised (top panel, lane 3) and its secretion abrogated (lane 7). When strains expressed the $VgrG5^{623}$-$VgrG4b^{187}$-chimera (lane 4), a band corresponding to its expected size was detected using the antibody against the C-terminus of VgrG4b (second panel). The same band was observed in the supernatant fraction (lane 8) confirming that the $VgrG5^{623}$-$VgrG4b^{187}$-chimera was secreted. A band corresponding to PldA-Bla_{TEM-1} was detected in the supernatant fractions of the same strain (top panel, lane 8) suggesting its secretion.

Competition assays against PldA-sensitive strains confirmed these results (Figure 5-20C). Strains expressing $VgrG5^{623}$-$VgrG4b^{187}$ (lane 12) showed a significant competitive advantage towards the prey strain similarly to the positive control (lane 10) suggesting that PldA was delivered using the chimera.

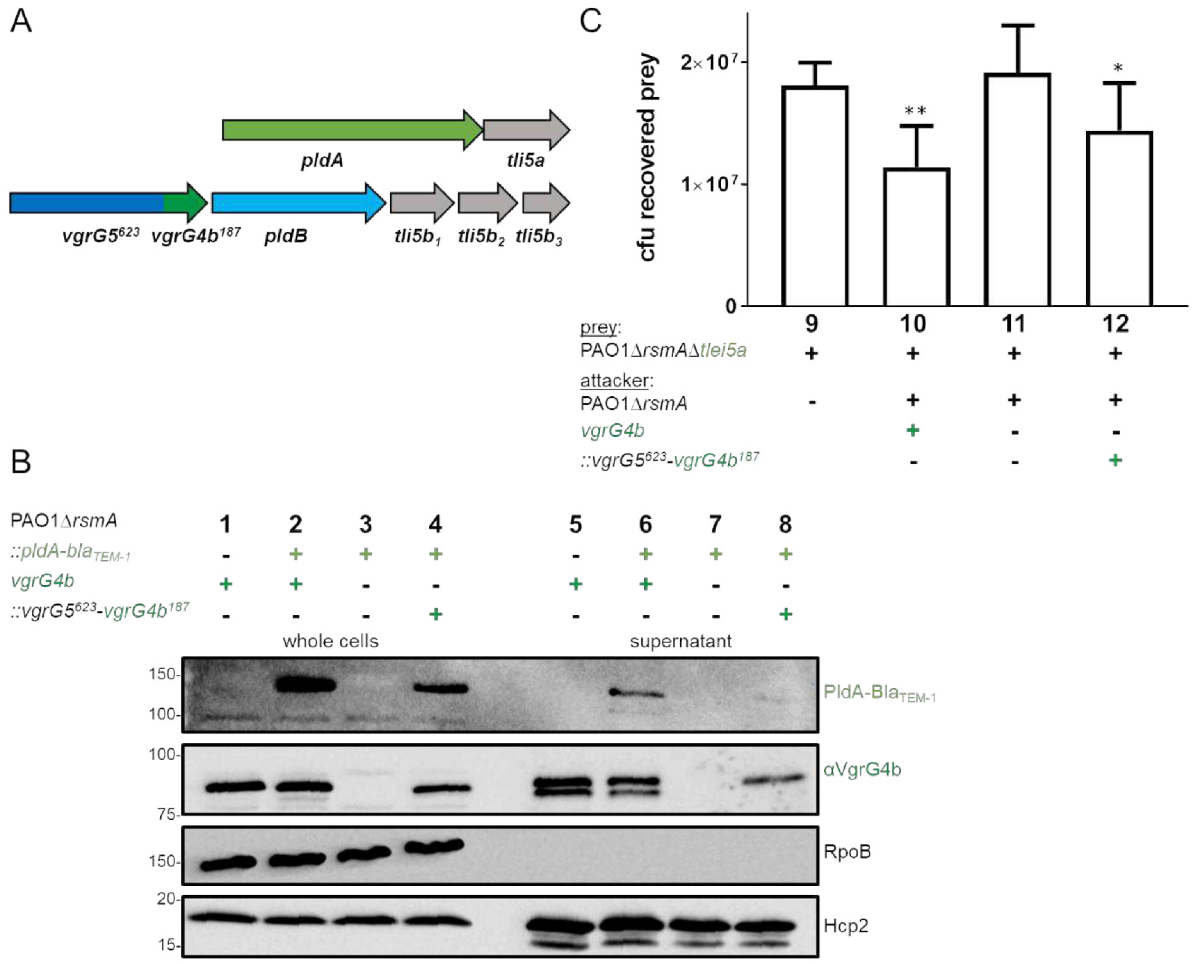


Figure 5-20. Substituting of the C-terminus of VgrG5 with the C-terminus of VgrG4b restores PldA secretion.

A: The here used mutants carry the gene sequence for a *vgrG5*^{623}-*vgrG4b*^{187}-chimera instead of the native *vgrG5* locus in absence of the native *vgrG4b* locus. B: Representative figure of a western blot from a secretion assay of PAO1Δ*rsmA::pldA-bla*$_{TEM-1}$ encoding native *vgrG4b* (+) or the *vgrG5*^{623}-*vgrG4b*^{187}-chimera (+). As a control for PldA-Bla$_{TEM-1}$ secretion, the parental strain was included (lane 6), while the negative control lacked the native *vgrG4b* (lane 7). Antibodies were used against Bla$_{TEM-1}$, VgrG4b-CT, Hcp2 and RpoB as indicated on the right. C: Plot of recovered cfu of prey strain PAO1Δ*rsmA*Δ*tlei5a::lacZ* after contact with the attacker strain that encoded native *vgrG4b* (+) or the *vgrG5*^{623}-*vgrG4b*^{187}-chimera (+). As a positive control for PldA-mediated killing, PAO1Δ*rsmA* was included (lane 10), while the negative control lacked *vgrG4b* (lane 11). Spots were incubated for 24 h at 25 °C in a 1:1 ratio. One-Way ANOVA analysis with Dunnett's multiple comparisons test was conducted on data set obtained from recovered prey on their own with **** $p<0.0001$.

We further wanted to corroborate these results and ensure that secretion of both the chimera and the effector are still mediated by the original T6SS machinery. Note, that since the VgrG5^{623}-VgrG4b^{187}-chimera carries the C-terminus of VgrG4b, its secretion can be monitored. Hence, strains were engineered that in addition to carrying *pldA-Bla$_{TEM-1}$* and *vgrG5^{623}-vgrG4b^{187}* also have deletions in *tssE2* or *tssK3*, leading to inactivation of H2- or H3-T6SS, respectively. Secretion assays were performed and a representative figure can be seen in Figure 5-21.

When cells expressed a non-functional H2-T6SS (lane 8), secretion of Hcp2 (bottom panel), PldA-Bla$_{TEM-1}$ (top panel) and VgrG4b (second panel) was abrogated. This was not the case in the parental strain (lane 7) or when cells had a non-functional H3-T6SS (lane 9), even though no control for H3-T6SS secretion is included here. Strains producing the VgrG5^{623}-VgrG4b^{187}-chimera showed bands for PldA-Bla$_{TEM-1}$ and the chimera both in the whole cells (lane 4) and in the supernatant fractions together with cleavage products (lane 10). These bands were less intense in the whole cell fractions of cells expressing a non-functional H2-T6SS (lane 5) and absent in the corresponding supernatant fractions (lane 11). Both bands could then be detected in the supernatant fractions of H3-T6SS inactive cells (lane 12), suggesting that secretion of VgrG5 is indeed H2-T6SS-dependent and PldA secretion using the VgrG5^{623}-VgrG4b^{187}-chimera remains H2-T6SS-dependent. A section of a Coomassie gel from the supernatant fractions ensured equal loading of supernatant fractions (bottom panel).

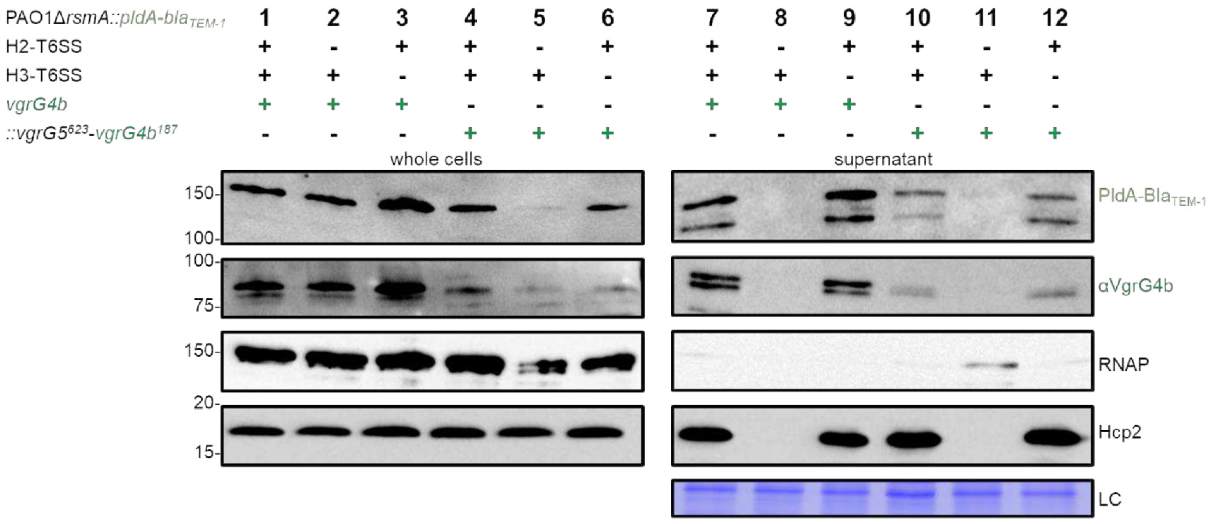


Figure 5-21. Swapping the VgrG vehicle for PldA secretion does not swap the T6SS machinery.

Representative figure of a western blot from a secretion assay of PAO1Δ*rsmA::pldA*$_{TEM-1}$ encoding native *vgrG4b* (+) or the *vgrG5*^{623}*-vgrG4b*^{187}-chimera (+) in presence of an active (+) or inactive (-) H2-T6SS or H3-T6SS. As a control for H2-T6SS-dependent PldA-Bla$_{TEM-1}$ secretion, the parental strain was included (lane 7), while the negative control expressed an inactive H2-T6SS (lane 8). Antibodies were used against Bla$_{TEM-1}$, VgrG4b-CT, Hcp2 and RpoB as indicated on the right. A section from a Coomassie gel was included to serve as a loading control (LC) for the supernatant fraction.

In this section we showed how the C-terminus of a VgrG can be used to effectively deliver a cognate effector, using the PldA/PldB couple, and switch the recognition motif on the VgrG protein. More specifically, we could successfully demonstrate that the presence of the C-terminus of VgrG4b specifically stabilises the cognate effector PldA. Furthermore, this interaction was shown to be sufficient to mediate delivery of PldA into target prey cells, once the C-terminus was plugged to the non-cognate VgrG5. Using this principle, we can gain further understanding on how the T6SS could be manipulated to deliver effectors of interest into target cells.

5.9.8. Summary: The C-termini of VgrG proteins are essential for effector delivery

In this chapter we have attempted multiple combinations that combined the structure of the VgrG shuttle, VgrG4b or VgrG5, with the fate of the respective cognate effectors PldA and PldB, including stability and secretion. The integration of all collected data resulted in the establishment of a summary model, which is shown in Figure 5-22. In the parental strain, PldA (bright green) interacts with the C-terminal TTR-like domain of VgrG4b (green arc) and PldB (cyan) interacts with the C-terminal TTR-like domain of VgrG5 (blue arc). VgrG4b and VgrG5 form functional heterotrimers that deliver their cognate effectors (Figure 5-22A). This model is in good agreement with a recent study from Flaugnatti and colleagues that showed that Tle1 from *E. coli* requires the interactions with the C-terminal domain of its cognate VgrG for its delivery [216].

We constructed strains that lack the native VgrG4b and produce VgrG5 with a substituted C-terminus of VgrG4b containing its TTR-like domain instead of its own (Figure 5-22B). We showed that this construct can no longer interact with PldB, abrogating its delivery (see 5.9.3). We, however, could successfully demonstrate that this chimera has a stabilising effect on PldA (Figure 5-18C), which is a sign for tight interactions between PldA and the C-terminus of VgrG4b. When challenged against PldA-sensitive strains, we monitored killing (Figure 5-20C), suggesting that PldA is indeed delivered. This is thus a very elegant demonstration of specificity switch through swapping of the VgrG C-termini.

Next, when VgrG4b carries the C-terminus of VgrG5 containing its TTR-like domain instead of its own (Figure 5-22C), we could not detect production of this construct. This chimera likely does not interact with PldA anymore, since no PldA delivery was observed (5.9.4). We further asked whether this chimera could be employed to deliver PldB, and in a *vgrG5* deficient background we observed interactions between PldB and the VgrG4b^{621}-

VgrG5^{169}-chimera (Figure 5-18A). However, no secretion of the effector could be monitored which is most likely due to the secretion defect of VgrG4b that we have observed in several instances in manipulated genetic backgrounds. To overcome this issue, and since the analysis was performed in a *vgrG5* mutant background, we attempted to co-express the VgrG5^{628} (Figure 5-22C), which did not rescue secretion of the tip complex or PldB (Figure 5-19). This was verified by the lack of VgrG5^{628} and PldB-Bla$_{TEM-1}$ in the supernatant fraction. This secretion defect was explained with the complexity associated with VgrG4b as the backbone of the shuttle.

We have proposed that one cognate PAAR protein specifically recognises the blunt VgrG end of a heterotrimer consisting of VgrG4b and VgrG5 (Figure 5-22A). Expressing both the VgrG4b^{621}-VgrG5^{169}-chimera and the truncation mutant VgrG5^{628} supposedly alters the recognition interface for the PAAR protein (Figure 5-22C). We propose that the cognate PAAR protein cannot bind such hetero-trimer as no efficient secretion of VgrG5^{628} was detected in the supernatant (Figure 5-19). Thus, we concluded that a hetero-trimer of VgrG4b^{621}-VgrG5^{169} and VgrG5^{628} is unlikely to assemble and form a functional T6SS tip.

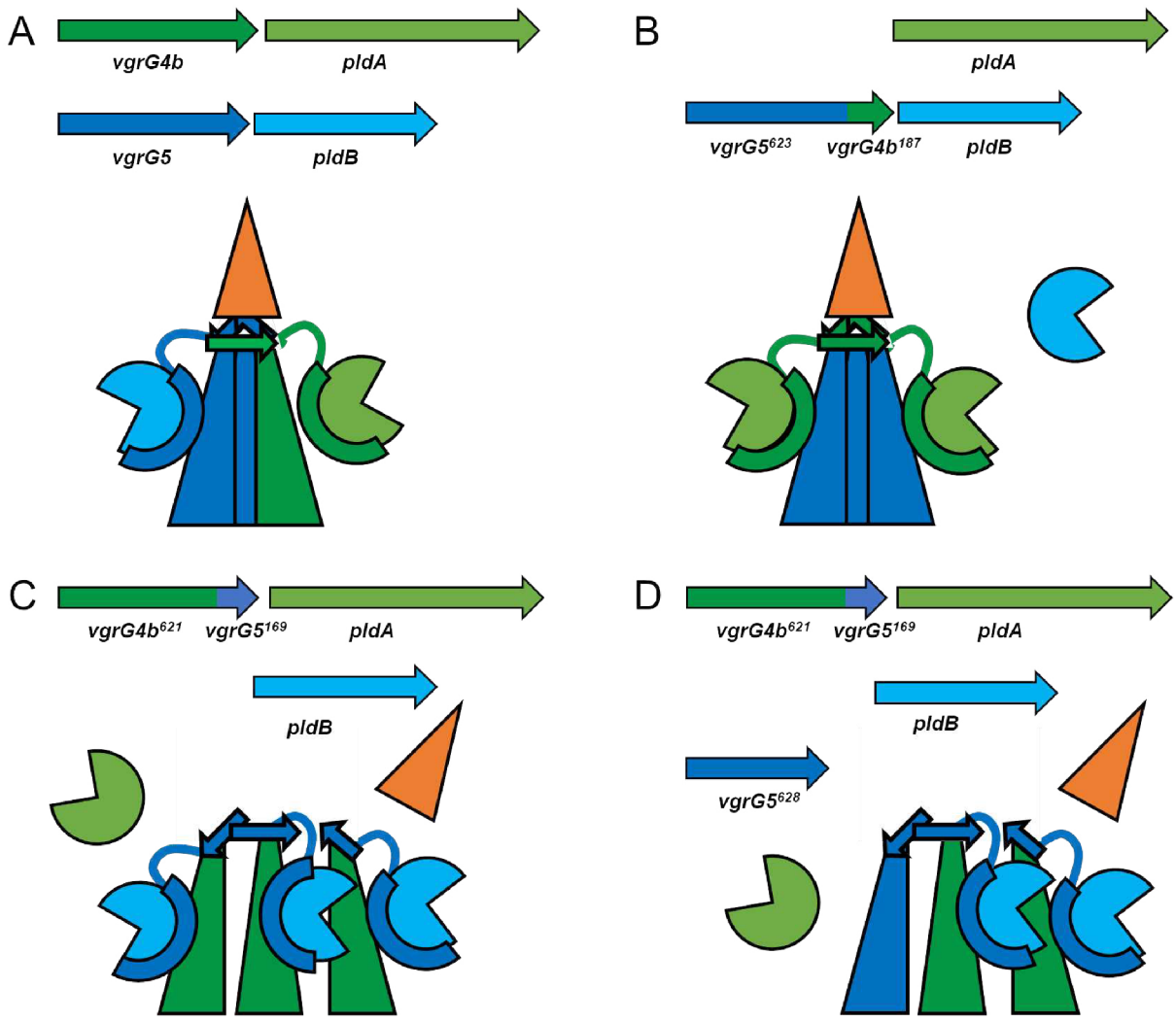


Figure 5-22. Model of the interactions between PldA and PldB and the C-terminal domains from their cognate VgrGs resulting in delivery shuttles of both effectors.

A: PldA (bright green) and PldB (cyan) interact with the C-termini containing the TTR-like domains of their cognate VgrGs, VgrG4b (green) and VgrG5 (blue), respectively. B: To connect PldA with VgrG5 as a vehicle, the C-terminus of VgrG5 was substituted with the C-terminus of VgrG4b in a *vgrG4b* deficient background. The VgrG5^{623}-VgrG4b^{187} chimerae can form a functional tip that recruits PldA, but not PldB, and delivers the cognate effector. C: To connect PldB with VgrG4b as a vehicle, the C-terminus of VgrG4b was substituted with the C-terminus of VgrG5 in a *vgrG5* deficient background. The VgrG4b^{621}-VgrG5^{169}-chimerae do not form a functional tip, but they interact with PldB and not with PldA. No effector is delivered with this construct. D: Expression of the N-terminus of VgrG5 did neither result in secretion of the VgrG complex nor in delivery of PldB.

5.10. Summary

In this chapter we have used two orphan *vgrG* clusters and performed in depth analysis of the specificity mechanism associated with the recognition of adaptor-less effectors by their cognate VgrG. Some information was already available from the literature but our study brought additional conceptual information, in several instances experimentally demonstrated what was only suggested so far and importantly challenged a few observations made in other studies. Firstly, we demonstrated that the *vgrG4b* and *vgrG5*-operons are activated in *P. aeruginosa* PAO1 strains lacking the master regulator RsmA. This is an important observation that pinpoints that RsmA not only is a regulator of all three *P. aeruginosa* T6SSs, but also of all orphan *vgrG* clusters. In other words, once RsmA repression is released, all T6SS-associated genes seem to be expressed and *P. aeruginosa* is ready to fire any T6SS weapon at its disposal to face competitors. When studying orphan *vgrG* clusters, the one major question to address is also what is the T6SS on which the VgrG and its cognate effector relies. Here, we showed without any ambiguity that both PldA and PldB are delivered by the H2-T6SS machinery, which was until now only speculations [186]. Next, we clearly demonstrated that as expected the cluster composition reflects the connection between a VgrG protein and its T6SS effector. It was thus demonstrated, that VgrG5 mediates delivery of PldB and VgrG4b of PldA. However, we made the puzzling observation that VgrG5 also impacts delivery of VgrG4b, and thus PldA, while the reverse was not true. This indirect impact on effector delivery is a novel concept and we propose that it underlies the formation of heterotrimeric VgrGs which is essential in some context but not in others. The requirement for hetero-trimerisation is not entirely clear but is likely to be connected with the formation of a compatible interface on which a PAAR protein would be fitted at the tip of the VgrG needle. Hence, using VgrG4b as a vehicle to deliver the C-terminus of VgrG5 and thus PldB was unsuccessful. Nevertheless, in the mirrored configuration, secretion of VgrG5 was definitely unaltered in absence of VgrG4b. This allowed the construction of a shuttle to switch the specific delivery

of PldA, which was to make it VgrG5-dependent simply by swapping the C terminus with the one of VgrG4b.

5.11. Discussion

5.11.1. A PAAR protein recognises a specific interface at the end of a VgrG trimer

In this study, we swapped the C-termini of two VgrG proteins and followed their fate in terms of secretion and effector recruitment. On the basis of the amino acid sequence alignment and structural models, we not only swapped the domains essential for effector recognition, but also the putative last β-strands that supposedly bind the cognate PAAR protein [141]. Since we have shown in chapter 4.3.1 that binding of the cognate PAAR protein onto the blunt end of the VgrG trimer is a requirement for secretion of the VgrG trimer, we can use VgrG secretion and effector delivery as a readout to reconstruct PAAR binding. The discussed concepts are sketched in Figure 5-23, while no C-terminal TTR-like domains and no effector binding is shown to focus on the recruitment of the cognate PAAR (orange) towards the blunt VgrG-end. The last β-strands are depicted as arrows in blue or green dependent on their VgrG4b (green) or VgrG5 (blue) origin.

In the parental strain, it can be assumed that VgrG4b and VgrG5 interact with each other and form a functional heterotrimer (Figure 5-23A). This results in a trimer that has a blunt end with at least one β-strand originally from VgrG4b (green) and one from VgrG5 (blue), while the third could be either. A cognate PAAR protein recognises this mixed (green-blue) blunt VgrG trimer, binds and delivers the complex together with the cognate effectors. We have sound evidence that VgrG4b on its own cannot form functional homotrimers (Figure 5-23B) indicating that no *P. aeruginosa* PAAR protein exists that recognises a blunt VgrG4b (green-

green) interface. This finding that a VgrG protein on its own is not being bound by a cognate PAAR protein is a novel concept. Furthermore, VgrG5 on its own can form homotrimers (Figure 5-23C), as suggested by the fact that PldB is delivered in the absence of VgrG4b. Hence, a PAAR protein exists that specifically recognises a blunt VgrG5 (blue-blue) end. This could be the same PAAR as in Figure 5-23A, recognising a VgrG4b-VgrG5 trimer, or a specific PAAR protein for VgrG5 homotrimers.

When swapping the C-termini between VgrG4b and VgrG5, we also modified the interface for PAAR recognition. A VgrG4b^{621}-VgrG5^{169}-chimera (Figure 5-23D) supposedly has the same blue-blue interface as a VgrG5 homotrimer (Figure 5-23C), which one would expect to be recognised by the same PAAR protein. However, we have no evidence that this chimera forms a functional trimer, suggesting that the cognate PAAR protein is unable to bind this chimera. In the reverse situation, the engineered VgrG5^{623}-VgrG4b^{187}-chimera exhibits a green-green VgrG4b-origin interface for the PAAR protein (Figure 5-23E). A green-green interface was shown before not to be recognised by a cognate PAAR (Figure 5-23B), however, we could observe secretion of the VgrG5^{623}-VgrG4b^{187}-chimera suggesting PAAR binding.

One possible explanation for this discrepancy is that the prediction of the PAAR binding β-strand within VgrG4b and VgrG5, as shown in Figure 5-15A with a purple line, was wrong. If by swapping the C-termini between VgrG4b and VgrG5, we indeed did not swap the PAAR binding β-strands, the binding interface for the PAAR protein would not be changed in the chimerae after all. This would then lead to an interface originally from VgrG4b (green-green) in the VgrG4b^{621}-VgrG5^{169}-chimera (Figure 5-23D) not being recognised by a cognate PAAR and an interface originally from VgrG5 (blue-blue) in the VgrG5^{623}-VgrG4b^{187}-chimera recognisable for the cognate PAAR (Figure 5-23E). This actually agrees with the findings in this study suggesting that the PAAR-binding β-strands of VgrG4b and VgrG5 were indeed miss-predicted. However, to completely resolve this issue and to identify the correct PAAR-

binding site, structural studies would need to be employed to solve the structure of a VgrG4b-VgrG5 trimer in complex with the cognate PAAR protein.

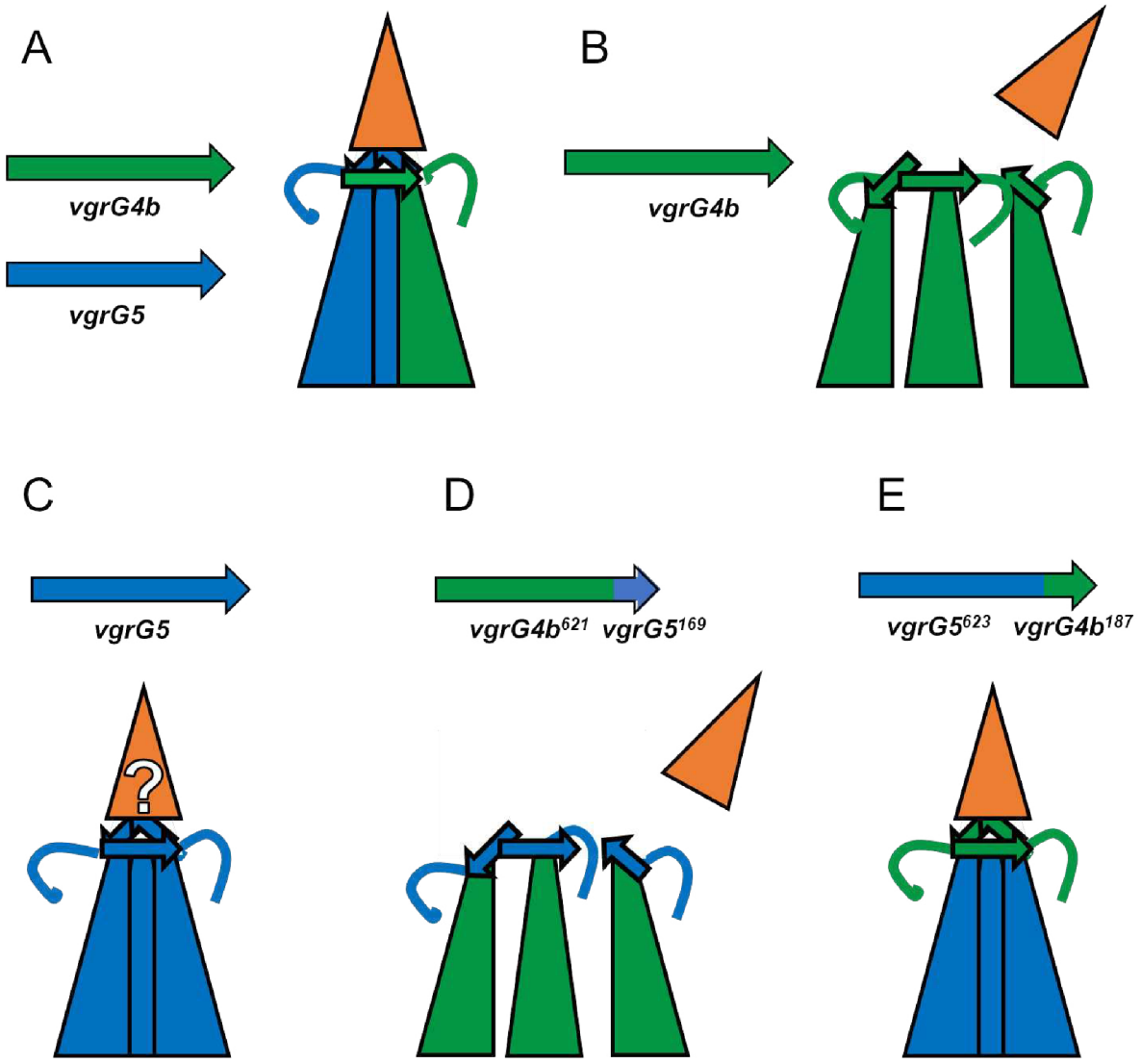


Figure 5-23. Models about contradictions in heterotrimer formation of VgrG4b and VgrG5.

A: In *P. aeruginosa* WT, VgrG4b (dark green) and VgrG5 (blue) form a functional heterotrimer topped up by a putative cognate PAAR (orange). B: In the absence of VgrG5, VgrG4b on its own cannot form a functional T6SS tip and is not secreted. C: In the absence of VgrG4b, VgrG5 might form a functional T6SS tip, although this has not been proven. D: When the C-terminus of VgrG4b is substituted with the one from VgrG5, the chimera most likely does not form a functional spike complex. E: When the C-terminus of VgrG5 was substituted with the C-terminus of VgrG4b, a functional trimer is formed and secreted.

5.11.2. *P. aeruginosa* fires its bullets with different efficiencies

Throughout this study we observed contradictions in the killing efficiency mediated by PldB and PldA, which we want to investigate here further. Delivery of PldB into prey strains susceptible for PldB in all cases led to efficient killing based on the recovered prey cfu. As can be seen in Figure 5-6B as an example, the parental strain as attacker leads to a massive drop of recovered prey due to PldB delivery. For this competition experiment, the competitive index was calculated by comparing the output ratio attacker/prey to the input ratio attacker/prey. A high competitive index reflects a competitive advantage of the attacker, while competitive parity correlates with a competitive index of 1. The competitive index of the parental strain in competition with the PldB-susceptible strain from the experiment in Figure 5-6B is 11, while the parental strain in competition with a PldA-susceptible strain from the corresponding experiment in Figure 5-5B has a competitive index of 3. This highlights that PldB-mediated delivery and thus killing is a lot more efficient than PldA-mediated delivery. This contradiction in delivery efficiency has not been addressed in previous studies that investigated the delivery of these effectors [188].

Here, we attempted to understand this discrepancy. Due to findings from this study, we reason that VgrG5 on its own can form homotrimers and recruit and deliver PldB as depicted in Figure 5-12B. VgrG4b and thus PldA can only be delivered together with VgrG5 as depicted in Figure 5-12A. Hence, a VgrG4b-VgrG5 heterotrimer always delivers at least one PldA and one PldB molecule into prey cells with the third one being either of them. A VgrG5 homotrimer is proposed to recruit and deliver three PldB molecules at once. Thus, there is always a higher statistical chance that PldB is recruited to a T6SS spike, leading to a higher rate of delivered PldB molecules into prey cells. This might ultimately lead to more efficient PldB-mediated killing and the observed higher competitive advantage.

Another explanation to understand this contradiction could be a hierarchy concept of delivered T6SS effectors which was also observed by other members of our lab (*unpublished data*) and was suggested in a recent study [220]. In this concept, which will be the basis of a publication, we reason that *P. aeruginosa* defines its effector repertoire by a hierarchy of PAAR proteins that are recruited towards the H2-T6SS machinery.

Our data suggest that a hierarchy in the recruitment of PAAR proteins exists that determines the preferred loading of a VgrG and thus firing of the cognate effector. If the preferred PAAR is missing from the cell, the next PAAR in line and its cognate VgrG and effector are recruited and fired [220]. This was supported by the finding that if a VgrG2b-PA1508 spike is not fired, PldA- and PldB- mediated killing are a lot more efficient (Thomas Wood, *unpublished data*) [220]. Considering the findings from this study, one may consider a yet unknown but preferably recruited PAAR protein that specifically recruits homotrimers of VgrG5 and the cognate PldB. A heterotrimer of VgrG4b and VgrG5 might be recognised by a different PAAR protein that is less efficiently recruited towards the H2-T6SS machinery. To unravel this mechanism in more detail, it should be the highest aim to identify the cognate PAAR protein for the VgrG5 homotrimer. Competition assays conducted in a background deleted for the *paar* gene might then unlock the less preferably recruited PAAR protein specific for the VgrG4b-VgrG5 heterotrimer. This would result in a more efficient delivery of PldA mirrored in a higher competitive index towards PldA-susceptible preys.

6. Results:

Taps and their role in effector delivery

6.1. Introduction

The “á la carte” effector delivery concept describes that a VgrG recruits and delivers one specific effector [175] and was proven valid for a range of T6SS effectors so far. Additionally, some T6SS effectors were identified that require additional proteins for their delivery [149, 200, 217, 218]. While in 4.6.2 we discussed that delivery of certain PAAR effectors requires the presence of additional proteins of the DUF1795 family, here we will focus on the contribution of proteins from the DUF4123 family on T6SS-mediated effector delivery.

DUF4123 genes can be found in the vicinity of a range of T6SS effectors, while nearby is usually the T6SS component encoded, *vgrG* or *paar*, which mediates delivery of the effector. Figure 6-13 displays operons encoding *tap* genes and the corresponding effector-immunity modules, that are crucial for this study. Two nomenclatures for DUF4123 gene products are generally used: Tap for **T**6SS-effector adaptor protein [217] and Tec for T6SS effector chaperone [218]. In this current work, we will generally name DUF4123 proteins Tap, unless another name for a gene or its product was proposed.

Tap components are highly hydrophobic proteins of around 30 – 40 kDa, whose presence was proven to be essential for the delivery of a range of effectors, like Tde1 from *A. tumefaciens*, TseL from *V. cholerae* or TseF from *P. aeruginosa* [149, 217, 218]. The current model suggests that a Tap binds and stabilises its cognate effector. The Tap then facilitates binding of the effector to the C-terminus of the cognate VgrG or PAAR protein and

subsequently dissociates from the tip. After dissociation of the Tap from the tip complex, the effector remains bound to the VgrG or PAAR protein and by delivering the spike complex, the effector is transported [149, 220].

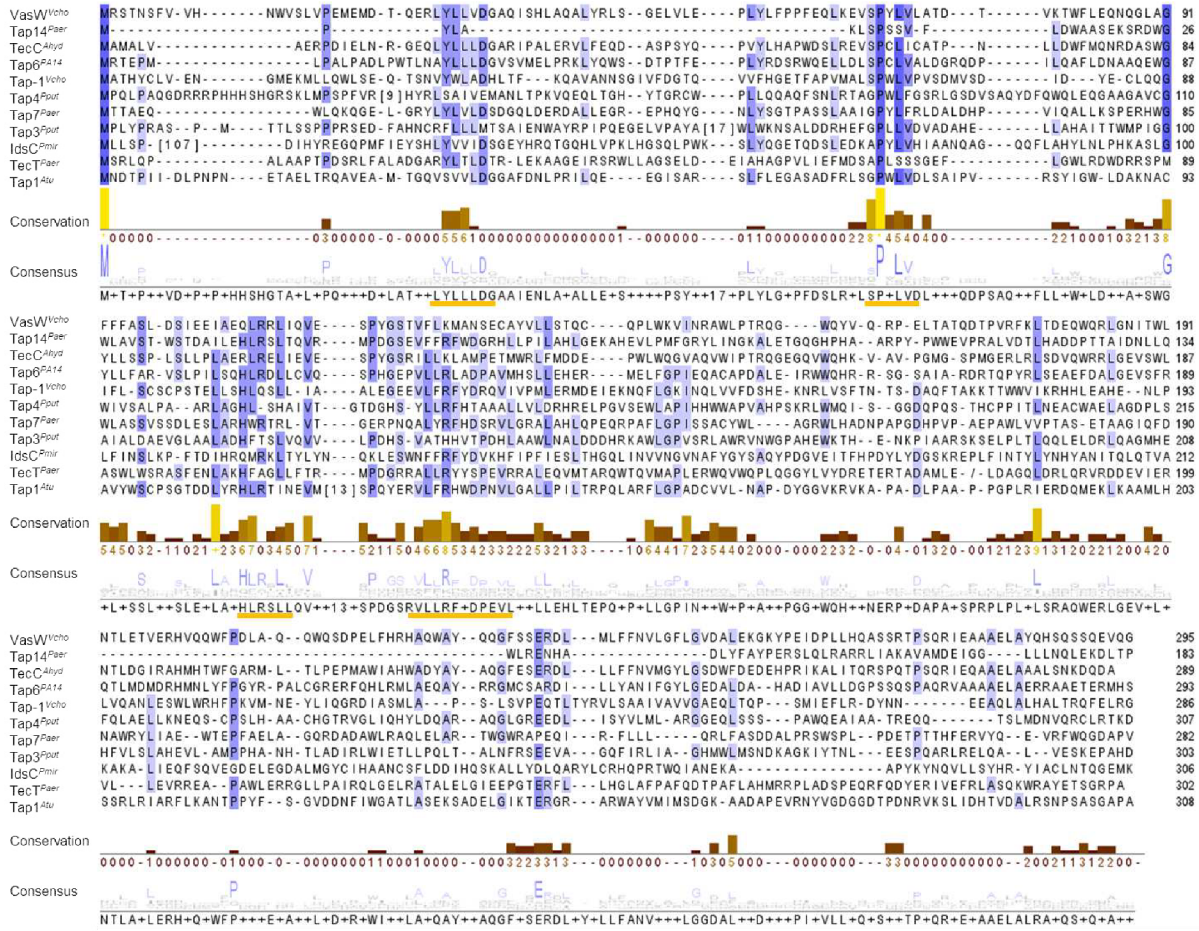


Figure 6-1. Taps contain highly conserved motifs within their N-termini.

Multiple sequence alignment of experimentally proven or proposed Taps. Within the N-termini, highly conserved motifs (orange lines) can be identified that are representative for DUF4123 domains. The C-termini are rather variable and thus might interact with the specific effector encoded downstream.

tap genes were described as chimerae, with a recombination site in the middle of the gene [217]. Unterweger and colleagues showed that the downstream region of the recombination site generally co-segregates with the downstream encoded effector gene (see

Figure 6-13). This might be the reason for the high variance of the C-terminal domains of Taps (Figure 6-1). Interestingly, the N-terminal domains of Taps contain the DUF4123 domains and thus the highly conserved motifs, as highlighted with orange lines in Figure 6-1. Furthermore, the N-terminal segments of Taps were shown to correlate with the specific C-terminal extension of VgrG proteins in *V. cholerae*. Thus, the authors proposed that the N-terminal Tap domain specifically interacts with the C-terminus of a VgrG protein, while the C-terminal Tap domain specifically binds the N-terminus of the cognate effector protein [217]. However, it is currently completely unclear, how this specificity is maintained and how Taps achieve the complex formation between VgrG and effector.

6.2. Aim of this chapter

This project aims at broadening our understanding on the molecular mechanisms associated with the delivery of Tap-dependent T6SS effectors. For this study, we focus on two effectors encoded downstream of *tap* genes. First, we want to investigate the secretion conditions of RhsP2, which is a unique effector of unknown function, encoded next to a *tap*, from *P. aeruginosa* PA14, to further elucidate its delivery mechanism. Next, we will elucidate what the basic requirements are for delivery of the Tap-dependent effector Tde1 from *A. tumefaciens*. To do this, we designed strategies to adapt Tde1 to the H1-T6SS of *P. aeruginosa* using the previously characterised VgrG1a as a shuttle to secrete and deliver Tde1 from the heterologous host.

Additionally, we will investigate molecular determinants of VgrG-Tap-effector complexes using bioinformatic analyses. We aim to shed light on the molecular features that determine recognition within VgrG-effector pairs with the help of Taps. With these results, we will propose a model for effector recruitment towards the VgrG spike facilitated by Taps and outline some strategies to prove our model. This knowledge will ultimately help understanding

the accommodation of effectors around the tip which in the long future could allow the design of specific effector shuttles.

6.3. *P. aeruginosa* PA14 expresses a putative Tap-dependent Rhs effector that is auto-cleaved

The involvement of Taps in delivering certain T6SS effectors again highlights the modularity of T6SS-mediated effector delivery. This section will now focus on the Rhs effector RhsP2 from *P. aeruginosa* PA14 whose delivery additionally seem to depend on a Tap. Interestingly, RhsP2 is, as far as our analysis can tell, the only example of an Rhs effector being encoded together with a *tap* gene.

RhsP2 is encoded within the unique *hcp2*-operon as sketched in Figure 6-2 [147]. Downstream of *hcp2* are encoded *vgrG14*, the DUF4123 gene *tap14* and the effector immunity module *rhsP2* and *rhsI2* (Figure 6-2). Because *hcp2* is 99% identical to the H2-T6SS-associated *hcpA*, *hcpB* and *hcpC* [147], an affiliation with the H2-T6SS was implied [146]. Furthermore, the fact that VgrG14 is 99% identical to VgrG5 [147] and in 5.6 we clearly demonstrated that VgrG5 is delivered by the H2-T6SS, VgrG14 is most likely also affiliated with the H2-T6SS machinery.

Rhs effectors are large polymorphic proteins comprised of N-terminal PAAR domains, massive Rhs core domains and C-terminal toxic domains of various functions [212]. In 4.6.1, we proposed a model for the delivery of such Rhs effectors *via* the T6SS. We suggest that the N-terminal PAAR domain allows an Rhs effector to bind on top of a VgrG trimer (see Figure 4-17). The shell-like Rhs domain might then wrap around the VgrG trimer and thus recruits the C-terminal toxic domain towards the tip. Remarkably, the N-terminal PAAR domain of RhsP2 is disrupted by a transthyretin-like domain (see Figure 4-16), which is a unique feature

of this Rhs effector. Thus, the presence of both the Tap14 and the transthyretin-like domain within RhsP2 begs the question of functionality of these components and thus the assembly of the effector around the VgrG spike.

Expression of this operon has been studied before in our laboratory by engineering an artificial arabinose promotor upstream of the *hcp-2* gene, however, secretion of neither VgrG14 nor RhsP2 could be shown [147]. Since recent work from our lab demonstrated that the H2-T6SS of *P. aeruginosa* PA14 is highly upregulated in absence of the regulator RsmA [146], we wanted to test whether such deletion mutant would have increased production and secretion levels of components of the *hcp-2* operon. If this was the case, we aimed at investigating the delivery mechanism of RhsP2 with special focus on the influence of Tap14.



Figure 6-2. The *hcp-2*-operon of *P. aeruginosa* PA14 [147].

hcp-2 (grey) is encoded upstream of *vgrG14* (green), followed by *tap14* (magenta) and the effector immuity module *rhsP2* (purple-red) and its cognate immunity *rhsI2* (cyan).

6.3.1. RhsP2 is expressed and cleaved but not secreted

To investigate the basic delivery mechanism of RhsP2 from *P. aeruginosa* PA14, we used mutants expressing chimeric chromosomal gene fusions to encode V5-tagged VgrG14 and RhsP2 [147] and deleted *rsmA* in those backgrounds. To understand whether VgrG14 and RhsP2 would be produced in higher amounts in the isogenic regulatory mutants, they were grown together with the parental strains at 25 °C and 37 °C for 24 h (Figure 6-3A and B). Using western blot analysis, we probed whole cell lysate containing membranes against the

V5-tag to detect VgrG14 and RhsP2 production (top panels) and against Hcp2 (bottom panels) to visualise expression of the H2-T6SS machinery. Hcp2 levels are drastically elevated in cells lacking the repressor RsmA (lanes 4 and 10), independent of the temperature, but not in the parental strain (lanes 1 and 7), which agrees with a previous study by our laboratory [146]. Furthermore, independent of the temperature, we could detect clear bands corresponding to VgrG14-V5 in strains deficient for *rsmA* (lanes 5 and 11), while these were absent or barely detectable in the parental strains (lanes 2 and 8). A band corresponding to the right size of RhsP2-V5 became only apparent when *rsmA* deficient cells were grown at 37 °C (lane 12). Interestingly, when we ran whole cell lysates grown at 25 °C on higher percentage gels to visualise smaller proteins, we could detect a smaller band in samples derived from RhsP2-V5 expressing strains (Figure 6-3C, top panel, lane 15). This band has a size of approximately 22 kDa, which corresponds to the size of the V5-tagged toxic domain of RhsP2 after auto-cleavage. Auto-cleavage was suggested to be a general feature of Rhs effectors [212], however, it has not been shown before under physiological conditions.

We then performed secretion assays at both 25 °C and 37 °C, while here only a representative figure derived from 25 °C grown samples is shown (Figure 6-3C). At neither of these temperatures, secretion of VgrG14 was detected (lane 17), and neither was full-length RhsP2 (not shown) nor the C-terminal RhsP2 domain (lane 18). Functionality of the H2-T6SS was confirmed with detection of Hcp2 in the supernatant fractions (bottom panel, lanes 16 - 18), thus, a non-functional H2-T6SS would not be the reason for the lack of secreted VgrG14 and RhsP2. Nevertheless, it needs to be stated at this point, that the Hcp2-antibody recognises the four species HcpA, HcpB, HcpC and Hcp2 present in PA14 [147], thus, any of the other three proteins might be detected in the supernatant and we have no means of distinguishing whether Hcp2 from the *hcp-2* operon was indeed secreted.

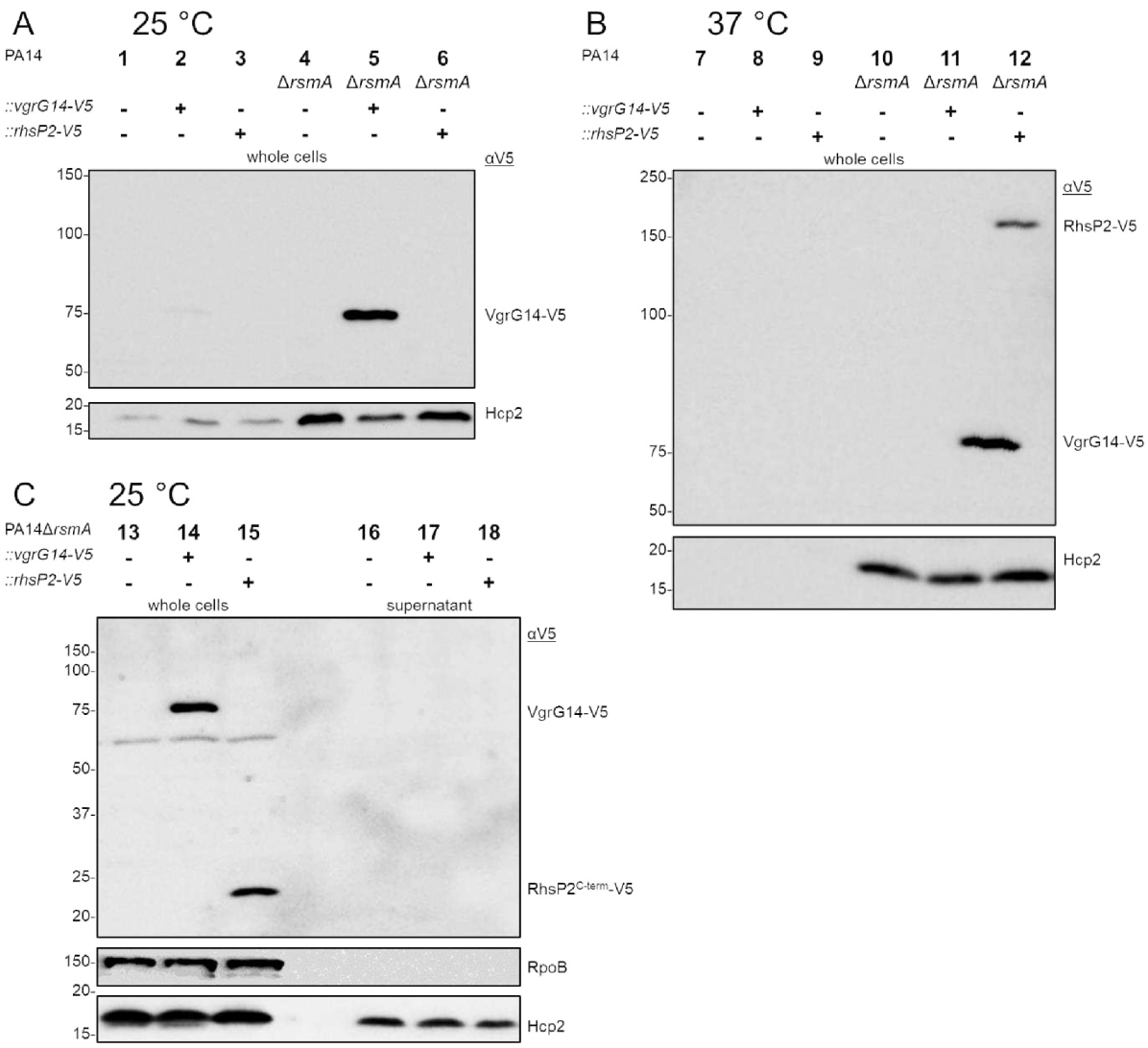


Figure 6-3. VgrG14 and RhsP2 are expressed in *P. aeruginosa* PA14.

Representative figures of western blots from A, B: whole cell lysates of PA14 WT and with deletions in *rsmA* grown at A: 25 °C or B: 37 °C and C: a secretion assay of PA14Δ*rsmA* grown at 25 °C. The strains expressed V5-tagged versions of VgrG14 (+) or RhsP2 (+). As a control for a functional H2-T6SS machinery blots showing Hcp2 production and secretion were included (bottom panels). Antibodies were used against V5, RpoB and Hcp2 as indicated on the right of each panel.

No secretion of VgrG14, full-length RhsP2 or the C-terminal domain of RhsP2 was observed, while secretion of a Rhs effector has yet only been shown in one instance, that is Tke2 from *Pseudomonas putida* [136]. In this study, the authors could detect full-length Tke2 in the supernatant fractions of *P. putida* after growth at 30 °C with no cleavage product being

identified [136]. Furthermore, other lab members attempted to show delivery of RhsP2 into prey *E. coli* cells, which was also unsuccessful (Luke Allsopp, Thomas Wood, *personal communication*). Hence, these results prevented us from further analysing this operon and from studies into the delivery mechanism of RhsP2.

6.4. The Tap-dependent effector Tde1 from *A. tumefaciens*

We then focussed on another Tap-dependent effector, Tde1 from *A. tumefaciens*, whose basic delivery system was studied in great detail by our collaborators [149, 153]. Tde1 was shown to be one of the major anti-bacterial toxins delivered by the T6SS from *A. tumefaciens* [153]. It is a DNase whose activity is counteracted by the immunity protein Tdi1 (Figure 6-4A) [153]. Delivery of Tde1 was shown to be dependent on gene products encoded within the same operon [149]. The current model of Tde1 recruitment to the tip states that VgrG1^A is assembled to a functional trimer and capped by the cognate PAAR1^A protein. The interactions between VgrG1^A and PAAR1^A are similar to the mode described in 4.4, in that PAAR1^A binds to the three last VgrG1^A β-strands. Concomitantly, Tap1 interacts with and stabilises Tde1 within the cell and the Tap1-Tde1 complex is then recruited to the C-terminal amino acids of VgrG1^A. Tap1 is released and Tde1 remains bound to the VgrG1^A spike, which is propelled into the surrounding and thus delivery of Tde1 into target cells occurs (Figure 6-4B) [149].

Here, we aim at further understanding what the minimal requirement is for having the heterologous effector Tde1 from *A. tumefaciens* secreted by the T6SS of *P. aeruginosa*. This project will give further clues about whether other components than Tap1 and the C-terminal amino acids of VgrG1^A are required to target Tde1 to a T6SS spike. For this project, plasmids containing the sequences for *tap1-tde1-tdi1-paar1*, *tap1-tde1(HADA)-tdi1-paar1*, in which two catalytic residues within *tde1* were mutated rendering it non-toxic, and *vgrG1^A* as well as

antibodies recognising Tde1 and VgrG1^{A} were kindly provided by Erh-Min Lai from Academia Sinica, Taipei [144, 153].

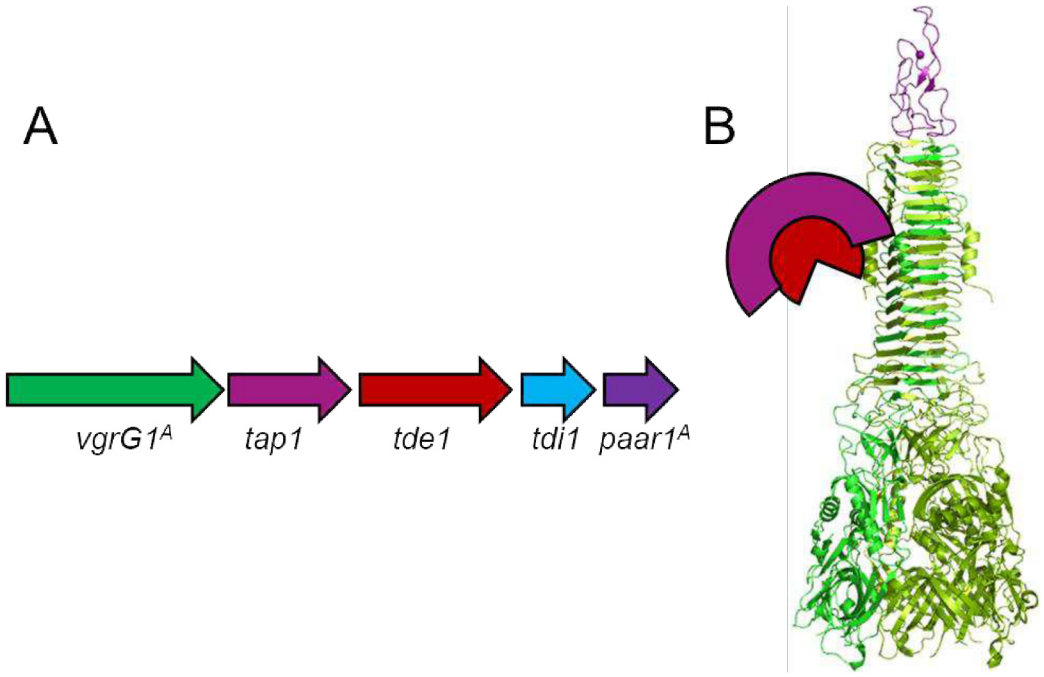


Figure 6-4. Tde1 from *A. tumefaciens* is secreted dependent on the genes encoded in its cluster [149].

A: *vgrG1*-operon from *A. tumefaciens* as published in [144]. *tde1* (red) is encoded downstream of its cognate *tap1* (magenta) and *vgrG1*^{A} (green) together with the cognate immunity *tdi1* (cyan) and *paar1* (purple). B: The Tap1-Tde1-complex (red-magenta) binds specifically to the C-terminus of VgrG1^{A} (green) which is capped by PAAR1^{A} (purple). Adapted from Bondage et.al. [149].

6.4.1. *P. aeruginosa* cannot secrete the heterologous effector Tde1

Before investigating how to connect the heterologous effector Tde1 with the T6SS in *P. aeruginosa*, it was explored whether *P. aeruginosa* is able to secrete Tde1. The plasmid pTrc200 containing the gene sequence for *tap1-tde1(HADA)-tdi1-paar1* (t-t-t-p) was introduced into *P. aeruginosa* PAKΔ*retS* and secretion assays performed under H1-T6SS

inducing conditions, that is growth at 37 °C until cells reached an OD_{600} of approximately 5 [140].

As can be seen in Figure 6-5, top panel, lane 2, Tde1 (red) is expressed in PAKΔ*retS.* In the supernatant fraction of a T6SS-active strain (lane 9), no band corresponding to Tde1 is detected, while a faint band for Tde1 is detected in the supernatant fraction of a H1-T6SS-inactive strain (lane 10). However, this correlates with elevated detection of RpoB (third panel) suggesting cell lysis. Since no efficient secretion of Tde1 was observed, we attempted to connect Tde1 with the H1-T6SS in *P. aeruginosa* by co-expressing the cognate *vgrG1*^{A} [149]. We additionally electroporated plasmid pRL662 containing the gene sequence for *vgrG1*^{A} into the above strains and repeated the secretion assays. What becomes immediately apparent is the fact that co-expression of VgrG1^A increases the intensity of the band corresponding to Tde1 (lane 6), which indicates specific interactions with and stabilisation of Tde1. While VgrG1^A was produced in detectable amounts in *P. aeruginosa* (second panel, lane 6), its secretion could not be observed (lane 13). However, secreted VgrG1^A in the supernatant fractions of *A. tumefaciens* is generally also barely detectable (Erh-Min Lai, *personal communication*), as is confirmed in Figure 6-9. Furthermore, even when cells co-express VgrG1^A and it likely interacts with Tde1, no secretion of Tde1 becomes apparent from H1-T6SS-active strains (lane 13). In the supernatant fractions of H1-T6SS-inactive strains (lane 14), a weak band for Tde1 is detectable, but this again correlates with elevated levels of RpoB (third panel) implying cell lysis. These results indicate that *P. aeruginosa* is not able to incorporate VgrG1^A into its T6SS and thus to recruit Tde1. This finding was not unexpected, as secretion of heterologous effectors is usually not a general feature of bacterial protein secretion systems [27, 40, 262]. However, one needs to consider that here we only tested growth conditions under which the H1-T6SS of *P. aeruginosa* PAKΔ*retS* is mainly active [140], while there might be a slight possibility that the H2-T6SS or H3-T6SS could mediate secretion of Tde1. We did not test these conditions, as we now wanted to understand how we could connect Tde1 to the H1-T6SS of *P. aeruginosa* to attain its delivery.

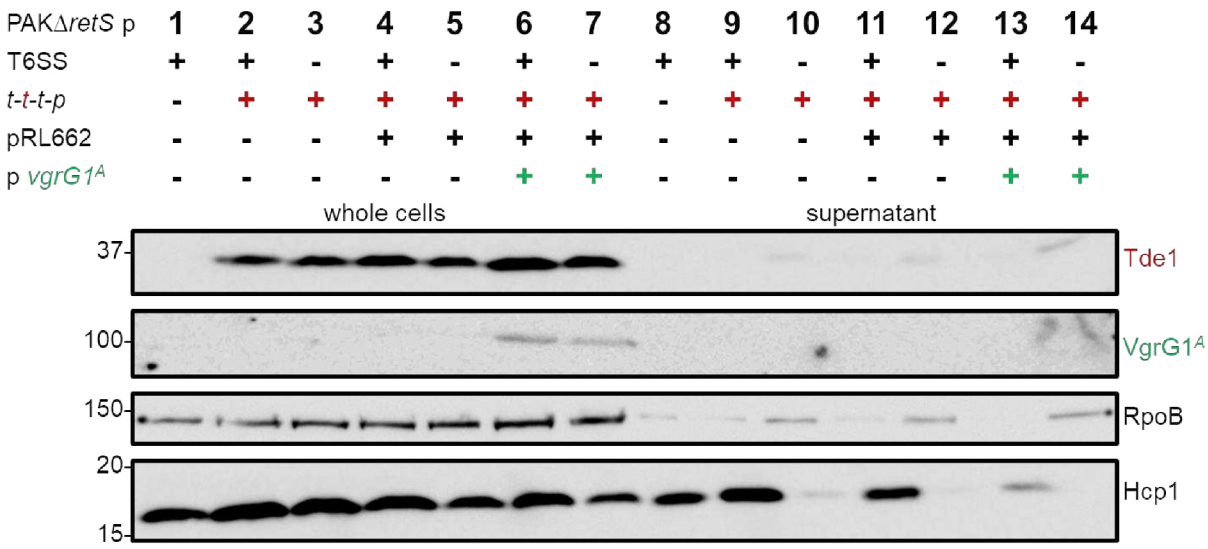


Figure 6-5. *P. aeruginosa* cannot incorporate heterologous VgrG1^A and secrete Tde1.

Representative figure of a western blot from a secretion assay of PAKΔ*retS* pTrc200 (p) with an active (+) or inactive (-) H1-T6SS expressing (+) *tap1-tde1(HADA)-tdi1-paar1* (*t-t-t-p*) or containing pRL662 (+) with *vgrG1*^{A} (+). As a control for H1-T6SS activity, a blot against Hcp1 was included (bottom panel). Antibodies were used against Tde1, VgrG1^A, RpoB and Hcp1 as indicated on the right.

6.4.2. Tde1 binds to the C-terminus of its cognate VgrG

As *P. aeruginosa* cannot secrete the heterologous effector Tde1, we further investigated whether targeting and secretion of Tde1 to the H1-T6SS machinery of *P. aeruginosa* could be adapted. As indicated, it was recently demonstrated, that the Tap1-Tde1-complex binds to the 31 C-terminal amino acids of VgrG1 in *A. tumefaciens* [149] which was shown to be the prerequisite for Tde1 delivery. In 4.4.3, we gave a comprehensive description of chimeric VgrG proteins between VgrG1a from *P. aeruginosa* (VgrG1a^P) and VgrG1 from *A. tumefaciens* (VgrG1^A) and we demonstrated their functionality. Here, we decided to employ these three chimeric constructs in an attempt to connect the heterologous Tde1 to the VgrG1a spike of *P. aeruginosa.* Briefly, construct A contains the full-length VgrG1a^P extended by the 31 Tde1-binding amino acids from VgrG1^A. Constructs B and C

cover the first 605 and 614 aa, respectively, from VgrG1a^{P} and 31 and 21 Tde1-binding amino acids from VgrG1^{A}, respectively (Figure 6-6).

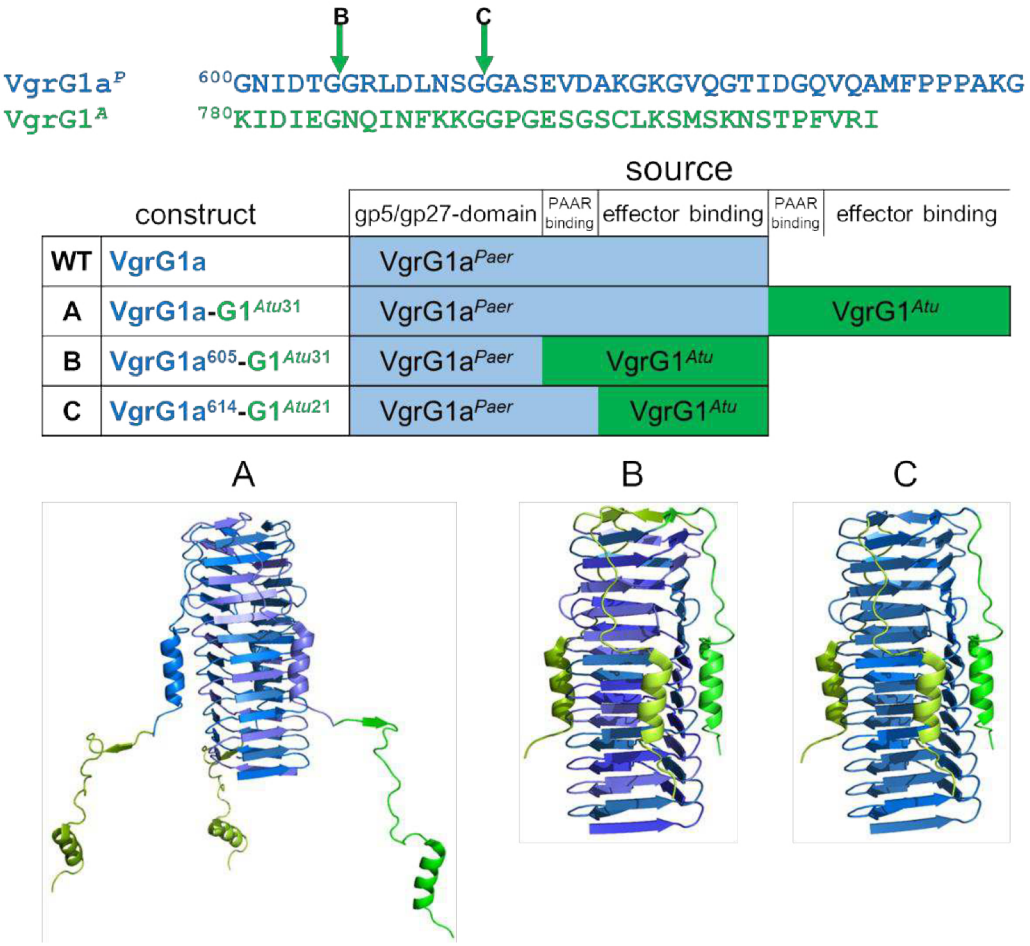


Figure 6-6. Overview of chimerae which were employed to connect Tde1 to the H1-T6SS in *P. aeruginosa*.

The top panel represents the amino acid sequences of the C-terminal extensions of VgrG1a^{P} (blue) and VgrG1^{A} (green) as well as the swapping points for chimerae B and C. Structural models of the needle parts of the chimerae are shown in the bottom panel. In construct A, the STOP codon of *vgrG1a*^{P} (blue) was replaced by the gene portion corresponding to the last 31 aa of VgrG1^{A} (green). Constructs B and C were designed by substituting the gene portions corresponding to the last 35 aa and 29 aa of *vgrG1a*^{P} with the gene portions corresponding to the last 31 aa and 21 aa, respectively, of VgrG1^{A}.

First, we assessed whether Tde1 could bind to the C-terminus of VgrG1^{A}, when the latter is fused to a different VgrG vehicle as is the case in these three chimeric constructs. We used a bacterial-two-hybrid (BTH) assay, in which all gene products carry the T18- or T25-domains (T18/25) at their C-termini (Figure 6-7A). Thus, a Tde1-T18/25-fusion protein would bind the VgrG-T18/25-fusion near its C-terminus and then brings the two adenylate cyclase domains close together for them to interact and to form a functional enzyme.

To circumvent toxicity of Tde1 on the producing strains, the gene sequence for the catalytic mutant of Tde1 (Tde1(M)) was cloned prior to the gene sequence corresponding to the T18/25-domains (Figure 6-7A). When we tested the interactions between Tde1(M) and any of the VgrG-constructs, no blue colonies appeared indicating that these two proteins did not interact (Figure 6-7B, right panel). Since it was proposed that Tde1 only binds VgrG1^{A} in presence of Tap1, we then included upstream of *tde1(M)* the gene sequence for *tap1* (Figure 6-7A) and tested for interactions (Figure 6-7B, left panel).

Our results show that Tde1 does not bind VgrG1a^{P} (WT). Instead, when Tap1 is present and any of the VgrG1a^{P}-G1^{A}-chimerae, dark blue spots could be readily observed suggesting strong interactions between Tde1 and more likely with the Tap1-Tde1 complex. The fact that construct C efficiently associates with Tap1-Tde1 suggests that as little as the 21 C-terminal amino acids of VgrG1^{A} are sufficient to mediate this interaction. Intriguingly, Tap1-Tde1 binds only very weakly to VgrG1^{A}, which might be due to the lack of the cognate PAAR1^{A} [149]. However, we did not quantify these results to gain statistical significance of these experiments.

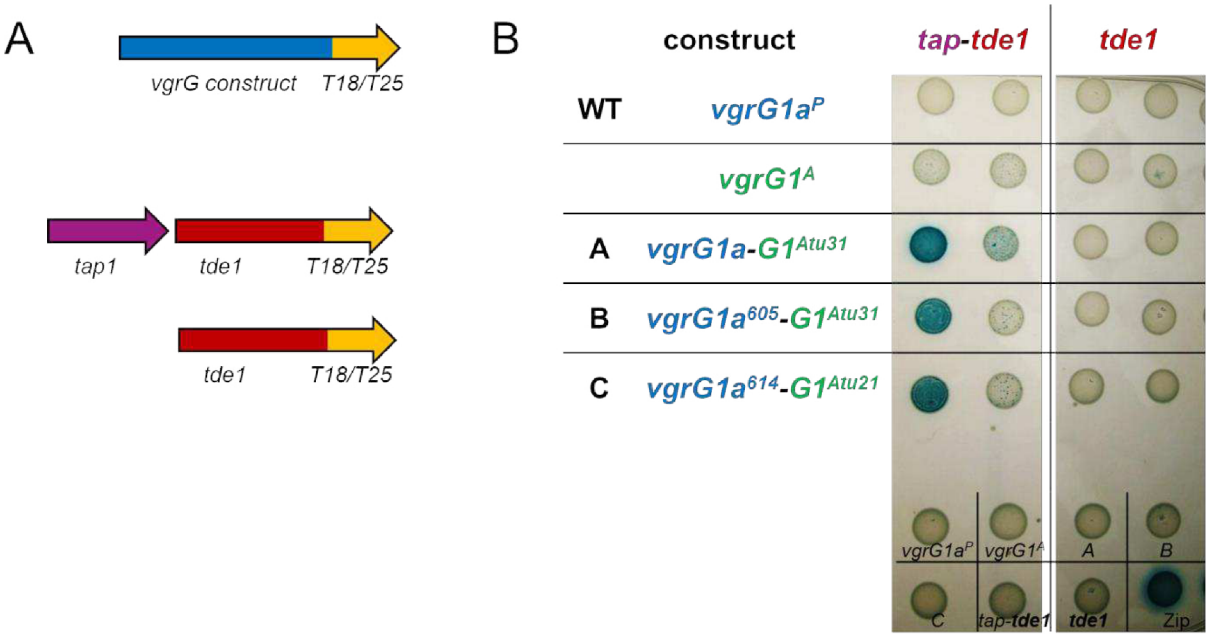


Figure 6-7. All chimerae interact with Tde1 in presence of Tap1 *in vitro*.

A: T25 and T18-domains (orange) were fused to the C-termini of either the *vgrG*-genes (blue) or a catalytic mutant of *tde1* (red) on its own or in presence of the cognate *tap1* (magenta). B: Representative bacterial-two-hybrid plate tested for interactions between VgrG1a^{P}-G1^{A}-chimerae and Tde1 in absence (right panel) and presence (left panel) of the essential Tap1 protein [149]. All interactions were tested with all gene sequences cloned into both pKT25 and pUT18C represented as two columns for each tested interaction while empty vector controls are shown in the bottom panel.

This result clearly demonstrates that Tap1-Tde1 could recognise the C-terminus of VgrG1^{A} even when it is plugged onto a heterologous VgrG core. We then investigated whether this interaction would also occur in *P. aeruginosa* cells, and whether this could potentially result in secretion of Tde1. For this, PAKΔ*retS* cells expressing WT VgrG1a^{P} or any of the chimerae (A/B/C) were grown for 5 h at 37 °C in the presence (+) or absence (-) of *tap1-tde1(HADA)-tdi1-paar1*. Western blot analysis was performed on whole cell lysates probed for Tde1 and VgrG1abc (Figure 6-8A) and images from three independent experiments were analysed using ImageJ. The intensity of the VgrG1a^{P} band in absence of Tde1 (lane 1) was quantified and served as a standard for VgrG1a^{P} stability, as this being the basic condition in WT cells. The intensities of all bands corresponding to VgrG1a^{P}/constructABC were quantified

and divided by the standard intensity of VgrG1a^{P} (Figure 6-8B). According to this calculation, the closer a ratio is to 1, the more stable a protein would be.

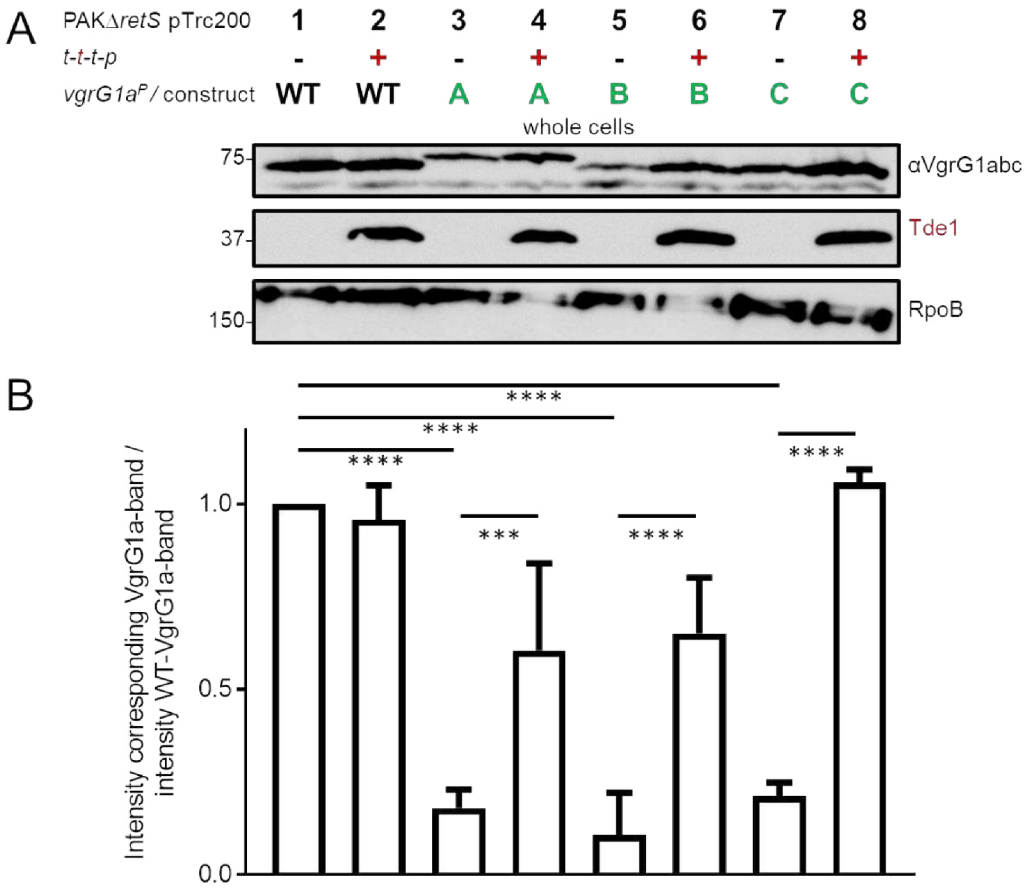


Figure 6-8. All chimerae likely interact with Tde1 in presence of Tap1 *in vivo.*

A: Representative Western blot of whole cell lysates of PAK*ΔretS* containing pTrc200 and expressing chimerae A, B, C between VgrG1a^{P} and VgrG1^{A} in absence (-) and presence (+) of *tap1-tde1(HADA)-tdi1-paar1* (*t-t-t-p*). As a control for VgrG1a stability, the parental strain was included and grown in absence and presence of *t-t-t-p* (lanes 1 and 2). Antibodies were used against VgrG1abc, Tde1 and RpoB as indicated on the right. B: Intensities of the corresponding VgrG1a^{P} bands from three independent experiments were quantified using ImageJ (https://imagej.nih.gov/ij/index.html) and divided by the intensity of the band belonging to WT VgrG1a^{P} in absence of Tde1 (lane 1) as a standard for VgrG1a stability. One-Way ANOVA with Tukey's multiple comparison test was conducted between datasets as indicated with **** $p<0.0001$.

Whereas no difference in intensity between the VgrG1a^{P} bands in absence (lanes 1) or presence (lane 2) of Tde1 was observed, the VgrG1a^{P}-G1^{A} chimerae show variability when comparing their stability in presence and absence of Tap1-Tde1. Indeed, a drastic decrease of their abundance is observed in absence of Tde1 (lanes 3, 5 and 7) while co-expression of Tap1-Tde1-Tdi1-PAAR1 (lanes 4, 6 and 8) led to a significant increase in intensity of the corresponding band. This change in intensity suggests a lack of stability of the chimeric VgrG in absence of the Tap1-Tde1 complex. This would suggest that the VgrG1a-chimerae are more stable upon interactions with Tap1-Tde1, which confirms the results obtained from the BTH (Figure 1-10).

6.4.3. Connecting an effector to the T6SS tip is not sufficient for its secretion

From the last section, we concluded that Tde1 might be connected to the VgrG1a tip in *P. aeruginosa*. Further, we could validate previous findings by our collaborators that the C-terminal amino acids of VgrG1^{A} are sufficient to recruit the Tap-Tde1 complex [149]. Next, we wanted to investigate whether interactions between Tde1 and the VgrG1a tip would be enough to allow proficient secretion in *P. aeruginosa* of this heterologous effector. Hence, standard secretion assays were performed of strains that either lacked *vgrG1b* and *vgrG1c* (Figure 6-9A) or not (Figure 6-9B) and expressed any of the chimerae between VgrG1a^{P} and VgrG1^{A} in presence of pTrc200 *tap1-tde1(HADA)-tdi1-paar1*. By testing two sets of strains in presence or absence of VgrG1b and VgrG1c, we wanted to confirm that the presence of the other two spike proteins will not have an impact on Tde1 secretion.

Figure 6-9 shows a representative figure of all Tde1 secretion assays conducted. This western blot revealed with an antibody against *P. aeruginosa* VgrG1a (second panels), that VgrG1a^{P} and all VgrG1a^{P}-chimerae are produced in significant amount (lanes 1, 3-5, 13-17). Using an antibody specifically against the C-terminal 31 aa of VgrG1^{A} (third panels), constructs

A, B as well as VgrG1^{A} were detected in whole cell fractions (lanes 3, 4 ,6, 15, 16 and 18), while VgrG1a^{P} was not, as expected (lanes 1 and 13). Construct C (lanes 5 and 17) was not detected with this antibody, probably because it only contains the last 21 aa of VgrG1^{A}. Upon analysis of the supernatant fractions of *vgrG1b*- and *vgrG1c*- deficient strains (Figure 6-9A), only VgrG1a^{P} (lane 7) and interestingly construct A (lane 9) could be detected. Hcp1 was also monitored as a readout of T6SS functionality (bottom panel) and is only seen in the supernatant when VgrG1a^{P} or the construct A is secreted but not with the other chimera which are not secreted. This suggests that only construct A is, similarly to WT VgrG1a^{P}, able to form a functional T6SS tip. This is in good correlation with results from 0, in which only construct A was secreted even in absence of Tap1-Tde1. Thus, even though construct A now binds to Tap-Tde1, its ability to form a functional T6SS is not affected.

We observed faint bands for Tde1 in the supernatant fractions of all tested strains, which we believe is unlikely being specific T6SS-dependent secretion. In particular, there is no particular increase in the intensity of the Tde1 band in presence of the secreted chimera A (lanes 9 and 21) as compared to other not secreted chimera (lanes 10, 11, 22 and 23). As a control for Tde1 secretion, *A. tumefaciens* was grown under T6SS-inducing conditions [144] displaying intense bands for Tde1 in the supernatant (lanes 12 and 24).

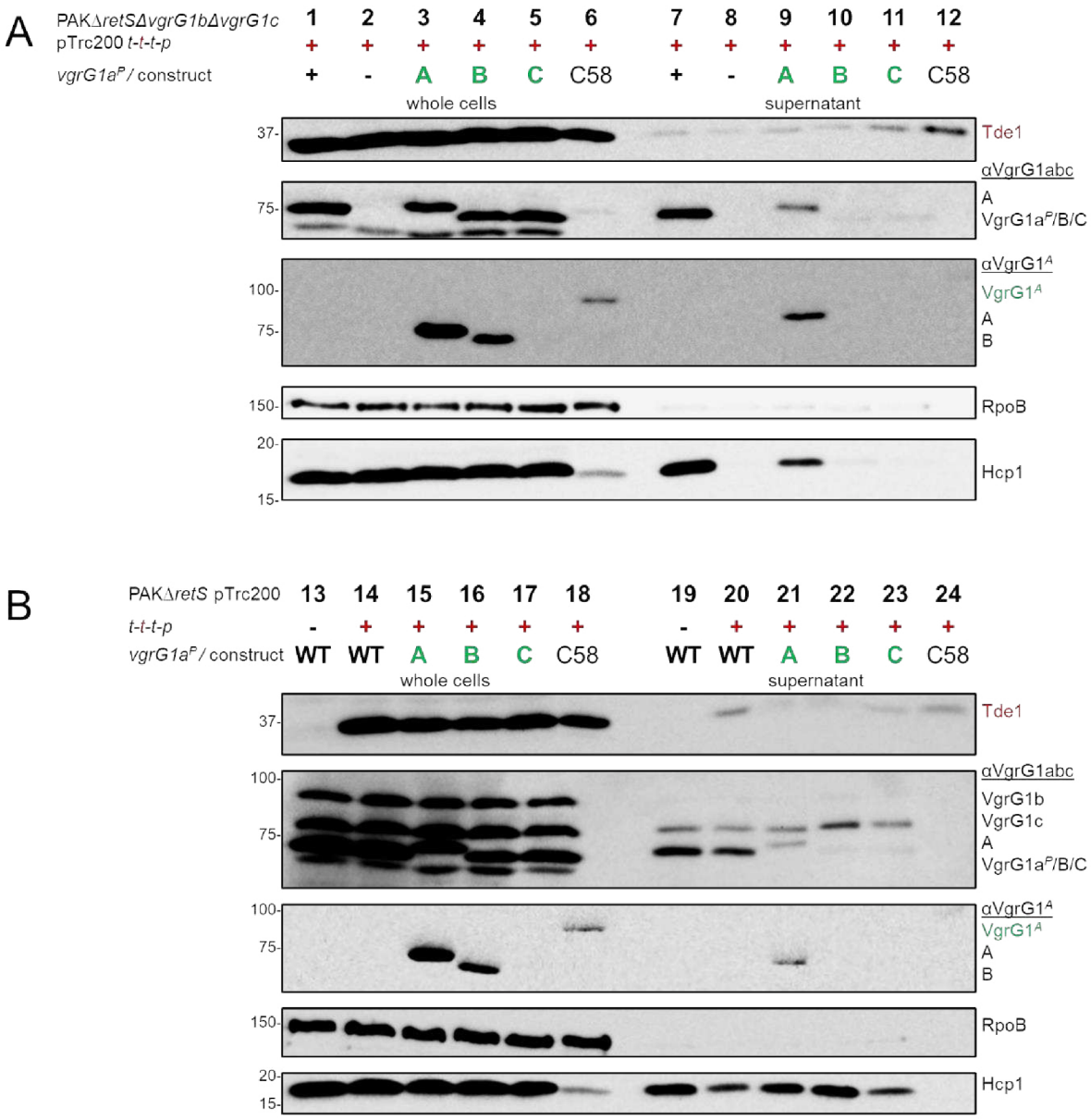


Figure 6-9. *P. aeruginosa* is not able to secrete the heterologous effector Tde1.

Representative figures of western blots from secretion assays of A: PAKΔ*retS pTrc200* and PAKΔ*retS*Δ*vgrG1b*Δ*vgrG1c* pTrc200 expressing chimerae A, B, C between VgrG1a^{P} and VgrG1^{A} in presence (+) of *tap1-tde1(HADA)-tdi1-paar1 (t-t-t-p)*. As a control for Tde1 secretion supernatant fractions of *A. tumefaciens* C58 were included (lanes 12 and 24). Antibodies were used against Tde1, VgrG1abc, VgrG1^{A}, RpoB and Hcp1 as indicated on the right of both panels.

To assess Tde1 delivery into nearby bacterial strains, we further performed competition assays. It was attempted to outcompete the parental PAKΔ*retS* by delivering Tde1 from

PAKΔ*retS* strains producing any of the VgrG1a-chimerae. Prey cell survival as well as attacker strain survival were highly variable and did not allow conclusive results (*data not shown*). When we further expressed the immunity Tdi1 in the prey strains, we could not recover any phenotype (*data not shown*), which did not allow us to draw any conclusions as to whether Tde1 delivery was successful or not.

The drawback of inconclusive competition assays might be explained with the toxicity of Tde1 [153]. We have noticed before that when *P. aeruginosa* cells grew in presence of pTrc200 containing *tap1-tde1-tdi1-paar1*, its growth was significantly affected (*data not shown*). This is likely due to the toxicity of Tde1 [153], even though its immunity was co-expressed. For all secretion assays conducted in this study, we grew *P. aeruginosa* cells in presence of the catalytic mutant of Tde1 (Tde1(M)), which resulted in growth phenotypes similar to the empty-vector controls. Now, to demonstrate Tde1 delivery, we wanted to make use of its toxic effect which required us to express WT Tde1. However, due to uncontrolled firing of the T6SS, *P. aeruginosa* not only delivers toxic Tde1 into prey cells, but also into its own sibling cells that might also be susceptible to Tde1 delivery. Hence, both attacking and prey strains survived in highly variable amounts which ultimately led to inconclusive data and prevented us from further experiments using this set up.

6.4.4. Does the tip get too bulky?

From the above section, we could anticipate that Tde1 delivery from *P. aeruginosa* was not successful as we have negative secretion assays and inconclusive competition assays. However, we could indeed demonstrate that Tde1 interacts with the VgrG1a spike in *P. aeruginosa* which is a major achievement. We further wanted to explore the reasons for this controversy. First, and as summarised in Figure 6-10, we noticed an impact on secretion efficiency of construct A in presence of Tap1-Tde1. We quantified these data by measuring

the intensities of the corresponding bands from the supernatant fractions from three independent experiments using ImageJ and plotted them in Figure 6-10C. One key observation was that secretion of chimera A in absence of Tap1-Tde1 is as efficient as secretion of VgrG1a^{P} and this is reproducible (Figure 6-10A, compare lanes 4 and 6). Around 60 % of VgrG1a^{P} and construct A are secreted into the supernatant in the absence of Tap1-Tde1 (Figure 6-10C, lanes 13 and 15). However, when both VgrG1a^{P} and construct A are expressed in presence of the Tap1-Tde1 complex, secretion of construct A is hampered in comparison to VgrG1a^{P} (Figure 6-10B, compare lanes 10 and 12). This correlates with a drop of secreted construct A to 20 % (Figure 6-10C, lane 16), while secretion of VgrG1a^{P} remains unaffected by presence of Tap1-Tde1 (lane 14). This is a remarkable finding which suggests that Tap1-Tde1 does interfere with construct A secretion but not with VgrG1a^{P}. This could then be correlated with the fact that Tap1-Tde1 interacts with construct A but not with VgrG1a^{P}.

If secretion of construct A is somehow impacted by the presence of Tap1-Tde1, one might assume that Tse6 delivery into prey cells is as well. As previously indicated, a bacterial competition assay is likely a more sensitive readout than analysing western blots for secreted effectors. The idea here is that in absence of the Tap1-Tde1 complex, VgrG1a^{P} and construct A are able to drive killing of Tse6-sensitive cells as shown in 4.4.4. Instead, in presence of Tap1-Tde1 such killing would be hampered due to the failure to bind and thus deliver Tse6 which might be trapped in the attacking cell.

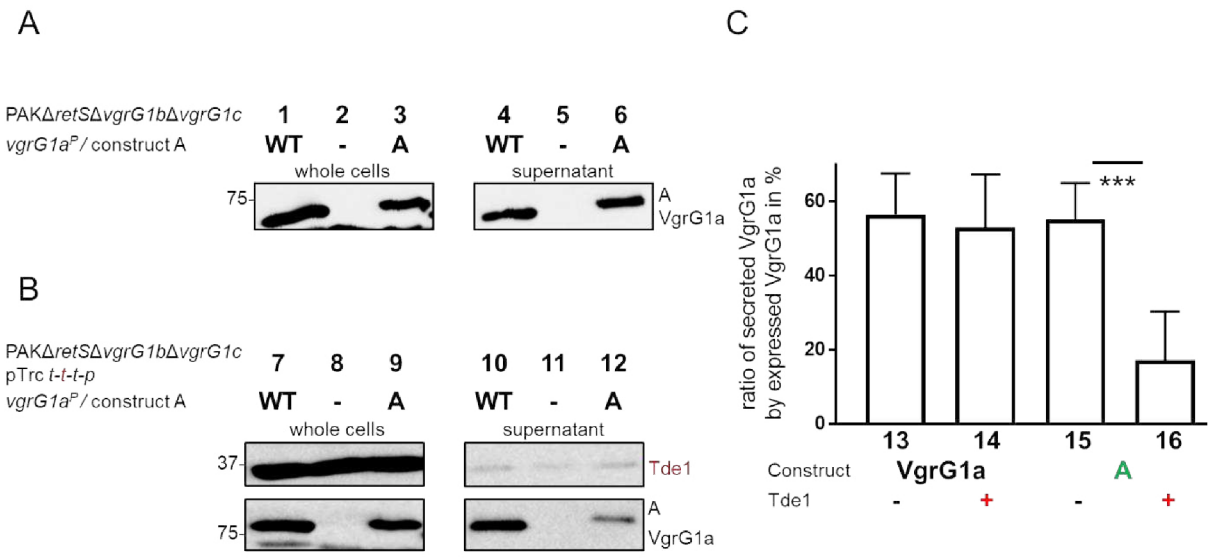


Figure 6-10. Presence of Tde1 interferes with secretion of construct A.

A, B: Sections of western blots from secretion assays of PAKΔ*retS*Δ*vgrG1b*Δ*vgrG1c* expressing chimerae A in A: absence and B: presence of *tap1-tde1-tdi1-paar1* from *pTrc200*. Chimera A secretion is massively reduced in presence of Tde1 (lane 12). C: Percentage of secreted VgrG1a or construct A in absence (-) or presence (+) of *tap1-tde1-tdi1-paar1*. Intensities of bands corresponding to VgrG1a were measured using ImageJ and plotted. Dunnett's multiple comparisons test was conducted with *** $p<0.001$.

We used as prey a strain lacking *tsei6* and thus immunity to Tse6, while the attacker uses either VgrG1a or construct A in presence or absence of Tde1. Note that a catalytic mutant of Tde1 (Tde1(HADA) was used to rule out any toxic effect on the prey in case Tde1 was delivered even in small amounts. Thus, to evaluate the impact of Tde1 binding on construct A delivery, prey survival numbers from three independent experiments were compared and plotted in Figure 6-11. As can be seen in lane 1, when attacking strains express VgrG1a^P, a decrease in recovered prey cfu can be observed due to Tse6 delivery which is not affected by Tde1 presence (lane 2). This outcompeting effect is abrogated when attacking strains lack *vgrG1a*^{P} (lanes 5 and 6). Instead, when attacking strains express construct A and no Tde1 (lane 3), Tse6-dependent killing is reflected by low prey survival similar to WT levels. This confirms that not only is construct A secreted, but it also drives delivery of Tse6 into prey cells,

corroborating its functionality despite the addition of C-terminal residues. Remarkably, co-expression of Tde1 (lane 4) leads to an intermediate phenotype suggesting that Tse6 delivery is affected but not completely abrogated. This would mean that either binding of Tap1-Tde1 to the tip composed of construct A does not entirely prevent Tse6 secretion, or that only a fraction of construct A is bound by Tap1-Tde1 and others which are associated with Tse6 could thus deliver Tse6.

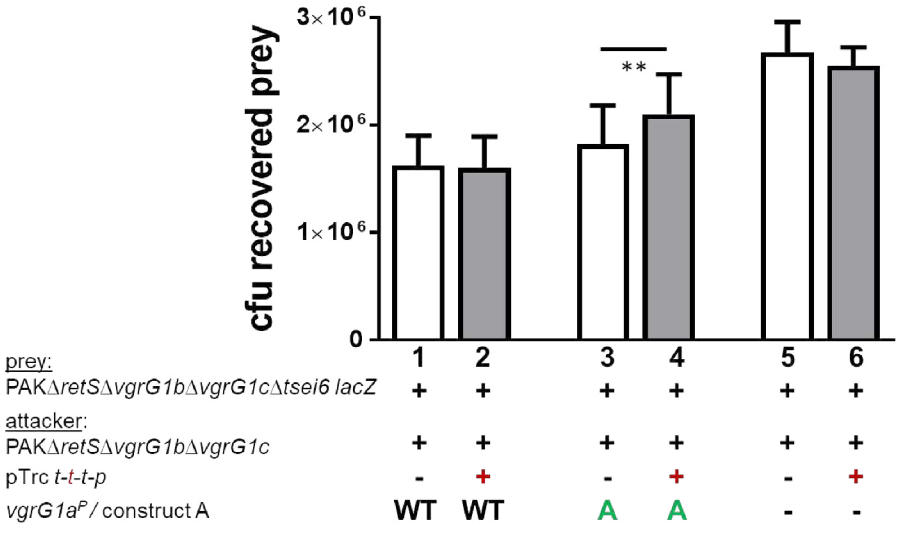


Figure 6-11. Presence of Tde1 interferes with delivery of Tse6 into prey cells.

Plot of recovered cfu of prey strain PAKΔ*retS*Δ*vgrG1b*Δ*vgrG1c*Δ*tsei6::lacZ* after contact with attacker strain that expressed VgrG1a^{P} (WT) or construct A in absence (-) or presence (+) of of *tap1-tde1(HADA)-tdi1-paar1* (*t-t-t-p*) from pTrc200. Spots were incubated for 5 h at 37 °C in a 5:1 ratio. One-Way ANOVA analysis with Sidak's multiple comparisons test was conducted between the datasets obtained from the two genetically same strain backgrounds with ** $p<0.01$.

These findings could be explained with the following concept as summarised in a model sketched in Figure 6-12. In an original *P. aeruginosa* context (Figure 6-12A), VgrG1a (blue) should interact with the PAAR domain of Tse6 (orange) *via* its last three β-strands as discussed in 4.4.1. Instead, the C-terminal domain of Tse6, which is the toxin domain

comprising of 260 aa, should expand beyond the tip, possibly bending along the side of the torch-like structure of the VgrG [202]. It was also shown in recent structural studies that EagT6 (magenta), which is about 16 kDa, and the Elongation factor 2 (Ef2, cyan), approximately 50 kDa, also tightly interact with the tip complex resulting in additional 80 kDa that sterically occupy space around the tip [202].

In the case of the chimera A, all of these components would still be interacting on the tip, since none of these interaction surfaces were modified (Figure 6-12B). Now, because of the addition of 31 aa derived from the C-terminus of VgrG1^{A} (green), one can assume that Tap1-Tde1 (purple-red) would bind to this region and would add another three complexes of 55 kDa surrounding the VgrG tip. All in all, we suggest that the steric hindrance due to a wealth of binding partners around the VgrG tip could be a limitation factor.

In light of these observations, one could envision that decreasing the steric hindrance at the tip of the construct A would be to prevent binding of Tse6 and its associated factors. Yet, for VgrG being able to act as a puncturing device, a PAAR protein is needed to bind onto the blunt end as discussed in 4.4. One genetic background which would allow to achieve this, would be to have a *tse6* gene truncated for the region encoding the toxic domain but intact for the PAAR domain, and this would give more sterical space around the VgrG1a tip to accommodate Tap1-Tde1 (Figure 6-12C). Due to time restrictions of this PhD project, these mutants could not be constructed, but are prospect of future work in the lab.

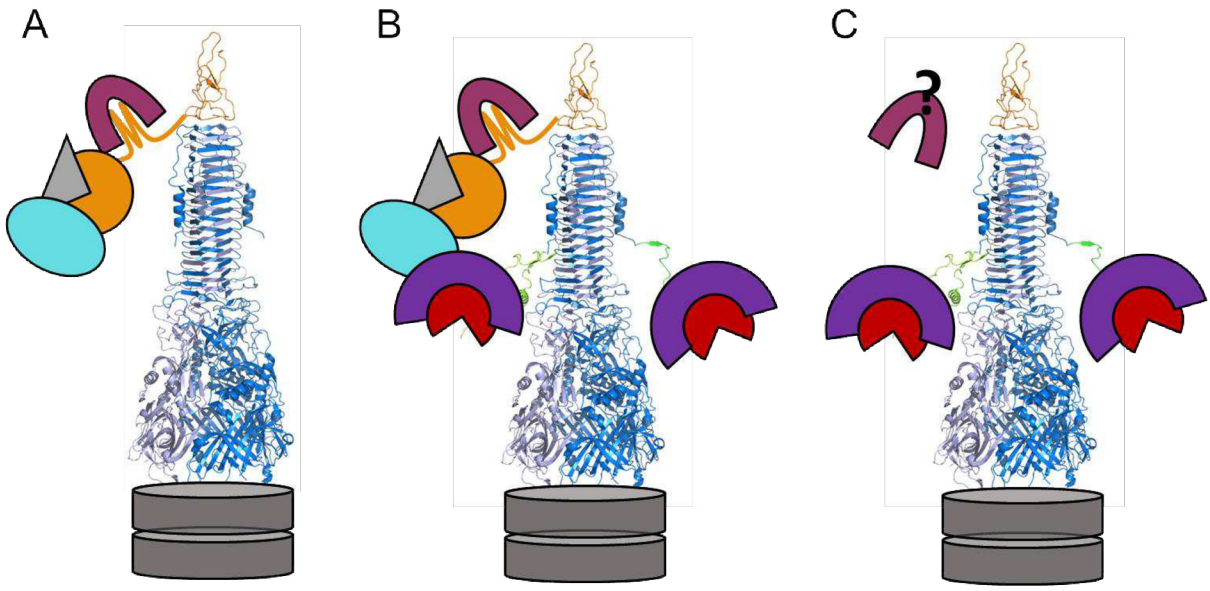


Figure 6-12. Model about the decoration of the VgrG1a/chimera A-tip in absence and presence of Tap-Tde1.

VgrG1a^{P} is represented as a blue trimer (pdb: 4mtk), topped up by the PAAR domain of Tse6 (orange) with the C-terminal domain of Tse6 floating around the tip bound to its cognate immunity Tsi6 (grey). The chaperone EagT6 (magenta) and EfTu2 (cyan) bind C-terminal Tse6. A: Configuration of the VgrG1a tip in the parental strain. B: VgrG1a is extended by 31 aa originally from VgrG1^{A} (green) resulting in the binding of Tap (purple) together with Tde1 (red) leading to a sterically complex tip. C: If the C-terminal domain of Tse6 was absent, it would give more space for the Tap-Tde1 complex to accommodate around the tip, probably resulting in secretion of the complex.

6.5. Bioinformatic analysis of recognition patterns within the VgrG-Tap-effector complex

In the previous section, we could experimentally demonstrate and confirm that Taps have essential functions in mediating the specific interactions between effectors and their cognate VgrG proteins [149, 217]. This crucial connecting role might be due to the genomic organisation of *tap* containing clusters, with *tap* genes usually being located between an effector gene and a *vgrG/paar* gene (Figure 6-13). Furthermore, a recombination site within the *tap-1* gene in *V. cholerae* was identified that is thought to be a key feature during the

genetic exchange of effector modules. It was shown that the 3' end of *tap-1* downstream of the recombination site generally co-segregates with the effector-encoding gene, which gave rise for the hypothesis that the C-terminal Tap domain binds the N-terminus of an effector. Accordingly, the N-terminal Tap domain, usually comprising the DUF4123, is proposed to specifically interact with the C-terminus of the cognate VgrG or PAAR protein [217]. This would bring VgrG or PAAR and effector into close proximity, which might lead to the formation of a deliverable VgrG/PAAR-effector-complex. The noticeable hydrophobic nature of Tap proteins might be an important asset in this complex formation process. Further, it remains elusive how this complex remains stable after the Tap dissociates and how Taps have evolved to specifically recognise both effector and VgrG/PAAR [217]. Here, we attempt to identify specific sequences within effector and VgrG proteins that would be crucial for Tap recognition as well as complex formation and stability.

With regards to the chimeric nature of Taps, we here want to briefly discuss one aspect of recent research. In a study by Burkinshaw and colleagues [220], the delivery mechanism of TseT from *P. aeruginosa* was investigated and the authors claimed that delivery of TseT depends on the proteins PAAR4, TecT and Co-TecT, of which all genes are encoded together with *tseT* (Figure 6-13). They showed that Co-TecT has a chaperoning role towards TecT and is required for functionality of TecT [220]. When analysing the amino acid sequences of TecT and Co-TecT, we noticed that TecT contains the conserved motifs of DUF4123 domains (Figure 6-1), while Co-TecT exhibits similar hydrophobic patterns as the C-terminal domains of Taps. Hence, we aligned Co-TecT as an extension of TecT, as seen in Figure 6-1, and based on the similarity, we claim that TecT and Co-TecT assemble to form one functional Tap that recruits TseT towards its cognate PAAR4.

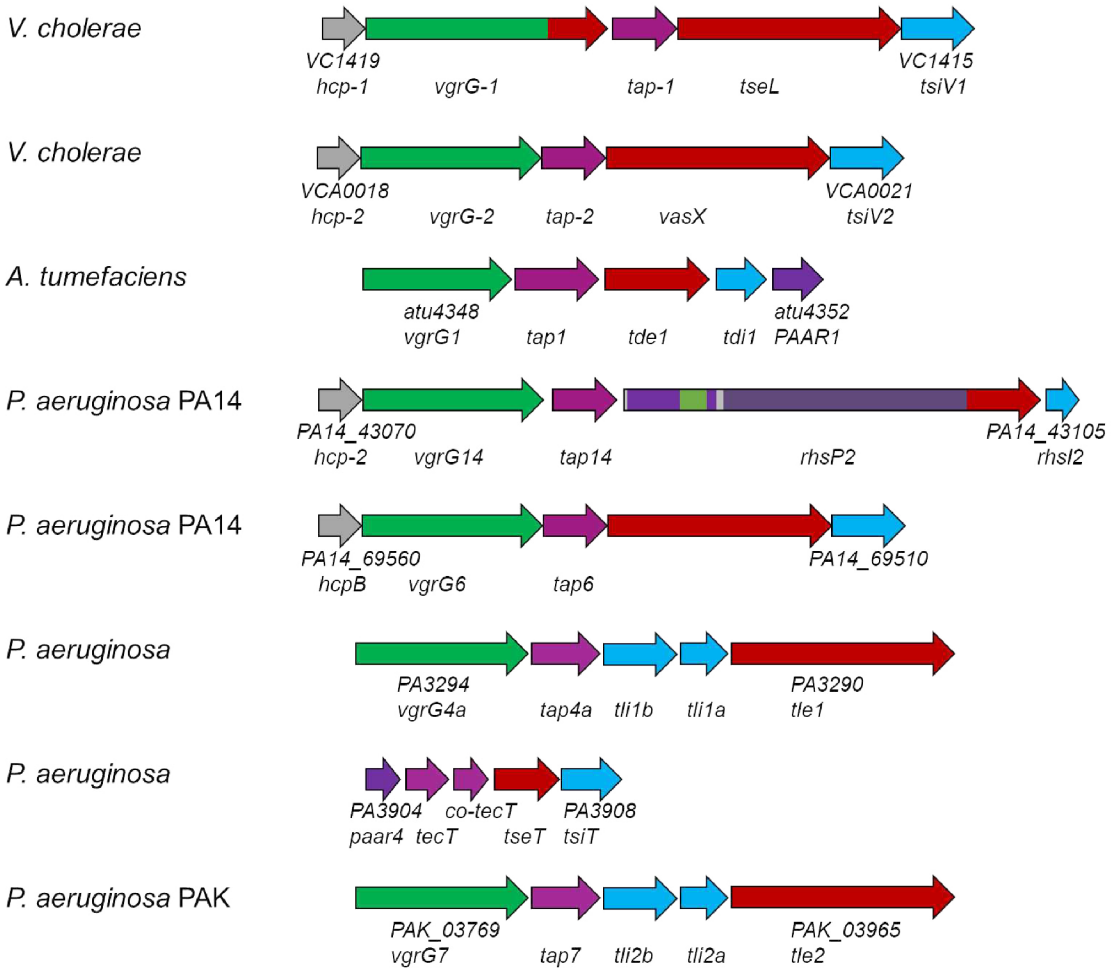


Figure 6-13. Genetic environments of Tap-dependent effectors from *Vibrio cholerae*, *Pseudomonas aeruginosa* and *Agrobacterium tumefaciens*.

Characterised and predicted Tap-containing operons adapted from [149, 217]. *hcp* genes are depicted in grey and are usually encoded upstream of *vgrG* genes (green) followed by *tap* genes (magenta) and effector-immunity modules (red-cyan).

6.5.1. Tap-dependent effectors contain conserved and accessible cysteines

Here, we aim to shed light on the basic aspects of Tap-mediated effector delivery using a bioinformatical approach. We chose effectors, that were experimentally proven to be delivered in a Tap-dependent manner or are encoded in *P. aeruginosa* and *P. putida* together with *tap* genes, and analysed them with special focus on their N-termini (Figure 6-14).

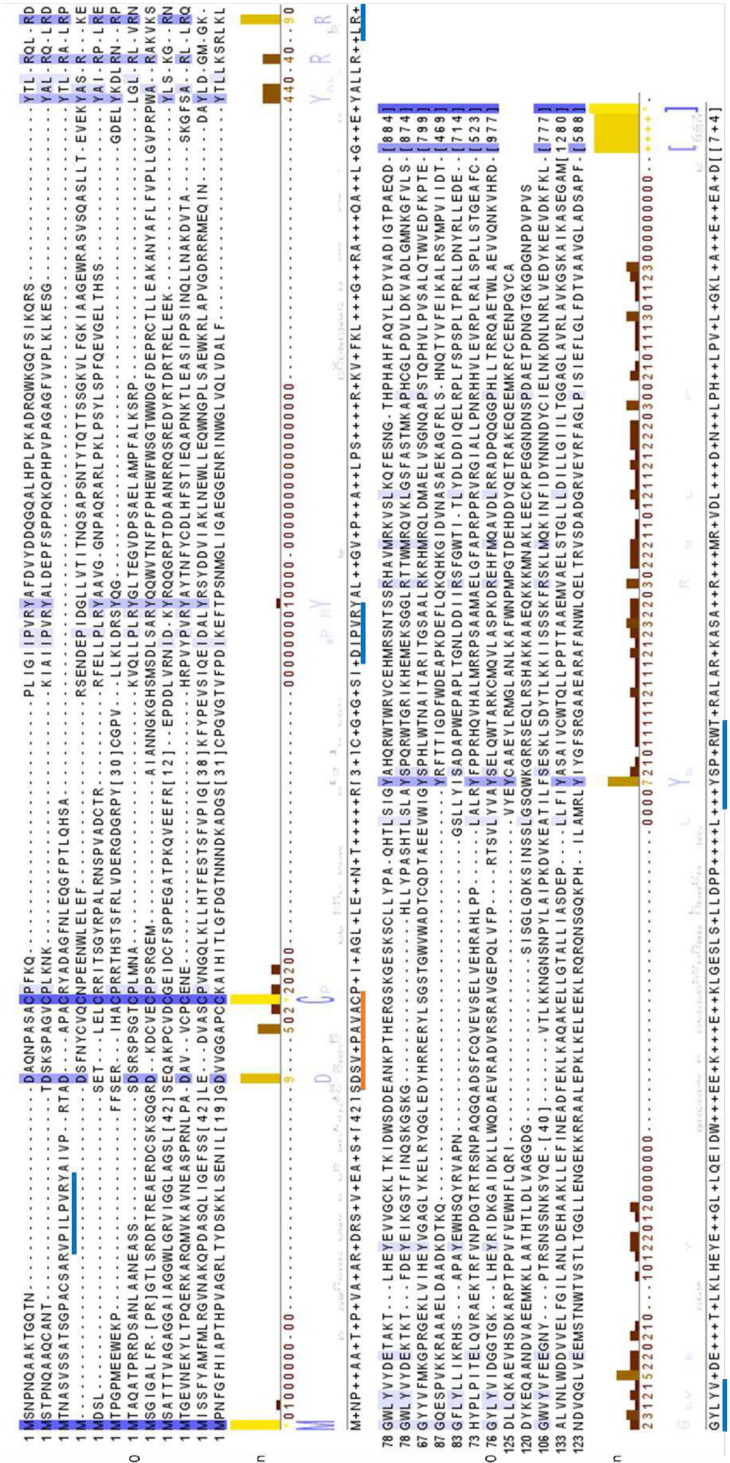


Figure 6-14. Tap-dependent effectors contain conserved cysteines.

Multiple sequence alignment of the N-terminus of effectors whose delivery depend on Tap proteins. At the beginning of the N-terminus, all effectors contain a 6-9 aa long sequence containing a conserved cysteine (orange line), which from now on will be called cysteine sequence. After that three less conserved MIX-like motifs can be identified (blue lines).

Examination of the N-termini of Tap-dependent effector proteins with protein-domain prediction and structural homology building tools did not point towards any common domains or structural folds (*data not shown*). However, a multiple sequence alignment of the N-termini of Tap-dependent effectors revealed a conserved aspartate or glutamate residue followed by up to 7 predominantly hydrophobic amino acids and a conserved cysteine (highlighted in orange in Figure 6-14). We termed this sequence “effector cysteine sequence” due to the prevalence of a highly conserved cysteine residue in those effectors as summarised in Table 6-1.

Subsequently, the location of the cysteine sequence on the tertiary protein structure was analysed. The structure for one Tap-dependent effector, Tle1^{Paer}, is known and shown in Figure 6-15 [190]. The cysteine sequence of Tle1^{Paer} contains two cysteine residues (see Table 6-1), highlighted in orange in Figure 6-15, that are located at the end of an unstructured and likely flexible loop. The rest of the flexible loop comprises the additional amino acid residues of the cysteine motif [190]. Thus, the presence of conserved sequences on the surface of Tap-dependent effectors hints towards an effector recognition site for a cognate interaction partner, which we will go into detail below.



Figure 6-15. Tap-dependent effectors contain easily accessible cysteines.

Close-up on the structure of Tle1 (PDB code: 4O5P) [190]. Two cysteine residues of the N-terminal cysteine sequence are highlighted in orange and are located just prior an unstructured loop that comprises the additional amino acids of the cysteine sequence. The central and the C-terminal MIX-like motifs are highlighted in blue.

6.5.2. Tap-dependent effectors contain hydrophobic MIX-like motifs

In the sequence alignment in Figure 6-14, we further identified three conserved clusters of variable lengths that are highlighted with blue lines. When further analysing these clusters, we realised that they not only comprise of mainly hydrophobic amino acids, but they also show a remarkable resemblance with the recently described MIX-motifs found in a subset of T6SS effectors [214].

The MIX motif was described in a work by Salomon *et.al.* as a conserved motif within a range of T6SS effectors of various organisms [214]. No genetic dependency or domain organisation of these MIX-containing effectors could be identified by the authors; thus, their prevalence is highly flexible and independent on any effector-associated genes. The MIX motif

was described as three sequences, with one being the conserved central motif hRXGhhYhh, with h representing hydrophobic residues, as well as the N-terminal shhPhR and the C-terminal hhF/YSXXXWS/T motif, with s representing small residues [214]. However, in that study, the authors did not demonstrate any functionality of these motifs or showed a specific role in effector recognition, function or delivery.

In the multiple sequence alignment in Figure 6-14, derivates of these three MIX motifs, henceforth termed MIX-like, are readily recognisable. The here identified central motif can be summarised to the sequence hRXshhYh, which is highly similar to the motif described by Salomon and colleagues [214]. The N-terminal motif in our case can be described as a sequence of hhPhR and the C-terminal as LhhhYSXXX, with the last two amino acid residues WT being present in only a subset of effectors.

When we mapped these MIX-like motifs onto the structure of Tle1^{Paer}, we observed that two of the motifs are located on the surface of the protein (Figure 6-15, highlighted in blue). The third one, the N-terminal hhPhR motif, is buried within the core of the protein (not shown) which implies an impact on protein folding or stabilisation. However, the fact that the central and the C-terminal MIX-like motifs are accessible for interaction partners might support their role in effector recognition by another T6SS component.

6.5.3. VgrGs delivering Tap-dependent effectors contain conserved cysteines

As some studies suggested already, it is thought that a Tap-effector complex specifically binds to the C-terminus of the cognate VgrG protein [149], but no clear details are available on how this interaction is facilitated. The identification of a conserved cysteine sequence and three conserved MIX-like motifs within the N-termini of Tap-dependent effectors led us to speculate that a similar conserved sequence could be identified within the C-termini

of VgrG proteins. We here focus our analysis on VgrG proteins that are encoded upstream of *tap* genes and that were shown or predicted to serve as the cognate VgrGs for the above analysed effectors (6.5.1, Table 6-1).

Modelling the C-termini of these VgrG proteins with the Phyre2 web tool or domain prediction tools showed that this protein region is predominantly disordered (*data not shown*). This is fitting to its assumed function as it would allow flexibility of the extension arm to interact with its target. A multiple sequence alignment of these VgrG proteins is displayed in Figure 6-16A and a high conservation within their gp5-/gp27-like domains can be observed (identical amino acids are highlighted with blue boxes); which correspond to the needle-like part of VgrG proteins (see Figure 6-4B). In 4.4, we discussed in detail and showed how the last VgrG β-strand is crucial for binding of the cognate PAAR protein. These last β-strands of all tested VgrG proteins can be identified in the sequence alignment with the help of structural modelling (not shown) and published literature [141, 149] and are highlighted with a purple line in Figure 6-16B. Following the putative last β-strands, all VgrG proteins display extensions of various lengths while only VgrG-1^{Vcho} contains an extension domain [181]. In all cases, the putative last β-strand is followed by an amino acid stretch rich in prolines and glycines (highlighted with a green line) that might give flexibility to the extension arm and positions it away from the VgrG spike [141]. Detailed examination of the C-terminal region of these extensions pinpointed a conserved sequence starting with a proline that is followed by four to seven primarily hydrophobic amino acids and a highly conserved cysteine (highlighted by an orange line, see Table 6-1). We then examined the C-terminal regions of various VgrG proteins that are not encoded upstream of *tap* genes and could not identify this sequence (not shown), suggesting that this cysteine sequence is a highly unique feature of VgrG proteins delivering Tap-dependent effectors.

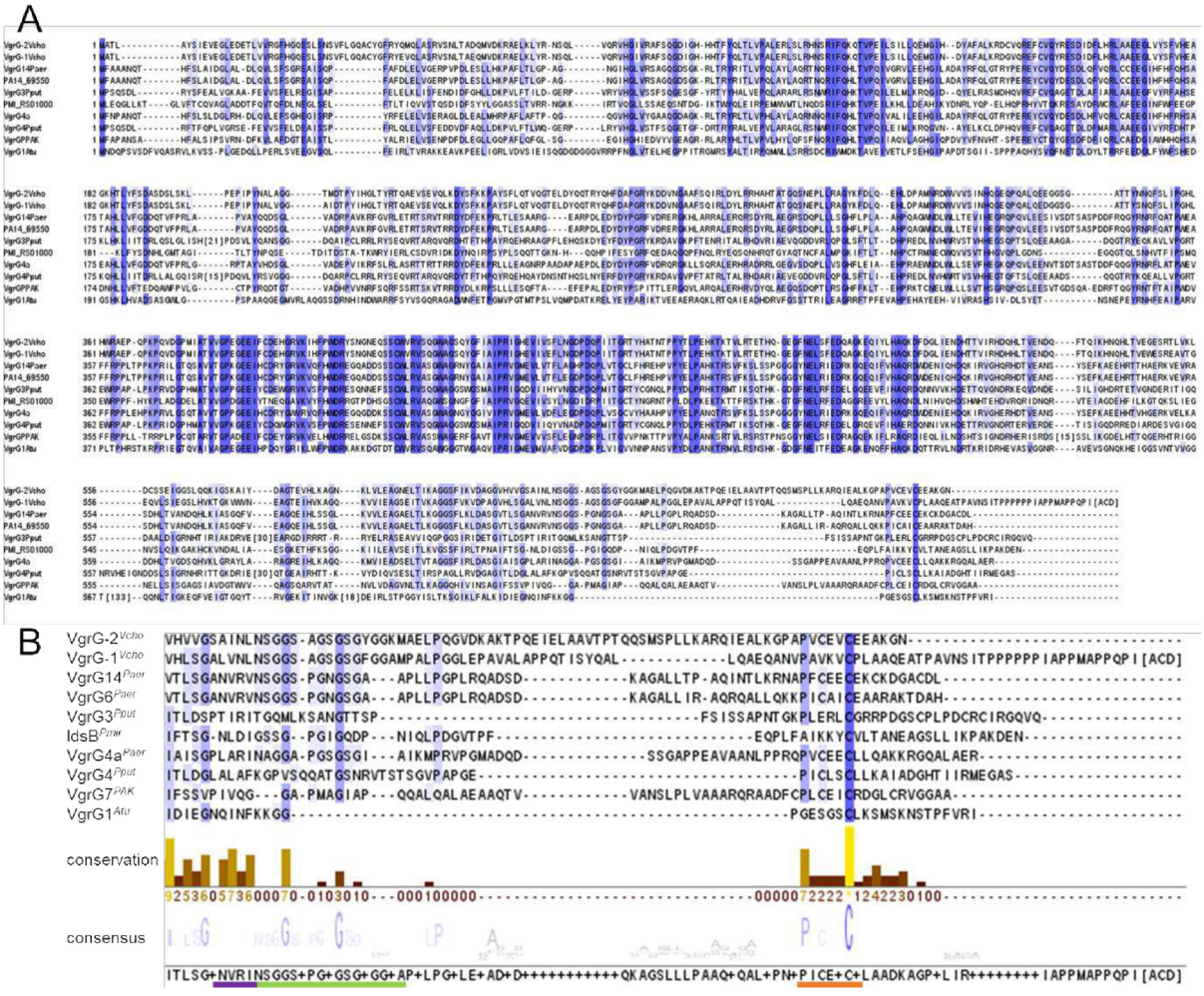


Figure 6-16. VgrGs delivering Tap effectors contain cysteine motifs.

Multiple sequence alignment of VgrG proteins involved in the delivery of Tap-dependent effectors. A: The gp27-/gp5-like domains are highly conserved as visualised by blue boxes for identical amino acids. B: The last predicted β-strand, probably binding the cognate PAAR, can be identified and is highlighted by a purple line. Then a proline and glycine rich stretch follows giving the extension structural flexibility. Subsequently, another cysteine sequence can be identified encompassing a conserved proline, followed by a range of hydrophobic amino acids and a conserved cysteine (highlighted with an orange line).

6.5.4. Effector recruitment via disulphide bonds – a novel concept

Here, we identified novel sequences within VgrG proteins and their cognate Tap-dependent effectors, as summarised in Table 6-1. The presence of highly conserved cysteines

within the N-termini of effectors and the C-termini of their cognate VgrG proteins allows for the hypothesis that these two proteins could form disulphide bonds as sketched in Figure 6-17.

Table 6-1. Overview of cysteine motifs within Tap-dependent effectors and their cognate VgrGs/PAARs.

Cysteine sequences were extracted from multiple sequence alignments shown in Figure 6-14 and Figure 6-16 and the effectors listed with their cognate Taps and VgrG or PAAR according to the available literature from [149, 217, 218, 220, 263]. Underlined are the conserved residues within both cysteine sequences, proline (P) and cysteine (C) within the C-terminus of the VgrG- or PAAR proteins and aspartate (D) or glutamate (E) and cysteine (C) within the N-terminus of the effectors.

organism	adaptor	cysteine sequence	Tap	effector	cysteine sequence
V. cholerae	VgrG-2	PVCEVC	Tap2/VasW	VasX	DAQNPASAC
A. hydrophila	VgrG1	PFCEEC	TecC	TseC	DSKSPAGVC
V. cholerae	VgrG-1	PAVKVC	Tap1	TseL	DSFNYCVQC
A. tumefaciens	VgrG1	PGESGSC	Tap1	Tde1	EQAKPCVDC
P. aeruginosa	VgrG7	PLCEIC	Tap7	Tle2^{PAK}	ERIHAC
P. aeruginosa	VgrG6^{PA14}	PICAIC	Tap6	PA14_69520	DSRSPSGTC
P. aeruginosa	PAAR4	PKLCLQC	(co-/)TecT	TseT	DKCVEC(^{93})
P. aeruginosa	VgrG4a	PVCEEC	Tap4a	Tle1	DVVGGAPCC
P. aeruginosa	VgrG14	PFCEEC	Tap14	RhsP2	EDVASC
P. mirabilis	IdsB	PLFAIKKYC	IdsC	IdsD	EDVASC
P. putida	VgrG3	PLERLC	Tap3	Tke5	DAPAC
P. putida	VgrG4	PICLSC	Tap4	Tke9	ETLELC

We propose that these specific disulphide bonds are required for effector delivery. Bond formation could be facilitated in the reducing cytoplasmic environment through interactions with the specific and hydrophobic Tap (Figure 6-17C). Protein-protein interactions lead to desolvation and increased hydrophobicity, an environment amenable for cysteine cross-linking [264]. A covalent bond between the VgrG and the effector might help explain how interactions between these two proteins are maintained in the absence of the Tap during

the secretion process (Figure 6-17F). After dissociation of the Tap, the VgrG-effector complex can be delivered by the T6SS into target prey cells, where it meets the reducing environment of the cytosol (Figure 6-17G). This might lead to reduction of the disulphides and thus the dissociation of the VgrG-effector complex allowing the effector to find its cellular target and exert toxicity.

This model needs to be supported by solid experimental data, however, due to time restrictions of this PhD project, this work could not be performed. The approach was to choose one effector, likely Tle1 from *P. aeruginosa,* that is encoded downstream of *vgrG4a* and *tap4a* (Figure 6-13 and Table 6-1). It would have been the rationale to first show that Tle1 delivery depends on VgrG4a and Tap4a. Further, the idea was to mutate the conserved cysteines within both VgrG4a and Tle1 to show their importance for Tle1 delivery, while confirming that Tle1 toxicity was not impacted. Further, structural studies into the VgrG4a-Tap4a-Tle1 complex could support this hypothesis and allow more definite conclusions about the spatial arrangement of the Tap4a-Tle1 complex around the VgrG4a tip.

Interestingly, a study by Unterweger and colleagues showed that delivery of TseL depends on its upstream encoded Tap1 as well as VgrG-1 in *V. cholerae* (Figure 6-13 and Table 6-1) [217]. They further adhered to a region of 37 aa after the gp5-/gp27-like domains of VgrG-1 and prior to the extension domain (see Figure 6-16). The authors could show that absence of this linker region abolished TseL delivery, while lack of solely the C-terminal effector domain had no effect [217]. Remarkably, the here identified cysteine sequence can be found within those described 37 aa (see Figure 6-16) supporting our idea that this sequence is crucial for effector recognition and delivery.

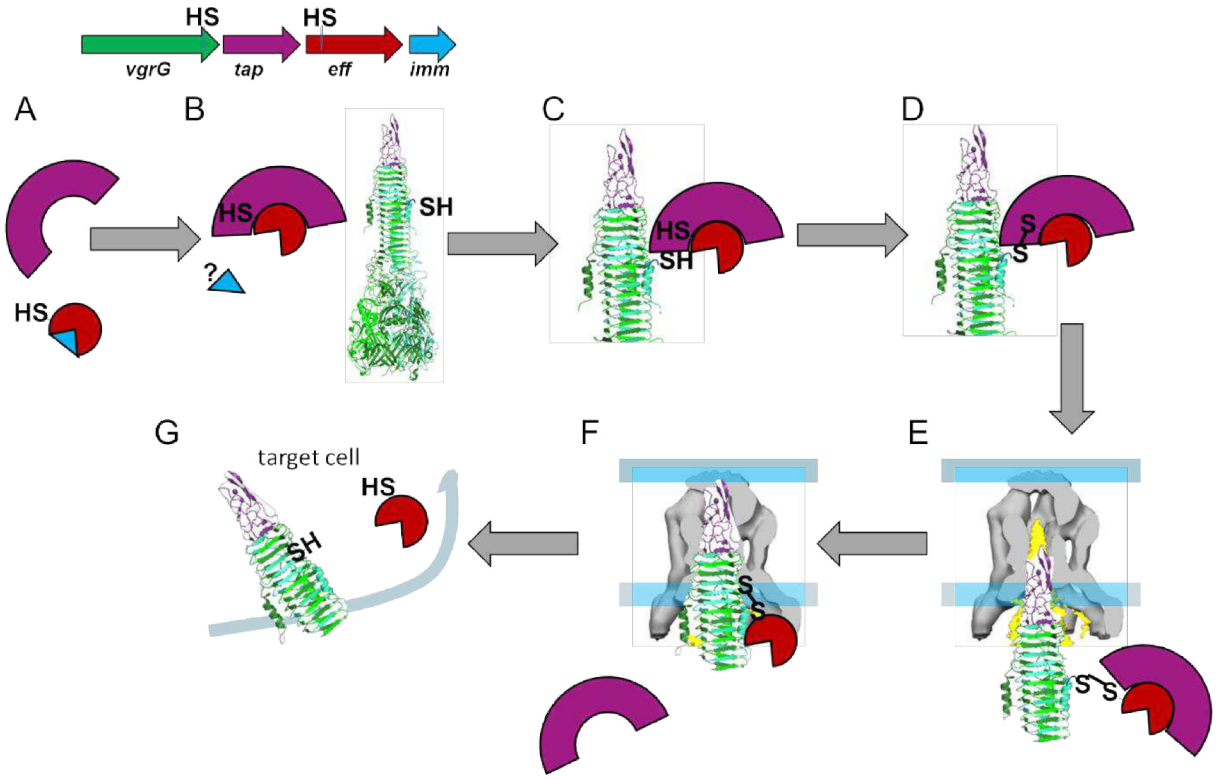


Figure 6-17. Model of disulphide formation between a VgrG and its cognate Tap-dependent effector.

VgrG proteins are shown in green (PDB: 4mtk) and contain a conserved cysteine within their C-termini. A: The cognate effector is shown in red and contains a conserved cysteine within its N-terminus. B: The hydrophobic Tap (magenta) binds the effector and C: recruits it to the C-terminus of the cognate VgrG. D: The Tap creates a hydrophobic environment which facilitates disulphide formation between the VgrG and the effector. E: This complex is recruited towards the membrane complex (grey, figure reproduced under a Creative Commons Attribution Licence from [115]), in which the disulphide bond might be stable, F: and the Tap dissociates. G: The VgrG-effector complex is delivered into prey cells, where it meets the reducing environment of the cytosol leading to dissociation of the disulphide bond and thus the two proteins, allowing the effector to meet its cellular target and exert toxicity.

Furthermore, a recent study brought detailed insights into the delivery mechanism of the Tap-dependent effector TseT in *P. aeruginosa* [220]. TseT is encoded together with *paar4, co-tecT* and *tecT*, a *DUF4123/tap* gene (Figure 6-13), and its delivery into prey cells was shown to be dependent on these three gene products as well as on VgrG4b and VgrG6. While neither VgrG4b nor VgrG6 contain the here described cysteine sequence, PAAR4 displays a

C-terminal extension, which is rather unusual for PAAR proteins, in which the cysteine sequence can be identified (Table 6-1).

The authors identified two cysteine residues within the N-terminus of TseT. One of these cysteines (cysteine^{93}) corresponds the conserved cysteine identified in the here described cysteine sequence (Table 6-1). When the authors mutated cysteine^{93}, they could show that TseT-mediated killing of TseT-sensitive prey cells was abolished [220]. They reasoned that somehow toxicity of TseT was impacted by the cysteine mutation, while we hypothesise that delivery of TseT into prey cells was most likely abolished. However, neither of these ideas are proven and thus remain elusive. This delivery mechanism demonstrates another remarkable concept for Tap-dependent effector delivery. In this case, the effector would not be covalently bound to the cognate VgrG protein, but to a PAAR protein. This would allow the additional recruitment of effector proteins by the VgrG protein and thus a highly variable decoration of the VgrG-PAAR spike complex.

Finally, it is important to discuss our attempt to connect Tde1 to VgrG1a^{P} using the C-terminus of VgrG1^{A}. We designed chimerae that expressed a part of VgrG1a^{P} and the 21 and 31 C-terminal residues from VgrG1^{A}. The cysteine sequence could also be identified in the C-terminus of VgrG1^{A} (Table 6-1) and, considering the swapping points of our chimerae (Figure 6-6), each of the designed chimerae contained the cysteine sequence derived from VgrG1^{A}. The presence of this sequence within the VgrG spike protein would be the prerequisite for efficient Tde1 recognition. This is in good agreement with the interactions we observed between any of our chimerae and Tde1 (Figure 6-7 and Figure 6-8).

6.5.5. Discussion: Using the chimeric nature of Taps to investigate Tap-dependent effector delivery

Another way to shed light on the delivery mechanism of Tap-dependent effectors is to make use of their chimeric nature [217]. Due to time restrictions of this PhD project, this strategy could not be pursued.

As it has been suggested by a couple of studies, the N-terminus of a Tap specifically recognises the C-terminus of a VgrG protein and the C-terminus of a Tap specifically recognises the N-terminus of the cognate effector (Figure 6-18A, black circles representing interactions) [217, 218]. On the basis of this concept, we developed three strategies that could broaden our knowledge on the delivery of Tap-dependent effectors as outlined in Figure 6-18.

All strategies aim at delivering the heterologous effector^{delivery} (yellow) using VgrG^{host} (green) as a vehicle (Figure 6-18A). One option is similar to the one adopted in this current study in which we substituted the C-terminus of VgrG^{host} with the C-terminus of VgrG^{delivery} (red). The substitution point would need to be determined carefully so that the PAAR-binding β-strand is not modified thus the cognate PAAR^{host} would remain the same. An advanced strategy could further be to solely substitute the cysteine sequence of VgrG^{host} with the one from VgrG^{delivery}. This strategy likely leads to specific recognition of the Tap^{delivery}-effector^{delivery}-complex by the C-terminus/cysteine sequence of VgrG^{delivery} resulting in delivery of effector^{delivery} (Figure 6-18B). However, in our case, this strategy proved unsuccessful probably due to the chosen VgrG vehicle. Thus, we propose to attempt the delivery of a Tap-dependent effector using a VgrG protein that does not bind and deliver any other large effectors as in our case VgrG1a delivering Tse6.

Another possibility could include the design of a Tap^{chimera} which consists of an N-terminal Tap^{host}-domain (blue) and a C-terminal Tap^{delivery}-domain (orange). While VgrG^{host}

would recognise and bind the N-terminal Tap^{host}-domain, the C-terminal Tap^{delivery}-domain would specifically bind the cognate effector^{delivery} (Figure 6-18C). This might very likely lead to delivery of effector^{delivery}.

A third option could be based on an effector^{chimera} that contains an N-terminal effector^{host} part (cyan) and the main effector domain from effector^{delivery}. Tap^{host} would probably bind the N-terminal effector^{host} domain and then recruit effector^{chimera} to VgrG^{host} which might lead to its delivery. Additionally, the cysteine sequence of effector^{host} could be substituted by the cysteine sequence of effector^{delivery} likely resulting in delivery of effector^{chimera}. This approach would further emphasise on the importance of the cysteine sequence in effector recognition.

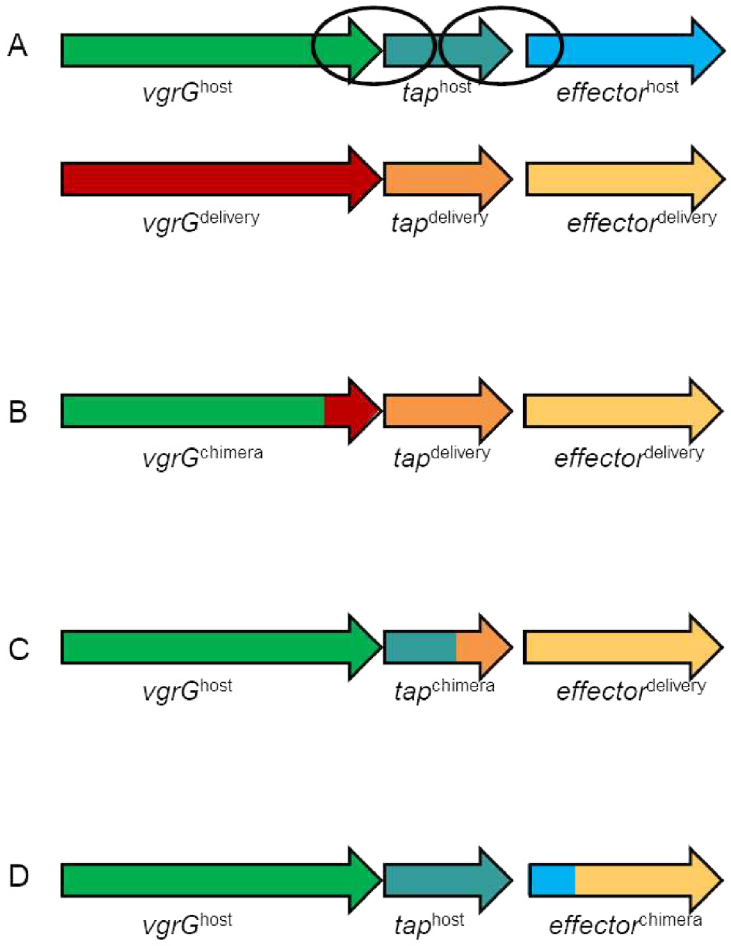


Figure 6-18. Strategy to elucidate the molecular mechanism of Tap-dependent effectors.

A: VgrG^{host} (green) mediates delivery of effector^{host} (cyan) dependent on tap^{host} (turquoise). VgrG^{delivery} (red) mediates delivery of the heterologous effector^{delivery} (yellow) dependent on tap^{delivery} (orange). B: In an attempt to deliver the heterologous effector^{delivery}, one could substitute the C-terminus of VgrG^{host} with the C-terminus of VgrG^{delivery} resulting in VgrG^{chimera}. This might the recognise its cognate Tap^{delivery} and effector^{delivery} leading to its delivery. C: Another approach could be to construct a chimera between Tap^{host} and Tap^{delivery} resulting in Tap^{chimera}. VgrG^{host} recognises the N-terminus of Tap^{chimera} (blue part) due to its *host* source. Effector^{delivery} is recognised by the C-terminus of Tap^{chimera} (orange part) due to its *delivery* source. D: A further approach might be to design an effector^{chimera} based on the N-terminus from effector^{host} and the effector domain from effector^{delivery}. Tap^{host} could specifically recognise the effector^{host} part and recruit the Tap-effector complex to VgrG^{host} which might lead to delivery of the complex.

6.6. Summary

In this chapter we attempted to gain molecular understanding on the T6SS-dependent delivery of effectors that rely on the presence of specific adaptor proteins called Tap. We assessed the mechanism by investigating the possibility of heterologous secretion in *P. aeruginosa* of the Tap-dependent effector Tde1 from *A. tumefaciens*. As is the case with this specific adaptor protein, the effector would need to first bind onto Tap before being able to bind to its cognate VgrG protein [217]. We demonstrated specific interactions between a Tap-dependent effector and the C-terminus of the VgrG protein, however delivery of the effector proved unsuccessful probably due to other limitations. Future work will attempt to circumvent these restrictions in an attempt to ultimately deliver the heterologous effector.

Further, we proposed a model for effector recruitment towards the VgrG tip which would involve the formation of a covalent disulphide bond facilitated by the hydrophobic Tap. We proposed strategies and experiments to support our model and if proven right, this would represent a completely novel principle of effector recruitment towards a bacterial protein secretion system.

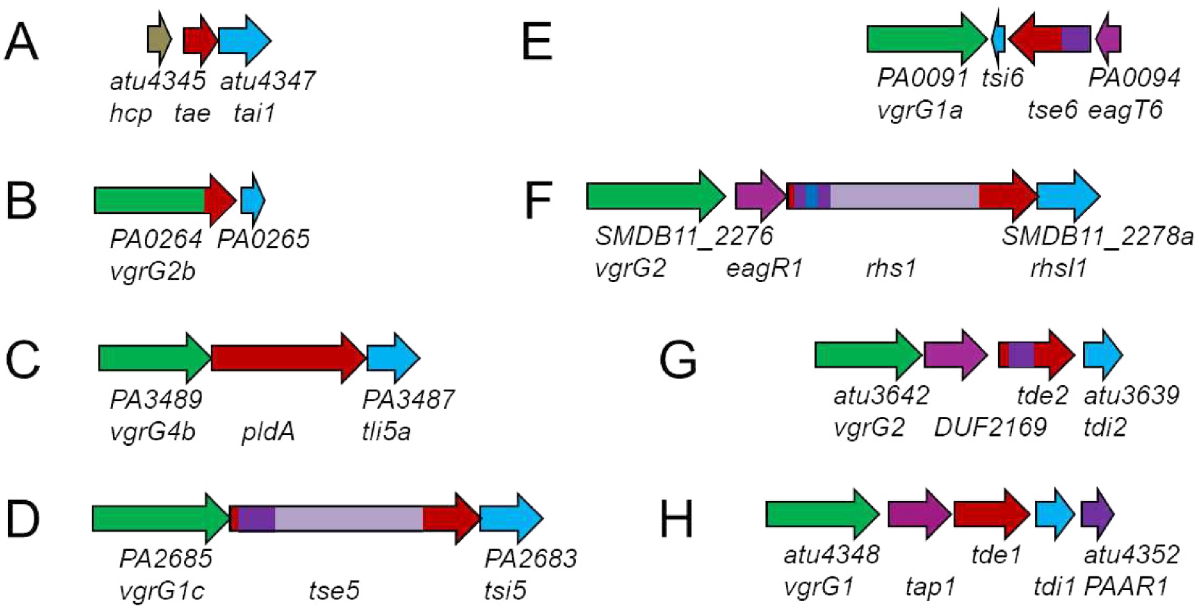
7. General discussion

The T6SS is a versatile secretion system, injecting effector proteins into target cells by using different delivery strategies. With this injection device, *P. aeruginosa* is well equipped to establish a niche in any given polymicrobial environment or modulate host cell responses. Loading a T6SS spike with various effectors carrying different enzymatic activities results in the release of a toxic cocktail causing a broad range of damages. This thesis set out with the aim of broadening our knowledge on the molecular mechanisms of T6SS effector delivery and possibilities of decorations of the T6SS spike. We studied four distinct concepts of the known T6SS-mediated delivery mechanisms and these findings are discussed here in a broader context while assessing their impact on the understanding of this fascinating nanomachine.

7.1. Mix'n'match – finding the right adaptor to a chaperone

This section discusses the requirement of so called adaptors and chaperones for effector delivery. Here, we coin the concept of an adaptor as a component that specifically connects a T6SS effector to the T6SS tip and is thus a requirement for effector recognition. As it was shown for example for Tde1 from *A. tumefaciens* that it would only bind to its cognate VgrG1^{Atu} in the presence of its adaptor protein Tap1^{Atu} [149]. In contrast, a chaperone is here defined as a component that specifically binds its cognate effector protein and stabilises it which is henceforth the prerequisite for effector recruitment towards the tip. For instance, it was demonstrated that Tde1^{Atu} is drastically stabilised by interactions with its cognate Tap1^{Atu} [153]. Results from this thesis demonstrated on multiple occasions that effector stability is influenced by the absence or presence of a cognate protein or protein domain, while we could also clearly show that to connect an effector to the T6SS tip, adaptors are required.

In this section, we will discuss a model that proposes that every T6SS effector requires a cognate chaperone and a cognate adaptor. While the chaperone module is essential for effector stability, the adaptor module is crucial for effector delivery. It is possible that both modules are combined within one protein, a concept that we here coin as a "**chadaptor**", while in other cases, two different proteins or domains exert these two functions. Remarkably, an effector is usually encoded close to both its adaptor and chaperone components and in many cases also to the T6SS component to which it is connected to, VgrG, PAAR or Hcp (Figure 7-1, top panel). The here described model integrates findings from this and previous studies which are summarised in Figure 7-1. We have classified the known delivery concepts into eight modes (A-H), with one effector and its genetic environment for each mode exemplified in the top panel in Figure 7-1 and the decoration of the tip sketched throughout this section.



Concept	Adaptor	Chaperone	Example/Effector
A	Hcp	Hcp	Tse1-4^{Paer} [208], Tae^{Atu} [149], Ssp2^{Smar}, Ssp4^{Smar} [148], TecA^{Bcen} [184], Tae^{Styp} [173]
B	VgrG	(linker)	VgrG2b^{Paer} [185], VgrG-1^{Vcho} [207], VgrG-3^{Vcho} [238], VgrG1^{Ahyd} [183], VgrG5^{Bpse} [182]
C	Transthyretin-like domain	Transthyretin-like domain	PldA^{Paer}, PldB^{Paer}, Tle1^{Eco} [216], (Tle3^{Paer}, TplE^{Paer}, Tle1^{Abau})
D	PAAR	Rhs	RhsP1^{Paer} [175]
E	PAAR	Eag	Tse6^{Paer} [202]
F	PAAR	Rhs, Eag	Rhs1^{Smar}, Rhs2^{Smar} [200], Rhs-CT3^{Eco} [209], RhsA^{Dda}, RhsB^{Dda} [199]
G	PAAR	(DUF2169 ?)	Tde2^{Atu} [149], (Tse7^{Paer})
H	Tap	Tap	Tde1^{Atu} [149], TseL^{Vcho}, VasX^{Vcho} [217], TseC^{Ahyd} [218], IdsD^{Pmir} [263], TseT^{Paer} [220]

Figure 7-1. T6SS effectors are encoded together with their adaptor and chaperone module.

All T6SS delivered effectors require an adaptor module to connect to the T6 tip, while additional components can take over the chaperoning function. For each T6SS effector modularity concept (A-H) at least one example from the literature is given with their genetic environment in the top panel and the assumed adaptor and chaperone functions listed in the bottom table. Superscripted abbreviations correspond to the organism the effector is encoded in and secreted from (*Paer – Pseudomonas aeruginosa; Vcho – Vibrio cholerae; Ahyd – Aeromonas hydrophila; Atu – Agrobacterium tumefaciens; Smar – Serratia marcescens; Bcen – Burkholderia cenocepacia; Styp – Salmonella enterica* spec. Typhimurium; *Eco – Escherichia coli; Abau – Acinetobacter baumannii; Dda – Dickeya dadantii; Pmir – Proteus mirabilis*). Effectors in brackets have not been proven experimentally, but there is empirical data or genetical links supporting the concept.

7.1.1. Concept A - Hcp rings can be adaptor and chaperone modules

It is a well understood concept that some T6SS effectors depend on Hcp as a chaperone. In *P. aeruginosa,* it has been shown that interactions between Tse1, Tse2 or Tse3 and conserved residues within the Hcp1 lumen protect the effector proteins from degradation [204]. In the current study, we fused Tse2 to another vehicle, VgrG1a, and obtained sound evidence that Hcp1 still interacts with the VgrG1a-Tse2 chimera. Moreover, abolishing this interaction by mutating a conserved residue within the Hcp lumen resulted in degradation of the chimera (Figure 3-13). This corroborates the concept of Hcp1 being a chaperone for Tse2.

In the study by Silverman and collaborators, Hcp1 was also coined as a receptor for Tse2 [204]. The here preferred term is adaptor, while the general concept is similar to that of a receptor. By binding within the lumen of the Hcp1 tube, Tse2 is able to dock into the T6SS machinery which is a prerequisite for its delivery (Figure 7-4A) [204]. In this current study, we attempted to replace Hcp1 as an adaptor module for Tse2 by fusing it covalently to VgrG1a. This way, VgrG1a functioned as an adaptor to connect Tse2 to the T6SS tip (see 7.1.2). However, the chaperone function of Hcp stabilising Tse2 appears to be still needed thus interfering with our rerouting concept. With this example, we could highlight the importance of Hcp as both a chaperone and an adaptor for its cognate effector.

7.1.2. Concept B - VgrG proteins can function as adaptor modules

The concept of evolved VgrGs is probably the simplest of all delivery mechanisms. Evolved VgrGs contain the gp5-/gp27-like domains working as the tip complex and a C-terminal extension carrying the effector domain that is delivered into target cells upon VgrG secretion [207, 239]. In the here proposed concept, a VgrG protein thus functions as an adaptor to connect the C-terminal effector domain to the T6SS tip. In chapter 3, we could show how different heterologous effector domains, like Bla_{TEM-1} or VgrG2b-CT, can be connected to the VgrG1a or VgrG4b canonical spike. This way, we used the VgrG proteins as adaptor modules and succeeded connecting Bla_{TEM-1} or VgrG2b-CT to the H1-T6SS or H2-T6SS tips of *P. aeruginosa.*

The chaperone module within the concept of evolved VgrGs, however, requires careful consideration. We designed five different fusions, and all of them, except the chimera VgrG1a-VgrG2b-CT, were unstable to certain extents, hence suggesting that the chaperone modules were somehow missing. For the VgrG1a-Tse2 fusion, we could establish that Hcp1 still works as a chaperone for Tse2 which we were unable to modify [204]. However, the VgrG1a-Bla_{TEM-1}, VgrG4b-Bla_{TEM-1} and VgrG4b-PldA chimerae are unstable fusion proteins probably lacking the chaperone modules (see Figure 3-6, Figure 3-8 and Figure 3-18). In case of the VgrG1a-VgrG2b-CT chimera, not only did we fuse the effector domain, as for Bla_{TEM-1}, but an additional 74 aa long region N-terminal to the effector domain VgrG2b-CT (see Figure 3-3). Considering the presence of this additional “linker domain” in this particular fusion (Figure 7-2A) and the positive impact on the stability of the chimeric protein, one might assume that it might contribute a type of chaperone module. This idea is further supported by the fact that all evolved VgrG proteins from various organisms contain flexible linker regions between the end of the gp5-like domain and the start of the effector domain (Figure 7-2B) [217, 238]. Examination of this linker region from evolved VgrG proteins shows that this region is rich in

serine and glycine residues allowing for flexibility, however no conserved sequence can be readily identified (Figure 7-2C). We speculate that this linker region somehow acts as an intramolecular chaperone module for the C-terminal effector domain (Figure 7-4B). Within the producing cell, the chaperone module could thus stabilise the C-terminal effector domain and upon delivery of the evolved VgrG protein into target prey cells, a change in the environment or proteolytic cleavage might occur that leads to dissociation of the effector domain from the VgrG spike protein. Interestingly, a recent study by the Mekalanos group proposed a hidden signal peptide within the linker region of VgrG-3^{Vcho}. After potential cleavage of the C-terminal effector domain, the signal peptide could allow recognition by the Tat complex exporting the effector domain into the periplasm where its target lies [238]. The question, however, remains what would trigger such release of the effector domain in the prey cell environment and whether the release of the chaperone linker then somehow activates the effector function.



Figure 7-2. Evolved VgrGs might contain intramolecular chaperones within their linker regions.

A: All evolved VgrG proteins contain the gp27-/gp5-like core domains (green), followed by a short linker region (grey) and a C-terminal extension domain (red). B: Alignment of evolved VgrG proteins from different organisms. C: close-up of the alignment of the linker region of evolved VgrG proteins. The linker region is present in all evolved VgrGs, but no sequence conservation can be identified.

7.1.3. Concept C - TTR-like domains serve as adaptor and chaperone modules

T6SS effectors were identified that do not contain any recognisable adaptor domain, like a PAAR, that might connect them to the T6SS tip. Nevertheless, these effectors are encoded downstream of *vgrG* genes, suggesting their delivery to be VgrG-dependent. In a

recent study, Flaugnatti *et.al* showed that Tle1 in *E. coli* specifically interacts with the C-terminal TTR-like domain of the upstream encoded VgrG1^{Eco} [216]. They also demonstrated that delivery of Tle1^{Eco} solely depends on the TTR-like domain. Our results showed that by swapping TTR-like domains between different VgrG proteins, the specificity of a VgrG for its effector could be swapped as well (5.9.7). This allows the assumption that the TTR-like domain of a VgrG serves as an adaptor module to connect an effector to its cognate VgrG tip.

Furthermore, our experiments showed that stability of an effector depends on the C-terminal TTR-like domain of its cognate VgrG. In other words, presence of the TTR-like domain, even though as part of a non-cognate VgrG, restored stability of the cognate effector (see 5.9.5). These findings support the hypothesis that TTR-like domains function as chaperone modules for T6SS effectors and we showed for the first time that effector stability can depend on the C-terminal domain of a VgrG protein.

We here propose that TTR-like domains of VgrG proteins have dual functions and can be thus called “chadaptors”. First, by binding the cognate effector, TTR-like domains adapt and connect the effector to the VgrG and thus to the T6SS tip (Figure 7-4C). Second, by binding the effector, TTR-like domains stabilise effector proteins and thus guarantee delivery.

Future studies ought to explore which part of the effector protein is recognised by the TTR-like domain, as now it is understood that the TTR-like domain interacts specifically with its cognate effector [216]. By swapping or deleting small fractions of the effector protein, one could pinpoint exactly at potential recognition motifs.

7.1.4. A PAAR domain functions as an adaptor

Evolved PAAR effectors come in different flavours (Figure 7-3, bottom panel). All evolved PAAR effectors contain an N-terminal PAAR domain that likely binds onto the blunt end of a VgrG spike [141], while the C-terminal domain carries the effector domain and in some cases an additional Rhs core domain. Hence, the N-terminal PAAR domain functions as the adaptor module to connect the C-terminal effector domain to the T6SS spike. In this study, we employed a PAAR protein shuttle in which we showed how the effector domain of Tse7, a DNase, can be connected to the VgrG1a spike using the cognate PAAR domain of Tse6 as an adaptor (0).

Concept D – Rhs domains as chaperone modules

PAAR effectors were characterised that additionally contain a large Rhs core (Figure 7-3D) [175]. The structure of such Rhs core domain was solved and showed that it forms a shell-like shape enclosing the C-terminal effector domain as described in 4.6.1 [212]. Here, the Rhs core domain can be considered as the chaperone module for the effector, while the N-terminal PAAR domain is the adaptor module for binding the VgrG tip. In this case, adaptor module and chaperone module are uncoupled, even though they are part of the same protein.

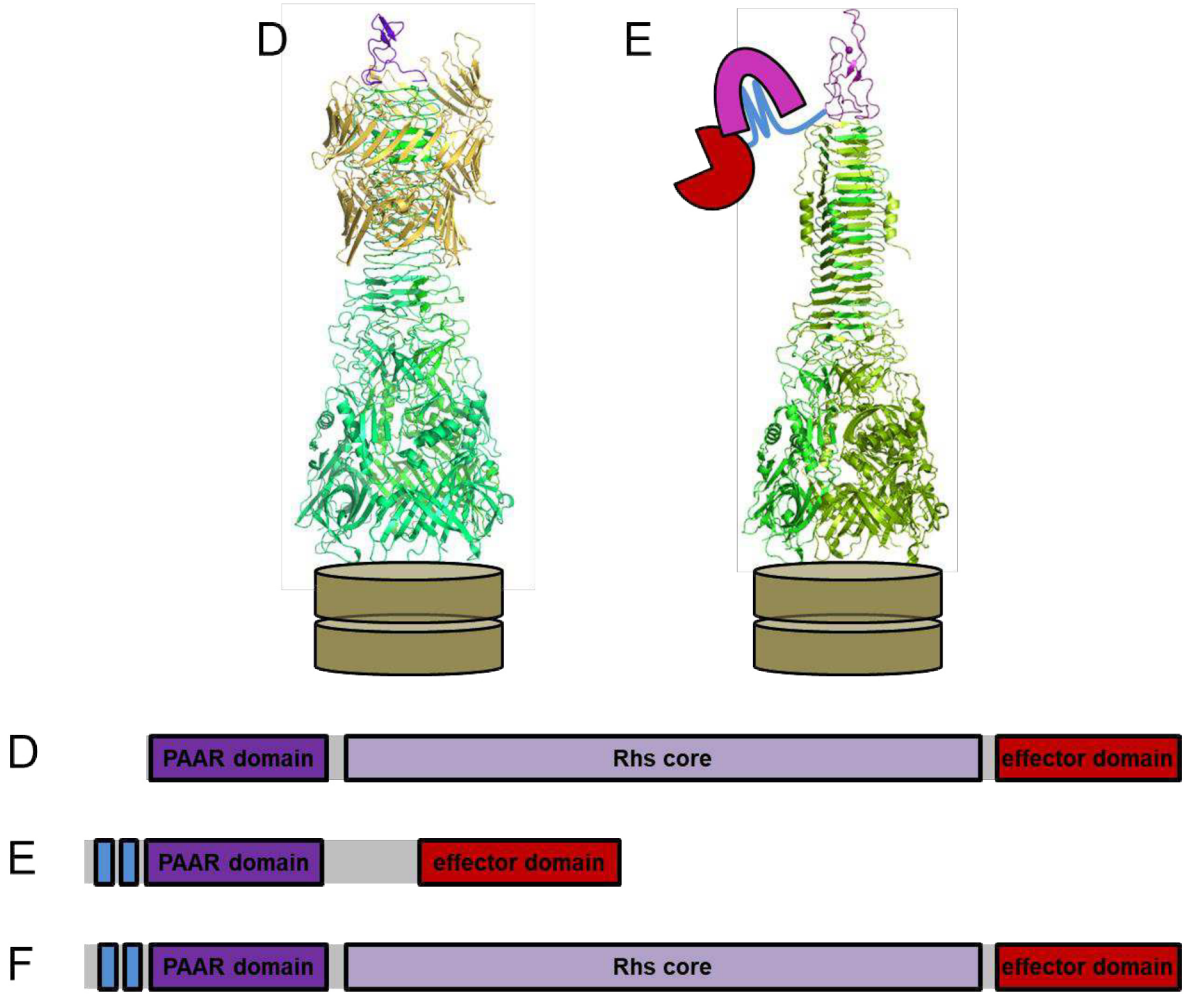


Figure 7-3. PAAR domains work as adaptors, while the chaperones can be of various nature.

Concept D: Rhs effectors contain N-terminal PAAR domains (purple) as adaptor modules and Rhs core domain (bright purple) as chaperone modules that might wrap around the VgrG trimer. Concept E: Eag-dependent PAAR effectors use the PAAR domains as adaptors while their N-terminal transmembrane domains (blue) require presence of an Eag protein as the chaperone module (not shown). Concept F: Rhs effectors contain PAAR domains as adaptor modules and additional N-terminal transmembrane domains requiring the presence of an Eag protein as the chaperone module while the Rhs core also functions as a chaperone module.

Concept E - Eag proteins as chaperone modules

The delivery of a wide range of PAAR effectors was shown to be dependent on Eag proteins [199, 200, 202, 209]. The Eag proteins EagR1 and EagR2 from *S. marcescens* were shown to specifically bind the N-terminal regions of their cognate effectors Rhs1 and Rhs2, respectively [148]. In our *in silico* studies in 4.6.1, we could further affirm previous assumptions that Eag-dependent effectors contain transmembrane helices (Figure 7-3E). We thus propose that transmembrane helices are a common feature of Eag-dependent PAAR effectors and that by binding to those transmembrane helices, intracellular aggregation might be prevented. Hence, Eag proteins can be considered as chaperone modules for PAAR effectors containing transmembrane helices.

Concept F – Rhs and Eag proteins as chaperones

Concept F adds up to the modularity and describes PAAR effectors that contain both Rhs domains and transmembrane helices (Figure 7-3F). In this case, both the Rhs core and the Eag protein would serve as chaperone modules while the PAAR domain at the N-terminus remains the adaptor module.

Concept G - DUF2169 proteins as putative adaptor modules

Another delivery mechanism of PAAR effectors was recently identified. Some PAAR effectors, like Tde2 from *A. tumefaciens*, require the presence of DUF2169 proteins for their delivery [149]. However, the molecular function of a DUF2169 protein and its detailed role in mediating effector delivery remains elusive. Furthermore, no molecular determinant within PAAR effectors could be identified that would emphasise the requirement for DUF2169

proteins (*data not shown*) as it is the case for Eag proteins and their correlation with transmembrane helices within their cognate effectors. Hence, it can only be speculated that DUF2169 proteins have stabilising and thus chaperoning functions on their cognate effectors.

7.1.5. Concept H - Tap proteins function both as adaptor and chaperone

Several reports have outlined the importance of DUF4123 proteins in effector delivery mediated by the T6SS. DUF4123 proteins were considered as chaperones for cognate effectors and termed Tec for type VI effector chaperone [218]. In another study, the adaptor function of DUF4123 proteins was pointed out resulting in naming them Tap for type VI adaptor protein [217]. The current study confirmed both concepts, which is why we propose that DUF4123 proteins could be coined as “chadaptor” proteins supporting their dual and chimeric function. As for nomenclature, we decided to continue calling DUF4123 proteins Taps.

Taps function as adaptors to connect effectors to the VgrG spike (Figure 7-4H). Previous studies showed that the effectors Tde1^{Atu} and TseL^{Vcho} would only bind to their cognate VgrG1^{Atu} and VgrG-1^{Vcho}, respectively, in presence of their cognate Taps [149, 217]. Furthermore, another study showed that the Tap TecT^{Paer} specifically recruits its cognate effector TseT^{Paer} to the C-terminus of PAAR4^{Paer} [220]. Here, we confirmed the concepts by demonstrating that Tde1^{Atu} binds the C-terminal end of its cognate VgrG1^{Atu}, even when fused to another VgrG vehicle, but this occurs only in presence of the cognate Tap1^{Atu} (see Figure 6-7). These results underline the adaptor function of Taps.

The chaperone function of Taps can also be confirmed with results from this and other studies. Previous research suggested that effectors are more stable in the presence of their cognate Taps indicating their chaperone function [153]. The current study did not directly investigate the stability of the effector Tde1^{Atu} dependent on the cognate Tap1^{Atu}. However,

we observed that each of our constructed chimerae between VgrG1a^{Paer} and a C-terminal portion of VgrG1^{Atu} was stabilised by the presence of the Tap1-Tde1 complex (Figure 6-8). Similarly, and in presence of Tap1^{Atu}, Tde1^{Atu} was revealed to be more stable when VgrG1^{Atu} was co-expressed in the heterologous *P. aeruginosa* host (Figure 6-5). Hence, these results highlight the stabilising effect of complex formation between a VgrG, the Tap and the cognate effector.

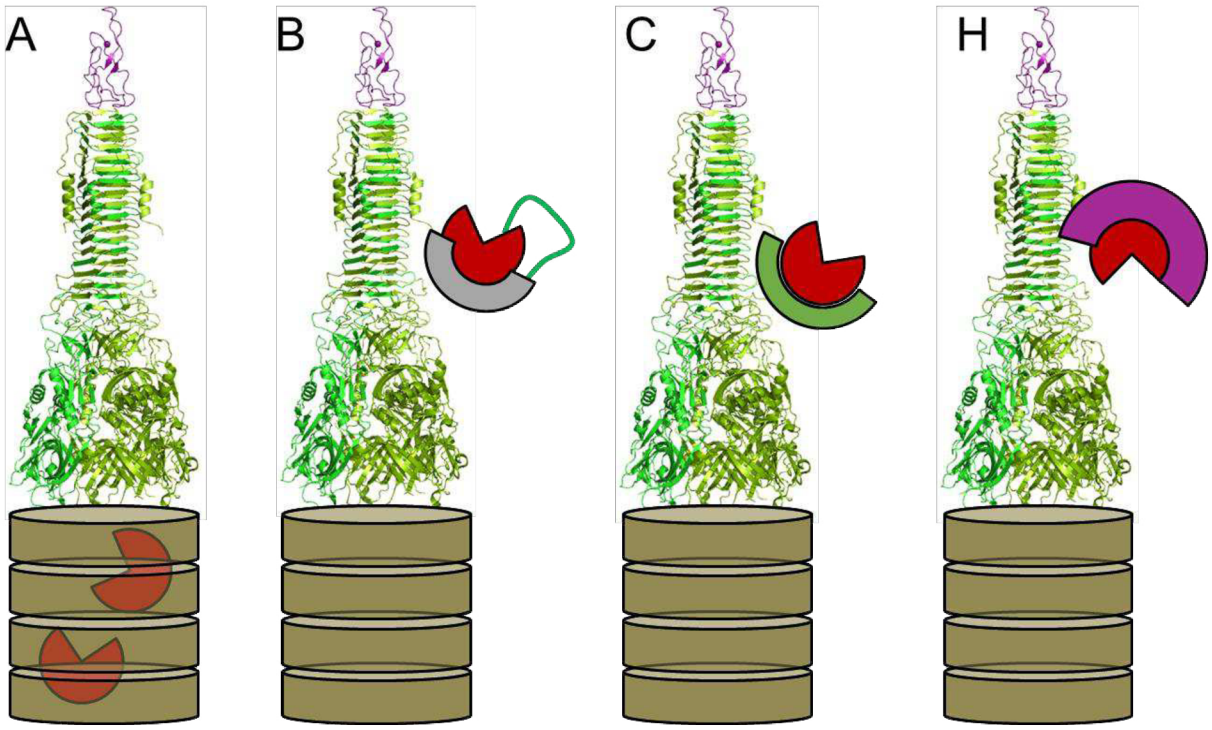


Figure 7-4. Effector proteins are chaperoned and connected to the T6SS tip by different mechanisms.

Concept A: T6SS effectors (red) are bound and stabilised by Hcp-hexamers (brown) and recruited towards the T6SS tip via assembly of the Hcp-tube. Concept B: An effector domain is part of an evolved VgrG (green, model PDB: 4mtk) and might be chaperoned by the flexible linker region (grey) present in all evolved VgrG proteins. Concept C: An effector directly interacts with the C-terminal TTR-like domain (green arc) of a VgrG that both connects it to the T6SS tip and stabilises the effector protein. Concept H: An effector directly interacts with its cognate Tap (magenta) which stabilises it and recruits the effector to the T6SS tip.

RhsP2 contains several adaptor and chaperone modules

One aspect that is worth mentioning at this stage is the issue of RhsP2 (see 6.3). RhsP2 contains a TTR-like domain (Figure 7-5, green) within its N-terminal PAAR domain (purple), which most likely functions as an adaptor module as discussed above. The Rhs core domain (bright purple) could be considered as the chaperone for the C-terminal effector domain (red), as previously described [147]. Yet, the gene upstream of *rhsP2*, is a *tap* gene whose product could be claimed to function as another adaptor module.

Considering what has been discussed above, it does not give a clear understanding of which of the many components associated with RhsP2 functions as adaptor or chaperone module. The presence of a Tap, a TTR-like domain and a PAAR as potential adaptor modules raises the question of specificity. This is further overstated by the presence of an Rhs core, a Tap and a TTR-like domain as putative chaperone modules. The sum of all these adaptor and chaperone modules might explain the difficulty to find appropriate conditions/genetic backgrounds to detect RhsP2 secretion which we have failed to monitor up to now (see Figure 6-3).



Figure 7-5. Predicted domains of RhsP2.

A TTR-like domain (green) lies within the N-terminal PAAR domain (purple), followed by an Rhs core domain (bright purple) and a C-terminal effector domain (red).

7.1.6. Adaptors and chaperones are common features of bacterial secretion systems

In this study, we introduced the concept of chaperone and adapter modules for T6SS-dependent effectors and supported this concept with results obtained in the current and from previous studies. Here, we proposed that an adaptor module can be a VgrG, its C-terminal TTR-domain, a PAAR domain, a Tap or an Hcp ring to connect an effector to the T6SS tip (see Figure 7-1). In contrast, a chaperone module can be a TTR-like domain, an Hcp ring, a Tap or an Eag protein to specifically stabilise the effector protein. We showed that each T6SS effector requires at least one adaptor and one chaperone module for its secretion and that in some cases both modules are combined in one protein and can thus be called "**chadaptor"**. Here, we will attempt to compare our above outlined concept with effector delivery mechanisms described in other bacterial protein secretion systems.

Adaptors are comparable to secretion signals

The main difference between T6SS-dependent substrates and substrates delivered by other protein secretion systems was long stated to be the absence of secretion signals. It was shown in substrates delivered by the T1SS, T2SS, T3SS, T4SS and T7SS, that they contain specific stretches of amino acids or structural motifs either within their N-termini or C-termini [27, 38, 47, 73]. The length and composition of these secretion signals depend on the cognate secretion system. It is understood, that these secretion signals are specifically recognised by a component of the cognate machinery which then leads to effector docking into the machinery with subsequent delivery.

For T6SS-dependent effectors, the question of a common secretion signal is still debatable even though none has been identified so far. Thus, the presence of adaptor

modules could be a specific feature of the T6SS as compared to other bacterial secretion systems. While secretion signals of effectors share a common motif dependent on the cognate secretion system and are less flexible, T6SS-adaptor modules can be of various nature, as discussed above. This allows the attachment of multiple effectors to one T6SS spike via different routes and gives higher flexibility for effector delivery as compared to other bacterial protein secretion system.

As mentioned in the introduction of this thesis, various attempts to use bacterial protein secretion systems to deliver heterologous effectors have been described. The basis of these strategies is similar to the one we used here. The secretion signal of a substrate targeted to a particular secretion system was covalently fused to a heterologous effector or effector domain. The secretion system then specifically recognised the cognate secretion signal present on the chimera, and recruited the unusual passenger domain to mediate its delivery [28, 40, 56, 57, 59, 73, 265]. In the evolved VgrG and PAAR chapters of this thesis, we similarly used an adaptor module, VgrG or PAAR, and fused a heterologous effector domain to it. The adaptor module was recognised by the cognate secretion machinery, the T6SS, which then mediated the delivery of the clandestine passenger. This highlights the universal principle of specific effector recognition within bacterial secretion systems.

Effector chaperones are essential for protein secretion systems

Previous studies proposed that chaperones are essential components for substrates delivered by the T2SS, T3SS, T4SS and T7SS [41-43, 60, 61, 66]. For the T3SS and the T4SS, it was described that effectors as YopE from *Y. pseudotuberculosis* [61] or VirE2 from *A. tumefaciens* [82, 84] require chaperones to make the connection with the cognate machinery (see Table 1-1). In both cases, the chaperone binds the effector towards its N-terminus and keeps it in a partially unfolded conformation before handing the effector over to

the secretion machinery. In the case of T7SS, chaperones are hypothesised to bind their cognate effectors near the N-terminus, however not much further data have been presented to have a clear and molecular idea of this interaction. T2SS-dependent effectors interact with their chaperones after translocation into the periplasm, where they are folded properly, thus forming the structural secretion signal which allows recruitment towards the secretin vestibule [43, 46]. Effector chaperones from the T2SS, T3SS and T4SS and also the T6SS have similar functions in facilitating folding and stabilisation of effector proteins, and thus they could be claimed as common features of bacterial effector proteins.

Another aspect worth discussing is the promiscuity of chaperone modules. Some chaperones in the T6SS, like Taps or TTRs, are thought to bind and stabilise one specific effector [149, 216, 217]. This was shown for the specific interactions between Tap1^{Atu} and Tde1^{Atu} [149], as well as the C-terminal TTR domain of VgrG4b^{Paer} and its cognate effector protein PldA^{Paer} (5.9.4). However, it was shown for Hcp1 in *P. aeruginosa* that it chaperones at least three different effectors, Tse1, Tse2 and Tse3 [204]. In the T2SS and the T4SS, chaperones also solely bind their cognate effectors [32, 82, 83], while T3SS chaperones can have multiple partners that they stabilise, as exemplified by the chaperone SpcS^{Paer} stabilising both ExoS^{Paer} and ExoT^{Paer} [60, 61, 69].

The specificity of T3SS chaperones was investigated in a recent study on the chaperone binding domain in *Salmonella enterica* T3SS effectors. The chaperone InvB mediates the delivery of the effector IpgB2, but not IpgB1. When the N-terminal conserved chaperone-binding domains between IpgB1 and IpgB2 were swapped, InvB-dependent secretion of IpgB1 could be achieved while secretion of IpgB2 was abolished [60]. This approach is similar to our strategy to design a protein shuttle based on the specificity between effectors, like PldA or Tde1, and components of the T6SS. Again, this highlights the methodology bacteria use to specifically bind and recruit their cognate effectors thus avoiding inappropriate transport.

7.2. Proteolytic cleavage of T6SS substrates

Another peculiar aspect of T6SS-mediated effector secretion will be discussed in this section since in multiple occasions throughout this study, we observed cleavage of T6SS secreted components. In chapter 3, we designed VgrG fusions with effector domains and noticed cleavage products of the VgrG1a-Bla_{TEM-1} (3.5.1), VgrG4b-Bla_{TEM-1} (3.5.2) and VgrG4b-PldA-fusions (3.7.1). In the culture supernatant fractions of these strains, proteins were detected that correspond to the size of the canonical domains of VgrGs once cleavage of the heterologous effector domains has occurred.

In several occasions throughout chapter 5, two bands corresponding to VgrG4b were detected in the supernatant fractions. This suggests that a proportionally small fragment (~5 kDa) of WT VgrG4b is cleaved upon arrival in the supernatant. Our antibody specifically recognises the C-terminal domain comprising 190 aa of VgrG4b. If a small fraction of this C-terminal domain was cleaved, it might still be recognised by the antibody. Hence, it is impossible to distinguish whether cleavage of VgrG4b occurred at the N-terminus or the C-terminus. These findings are in good agreement with observations from other lab members, that detected cleavage products of other VgrGs, such as VgrG2b and VgrG2a, in the supernatant fractions of *P. aeruginosa* strains (Thomas Wood, *personal communication*).

Additionally, whenever PldB-Bla_{TEM-1} was detected in the supernatant fractions, we only detected bands that were about 30 kDa smaller than the originally produced protein (Figure 5-7B). Furthermore, cleavage products corresponding to PldA-Bla_{TEM-1} were detected in the supernatant fractions in some instances (Figure 5-20B). These were less abundant and intense than the bands corresponding to PldB-Bla_{TEM-1}. Cleavage of both PldA-Bla_{TEM-1} and PldB-Bla_{TEM-1} must have happened at the N-termini of the effector proteins due to the presence of the Bla_{TEM-1}-domains at the C-termini of the chimerae. Since cleavage of PldA-Bla_{TEM-1} was not observed in all experiments, it suggests that this was triggered by an unknown but slightly

variable factor associated with the growth conditions, like differences in the pH or salt content of the medium, or preparation of the supernatant samples. Additionally, there is a chance that any of the abundant extracellular proteases of *P. aeruginosa* might mediate cleavage of secreted substrates [266].

Remarkably, Rhs proteins, that were confirmed to be T6SS substrates, are known to be products of auto-proteolysis [212]. We detected intracellular cleavage of the Rhs protein RhsP2 most likely releasing its C-terminal toxin domain (Figure 6-3). This cleavage only occurred when cells were grown at 25 °C, but not when grown at 37 °C. A study by Busby and colleagues showed that the C-terminal toxin domain of a Rhs protein is released at a lower pH and otherwise remains sequestered within the Rhs shell [212]. This might be in accordance to our results, as an intracellular temperature drop might lead to a pH change sufficient to activate the auto-proteolysis activity of RhsP2. However, this hypothesis would need to be tested in detail and expanded on the second Rhs protein from *P. aeruginosa*, the VgrG1c-dependent RhsP1 [175]. Growth and secretion experiments at different temperatures and different pHs with both N-terminal and C-terminal tagged versions of RhsP1 would begin to unravel the cleavage profile of this T6SS effector. Furthermore, one could think of site-directed mutagenesis within RhsP1 and RhsP2 or a genetic background that abolishes cleavage of the Rhs proteins.

7.3. Molecular details of T6SS-mediated effector delivery

7.3.1. Space around the VgrG tip

This PhD thesis set out to shed light on the molecular mechanism of effector delivery by the *P. aeruginosa* T6SS. Results from our study emphasised one limitation of T6SS-mediated effector delivery, which is the available space around the VgrG tip (Figure 7-6B) and

probably within the membrane complex (Figure 7-6A, C). Recent studies from the Basler and the Cascales groups visualised the baseplate structure [267] and the membrane complex [115] of the T6SS, respectively, which are shown in Figure 7-6A and C. Both groups managed to map VgrG-PAAR spikes into the cryo-EM densities and identified cavities around the spike complexes which were unoccupied (green in Figure 7-6A and unoccupied space close to the yellow spike fit in Figure 7-6C). They claimed, that these cavities would allow the accommodation of effector proteins. However, the baseplate structure originates from *V. cholerae* while the membrane complex is adapted from *E. coli* and it is not yet entirely clear whether molecular differences in the structure of T6SS machineries from different bacterial organisms exist or not and how this would impact the overall structure.

We attempted to connect Tse2 and the heterologous effector Tde1 to the tip in *P. aeruginosa* by accommodating these effectors around the VgrG spike. In experiments monitoring VgrG and effector delivery, we observed a severe impact on delivery of these components (see 3.6.1 and 6.4.2). In these cases, we have to consider that in *P. aeruginosa* at least three components bind to the VgrG1a tip (Figure 7-6B), these are Tsi6 (purple), EagT6 (red) and Ef-Tu (blue) [202]. Hence, the additional recruitment of protein components towards the tip, would probably result in sterical hindrance around the tip complex and thus blockage of the T6SS secretion. Such concept could be used to completely lock the tip into the membrane complex and in a pull-down assay identify all binding partners and thus the entire machinery.

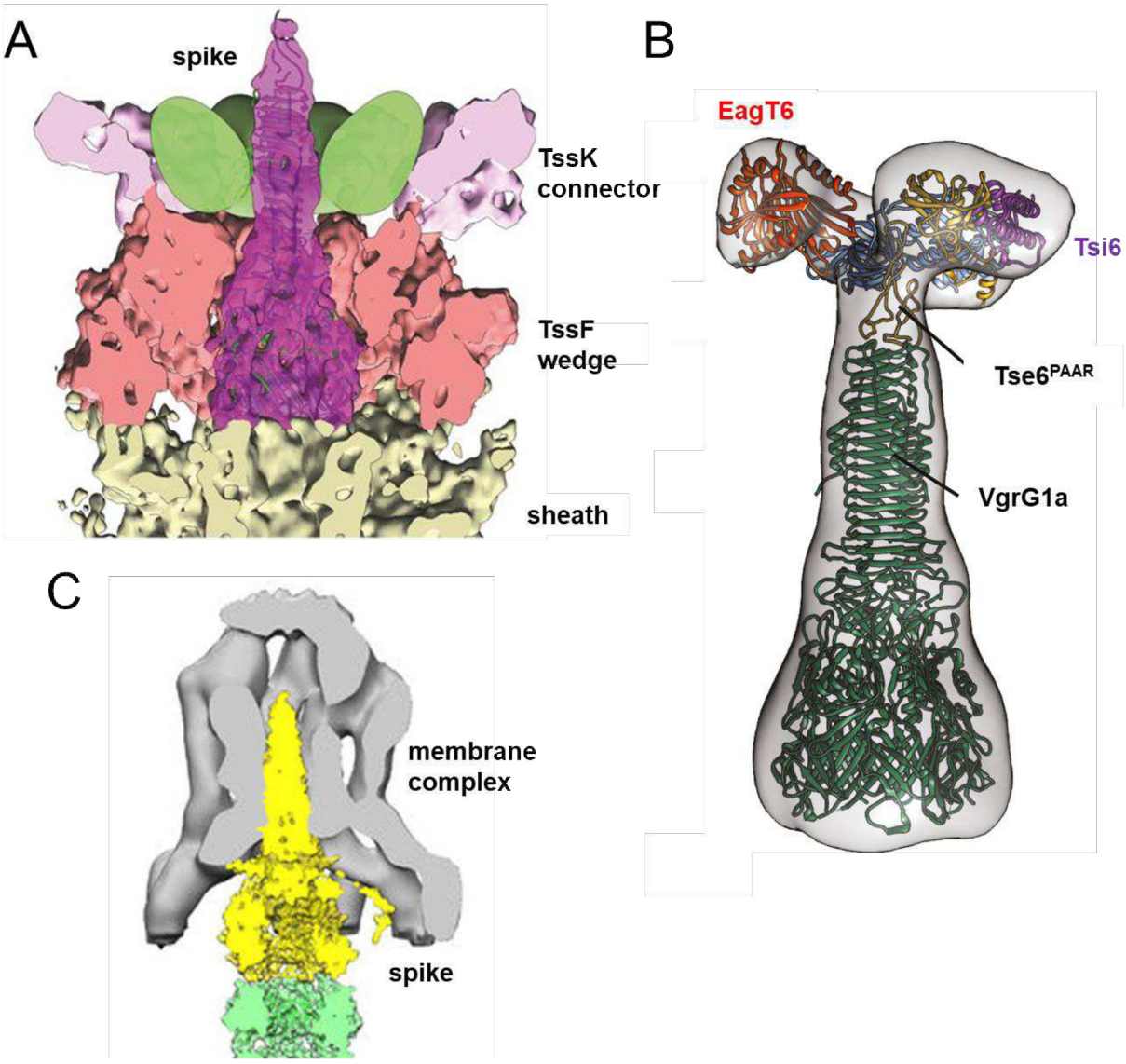


Figure 7-6. Space around the VgrG spike is limited.

A: Reconstruction of the elongated sheath (yellow), the baseplate components in red and pink and the spike consisting of VgrG and PAAR (purple). A possible cavity around the spike for effector protein assembly is shown in green. B: Reconstructed 3D density map and molecular fitting of the spike complex consisting of VgrG1a (green), Tse6 (yellow), Tsi6 (purple), EagT6 (red) and Ef-Tu (blue). C: 3D reconstruction of the membrane complex (grey) consisting of TssJLM with fitted into the VgrG spike (yellow) and Hcp tube (green). These figures were reproduced under a Creative Commons Attribution Licence from A: [267], B: [202] and C: [115].

The concept of restricted space around the VgrG tip further raises the question about how large Rhs proteins are transported by the T6SS. We have shown in 4.6.1 that Rhs

effectors most likely connect to the VgrG spike *via* their PAAR domains. Yet, our hypothesis that the Rhs core domain wraps around the VgrG spike (Figure 7-3D) could be in good agreement with the identified cavity around the VgrG spike from the cryo-EM data. However, this remains a model and needs further investigations into the structure and assembly of such VgrG-Rhs complexes.

7.3.2. Heterologous secretion is not a common feature of bacterial protein secretion systems

Another aspect of this PhD thesis meant to address how heterologous effector proteins could be connected to the T6SS tip of *P. aeruginosa.* Our strategy was the design of protein shuttles based on our knowledge on the molecular mechanisms of effector recruitment towards the T6SS tip. In each of our protein shuttles, we changed different levels of effector recognition. In this section and as summarised in Table 7-1, we define the level of effector recognition as a parameter of one of these four aspects: the delivery route of an effector (cargo or fusion), the T6SS component the delivery depends on (a specific VgrG, PAAR or Hcp), the T6SS machinery mediating the delivery (H1-T6SS or H2-T6SS) or the bacterial strain delivering the effector (*P. aeruginosa* PAK or PAO1 or *A. tumefaciens*). We listed these parameters for each designed protein shuttle and distinguished between original and modified route (see the two columns in Table 7-1). The column “original route” displays those parameters under which the effector is originally delivered from the host strain, while the column “modified route” lists those parameters that we employed to deliver the effector in our protein shuttle in a heterologous environment. In each cell within these two columns, the first line corresponds to the parameter bacterial strain, the second line to the associated T6SS machinery, the third line to the delivery-dependent T6SS component and the bottom line to the delivery route. We further highlighted those parameters in bold that differed between the original and the modified route. According to how many of these parameters were changed

between the two routes, we classified our protein shuttles. While in a class 1 shuttle, only one recognition level was changed (highlighted in bold), in a class 2 shuttle, two levels were changed and similarly for levels 3 and 4 (Table 7-1). The different protein shuttles were further labelled A-D to better follow which shuttle is currently described, as exemplified in the first column with 1A for the PldA-VgrG4b shuttle. The designed protein shuttles according to the modified effector recognition levels and the caveats of each shuttle will be discussed below.

In the simplest attempt to modify effector delivery, we wanted to deliver PldA as a fusion to VgrG4b, instead of having it as a cargo effector that requires specific interactions (1A) [146]. Thus, solely changing the delivery mechanism of PldA, while all other parameters, as essential T6SS component VgrG4b, the associated machinery H2-T6SS and the delivering strain being PAO1, remained the same (class 1 shuttle), was successful (see 3.7.1). This suggested that modification of this basic level of effector recognition had no negative influence on effector delivery. Next, we changed a different level of effector recognition namely the T6SS component that the delivery of the effector depended on. We successfully delivered the extension domain of the evolved PAAR effector Tse7 via another PAAR domain (1B, see 0) and we also managed to deliver the cargo effector PldA via another VgrG (1C, see 5.9.7). The attempt to alter the same parameter for PldB (1D) and thus deliver it via a different VgrG, however, highlighted another limitation that we had not anticipated (see 5.9.6). This was a co-dependency on more than one VgrG protein and we could not resolve this issue to achieve a successful shuttle. Nevertheless, it can be put forward that overall the parameter delivery-dependent T6SS component can be easily modified in order to achieve effector delivery.

In class 2 protein shuttles, we modified two effector recognition parameters to swap effector delivery. In an attempt to manipulate the delivery of Tse2 (2A) we modified the delivery mode (from cargo to fusion) and the delivering component (from Hcp1 to VgrG1a) [204] with only a limited success rate (3.6.4). In another shuttle, we modified effector recognition for PldA (2B) by altering the T6SS machinery (from H2-T6SS to H1-T6SS) and the required VgrG, by

designing a chimera between VgrG1a and the C-terminal portion of VgrG4b, and in this context delivery could not be monitored (5.9.7). This was probably caused by the inability to secrete the VgrG1a-VgrG4b chimera. It could be assumed that under the H1-T6SS inducing conditions, the VgrG1a-VgrG4b chimera was produced due to its H1-T6SS affiliation. However, the cognate PAAR protein might not be expressed under these conditions and is thus not present to bind to the chimera and facilitate its secretion. From these results one can propose that changing two effector recognition parameters already limits the chance of success for efficient effector delivery.

Moreover, we changed three parameters, thus resulting in class 3 shuttles, while keeping just one level of effector recognition, the delivery route. First, we attempted to deliver VgrG2b-CT (3A) from a different *P. aeruginosa* strain (PAO1 to PAK) with a different T6SS machinery (H2-T6SS to H1-T6SS) using a different VgrG vehicle (VgrG2b to VgrG1a) [146] and succeeded (see 3.4.1). Second, the attempt to deliver PldA changing the same parameters (3B) was not successful (*data not shown*). In this case, however, delivery might have been restricted by absence of the cognate PAAR protein, that is likely to be produced under different conditions, to mediate delivery of the VgrG1a-VgrG4b chimera similar as described for the 2B shuttle. Third, Tde1 (3C) is originally secreted from a different bacterial organism (*A. tumefaciens* instead of *P. aeruginosa*) [149] and uses a different T6SS machinery and VgrG protein. Even though, we managed to dock the effector into the *P. aeruginosa* T6SS using the same delivery mechanism, secretion could not be achieved (see 6.4.3).

Interestingly, delivery of the T6SS-unrelated Bla_{TEM-1} effector domain (class 4 shuttles) in two occasions, to VgrG1a (3.5.1) and VgrG4b (3.5.2), as covalent fusions proved successful. This highlights the power of a C-terminal extension domain as a delivery route likely due to the covalent link between the two proteins or domains. Taking these results together, one can conclude that the delivery route is the most restricting level of effector

recognition and connecting an effector to the T6SS with a covalent fusion is the most promising strategy.

Table 7-1. Overview of results from this thesis.

Listed are the delivered effector and which chapter the shuttle refers to. The original route and the modified route are classified according to the discussed specificity levels; 1.: the here used *P. aeruginosa* strain; 2.: the machinery that mediates delivery of the effector; 3.: the essential T6SS component delivering the effector and 4.: whether the delivery mode is by non-covalent interactions (cargo) or extension (fusion). Highlighted in bold are the levels of specificity that were changed in the protein shuttle attempt. The last column highlights whether delivery or secretion of the protein shuttle was successful as referred to in the individual chapters. A (yes) implies that the result was shown indirectly or not completely convincing.

shuttle	delivered effector	chapter	original route	modified route	success?
1A	**PldA**	3.7	PAO1 H2-T6SS VgrG4b cargo	PAO1 H2-T6SS VgrG4b **fusion**	yes
1B	**Tse7-CT**	0	PAK H1-T6SS VgrG1b PAAR fusion	PAK H1-T6SS **VgrG1a** PAAR fusion	(yes)
1C	**PldA**	5.9.7	PAO1 H2-T6SS VgrG4b cargo	PAO1 H2-T6SS **VgrG5** cargo	yes
1D	**PldB**	5.9.6	PAO1 H2-T6SS VgrG5 cargo	PAO1 H2-T6SS **VgrG4b** cargo	no
2A	**Tse2**	0	PAK H1-T6SS Hcp1 cargo	PAK H1-T6SS **VgrG1a** **fusion**	(yes)
2B	**PldA**	5.9.7	PAO1 H2-T6SS VgrG4b cargo	PAO1 **H1-T6SS** **VgrG1a** cargo	no

shuttle	delivered effector	chapter	original route	modified route	success?
3A	**VgrG2b-CT**	3.4	PAO1 H2-T6SS VgrG2b fusion	**PAK H1-T6SS VgrG1a** fusion	yes
3B	**PldA**	(not shown)	PAO1 H2-T6SS VgrG4b cargo	**PAK H1-T6SS VgrG1a** cargo	no
3C	**Tde1**	0	*A. tumefaciens* T6SS VgrG1^{A} cargo	**PAK H1-T6SS VgrG1a** cargo	no
4A	**Bla$_{TEM-1}$**	3.5.1	*E. coli*	**PAK H1-T6SS VgrG1a fusion**	yes
4B	**Bla$_{TEM-1}$**	3.5.2	*E. coli*	**PAO1 H2-T6SS VgrG4b fusion**	yes

7.3.3. Basis of the “á la carte” effector delivery lies within the VgrG C-terminus

The concept of the “á la carte” effector delivery has first been put forward in a study by our group [175] and was a major pillar of this PhD thesis. This concept is about the fact that a VgrG protein specifically mediates delivery of a cognate effector. Results from this current study generally support the “á la carte” concept, and recommend that the delivered cognate effectors are classified into two groups: PAAR effectors and cargo effectors. While the study by Hachani *et.al* showed the “á la carte” delivery of the evolved PAAR effectors Tse5, Tse6 and Tse7 [175], we here claim that this concept must be expanded to include cargo effectors that directly bind the C-terminus of VgrG proteins.

This current study showed how a VgrG protein is used as a vehicle to connect and subsequently deliver a cognate effector. In all cases we were able to show that the C-terminal

region of a VgrG protein plays a crucial role in effector binding and supports subsequent delivery. These findings are in good agreement with what has been shown in earlier studies. In *A. tumefaciens*, the “chadaptor”-effector complex Tap1-Tde1 specifically binds to the 31 C-terminal amino acids of its cognate VgrG1^{Atu} [149], while in *E. coli*, the lipase Tle1 was shown to interact with the C-terminal TTR-like domain of its cognate VgrG1^{Eco} [216]. Here, we could expand this concept and show for Tde1, that even 21 of the C-terminal amino acids are sufficient to mediate the interactions with the cognate VgrG, while we also demonstrate that TTR-like domains are crucial components for effector binding, stabilisation and delivery.

7.3.4. *P. aeruginosa* T6SS machineries can fire multiple VgrG-effector spikes

In this study we investigated the decoration of VgrG-PAAR spikes as a means for effector delivery based on the “á la carte” concept. We could prove that due to the versatility of adaptor modules connecting an effector to the T6SS (see 7.1), different combinations of effector attachment are possible. The study expanded on the *P. aeruginosa* effector recognition mechanisms with a special focus on the H2-T6SS, which we will summarise at this point and evaluate its implication for *P. aeruginosa* virulence.

A study from our group showed that *P. aeruginosa* uses its H1-T6SS to deliver at least three different VgrG-dependent antibacterial effectors into target prey cells, namely Tse5, Tse6 and Tse7 [175]. All of these effectors are evolved PAARs that connect to their cognate VgrG, VgrG1c, VgrG1a and VgrG1b, respectively, via their N-terminal PAAR domains (Figure 7-7A, B and C). Within the H3-T6SS cluster, *vgrG3* as well as the effector *tseF* are encoded (Figure 7-7F) [166]. A VgrG3 trimer is possibly topped by PAAR PA2375 considering the genetic linkage and delivers TseF, however, this has not been experimentally proven yet.

As for the H2-T6SS, delivery of VgrG4b, VgrG5, VgrG2a and VgrG2b and their associated effectors were experimentally proven either in this study or in another study concomitantly conducted by a lab member (Thomas Wood, *unpublished data*). Additionally, VgrG4a, which is encoded on another remote *vgrG* island, is also likely affiliated with the H2-T6SS due to a sequence identity of 97 % with VgrG4b (see Table 5-1) [146]. Downstream of *vgrG4a,* another effector, Tle1, is encoded (Figure 7-7G), and due to the genetic link, most likely delivered dependent on VgrG4a. VgrG6, encoded on yet another satellite *vgrG* island, is genetically linked to *hcpB* (Figure 7-7J), which is a convincing sign for its association with the H2-T6SS due to its homology to *hcpA* and *hcpC* [147]. However, there is no data yet about the toxicity of the downstream encoded effector of VgrG6, but in any case, it can be assumed that its delivery likely depends on VgrG6. Furthermore, a *paar* cluster has been connected to the H2-T6SS, whose gene product PAAR4 mediates delivery of TseT in a TecT, Co-TecT-, VgrG4b- and VgrG6-dependent fashion (Figure 7-7L) [220]. PAAR2, encoded on yet another orphan island (Figure 7-7K), was shown to be able to functionally replace PAAR4 [220], hence its affiliation with the H2-T6SS is implied as well.

Combining these data, it can be assumed that *P. aeruginosa* uses its H2-T6SS machinery to deliver a multitude of different spikes decorated with various effectors as listed in Table 7-2. VgrG2a and VgrG2b were shown to be mutually independent delivering their cargo effectors Tle4 and Tle3 (Figure 7-7D and E), respectively, while PA1508 as the cognate PAAR for a VgrG2b trimer was identified (Thomas Wood, *unpublished data*). We have shown that a VgrG5 homotrimer delivers PldB, although we have no evidence about the cognate PAAR protein.

Additionally, VgrG2b contains a C-terminal extension domain (Figure 7-7E), thus one VgrG2b trimer can not only deliver three covalently linked effector domains but also three cargo components of Tle3 [185]. This concept is similar to the effector recognition of VgrG-1 from *V. cholerae*, for which it was shown that in addition to a C-terminal ACD domain, it also

delivers the Tap-dependent cargo effector TseL [217]. Considering this, six effector molecules with two different enzymatic activities can be attached to one VgrG spike and are delivered in one firing process.

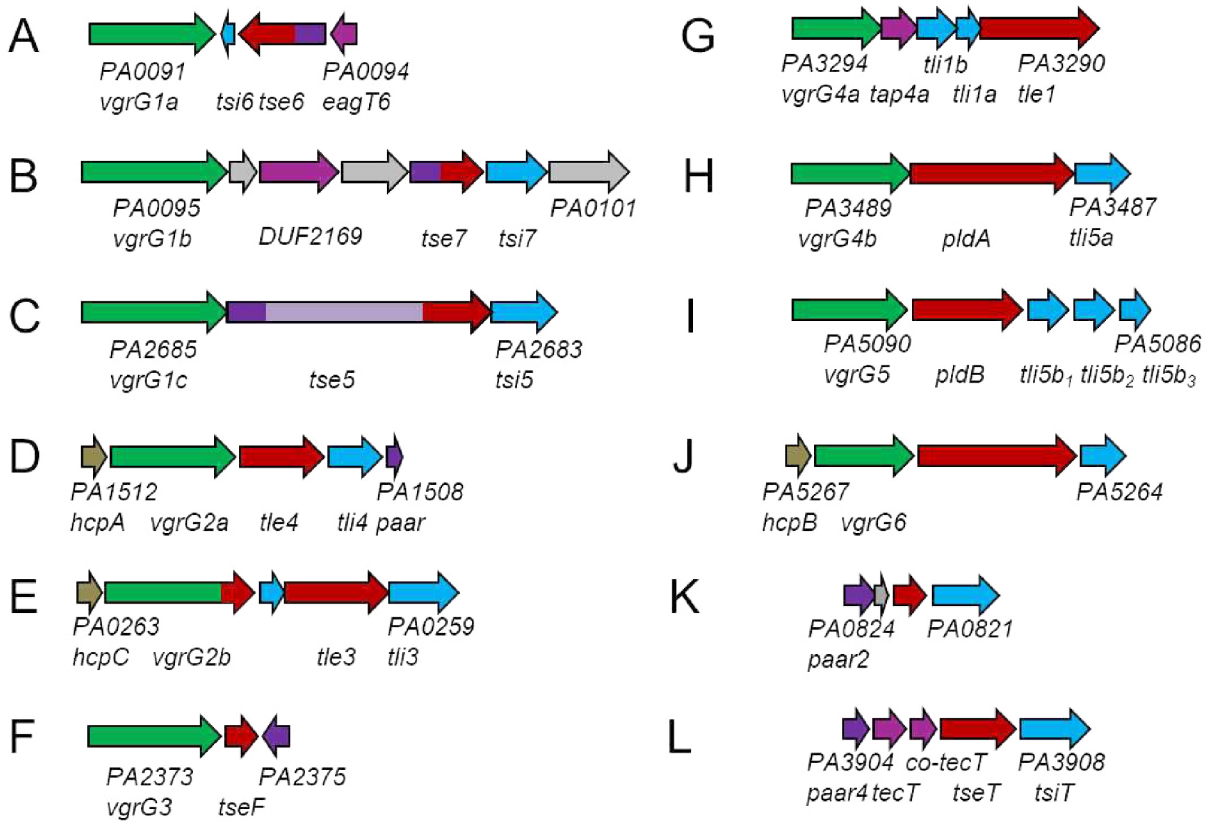


Figure 7-7. Operons containing *vgrG* or *paar* genes within *P. aeruginosa* PAO1.

vgrG genes are shown in green, effector genes in red, cognate immunities in cyan, *hcp* genes in grey, *paar* genes in purple and *tap* genes in magenta.

Furthermore, our data suggest that heterotrimers are an important aspect of assembled H2-T6SS spikes. There seems to be sufficient experimental proof that VgrG4b forms heterotrimers with at least two VgrG proteins, VgrG5 (5.8.1) and VgrG6 [220]. Due to high sequence identities between VgrG4a and VgrG4b, these two proteins might also form heterotrimers, but no experimental data are currently available supporting this hypothesis. As

we have shown here, a VgrG4b-VgrG5 heterotrimer delivers PldA (5.8.2) and there is strong evidence indicating that the C-termini of both VgrGs are required for PldA delivery, while no cognate PAAR protein is currently known. Additionally, a recent study revealed that a VgrG4b-VgrG6 heterotrimer is capped by PAAR4 and by interacting with the chaperone TecT-Co-TecT this complex delivers the effector TseT [220]. Interestingly, we have seen that VgrG4b secretion is impacted by the absence of VgrG5, hence VgrG6 on its own can probably not mediate delivery of VgrG4b under our tested conditions [220]. This leads to the question whether VgrG6 secretion would also be impacted by VgrG5 absence. If this was the case, one might speculate about a functional heterotrimer composed of VgrG4b, VgrG5 and VgrG6, capped by PAAR4 and delivering PldA, PldB, TseT and probably the VgrG6-affiliated effector PA5265. However, this complex and interesting concept and all the molecular details require further experiments to prove interactions between those components as well as competition assays in backgrounds lacking any of these components.

With such a broad spike repertoire, *P. aeruginosa* has a lot of options available to load its H2-T6SS weapon that might confer a competitive advantage in a polymicrobial environment. This also doubts the presumption of the H1-T6SS being the major antibacterial T6SS of *P. aeruginosa* [175]. In any case, the H2-T6SS gives *P. aeruginosa* the prospect to fire various effectors into competing prey cells. Interestingly, five (PldA, PldB, Tle3, Tle4 and Tle1) out of seven H2-T6SS-dependent effectors are lipases either experimentally proven [186, 188, 268] or proposed due to the presence of the lipase-specific DUF2235 domain. The affiliation of at least five lipases, with one T6SS machinery begs the question of why there would be such effector redundancy.

Table 7-2. VgrG spike compositions in *P. aeruginosa* PAO1.

Homotrimers of VgrG1a, VgrG1b and VgrG1c are topped by their cognate PAAR effectors Tse6, Tse7 and Tse5, respectively. A VgrG3 spike is most likely capped by PAAR PA2375 delivering TseF. The following H2-T6SS delivered spikes can be considered: VgrG4b, VgrG5 and VgrG6 likely form heterotrimers topped up by PAAR4 or PAAR2 and mediate delivery of PldA, PldB and TseT (this study and [220]. VgrG5 can form homotrimers with an unknown PAAR protein delivering PldB. VgrG2b forms homotrimers topped by PA1508 delivering Tle3. VgrG2a forms homotrimers topped by an unknown PAAR delivering Tle4. VgrG4a most likely mediate delivery of the downstream encoded Tle1 with the help of the nearby encoded Tap4a. VgrG6 is probably required to deliver its downstream encoded effector of unknown function.

VgrG spike	cognate PAAR	delivered effector	reference
VgrG1a	Tse6	Tse6	[175, 208]
VgrG1b	Tse7	Tse7	[175, 208]
VgrG1c	Tse5	Tse5	[175, 208]
VgrG2a	?	Tle4	Thomas Wood, *unpublished*
VgrG2b	PA1508	Tle3, VgrG2b-CT	Thomas Wood, *unpublished*
VgrG3	(PA2375)	TseF	[166]
VgrG4a	?	(Tle1)	
VgrG4b/VgrG6/VgrG5	PAAR4, PAAR2	TseT, PldA, PldB, (PA5265)	This study, [220]
VgrG5	?	PldB	This study

7.3.5. Specificity between VgrG and Hcp proteins

Another aspect of having this multitude of available VgrG spikes ready to fire asks for the specificity of interactions with Hcp proteins. The current model agrees on Hcp hexamers that stack in a head-to-tail fashion resulting in a tube on which the VgrG spike complex sits [114, 127] (see Figure 7-4). The *P. aeruginosa* H1-T6SS machinery was shown to specifically deliver Hcp1, which is encoded within the H1-T6SS-cluster [114], while Hcp3, encoded within the H3-T6SS-cluster, is delivered by the H3-T6SS-machinery [146]. From this,

one can assume that a tip consisting of VgrG1a, VgrG1b or VgrG1c specifically sits on top of a Hcp1 tube and the H3-T6SS-dependent VgrG3 on top of a Hcp3 tube.

Considering in *P. aeruginosa* strains PAK and PAO1, three Hcp proteins, HcpA, HcpB and HcpC (HcpABC), were connected with the H2-T6SS machinery [147]. Hence, an interesting question remains whether a Hcp tube affiliated with the H2-T6SS machinery would be a mixture of HcpA, HcpB and HcpC proteins, on which any of the H2-T6SS-affiliated VgrG trimers can sit. In another scenario, a tube of HcpA proteins might be specifically topped up with VgrG2a trimers due to their genetic linkage (Figure 7-7D), a tube of HcpB with VgrG2b trimers (Figure 7-7E) and a tube of HcpC with VgrG6 trimers (Figure 7-7J). This model, however, would leave out VgrG4b, VgrG5 and VgrG4a and begs the question of how these proteins together with their cognate effectors could leave the cell. To shed light on this research question, one would need to delete each single *hcpA*, *hcpB* and *hcpC* gene and monitor secretion of every H2-T6SS-dependent VgrG protein. This would give hints about the affiliation of each VgrG secretion to a specific *hcp* gene and thus to a specific Hcp tube.

Furthermore, mutants lacking all of the H2-T6SS affiliated *vgrG* and/or *paar* genes ought to be tested for their ability to secrete HcpABC. In our study we observed that HcpABC secretion was not affected by the absence of neither VgrG4b or VgrG5 (Figure 5-9) and other studies from our lab confirmed those results in the absence of VgrG2a or VgrG2b (Thomas Wood, *unpublished data*). However, the HcpABC-antibody recognises all three Hcp species and lack of one could be accompanied with higher abundance of another one, which might not alter the general HcpABC profile on a western blot.

Results from this study are thus also in good agreement with studies investigating the spike compositions in other T6SS-active organisms. Here, we showed that absence of one VgrG protein does not shut down activity of the H2-T6SS machinery. For the *P. aeruginosa* H1-T6SS it was shown that either VgrG1a^{Paer} or VgrG1c^{Paer} are required to form a functional

H1-T6SS-machinery [140]. In *S. marcescens* it was also shown, that at least one functional VgrG-PAAR assembly is required for a functional T6SS machinery and thus Hcp secretion [200]. *V. cholerae* encodes three VgrG proteins for its unique T6SS for which VgrG2^{Vcho}, the only canonical VgrG of *V. cholerae*, appears to be the only one essential, while VgrG1^{Vcho} and VgrG3^{Vcho} are not [207]. Hence, it could be concluded that VgrG2^{Vcho} is indeed the structurally essential component to plug onto the Hcp tube. The authors concluded that VgrG1^{Vcho} and VgrG3^{Vcho} form heterotrimers with VgrG2^{Vcho} to reach the supernatant [207]. With this mechanism, the bacteria seem to reassure that activity of the machinery does not solely rely on one spike but lack of one could be compensated by alternative options. In absence of one VgrG, another VgrG and its cognate effector can easily substitute and assure functionality of the machinery and thus competitor killing.

Table 7-3. List of T6SS substrates and their activities and delivery modes.

Only well described T6SS substrates from the literature are listed here and this list does not compose of all identified T6SS substrates. Commonly used names for T6SS substrates are listed as well as their immunity proteins and the host organism. For each substrate, its enzymatic activity is listed, as well as their delivery mode in terms of their adaptor and chaperone module, as will be discussed in detail in 7.1. Statements in brackets imply that there is a functional link due to genetic neighbourhood, however no experiments proved this yet.

effector	immunity	organism	enzymatic activity	adaptor	chaperone	delivery dependent on
VgrG2b		*P. aeruginosa*	Zn-dependent metallopeptidase [185]	VgrG		
Tse1	Tsi1	*P. aeruginosa*	endopeptidase [176, 245]	Hcp1	Hcp1	Hcp1 [269]
Tse2	Tsi2	*P. aeruginosa*	putative ADP-ribosylase [203]	Hcp1	Hcp1	Hcp1 [269]
Tse3	Tsi3	*P. aeruginosa*	muramidase [176]	Hcp1	Hcp1	Hcp1 [175, 269]
Tse4	Tsi4	*P. aeruginosa*	pore-forming [193, 208]	Hcp1	Hcp1	Hcp1 [208]

effector	immunity	organism	enzymatic activity	adaptor	chaperone	delivery dependent on
Tse5/RhsP1	Tsi5, RhsI1	*P. aeruginosa*	periplasmic toxicity [208]	PAAR	Rhs	VgrG1c [175, 208]
Tse6/Tne1	Tsi6	*P. aeruginosa*	NAD(P)+-glycohydrolase [201, 202]	PAAR	EagT6	VgrG1a [175, 208], EagT6 [202]
Tse7	Tsi7	*P. aeruginosa*	putative nuclease [175]	PAAR	(DUF2169)	VgrG1b [175]
Tle1	Tli1	*P. aeruginosa*	lipase [198]	(Tap4a)	(Tap4a)	(VgrG4a)
Tle3	Tli3	*P. aeruginosa*	lipase [198]	(TTR-like)	(TTR-like)	(VgrG2b)
PldA/Tle5a	Tli5a	*P. aeruginosa*	phospholipase D [186, 255]	(TTR-like)	(TTR-like)	VgrG4b [146]
Tle4/TplE	Tli4	*P. aeruginosa*	induces autophagy [268]	(TTR-like)	(TTR-like)	(VgrG2a)
PldB/Tle5b	$Tli5b_{123}$	*P. aeruginosa*	phospholipase D [188]	(TTR-like)	(TTR-like)	VgrG5 (this study)
TseF	na	*P. aeruginosa*	binds PQS, incorporated into OMVs [166]			interacts w VgrG1b, VgrG3 [166]
TseT	TsiT	*P. aeruginosa*	TOX-REase-5	TecT, Co-TecT	TecT, Co-TecT	(Co-)TecT, PAAR4, VgrG4b, VgrG6 [220]
RhsP2	RhsI2	*P. aeruginosa* PA14	toxic in *E coli* [175]	PAAR, (Tap14)	Rhs, (Tap14)	
Tke1	Tki1	*P. putida* KT2440	Tox-61 motif [136]			
Tke2	Tki2	*P. putida* KT2440	HNH motif [136]	PAAR	Rhs	[136] (VgrG1)
Tke3	Tki3	*P. putida* KT2440				
Tke4	Tki4	*P. putida* KT2440	SHH motif [136]	PAAR	Rhs	(VgrG2)
Tke5	Tki5	*P. putida* KT2440		(Tap3)	(Tap3)	(VgrG3)
Tke6	Tki6	*P. putida* KT2440	colicin-like [136]	PAAR		
Tke7	Tki7	*P. putida* KT2440	colicin-like [136]	(Hcp5)	(Hcp5)	(Hcp5)
Tke8	Tki8	*P. putida* KT2440	colicin-like [136]	(Hcp6)	(Hcp6)	(Hcp6)
Tke9	Tki9	*P. putida* KT2440		(Tap4)	(Tap4)	(VgrG4)
Tke10	Tki9	*P. putida* KT2440	REase motif [136]	(TTR-like)	(TTR-like)	(VgrG5)
VasX	TsiV2	*V. cholerae* V52	colicin-like [192]	VasW/Tap2	VasW/Tap2	VgrG-2 [270], VasW [192, 217]
TseL	TsiV1	*V. cholerae* V52	lipase [187]	Tap1	Tap1	Tap1, VgrG1 [217]
TseH	TsiH	*V. cholerae* V52	putative peptidase [271]			
VgrG-3	TsiV3	*V. cholerae* V52	peptidoglycan binding domain	VgrG		

effector	immunity	organism	enzymatic activity	adaptor	chaperone	delivery dependent on
VgrG-1	na	*V. cholerae* V52	actin-crosslinking [207, 248, 249]	VgrG		
Tde1	Tdi1	*A. tumefaciens* C58	HxxD-nuclease [272]	Tap1	Tap1	VgrG1, Tap-1, PAAR [149]
Tde2	Tdi2	*A. tumefaciens* C58	nuclease [272]	PAAR-like	(DUF2169)	VgrG2, DUF2169 [149]
Tae	Tai	*A. tumefaciens* C58	amidase [272]	Hcp	Hcp	Hcp [149]
RhsA	RhsIA	*D. dadantii*	nuclease [273]	PAAR	Rhs, DUF1795	VgrGA [199]
RhsB	RhsIB	*D. dadantii*	nuclease [273]	PAAR	Rhs, DUF1795	VgrGB [199]
RhsC		*D. dadantii*		PAAR	Rhs	
Ssp1	Rap1a	*S. marcescens*	amidase [194, 195]			
Ssp2	Rap2a	*S. marcescens*	amidase [194, 195]	Hcp1	Hcp1	Hcp1 [148]
Ssp3		*S. marcescens*				
Ssp4	Sip4	*S. marcescens*		Hcp1	Hcp1	Hcp1 [148]
Ssp5		*S. marcescens*				
Ssp6		*S. marcescens*				
Slp		*S. marcescens*	lipase			VgrG2 [148]
Rhs2	RhsI2	*S. marcescens*	DNase [200]	PAAR	Rhs, EagR2	VgrG2, EagR2 [148]
Rhs1	RhsI1	*S. marcescens*		PAAR	Rhs, EagR1	EagR1 [200] VgrG2 [148]
VgrG1		*A. hydrophila*	actin ADP-ribosylase [183]	VgrG		
TseC	TseI	*A. hydrophila*		TecC	TecC	TecC [218]
Tle1	Tli1	*E. coli*	phospholipase [216]	(TTR-like)	(TTR-like)	VgrG1 [216]
Rhs-CT1	CTI1	*E. coli* STEC004	putative zincin-like metallo-peptidase [209]	PAAR	Rhs	VgrG2 [209]
Rhs-CT3	CTI3	*E. coli* PE027	putative REase-3 [209]	PAAR	Rhs	VgrG1, EagR [209]
Rhs-CT5	CTI5	*E. coli* O157	putative RNase [209]	PAAR	Rhs	VgrG2 [209]
Hcp-ET1	ETI1	*E. coli* STEC004	HNH-DNase [206]	Hcp	Hcp	
Hcp-ET2		*E. coli* PE321	phospholipase, [206]	Hcp	Hcp	
Hcp-ET3	ETI3/4	*E. coli* PE086	DNase activity [206]	Hcp	Hcp	

effector	immunity	organism	enzymatic activity	adaptor	chaperone	delivery dependent on
ET4		*E. coli* PE086	colicin-DNase toxin [206]	Hcp	Hcp	
KatN		*E. coli* EDL933	catalase [274]			
Tae4	Tai4	*E. cloacae*	hydrolysis of PG [275]			
RhsA	RhsIa	*E. cloacae*		PAAR	Rhs	VgrG2 [208]
RhsB	RhsIb	*E. cloacae*	Tox-GHH [225]	PAAR	Rhs	VgrG1 [208]
TecA		*B. cenocepacia*	inactivation of Rho GTPases [184]	Hcp	Hcp	Hcp [184]
VgrG5		*B. pseudomallei*	membrane fusion [182]	VgrG		
Tge2	Tgi2	*P. protegens*	N-acetyl-glycosaminidase [269]	Hcp	Hcp	
Tse4	Tsi4	*P. protegens*		Hcp	Hcp	
Tae3	Tai3	*P. protegens*		Hcp	Hcp	
RhsA	RhsI	*P. protegens*	REase [201]	PAAR	Rhs	
Tne2	Tni2	*P. protegens*	NADase [201]	PAAR		
IdsD		*P. mirabilis*		(IdsC)	(IdsC)	(IdsC)
Va16922	Va16927	*V. alginolyticus*	putative nuclease [215]			
Va18287	Va18282	*V. alginolyticus*	putative nuclease [215]	PAAR	Rhs	
Va03175	Va03170	*V. alginolyticus*	putative pore-forming [215]			
Va16152	Va16147	*V. alginolyticus*	putative pore-forming [215]	(MIX IV)		
Va01565	Va01560	*V. alginolyticus*		(MIX I)		
Va01435	Va01430	*V. alginolyticus*	putative PG-hydrolase[215]			
Va1565	Va1560	*V. alginolyticus*		(MIX)		
VP1390	VP1389	*V. parahaemolyticus*	[214]	(MIX)		
VPA1263	Vti2	*V. parahaemolyticus*	putative colicin [214]	(MIX V)		
VP1415	VP1416	*V. parahaemolyticus*	putative AHH-nuclease [214]	PAAR		
VgrG2		*V. parahaemolyticus*	induces autophagy [276]	VgrG		
VgrG1		*V. parahaemolyticus*	haemagglutinin repeat	VgrG		

7.4. Conclusions

This thesis made important advancements in the understanding of the molecular mechanisms of T6SS-mediated effector delivery. We showed how T6SS spike proteins can be extended by covalently fusing effector domains to them and have them delivered. Furthermore, we shed some light on the molecular determinants of the two spike components, VgrG and PAAR proteins, and pinpointed at amino acid residues mediating specific recognition of both VgrG and PAAR proteins. We then demonstrated how C-terminal residues of VgrG proteins mediate the specific binding and stabilisation of effector proteins. These results led us to propose a model describing how all T6SS effectors require adaptors to connect them to the T6SS spike and chaperones to maintain effector stability. We could also show some limitations of T6SS-mediated effector delivery that might need to be taken into account if one considers employing the T6SS as a protein shuttle to deliver heterologous passenger proteins. In all, the research presented here progresses our understanding of this fascinating secretion system and its versatility.

8. Bibliography

1. Silby, M.W., et al., Pseudomonas *genomes: diverse and adaptable.* FEMS Microbiol Rev, 2011. **35**(4): p. 652-80.
2. Gellatly, S.L. and R.E. Hancock, Pseudomonas *aeruginosa: new insights into pathogenesis and host defenses.* Pathog Dis, 2013. **67**(3): p. 159-73.
3. Klockgether, J. and B. Tummler, *Recent advances in understanding* Pseudomonas aeruginosa *as a pathogen.* F1000Res, 2017. **6**: p. 1261.
4. Valentini, M., et al., *Lifestyle transitions and adaptive pathogenesis of* Pseudomonas *aeruginosa.* Curr Opin Microbiol, 2017. **41**: p. 15-20.
5. Huber, P., et al., Pseudomonas aeruginosa *renews its virulence factors.* Environ Microbiol Rep, 2016.
6. Palmer, G.C. and M. Whiteley, *Metabolism and pathogenicity of* Pseudomonas aeruginosa *infections in the lungs of individuals with cystic fibrosis.* Microbiol Spectr, 2015. **3**(4).
7. Morita, Y., J. Tomida, and Y. Kawamura, *Responses of* Pseudomonas aeruginosa *to antimicrobials.* Front Microbiol, 2014. **4**: p. 422.
8. Masuda, N., et al., *Contribution of the MexX-MexY-oprM efflux system to intrinsic resistance in* Pseudomonas aeruginosa. Antimicrob Agents Chemother, 2000. **44**(9): p. 2242-6.
9. Hancock, R.E. and F.S. Brinkman, *Function of* pseudomonas *porins in uptake and efflux.* Annu Rev Microbiol, 2002. **56**: p. 17-38.
10. Poole, K., Pseudomonas aeruginosa*: resistance to the max.* Front Microbiol, 2011. **2**: p. 65.
11. Poole, K., *Aminoglycoside resistance in* Pseudomonas aeruginosa*.* Antimicrob Agents Chemother, 2005. **49**(2): p. 479-87.
12. Herrmann, G., et al., *Colistin-tobramycin combinations are superior to monotherapy concerning the killing of biofilm* Pseudomonas aeruginosa. J Infect Dis, 2010. **202**(10): p. 1585-92.
13. Lee, D.G., et al., *Genomic analysis reveals that* Pseudomonas aeruginosa *virulence is combinatorial.* Genome Biol, 2006. **7**(10): p. R90.
14. Lassek, C., et al., *Proteome and carbon flux analysis of* Pseudomonas aeruginosa *clinical isolates from different infection sites.* Proteomics, 2016. **16**(9): p. 1381-5.
15. Filloux, A., *Secretion signal and protein targeting in bacteria: a biological puzzle.* J Bacteriol, 2010. **192**(15): p. 3847-9.
16. Filloux, A., *Protein Secretion Systems in* Pseudomonas aeruginosa*: An Essay on Diversity, Evolution, and Function.* Front Microbiol, 2011. **2**: p. 155.
17. Stathopoulos, C., et al., *Secretion of virulence determinants by the general secretory pathway in gram-negative pathogens: an evolving story.* Microbes Infect, 2000. **2**(9): p. 1061-72.
18. Papanikou, E., S. Karamanou, and A. Economou, *Bacterial protein secretion through the translocase nanomachine.* Nat Rev Microbiol, 2007. **5**(11): p. 839-51.
19. Palmer, T. and B.C. Berks, *The twin-arginine translocation (Tat) protein export pathway.* Nat Rev Microbiol, 2012. **10**(7): p. 483-96.
20. Koronakis, V., E. Koronakis, and C. Hughes, *Isolation and analysis of the C-terminal signal directing export of* Escherichia coli *hemolysin protein across both bacterial membranes.* EMBO J, 1989. **8**(2): p. 595-605.
21. Binet, R., et al., *Protein secretion by gram-negative bacterial ABC exporters.* Folia Microbiol (Praha), 1997. **42**(3): p. 179-83.
22. Duong, F., et al., *The AprX protein of* Pseudomonas aeruginosa: *a new substrate for the Apr type I secretion system.* Gene, 2001. **262**(1-2): p. 147-53.

23. Guzzo, J., et al., Pseudomonas aeruginosa *alkaline protease: evidence for secretion genes and study of secretion mechanism.* J Bacteriol, 1991. **173**(17): p. 5290-7.
24. Letoffe, S., V. Redeker, and C. Wandersman, *Isolation and characterization of an extracellular haem-binding protein from* Pseudomonas aeruginosa t*hat shares function and sequence similarities with the* Serratia marcescens *HasA haemophore.* Mol Microbiol, 1998. **28**(6): p. 1223-34.
25. Rybtke, M., et al., *The LapG protein plays a role in* Pseudomonas aeruginosa *biofilm formation by controlling the presence of the CdrA adhesin on the cell surface.* Microbiologyopen, 2015. **4**(6): p. 917-30.
26. Thanabalu, T., et al., *Substrate-induced assembly of a contiguous channel for protein export from* E.coli*: reversible bridging of an inner-membrane translocase to an outer membrane exit pore.* EMBO J, 1998. **17**(22): p. 6487-96.
27. Duong, F., A. Lazdunski, and M. Murgier, *Protein secretion by heterologous bacterial ABC-transporters: the C-terminus secretion signal of the secreted protein confers high recognition specificity.* Mol Microbiol, 1996. **21**(3): p. 459-70.
28. Hahn, H.P. and B.U. von Specht, *Secretory delivery of recombinant proteins in attenuated* Salmonella *strains: potential and limitations of Type I protein transporters.* FEMS Immunol Med Microbiol, 2003. **37**(2-3): p. 87-98.
29. Bleves, S., et al., *Protein secretion systems in* Pseudomonas aeruginosa*: A wealth of pathogenic weapons.* Int J Med Microbiol, 2010. **300**(8): p. 534-43.
30. Hay, I.D., et al., *Structure and Membrane Topography of the Vibrio-Type Secretin Complex from the Type 2 Secretion System of Enteropathogenic* Escherichia col*i.* J Bacteriol, 2018. **200**(5).
31. Douzi, B., A. Filloux, and R. Voulhoux, *On the path to uncover the bacterial type II secretion system.* Philos Trans R Soc Lond B Biol Sci, 2012. **367**(1592): p. 1059-72.
32. Thomassin, J.L., et al., *The trans-envelope architecture and function of the type 2 secretion system: new insights raising new questions.* Mol Microbiol, 2017. **105**(2): p. 211-226.
33. Costa, T.R., et al., *Secretion systems in Gram-negative bacteria: structural and mechanistic insights.* Nat Rev Microbiol, 2015. **13**(6): p. 343-59.
34. Ball, G., et al., *A novel type II secretion system in* Pseudomonas aeruginosa*.* Mol Microbiol, 2002. **43**(2): p. 475-85.
35. Olson, J.C. and D.E. Ohman, *Efficient production and processing of elastase and LasA by* Pseudomonas aeruginosa *require zinc and calcium ions.* J Bacteriol, 1992. **174**(12): p. 4140-7.
36. Lu, H.M., S. Mizushima, and S. Lory, *A periplasmic intermediate in the extracellular secretion pathway of* Pseudomonas aeruginosa *exotoxin A.* J Bacteriol, 1993. **175**(22): p. 7463-7.
37. Douzi, B., et al., *Deciphering the Xcp* Pseudomonas aeruginosa *type II secretion machinery through multiple interactions with substrates.* J Biol Chem, 2011. **286**(47): p. 40792-801.
38. Francetic, O. and A.P. Pugsley, *Towards the identification of type II secretion signals in a nonacylated variant of pullulanase from* Klebsiella oxytoca*.* J Bacteriol, 2005. **187**(20): p. 7045-55.
39. Gerard-Vincent, M., et al., *Identification of XcpP domains that confer functionality and specificity to the* Pseudomonas aeruginosa t*ype II secretion apparatus.* Mol Microbiol, 2002. **44**(6): p. 1651-65.
40. Zhou, L., et al., *Secretory delivery of heterologous proteins in attenuated* Vibrio anguillarum *for potential use in vaccine design.* Appl Microbiol Biotechnol, 2008. **79**(6): p. 1027-34.
41. Harding, C.M., et al., *Medically relevant* Acinetobacter *species require a type II secretion system and specific membrane-associated chaperones for the export of multiple substrates and full virulence.* PLoS Pathog, 2016. **12**(1): p. e1005391.

42. Oshima-Hirayama, N., et al., *Lipase from* Pseudomonas aeruginosa*. Production in Escherichia coli and activation in vitro with a protein from the downstream gene.* Eur J Biochem, 1993. **215**(2): p. 239-46.
43. El Khattabi, M., et al., *Role of the lipase-specific foldase of* Burkholderia glumae *as a steric chaperone.* J Biol Chem, 2000. **275**(35): p. 26885-91.
44. Kinsella, R.L., et al., *Defining the interaction of the protease CpaA with its type II secretion chaperone CpaB and its contribution to virulence in* Acinetobacter *species.* J Biol Chem, 2017. **292**(48): p. 19628-19638.
45. Pauwels, K., et al., *Structure of a membrane-based steric chaperone in complex with its lipase substrate.* Nat Struct Mol Biol, 2006. **13**(4): p. 374-5.
46. Braun, P., J. Tommassen, and A. Filloux, *Role of the propeptide in folding and secretion of elastase of* Pseudomonas aeruginosa. Mol Microbiol, 1996. **19**(2): p. 297-306.
47. Galan, J.E., et al., *Bacterial type III secretion systems: specialized nanomachines for protein delivery into target cells.* Annu Rev Microbiol, 2014. **68**: p. 415-38.
48. Galle, C., Beyaert, *Structure and Function of the Type III Secretion System of* Pseudomonas aeruginosa. Current Protein and Peptide Science, 2012. **13**: p. 831-842.
49. Burstein, D., et al., *Novel type III effectors in* Pseudomonas aeruginosa*.* MBio, 2015. **6**(2): p. e00161.
50. Feltman, H., et al., *Prevalence of type III secretion genes in clinical and environmental isolates of* Pseudomonas aeruginosa*.* Microbiology, 2001. **147**(Pt 10): p. 2659-69.
51. Hauser, A.R., *The type III secretion system of* Pseudomonas aeruginosa: *infection by injection.* Nat Rev Microbiol, 2009. **7**(9): p. 654-65.
52. Radke, J., K.J. Pederson, and J.T. Barbieri, Pseudomonas aeruginosa *exoenzyme S is a biglutamic acid ADP-ribosyltransferase.* Infect Immun, 1999. **67**(3): p. 1508-10.
53. Dortet, L., et al., *Pore-forming activity of the* Pseudomonas aeruginosa *type III secretion system translocon alters the host epigenome.* Nat Microbiol, 2018. **3**(3): p. 378-386.
54. McDermott, J.E., et al., *Computational prediction of type III and IV secreted effectors in gram-negative bacteria.* Infect Immun, 2011. **79**(1): p. 23-32.
55. Anderson, D.M. and O. Schneewind, *A mRNA signal for the type III secretion of Yop proteins by* Yersinia enterocolitica*.* Science, 1997. **278**(5340): p. 1140-3.
56. Epaulard, O., et al., *Anti-tumor immunotherapy via antigen delivery from a live attenuated genetically engineered* Pseudomonas aeruginosa *type III secretion system-based vector.* Mol Ther, 2006. **14**(5): p. 656-61.
57. Nishikawa, H., et al., *In vivo antigen delivery by a* Salmonella typhimurium *type III secretion system for therapeutic cancer vaccines.* J Clin Invest, 2006. **116**(7): p. 1946-54.
58. Russmann, H., Yersinia *outer protein E, YopE. A versatile type III effector molecule for cytosolic targeting of heterologous antigens by attenuated Salmonella.* Adv Exp Med Biol, 2003. **529**: p. 407-13.
59. Wieser, A., et al., *First multi-epitope subunit vaccine against extraintestinal pathogenic* Escherichia coli *delivered by a bacterial type-3 secretion system (T3SS).* Int J Med Microbiol, 2012. **302**(1): p. 10-8.
60. Costa, S.C., et al., *A new means to identify type 3 secreted effectors: functionally interchangeable class IB chaperones recognize a conserved sequence.* MBio, 2012. **3**(1).
61. Birtalan, S.C., R.M. Phillips, and P. Ghosh, *Three-dimensional secretion signals in chaperone-effector complexes of bacterial pathogens.* Mol Cell, 2002. **9**(5): p. 971-80.
62. Stebbins, C.E. and J.E. Galan, *Maintenance of an unfolded polypeptide by a cognate chaperone in bacterial type III secretion.* Nature, 2001. **414**(6859): p. 77-81.
63. Lilic, M., M. Vujanac, and C.E. Stebbins, *A common structural motif in the binding of virulence factors to bacterial secretion chaperones.* Mol Cell, 2006. **21**(5): p. 653-64.

64. Akeda, Y. and J.E. Galan, *Chaperone release and unfolding of substrates in type III secretion.* Nature, 2005. **437**(7060): p. 911-5.
65. Gauthier, A. and B.B. Finlay, *Translocated intimin receptor and its chaperone interact with ATPase of the type III secretion apparatus of enteropathogenic* Escherichia coli. J Bacteriol, 2003. **185**(23): p. 6747-55.
66. Parsot, C., C. Hamiaux, and A.L. Page, *The various and varying roles of specific chaperones in type III secretion systems.* Curr Opin Microbiol, 2003. **6**(1): p. 7-14.
67. Sory, M.P., et al., *Identification of the YopE and YopH domains required for secretion and internalization into the cytosol of macrophages, using the cyaA gene fusion approach.* Proc Natl Acad Sci U S A, 1995. **92**(26): p. 11998-2002.
68. Cornelis, G.R. and F. Van Gijsegem, *Assembly and function of type III secretory systems.* Annu Rev Microbiol, 2000. **54**: p. 735-74.
69. Shen, D.K., et al., *Orf1/SpcS chaperones ExoS for type three secretion by* Pseudomonas aeruginosa. Biomed Environ Sci, 2008. **21**(2): p. 103-9.
70. Finck-Barbancon, V., T.L. Yahr, and D.W. Frank, *Identification and characterization of SpcU, a chaperone required for efficient secretion of the ExoU cytotoxin.* J Bacteriol, 1998. **180**(23): p. 6224-31.
71. Yahr, T.L., J. Goranson, and D.W. Frank, *Exoenzyme S of* Pseudomonas aeruginosa *is secreted by a type III pathway.* Molecular Microbiology, 1996. **22**(5): p. 991-1003.
72. Christie, P.J., *The mosaic type IV secretion systems.* EcoSal Plus, 2016. **7**(1).
73. Christie, P.J., N. Whitaker, and C. Gonzalez-Rivera, *Mechanism and structure of the bacterial type IV secretion systems.* Biochim Biophys Acta, 2014. **1843**(8): p. 1578-91.
74. Souza, D.P., et al., *Bacterial killing via a type IV secretion system.* Nat Commun, 2015. **6**: p. 6453.
75. Terradot, L. and G. Waksman, *Architecture of the Helicobacter pylori Cag-type IV secretion system.* FEBS J, 2011. **278**(8): p. 1213-22.
76. Whitaker, N., et al., *Chimeric coupling proteins mediate transfer of heterologous type IV effectors through the* Escherichia coli *pKM101-encoded conjugation machine.* J Bacteriol, 2016. **198**(19): p. 2701-18.
77. Fronzes, R., et al., *Structure of a type IV secretion system core complex.* Science, 2009. **323**(5911): p. 266-8.
78. Wallden, K., A. Rivera-Calzada, and G. Waksman, *Type IV secretion systems: versatility and diversity in function.* Cell Microbiol, 2010. **12**(9): p. 1203-12.
79. Hohlfeld, S., et al., *A C-terminal translocation signal is necessary, but not sufficient for type IV secretion of the* Helicobacter pylori *CagA protein.* Mol Microbiol, 2006. **59**(5): p. 1624-37.
80. Vergunst, A.C., et al., *VirB/D4-dependent protein translocation from* Agrobacterium *into plant cells.* Science, 2000. **290**(5493): p. 979-82.
81. Schmid, M.C., et al., *The VirB type IV secretion system of* Bartonella henselae *mediates invasion, proinflammatory activation and antiapoptotic protection of endothelial cells.* Mol Microbiol, 2004. **52**(1): p. 81-92.
82. Sutherland, M.C., et al., *The* Legionella *IcmSW complex directly interacts with DotL to mediate translocation of adaptor-dependent substrates.* PLoS Pathog, 2012. **8**(9): p. e1002910.
83. Atmakuri, K., Z. Ding, and P.J. Christie, *VirE2, a type IV secretion substrate, interacts with the VirD4 transfer protein at cell poles of* Agrobacterium tumefaciens. Mol Microbiol, 2003. **49**(6): p. 1699-713.
84. Zhao, Z., et al., *Activities of virE1 and the VirE1 secretion chaperone in export of the multifunctional VirE2 effector via an* Agrobacterium *type IV secretion pathway.* J Bacteriol, 2001. **183**(13): p. 3855-65.
85. Couturier, M.R., et al., *Interaction with CagF is required for translocation of CagA into the host via the* Helicobacter pylori *type IV secretion system.* Infect Immun, 2006. **74**(1): p. 273-81.
86. Kessler, E., et al., *Elastase and the LasA protease of* Pseudomonas aeruginosa *are secreted with their propeptides.* J Biol Chem, 1998. **273**(46): p. 30225-31.

87. Luo, Y., et al., *Structural and biochemical characterization of the type III secretion chaperones CesT and SigE.* Nat Struct Biol, 2001. **8**(12): p. 1031-6.
88. Cambronne, E.D. and C.R. Roy, *The* Legionella pneumophila *IcmSW complex interacts with multiple Dot/Icm effectors to facilitate type IV translocation.* PLoS Pathog, 2007. **3**(12): p. e188.
89. Daleke, M.H., et al., *Specific chaperones for the type VII protein secretion pathway.* J Biol Chem, 2012. **287**(38): p. 31939-47.
90. Cao, Z., et al., *The type VII secretion system of* Staphylococcus aureus *secretes a nuclease toxin that targets competitor bacteria.* Nat Microbiol, 2016. **2**: p. 16183.
91. Guerin, J., et al., *Two-partner secretion: combining efficiency and simplicity in the secretion of large proteins for bacteria-host and bacteria-bacteria interactions.* Front Cell Infect Microbiol, 2017. **7**: p. 148.
92. van Ulsen, P., et al., *Type V secretion: from biogenesis to biotechnology.* Biochim Biophys Acta, 2014. **1843**(8): p. 1592-611.
93. Wilhelm, S., et al., *The autotransporter esterase EstA of* Pseudomonas aeruginosa *is required for rhamnolipid production, cell motility, and biofilm formation.* J Bacteriol, 2007. **189**(18): p. 6695-703.
94. Salacha, R., et al., *The* Pseudomonas aeruginosa *patatin-like protein PlpD is the archetype of a novel Type V secretion system.* Environ Microbiol, 2010. **12**(6): p. 1498-512.
95. Ruer, S., et al., *Assembly of fimbrial structures in* Pseudomonas aeruginosa: *functionality and specificity of chaperone-usher machineries.* J Bacteriol, 2007. **189**(9): p. 3547-55.
96. Jamet, A. and X. Nassif, *New players in the toxin field: polymorphic toxin systems in bacteria.* MBio, 2015. **6**(3).
97. Jones, A.M., D.A. Low, and C.S. Hayes, *Can't you hear me knocking: contact-dependent competition and cooperation in bacteria.* Emerg Top Life Sci, 2017. **1**(1): p. 75-83.
98. Aoki, S.K., et al., *Contact-dependent inhibition of growth in* Escherichia coli. Science, 2005. **309**(5738): p. 1245-8.
99. Beck, C.M., et al., *CdiA from* Enterobacter cloacae *delivers a toxic ribosomal RNase into target bacteria.* Structure, 2014. **22**(5): p. 707-18.
100. Aoki, S.K., et al., *Contact-dependent growth inhibition causes reversible metabolic downregulation in* Escherichia coli. J Bacteriol, 2009. **191**(6): p. 1777-86.
101. Mercy, C., et al., *Functional Characterization of* Pseudomonas *Contact Dependent Growth Inhibition (CDI) Systems.* PLoS One, 2016. **11**(1): p. e0147435.
102. Webb, J.S., et al., *Delivery of CdiA nuclease toxins into target cells during contact-dependent growth inhibition.* PLoS One, 2013. **8**(2): p. e57609.
103. Willett, J.L., et al., *Contact-dependent growth inhibition toxins exploit multiple independent cell-entry pathways.* Proc Natl Acad Sci U S A, 2015. **112**(36): p. 11341-6.
104. Aoki, S.K., et al., *Contact-dependent growth inhibition requires the essential outer membrane protein BamA (YaeT) as the receptor and the inner membrane transport protein AcrB.* Mol Microbiol, 2008. **70**(2): p. 323-40.
105. Ruhe, Z.C., et al., *The proton-motive force is required for translocation of CDI toxins across the inner membrane of target bacteria.* Mol Microbiol, 2014. **94**(2): p. 466-81.
106. Aoki, S.K., et al., *A widespread family of polymorphic contact-dependent toxin delivery systems in bacteria.* Nature, 2010. **468**(7322): p. 439-42.
107. Stanley, S.A., et al., *Acute infection and macrophage subversion by* Mycobacterium tuberculosis *require a specialized secretion system.* Proc Natl Acad Sci U S A, 2003. **100**(22): p. 13001-6.
108. Burts, M.L., et al., *EsxA and EsxB are secreted by an ESAT-6-like system that is required for the pathogenesis of* Staphylococcus aureus *infections.* Proc Natl Acad Sci U S A, 2005. **102**(4): p. 1169-74.

109. Jager, F., et al., *Membrane interactions and self-association of components of the Ess/Type VII secretion system of* Staphylococcus aureus. FEBS Lett, 2016. **590**(3): p. 349-57.
110. Daleke, M.H., et al., *General secretion signal for the mycobacterial type VII secretion pathway.* Proc Natl Acad Sci U S A, 2012. **109**(28): p. 11342-7.
111. Rosenberg, O.S., et al., *Substrates control multimerization and activation of the multi-domain ATPase motor of type VII secretion.* Cell, 2015. **161**(3): p. 501-512.
112. Bingle, L.E., C.M. Bailey, and M.J. Pallen, *Type VI secretion: a beginner's guide.* Curr Opin Microbiol, 2008. **11**(1): p. 3-8.
113. Basler, M., B.T. Ho, and J.J. Mekalanos, *Tit-for-tat: type VI secretion system counterattack during bacterial cell-cell interactions.* Cell, 2013. **152**(4): p. 884-94.
114. Mougous, J.D., et al., *A virulence locus of* Pseudomonas aeruginosa *encodes a protein secretion apparatus.* Science, 2006. **312**(5779): p. 1526-30.
115. Durand, E., et al., *Biogenesis and structure of a type VI secretion membrane core complex.* Nature, 2015.
116. Durand, E., et al., *Structural characterization and oligomerization of the TssL protein, a component shared by bacterial type VI and type IVb secretion systems.* J Biol Chem, 2012. **287**(17): p. 14157-68.
117. Felisberto-Rodrigues, C., et al., *Towards a structural comprehension of bacterial type VI secretion systems: characterization of the TssJ-TssM complex of an* Escherichia coli *pathovar.* PLoS Pathog, 2011. **7**(11): p. e1002386.
118. Mariano, G., L. Monlezun, and S.J. Coulthurst, *Dual Role for DsbA in Attacking and Targeted Bacterial Cells during Type VI Secretion System-Mediated Competition.* Cell Rep, 2018. **22**(3): p. 774-785.
119. Brunet, Y.R., et al., *The type VI secretion TssEFGK-VgrG phage-like baseplate is recruited to the TssJLM membrane complex via multiple contacts and serves as assembly platform for tail tube/sheath polymerization.* PLoS Genet, 2015. **11**(10): p. e1005545.
120. Planamente, S., et al., *TssA forms a gp6-like ring attached to the type VI secretion sheath.* EMBO J, 2016. **35**(15): p. 1613-27.
121. Taylor, N.M., et al., *Structure of the T4 baseplate and its function in triggering sheath contraction.* Nature, 2016. **533**(7603): p. 346-52.
122. Zoued, A., et al., *TssK is a trimeric cytoplasmic protein interacting with components of both phage-like and membrane anchoring complexes of the type VI secretion system.* J Biol Chem, 2013. **288**(38): p. 27031-41.
123. Zoued, A., et al., *Priming and polymerization of a bacterial contractile tail structure.* Nature, 2016. **531**(7592): p. 59-63.
124. Leiman, P.G., et al., *Type VI secretion apparatus and phage tail-associated protein complexes share a common evolutionary origin.* Proc Natl Acad Sci U S A, 2009. **106**(11): p. 4154-9.
125. Lossi, N.S., et al., *The HsiB1C1 (TssB-TssC) complex of the* Pseudomonas aeruginosa *type VI secretion system forms a bacteriophage tail sheathlike structure.* J Biol Chem, 2013. **288**(11): p. 7536-48.
126. Förster, A., et al., *Coevolution of the ATPase ClpV, the sheath proteins TssB and TssC and the accessory protein TagJ/HsiE1 distinguishes type VI secretion classes.* J Biol Chem, 2014.
127. Brunet, Y.R., et al., *Type VI secretion and bacteriophage tail tubes share a common assembly pathway.* EMBO Rep, 2014. **15**(3): p. 315-21.
128. Boenemann, G., et al., *Remodelling of VipA/VipB tubules by ClpV-mediated threading is crucial for type VI protein secretion.* The EMBO Journal, 2009. **28**: p. 315-325.
129. Vettiger, A., et al., *The type VI secretion system sheath assembles at the end distal from the membrane anchor.* Nat Commun, 2017. **8**: p. 16088.
130. Basler, M., et al., *Type VI secretion requires a dynamic contractile phage tail-like structure.* Nature, 2012. **483**(7388): p. 182-6.

131. Pukatzki, S., et al., *Identification of a conserved bacterial protein secretion system in* Vibrio cholerae *using the Dictyostelium host model system.* Proc Natl Acad Sci U S A, 2006. **103**(5): p. 1528-33.
132. Cascales, E. and C. Cambillau, *Structural biology of type VI secretion systems.* Philos Trans R Soc Lond B Biol Sci, 2012. **367**(1592): p. 1102-11.
133. Kapitein, N., et al., *ClpV recycles VipA/VipB tubules and prevents non-productive tubule formation to ensure efficient type VI protein secretion.* Mol Microbiol, 2013. **87**(5): p. 1013-28.
134. Kudryashev, M., et al., *Structure of the type VI secretion system contractile sheath.* Cell, 2015. **160**(5): p. 952-62.
135. Zheng, J., B. Ho, and J.J. Mekalanos, *Genetic analysis of anti-amoebae and anti-bacterial activities of the type VI secretion system in* Vibrio cholerae. PLoS One, 2011. **6**(8): p. e23876.
136. Bernal, P., et al., *The* Pseudomonas putida *T6SS is a plant warden against phytopathogens.* ISME J, 2017.
137. Kanamaru, S., et al., *Structure of the cell-puncturing device of bacteriophage T4.* Nature, 2002. **415**(6871): p. 553-7.
138. Buth, S.A., et al., *Structure and biophysical properties of a triple-stranded beta-helix comprising the central spike of bacteriophage T4.* Viruses, 2015. **7**(8): p. 4676-706.
139. Uchida, K., et al., *Structure and properties of the C-terminal beta-helical domain of VgrG protein from* Escherichia coli *O157.* J Biochem, 2014. **155**(3): p. 173-82.
140. Hachani, A., et al., *Type VI secretion system in* Pseudomonas aeruginosa*: secretion and multimerization of VgrG proteins.* J Biol Chem, 2011. **286**(14): p. 12317-27.
141. Shneider, M.M., et al., *PAAR-repeat proteins sharpen and diversify the type VI secretion system spike.* Nature, 2013. **500**(7462): p. 350-3.
142. Browning, C., et al., *Phage pierces the host cell membrane with the iron-loaded spike.* Structure, 2012. **20**(2): p. 326-39.
143. Murdoch, S.L., et al., *The opportunistic pathogen Serratia marcescens utilizes type VI secretion to target bacterial competitors.* J Bacteriol, 2011. **193**(21): p. 6057-69.
144. Lin, J.S., L.S. Ma, and E.M. Lai, *Systematic dissection of the agrobacterium type VI secretion system reveals machinery and secreted components for subcomplex formation.* PLoS One, 2013. **8**(7): p. e67647.
145. Schell, M.A., et al., *Type VI secretion is a major virulence determinant in* Burkholderia mallei*.* Mol Microbiol, 2007. **64**(6): p. 1466-85.
146. Allsopp, L.P., et al., *RsmA and AmrZ orchestrate the assembly of all three type VI secretion systems in* Pseudomonas aeruginosa*.* Proc Natl Acad Sci U S A, 2017.
147. Jones, C., et al., *An rhs gene linked to the second type VI secretion cluster is a feature of the* Pseudomonas aeruginosa *strain PA14.* Journal of Bacteriology, 2013: p. 800-810.
148. Cianfanelli, F.R., et al., *VgrG and PAAR Proteins Define Distinct Versions of a Functional Type VI Secretion System.* PLoS Pathog, 2016. **12**(6): p. e1005735.
149. Bondage, D.D., et al., *VgrG C terminus confers the type VI effector transport specificity and is required for binding with PAAR and adaptor-effector complex.* Proc Natl Acad Sci U S A, 2016.
150. Jones, C., et al., *Subinhibitory concentration of kanamycin induces the* Pseudomonas aeruginosa *type VI secretion system.* PLoS One, 2013. **8**(11): p. e81132.
151. Bachmann, V., et al., *Bile Salts Modulate the Mucin-Activated Type VI Secretion System of Pandemic* Vibrio cholerae*.* PLoS Negl Trop Dis, 2015. **9**(8): p. e0004031.
152. Sana, T.G., et al., *The second type VI secretion system of* Pseudomonas aeruginosa *strain PAO1 is regulated by quorum sensing and Fur and modulates internalization in epithelial cells.* J Biol Chem, 2012. **287**(32): p. 27095-105.
153. Ma, L.S., et al., Agrobacterium tumefaciens *deploys a superfamily of type VI secretion DNase effectors as weapons for interbacterial competition in planta.* Cell Host Microbe, 2014. **16**(1): p. 94-104.

154. Gerc, A.J., et al., *Visualization of the* Serratia *Type VI Secretion System Reveals Unprovoked Attacks and Dynamic Assembly.* Cell Rep, 2015. **12**(12): p. 2131-42.
155. Lin, J.S., et al., *TagF-mediated repression of bacterial type VI secretion systems involves a direct interaction with the cytoplasmic protein Fha.* J Biol Chem, 2018.
156. Mougous, J.D., et al., *Threonine phosphorylation post-translationally regulates protein secretion in* Pseudomonas aeruginosa*.* Nat Cell Biol, 2007. **9**(7): p. 797-803.
157. Casabona, M.G., et al., *An ABC transporter and an outer membrane lipoprotein participate in posttranslational activation of type VI secretion in* Pseudomonas aeruginosa*.* Environ Microbiol, 2013. **15**(2): p. 471-86.
158. Hsu, F., S. Schwarz, and J.D. Mougous, *TagR promotes PpkA-catalysed type VI secretion activation in* Pseudomonas aeruginosa. Mol Microbiol, 2009. **72**(5): p. 1111-25.
159. Brencic, A. and S. Lory, *Determination of the regulon and identification of novel mRNA targets of* Pseudomonas aeruginosa *RsmA.* Mol Microbiol, 2009. **72**(3): p. 612-32.
160. Goodman, A.L., et al., *A signaling network reciprocally regulates genes associated with acute infection and chronic persistence in* Pseudomonas aeruginosa. Dev Cell, 2004. **7**(5): p. 745-54.
161. Goodman, A.L., et al., *Direct interaction between sensor kinase proteins mediates acute and chronic disease phenotypes in a bacterial pathogen.* Genes Dev, 2009. **23**(2): p. 249-59.
162. Moscoso, J.A., et al., *The* Pseudomonas aeruginosa *sensor RetS switches type III and type VI secretion via c-di-GMP signalling.* Environ Microbiol, 2011. **13**(12): p. 3128-38.
163. Hood, R.D., et al., *A type VI secretion system of* Pseudomonas aeruginosa *targets a toxin to bacteria.* Cell Host Microbe, 2010. **7**(1): p. 25-37.
164. LeRoux, M., et al., *Kin cell lysis is a danger signal that activates antibacterial pathways of P*seudomonas aeruginosa*.* Elife, 2015. **4**.
165. Borgeaud, S., et al., *The type VI secretion system of* Vibrio cholerae *fosters horizontal gene transfer.* Science, 2015. **347**(6217): p. 63-7.
166. Lin, J., et al., *A* Pseudomonas *T6SS effector recruits PQS-containing outer membrane vesicles for iron acquisition.* Nat Commun, 2017. **8**: p. 14888.
167. Cianfanelli, F.R., L. Monlezun, and S.J. Coulthurst, *Aim, Load, Fire: The Type VI Secretion System, a Bacterial Nanoweapon.* Trends Microbiol, 2016. **24**(1): p. 51-62.
168. Sana, T.G., K.A. Lugo, and D.M. Monack, *T6SS: The bacterial "fight club" in the host gut.* PLoS Pathog, 2017. **13**(6): p. e1006325.
169. Verster, A.J., et al., *The Landscape of Type VI Secretion across Human Gut Microbiomes Reveals Its Role in Community Composition.* Cell Host Microbe, 2017. **22**(3): p. 411-419 e4.
170. Coyne, M.J., K.G. Roelofs, and L.E. Comstock, *Type VI secretion systems of human gut Bacteroidales segregate into three genetic architectures, two of which are contained on mobile genetic elements.* BMC Genomics, 2016. **17**: p. 58.
171. Chatzidaki-Livanis, M., N. Geva-Zatorsky, and L.E. Comstock, Bacteroides fragilis *type VI secretion systems use novel effector and immunity proteins to antagonize human gut Bacteroidales species.* Proc Natl Acad Sci U S A, 2016. **113**(13): p. 3627-32.
172. Hecht, A.L., et al., *Strain competition restricts colonization of an enteric pathogen and prevents colitis.* EMBO Rep, 2016. **17**(9): p. 1281-91.
173. Sana, T.G., et al., Salmonella Typhimurium *utilizes a T6SS-mediated antibacterial weapon to establish in the host gut.* Proc Natl Acad Sci U S A, 2016.
174. Anderson, M.C., et al., Shigella sonnei *encodes a functional T6SS used for interbacterial competition and niche occupancy.* Cell Host Microbe, 2017. **21**(6): p. 769-776 e3.
175. Hachani, A., et al., *The VgrG proteins are "á la carte" delivery systems for bacterial type VI effectors.* J Biol Chem, 2014. **289**(25): p. 17872-84.
176. Russell, A.B., et al., *Type VI secretion delivers bacteriolytic effectors to target cells.* Nature, 2011. **475**(7356): p. 343-7.

177. Li, M., et al., *Structural basis for type VI secretion effector recognition by a cognate immunity protein.* PLoS Pathog, 2012. **8**(4): p. e1002613.
178. Dong, C., et al., *Structural insights into the inhibition of type VI effector Tae3 by its immunity protein Tai3.* Biochem J, 2013. **454**(1): p. 59-68.
179. MacIntyre, D.L., et al., *The* Vibrio cholerae *type VI secretion system displays antimicrobial properties.* Proceedings of the National Academy of Sciences of the United States of America, 2010. **107**(45): p. 19520-19524.
180. Hachani, A., T.E. Wood, and A. Filloux, *Type VI secretion and anti-host effectors.* Curr Opin Microbiol, 2016. **29**: p. 81-93.
181. Ma, A.T., et al., *Translocation of a* Vibrio cholerae *type VI secretion effector requires bacterial endocytosis by host cells.* Cell Host Microbe, 2009. **5**(3): p. 234-43.
182. Toesca, I.J., C.T. French, and J.F. Miller, *The Type VI secretion system spike protein VgrG5 mediates membrane fusion during intercellular spread by pseudomallei group* Burkholderia *species.* Infect Immun, 2014. **82**(4): p. 1436-44.
183. Suarez, G., et al., *A type VI secretion system effector protein, VgrG1, from* Aeromonas hydrophila *that induces host cell toxicity by ADP ribosylation of actin.* J Bacteriol, 2010. **192**(1): p. 155-68.
184. Aubert, D.F., et al., *A* Burkholderia *type VI effector deamidates Rho GTPases to activate the pyrin inflammasome and trigger inflammation.* Cell Host Microbe, 2016.
185. Sana, T.G., et al., *Internalization of* Pseudomonas aeruginosa *strain PAO1 into epithelial cells is promoted by interaction of a T6SS effector with the microtubule network.* MBio, 2015. **6**(3).
186. Russell, A.B., et al., *Diverse type VI secretion phospholipases are functionally plastic antibacterial effectors.* Nature, 2013. **496**(7446): p. 508-12.
187. Dong, T.G., et al., *Identification of T6SS-dependent effector and immunity proteins by Tn-seq in Vibrio cholerae.* Proc Natl Acad Sci U S A, 2013. **110**(7): p. 2623-8.
188. Jiang, F., et al., *A* Pseudomonas aeruginosa *type VI secretion phospholipase D effector targets both prokaryotic and eukaryotic cells.* Cell Host Microbe, 2014. **15**(5): p. 600-10.
189. Durand, E., et al., *VgrG, Tae, Tle, and beyond: the versatile arsenal of Type VI secretion effectors.* Trends Microbiol, 2014. **22**(9): p. 498-507.
190. Hu, H., et al., *Structure of the type VI secretion phospholipase effector Tle1 provides insight into its hydrolysis and membrane targeting.* Acta Crystallogr D Biol Crystallogr, 2014. **70**(Pt 8): p. 2175-85.
191. Lery, L.M., et al., *Comparative analysis of* Klebsiella pneumoniae *genomes identifies a phospholipase D family protein as a novel virulence factor.* BMC Biol, 2014. **12**: p. 41.
192. Miyata, S.T., et al., *Dual expression profile of type VI secretion system immunity genes protects pandemic* Vibrio cholerae*.* PLoS Pathog, 2013. **9**(12): p. e1003752.
193. LaCourse, K.D., et al., *Conditional toxicity and synergy drive diversity among antibacterial effectors.* Nat Microbiol, 2018.
194. Srikannathasan, V., et al., *Structural basis for type VI secreted peptidoglycan DL-endopeptidase function, specificity and neutralization in* Serratia marcescens. Acta Crystallogr D Biol Crystallogr, 2013. **69**(Pt 12): p. 2468-82.
195. English, G., et al., *New secreted toxins and immunity proteins encoded within the Type VI secretion system gene cluster of* Serratia marcescens. Mol Microbiol, 2012. **86**(4): p. 921-36.
196. Wang, T., et al., *Complex structure of type VI peptidoglycan muramidase effector and a cognate immunity protein.* Acta Crystallogr D Biol Crystallogr, 2013. **69**(Pt 10): p. 1889-900.
197. Li, L., et al., *Structural Insights on the bacteriolytic and self-protection mechanism of muramidase effector Tse3 in* Pseudomonas aeruginosa*.* J Biol Chem, 2013. **288**(42): p. 30607-13.
198. Russell, A.B., S.B. Peterson, and J.D. Mougous, *Type VI secretion system effectors: poisons with a purpose.* Nat Rev Microbiol, 2014. **12**(2): p. 137-48.

199. Koskiniemia, S., et al., *Rhs proteins from diverse bacteria mediate intercellular competition.* 2013.
200. Diniz, J.A. and S.J. Coulthurst, *Intra-species competition in* Serratia marcescens *is mediated by type VI secretion Rhs effectors and a conserved effector-associated accessory protein.* J Bacteriol, 2015.
201. Tang, J.Y., et al., *Diverse NADase effector families mediate interbacterial antagonism via the type VI secretion system.* J Biol Chem, 2017.
202. Whitney, J.C., et al., *An interbacterial NAD(P)(+) glycohydrolase toxin requires elongation factor Tu for delivery to target cells.* Cell, 2015. **163**(3): p. 607-19.
203. Robb, C.S., et al., *The structure of the toxin and type six secretion system substrate Tse2 in complex with its immunity protein.* Structure, 2015.
204. Silverman, J.M., et al., *Haemolysin coregulated protein is an exported receptor and chaperone of type VI secretion substrates.* Mol Cell, 2013. **51**(5): p. 584-93.
205. Blondel, C.J., et al., *Comparative genomic analysis uncovers 3 novel loci encoding type six secretion systems differentially distributed in* Salmonella *serotypes.* BMC Genomics, 2009. **10**: p. 354.
206. Ma, J., et al., *The Hcp proteins fused with diverse extended-toxin domains represent a novel pattern of antibacterial effectors in type VI secretion systems.* Virulence, 2017: p. 0.
207. Pukatzki, S., et al., *Type VI secretion system translocates a phage tail spike-like protein into target cells where it cross-links actin.* Proc Natl Acad Sci U S A, 2007. **104**(39): p. 15508-13.
208. Whitney, J.C., et al., *Genetically distinct pathways guide effector export through the type VI secretion system.* Mol Microbiol, 2014. **92**(3): p. 529-42.
209. Ma, J., et al., *PAAR-Rhs proteins harbor various C-terminal toxins to diversify the antibacterial pathways of type VI secretion systems.* Environ Microbiol, 2016.
210. Jackson, A.P., et al., *Evolutionary diversification of an ancient gene family (rhs) through C-terminal displacement.* BMC Genomics, 2009. **10**: p. 584.
211. Zhang, D., et al., *Polymorphic toxin systems: comprehensive characterization of trafficking modes, processing, mechanisms of action, immunity and ecology using comparative genomics.* Biol Direct, 2012. **7**: p. 18.
212. Busby, J.N., et al., *The BC component of ABC toxins is an RHS-repeat-containing protein encapsulation device.* Nature, 2013. **501**(7468): p. 547-50.
213. Wang, Y.D., S. Zhao, and C.W. Hill, *Rhs elements comprise three subfamilies which diverged prior to acquisition by* Escherichia coli. J Bacteriol, 1998. **180**(16): p. 4102-10.
214. Salomon, D., et al., *Marker for type VI secretion system effectors.* Proc Natl Acad Sci U S A, 2014. **111**(25): p. 9271-6.
215. Salomon, D., et al., *Type VI secretion system toxins horizontally shared between marine bacteria.* PLoS Pathog, 2015. **11**(8): p. e1005128.
216. Flaugnatti, N., et al., *A phospholipase A anti-bacterial T6SS effector interacts directly with the C-terminal domain of the VgrG spike protein for delivery.* Mol Microbiol, 2015.
217. Unterweger, D., et al., *Chimeric adaptor proteins translocate diverse type VI secretion system effectors in Vibrio cholerae.* EMBO J, 2015. **34**(16): p. 2198-210.
218. Liang, X., et al., *Identification of divergent type VI secretion effectors using a conserved chaperone domain.* Proc Natl Acad Sci U S A, 2015.
219. Unterweger, D., et al., *The* Vibrio cholerae *type VI secretion system employs diverse effector modules for intraspecific competition.* Nat Commun, 2014. **5**: p. 3549.
220. Burkinshaw, B.J., et al., *A type VI secretion system effector delivery mechanism dependent on PAAR and a chaperone-co-chaperone complex.* Nat Microbiol, 2018.
221. Lossi, N.S., et al., *The archetype* Pseudomonas aeruginosa *proteins TssB and TagJ form a novel subcomplex in the bacterial type VI secretion system.* Mol Microbiol, 2012. **86**(2): p. 437-56.

222. Miller, V.L. and J.J. Mekalanos, *A novel suicide vector and its use in construction of insertion mutations: osmoregulation of outer membrane proteins and virulence determinants in* Vibrio cholerae *requires toxR.* J Bacteriol, 1988. **170**(6): p. 2575-83.
223. Herrero, M., V. de Lorenzo, and K.N. Timmis, *Transposon vectors containing non-antibiotic resistance selection markers for cloning and stable chromosomal insertion of foreign genes in gram-negative bacteria.* J Bacteriol, 1990. **172**(11): p. 6557-67.
224. Karimova, G., et al., *A bacterial two-hybrid system based on a reconstituted signal transduction pathway.* Proc Natl Acad Sci U S A, 1998. **95**(10): p. 5752-6.
225. Figurski, D.H. and D.R. Helinski, *Replication of an origin-containing derivative of plasmid RK2 dependent on a plasmid function provided in trans.* Proc Natl Acad Sci U S A, 1979. **76**(4): p. 1648-52.
226. Schmidt-Eisenlohr, H., N. Domke, and C. Baron, *TraC of IncN plasmid pKM101 associates with membranes and extracellular high-molecular-weight structures in* Escherichia coli. J Bacteriol, 1999. **181**(18): p. 5563-71.
227. Kovach, M.E., et al., *Four new derivatives of the broad-host-range cloning vector pBBR1MCS, carrying different antibiotic-resistance cassettes.* Gene, 1995. **166**(1): p. 175-6.
228. Becher, A. and H.P. Schweizer, *Integration-proficient* Pseudomonas aeruginosa *vectors for isolation of single-copy chromosomal lacZ and lux gene fusions.* Biotechniques, 2000. **29**(5): p. 948-50, 952.
229. Untergasser, A., et al., *Primer3--new capabilities and interfaces.* Nucleic Acids Res, 2012. **40**(15): p. e115.
230. Kaniga, K., I. Delor, and G.R. Cornelis, *A wide-host-range suicide vector for improving reverse genetics in gram-negative bacteria: inactivation of the blaA gene of* Yersinia enterocolitica. Gene, 1991. **109**(1): p. 137-41.
231. Charpentier, X. and E. Oswald, *Identification of the secretion and translocation domain of the enteropathogenic and enterohemorrhagic* Escherichia coli *effector Cif, using TEM-1 beta-lactamase as a new fluorescence-based reporter.* J Bacteriol, 2004. **186**(16): p. 5486-95.
232. Waterhouse, A.M., et al., *Jalview Version 2--a multiple sequence alignment editor and analysis workbench.* Bioinformatics, 2009. **25**(9): p. 1189-91.
233. Notredame, C., D.G. Higgins, and J. Heringa, *T-Coffee: A novel method for fast and accurate multiple sequence alignment.* J Mol Biol, 2000. **302**(1): p. 205-17.
234. Krogh, A., et al., *Predicting transmembrane protein topology with a hidden Markov model: application to complete genomes.* J Mol Biol, 2001. **305**(3): p. 567-80.
235. Kelley, L.A., et al., *The Phyre2 web portal for protein modeling, prediction and analysis.* Nat Protoc, 2015. **10**(6): p. 845-58.
236. Schrodinger, L., *The PyMOL Molecular Graphics System, Version 1.8*. 2015.
237. Brooks, T.M., et al., *Lytic activity of the Vibrio cholerae type VI secretion toxin VgrG-3 is inhibited by the antitoxin TsaB.* J Biol Chem, 2013. **288**(11): p. 7618-25.
238. Ho, B.T., et al., *Vibrio cholerae type 6 secretion system effector trafficking in target bacterial cells.* Proc Natl Acad Sci U S A, 2017. **114**(35): p. 9427-9432.
239. Vettiger, A. and M. Basler, *Type VI secretion system substrates are transferred and reused among sister cells.* Cell, 2016. **167**(1): p. 99-110 e12.
240. Sheahan, K.L., C.L. Cordero, and K.J. Satchell, *Identification of a domain within the multifunctional Vibrio cholerae RTX toxin that covalently cross-links actin.* Proc Natl Acad Sci U S A, 2004. **101**(26): p. 9798-803.
241. Russell, A.B., et al., *A widespread bacterial type VI secretion effector superfamily identified using a heuristic approach.* Cell Host Microbe, 2012. **11**(5): p. 538-49.
242. Wexler, A.G., et al., *Human symbionts inject and neutralize antibacterial toxins to persist in the gut.* Proc Natl Acad Sci U S A, 2016. **113**(13): p. 3639-44.
243. Bröms, J.E., et al., *Unique substrates secreted by the type VI secretion system of* Francisella tularensis *during intramacrophage infection.* PLoS One, 2012. **7**(11): p. e50473.

244. Schroeder, G.N., et al., Legionella pneumophila *strain 130b possesses a unique combination of type IV secretion systems and novel Dot/Icm secretion system effector proteins.* J Bacteriol, 2010. **192**(22): p. 6001-16.
245. Ding, J., et al., *Structural insights into the* Pseudomonas aeruginosa *type VI virulence effector Tse1 bacteriolysis and self-protection mechanisms.* J Biol Chem, 2012. **287**(32): p. 26911-20.
246. Zhang, H., et al., *Crystal structure of type VI effector Tse1 from* Pseudomonas aeruginosa*.* FEBS Lett, 2012. **586**(19): p. 3193-9.
247. Hachani, A., N.S. Lossi, and A. Filloux, *A visual assay to monitor T6SS-mediated bacterial competition.* J Vis Exp, 2013(73): p. e50103.
248. Ma, A.T. and J.J. Mekalanos, *In vivo actin cross-linking induced by* Vibrio cholerae *type VI secretion system is associated with intestinal inflammation.* Proc Natl Acad Sci U S A, 2010. **107**(9): p. 4365-70.
249. Durand, E., et al., *Crystal structure of the VgrG1 actin cross-linking domain of the* Vibrio cholerae *type VI secretion system.* J Biol Chem, 2012. **287**(45): p. 38190-9.
250. Rigard, M., et al., *Francisella tularensis IglG Belongs to a Novel Family of PAAR-Like T6SS Proteins and Harbors a Unique N-terminal Extension Required for Virulence.* PLoS Pathog, 2016. **12**(9): p. e1005821.
251. Bordi, C., et al., *Regulatory RNAs and the HptB/RetS signalling pathways fine-tune* Pseudomonas aeruginosa *pathogenesis.* Mol Microbiol, 2010. **76**(6): p. 1427-43.
252. Poole, S.J., et al., *Identification of functional toxin/immunity genes linked to contact-dependent growth inhibition (CDI) and rearrangement hotspot (Rhs) systems.* PLoS Genet, 2011. **7**(8): p. e1002217.
253. Spinola-Amilibia, M., et al., *The structure of VgrG1 from* Pseudomonas aeruginosa, *the needle tip of the bacterial type VI secretion system.* Acta Crystallogr D Struct Biol, 2016. **72**(Pt 1): p. 22-33.
254. Hennebry, S.C., et al., *The crystal structure of the transthyretin-like protein from Salmonella dublin, a prokaryote 5-hydroxyisourate hydrolase.* J Mol Biol, 2006. **359**(5): p. 1389-99.
255. Spencer, C. and H.A. Brown, *Biochemical characterization of a* Pseudomonas aeruginosa *phospholipase D.* Biochemistry, 2015. **54**(5): p. 1208-18.
256. Tang, L., et al., *Commentary: The icmF3 Locus is Involved in Multiple Adaptation- and Virulence-related Characteristics in* Pseudomonas aeruginosa *PAO1.* Front Cell Infect Microbiol, 2015. **5**: p. 83.
257. Burrowes, E., et al., *Influence of the regulatory protein RsmA on cellular functions in* Pseudomonas aeruginosa *PAO1, as revealed by transcriptome analysis.* Microbiology, 2006. **152**(Pt 2): p. 405-18.
258. Buxbaum, J.N. and N. Reixach, *Transthyretin: the servant of many masters.* Cell Mol Life Sci, 2009. **66**(19): p. 3095-101.
259. Ingenbleek, Y. and L.H. Bernstein, *Plasma Transthyretin as a Biomarker of Lean Body Mass and Catabolic States.* Adv Nutr, 2015. **6**(5): p. 572-80.
260. Lee, Y., et al., *Transthyretin-related proteins function to facilitate the hydrolysis of 5-hydroxyisourate, the end product of the uricase reaction.* FEBS Lett, 2005. **579**(21): p. 4769-74.
261. Hennebry, S.C., et al., *Structural and functional evolution of transthyretin and transthyretin-like proteins.* Proteins, 2006. **64**(4): p. 1024-45.
262. Zhu, C., et al., *Delivery of heterologous protein antigens via hemolysin or autotransporter systems by an attenuated ler mutant of rabbit enteropathogenic Escherichia coli.* Vaccine, 2006. **24**(18): p. 3821-31.
263. Zepeda-Rivera, M.A., C.C. Saak, and K.A. Gibbs, *A proposed chaperone of the bacterial type VI secretion system functions to constrain a self-identity protein.* J Bacteriol, 2018.
264. Mavridou, D.A., et al., *Oxidation state-dependent protein-protein interactions in disulfide cascades.* J Biol Chem, 2011. **286**(28): p. 24943-56.

265. Russmann, H., et al., *Yersinia enterocolitica-mediated translocation of defined fusion proteins to the cytosol of mammalian cells results in peptide-specific MHC class I-restricted antigen presentation.* Eur J Immunol, 2000. **30**(5): p. 1375-84.
266. Matsumoto, K., *Role of bacterial proteases in pseudomonal and serratial keratitis.* Biol Chem, 2004. **385**(11): p. 1007-16.
267. Nazarov, S., et al., *Cryo-EM reconstruction of type VI secretion system baseplate and sheath distal end.* EMBO J, 2018. **37**(4).
268. Jiang, F., et al., *The Pseudomonas aeruginosa type VI secretion PGAP1-like effector induces host autophagy by activating endoplasmic reticulum stress.* Cell Rep, 2016.
269. Whitney, J.C., et al., *Identification, structure, and function of a novel type VI secretion peptidoglycan glycoside hydrolase effector-immunity pair.* J Biol Chem, 2013. **288**(37): p. 26616-24.
270. Miyata, S.T., et al., Vibrio cholerae *requires the type VI secretion system virulence factor VasX to kill* Dictyostelium discoideum. Infect Immun, 2011. **79**(7): p. 2941-9.
271. Altindis, E., et al., *Secretome analysis of Vibrio cholerae type VI secretion system reveals a new effector-immunity pair.* MBio, 2015. **6**(2): p. e00075.
272. Ma, J., et al., *Two functional type VI secretion systems in avian pathogenic* Escherichia coli *are involved in different pathogenic pathways.* Infect Immun, 2014. **82**(9): p. 3867-79.
273. Koskiniemi, S., et al., *Rhs proteins from diverse bacteria mediate intercellular competition.* Proc Natl Acad Sci U S A, 2013. **110**(17): p. 7032-7.
274. Wan, B., et al., *Type VI secretion system contributes to Enterohemorrhagic* Escherichia coli *virulence by secreting catalase against host reactive oxygen species (ROS).* PLoS Pathog, 2017. **13**(3): p. e1006246.
275. Zhang, H., et al., *Structure of the type VI effector-immunity complex (Tae4-Tai4) provides novel insights into the inhibition mechanism of the effector by its immunity protein.* J Biol Chem, 2013. **288**(8): p. 5928-39.
276. Yu, Y., et al., *VgrG2 of type VI secretion system 2 of* Vibrio parahaemolyticus *induces autophagy in macrophages.* Front Microbiol, 2015. **6**: p. 168.

9. Appendix

9.1. Figure permissions

JOHN WILEY AND SONS LICENSE TERMS AND CONDITIONS

Apr 21, 2018

This Agreement between Ms. Sarah Wettstadt ("You") and John Wiley and Sons ("John Wiley and Sons") consists of your license details and the terms and conditions provided by John Wiley and Sons and Copyright Clearance Center.

License Number	4333580590252
License date	Apr 21, 2018
Licensed Content Publisher	John Wiley and Sons
Licensed Content Publication	The EMBO Journal
Licensed Content Title	Substrate-induced assembly of a contiguous channel for protein export from E.coli: reversible bridging of an inner-membrane translocase to an outer membrane exit pore
Licensed Content Author	Thirumaran Thanabalu, Eva Koronakis, Colin Hughes, et al
Licensed Content Date	Nov 16, 1998
Licensed Content Volume	17
Licensed Content Issue	22
Licensed Content Pages	10
Type of use	Dissertation/Thesis
Requestor type	University/Academic
Format	Print and electronic
Portion	Figure/table
Number of figures/tables	1
Original Wiley figure/table number(s)	Figure 10
Will you be translating?	No
Title of your thesis / dissertation	Using the Pseudomonas aeruginosa T6SS as a protein shuttle to deliver effectors
Expected completion date	Apr 2018
Expected size (number of pages)	300
Requestor Location	Ms. Sarah Wettstadt 3 Adelaide Grove Red door London, W12 0JU United Kingdom Attn: Ms. Sarah Wettstadt
Publisher Tax ID	EU826007151
Total	0.00 GBP
Terms and Conditions	

TERMS AND CONDITIONS

This copyrighted material is owned by or exclusively licensed to John Wiley & Sons, Inc. or one of its group companies (each a"Wiley Company") or handled on behalf of a society with which a Wiley Company has exclusive publishing rights in relation to a particular work (collectively "WILEY"). By clicking "accept" in connection with completing this licensing transaction, you agree that the following terms and conditions apply to this transaction

ELSEVIER LICENSE
TERMS AND CONDITIONS

Apr 21, 2018

This Agreement between Ms. Sarah Wettstadt ("You") and Elsevier ("Elsevier") consists of your license details and the terms and conditions provided by Elsevier and Copyright Clearance Center.

License Number	4333751147011
License date	Apr 21, 2018
Licensed Content Publisher	Elsevier
Licensed Content Publication	Molecular Cell
Licensed Content Title	Three-Dimensional Secretion Signals in Chaperone-Effector Complexes of Bacterial Pathogens
Licensed Content Author	Sara C Birtalan,Rebecca M Phillips,Partho Ghosh
Licensed Content Date	May 1, 2002
Licensed Content Volume	9
Licensed Content Issue	5
Licensed Content Pages	10
Start Page	971
End Page	980
Type of Use	reuse in a thesis/dissertation
Intended publisher of new work	other
Portion	figures/tables/illustrations
Number of figures/tables/illustrations	1
Format	both print and electronic
Are you the author of this Elsevier article?	No
Will you be translating?	No
Original figure numbers	Figure 1
Title of your thesis/dissertation	Using the Pseudomonas aeruginosa T6SS as a protein shuttle to deliver effectors
Publisher of new work	Imperial College London
Expected completion date	Apr 2018
Estimated size (number of pages)	300
Requestor Location	Ms. Sarah Wettstadt 3 Adelaide Grove Red door London, W12 0JU United Kingdom Attn: Ms. Sarah Wettstadt
Publisher Tax ID	GB 494 6272 12
Total	0.00 GBP
Terms and Conditions	

ELSEVIER LICENSE
TERMS AND CONDITIONS

Apr 21, 2018

This Agreement between Ms. Sarah Wettstadt ("You") and Elsevier ("Elsevier") consists of your license details and the terms and conditions provided by Elsevier and Copyright Clearance Center.

License Number	4333750848402
License date	Apr 21, 2018
Licensed Content Publisher	Elsevier
Licensed Content Publication	Molecular Cell
Licensed Content Title	Three-Dimensional Secretion Signals in Chaperone-Effector Complexes of Bacterial Pathogens
Licensed Content Author	Sara C Birtalan,Rebecca M Phillips,Partho Ghosh
Licensed Content Date	May 1, 2002
Licensed Content Volume	9
Licensed Content Issue	5
Licensed Content Pages	10
Start Page	971
End Page	980
Type of Use	reuse in a thesis/dissertation
Intended publisher of new work	other
Portion	figures/tables/illustrations
Number of figures/tables/illustrations	1
Format	both print and electronic
Are you the author of this Elsevier article?	No
Will you be translating?	No
Original figure numbers	Figure 2
Title of your thesis/dissertation	Using the Pseudomonas aeruginosa T6SS as a protein shuttle to deliver effectors
Publisher of new work	Imperial College London
Expected completion date	Apr 2018
Estimated size (number of pages)	300
Requestor Location	Ms. Sarah Wettstadt 3 Adelaide Grove Red door London, W12 0JU United Kingdom Attn: Ms. Sarah Wettstadt
Publisher Tax ID	GB 494 6272 12
Total	0.00 GBP
Terms and Conditions	

SPRINGER NATURE LICENSE TERMS AND CONDITIONS

Apr 25, 2018

This Agreement between Ms. Sarah Wettstadt ("You") and Springer Nature ("Springer Nature") consists of your license details and the terms and conditions provided by Springer Nature and Copyright Clearance Center.

License Number	4335840117905
License date	Apr 25, 2018
Licensed Content Publisher	Springer Nature
Licensed Content Publication	Nature
Licensed Content Title	Structure of the cell-puncturing device of bacteriophage T4
Licensed Content Author	Shuji Kanamaru, Petr G. Leiman, Victor A. Kostyuchenko, Paul R. Chipman, Vadim V. Mesyanzhinov et al.
Licensed Content Date	Jan 31, 2002
Licensed Content Volume	415
Licensed Content Issue	6871
Type of Use	Thesis/Dissertation
Requestor type	academic/university or research institute
Format	print and electronic
Portion	figures/tables/illustrations
Number of figures/tables/illustrations	2
High-res required	no
Will you be translating?	no
Circulation/distribution	<501
Author of this Springer Nature content	no
Title	Using the Pseudomonas aeruginosa T6SS as a protein shuttle to deliver effectors
Instructor name	n/a
Institution name	Imperial College London
Expected presentation date	Apr 2018
Portions	Figure 1 Figure 2
Requestor Location	Ms. Sarah Wettstadt 3 Adelaide Grove Red door London, W12 0JU United Kingdom Attn: Ms. Sarah Wettstadt
Billing Type	Invoice
Billing Address	Ms. Sarah Wettstadt 3 Adelaide Grove Red door London, United Kingdom W12 0JU Attn: Ms. Sarah Wettstadt

SPRINGER NATURE LICENSE TERMS AND CONDITIONS

Apr 21, 2018

This Agreement between Ms. Sarah Wettstadt ("You") and Springer Nature ("Springer Nature") consists of your license details and the terms and conditions provided by Springer Nature and Copyright Clearance Center.

License Number	4333641121997
License date	Apr 21, 2018
Licensed Content Publisher	Springer Nature
Licensed Content Publication	Nature Structural & Molecular Biology
Licensed Content Title	Structure of a membrane-based steric chaperone in complex with its lipase substrate
Licensed Content Author	Kris Pauwels, Ariel Lustig, Lode Wyns, Jan Tommassen, Savvas N Savvides et al.
Licensed Content Date	Mar 5, 2006
Licensed Content Volume	13
Licensed Content Issue	4
Type of Use	Thesis/Dissertation
Requestor type	academic/university or research institute
Format	print and electronic
Portion	figures/tables/illustrations
Number of figures/tables/illustrations	2
High-res required	no
Will you be translating?	no
Circulation/distribution	<501
Author of this Springer Nature content	no
Title	Using the Pseudomonas aeruginosa T6SS as a protein shuttle to deliver effectors
Instructor name	n/a
Institution name	Imperial College London
Expected presentation date	Apr 2018
Portions	Figure 1, Figure 2
Requestor Location	Ms. Sarah Wettstadt 3 Adelaide Grove Red door London, W12 0JU United Kingdom Attn: Ms. Sarah Wettstadt
Billing Type	Invoice
Billing Address	Ms. Sarah Wettstadt 3 Adelaide Grove Red door London, United Kingdom W12 0JU Attn: Ms. Sarah Wettstadt

SPRINGER NATURE LICENSE TERMS AND CONDITIONS

Apr 20, 2018

This Agreement between Ms. Sarah Wettstadt ("You") and Springer Nature ("Springer Nature") consists of your license details and the terms and conditions provided by Springer Nature and Copyright Clearance Center.

License Number	4333010495020
License date	Apr 20, 2018
Licensed Content Publisher	Springer Nature
Licensed Content Publication	Nature Reviews Microbiology
Licensed Content Title	Bacterial protein secretion through the translocase nanomachine
Licensed Content Author	Effrosyni Papanikou, Spyridoula Karamanou, Anastassios Economou
Licensed Content Date	Nov 1, 2007
Licensed Content Volume	5
Licensed Content Issue	11
Type of Use	Thesis/Dissertation
Requestor type	academic/university or research institute
Format	print and electronic
Portion	figures/tables/illustrations
Number of figures/tables/illustrations	1
High-res required	no
Will you be translating?	no
Circulation/distribution	<501
Author of this Springer Nature content	no
Title	Using the Pseudomonas aeruginosa T6SS as a protein shuttle to deliver effectors
Instructor name	n/a
Institution name	Imperial College London
Expected presentation date	Apr 2018
Portions	Figure 1
Requestor Location	Ms. Sarah Wettstadt 3 Adelaide Grove Red door London, W12 0JU United Kingdom Attn: Ms. Sarah Wettstadt
Billing Type	Invoice
Billing Address	Ms. Sarah Wettstadt 3 Adelaide Grove Red door London, United Kingdom W12 0JU Attn: Ms. Sarah Wettstadt
Total	0.00 GBP

THE AMERICAN ASSOCIATION FOR THE ADVANCEMENT OF SCIENCE LICENSE TERMS AND CONDITIONS

Apr 21, 2018

This Agreement between Ms. Sarah Wettstadt ("You") and The American Association for the Advancement of Science ("The American Association for the Advancement of Science") consists of your license details and the terms and conditions provided by The American Association for the Advancement of Science and Copyright Clearance Center.

License Number	4333771123218
License date	Apr 21, 2018
Licensed Content Publisher	The American Association for the Advancement of Science
Licensed Content Publication	Science
Licensed Content Title	Structure of a Type IV Secretion System Core Complex
Licensed Content Author	Rémi Fronzes,Eva Schäfer,Luchun Wang,Helen R. Saibil,Elena V. Orlova,Gabriel Waksman
Licensed Content Date	Jan 9, 2009
Licensed Content Volume	323
Licensed Content Issue	5911
Volume number	323
Issue number	5911
Type of Use	Thesis / Dissertation
Requestor type	Scientist/individual at a research institution
Format	Print and electronic
Portion	Figure
Number of figures/tables	2
Order reference number	
Title of your thesis / dissertation	Using the Pseudomonas aeruginosa T6SS as a protein shuttle to deliver effectors
Expected completion date	Apr 2018
Estimated size(pages)	300
Requestor Location	Ms. Sarah Wettstadt 3 Adelaide Grove Red door London, W12 0JU United Kingdom Attn: Ms. Sarah Wettstadt
Billing Type	Invoice
Billing Address	Ms. Sarah Wettstadt 3 Adelaide Grove Red door London, United Kingdom W12 0JU Attn: Ms. Sarah Wettstadt
Total	0.00 GBP

Terms and Conditions

American Association for the Advancement of Science TERMS AND CONDITIONS

JOHN WILEY AND SONS LICENSE TERMS AND CONDITIONS

Apr 21, 2018

This Agreement between Ms. Sarah Wettstadt ("You") and John Wiley and Sons ("John Wiley and Sons") consists of your license details and the terms and conditions provided by John Wiley and Sons and Copyright Clearance Center.

License Number	4333770903538
License date	Apr 21, 2018
Licensed Content Publisher	John Wiley and Sons
Licensed Content Publication	Cellular Microbiology
Licensed Content Title	Microreview: Type IV secretion systems: versatility and diversity in function
Licensed Content Author	Karin Wallden,Angel Rivera-Calzada,Gabriel Waksman
Licensed Content Date	Jul 20, 2010
Licensed Content Pages	10
Type of use	Dissertation/Thesis
Requestor type	University/Academic
Format	Print and electronic
Portion	Figure/table
Number of figures/tables	1
Original Wiley figure/table number(s)	Figure 1
Will you be translating?	No
Title of your thesis / dissertation	Using the Pseudomonas aeruginosa T6SS as a protein shuttle to deliver effectors
Expected completion date	Apr 2018
Expected size (number of pages)	300
Requestor Location	Ms. Sarah Wettstadt 3 Adelaide Grove Red door London, W12 0JU United Kingdom Attn: Ms. Sarah Wettstadt
Publisher Tax ID	EU826007151
Total	0.00 GBP
Terms and Conditions	

TERMS AND CONDITIONS

This copyrighted material is owned by or exclusively licensed to John Wiley & Sons, Inc. or one of its group companies (each a"Wiley Company") or handled on behalf of a society with which a Wiley Company has exclusive publishing rights in relation to a particular work (collectively "WILEY"). By clicking "accept" in connection with completing this licensing transaction, you agree that the following terms and conditions apply to this transaction (along with the billing and payment terms and conditions established by the Copyright Clearance Center Inc., ("CCC's Billing and Payment terms and conditions"), at the time that you opened your RightsLink account (these are available at any time at http://myaccount.copyright.com).

11200 Rockville Pike
Suite 302
Rockville, Maryland 20852

August 19, 2011

American Society for Biochemistry and Molecular Biology

To whom it may concern,

It is the policy of the American Society for Biochemistry and Molecular Biology to allow reuse of any material published in its journals (the Journal of Biological Chemistry, Molecular & Cellular Proteomics and the Journal of Lipid Research) in a thesis or dissertation at no cost and with no explicit permission needed. Please see our copyright permissions page on the journal site for more information.

Best wishes,

Sarah Crespi

American Society for Biochemistry and Molecular Biology
11200 Rockville Pike, Rockville, MD
Suite 302
240-283-6616
JBC | MCP | JLR

Copyright Clearance Center

Note: Copyright.com supplies permissions but not the copyrighted content itself.

1 PAYMENT 2 REVIEW 3 CONFIRMATION

Step 3: Order Confirmation

Thank you for your order! A confirmation for your order will be sent to your account email address. If you have questions about your order, you can call us 24 hrs/day, M-F at +1.855.239.3415 Toll Free; or write to us at info@copyright.com. This is not an invoice.

Confirmation Number: 11712853
Order Date: 04/21/2018

If you paid by credit card, your order will be finalized and your card will be charged within 24 hours. If you choose to be invoiced, you can change or cancel your order until the invoice is generated.

Payment Information

Sarah Wettstadt
sw6314@ic.ac.uk
+44 7821235094
Payment Method: n/a

Order Details

CURRENT PROTEIN AND PEPTIDE SCIENCE

Order detail ID:	71135928
Order License Id:	4333680545584
ISSN:	1389-2037
Publication Type:	Journal
Volume:	
Issue:	
Start page:	
Publisher:	BENTHAM SCIENCE PUBLISHERS LTD.

Permission Status:	Granted
Permission type:	Republish or display content
Type of use:	Thesis/Dissertation
Requestor type	Academic institution
Format	Print, Electronic
Portion	chart/graph/table/figure
Number of charts/graphs/tables/figures	1
The requesting person/organization	Sarah Wettstadt
Title or numeric reference of the portion(s)	Figure 1
Title of the article or chapter the portion is from	Structure and Function of the Type III Secretion System of Pseudomonas aeruginosa
Editor of portion(s)	N/A
Author of portion(s)	Beyaert, Rudi ; Carpentier, Isabelle ; Galle, Marlies
	13

SPRINGER NATURE LICENSE TERMS AND CONDITIONS

Apr 20, 2018

This Agreement between Ms. Sarah Wettstadt ("You") and Springer Nature ("Springer Nature") consists of your license details and the terms and conditions provided by Springer Nature and Copyright Clearance Center.

License Number	4333060531025
License date	Apr 20, 2018
Licensed Content Publisher	Springer Nature
Licensed Content Publication	Nature Reviews Microbiology
Licensed Content Title	The twin-arginine translocation (Tat) protein export pathway
Licensed Content Author	Tracy Palmer, Ben C. Berks
Licensed Content Date	Jun 11, 2012
Licensed Content Volume	10
Licensed Content Issue	7
Type of Use	Thesis/Dissertation
Requestor type	academic/university or research institute
Format	print and electronic
Portion	figures/tables/illustrations
Number of figures/tables/illustrations	1
High-res required	no
Will you be translating?	no
Circulation/distribution	<501
Author of this Springer Nature content	no
Title	Using the Pseudomonas aeruginosa T6SS as a protein shuttle to deliver effectors
Instructor name	n/a
Institution name	Imperial College London
Expected presentation date	Apr 2018
Portions	Figure 2
Requestor Location	Ms. Sarah Wettstadt 3 Adelaide Grove Red door London, W12 0JU United Kingdom Attn: Ms. Sarah Wettstadt
Billing Type	Invoice
Billing Address	Ms. Sarah Wettstadt 3 Adelaide Grove Red door London, United Kingdom W12 0JU Attn: Ms. Sarah Wettstadt
Total	0.00 GBP

ELSEVIER LICENSE
TERMS AND CONDITIONS

Apr 26, 2018

This Agreement between Ms. Sarah Wettstadt ("You") and Elsevier ("Elsevier") consists of your license details and the terms and conditions provided by Elsevier and Copyright Clearance Center.

License Number	4336540386131
License date	Apr 26, 2018
Licensed Content Publisher	Elsevier
Licensed Content Publication	Molecular Cell
Licensed Content Title	Haemolysin Coregulated Protein Is an Exported Receptor and Chaperone of Type VI Secretion Substrates
Licensed Content Author	Julie M. Silverman,Danielle M. Agnello,Hongjin Zheng,Benjamin T. Andrews,Mo Li,Carlos E. Catalano,Tamir Gonen,Joseph D. Mougous
Licensed Content Date	Sep 12, 2013
Licensed Content Volume	51
Licensed Content Issue	5
Licensed Content Pages	10
Start Page	584
End Page	593
Type of Use	reuse in a thesis/dissertation
Intended publisher of new work	other
Portion	figures/tables/illustrations
Number of figures/tables/illustrations	1
Format	both print and electronic
Are you the author of this Elsevier article?	No
Will you be translating?	No
Original figure numbers	Figure 3
Title of your thesis/dissertation	Using the Pseudomonas aeruginosa T6SS as a protein shuttle to deliver effectors
Publisher of new work	Imperial College London
Expected completion date	Apr 2018
Estimated size (number of pages)	300
Requestor Location	Ms. Sarah Wettstadt 3 Adelaide Grove Red door London, W12 0JU United Kingdom Attn: Ms. Sarah Wettstadt
Publisher Tax ID	GB 494 6272 12
Total	0.00 GBP
Terms and Conditions	

SPRINGER NATURE LICENSE TERMS AND CONDITIONS

Apr 17, 2018

This Agreement between Ms. Sarah Wettstadt ("You") and Springer Nature ("Springer Nature") consists of your license details and the terms and conditions provided by Springer Nature and Copyright Clearance Center.

License Number	4331540852514
License date	Apr 17, 2018
Licensed Content Publisher	Springer Nature
Licensed Content Publication	Nature
Licensed Content Title	Biogenesis and structure of a type VI secretion membrane core complex
Licensed Content Author	Eric Durand, Van Son Nguyen, Abdelrahim Zoued, Laureen Logger, Gérard Péhau-Arnaudet et al.
Licensed Content Date	Jul 22, 2015
Licensed Content Volume	523
Licensed Content Issue	7562
Type of Use	Thesis/Dissertation
Requestor type	academic/university or research institute
Format	print and electronic
Portion	figures/tables/illustrations
Number of figures/tables/illustrations	1
High-res required	no
Will you be translating?	no
Circulation/distribution	<501
Author of this Springer Nature content	no
Title	Using the Pseudomonas aeruginosa T6SS as a protein shuttle to deliver effectors
Instructor name	n/a
Institution name	n/a
Expected presentation date	Apr 2018
Portions	Extended Data Figure 7
Requestor Location	Ms. Sarah Wettstadt 3 Adelaide Grove Red door London, W12 0JU United Kingdom Attn: Ms. Sarah Wettstadt
Billing Type	Invoice
Billing Address	Ms. Sarah Wettstadt 3 Adelaide Grove Red door London, United Kingdom W12 0JU Attn: Ms. Sarah Wettstadt

ELSEVIER LICENSE
TERMS AND CONDITIONS

Apr 18, 2018

This Agreement between Ms. Sarah Wettstadt ("You") and Elsevier ("Elsevier") consists of your license details and the terms and conditions provided by Elsevier and Copyright Clearance Center.

License Number	4332071498598
License date	Apr 18, 2018
Licensed Content Publisher	Elsevier
Licensed Content Publication	Cell
Licensed Content Title	An Interbacterial NAD(P)+ Glycohydrolase Toxin Requires Elongation Factor Tu for Delivery to Target Cells
Licensed Content Author	John C. Whitney,Dennis Quentin,Shin Sawai,Michele LeRoux,Brittany N. Harding,Hannah E. Ledvina,Bao Q. Tran,Howard Robinson,Young Ah Goo,David R. Goodlett,Stefan Raunser,Joseph D. Mougous
Licensed Content Date	Oct 22, 2015
Licensed Content Volume	163
Licensed Content Issue	3
Licensed Content Pages	13
Start Page	607
End Page	619
Type of Use	reuse in a thesis/dissertation
Portion	figures/tables/illustrations
Number of figures/tables/illustrations	1
Format	both print and electronic
Are you the author of this Elsevier article?	No
Will you be translating?	No
Original figure numbers	Figure 6
Title of your thesis/dissertation	Using the Pseudomonas aeruginosa T6SS as a protein shuttle to deliver effectors
Expected completion date	Apr 2018
Estimated size (number of pages)	300
Requestor Location	Ms. Sarah Wettstadt 3 Adelaide Grove Red door London, W12 0JU United Kingdom Attn: Ms. Sarah Wettstadt
Publisher Tax ID	GB 494 6272 12
Total	0.00 GBP
Terms and Conditions	

ELSEVIER LICENSE
TERMS AND CONDITIONS

Apr 26, 2018

This Agreement between Ms. Sarah Wettstadt ("You") and Elsevier ("Elsevier") consists of your license details and the terms and conditions provided by Elsevier and Copyright Clearance Center.

License Number	4336441437658
License date	Apr 26, 2018
Licensed Content Publisher	Elsevier
Licensed Content Publication	Structure
Licensed Content Title	The Structure of the Toxin and Type Six Secretion System Substrate Tse2 in Complex with Its Immunity Protein
Licensed Content Author	Craig S. Robb,Melissa Robb,Francis E. Nano,Alisdair B. Boraston
Licensed Content Date	Feb 2, 2016
Licensed Content Volume	24
Licensed Content Issue	2
Licensed Content Pages	8
Start Page	277
End Page	284
Type of Use	reuse in a thesis/dissertation
Portion	figures/tables/illustrations
Number of figures/tables/illustrations	1
Format	both print and electronic
Are you the author of this Elsevier article?	No
Will you be translating?	No
Original figure numbers	Figure 1
Title of your thesis/dissertation	Using the Pseudomonas aeruginosa T6SS as a protein shuttle to deliver effectors
Publisher of new work	Imperial College London
Expected completion date	Apr 2018
Estimated size (number of pages)	300
Requestor Location	Ms. Sarah Wettstadt 3 Adelaide Grove Red door London, W12 0JU United Kingdom Attn: Ms. Sarah Wettstadt
Publisher Tax ID	GB 494 6272 12
Total	0.00 GBP
Terms and Conditions	

INTRODUCTION

SPRINGER NATURE LICENSE TERMS AND CONDITIONS

Apr 22, 2018

This Agreement between Ms. Sarah Wettstadt ("You") and Springer Nature ("Springer Nature") consists of your license details and the terms and conditions provided by Springer Nature and Copyright Clearance Center.

License Number	4334261472318
License date	Apr 22, 2018
Licensed Content Publisher	Springer Nature
Licensed Content Publication	Nature Microbiology
Licensed Content Title	The type VII secretion system of Staphylococcus aureus secretes a nuclease toxin that targets competitor bacteria
Licensed Content Author	Zhenping Cao, M. Guillermina Casabona, Holger Kneuper, James D. Chalmers, Tracy Palmer
Licensed Content Date	Oct 10, 2016
Licensed Content Volume	2
Licensed Content Issue	1
Type of Use	Thesis/Dissertation
Requestor type	academic/university or research institute
Format	print and electronic
Portion	figures/tables/illustrations
Number of figures/tables/illustrations	2
High-res required	no
Will you be translating?	no
Circulation/distribution	<501
Author of this Springer Nature content	no
Title	Using the Pseudomonas aeruginosa T6SS as a protein shuttle to deliver effectors
Instructor name	n/a
Institution name	Imperial College London
Expected presentation date	Apr 2018
Portions	Figure 4 Supplementary figure 1
Requestor Location	Ms. Sarah Wettstadt 3 Adelaide Grove Red door London, W12 0JU United Kingdom Attn: Ms. Sarah Wettstadt
Billing Type	Invoice
Billing Address	Ms. Sarah Wettstadt 3 Adelaide Grove Red door

JOHN WILEY AND SONS LICENSE TERMS AND CONDITIONS

Mar 28, 2018

This Agreement between Ms. Sarah Wettstadt ("You") and John Wiley and Sons ("John Wiley and Sons") consists of your license details and the terms and conditions provided by John Wiley and Sons and Copyright Clearance Center.

License Number	4317600821296
License date	Mar 28, 2018
Licensed Content Publisher	John Wiley and Sons
Licensed Content Publication	The EMBO Journal
Licensed Content Title	Cryo-EM reconstruction of Type VI secretion system baseplate and sheath distal end
Licensed Content Author	Sergey Nazarov, Johannes P Schneider, Maximilian Brackmann, et al
Licensed Content Date	Dec 18, 2017
Licensed Content Volume	37
Licensed Content Issue	4
Licensed Content Pages	14
Type of use	Dissertation/Thesis
Requestor type	University/Academic
Format	Print and electronic
Portion	Figure/table
Number of figures/tables	1
Original Wiley figure/table number(s)	Figure 3.
Will you be translating?	No
Title of your thesis / dissertation	Using the Pseudomonas aeruginosa T6SS as a protein shuttle to deliver effectors
Expected completion date	Apr 2018
Expected size (number of pages)	300
Requestor Location	Ms. Sarah Wettstadt 3 Adelaide Grove Red door London, W12 0JU United Kingdom Attn: Ms. Sarah Wettstadt
Publisher Tax ID	EU826007151
Total	0.00 GBP
Terms and Conditions	

ELSEVIER LICENSE
TERMS AND CONDITIONS

Apr 28, 2018

This Agreement between Ms. Sarah Wettstadt ("You") and Elsevier ("Elsevier") consists of your license details and the terms and conditions provided by Elsevier and Copyright Clearance Center.

License Number	4337581381008
License date	Apr 28, 2018
Licensed Content Publisher	Elsevier
Licensed Content Publication	Current Opinion in Structural Biology
Licensed Content Title	Towards a complete structural deciphering of Type VI secretion system
Licensed Content Author	Van Son Nguyen,Badreddine Douzi,Eric Durand,Alain Roussel,Eric Cascales,Christian Cambillau
Licensed Content Date	Apr 1, 2018
Licensed Content Volume	49
Licensed Content Issue	n/a
Licensed Content Pages	8
Start Page	77
End Page	84
Type of Use	reuse in a thesis/dissertation
Portion	figures/tables/illustrations
Number of figures/tables/illustrations	1
Format	both print and electronic
Are you the author of this Elsevier article?	No
Will you be translating?	No
Original figure numbers	Figure 1
Title of your thesis/dissertation	Using the Pseudomonas aeruginosa T6SS as a protein shuttle to deliver effectors
Publisher of new work	Imperial College London
Expected completion date	Apr 2018
Estimated size (number of pages)	300
Requestor Location	Ms. Sarah Wettstadt 3 Adelaide Grove Red door London, W12 0JU United Kingdom Attn: Ms. Sarah Wettstadt
Publisher Tax ID	GB 494 6272 12
Total	0.00 GBP
Terms and Conditions	